INTERNATIONAL REVIEW OF CELL AND MOLECULAR BIOLOGY

Edited by

Kwang W. Jeon

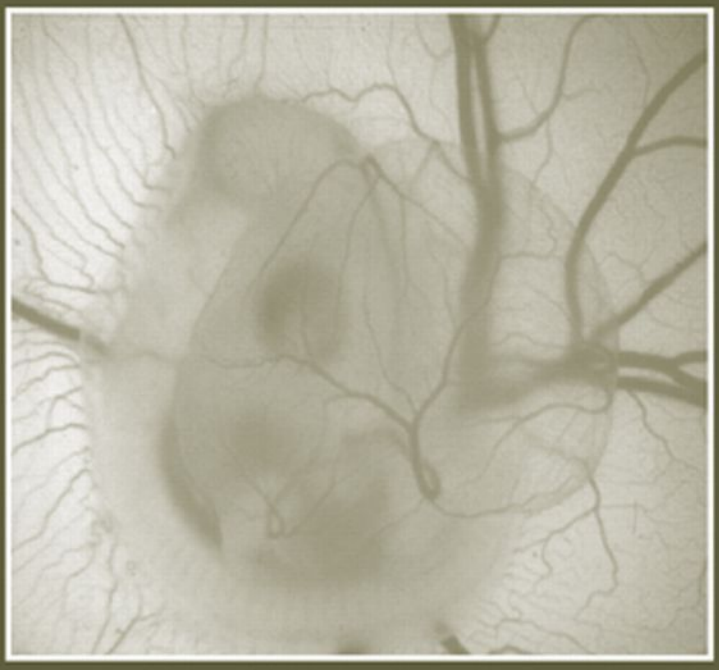

Volume 270

VOLUME TWO SEVENTY

International Review of CELL AND MOLECULAR BIOLOGY

INTERNATIONAL REVIEW OF CELL AND MOLECULAR BIOLOGY

VOLUME TWO SEVENTY

International Review of CELL AND MOLECULAR BIOLOGY

EDITED BY

KWANG W. JEON
Department of Biochemistry
University of Tennessee
Knoxville, Tennessee

ELSEVIER

AMSTERDAM • BOSTON • HEIDELBERG • LONDON
NEW YORK • OXFORD • PARIS • SAN DIEGO
SAN FRANCISCO • SINGAPORE • SYDNEY • TOKYO
Academic Press is an imprint of Elsevier

Front Cover Photography: Cover figure by Domenico Ribatti.

Academic Press is an imprint of Elsevier
525 B Street, Suite 1900, San Diego, CA 92101-4495, USA
30 Corporate Drive, Suite 400, Burlington, MA 01803, USA
32, Jamestown Road, London NW1 7BY, UK
Radarweg 29, PO Box 211, 1000 AE Amsterdam, The Netherlands

First edition 2008

British Library Cataloguing in Publication Data
A catalogue record for this book is available from the British Library

Library of Congress Cataloging-in-Publication Data
A catalog record for this book is available from the Library of Congress

For information on all Academic Press publications
visit our website at elsevierdirect.com

ISBN: 978-0-12-374583-5

PRINTED AND BOUND IN UNITED STATES OF AMERICA
08 09 10 11 12 10 9 8 7 6 5 4 3 2 1

Contents

This page intentionally left blank

Contributors

Michael J. Caplan
Department of Cellular and Molecular Physiology, Yale University School of Medicine, New Haven, Connecticut 06520

Amy Duffield
Department of Pathology, Johns Hopkins Medical Institutions, Baltimore, Maryland 21287, and Department of Cellular and Molecular Physiology, Yale University School of Medicine, New Haven, Connecticut 06520

Olivier Dussurget
Institut Pasteur, Unité des Interactions Bactéries-Cellules, Inserm, U604, and INRA, USC2020, Paris F-75015, France

Ilya Gadjev
Department of Plant Physiology and Plant Molecular Biology, University of Plovdiv, Plovdiv 4000, Bulgaria

Tsanko S. Gechev
Department of Plant Physiology and Plant Molecular Biology, University of Plovdiv, Plovdiv 4000, Bulgaria

Michio Homma
Division of Biological Science, Graduate School of Science, Nagoya University, Nagoya, Japan

Seiji Kojima
Division of Biological Science, Graduate School of Science, Nagoya University, Nagoya, Japan

Theodore R. Muth
Department of Biology, Brooklyn College, City University of New York, Brooklyn, New York 11210

Domenico Ribatti
Department of Human Anatomy and Histology, University of Bari Medical School, I-70124 Bari, Italy

Alexei P. Ryskov
Institute of Gene Biology, Russian Academy of Sciences, 119334 Moscow, Russia

Julie M. Stone
Department of Biochemistry and Center for Plant Science Innovation, University of Nebraska – Lincoln N230 Beadle Center, Lincoln, Nebraska 68588

Andrei Surguchov
Retinal Biology Research Laboratory, VA Medical Center, Kansas City, Missouri 64128, and Kansas University Medical Center, Kansas City, Kansas, Missouri 66148

Hiroyuki Terashima
Division of Biological Science, Graduate School of Science, Nagoya University, Nagoya, Japan

CHAPTER ONE

New Insights into Determinants of *Listeria Monocytogenes* Virulence

Olivier Dussurget[*,†,‡]

Contents

* Institut Pasteur, Unité des Interactions Bactéries-Cellules, Paris F-75015, France
† Inserm, U604, Paris F-75015, France
‡ INRA, USC2020, Paris F-75015, France

International Review of Cell and Molecular Biology, Volume 270
ISSN 1937-6448, DOI: 10.1016/S1937-6448(08)01401-9

Abstract

Listeria monocytogenes is the causative agent of human listeriosis, a potentially fatal foodborne infection. Clinical manifestations range from febrile gastroenteritis to more severe invasive forms including meningitis, encephalitis, abortions, and perinatal infections. This Gram-positive facultative intracellular pathogen has evolved multiple strategies to face extracellular innate defense mechanisms of the host and to invade and multiply intracellularly within macrophages and nonphagocytic cells. This chapter provides an updated panorama of recent advances in the characterization of *L. monocytogenes* virulence determinants in the postgenomic era.

Key Words: Listeriosis, *Listeria monocytogenes*, Virulence, Genome, Cell invasion, Immunity, Pathophysiology.

1. Introduction

The *Listeria* genus is composed of six species: *L. monocytogenes*, *L. ivanovii*, *L. innocua*, *L. seeligeri*, *L. welshimeri*, and *L. grayi* (Vazquez-Boland *et al.*, 2001b). The pathogenic species *L.monocytogenes* causes disease in humans and animals. The second pathogenic species, *L. ivanovii*, causes disease in animals. *L. innocua*, *L. seeligeri*, *L. welshimeri*, and *L. grayi* are four nonpathogenic species. *Listeria* spp. are flagellated and motile Gram-positive, nonsporeforming, facultative anaerobic bacilli of low GC content (Seeliger and Jones, 1986). These ubiquitous bacteria are commonly isolated from multiple sources such as plants, soil, and water. *L. monocytogenes* can contaminate the agricultural environment, animal feed, and food at various stages of the production process leading to recalls (Orndorff *et al.*, 2006; Roberts and Wiedmann, 2003). It is thus a major problem in the food industry. Ingestion of food contaminated with *L. monocytogenes* is the primary route of transmission to humans. *L. monocytogenes* is the causative agent of listeriosis. Although the incidence of the disease is low (0.1 to 11.3/1,000,000), it is a public health concern because of a high mortality rate (20–30%) and high occurrence of *Listeria* in food (Swaminathan and Gerner-Smidt, 2007).

L. monocytogenes causes two forms of listeriosis depending on the immunological status of the host, the pathogenic potential of the bacterial strain, and the infectious dose: noninvasive gastrointestinal listeriosis and invasive listeriosis (Vazquez-Boland *et al.*, 2001b). In immunocompetent individuals, noninvasive listeriosis develops as a typical febrile gastroenteritis. In immunocompromised adults such as the elderly, patients with genetic or acquired defects in immunity and patients receiving immunosuppressive agents, listeriosis can manifest as septicemia and/or meningoencephalitis.

Invasive listeriosis can also be acquired by the fetus from the infected mother by transplacental transmission. Perinatal listeriosis can lead to abortion, birth of a stillborn fetus or a baby with generalized infection (granulomatosis infanseptica), and meningitis in neonates. Clinical features of invasive listeriosis derive from the unique capacity of *L. monocytogenes* to cross three barriers: the intestinal, blood–brain, and placental barriers (Lecuit, 2005). The clinical outcome of listeriosis is influenced by the pathogenic potential of the infecting strain. Among *L. monocytogenes* strains, those of the serovars 1/2a, 1/2b, and 4b are responsible for 95% of human infections and most outbreaks are caused by strains of serovar 4b (Swaminathan and Gerner-Smidt, 2007). The remarkable capacity of *L. monocytogenes* to invade and multiply in epithelial cells and professional phagocytic cells is central to listeriosis pathophysiology (Fig. 1.1). *L. monocytogenes* uses various receptors to enter these cells. After internalization, the bacterium lyzes the vacuole, escapes in the cytosol, and replicates. *L. monocytogenes* then exploits the actin machinery to move within the cell and to neighboring cells where it is internalized in a double-membrane vacuole that is lyzed, allowing the bacterium to access the cytosol and start a new intracellular infection cycle (Tilney and Portnoy, 1989).

For more than 40 years, *L. monocytogenes* and experimental listeriosis have been used to study the immune response and the biology of the cell leading to major discoveries (Cossart, 2007; Garifulin and Boyartchuk, 2005; Hamon *et al.*, 2006; Mackaness, 1962; Pamer, 2004). More recently, the extensive characterization of the mechanisms used by *L. monocytogenes* to

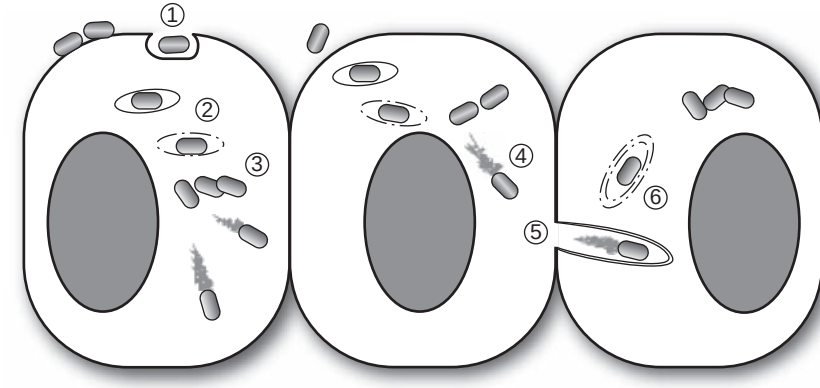

Figure 1.1 Schematic representation of the infectious cycle of *Listeria monocytogenes*. Bacteria first adhere to cells, induce entry, and are internalized in a vacuole (1). The vacuole is lyzed by *L. monocytogenes* virulence factors (2). Once free in the cell cytoplasm, bacteria start to replicate (3). *L. monocytogenes* then exploits the actin polymerization machinery of the cell to propel itself (4). When bacteria reach a neighboring cell, they induce the formation of a protrusion characterized by a double membrane (5). This secondary vacuole is finally lyzed (6), allowing a new infection cycle.

manipulate the host cell contributed to the creation of the field of cellular microbiology (Cossart *et al.*, 1996). The advanced knowledge of the specificity of *L. monocytogenes* interactions with the host culminated in 2001, with the creation of the first transgenic mouse to model human listeriosis in animals (Lecuit, 2007; Lecuit and Cossart, 2002; Lecuit *et al.*, 2001). The same year, the first comparison of the genome sequences of a pathogenic bacterium and a related nonpathogenic species, *L. monocytogenes* and *L. innocua*, respectively, allowed to envision the identification of the complete arsenal used by *Listeria* to cause disease (Dussurget *et al.*, 2004; Glaser *et al.*, 2001). Here, we review *L. monocytogenes* major virulence determinants that have been currently characterized.

2. Acquisition of Virulence Genes and Their Expression

2.1. Acquisition of virulence genes

Acquisition and loss of genetic elements lead to bacterial speciation and provide the properties necessary for a particular lifestyle. Cumulative acquisition of virulence genes provides pathogenic bacteria the functions required for survival, growth and damage in the infected host.

The genome organization is remarkably conserved between different *Listeria* species (Hain *et al.*, 2007; Schmid *et al.*, 2005). However, comparative genomic analysis of pathogenic and nonpathogenic *Listeria* species reveals scattered genes specific to virulent strains that are isolated or form pathogenicity islands (Glaser *et al.*, 2001; Vazquez-Boland *et al.*, 2001a). The unusual base composition of some of these sequences could be the consequence of horizontal transfer (Begley *et al.*, 2005; Dussurget *et al.*, 2002). Interestingly, *Listeria* genomes contain open reading frames homologous to *Bacillus subtilis* competence genes (Buchrieser, 2007; Glaser *et al.*, 2001). Although the function of this putative DNA uptake system has not been demonstrated yet, it could be hypothesized that competence may play a role in acquisition of virulence genes by *L. monocytogenes*. Lysogenic bacteriophages, plasmids, and transposons, which could play critical roles in the evolution of pathogenicity, have been characterized in *Listeria* species but they have not been associated to virulence (Hain *et al.*, 2007). Nonpathogenic species, including *L. innocua* appear to have evolved from a *L. monocytogenes* ancestor after multiple deletions of virulence genes (Buchrieser, 2007; Hain *et al.*, 2006). Recently, analysis of the complete genome sequence of the nonpathogenic *L. welshimeri* revealed deletions of all the genes required for virulence and of some genes encoding

transcription factors, surface proteins, and proteins involved in carbohydrate transport and metabolism (Hain *et al.*, 2006). Comparison of *L. welshimeri* and *L. innocua* suggests similar evolutionary paths from an ancestor.

2.2. Regulation of virulence gene expression

Adaptability of *L. monocytogenes* that is central to the infectious process is determined by the genetic elements allowing bacteria to survive and multiply within multiple tissues and by the mechanisms required for the tight and coordinate regulation of their expression.

2.2.1. PrfA

PrfA is the master regulator of virulence gene expression in *L. monocytogenes*. PrfA is a protein of 233 amino acids that binds to a 14-bp palindromic sequence in the −41 region of the genes from the PrfA regulon and activates their transcription. The activity of PrfA itself is tightly controlled by multiple mechanisms (Vazquez-Boland *et al.*, 2001b). Translation of PrfA is regulated by temperature (Johansson and Cossart, 2003; Johansson *et al.*, 2002). At a temperature lower than 30 °C, the untranslated region of *prfA* mRNA adopts a stable secondary structure that prevents binding of the ribosome and blocks translation. In the host, the temperature of 37 °C induces melting of the secondary structure. Consequently, PrfA is translated and activates virulence gene expression. Determination of *L. monocytogenes* genome sequence allowed analysis of the transcriptome and identification of the PrfA regulon (Milohanic *et al.*, 2003). The transcriptomic analysis identified a total of 73 genes regulated directly or indirectly by PrfA. This study confirmed that the expression of important virulence genes such as *hly*, *actA*, *plcA*, *plcB*, *mpl*, *inlA*, *inlB*, *inlC*, *hpt*, and *prfA* itself is activated by PrfA. Interestingly, the expression of all these genes is increased intracellularly after infection of macrophages and epithelial cells (Chatterjee *et al.*, 2006; Joseph *et al.*, 2006).

2.2.2. Sigma B

Other regulatory elements have been demonstrated to be necessary for full virulence of *L. monocytogenes*. The stress-responsive alternative sigma factor encoded by *sigB* contributes to invasion (Kim *et al.*, 2004) and virulence (Garner *et al.*, 2006; Nadon *et al.*, 2002). The sigma B regulon contains stress response and virulence genes such as *gadB*, *opuCA*, *bsh*, *inlA*, and *inlB* (Kazmierczak *et al.*, 2003; McGann *et al.*, 2007; Sue *et al.*, 2003) and stress and virulence gene regulators Hfq (Christiansen *et al.*, 2004; Nadon *et al.*, 2002) and PrfA (Nadon *et al.*, 2002).

2.2.3. MogR

Temperature-dependent expression of the flagellin gene *flaA* is controlled by the transcriptional regulator DegU and by the antagonist activity of the repressor MogR (Grundling *et al.*, 2004). At 37 °C, flagellin synthesis is repressed by the regulator MogR. At 30 °C and below, DegU activates expression of GmaR that forms a complex with MogR and prevents binding of the repressor to its target DNA sequences (Shen *et al.*, 2006). GmaR is a bifunctional protein that functions as an antirepressor and an O-linked *N*-acetylglucosamine transferase that glycosylates flagellin (Schirm *et al.*, 2005; Shen *et al.*, 2006). The role of flagellin glycosylation remains to be determined. MogR contributes to *L. monocytogenes* virulence (Grundling *et al.*, 2004; Shen and Higgins, 2006) and its expression is induced in macrophages (Chatterjee *et al.*, 2006). Overproduction of FlaA in *mogR* mutants leads to defects in bacterial division, intracellular spread, and virulence in mice.

2.2.4. CtsR

The class III stress gene repressor CtsR regulates the expression of class III heat-shock genes encoding the Clp ATPases ClpB, ClpC, ClpE, and ClpP, which are required for virulence (Chastanet *et al.*, 2004; Gaillot *et al.*, 2000; Nair *et al.*, 1999, 2000; Rouquette *et al.*, 1998). Interestingly, the expression of CtsR and the four ATPases is induced in infected macrophages (Chatterjee *et al.*, 2006).

2.2.5. PerR and Fur

The Fur family of regulators includes sensors of iron (Fur), zinc (Zur), manganese (Mur), nickel (Nur), as well as metal-dependent reactive oxygen species sensors such as the peroxide sensor PerR (Lee and Helmann, 2007). The iron-responsive transcriptional regulator Fur is responsible for coordinating the expression of genes involved in iron uptake and storage (Lee and Helmann, 2007). The regulator PerR senses peroxides by metal-catalyzed oxidation and regulates the expression of inducible genes involved in defense against reactive oxygen species (Lee and Helmann, 2006). *L. monocytogenes perR* and *fur* mutants are more sensitive to hydrogen peroxide and have a significantly reduced virulence of in mice (Rea *et al.*, 2004, 2005). Interestingly, the PerR regulon includes the ferritin gene *fri* that contributes to survival of *L. monocytogenes in vivo* (Dussurget *et al.*, 2005; Mohamed *et al.*, 2006; Olsen *et al.*, 2005). Thus, regulation of iron uptake and oxidative stress response is an important determinant for the infectious process.

2.2.6. LisRK, AgrA, VirR, and DegU

Several two-component regulatory systems contribute to *L. monocytogenes* survival in the infected host. LisRK is important for bacterial response to acid and hydrogen peroxide stresses and for osmotolerance mediated by the

HtrA-like serine protease (Cotter *et al.*, 1999; Stack *et al.*, 2005). The response regulators AgrA (Autret *et al.*, 2003) and VirR (Mandin *et al.*, 2005) play a role in virulence, which was identified by signature-tagged mutagenesis. A transcriptomic approach led to the identification of 12 genes regulated by VirR, including the *dlt* operon, which is required for *L. monocytogenes* full virulence. However, a *dltA* mutant is not as impaired in virulence as a *virR* mutant, suggesting that the response regulator may control the expression of other virulence determinants (Mandin *et al.*, 2005). Indeed, another member of the VirR regulon, the *mprF* gene, has recently been shown to contribute to *L. monocytogenes* virulence (Thedieck *et al.*, 2006). The response regulator DegU is a transcriptional activator of the expression of the flagellin gene *flaA* at low temperature and regulates virulence-associated genes (Knudsen *et al.*, 2004; Williams *et al.*, 2005).

2.2.7. Stp

Analysis of *L. monocytogenes* genome sequence revealed 9 signal transduction systems based on reversible phosphorylation in addition to the 16 two-component systems: 4 putative tyrosine phosphatases, 3 putative serine-threonine kinases, and 2 putative serine-threonine phosphatases (Archambaud *et al.*, 2005; Glaser *et al.*, 2001). One of the latter enzyme is an Mn^{2+}-dependent serine-threonine phosphatase that has an important role in regulating the elongation factor EF-Tu and controlling bacterial survival in the infected host (Archambaud *et al.*, 2005). Stp was recently shown to control L. monocytogenes manganese dependent-superoxide dismutase (MnSOD) an enzyme that is required for full virulence (Archambaud *et al.*, 2006).

2.2.8. Hfq

The RNA-binding protein Hfq regulates multiple important processes such as stress tolerance and virulence. Hfq contributes to virulence in mice possibly by interacting with mRNA and/or small regulatory RNA, playing a role in the survival and multiplication of *L. monocytogenes in vivo* (Christiansen *et al.*, 2004; Mandin *et al.*, 2007).

3. Adaptation to Host Extracellular Compartments

Following ingestion, the capacity of *L. monocytogenes* to survive and multiply successfully under the multiple and dynamic environments found in the host is an essential factor in the infectious process.

3.1. GAD

The glutamate decarboxylase system GAD is essential for survival in the stomach after ingestion (Cotter *et al.*, 2001). Depending on the strain, it is composed of two or three glutamate decarboxylases and one or two glutamate/γ-aminobutyrate antiporters (Cotter *et al.*, 2005). The GAD system transports and converts glutamate to γ-aminobutyrate consuming a proton, allowing *L. monocytogenes* to survive in acidic environments.

3.2. BSH

Bile is essential to emulsify lipids and has important antimicrobial properties. *L. monocytogenes* is well equipped to tolerate high concentration of bile (Begley *et al.*, 2002, 2003, 2005; Dussurget *et al.*, 2002; Sleator *et al.*, 2005). Analysis of *L. monocytogenes* genome sequence revealed the presence of a gene encoding a bile salt hydrolase (BSH) that was absent from the genome of the nonpathogenic species *L. innocua* (Dussurget *et al.*, 2002). BSH is produced by commensal enteric bacteria and lactic bacteria. Deconjugation of conjugated bile salts by BSH could be a protective mechanism against bile toxicity. *L. monocytogenes* BSH is controlled by sigma B (Kazmierczak *et al.*, 2003; Sue *et al.*, 2003) and activated by PrfA (Dussurget *et al.*, 2002). Its activity is induced at low oxygen tension that could be a signal sensed by bacteria after ingestion to express the *bsh* as well as other virulence genes (Dussurget *et al.*, 2002). *L. monocytogenes* BSH confers resistance to bile (Begley *et al.*, 2005; Dussurget *et al.*, 2002). Deletion of the *bsh* gene results in dramatically reduced fecal carriage in guinea pigs after intragastric inoculation and decreased survival in the liver of mice after intravenous injection (Dussurget *et al.*, 2002). BSH is therefore a new type of virulence determinant that is important for both intestinal persistence and hepatic colonization.

3.3. BilE

Analysis of *L. monocytogenes* genome revealed a two-gene operon, *bilEA–bilEB*, which is critical for bile tolerance (Sleator *et al.*, 2005). The expression of the operon is controlled by sigma B and PrfA. The operon encodes a bile exclusion system providing a protection against bile and contributing to *L. monocytogenes* virulence in mice infected orally.

3.4. BtlB

A third locus, *btlB*, has been shown to contribute to bile tolerance and *L. monocytogenes* virulence in mice (Begley *et al.*, 2005). BtlA and Pva that encode a putative transporter and a penicillin V amidase, respectively, are other important determinants conferring tolerance to bile but do not contribute significantly to virulence in mice (Begley *et al.*, 2003, 2005).

3.5. OpuC

Once in the intestinal lumen, *L. monocytogenes* has to cope not only with the presence of bile salts but also with an increased osmolarity. *L. monocytogenes* produces several osmolyte uptake systems increasing osmotolerance, such as the glycine betaine transporters BetL and Gbu and the carnitine transporter OpuC (Ko and Smith, 1999; Sleator *et al.*, 1999, 2001; Wemekamp-Kamphuis *et al.*, 2002). While deletion of *betL* and *gbu* does not affect virulence, OpuC is required for full virulence in mice infected orally (Sleator *et al.*, 2001; Wemekamp-Kamphuis *et al.*, 2002).

3.6. OppA

Uptake of oligopeptides by the OppA transporter could also contribute to osmotolerance and is required for intracellular survival in macrophages and bacterial growth in mice (Borezee *et al.*, 2000).

4. Adhesion, Cell Invasion, and Intracellular Multiplication

Following gastrointestinal passage of *L. monocytogenes*, some of the bacteria that survived nonspecific defense mechanisms of the host in the stomach and intestinal lumen invade the intestinal tissue. Crossing of the intestinal barrier prevents their mechanical elimination by peristalsis and competition with the commensal flora. *L. monocytogenes* has the capacity to invade both intestinal epithelial cells and M cells of Peyer's patches. After intestinal translocation, bacteria reach the liver, spleen, and mesenteric lymph nodes by the blood and lymph. In the liver, the major site of *L. monocytogenes* multiplication is the hepatocyte. If the multiplication is not controlled by the host immune response, bacteria access the blood-stream and infect secondary target organs. Although *L. monocytogenes* has a strong neurotropism, it can infect a wide range of tissues (Vazquez-Boland *et al.*, 2001b). *L. monocytogenes* has an exceptional repertoire of virulence determinants involved in cellular adhesion, entry, and survival (Bierne and Cossart, 2007; Hamon *et al.*, 2006; Seveau *et al.*, 2007).

4.1. Adhesion

4.1.1. Ami

Ami is a 102-kDa autolytic amidase of 917 amino acids that is involved in adhesion to cells and virulence (Milohanic *et al.*, 2000, 2001). It was identified by transposon mutagenesis in an *inlAB* deletion mutant

(Milohanic *et al.*, 2000, 2001). One of the mutants severely defective in adhesion to eukaryotic cells had five insertions, one of which was upstream from the *ami* gene. Construction of an *ami* null mutant demonstrated that Ami significantly contributed to *L. monocytogenes* adhesion capacity (Milohanic *et al.*, 2000, 2001). Ami has an N-terminal region containing the amidase domain and C-terminal cell wall-anchoring domain composed of eight modules containing the dipeptide GW (Milohanic *et al.*, 2004). Adhesion to cells is promoted by the cell wall-anchoring domain (Milohanic *et al.*, 2000, 2001). *L. monocytogenes* attachment mediated by Ami may contribute to colonization of host tissues.

4.1.2. DltA

Lipoteichoic acids are highly anionic cell wall-associated polymers. The *dltABCD* operon is responsible for D-alanine esterification of lipoteichoic acids. Inactivation of the D-alanine-polyphosphoribitol ligase gene *dltA*, leading to synthesis of D-alanine-deficient lipoteichoic acids, attenuates *L. monocytogenes* virulence in mice (Abachin *et al.*, 2002; Mandin *et al.*, 2005). DltA deficiency decreases adherence of bacteria to macrophages, hepatocytes, and epithelial cells, possibly by modulation of the charge of the bacterial surface and/or by alteration of adhesin-binding activity (Abachin *et al.*, 2002).

4.1.3. FbpA

FbpA is an adhesin that is important for *L. monocytogenes* pathogenesis. FbpA has been identified using signature-tagged mutagenesis (Dramsi *et al.*, 2004). It was shown to be required for liver colonization of mice inoculated intravenously as well as intestinal and liver colonization of mice expressing human E-cadherin after intragastric inoculation. FbpA is a protein of 570 amino acids homologous to atypical fibronectin-binding proteins. It binds to human fibronectin and increases *L. monocytogenes* adhesion to eukaryotic cells in the presence of exogenous fibronectin. FbpA is secreted by the SecA2 pathway and exposed on the bacterial surface. In addition to its fibronectin-binding capacity, FbpA coprecipitates with the virulence factors listeriolysin O (LLO) and InlB. Expression of FbpA modulates the protein levels of LLO and InlB, suggesting that it could function as a chaperone to prevent the degradation of virulence factors (Dramsi *et al.*, 2004).

4.1.4. Flagella

L. monocytogenes produces up to six peritrichous flagella (Leifson and Palen, 1955). Flagella are composed of a basal body, hook/junction proteins, a flagellar motor/switch, a flagella export apparatus, and a flagellar filament containing mostly the flagellin protein FlaA. Flagellin is a potent proinflammatory protein that activates Toll-like receptor (TLR) 5 (Hayashi *et al.*, 2001). Moreover, flagellin has been reported to have peptidoglycan

hydrolyzing activity (Popowska and Markiewicz, 2004). While many flagella are produced at 20 °C, the expression of flagellar motility genes is repressed at 37 °C (Griffin and Robbins, 1944; Grundling *et al.*, 2004; Peel *et al.*, 1988; Way *et al.*, 2004). However, the temperature control of flagellar motility is less stringent in some *L. monocytogenes* strains (Grundling *et al.*, 2004; Way *et al.*, 2004). Flagellin expression at 37 °C is maintained in 20% of clinical isolates (Bigot *et al.*, 2005; Way *et al.*, 2004). Flagella contribute to *L. monocytogenes* adhesion and invasion of epithelial cells. Indeed, the nonmotile *flaA* mutant, *fliF* and *fliI* mutants, lacking the basal body and the ATPase of the flagellar export apparatus, and the *cheYA* chemotaxis mutant are strongly impaired in adhesion and invasion (Bigot *et al.*, 2005; Dons *et al.*, 2004). It has recently been demonstrated that flagella do not function as adhesins but that flagella-dependent motility promotes *L. monocytogenes* invasion of epithelial cells (O'Neil and Marquis, 2006). The specific role of flagellar motility and flagellin in the infectious process is not completely understood. Liver and spleen colonization of a *flaA* deletion mutant has been shown to be similar to that of a parental strain expressing flagellin constitutively, after intravenous infection of mice (Way *et al.*, 2004). However, survival of the parental strain producing flagellin seemed to be decreased compared with that of the *flaA* mutant, 7 days after intragastric inoculation of mice. The LD50 of *fliF* and *fliI* mutants was very modestly affected compared with that of the EGDe wild-type strain after intravenous infection of Swiss mice (Bigot *et al.*, 2005). Interestingly, the survival of the wild-type strain was lower than that of the *fliF* mutant in the spleen of BALB/c mice, 3 days after intragastric infection. A similar observation was reported with a *flaA* mutant that was recovered in higher numbers than the wild-type strain from the spleen of BALB/c mice, 3 days after intragastric inoculation (Dons *et al.*, 2004). However, the fact that this difference was not detected at 1 or 7 days postinfection is puzzling. Recently, flagellin was shown to be required for intestinal and liver colonization in the early phase of murine listeriosis, between 4 and 18 h after intragastric inoculation (O'Neil and Marquis, 2006). It could be hypothesized that *L. monocytogenes* regulates flagella synthesis in time and space, producing flagella to colonize the gastrointestinal tract after ingestion and repressing their synthesis as a means of innate immune evasion at later stages of the infectious process.

4.2. Internalization

4.2.1. Internalin

The internalin is a protein of 800 amino acids encoded by the *inlA* gene. It is composed of a typical N-terminal signal sequence followed by 15 leucine-rich repeats (LRRs) of 22 amino acids, a conserved interrepeat region and a second repeat region, the B repeat region. The C-terminus displays the

sequence LPTTG, which is recognized by the sortase A, a transamidase that covalently links LPXTG-containing proteins to the peptidoglycan. This surface protein is an invasin that mediates internalization of *L. monocytogenes* in epithelial cells. It was identified by screening a bank of transposon mutants for reduced entry in Caco-2 cells (Gaillard *et al.*, 1991). The intercellular adhesion glycoprotein E-cadherin was subsequently identified as the internalin ligand using affinity chromatography (Mengaud *et al.*, 1996). If E-cadherin ectodomain is sufficient for adherence of *L. monocytogenes* to cells, the intracytoplasmic β-catenin-binding domain is required for entry (Lecuit *et al.*, 2000). Bacterial interaction with E-cadherin triggers actin polymerization mediated by β-catenin and α-catenin interaction, leading to membrane extension and internalization. Recently, ARHGAP10, a Rho-GAP domain protein that interacts with the small GTP-binding protein Arf6 and is a new ligand of α-catenin identified by a two-hybrid screen, has been shown to be critical for recruitment of α-catenin and bacterial entry (Sousa *et al.*, 2005). The internalin-dependent entry pathway requires several other proteins including myosin VIIA, Src, cortactin, and Arp2/3. The myosin VIIA, a molecular motor recruited at adherens junctions by the transmembrane protein vezatin, could contribute to the contractile force necessary for internalization of *L. monocytogenes* (Sousa *et al.*, 2004). The tyrosine kinase Src and the small GTPase Rac1 promote the recruitment of cortactin leading to activation of the actin nucleator Arp2/3 necessary for E-cadherin-mediated bacterial entry (Sousa *et al.*, 2007).

Although internalin plays a major role in bacterial internalization into specific cell lines, the protein had a minor contribution to virulence in the murine models that were first used, irrespective of the route of infection, that is intravenous or intragastric inoculations (Gaillard *et al.*, 1996). It was later shown that the mouse E-cadherin does not interact efficiently with InlA (Lecuit *et al.*, 1999). Indeed, the interaction requires recognition of the proline 16 of the first extracellular domain of E-cadherin as found in human or guinea pig E-cadherins. However, the murine E-cadherin has a glutamic acid at position 16. A transgenic mouse expressing the human E-cadherin in the intestine was created and used to demonstrate the major role of internalin in the specific crossing of the intestinal barrier by *L. monocytogenes* (Lecuit *et al.*, 2001). Recently, a strain of *L. monocytogenes* expressing an internalin with two amino acid substitutions allowing efficient binding to murine E-cadherine was created (Wollert *et al.*, 2007). This new strain could be a powerful tool to study listeriosis in nontransgenic mice, circumventing limitations, and problems inherent to humanized mice.

In addition to its established role in crossing of the intestinal barrier, InlA is involved in the crossing of the maternofetal barrier (Lecuit *et al.*, 2004). Internalin is required for *L. monocytogenes* entry into E-cadherin-expressing syncytiotrophoblasts and crossing of the trophoblastic barrier in human placental explants (Lecuit *et al.*, 2004). Interestingly, the InlA protein is

truncated in some *L. monocytogenes* isolates. Truncation of InlA has been involved in defective invasion capacity of *L. monocytogenes* isolates from healthy carriers (Olier *et al.*, 2003). An epidemiological survey demonstrated that a full-length InlA was produced by 96% of *L. monocytogenes* clinical isolates and only 65% of the strains isolated from food products (Jacquet *et al.*, 2004). Another study confirmed that *inlA* mutations leading to premature stop codons were common in food isolates but rare in clinical isolates (Nightingale *et al.*, 2005). These results strongly suggest that a functional internalin is a key determinant in the pathogenesis of human listeriosis.

4.2.2. InlB

InlB is a 630-amino acid protein encoded by the gene *inlB*, which is located directly downstream of *inlA* in a two-gene operon (Gaillard *et al.*, 1991). The operon is regulated by PrfA and absent from *L. innocua* (Dramsi *et al.*, 1993; Glaser *et al.*, 2001; Lingnau *et al.*, 1995; Milohanic *et al.*, 2003). In contrast to internalin, InlB is required for *L. monocytogenes* internalization into a wide range of cells including epithelial cells, endothelial cells, hepatocytes, and fibroblasts (Braun *et al.*, 1998; Dramsi *et al.*, 1995; Greiffenberg *et al.*, 1998; Parida *et al.*, 1998). The InlB protein displays a signal sequence followed by seven LRRs, a B repeat, and three C-terminal GW modules. The GW modules interact noncovalently with lipoteichoic acids mediating loose attachment of InlB to the bacterial cell wall (Jonquieres *et al.*, 1999). The LRR region of the protein is sufficient to allow entry of noninvasive *L. innocua* or latex beads into cells (Braun *et al.*, 1999). However, the GW modules enhance internalization triggered by the LRR region. Binding of InlB to cellular glycosaminoglycans by its GW modules is required for efficient invasion (Banerjee *et al.*, 2004; Jonquieres *et al.*, 2001; Marino *et al.*, 2000, 2002, 2004). The GW modules of InlB also interact with the receptor for the globular head domain of the complement component C1q, gC1qR (Braun *et al.*, 2000). This interaction is not sufficient to allow entry but cooperates with the hepatocyte growth factor, also known as the tyrosine kinase receptor Met, for invasion (Khelef *et al.*, 2006). Met has been identified as the main receptor of InlB (Shen *et al.*, 2000). Interaction of InlB and Met results in transient phosphorylation of Met (Shen *et al.*, 2000), and recruitment and phosphorylation of the adaptor proteins Cbl, Gab1, and Shc leading to activation of the PI3-kinase (Ireton *et al.*, 1996, 1999). The PI3-kinase converts PI(4,5)P2 into PI(3,4,5)P3, which results in successive activation of Rac and LIM kinase. The LIM kinase regulates the actin depolymerizing factor cofilin and thus internalization of *L. monocytogenes* (Bierne *et al.*, 2001). The WAVE complex, N-WASP, Ena/VASP, and the Arp2/3 complex are other key effectors of the Met signaling pathway that are important for cytoskeletal rearrangements necessary for InlB-mediated entry (Bierne *et al.*, 2005). It has been demonstrated that

InlB induces monoubiquitination of Met by the ubiquitin ligase Cbl resulting in endocytosis of Met (Veiga and Cossart, 2005). *L. monocytogenes* exploits the endocytic machinery to invade the cell (Bonazzi and Cossart, 2006; Veiga and Cossart, 2006). Indeed, bacterial internalization was shown to be dependent on major components of the endocytic machinery such as clathrin, dynamin, eps15, Grb2, CIN85, cortactin, and Hrs (Veiga and Cossart, 2005, 2006; Veiga *et al.*, 2007).

Activation of Met by InlB is species-specific (Khelef *et al.*, 2006). InlB activates human and murine Met but not guinea pig and rabbit Met. In mice, InlB contributes slightly to colonization of the liver and spleen. In contrast, a role for InlB in *L. monocytogenes* virulence could not be detected in guinea pigs and rabbits (Khelef *et al.*, 2006).

4.2.3. SrtA and SrtB

Surface proteins displaying a C-terminal LPXTG motif are covalently linked to the bacterial cell wall peptidoglycan by sortases. Analysis of *L. monocytogenes* genome sequence revealed the presence of two genes encoding sortases, *srtA* and *srtB* (Bierne *et al.*, 2002). SrtA anchors InlA and several other LPXTG proteins to the peptidoglycane (Bierne *et al.*, 2002; Garandeau *et al.*, 2002; Pucciarelli *et al.*, 2005). Consequently, the sortase A is necessary for efficient entry into epithelial cells (Bierne *et al.*, 2002; Garandeau *et al.*, 2002). Interestingly, it has been shown that in contrast to deletion of *inlA*, inactivation of *srtA* leads to impaired colonization of the liver and spleen of mice after intragastric inoculation (Bierne *et al.*, 2002). Thus, the sortase A could be required for the anchoring of additional LPXTG proteins involved in virulence.

In *L. monocytogenes*, SrtB anchors a small group of proteins and may recognize two different sorting motifs, NXZTN and NPKXZ (Pucciarelli *et al.*, 2005). Inactivation of *L. monocytogenes* SrtB does not affect virulence in mice after intravenous inoculation (Bierne *et al.*, 2004). One of SrtB substrate is SvpA (Bierne *et al.*, 2004), a surface protein first reported to be involved in bacterial escape from the phagosome of macrophages and in virulence (Borezee *et al.*, 2001). It was later shown that the *svpA-srtB* locus does not contribute to virulence in mice after intravenous inoculation, but is required for efficient colonization of the liver, spleen, and intestine of mice infected by the oral route (Newton *et al.*, 2005).

4.2.4. Auto

The gene *aut* was identified by a comparative genomic approach (Cabanes *et al.*, 2002, 2004; Glaser *et al.*, 2001). It is absent from the genome of the nonpathogenic species *L. innocua*. It encodes Auto, a surface protein of 572 amino acids. The N-terminus of the protein contains a signal sequence and

an autolysin domain. The C-terminus displays a cell wall attachment domain composed of four GW modules. Inactivation of Auto decreases bacterial entry into cells. However, expression of the autolysin in *L. innocua* does not confer invasivity. Thus, Auto is necessary but not sufficient for entry. The decreased invasive potential of the *aut* deletion mutant correlates with its attenuation *in vivo*. Indeed, Auto is required for *L. monocytogenes* virulence in mice infected intravenously and in guinea pigs after intragastric inoculation (Cabanes *et al.*, 2004). The precise function of Auto remains to be determined. The autolytic activity of the protein could possibly play a role in pathogenicity, for example, by controlling the composition and structure of the bacterial surface during the infectious process.

4.2.5. Vip

The gene encoding the surface protein Vip was also identified by comparative genomics of *Listeria* species (Cabanes *et al.*, 2002, 2005; Glaser *et al.*, 2001). PrfA regulates the expression of the gene *vip*, which is absent from the genome of *L. innocua* (Cabanes *et al.*, 2005). The Vip protein contains a C-terminal LPXTG motif and is anchored to the peptidoglycane by the sortase A (Cabanes *et al.*, 2005). Vip is required for invasion of several cell lines and contributes to virulence in mice infected intravenously. In contrast to InlA, it is required for virulence in mice after intragastric inoculation independently of the expression of human E-cadherin at the intestinal level. It is also an important determinant of virulence in the guinea pig. The endoplasmic reticulum resident chaperone Gp96 has been identified as a ligand of Vip (Cabanes *et al.*, 2005). Recently, the creation of a macrophage-specific gp96-deficient mouse allowed to establish that Gp96 is an important chaperone for all TLRs that have been tested (Yang *et al.*, 2007). Interestingly, these gp96-deficient mice were highly susceptible to listeriosis. In wild-type mice, interaction of Vip with Gp96 could possibly interfere with TLRs trafficking resulting in the control of the innate immune response by *L. monocytogenes*.

4.2.6. LpeA

The *lpeA* gene encoding a 35-kDa lipoprotein was identified by analysis of *L. monocytogenes* genome sequence (Glaser *et al.*, 2001; Reglier-Poupet *et al.*, 2003b). The LpeA (for lipoprotein promoting entry) protein is homologous to PsaA, a lipoprotein involved in *Streptococcus pneumoniae* adherence to cells. LpeA is not involved in adherence but is required for entry of *L. monocytogenes* into nonprofessional phagocytic cells. However, the impaired invasion of an *lpeA* mutant is not correlated with a decrease in virulence in mice (Reglier-Poupet *et al.*, 2003b).

4.3. Vacuolar escape, intracellular survival and multiplication

4.3.1. Listeriolysin O

Listeriolysin O (LLO) is one of the major virulence determinants of *L. monocytogenes* (Kayal and Charbit, 2006; Schnupf and Portnoy, 2007; Vazquez-Boland *et al.*, 2001b). The *hly* gene encoding LLO was the first virulence gene identified in *Listeria*. Identification was based on transposon mutagenesis. Characterization of the *hly* genomic locus led to identification of the *L. monocytogenes* main virulence gene cluster composed of *prfA*, *plcA*, *hly*, *mpl*, *actA*, *plcB*, and *orfX*. LLO is a secreted protein that belongs to the cholesterol-dependent cytolysin (CDC) toxin family. It is responsible for bacterial escape from primary and secondary vacuoles (Gedde *et al.*, 2000; Portnoy *et al.*, 1988). *L. monocytogenes* mutants lacking LLO fail to reach the cytoplasm and are nonvirulent (Cossart *et al.*, 1989; Gaillard *et al.*, 1986, 1987; Kathariou *et al.*, 1987; Portnoy *et al.*, 1988). The activity of LLO is optimal at the acidic pH of the phagosome. It is less active at the neutral pH of the cytoplasm, preventing excessive cell damage. LLO binds to the cell plasma membrane as monomers that oligomerize into large complexes that penetrate the membrane and contribute to pore formation. As other CDCs, LLO is a potent signaling protein that can activate important signaling pathways such as NF-κB (Kayal *et al.*, 1999), MAP kinase (Tang *et al.*, 1996), and protein kinase C (Wadsworth and Goldfine, 2002) and induce proinflammatory cytokine secretion (Kayal *et al.*, 1999). Interestingly, LLO is also required for *L. monocytogenes* entry into cells (Dramsi and Cossart, 2003). The specific functions of LLO in the signaling and entry processes remain to be elucidated.

4.3.2. Phospholipases

L. monocytogenes secretes two phospholipases C (PLC), PlcA and PlcB, involved in the bacterial escape from the vacuoles (Goldfine *et al.*, 1998). PlcA is a secreted phosphatidylinositol-specific PLC (PI-PLC) encoded by the *plcA* gene (Leimeister-Wachter *et al.*, 1991; Mengaud *et al.*, 1991). PlcB is a secreted phosphatidylcholine PLC (PC-PLC) of broad substrate range encoded by the *plcB* gene (Geoffroy *et al.*, 1991; Vazquez-Boland *et al.*, 1992). PlcB is expressed as a proenzyme. The zinc metalloprotease encoded by the gene *mpl* is required for maturation of PlcB (Domann *et al.*, 1991; Raveneau *et al.*, 1992). The two phospholipases act in synergy with LLO to lyze primary and secondary vacuoles allowing *L. monocytogenes* to escape into the cytoplasm (Camilli *et al.*, 1993; Grundling *et al.*, 2003; Smith *et al.*, 1995). PlcB can also promote lysis of the primary vacuole in the absence of LLO (Grundling *et al.*, 2003; Marquis *et al.*, 1995). Both phospholipases are required for virulence in mice (Camilli *et al.*, 1991, 1993; Raveneau *et al.*, 1992; Schluter *et al.*, 1998; Smith *et al.*, 1995).

Recently, it has been demonstrated that *L. monocytogenes* phospholipases are necessary for evasion of autophagy (Birmingham *et al.*, 2007; Py *et al.*, 2007). Cellular invasion by *L. monocytogenes* first induces autophagy, a host degradative pathway important for both cell physiology and innate immunity. Expression of LLO is necessary for the induction of the autophagic response at the early time points after infection, suggesting a role for permeabilization of the vacuole in the induction of the degradative pathway. The expression PlcA and PlcB is then required for *L. monocytogenes* escape from autophagic degradation in nonprofessional phagocytic cells and macrophages (Birmingham *et al.*, 2007; Py *et al.*, 2007). The phospholipases may prevent autophagic killing by mediating escape from the double-membrane autophagosome or by inhibiting recognition of the target of the degradative pathway.

4.3.3. Lsp

The signal peptidase II Lsp is responsible for the maturation of lipoproteins in *L. monocytogenes* (Desvaux and Hebraud, 2006; Reglier-Poupet *et al.*, 2003a). A deletion mutant of the *lsp* gene fails to process lipoproteins and has a reduced virulence. Interestingly, the expression of *lsp* is strongly induced in the phagosome of infected macrophages. This induction correlates with the important role of Lsp, and thus lipoprotein maturation, in *L. monocytogenes* escape from the phagosome (Reglier-Poupet *et al.*, 2003a).

4.3.4. SipX and SipZ

L. monocytogenes genome contains three contiguous type I signal peptidase genes, *sipX*, *sipY*, and *sipZ*, for cleavage of signal peptides proteins exported and secreted by the general secretory pathway (Bonnemain *et al.*, 2004; Desvaux and Hebraud, 2006). The expression of the three genes is induced in the phagosome of infected cells (Raynaud and Charbit, 2005). The signal peptidases SipX and SipZ are required for full virulence (Bonnemain *et al.*, 2004). In contrast, inactivation of SipY did not impaired *L. monocytogenes* virulence. In addition, SipZ is required for efficient secretion of LLO and PC-PLC. Consequently, inactivation of SipZ restricts bacterial intracellular multiplication (Bonnemain *et al.*, 2004).

4.3.5. Hpt

Once free in the cytoplasm, *L. monocytogenes* expresses specific determinants to acquire nutrients necessary for intracellular multiplication. Uptake of glucose-1-phosphate, a source of carbon and energy available in the cytosol, depends on the PrfA-regulated hexose phosphate transporter Hpt (Chico-Calero *et al.*, 2002). Interestingly, Hpt is a structural and functional homologue of the eukaryotic glucose-6-phosphate translocase required for transport of glucose-6-phosphate from the cytosol into the endoplasmic

reticulum. Hpt has been shown to be required for intracellular replication of *L. monocytogenes* and for virulence in mice (Chico-Calero *et al.*, 2002).

4.3.6. LplA1

L. monocytogenes is a lipoate auxotroph. In order to scavenge this important cofactor, bacteria produce lipoate ligases to lipoylate specific metabolic enzymes. Analysis of *L. monocytogenes* genome sequence reveals two genes encoding putative lipoate ligases, *lplA1* and *lplA2* (Keeney *et al.*, 2007). However, only *lplA1* is required for intracellular replication and virulence (Keeney *et al.*, 2007; O'Riordan *et al.*, 2003). LplA1 is critical for utilization of host lipoyl peptides as a source of lipoate by *L. monocytogenes*.

4.3.7. Fri

L. monocytogenes genome encodes a single ferritin, Fri, which is involved in iron storage. Expression of the *fri* gene is controlled by the hydrogen peroxide regulator PerR and sigma B (Olsen *et al.*, 2005). The ferritin is required for protection against reactive oxygen species and contributes to *L. monocytogenes* survival and replication in macrophages and nonprofessional phagocytic cells (Dussurget *et al.*, 2005; Mohamed *et al.*, 2006; Olsen *et al.*, 2005). The impaired survival of a *fri* deletion mutant in macrophages correlates with decreased virulence of the mutant in mice (Dussurget *et al.*, 2005; Mohamed *et al.*, 2006; Olsen *et al.*, 2005). The capacity to prevent excessive production of reactive oxygen species and control the level of iron is an important component of *L. monocytogenes* intracellular survival strategy.

4.3.8. HupC

L. monocytogenes does not secrete siderophores but can use siderophores from other microorganisms or transferrin, hemin, and hemoglobin to obtain iron (Jin *et al.*, 2006; Newton *et al.*, 2005; Simon *et al.*, 1995). The permease HupC is an ABC transporter required for hemin and hemoglobin uptake (Jin *et al.*, 2006; Newton *et al.*, 2005). The LD50 of a mutant *L. monocytogenes* lacking *hupC* was strongly increased in Swiss mice infected intravenously, suggesting that acquisition of iron from blood or other infected sites facilitates *L. monocytogenes* host colonization.

4.3.9. MnSOD

SOD plays an important role in protection against oxidative stress and has been shown to contribute to the pathogenic potential of many bacterial species. *L. monocytogenes* produces a single MnSOD encoded by the gene *sod* (Archambaud *et al.*, 2006; Brehm *et al.*, 1992; Glaser *et al.*, 2001). A *sod* deletion mutant is impaired in survival within macrophages and in virulence in mice (Archambaud *et al.*, 2006). Cytoplasmic MnSOD is phosphorylated on serine and threonine residues and can be dephosphorylated by the serine/threonine phosphatase Stp resulting in an increased SOD activity

(Archambaud *et al.*, 2006). *L. monocytogenes* MnSOD is the first bacterial SOD shown to be regulated by phosphorylation. The most active nonphosphorylated form of MnSOD is secreted via the SecA2 pathway in infected cells where it can protect *L. monocytogenes* from reactive oxygen species. Interestingly, the MnSOD becomes phosphorylated in the host cell by a putative host kinase that could control the enzyme activity (Archambaud *et al.*, 2006), suggesting a new innate mechanism of the cell to counteract an important bacterial determinant of the infectious process.

4.3.10. RelA

The *relA* gene encodes a (p)ppGpp synthetase. An *L. monocytogenes relA* transposon insertion mutant was unable to accumulate (p)ppGpp in response to amino acid starvation (Taylor *et al.*, 2002). The virulence of the mutant was strongly attenuated in mice, indicating an essential role of the stringent response in the survival and multiplication of *L. monocytogenes* in the host. Recently, RelA has been shown to be important for bacterial growth in macrophages and nonprofessional phagocytic cells, suggesting that the ability of *L. monocytogenes* to mount a stringent response is required for efficient intracellular multiplication (Bennett *et al.*, 2007).

4.3.11. Lgt

The lipoprotein diacylglyceryl transferase Lgt catalyzes transfer of an *N*-acyl diglyceride group from a glycerophospholipid to the sulfhydryl moiety of a cysteine residue conserved in the signal peptides of lipoprotein precursors. The product of the reaction is then cleaved by the signal peptidase Lsp. Deletion of *lgt* impairs intracellular growth of *L. monocytogenes* (Baumgartner *et al.*, 2007), confirming the importance of lipoprotein processing for pathogenicity (Reglier-Poupet *et al.*, 2003a).

4.4. Cell–cell spread

4.4.1. ActA

After synthesis of the determinants responsible for entry, intracellular survival, lysis of the vacuole, and cytosolic replication, *L. monocytogenes* induces polymerization of actin filaments to move in the cytoplasm and to spread from cell to cell (Mounier *et al.*, 1990; Theriot *et al.*, 1992; Tilney and Portnoy, 1989; Tilney *et al.*, 1990). The surface protein ActA is the only bacterial determinant necessary for actin-based motility of *L. monocytogenes* (Fig. 1.2) (Domann *et al.*, 1992; Kocks *et al.*, 1992). Indeed, *L. innocua* expressing ActA and latex beads coated with ActA acquire the capacity to polymerize actin and move (Cameron *et al.*, 1999; Kocks *et al.*, 1995). ActA is one of the major virulence determinants of *L. monocytogenes* (Domann *et al.*, 1992). ActA is a protein of 639 amino acids containing an N-terminal signal sequence and a C-terminal transmembrane domain (Domann *et al.*,

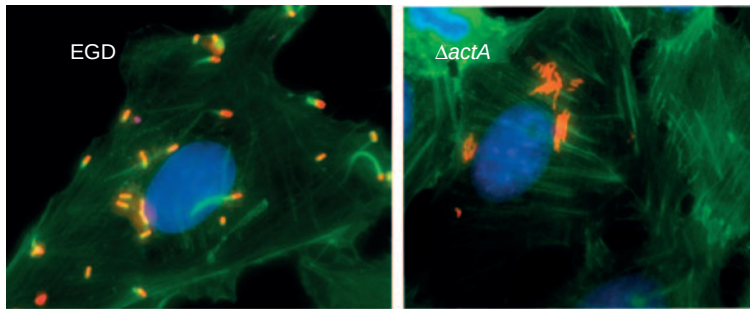

Figure 1.2 Vero cells infected with *L. monocytogenes* EGD (left panel) or its isogenic *actA* mutant (right panel). Cells were processed for triple fluorescence microscopy 5 h after infection. Bacteria were labeled with a polyclonal anti-*Listeria* antibody (black), actin with FITC-phalloidin (dark gray), and nuclei with DAPI (light gray). Actin accumulates around the parental strain EGD, leading to the formation of typical comet tails. In cells infected with the *actA* mutant, bacteria are unable to induce actin polymerization and multiply in the cytoplasm forming perinuclear microcolonies.

1992; Kocks *et al.*, 1992). The central part of the protein presents a domain composed of four proline-rich repeats that binds proteins of the Ena/VASP family, which modulate speed and directionality of bacterial movement (Auerbuch *et al.*, 2003; Chakraborty *et al.*, 1995; Geese *et al.*, 2002; Lasa *et al.*, 1995; Laurent *et al.*, 1999; Niebuhr *et al.*, 1997). The N-terminal region of ActA is sufficient to induce motility (Lasa *et al.*, 1997). It binds and activates the Arp2/3 complex inducing actin polymerization, mimicking proteins of the WASP family (Boujemaa-Paterski *et al.*, 2001; Skoble *et al.*, 2000, 2001). Actin tails induced by *L. monocytogenes* are composed of branched filaments similar to those of *Shigella flexneri*, in contrast to *Rickettsia conorii* actin tails which contain long and unbranched filaments (Gouin *et al.*, 1999, 2004, 2005).

ActA is also involved in cell attachment and entry by recognition of heparan sulfate (Alvarez-Dominguez *et al.*, 1997). Inactivation of ActA impairs *L. monocytogenes* invasion in macrophages and epithelial cells (Alvarez-Dominguez *et al.*, 1997; Suarez *et al.*, 2001). In addition, expression of ActA in *L. innocua* is sufficient to confer the capacity to enter epithelial cells (Suarez *et al.*, 2001).

A third role has been assigned to ActA in preventing bacterial autophagy in the cytosol of macrophages (Birmingham *et al.*, 2007; Rich *et al.*, 2003). Some *L. monocytogenes* are targeted by autophagy during early stages of infection by an LLO-dependent process. ActA expression is sufficient to promote autophagy evasion in the cytosol at later stages of infection (Birmingham *et al.*, 2007). ActA could possibly lead to escape from autophagy by actin-based movement or by actin masking of the bacteria, inhibiting recognition of autophagy targets.

4.4.2. SecA2

The auxiliary SecA paralogue protein SecA2 was identified by analysis of spontaneous rough variants of *L. monocytogenes*, which grew in chains (Lenz and Portnoy, 2002). In contrast to SecA, SecA2 is not essential for cell viability. SecA2 is required for virulence in mice and cell–cell spread in cultured cells (Lenz and Portnoy, 2002; Lenz *et al.*, 2003). Using a proteomic approach, 17 SecA2-dependent secreted and surface proteins were identified including the autolysin p60 and the *N*-acetylmuramidase NamA (Lenz *et al.*, 2003). These two peptidoglycane hydrolases and other SecA2 targets, such FbpA (Dramsi *et al.*, 2004) and MnSOD (Archambaud *et al.*, 2006), are important determinants of the infectious process. Thus, SecA2 could have evolved in part to mediate secretion of a subset of proteins contributing to virulence.

5. Immunomodulation and Persistence

5.1. Evasion and manipulation of host immune response

5.1.1. PgdA

Bacterial cell wall peptidoglycan is the pathogen-associated molecular pattern detected by the nucleotide-binding oligomerization domain (NOD) protein family of pattern-recognition receptors, resulting in activation of the NF-κB pathway (Chamaillard *et al.*, 2003; Girardin *et al.*, 2003a,b, Inohara *et al.*, 2003). Analysis of *L. monocytogenes* peptidoglycan revealed deacetylation of *N*-acetylglucosamine residues (Boneca *et al.*, 2007; Kamisango *et al.*, 1982). *L. monocytogenes* genome contains a single peptidoglycane *N*-deacetylase gene, *pgdA* (Boneca *et al.*, 2007; Glaser *et al.*, 2001). Inactivation of *pgdA* dramatically increases *L. monocytogenes* sensitivity to lyzozyme *in vitro* and strongly attenuates virulence in mice infected intravenously and in transgenic mice expressing human E-cadherin after intragastric inoculation (Boneca *et al.*, 2007). PgdA is required for survival within macrophage vacuoles (Fig. 1.3) and prevents proinflammatory cytokine and interferon-β secretion (Boneca *et al.*, 2007). Thus, peptidoglycan *N*-deacetylation is critical for evasion of host innate defenses.

5.1.2. p60

The autolysin p60, also known as the invasion-associated protein Iap or the cell wall hydrolase A CwhA, is a 60-kDa protein secreted by the SecA2 pathway. This peptidoglycan hydrolase promotes *L. monocytogenes* infection *in vivo* (Faith *et al.*, 2007; Lenz *et al.*, 2003). The mechanism of virulence attenuation of p60-deficient mutants is not completely understood. Recently, the reduced capacity of a p60 mutant to cause systemic infection

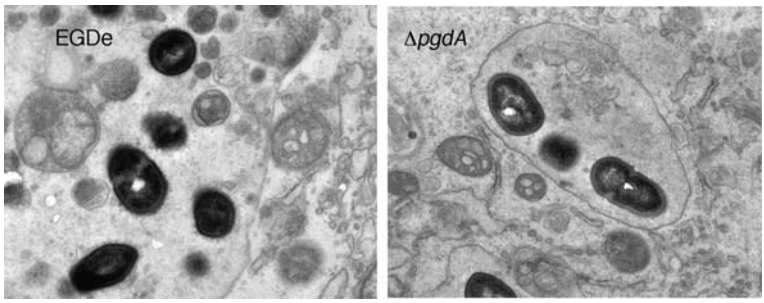

Figure 1.3 RAW264.7 macrophages infected with *L. monocytogenes* EGDe (left panel) or the *pgdA* deletion mutant (right panel). Cells were processed for electron microscopy 4 h after infection. Impaired survival of the *pgdA* mutant was correlated with delay in escape from the phagosome compared with the parental strain that was free in the cytoplasm.

of mice after intragastric inoculation was correlated to a diminished ability to enter and multiply within epithelial cells (Faith *et al.*, 2007). Interestingly, p60 has also been shown to indirectly increase NK cell activation and interferon-γ production (Humann *et al.*, 2007). It was suggested that p60 could promote early bacterial multiplication by subversion of interferon-γ-mediated immune responses and manipulation of deleterious and protective effects of interferon-γ production. The bacterial components that are released by the catalytic activity of p60 and directly modulate host innate response remain to be identified.

5.1.3. LLO

L. monocytogenes infection leads to modulation of expression of host genes. Posttranslational modifications of histones play an essential role in chromatin remodeling and gene expression regulation. It has been shown that infection of human endothelial cells by *L. monocytogenes* induces a p38 MAPK and MEK1-dependent acetylation of histone H4 and phosphorylation and acetylation of histone H3 globally as well as specifically at the promoter of IL8 (Schmeck *et al.*, 2005). LLO is required for upregulation of adhesion molecules and chemokines in endothelial cells infected by *L. monocytogenes* (Kayal *et al.*, 1999). Recently, LLO was shown to be critical for dephosphorylation of histone H3 and deacetylation of histone H4 during early phase of infection (Hamon *et al.*, 2007). Indeed, decreased LLO-mediated histone modifications were associated to modulation of host cell gene expression (Hamon *et al.*, 2007). Interestingly, transcription of the chemokine gene *cxcl2* and of other specific immunity genes was decreased, suggesting that LLO genetic reprogramming of the host cell could be an additional mechanism by which *L. monocytogenes* manipulate the host immune response.

5.1.4. MprF

L. monocytogenes multiple peptide resistance factor MprF is a membrane protein of 98 kDa regulated by the response regulator VirR (Mandin *et al.*, 2005; Thedieck *et al.*, 2006). MprF is required for synthesis of lysylphosphatidylglycerol and for lysinylation of diphosphatidylglycerol, two-membrane phospholipids (Thedieck *et al.*, 2006). Inactivation of MprF results in a decreased invasivity in both epithelial cells and macrophages and in attenuation of the virulence in mice. MprF is critical for resistance to cationic antimicrobial peptides and could be another mechanism of *L. monocytogenes* to escape host innate immune response.

5.2. Persistence

L. monocytogenes is a common transient colonizer of the human gastrointestinal tract that does not cause invasive disease unless a combination of host susceptibility factors, bacterial virulence determinants, and a high infective dose is met. Asymptomatic fecal carriage in healthy individuals has a prevalence of 2–10% (Schlech, 2000). The mechanisms used by *L. monocytogenes* to persist in the host are not fully understood.

L. monocytogenes infection of the gallbladder has been documented in humans (Allerberger *et al.*, 1989; Gluck *et al.*, 2002; Gordon and Singer, 1986; Loupa *et al.*, 2007). In addition, *L. monocytogenes* was isolated from liver, bile, and feces of mice inoculated subcutaneously, suggesting that bacteria reached the intestine by biliary excretion (Briones *et al.*, 1992). *L. monocytogenes* can replicate extracellularly in the gallbladder of mice after oral or intravenous inoculation (Hardy *et al.*, 2004). Bacteria growing in the lumen of the gallbladder can transit through the bile duct into the intestine as soon as 5 min after induction of gallbladder contraction by food or cholecystokinin (Hardy *et al.*, 2006). Bacteria then move through the intestinal lumen, are excreted in the environment, and possibly reinfect mice. *L. monocytogenes* strains causing human disease express a BSH conferring resistance to bile antimicrobial activity and the capacity to colonize the gastrointestinal tract (Dussurget *et al.*, 2002). *L. monocytogenes* is particularly well equipped to survive in presence of bile as several other important genetic loci involved in bile resistance have been identified (Begley *et al.*, 2002, 2003, 2005; Sleator *et al.*, 2005). Thus, gallbladder could represent a niche where *L. monocytogenes* grows in the absence of commensal competitors and specific immune response. Dissemination of *L. monocytogenes* from the gallbladder to the intestine and the environment could play an important role in transient or chronic shedding and in transmission.

6. Virulence Determinants of Unknown Function

6.1. InlC

InlC (also designated internalin-related protein A, IrpA) is a secreted protein of 297 amino acids containing a central region composed of 6 LRRs followed by a C-terminal Ig-like domain (Domann *et al.*, 1997; Engelbrecht *et al.*, 1996; Ooi *et al.*, 2006). The *inlC* gene, which is absent from the genome of *L. innocua*, is transcribed by PrfA-dependent and -independent mechanisms (Domann *et al.*, 1997; Luo *et al.*, 2004). InlC contributes to *L. monocytogenes* virulence in mice (Domann *et al.*, 1997; Engelbrecht *et al.*, 1996). The expression of *inlC* is strongly induced in the cytoplasm of infected macrophages (Engelbrecht *et al.*, 1996). However, deletion of *inlC* does not affect invasion, intracellular survival, or cell spread (Domann *et al.*, 1997; Engelbrecht *et al.*, 1996; Greiffenberg *et al.*, 1998). The function and binding partners of InlC have yet to be discovered.

6.2. InlGHE

A gene cluster encoding the three internalins InlG, InlH, and InlE has been identified in some *L. monocytogenes* strains (Raffelsbauer *et al.*, 1998). An in-frame deletion of the *inlGHE* operon had no effect on cellular invasion and its function remains unknown. However, the mutant showed reduced colonization of the spleen and liver after infection of mice by the oral route (Raffelsbauer *et al.*, 1998). A specific role for InlH in virulence was later demonstrated in mice infected intravenously (Schubert *et al.*, 2001).

6.3. InlJ

Another internalin encoding gene, *inlJ*, was identified by analyzing *L. monocytogenes* genome sequence (Cabanes *et al.*, 2002; Glaser *et al.*, 2001; Sabet *et al.*, 2005). InlJ is required for full virulence of *L. monocytogenes* in mice infected intravenously and after intragastric inoculation in transgenic mice expressing the human E-cadherin at the level of the intestine (Sabet *et al.*, 2005). However, inactivation of *inlJ* does not affect *L. monocytogenes* capacity to infect cells. The function of this internalin remains to be determined.

7. Conclusion

The advent of comparative genomics and transcriptomic technologies allowing analysis of host cell and bacterial gene expression during the infectious cycle coupled to the development of new animal models of

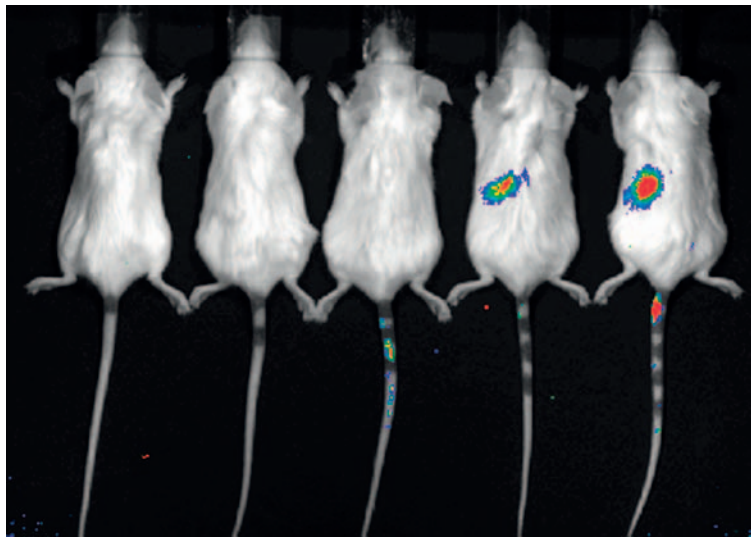

Figure 1.4 Noninvasive bioluminescence imaging of listeriosis in BALB/c mice. Bioluminescent splenic signals corresponding to bacterial replication foci were detected 48 h after intravenous inoculation of 8×10^3, 4×10^4, 2×10^5, 10^6, and 5×10^6 *L. monocytogenes* from left to right.

infection have greatly improved our knowledge of *L. monocytogenes* pathogenesis. Here, we have highlighted some of the important bacterial determinants that have been involved in the infectious process. However, our understanding of listeriosis is still far from complete. As more virulence determinants are identified, determination of their specific function, their host partners, and where and when they are expressed during the infectious process will become the next challenge. Identification of the key components of host immune response involved in listeriosis and how they can be manipulated by *L. monocytogenes* should benefit from the recent advances in the field of innate immunity. Dynamic gene profiling *in vivo*, noninvasive imaging in relevant animal models (Fig. 1.4), and real-time imaging in living cells will surely help to address the complexity of *L. monocytogenes* interactions with the host and bring us a step closer to a comprehensive understanding of the disease.

ACKNOWLEDGMENTS

I apologize to authors whose relevant work could not be cited owing to space limitations. Past and present colleagues of the Cossart laboratory and the *Listeria* genome consortium are gratefully acknowledged for contributing to the work described in this chapter and for many valuable discussions over the last years. Research in the laboratory is supported by the Pasteur Institute, INRA, Inserm, ANR, EU FP6, and HHMI.

REFERENCES

Abachin, E., Poyart, C., Pellegrini, E., Milohanic, E., Fiedler, F., Berche, P., and Trieu-Cuot, P. (2002). Formation of D-alanyl-lipoteichoic acid is required for adhesion and virulence of *Listeria monocytogenes*. *Mol. Microbiol.* **43,** 1–14.

Allerberger, F., Langer, B., Hirsch, O., Dierich, M. P., and Seeliger, H. P. (1989). *Listeria monocytogenes* cholecystitis. *Z. Gastroenterol.* **27,** 145–147.

Alvarez-Dominguez, C., Vazquez-Boland, J. A., Carrasco-Marin, E., Lopez-Mato, P., and Leyva-Cobian, F. (1997). Host cell heparan sulfate proteoglycans mediate attachment and entry of *Listeria monocytogenes*, and the listerial surface protein ActA is involved in heparan sulfate receptor recognition. *Infect. Immun.* **65,** 78–88.

Archambaud, C., Gouin, E., Pizarro-Cerda, J., Cossart, P., and Dussurget, O. (2005). Translation elongation factor EF-Tu is a target for Stp, a serine-threonine phosphatase involved in virulence of *Listeria monocytogenes*. *Mol. Microbiol.* **56,** 383–396.

Archambaud, C., Nahori, M. A., Pizarro-Cerda, J., Cossart, P., and Dussurget, O. (2006). Control of *Listeria* superoxide dismutase by phosphorylation. *J. Biol. Chem.* **281,** 31812–31822.

Auerbuch, V., Loureiro, J. J., Gertler, F. B., Theriot, J. A., and Portnoy, D. A. (2003). Ena/VASP proteins contribute to *Listeria monocytogenes* pathogenesis by controlling temporal and spatial persistence of bacterial actin-based motility. *Mol. Microbiol.* **49,** 1361–1375.

Autret, N., Raynaud, C., Dubail, I., Berche, P., and Charbit, A. (2003). Identification of the agr locus of *Listeria monocytogenes*: Role in bacterial virulence. *Infect. Immun.* **71,** 4463–4471.

Banerjee, M., Copp, J., Vuga, D., Marino, M., Chapman, T., van der Geer, P., and Ghosh, P. (2004). GW domains of the *Listeria monocytogenes* invasion protein InlB are required for potentiation of Met activation. *Mol. Microbiol.* **52,** 257–271.

Baumgartner, M., Karst, U., Gerstel, B., Loessner, M., Wehland, J., and Jansch, L. (2007). Inactivation of Lgt allows systematic characterization of lipoproteins from *Listeria monocytogenes*. *J. Bacteriol.* **189,** 313–324.

Begley, M., Gahan, C. G., and Hill, C. (2002). Bile stress response in *Listeria monocytogenes* LO28: Adaptation, cross-protection, and identification of genetic loci involved in bile resistance. *Appl. Environ. Microbiol.* **68,** 6005–6012.

Begley, M., Hill, C., and Gahan, C. G. (2003). Identification and disruption of btlA, a locus involved in bile tolerance and general stress resistance in *Listeria monocytogenes*. *FEMS Microbiol. Lett.* **218,** 31–38.

Begley, M., Sleator, R. D., Gahan, C. G., and Hill, C. (2005). Contribution of three bile-associated loci, bsh, pva, and btlB, to gastrointestinal persistence and bile tolerance of *Listeria monocytogenes*. *Infect. Immun.* **73,** 894–904.

Bennett, H. J., Pearce, D. M., Glenn, S., Taylor, C. M., Kuhn, M., Sonenshein, A. L., Andrew, P. W., and Roberts, I. S. (2007). Characterization of relA and codY mutants of *Listeria monocytogenes*: Identification of the CodY regulon and its role in virulence. *Mol. Microbiol.* **63,** 1453–1467.

Bierne, H., and Cossart, P. (2007). *Listeria monocytogenes* surface proteins: From genome predictions to function. *Microbiol. Mol. Biol. Rev.* **71,** 377–397.

Bierne, H., Gouin, E., Roux, P., Caroni, P., Yin, H. L., and Cossart, P. (2001). A role for cofilin and LIM kinase in *Listeria*-induced phagocytosis. *J. Cell Biol.* **155,** 101–112.

Bierne, H., Mazmanian, S. K., Trost, M., Pucciarelli, M. G., Liu, G., Dehoux, P., Jansch, L., Garcia-del Portillo, F., Schneewind, O., and Cossart, P. (2002). Inactivation of the srtA gene in *Listeria monocytogenes* inhibits anchoring of surface proteins and affects virulence. *Mol. Microbiol.* **43,** 869–881.

Bierne, H., Garandeau, C., Pucciarelli, M. G., Sabet, C., Newton, S., Garcia-del Portillo, F., Cossart, P., and Charbit, A. (2004). Sortase B, a new class of sortase in *Listeria monocytogenes*. *J. Bacteriol.* **186,** 1972–1982.

Bierne, H., Miki, H., Innocenti, M., Scita, G., Gertler, F. B., Takenawa, T., and Cossart, P. (2005). WASP-related proteins, Abi1 and Ena/VASP are required for *Listeria* invasion induced by the Met receptor. *J. Cell Sci.* **118,** 1537–1547.

Bigot, A., Pagniez, H., Botton, E., Frehel, C., Dubail, I., Jacquet, C., Charbit, A., and Raynaud, C. (2005). Role of FliF and FliI of *Listeria monocytogenes* in flagellar assembly and pathogenicity. *Infect. Immun.* **73,** 5530–5539.

Birmingham, C. L., Canadien, V., Gouin, E., Troy, E. B., Yoshimori, T., Cossart, P., Higgins, D. E., and Brumell, J. H. (2007). *Listeria monocytogenes* evades killing by autophagy during colonization of host cells. *Autophagy* **3,** 442–451.

Bonazzi, M., and Cossart, P. (2006). Bacterial entry into cells: A role for the endocytic machinery. *FEBS Lett.* **580,** 2962–2967.

Boneca, I. G., Dussurget, O., Cabanes, D., Nahori, M. A., Sousa, S., Lecuit, M., Psylinakis, E., Bouriotis, V., Hugot, J. P., Giovannini, M., Coyle, A., Bertin, J., *et al.* (2007). A critical role for peptidoglycan *N*-deacetylation in *Listeria* evasion from the host innate immune system. *Proc. Natl. Acad. Sci. USA* **104,** 997–1002.

Bonnemain, C., Raynaud, C., Reglier-Poupet, H., Dubail, I., Frehel, C., Lety, M. A., Berche, P., and Charbit, A. (2004). Differential roles of multiple signal peptidases in the virulence of *Listeria monocytogenes*. *Mol. Microbiol.* **51,** 1251–1266.

Borezee, E., Pellegrini, E., and Berche, P. (2000). OppA of *Listeria monocytogenes*, an oligopeptide-binding protein required for bacterial growth at low temperature and involved in intracellular survival. *Infect. Immun.* **68,** 7069–7077.

Borezee, E., Pellegrini, E., Beretti, J. L., and Berche, P. (2001). SvpA, a novel surface virulence-associated protein required for intracellular survival of *Listeria monocytogenes*. *Microbiology* **147,** 2913–2923.

Boujemaa-Paterski, R., Gouin, E., Hansen, G., Samarin, S., Le Clainche, C., Didry, D., Dehoux, P., Cossart, P., Kocks, C., Carlier, M. F., and Pantaloni, D. (2001). *Listeria* protein ActA mimics WASp family proteins: It activates filament barbed end branching by Arp2/3 complex. *Biochemistry* **40,** 11390–11404.

Braun, L., Ohayon, H., and Cossart, P. (1998). The InIB protein of *Listeria monocytogenes* is sufficient to promote entry into mammalian cells. *Mol. Microbiol.* **27,** 1077–1087.

Braun, L., Nato, F., Payrastre, B., Mazie, J. C., and Cossart, P. (1999). The 213-amino-acid leucine-rich repeat region of the *Listeria monocytogenes* InlB protein is sufficient for entry into mammalian cells, stimulation of PI 3-kinase and membrane ruffling. *Mol. Microbiol.* **34,** 10–23.

Braun, L., Ghebrehiwet, B., and Cossart, P. (2000). gC1q-R/p32, a C1q-binding protein, is a receptor for the InlB invasion protein of *Listeria monocytogenes*. *EMBO J.* **19,** 1458–1466.

Brehm, K., Haas, A., Goebel, W., and Kreft, J. (1992). A gene encoding a superoxide dismutase of the facultative intracellular bacterium *Listeria monocytogenes*. *Gene* **118,** 121–125.

Briones, V., Blanco, M. M., Marco, A., Prats, N., Fernandez-Garayzabal, J. F., Suarez, G., Domingo, M., and Dominguez, L. (1992). Biliary excretion as possible origin of *Listeria monocytogenes* in fecal carriers. *Am. J. Vet. Res.* **53,** 191–193.

Buchrieser, C. (2007). Biodiversity of the species *Listeria monocytogenes* and the genus *Listeria*. *Microbes Infect.* **9,** 1147–1155.

Cabanes, D., Dehoux, P., Dussurget, O., Frangeul, L., and Cossart, P. (2002). Surface proteins and the pathogenic potential of *Listeria monocytogenes*. *Trends Microbiol* **10,** 238–245.

Cabanes, D., Dussurget, O., Dehoux, P., and Cossart, P. (2004). Auto, a surface associated autolysin of *Listeria monocytogenes* required for entry into eukaryotic cells and virulence. *Mol. Microbiol.* **51,** 1601–1614.

Cabanes, D., Sousa, S., Cebria, A., Lecuit, M., Garcia-del Portillo, F., and Cossart, P. (2005). Gp96 is a receptor for a novel *Listeria monocytogenes* virulence factor, Vip, a surface protein. *EMBO J.* **24,** 2827–2838.

Cameron, L. A., Footer, M. J., van Oudenaarden, A., and Theriot, J. A. (1999). Motility of ActA protein-coated microspheres driven by actin polymerization. *Proc. Natl. Acad. Sci. USA* **96,** 4908–4913.

Camilli, A., Goldfine, H., and Portnoy, D. A. (1991). *Listeria monocytogenes* mutants lacking phosphatidylinositol-specific phospholipase C are avirulent. *J. Exp. Med.* **173,** 751–754.

Camilli, A., Tilney, L. G., and Portnoy, D. A. (1993). Dual roles of plcA in *Listeria monocytogenes* pathogenesis. *Mol. Microbiol.* **8,** 143–157.

Chakraborty, T., Ebel, F., Domann, E., Niebuhr, K., Gerstel, B., Pistor, S., Temm-Grove, C. J., Jockusch, B. M., Reinhard, M., Walter, U., and Wehland, J. (1995). A focal adhesion factor directly linking intracellularly motile *Listeria monocytogenes* and *Listeria ivanovii* to the actin-based cytoskeleton of mammalian cells. *EMBO J.* **14,** 1314–1321.

Chamaillard, M., Hashimoto, M., Horie, Y., Masumoto, J., Qiu, S., Saab, L., Ogura, Y., Kawasaki, A., Fukase, K., Kusumoto, S., Valvano, M. A., Foster, S. J., *et al.* (2003). An essential role for NOD1 in host recognition of bacterial peptidoglycan containing diaminopimelic acid. *Nat. Immunol.* **4,** 702–707.

Chastanet, A., Derre, I., Nair, S., and Msadek, T. (2004). clpB, a novel member of the *Listeria monocytogenes* CtsR regulon, is involved in virulence but not in general stress tolerance. *J. Bacteriol.* **186,** 1165–1174.

Chatterjee, S. S., Hossain, H., Otten, S., Kuenne, C., Kuchmina, K., Machata, S., Domann, E., Chakraborty, T., and Hain, T. (2006). Intracellular gene expression profile of *Listeria monocytogenes*. *Infect. Immun.* **74,** 1323–1338.

Chico-Calero, I., Suarez, M., Gonzalez-Zorn, B., Scortti, M., Slaghuis, J., Goebel, W., and Vazquez-Boland, J. A. (2002). Hpt, a bacterial homolog of the microsomal glucose-6-phosphate translocase, mediates rapid intracellular proliferation in *Listeria*. *Proc. Natl. Acad. Sci. USA* **99,** 431–436.

Christiansen, J. K., Larsen, M. H., Ingmer, H., Sogaard-Andersen, L., and Kallipolitis, B. H. (2004). The RNA-binding protein Hfq of *Listeria monocytogenes*: Role in stress tolerance and virulence. *J. Bacteriol.* **186,** 3355–3362.

Cossart, P. (2007). Listeriology (1926–2007): The rise of a model pathogen. *Microbes Infect.* **9,** 1143–1146.

Cossart, P., Vicente, M. F., Mengaud, J., Baquero, F., Perez-Diaz, J. C., and Berche, P. (1989). Listeriolysin O is essential for virulence of *Listeria monocytogenes*: Direct evidence obtained by gene complementation. *Infect. Immun.* **57,** 3629–3636.

Cossart, P., Boquet, P., Normark, S., and Rappuoli, R. (1996). Cellular microbiology emerging. *Science* **271,** 315–316.

Cotter, P. D., Emerson, N., Gahan, C. G., and Hill, C. (1999). Identification and disruption of lisRK, a genetic locus encoding a two-component signal transduction system involved in stress tolerance and virulence in *Listeria monocytogenes*. *J. Bacteriol.* **181,** 6840–6843.

Cotter, P. D., Gahan, C. G., and Hill, C. (2001). A glutamate decarboxylase system protects *Listeria monocytogenes* in gastric fluid. *Mol. Microbiol.* **40,** 465–475.

Cotter, P. D., Ryan, S., Gahan, C. G., and Hill, C. (2005). Presence of GadD1 glutamate decarboxylase in selected *Listeria monocytogenes* strains is associated with an ability to grow at low pH. *Appl. Environ. Microbiol.* **71,** 2832–2839.

Desvaux, M., and Hebraud, M. (2006). The protein secretion systems in *Listeria*: Inside out bacterial virulence. *FEMS Microbiol. Rev.* **30,** 774–805.

Domann, E., Leimeister-Wachter, M., Goebel, W., and Chakraborty, T. (1991). Molecular cloning, sequencing, and identification of a metalloprotease gene from *Listeria monocytogenes* that is species specific and physically linked to the listeriolysin gene. *Infect. Immun.* **59,** 65–72.

Domann, E., Wehland, J., Rohde, M., Pistor, S., Hartl, M., Goebel, W., Leimeister-Wachter, M., Wuenscher, M., and Chakraborty, T. (1992). A novel bacterial virulence gene in *Listeria monocytogenes* required for host cell microfilament interaction with homology to the proline-rich region of vinculin. *EMBO J.* **11,** 1981–1990.

Domann, E., Zechel, S., Lingnau, A., Hain, T., Darji, A., Nichterlein, T., Wehland, J., and Chakraborty, T. (1997). Identification and characterization of a novel PrfA-regulated gene in *Listeria monocytogenes* whose product, IrpA, is highly homologous to internalin proteins, which contain leucine-rich repeats. *Infect. Immun.* **65,** 101–109.

Dons, L., Eriksson, E., Jin, Y., Rottenberg, M. E., Kristensson, K., Larsen, C. N., Bresciani, J., and Olsen, J. E. (2004). Role of flagellin and the two-component CheA/CheY system of *Listeria monocytogenes* in host cell invasion and virulence. *Infect. Immun.* **72,** 3237–3244.

Dramsi, S., and Cossart, P. (2003). Listeriolysin O-mediated calcium influx potentiates entry of *Listeria monocytogenes* into the human Hep-2 epithelial cell line. *Infect. Immun.* **71,** 3614–3618.

Dramsi, S., Kocks, C., Forestier, C., and Cossart, P. (1993). Internalin-mediated invasion of epithelial cells by *Listeria monocytogenes* is regulated by the bacterial growth state, temperature and the pleiotropic activator prfA. *Mol. Microbiol.* **9,** 931–941.

Dramsi, S., Biswas, I., Maguin, E., Braun, L., Mastroeni, P., and Cossart, P. (1995). Entry of *Listeria monocytogenes* into hepatocytes requires expression of inIB, a surface protein of the internalin multigene family. *Mol. Microbiol.* **16,** 251–261.

Dramsi, S., Bourdichon, F., Cabanes, D., Lecuit, M., Fsihi, H., and Cossart, P. (2004). FbpA, a novel multifunctional *Listeria monocytogenes* virulence factor. *Mol. Microbiol.* **53,** 639–649.

Dussurget, O., Cabanes, D., Dehoux, P., Lecuit, M., Buchrieser, C., Glaser, P., and Cossart, P. (2002). *Listeria monocytogenes* bile salt hydrolase is a PrfA-regulated virulence factor involved in the intestinal and hepatic phases of listeriosis. *Mol. Microbiol.* **45,** 1095–1106.

Dussurget, O., Pizarro-Cerda, J., and Cossart, P. (2004). Molecular determinants of *Listeria monocytogenes* virulence. *Annu. Rev. Microbiol.* **58,** 587–610.

Dussurget, O., Dumas, E., Archambaud, C., Chafsey, I., Chambon, C., Hebraud, M., and Cossart, P. (2005). *Listeria monocytogenes* ferritin protects against multiple stresses and is required for virulence. *FEMS Microbiol. Lett.* **250,** 253–261.

Engelbrecht, F., Chun, S. K., Ochs, C., Hess, J., Lottspeich, F., Goebel, W., and Sokolovic, Z. (1996). A new PrfA-regulated gene of *Listeria monocytogenes* encoding a small, secreted protein which belongs to the family of internalins. *Mol. Microbiol.* **21,** 823–837.

Faith, N. G., Kathariou, S., Neudeck, B. L., Luchansky, J. B., and Czuprynski, C. J. (2007). A p60 mutant of *Listeria monocytogenes* is impaired in its ability to cause infection in intragastrically inoculated mice. *Microb. Pathog.* **42,** 237–241.

Gaillard, J. L., Berche, P., and Sansonetti, P. (1986). Transposon mutagenesis as a tool to study the role of hemolysin in the virulence of *Listeria monocytogenes*. *Infect. Immun.* **52,** 50–55.

Gaillard, J. L., Berche, P., Mounier, J., Richard, S., and Sansonetti, P. (1987). *In vitro* model of penetration and intracellular growth of *Listeria monocytogenes* in the human enterocyte-like cell line Caco-2. *Infect. Immun.* **55,** 2822–2829.

Gaillard, J. L., Berche, P., Frehel, C., Gouin, E., and Cossart, P. (1991). Entry of *L. monocytogenes* into cells is mediated by internalin, a repeat protein reminiscent of surface antigens from gram-positive cocci. *Cell* **65,** 1127–1141.

Gaillard, J. L., Jaubert, F., and Berche, P. (1996). The inlAB locus mediates the entry of *Listeria monocytogenes* into hepatocytes *in vivo*. *J. Exp. Med.* **183,** 359–369.

Gaillot, O., Pellegrini, E., Bregenholt, S., Nair, S., and Berche, P. (2000). The ClpP serine protease is essential for the intracellular parasitism and virulence of *Listeria monocytogenes*. *Mol. Microbiol.* **35,** 1286–1294.

Garandeau, C., Reglier-Poupet, H., Dubail, I., Beretti, J. L., Berche, P., and Charbit, A. (2002). The sortase SrtA of *Listeria monocytogenes* is involved in processing of internalin and in virulence. *Infect. Immun.* **70,** 1382–1390.

Garifulin, O., and Boyartchuk, V. (2005). *Listeria monocytogenes* as a probe of immune function. *Brief. Funct. Genomic. Proteomic.* **4,** 258–269.

Garner, M. R., Njaa, B. L., Wiedmann, M., and Boor, K. J. (2006). Sigma B contributes to *Listeria monocytogenes* gastrointestinal infection but not to systemic spread in the guinea pig infection model. *Infect. Immun.* **74,** 876–886.

Gedde, M. M., Higgins, D. E., Tilney, L. G., and Portnoy, D. A. (2000). Role of listeriolysin O in cell-to-cell spread of *Listeria monocytogenes*. *Infect. Immun.* **68,** 999–1003.

Geese, M., Loureiro, J. J., Bear, J. E., Wehland, J., Gertler, F. B., and Sechi, A. S. (2002). Contribution of Ena/VASP proteins to intracellular motility of *Listeria* requires phosphorylation and proline-rich core but not F-actin binding or multimerization. *Mol. Biol. Cell* **13,** 2383–2396.

Geoffroy, C., Raveneau, J., Beretti, J. L., Lecroisey, A., Vazquez-Boland, J. A., Alouf, J. E., and Berche, P. (1991). Purification and characterization of an extracellular 29-kilodalton phospholipase C from *Listeria monocytogenes*. *Infect. Immun.* **59,** 2382–2388.

Girardin, S. E., Boneca, I. G., Carneiro, L. A., Antignac, A., Jehanno, M., Viala, J., Tedin, K., Taha, M. K., Labigne, A., Zahringer, U., Coyle, A. J., DiStefano, P. S., *et al.* (2003a). Nod1 detects a unique muropeptide from gram-negative bacterial peptidoglycan. *Science* **300,** 1584–1587.

Girardin, S. E., Boneca, I. G., Viala, J., Chamaillard, M., Labigne, A., Thomas, G., Philpott, D. J., and Sansonetti, P. J. (2003b). Nod2 is a general sensor of peptidoglycan through muramyl dipeptide (MDP) detection. *J. Biol. Chem.* **278,** 8869–8872.

Glaser, P., Frangeul, L., Buchrieser, C., Rusniok, C., Amend, A., Baquero, F., Berche, P., Bloecker, H., Brandt, P., Chakraborty, T., Charbit, A., Chetouani, F., *et al.* (2001). Comparative genomics of *Listeria* species. *Science* **294,** 849–852.

Gluck, T., Linde, H. J., Scholmerich, J., Muller-Ladner, U., Fiehn, C., and Bohland, P. (2002). Anti-tumor necrosis factor therapy and *Listeria monocytogenes* infection: Report of two cases. *Arthritis Rheum.* **46,** 2255–2257.

Goldfine, H., Bannam, T., Johnston, N. C., and Zuckert, W. R. (1998). Bacterial phospholipases and intracellular growth: The two distinct phospholipases C of *Listeria monocytogenes*. *Symp. Ser. Soc. Appl. Microbiol.* **27,** 7S–14S.

Gordon, S., and Singer, C. (1986). *Listeria monocytogenes* cholecystitis. *J. Infect. Dis.* **154,** 918–919.

Gouin, E., Gantelet, H., Egile, C., Lasa, I., Ohayon, H., Villiers, V., Gounon, P., Sansonetti, P. J., and Cossart, P. (1999). A comparative study of the actin-based motilities of the pathogenic bacteria *Listeria monocytogenes*, *Shigella flexneri* and *Rickettsia conorii*. *J. Cell Sci.* **112**(Pt 11), 1697–1708.

Gouin, E., Egile, C., Dehoux, P., Villiers, V., Adams, J., Gertler, F., Li, R., and Cossart, P. (2004). The RickA protein of Rickettsia conorii activates the Arp2/3 complex. *Nature* **427,** 457–461.

Gouin, E., Welch, M. D., and Cossart, P. (2005). Actin-based motility of intracellular pathogens. *Curr. Opin. Microbiol.* **8,** 35–45.

Greiffenberg, L., Goebel, W., Kim, K. S., Weiglein, I., Bubert, A., Engelbrecht, F., Stins, M., and Kuhn, M. (1998). Interaction of *Listeria monocytogenes* with human brain microvascular endothelial cells: InlB-dependent invasion, long-term intracellular growth, and spread from macrophages to endothelial cells. *Infect. Immun.* **66,** 5260–5267.

Griffin, A. M., and Robbins, M. L. (1944). The flagellation of *Listeria monocytogenes*. *J. Bacteriol.* **48,** 114–115.

Grundling, A., Gonzalez, M. D., and Higgins, D. E. (2003). Requirement of the *Listeria monocytogenes* broad-range phospholipase PC-PLC during infection of human epithelial cells. *J. Bacteriol.* **185,** 6295–6307.

Grundling, A., Burrack, L. S., Bouwer, H. G., and Higgins, D. E. (2004). *Listeria monocytogenes* regulates flagellar motility gene expression through MogR, a transcriptional repressor required for virulence. *Proc. Natl. Acad. Sci. USA* **101,** 12318–12323.

Hain, T., Steinweg, C., Kuenne, C. T., Billion, A., Ghai, R., Chatterjee, S. S., Domann, E., Karst, U., Goesmann, A., Bekel, T., Bartels, D., Kaiser, O., *et al.* (2006). Whole-genome sequence of *Listeria welshimeri* reveals common steps in genome reduction with *Listeria innocua* as compared to *Listeria monocytogenes*. *J. Bacteriol.* **188,** 7405–7415.

Hain, T., Chatterjee, S. S., Ghai, R., Kuenne, C. T., Billion, A., Steinweg, C., Domann, E., Karst, U., Jansch, L., Wehland, J., Eisenreich, W., Bacher, A., *et al.* (2007). Pathogenomics of *Listeria* spp. *Int. J. Med. Microbiol.* **297,** 541–557.

Hamon, M., Bierne, H., and Cossart, P. (2006). *Listeria monocytogenes*: A multifaceted model. *Nat. Rev. Microbiol.* **4,** 423–434.

Hamon, M. A., Batsche, E., Regnault, B., Tham, T. N., Seveau, S., Muchardt, C., and Cossart, P. (2007). Histone modifications induced by a family of bacterial toxins. *Proc. Natl. Acad. Sci. USA* **104,** 13467–13472.

Hardy, J., Francis, K. P., DeBoer, M., Chu, P., Gibbs, K., and Contag, C. H. (2004). Extracellular replication of *Listeria monocytogenes* in the murine gallbladder. *Science* **303,** 851–853.

Hardy, J., Margolis, J. J., and Contag, C. H. (2006). Induced biliary excretion of *Listeria monocytogenes*. *Infect. Immun.* **74,** 1819–1827.

Hayashi, F., Smith, K. D., Ozinsky, A., Hawn, T. R., Yi, E. C., Goodlett, D. R., Eng, J. K., Akira, S., Underhill, D. M., and Aderem, A. (2001). The innate immune response to bacterial flagellin is mediated by Toll-like receptor 5. *Nature* **410,** 1099–1103.

Humann, J., Bjordahl, R., Andreasen, K., and Lenz, L. L. (2007). Expression of the p60 autolysin enhances NK cell activation and is required for *Listeria monocytogenes* expansion in IFN-gamma-responsive mice. *J. Immunol.* **178,** 2407–2414.

Inohara, N., Ogura, Y., Fontalba, A., Gutierrez, O., Pons, F., Crespo, J., Fukase, K., Inamura, S., Kusumoto, S., Hashimoto, M., Foster, S. J., Moran, A. P., *et al.* (2003). Host recognition of bacterial muramyl dipeptide mediated through NOD2. Implications for Crohn's disease. *J. Biol. Chem.* **278,** 5509–5512.

Ireton, K., Payrastre, B., Chap, H., Ogawa, W., Sakaue, H., Kasuga, M., and Cossart, P. (1996). A role for phosphoinositide 3-kinase in bacterial invasion. *Science* **274,** 780–782.

Ireton, K., Payrastre, B., and Cossart, P. (1999). The *Listeria monocytogenes* protein InlB is an agonist of mammalian phosphoinositide 3-kinase. *J. Biol. Chem.* **274,** 17025–17032.

Jacquet, C., Doumith, M., Gordon, J. I., Martin, P. M., Cossart, P., and Lecuit, M. (2004). A molecular marker for evaluating the pathogenic potential of foodborne *Listeria monocytogenes*. *J. Infect. Dis.* **189,** 2094–2100.

Jin, B., Newton, S. M., Shao, Y., Jiang, X., Charbit, A., and Klebba, P. E. (2006). Iron acquisition systems for ferric hydroxamates, haemin and haemoglobin in *Listeria monocytogenes*. *Mol. Microbiol.* **59,** 1185–1198.

Johansson, J., and Cossart, P. (2003). RNA-mediated control of virulence gene expression in bacterial pathogens. *Trends Microbiol.* **11,** 280–285.

Johansson, J., Mandin, P., Renzoni, A., Chiaruttini, C., Springer, M., and Cossart, P. (2002). An RNA thermosensor controls expression of virulence genes in *Listeria monocytogenes*. *Cell* **110,** 551–561.

Jonquieres, R., Bierne, H., Fiedler, F., Gounon, P., and Cossart, P. (1999). Interaction between the protein InlB of *Listeria monocytogenes* and lipoteichoic acid: A novel mechanism of protein association at the surface of gram-positive bacteria. *Mol. Microbiol.* **34,** 902–914.

Jonquieres, R., Pizarro-Cerda, J., and Cossart, P. (2001). Synergy between the N- and C-terminal domains of InlB for efficient invasion of non-phagocytic cells by *Listeria monocytogenes*. *Mol. Microbiol.* **42,** 955–965.

Joseph, B., Przybilla, K., Stuhler, C., Schauer, K., Slaghuis, J., Fuchs, T. M., and Goebel, W. (2006). Identification of *Listeria monocytogenes* genes contributing to intracellular replication by expression profiling and mutant screening. *J. Bacteriol.* **188,** 556–568.

Kamisango, K., Saiki, I., Tanio, Y., Okumura, H., Araki, Y., Sekikawa, I., Azuma, I., and Yamamura, Y. (1982). Structures and biological activities of peptidoglycans of *Listeria monocytogenes* and *Propionibacterium acnes*. *J. Biochem.* **92,** 23–33.

Kathariou, S., Metz, P., Hof, H., and Goebel, W. (1987). Tn916-induced mutations in the hemolysin determinant affecting virulence of *Listeria monocytogenes*. *J. Bacteriol.* **169,** 1291–1297.

Kayal, S., and Charbit, A. (2006). Listeriolysin O: A key protein of *Listeria monocytogenes* with multiple functions. *FEMS Microbiol. Rev.* **30,** 514–529.

Kayal, S., Lilienbaum, A., Poyart, C., Memet, S., Israel, A., and Berche, P. (1999). Listeriolysin O-dependent activation of endothelial cells during infection with *Listeria monocytogenes*: Activation of NF-kappa B and upregulation of adhesion molecules and chemokines. *Mol. Microbiol.* **31,** 1709–1722.

Kazmierczak, M. J., Mithoe, S. C., Boor, K. J., and Wiedmann, M. (2003). *Listeria monocytogenes* sigma B regulates stress response and virulence functions. *J. Bacteriol.* **185,** 5722–5734.

Keeney, K. M., Stuckey, J. A., and O'Riordan, M. X. (2007). LplA1-dependent utilization of host lipoyl peptides enables *Listeria* cytosolic growth and virulence. *Mol. Microbiol.* **66,** 758–770.

Khelef, N., Lecuit, M., Bierne, H., and Cossart, P. (2006). Species specificity of the *Listeria monocytogenes* InlB protein. *Cell. Microbiol.* **8,** 457–470.

Kim, H., Boor, K. J., and Marquis, H. (2004). *Listeria monocytogenes* sigmaB contributes to invasion of human intestinal epithelial cells. *Infect. Immun.* **72,** 7374–7378.

Knudsen, G. M., Olsen, J. E., and Dons, L. (2004). Characterization of DegU, a response regulator in *Listeria monocytogenes*, involved in regulation of motility and contributes to virulence. *FEMS Microbiol. Lett.* **240,** 171–179.

Ko, R., and Smith, L. T. (1999). Identification of an ATP-driven, osmoregulated glycine betaine transport system in *Listeria monocytogenes*. *Appl. Environ. Microbiol.* **65,** 4040–4048.

Kocks, C., Gouin, E., Tabouret, M., Berche, P., Ohayon, H., and Cossart, P. (1992). *L. monocytogenes*-induced actin assembly requires the actA gene product, a surface protein. *Cell* **68,** 521–531.

Kocks, C., Marchand, J. B., Gouin, E., d'Hauteville, H., Sansonetti, P. J., Carlier, M. F., and Cossart, P. (1995). The unrelated surface proteins ActA of *Listeria monocytogenes* and IcsA of *Shigella flexneri* are sufficient to confer actin-based motility on *Listeria innocua* and *Escherichia coli* respectively. *Mol. Microbiol.* **18,** 413–423.

Lasa, I., David, V., Gouin, E., Marchand, J. B., and Cossart, P. (1995). The amino-terminal part of ActA is critical for the actin-based motility of *Listeria monocytogenes*; the central proline-rich region acts as a stimulator. *Mol. Microbiol.* **18,** 425–436.

Lasa, I., Gouin, E., Goethals, M., Vancompernolle, K., David, V., Vandekerckhove, J., and Cossart, P. (1997). Identification of two regions in the N-terminal domain of ActA involved in the actin comet tail formation by *Listeria monocytogenes*. *EMBO J.* **16,** 1531–1540.

Laurent, V., Loisel, T. P., Harbeck, B., Wehman, A., Grobe, L., Jockusch, B. M., Wehland, J., Gertler, F. B., and Carlier, M. F. (1999). Role of proteins of the Ena/VASP family in actin-based motility of *Listeria monocytogenes*. *J. Cell Biol.* **144,** 1245–1258.

Lecuit, M. (2005). Understanding how *Listeria monocytogenes* targets and crosses host barriers. *Clin. Microbiol. Infect.* **11,** 430–436.

Lecuit, M. (2007). Human listeriosis and animal models. *Microbes Infect.* **9,** 1216–1225.

Lecuit, M., and Cossart, P. (2002). Genetically-modified-animal models for human infections: The *Listeria* paradigm. *Trends Mol. Med.* **8,** 537–542.

Lecuit, M., Dramsi, S., Gottardi, C., Fedor-Chaiken, M., Gumbiner, B., and Cossart, P. (1999). A single amino acid in E-cadherin responsible for host specificity towards the human pathogen *Listeria monocytogenes*. *EMBO J.* **18,** 3956–3963.

Lecuit, M., Hurme, R., Pizarro-Cerda, J., Ohayon, H., Geiger, B., and Cossart, P. (2000). A role for alpha-and beta-catenins in bacterial uptake. *Proc. Natl. Acad. Sci. USA* **97,** 10008–10013.

Lecuit, M., Vandormael-Pournin, S., Lefort, J., Huerre, M., Gounon, P., Dupuy, C., Babinet, C., and Cossart, P. (2001). A transgenic model for listeriosis: Role of internalin in crossing the intestinal barrier. *Science* **292,** 1722–1725.

Lecuit, M., Nelson, D. M., Smith, S. D., Khun, H., Huerre, M., Vacher-Lavenu, M. C., Gordon, J. I., and Cossart, P. (2004). Targeting and crossing of the human maternofetal barrier by *Listeria monocytogenes*: Role of internalin interaction with trophoblast E-cadherin. *Proc. Natl. Acad. Sci. USA* **101,** 6152–6157.

Lee, J. W., and Helmann, J. D. (2006). The PerR transcription factor senses H2O2 by metal-catalysed histidine oxidation. *Nature* **440,** 363–367.

Lee, J. W., and Helmann, J. D. (2007). Functional specialization within the Fur family of metalloregulators. *Biometals* **20,** 485–499.

Leifson, E., and Palen, M. I. (1955). Variations and spontaneous mutations in the genus *Listeria* in respect to flagellation and motility. *J. Bacteriol.* **70,** 233–240.

Leimeister-Wachter, M., Domann, E., and Chakraborty, T. (1991). Detection of a gene encoding a phosphatidylinositol-specific phospholipase C that is co-ordinately expressed with listeriolysin in *Listeria monocytogenes*. *Mol. Microbiol.* **5,** 361–366.

Lenz, L. L., and Portnoy, D. A. (2002). Identification of a second *Listeria* secA gene associated with protein secretion and the rough phenotype. *Mol. Microbiol.* **45,** 1043–1056.

Lenz, L. L., Mohammadi, S., Geissler, A., and Portnoy, D. A. (2003). SecA2-dependent secretion of autolytic enzymes promotes *Listeria monocytogenes* pathogenesis. *Proc. Natl. Acad. Sci. USA* **100,** 12432–12437.

Lingnau, A., Domann, E., Hudel, M., Bock, M., Nichterlein, T., Wehland, J., and Chakraborty, T. (1995). Expression of the *Listeria monocytogenes* EGD inlA and inlB genes, whose products mediate bacterial entry into tissue culture cell lines, by PrfA-dependent and -independent mechanisms. *Infect. Immun.* **63,** 3896–3903.

Loupa, C. V., Kouppar, G., Kosionis, N., Zouberi Koliomichali, M., and Lelekis, M. I. (2007). Biliary tract infection caused by *Listeria monocytogenes*. *Clin. Microbiol. Newsl.* **29,** 6–8.

Luo, Q., Rauch, M., Marr, A. K., Muller-Altrock, S., and Goebel, W. (2004). *In vitro* transcription of the *Listeria monocytogenes* virulence genes inlC and mpl reveals overlapping PrfA-dependent and -independent promoters that are differentially activated by GTP. *Mol. Microbiol.* **52,** 39–52.

Mackaness, G. B. (1962). Cellular resistance to infection. *J. Exp. Med.* **116,** 381–406.
Mandin, P., Fsihi, H., Dussurget, O., Vergassola, M., Milohanic, E., Toledo-Arana, A., Lasa, I., Johansson, J., and Cossart, P. (2005). VirR, a response regulator critical for *Listeria monocytogenes* virulence. *Mol. Microbiol.* **57,** 1367–1380.
Mandin, P., Repoila, F., Vergassola, M., Geissmann, T., and Cossart, P. (2007). Identification of new noncoding RNAs in *Listeria monocytogenes* and prediction of mRNA targets. *Nucleic Acids Res.* **35,** 962–974.
Marino, M., Braun, L., Cossart, P., and Ghosh, P. (2000). A framework for interpreting the leucine-rich repeats of the *Listeria internalins*. *Proc. Natl. Acad. Sci. USA* **97,** 8784–8788.
Marino, M., Banerjee, M., Jonquieres, R., Cossart, P., and Ghosh, P. (2002). GW domains of the *Listeria monocytogenes* invasion protein InlB are SH3-like and mediate binding to host ligands. *EMBO J.* **21,** 5623–5634.
Marino, M., Banerjee, M., Copp, J., Dramsi, S., Chapman, T., van der Geer, P., Cossart, P., and Ghosh, P. (2004). Characterization of the calcium-binding sites of *Listeria monocytogenes* InlB. *Biochem. Biophys. Res. Commun.* **316,** 379–386.
Marquis, H., Doshi, V., and Portnoy, D. A. (1995). The broad-range phospholipase C and a metalloprotease mediate listeriolysin O-independent escape of *Listeria monocytogenes* from a primary vacuole in human epithelial cells. *Infect. Immun.* **63,** 4531–4534.
McGann, P., Wiedmann, M., and Boor, K. J. (2007). The alternative sigma factor sigma B and the virulence gene regulator PrfA both regulate transcription of *Listeria monocytogenes* internalins. *Appl. Environ. Microbiol.* **73,** 2919–2930.
Mengaud, J., Braun-Breton, C., and Cossart, P. (1991). Identification of phosphatidylinositol-specific phospholipase C activity in *Listeria monocytogenes*: A novel type of virulence factor? *Mol. Microbiol.* **5,** 367–372.
Mengaud, J., Ohayon, H., Gounon, P., Mege, R. M., and Cossart, P. (1996). E-cadherin is the receptor for internalin, a surface protein required for entry of *L. monocytogenes* into epithelial cells. *Cell* **84,** 923–932.
Milohanic, E., Pron, B., Berche, P., and Gaillard, J. L. (2000). Identification of new loci involved in adhesion of *Listeria monocytogenes* to eukaryotic cells. European *Listeria* Genome Consortium. *Microbiology* **146**(Pt 3), 731–739.
Milohanic, E., Jonquieres, R., Cossart, P., Berche, P., and Gaillard, J. L. (2001). The autolysin Ami contributes to the adhesion of *Listeria monocytogenes* to eukaryotic cells via its cell wall anchor. *Mol. Microbiol.* **39,** 1212–1224.
Milohanic, E., Glaser, P., Coppee, J. Y., Frangeul, L., Vega, Y., Vazquez-Boland, J. A., Kunst, F., Cossart, P., and Buchrieser, C. (2003). Transcriptome analysis of *Listeria monocytogenes* identifies three groups of genes differently regulated by PrfA. *Mol. Microbiol.* **47,** 1613–1625.
Milohanic, E., Jonquieres, R., Glaser, P., Dehoux, P., Jacquet, C., Berche, P., Cossart, P., and Gaillard, J. L. (2004). Sequence and binding activity of the autolysin-adhesin Ami from epidemic *Listeria monocytogenes* 4b. *Infect. Immun.* **72,** 4401–4409.
Mohamed, W., Darji, A., Domann, E., Chiancone, E., and Chakraborty, T. (2006). The ferritin-like protein Frm is a target for the humoral immune response to *Listeria monocytogenes* and is required for efficient bacterial survival. *Mol. Genet. Genomics* **275,** 344–353.
Mounier, J., Ryter, A., Coquis-Rondon, M., and Sansonetti, P. J. (1990). Intracellular and cell-to-cell spread of *Listeria monocytogenes* involves interaction with F-actin in the enterocytelike cell line Caco-2. *Infect. Immun.* **58,** 1048–1058.
Nadon, C. A., Bowen, B. M., Wiedmann, M., and Boor, K. J. (2002). Sigma B contributes to PrfA-mediated virulence in *Listeria monocytogenes*. *Infect. Immun.* **70,** 3948–3952.
Nair, S., Frehel, C., Nguyen, L., Escuyer, V., and Berche, P. (1999). ClpE, a novel member of the HSP100 family, is involved in cell division and virulence of *Listeria monocytogenes*. *Mol. Microbiol.* **31,** 185–196.

Nair, S., Milohanic, E., and Berche, P. (2000). ClpC ATPase is required for cell adhesion and invasion of *Listeria monocytogenes*. *Infect. Immun.* **68,** 7061–7068.

Newton, S. M., Klebba, P. E., Raynaud, C., Shao, Y., Jiang, X., Dubail, I., Archer, C., Frehel, C., and Charbit, A. (2005). The svpA-srtB locus of *Listeria monocytogenes*: Fur-mediated iron regulation and effect on virulence. *Mol. Microbiol.* **55,** 927–940.

Niebuhr, K., Ebel, F., Frank, R., Reinhard, M., Domann, E., Carl, U. D., Walter, U., Gertler, F. B., Wehland, J., and Chakraborty, T. (1997). A novel proline-rich motif present in ActA of *Listeria monocytogenes* and cytoskeletal proteins is the ligand for the EVH1 domain, a protein module present in the Ena/VASP family. *EMBO J.* **16,** 5433–5444.

Nightingale, K. K., Windham, K., Martin, K. E., Yeung, M., and Wiedmann, M. (2005). Select *Listeria monocytogenes* subtypes commonly found in foods carry distinct nonsense mutations in inlA, leading to expression of truncated and secreted internalin A, and are associated with a reduced invasion phenotype for human intestinal epithelial cells. *Appl. Environ. Microbiol.* **71,** 8764–8772.

O'Neil, H. S., and Marquis, H. (2006). *Listeria monocytogenes* flagella are used for motility, not as adhesins, to increase host cell invasion. *Infect. Immun.* **74,** 6675–6681.

O'Riordan, M., Moors, M. A., and Portnoy, D. A. (2003). *Listeria* intracellular growth and virulence require host-derived lipoic acid. *Science* **302,** 462–464.

Olier, M., Pierre, F., Rousseaux, S., Lemaitre, J. P., Rousset, A., Piveteau, P., and Guzzo, J. (2003). Expression of truncated Internalin A is involved in impaired internalization of some *Listeria monocytogenes* isolates carried asymptomatically by humans. *Infect. Immun.* **71,** 1217–1224.

Olsen, K. N., Larsen, M. H., Gahan, C. G., Kallipolitis, B., Wolf, X. A., Rea, R., Hill, C., and Ingmer, H. (2005). The Dps-like protein Fri of *Listeria monocytogenes* promotes stress tolerance and intracellular multiplication in macrophage-like cells. *Microbiology* **151,** 925–933.

Ooi, A., Hussain, S., Seyedarabi, A., and Pickersgill, R. W. (2006). Structure of internalin C from *Listeria monocytogenes*. *Acta Crystallogr. D Biol. Crystallogr.* **62,** 1287–1293.

Orndorff, P. E., Hamrick, T. S., Smoak, I. W., and Havell, E. A. (2006). Host and bacterial factors in listeriosis pathogenesis. *Vet. Microbiol.* **114,** 1–15.

Pamer, E. G. (2004). Immune responses to *Listeria monocytogenes*. *Nat. Rev. Immunol.* **4,** 812–823.

Parida, S. K., Domann, E., Rohde, M., Muller, S., Darji, A., Hain, T., Wehland, J., and Chakraborty, T. (1998). Internalin B is essential for adhesion and mediates the invasion of *Listeria monocytogenes* into human endothelial cells. *Mol. Microbiol.* **28,** 81–93.

Peel, M., Donachie, W., and Shaw, A. (1988). Temperature-dependent expression of flagella of *Listeria monocytogenes* studied by electron microscopy, SDS-PAGE and western blotting. *J. Gen. Microbiol.* **134,** 2171–2178.

Popowska, M., and Markiewicz, Z. (2004). Murein-hydrolyzing activity of flagellin FlaA of *Listeria monocytogenes*. *Pol. J. Microbiol.* **53,** 237–241.

Portnoy, D. A., Jacks, P. S., and Hinrichs, D. J. (1988). Role of hemolysin for the intracellular growth of *Listeria monocytogenes*. *J. Exp. Med.* **167,** 1459–1471.

Pucciarelli, M. G., Calvo, E., Sabet, C., Bierne, H., Cossart, P., and Garcia-del Portillo, F. (2005). Identification of substrates of the *Listeria monocytogenes* sortases A and B by a non-gel proteomic analysis. *Proteomics* **5,** 4808–4817.

Py, B. F., Lipinski, M. M., and Yuan, J. (2007). Autophagy limits *Listeria monocytogenes* intracellular growth in the early phase of primary infection. *Autophagy* **3,** 117–125.

Raffelsbauer, D., Bubert, A., Engelbrecht, F., Scheinpflug, J., Simm, A., Hess, J., Kaufmann, S. H., and Goebel, W. (1998). The gene cluster inlC2DE of *Listeria monocytogenes* contains additional new internalin genes and is important for virulence in mice. *Mol. Gen. Genet.* **260,** 144–158.

Raveneau, J., Geoffroy, C., Beretti, J. L., Gaillard, J. L., Alouf, J. E., and Berche, P. (1992). Reduced virulence of a *Listeria monocytogenes* phospholipase-deficient mutant obtained by transposon insertion into the zinc metalloprotease gene. *Infect. Immun.* **60,** 916–921.

Raynaud, C., and Charbit, A. (2005). Regulation of expression of type I signal peptidases in *Listeria monocytogenes*. *Microbiology* **151,** 3769–3776.

Rea, R. B., Gahan, C. G., and Hill, C. (2004). Disruption of putative regulatory loci in *Listeria monocytogenes* demonstrates a significant role for Fur and PerR in virulence. *Infect. Immun.* **72,** 717–727.

Rea, R. B., Hill, C., and Gahan, C. G. (2005). *Listeria monocytogenes* PerR mutants display a small-colony phenotype, increased sensitivity to hydrogen peroxide, and significantly reduced murine virulence. *Appl. Environ. Microbiol.* **71,** 8314–8322.

Reglier-Poupet, H., Frehel, C., Dubail, I., Beretti, J. L., Berche, P., Charbit, A., and Raynaud, C. (2003a). Maturation of lipoproteins by type II signal peptidase is required for phagosomal escape of *Listeria monocytogenes*. *J. Biol. Chem.* **278,** 49469–49477.

Reglier-Poupet, H., Pellegrini, E., Charbit, A., and Berche, P. (2003b). Identification of LpeA, a PsaA-like membrane protein that promotes cell entry by *Listeria monocytogenes*. *Infect. Immun.* **71,** 474–482.

Rich, K. A., Burkett, C., and Webster, P. (2003). Cytoplasmic bacteria can be targets for autophagy. *Cell. Microbiol.* **5,** 455–468.

Roberts, A. J., and Wiedmann, M. (2003). Pathogen, host and environmental factors contributing to the pathogenesis of listeriosis. *Cell. Mol. Life Sci.* **60,** 904–918.

Rouquette, C., de Chastellier, C., Nair, S., and Berche, P. (1998). The ClpC ATPase of *Listeria monocytogenes* is a general stress protein required for virulence and promoting early bacterial escape from the phagosome of macrophages. *Mol. Microbiol.* **27,** 1235–1245.

Sabet, C., Lecuit, M., Cabanes, D., Cossart, P., and Bierne, H. (2005). LPXTG protein InlJ, a newly identified internalin involved in *Listeria monocytogenes* virulence. *Infect. Immun.* **73,** 6912–6922.

Schirm, M., Schoenhofen, I. C., Logan, S. M., Waldron, K. C., and Thibault, P. (2005). Identification of unusual bacterial glycosylation by tandem mass spectrometry analyses of intact proteins. *Anal. Chem.* **77,** 7774–7782.

Schlech, W. F., 3rd (2000). Foodborne listeriosis. *Clin. Infect. Dis.* **31,** 770–775.

Schluter, D., Domann, E., Buck, C., Hain, T., Hof, H., Chakraborty, T., and Deckert-Schluter, M. (1998). Phosphatidylcholine-specific phospholipase C from *Listeria monocytogenes* is an important virulence factor in murine cerebral listeriosis. *Infect. Immun.* **66,** 5930–5938.

Schmeck, B., Beermann, W., van Laak, V., Zahlten, J., Opitz, B., Witzenrath, M., Hocke, A. C., Chakraborty, T., Kracht, M., Rosseau, S., Suttorp, N., and Hippenstiel, S. (2005). Intracellular bacteria differentially regulated endothelial cytokine release by MAPK-dependent histone modification. *J. Immunol.* **175,** 2843–2850.

Schmid, M. W., Ng, E. Y., Lampidis, R., Emmerth, M., Walcher, M., Kreft, J., Goebel, W., Wagner, M., and Schleifer, K. H. (2005). Evolutionary history of the genus *Listeria* and its virulence genes. *Syst. Appl. Microbiol.* **28,** 1–18.

Schnupf, P., and Portnoy, D. A. (2007). Listeriolysin O: A phagosome-specific lysin. *Microbes Infect.* **9,** 1176–1187.

Schubert, W. D., Gobel, G., Diepholz, M., Darji, A., Kloer, D., Hain, T., Chakraborty, T., Wehland, J., Domann, E., and Heinz, D. W. (2001). Internalins from the human pathogen *Listeria monocytogenes* combine three distinct folds into a contiguous internalin domain. *J. Mol. Biol.* **312,** 783–794.

Seeliger, H. P. R., and Jones, D. (1986). The genus *Listeria*. *In* "Bergey's Manual of Systematic Bacteriology," pp. 1235–1245. Williams and Wilkins, Baltimore.

Seveau, S., Pizarro-Cerda, J., and Cossart, P. (2007). Molecular mechanisms exploited by *Listeria monocytogenes* during host cell invasion. *Microbes Infect.* **9,** 1167–1175.

Shen, A., and Higgins, D. E. (2006). The MogR transcriptional repressor regulates nonhierarchal expression of flagellar motility genes and virulence in *Listeria monocytogenes*. *PLoS Pathog*. **2,** e30.

Shen, Y., Naujokas, M., Park, M., and Ireton, K. (2000). InIB-dependent internalization of *Listeria* is mediated by the Met receptor tyrosine kinase. *Cell* **103,** 501–510.

Shen, A., Kamp, H. D., Grundling, A., and Higgins, D. E. (2006). A bifunctional O-GlcNAc transferase governs flagellar motility through anti-repression. *Genes Dev*. **20,** 3283–3295.

Simon, N., Coulanges, V., Andre, P., and Vidon, D. J. (1995). Utilization of exogenous siderophores and natural catechols by *Listeria monocytogenes*. *Appl. Environ. Microbiol*. **61,** 1643–1645.

Skoble, J., Portnoy, D. A., and Welch, M. D. (2000). Three regions within ActA promote Arp2/3 complex-mediated actin nucleation and *Listeria monocytogenes* motility. *J. Cell Biol*. **150,** 527–538.

Skoble, J., Auerbuch, V., Goley, E. D., Welch, M. D., and Portnoy, D. A. (2001). Pivotal role of VASP in Arp2/3 complex-mediated actin nucleation, actin branch-formation, and *Listeria monocytogenes* motility. *J. Cell Biol*. **155,** 89–100.

Sleator, R. D., Gahan, C. G., Abee, T., and Hill, C. (1999). Identification and disruption of BetL, a secondary glycine betaine transport system linked to the salt tolerance of *Listeria monocytogenes* LO28. *Appl. Environ. Microbiol*. **65,** 2078–2083.

Sleator, R. D., Wouters, J., Gahan, C. G., Abee, T., and Hill, C. (2001). Analysis of the role of OpuC, an osmolyte transport system, in salt tolerance and virulence potential of *Listeria monocytogenes*. *Appl. Environ. Microbiol*. **67,** 2692–2698.

Sleator, R. D., Wemekamp-Kamphuis, H. H., Gahan, C. G., Abee, T., and Hill, C. (2005). A PrfA-regulated bile exclusion system (BilE) is a novel virulence factor in *Listeria monocytogenes*. *Mol. Microbiol*. **55,** 1183–1195.

Smith, G. A., Marquis, H., Jones, S., Johnston, N. C., Portnoy, D. A., and Goldfine, H. (1995). The two distinct phospholipases C of *Listeria monocytogenes* have overlapping roles in escape from a vacuole and cell-to-cell spread. *Infect. Immun*. **63,** 4231–4237.

Sousa, S., Cabanes, D., El-Amraoui, A., Petit, C., Lecuit, M., and Cossart, P. (2004). Unconventional myosin VIIa and vezatin, two proteins crucial for *Listeria* entry into epithelial cells. *J. Cell Sci*. **117,** 2121–2130.

Sousa, S., Cabanes, D., Archambaud, C., Colland, F., Lemichez, E., Popoff, M., Boisson-Dupuis, S., Gouin, E., Lecuit, M., Legrain, P., and Cossart, P. (2005). ARHGAP10 is necessary for alpha-catenin recruitment at adherens junctions and for *Listeria* invasion. *Nat. Cell Biol*. **7,** 954–960.

Sousa, S., Cabanes, D., Bougneres, L., Lecuit, M., Sansonetti, P., Tran-Van-Nhieu, G., and Cossart, P. (2007). Src, cortactin and Arp2/3 complex are required for E-cadherin-mediated internalization of *Listeria* into cells. *Cell. Microbiol*. **9,** 2629–2643.

Stack, H. M., Sleator, R. D., Bowers, M., Hill, C., and Gahan, C. G. (2005). Role for HtrA in stress induction and virulence potential in *Listeria monocytogenes*. *Appl. Environ. Microbiol*. **71,** 4241–4247.

Suarez, M., Gonzalez-Zorn, B., Vega, Y., Chico-Calero, I., and Vazquez-Boland, J. A. (2001). A role for ActA in epithelial cell invasion by *Listeria monocytogenes*. *Cell. Microbiol*. **3,** 853–864.

Sue, D., Boor, K. J., and Wiedmann, M. (2003). Sigma(B)-dependent expression patterns of compatible solute transporter genes opuCA and lmo1421 and the conjugated bile salt hydrolase gene bsh in *Listeria monocytogenes*. *Microbiology* **149,** 3247–3256.

Swaminathan, B., and Gerner-Smidt, P. (2007). The epidemiology of human listeriosis. *Microbes Infect*. **9,** 1236–1243.

Tang, P., Rosenshine, I., Cossart, P., and Finlay, B. B. (1996). Listeriolysin O activates mitogen-activated protein kinase in eucaryotic cells. *Infect. Immun*. **64,** 2359–2361.

Taylor, C. M., Beresford, M., Epton, H. A., Sigee, D. C., Shama, G., Andrew, P. W., and Roberts, I. S. (2002). *Listeria monocytogenes* relA and hpt mutants are impaired in surface-attached growth and virulence. *J. Bacteriol.* **184,** 621–628.

Thedieck, K., Hain, T., Mohamed, W., Tindall, B. J., Nimtz, M., Chakraborty, T., Wehland, J., and Jansch, L. (2006). The MprF protein is required for lysinylation of phospholipids in listerial membranes and confers resistance to cationic antimicrobial peptides (CAMPs) on *Listeria monocytogenes*. *Mol. Microbiol.* **62,** 1325–1339.

Theriot, J. A., Mitchison, T. J., Tilney, L. G., and Portnoy, D. A. (1992). The rate of actin-based motility of intracellular *Listeria monocytogenes* equals the rate of actin polymerization. *Nature* **357,** 257–260.

Tilney, L. G., and Portnoy, D. A. (1989). Actin filaments and the growth, movement, and spread of the intracellular bacterial parasite, *Listeria monocytogenes*. *J. Cell Biol.* **109,** 1597–1608.

Tilney, L. G., Connelly, P. S., and Portnoy, D. A. (1990). Actin filament nucleation by the bacterial pathogen, *Listeria monocytogenes*. *J. Cell Biol.* **111,** 2979–2988.

Vazquez-Boland, J. A., Kocks, C., Dramsi, S., Ohayon, H., Geoffroy, C., Mengaud, J., and Cossart, P. (1992). Nucleotide sequence of the lecithinase operon of *Listeria monocytogenes* and possible role of lecithinase in cell-to-cell spread. *Infect. Immun.* **60,** 219–230.

Vazquez-Boland, J. A., Dominguez-Bernal, G., Gonzalez-Zorn, B., Kreft, J., and Goebel, W. (2001a). Pathogenicity islands and virulence evolution in *Listeria*. *Microbes Infect.* **3,** 571–584.

Vazquez-Boland, J. A., Kuhn, M., Berche, P., Chakraborty, T., Dominguez-Bernal, G., Goebel, W., Gonzalez-Zorn, B., Wehland, J., and Kreft, J. (2001b). *Listeria* pathogenesis and molecular virulence determinants. *Clin. Microbiol. Rev.* **14,** 584–640.

Veiga, E., and Cossart, P. (2005). *Listeria* hijacks the clathrin-dependent endocytic machinery to invade mammalian cells. *Nat. Cell Biol.* **7,** 894–900.

Veiga, E., and Cossart, P. (2006). The role of clathrin-dependent endocytosis in bacterial internalization. *Trends Cell Biol.* **16,** 499–504.

Veiga, E., Guttman, J. A., Bonazzi, M., Boucrot, E., Toledo-Arana, A., Lin, A. E., Enninga, J., Pizarro-Cerda, J., Finlay, B. B., Kirchhausen, T., and Cossart, P. (2007). Invasive and adherent bacterial pathogens co-opt host clathrin for infection. *Cell Host Microbe* **2,** 340–351.

Wadsworth, S. J., and Goldfine, H. (2002). Mobilization of protein kinase C in macrophages induced by *Listeria monocytogenes* affects its internalization and escape from the phagosome. *Infect. Immun.* **70,** 4650–4660.

Way, S. S., Thompson, L. J., Lopes, J. E., Hajjar, A. M., Kollmann, T. R., Freitag, N. E., and Wilson, C. B. (2004). Characterization of flagellin expression and its role in *Listeria monocytogenes* infection and immunity. *Cell. Microbiol.* **6,** 235–242.

Wemekamp-Kamphuis, H. H., Wouters, J. A., Sleator, R. D., Gahan, C. G., Hill, C., and Abee, T. (2002). Multiple deletions of the osmolyte transporters BetL, Gbu, and OpuC of *Listeria monocytogenes* affect virulence and growth at high osmolarity. *Appl. Environ. Microbiol.* **68,** 4710–4716.

Williams, T., Joseph, B., Beier, D., Goebel, W., and Kuhn, M. (2005). Response regulator DegU of *Listeria monocytogenes* regulates the expression of flagella-specific genes. *FEMS Microbiol. Lett.* **252,** 287–298.

Wollert, T., Pasche, B., Rochon, M., Deppenmeier, S., van den Heuvel, J., Gruber, A. D., Heinz, D. W., Lengeling, A., and Schubert, W. D. (2007). Extending the host range of *Listeria monocytogenes* by rational protein design. *Cell* **129,** 891–902.

Yang, Y., Liu, B., Dai, J., Srivastava, P. K., Zammit, D. J., Lefrancois, L., and Li, Z. (2007). Heat shock protein gp96 is a master chaperone for toll-like receptors and is important in the innate function of macrophages. *Immunity* **26,** 215–226.

CHAPTER TWO

Flagellar Motility in Bacteria: Structure and Function of Flagellar Motor

Hiroyuki Terashima,* Seiji Kojima,* *and* Michio Homma*

Contents

Abstract

Bacterial flagella are filamentous organelles that drive cell locomotion. They thrust cells in liquids (swimming) or on surfaces (swarming) so that cells can move toward favorable environments. At the base of each flagellum, a reversible rotary motor, which is powered by the proton- or the sodium-motive force,

* Division of Biological Science, Graduate School of Science, Nagoya University, Nagoya, Japan

International Review of Cell and Molecular Biology, Volume 270
ISSN 1937-6448, DOI: 10.1016/S1937-6448(08)01402-0

is embedded in the cell envelope. The motor consists of two parts: the rotating part, or rotor, that is connected to the hook and the filament, and the nonrotating part, or stator, that conducts coupling ion and is responsible for energy conversion. Intensive genetic and biochemical studies of the flagellum have been conducted in *Salmonella typhimurium* and *Escherichia coli*, and more than 50 gene products are known to be involved in flagellar assembly and function. The energy-coupling mechanism, however, is still not known. In this chapter, we survey our current knowledge of the flagellar system, based mostly on studies from *Salmonella*, *E. coli*, and marine species *Vibrio alginolyticus*, supplemented with distinct aspects of other bacterial species revealed by recent studies.

Key Words: Proton motive force, Sodium motive force, Energy transduction, *Vibrio alginolyticus*, *Salmonella typhimurium*, *Escherichia coli*.

1. Introduction

1.1. Molecular architecture of flagella

The flagellum consists of three parts: the filament (helical propeller), the hook (universal joint), and the basal structure (rotary motor) (Fig. 2.1). The largest part of the flagellum is the filament, a helical structure whose shape can vary among different helical forms, a phenomenon termed polymorphism (Asakura, 1970). This polymorphic alteration of flagellar shape is associated with phase variation (Iino, 1969). When the cell swims, the flagellar filament serves as a screw propeller to convert rotary motion of the motor into thrust (Berg and Anderson, 1973). In *Salmonella*, it grows to a length of around 15 μm and is composed of as many as 30,000 copies of a single protein named flagellin (Minamino and Namba, 2004). Some bacteria, for example *Vibrio*, have several closely related flagellins that form the filament (McCarter, 2001). The flagellin subunits (FliC in *Escherichia coli* and *Salmonella*) are self-assembled to form a hollow concentric double-tubular structure (inner and outer tubes) consisting of 11 protofilaments, which are arranged approximately parallel to the filament axis (Mimori *et al.*, 1995; Morgan *et al.*, 1995). Formation of a helical structure is achieved by a mixture of the protofilaments of two distinct conformations, the R- and L-type, distinguished by their helical handedness right or left (Asakura, 1970; Calladine, 1978). Each protofilament switches between these two conformations by responding to a variety of factors including pH, ionic strength, mechanical stress, and mutations (Kamiya and Asakura, 1976; Macnab and Ornston, 1977). Later, X-ray fiber diffraction studies revealed slightly different subunit packing between the R- and L-type, whose repeat distances are 51.9 and 52.7 Å, respectively (Yamashita *et al.*, 1998). To

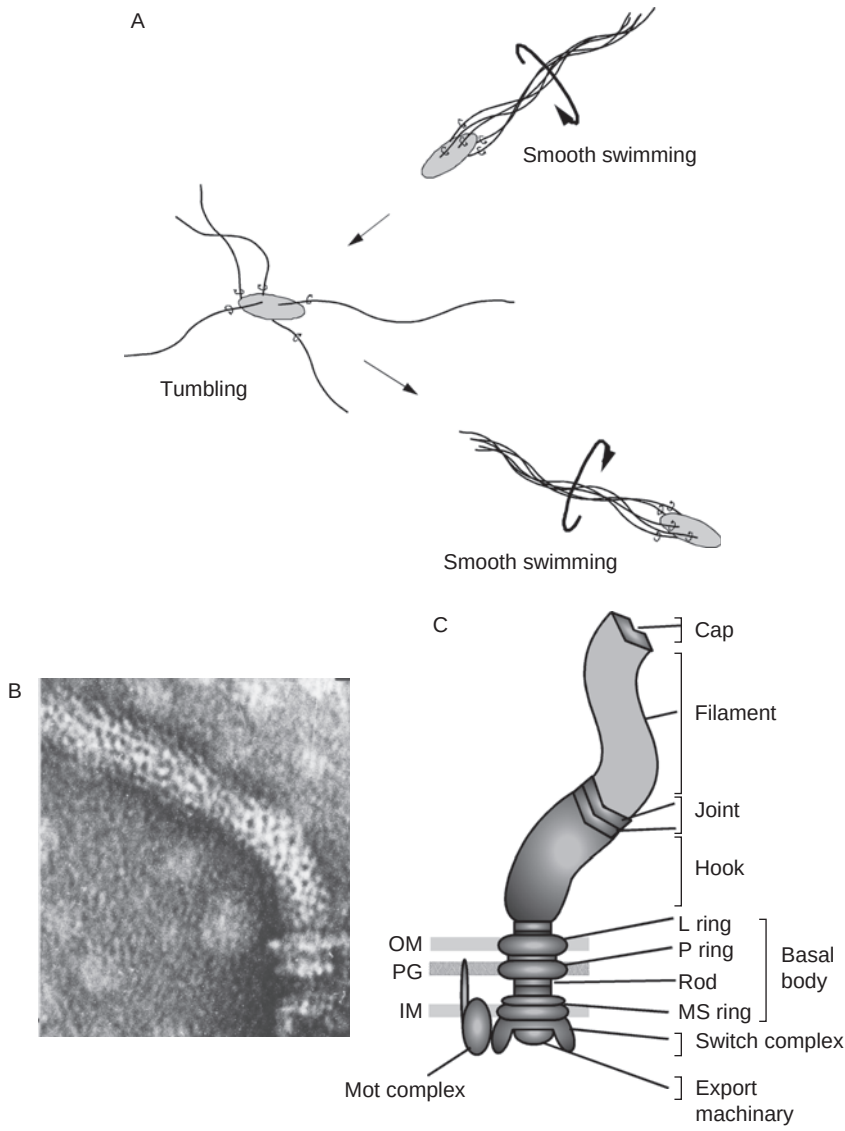

Figure 2.1 (A) Behavior of bacterial cells. (B) Electron micrograph of flagella isolated from *Salmonella typhimurium*. (C) Schematic diagram of flagellar structure of Gram-negative bacteria.

understand the polymorphic switching mechanism, the crystal structure of fragment containing most of the flagellin protein (F41 fragment of FliC) was solved at 2 Å (Samatey *et al.*, 2001). In the crystal, F41 fragments of the R-type conformation form protofilaments arranged in an antiparallel

manner, and simulation using atomic model revealed that a small, distinct conformational changes in the β-hairpin in D1, the domain that contributes to outer tube structure, is responsible for the conformational switching between L- and R-type protofilament. The crystal structure of F41 fragment lacks the D0 domain that forms inner tube structure. Later, electron cryomicroscopy and helical image analysis made it possible to build complete atomic model of the R-type filament structure including D0 domain of flagellin, revealing that intersubunit hydrophobic interactions in the inner tube (domain D0) make the filament structure mechanically stable, and the diameter of central channel is only 2 nm (Yonekura *et al.*, 2003). This central channel serves as a transport pathway of flagellins that will polymerize at the tip of the growing filament (Fig. 2.2).

The base of the filament is connected to the short tubular structure called the hook, which is thought to function as a universal joint to smoothly transmit the torque produced by the motor to the filament. The hook structure of *Salmonella* is composed of about 120 copies of a single protein FlgE and its length is controlled at 55 ($\pm$6) nm (Hirano *et al.*, 1994). The core structure of the hook protein was solved by X-ray crystallography, and its atomic model was docked onto the density map of the hook obtained by electron cryomicroscopy (Samatey *et al.*, 2004).

The junction between hook and filament consists of the two proteins, FlgK (HAP1) and FlgL (HAP3) (Homma and Iino, 1985; Ikeda *et al.*, 1985). About 13 molecules of each protein are present in each flagellum (Ikeda *et al.*, 1987). Mutational studies suggested that the junction acts as a buffering structure connecting two filamentous structures (hook and filament) with distinct mechanical properties (Fahrner *et al.*, 1994).

The proximal end of the hook is connected to the basal body structure, consisting of the rod and three coaxially mounted rings, termed as MS, P, and L ring. The MS ring is embedded in the cytoplasmic membrane and made of a single protein FliF (Ueno *et al.*, 1992), the P and L rings are associated with the peptidoglycan layer and the outer membrane, respectively, and are composed of FlgI and FlgH (Homma *et al.*, 1987; Schoenhals and Macnab, 1996). The rod structure is composed of three proximal rod proteins FlgB, FlgC, FlgF, and a distal rod protein FlgG, and fully traverses the periplasmic space. The L and P rings together form a quite rigid assembly resistant to stringent chemical treatments, and the LP-ring complex is believed to act as a molecular bushing for the flagellar axial structure (Akiba *et al.*, 1991). The basal body of Gram-positive bacteria is composed of only the MS ring and rod, and the LP ring is not present (Kobayashi *et al.*, 2003), probably because Gram-positive bacteria do not have the outer membrane but have a thick peptidoglycan layer. When the basal body is isolated with more gentle treatment, a drum-shaped structure, called C ring, was found on the MS ring facing the cytoplasm (Francis *et al.*, 1994). It is composed mostly of FliM and FliN proteins (Thomas *et al.*, 2006; Zhao

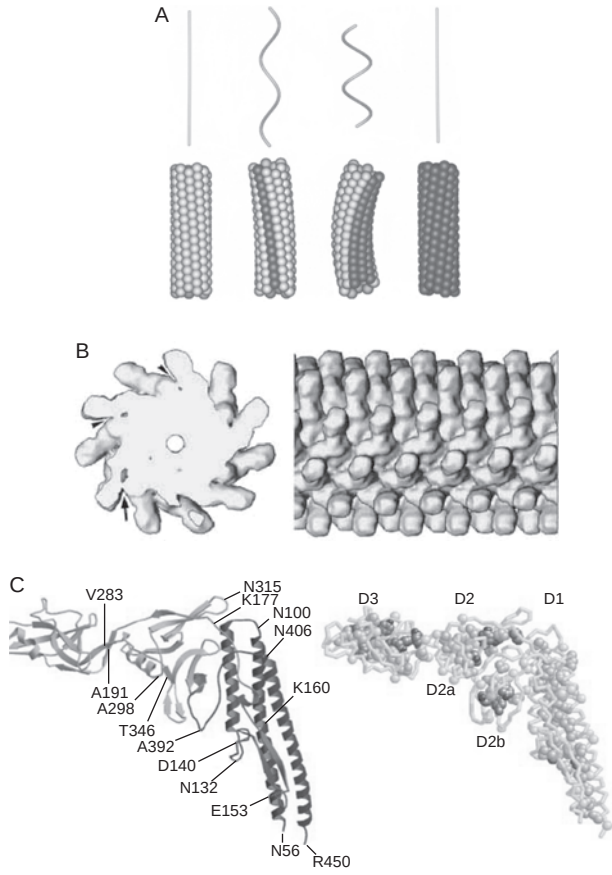

Figure 2.2 (A) Polymorphic structure of the flagellar filament. The filaments of L-type straight, normal, curly, and R-type straight are shown by the left to right in this order. (B) The flagellar filament structure revealed by electron cryomicroscopy. The end-on view of the cross section (left) and the side view of long segment (right). (C) The backbone trace of the flagellin (FliC) molecule of *Salmonella typhimurium*. The figures were kindly supplied by K. Namba.

et al., 1996a,b). These proteins, together with FliG which is located beneath the MS ring, have been known to form a complex, referred to as the switch complex. Mutations in each of these three proteins cause defects in switching the rotational direction of the motor (Yamaguchi *et al.*, 1986a). They are also important for rotation, and mutational studies revealed that FliG most closely participates in torque generation (Lloyd *et al.*, 1996). Careful preparation of the basal structure further revealed a central protrusion within the C ring, that is probably the export apparatus essential for assembly of flagellum (Katayama *et al.*, 1996).

1.2. Gene regulation

More than 50 genes are required for flagellar formation and function (Macnab, 2003). Because the flagellum is such a big organelle, a large amount of energy is consumed during the assembly process. Bacteria deal with this problem by developing highly organized and regulated systems for flagellar assembly. Its characteristic feature is that the flagellar gene regulation temporally and tightly couples to the assembly process. Here we survey this regulatory mechanism in *Salmonella*, which has been most extensively studied. For further details of flagellar gene regulations in *Salmonella enterica* serovar *typhimurium* and *E. coli* as well as the other bacteria, such as *Caulobacter cresentus* and *Vibrio* spp., see the reviews cited in Chilcott and Hughes (2000), McCarter (2004), Wolfe and Visick (2008), and Wu and Newton (1997).

In *Salmonella*, the flagellar/motility/chemotaxis genes constitute a regulon, and they are arranged in hierarchical order into three classes, early, middle, and late (Fig. 2.3) (Kutsukake *et al.*, 1990). At the top of the hierarchy is a single operon (class 1 master operon) containing the *flhDC* genes (Liu and Matsumura, 1994). The FlhC and FlhD proteins form a heterotetrametic complex $FlhC_2FlhD_2$ that direct σ^{70}-RNA polymerase complex to activate transcription from class 2 promoters upstream of the

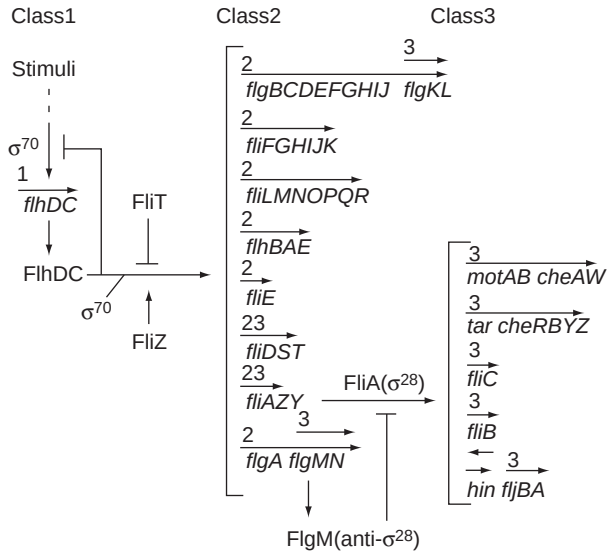

Figure 2.3 Regulation of transcription of the flagellar regulon. The flagellar operons are indicated by arrows. The numbers on the arrows show the class of transcriptional hierarchy in the flagellar regulon. Descriptions of the transcriptional regulation and the function of the gene products are described in text.

middle gene operons. The *flhDC* operon is tightly regulated under the control of a number of global regulatory signals such as cAMP-CRP, heat shock, DNA supercoiling, growth phase, surface-liquid transition, ClpXP protease, and c-di-GMP (reviewed in Chilcott and Hughes, 2000; Wolfe and Visick, 2008). Expression of *flhDC* is also linked to the cell cycle, showing that flagellation and cell cycle are interdependent processes (Pruss and Matsumura, 1996, 1997).

More than 30 middle gene products from class 2 operons are primarily required for the structure and assembly of the hook and basal body, and include regulatory proteins that control transcription of the genes from class 3 operons. Class 3 operons encode for proteins required late in the assembly process, including flagellin, hook-associated proteins (HAPs), stator components, and chemosensory systems. Expression of class 3 operons is positively controlled by FliA and negatively by FlgM (Gillen and Hughes, 1991; Kutsukake and Iino, 1994). FliA is the flagellum-specific transcription factor σ^{28} (Ohnishi *et al.*, 1990), and it leads σ^{28}-RNA polymerase complex to transcribe class 3 late gene operons, whereas FlgM is an anti-σ^{28} factor specific for FliA (Ohnishi *et al.*, 1992). Since filament formation requires large resources of the cells, the stage to initiate expression of class 3 operons is a critical checkpoint for flagellar gene regulation. Actually, what happens *in vivo* is that the late genes are not transcribed until the assembly of hook-basal body structures has been completed. Mutations in any one of the hook-basal body genes prevent the transcription of class 3 operons to avoid unnecessary late gene expression that would cause an energy drain in the cell. This remarkable coupling between structure and gene expression is achieved by the balance of FliA and FlgM. FlgM inhibits FliA for the expression of class 3 operons until hook-basal body completion, at which time FlgM is secreted out from the cells through hook-basal body structure and released FliA turns on transcription of class 3 operons to achieve filament formation and motor assembly (Hughes *et al.*, 1993; Kutsukake, 1994). Such a controlled expression is coupled to the ordered secretion of each gene products by the flagellum-specific export apparatus, putatively located inside of the MS ring, to complete the self-assembly of flagella.

As described above, sensing hook-basal body completion followed by FlgM secretion is such a critical checkpoint; *Salmonella* utilizes another factor involved in negative regulation in FlgM secretion. This gene, *flk* (Karlinsey *et al.*, 1997), also called as *rflH* (Kutsukake, 1997), was identified as the factor that allows expression of class 3 operons only when mutated in strains defective in LP ring assembly. Flk is a cytoplasmic-facing protein anchored to the inner membrane by a single, C-terminal transmembrane domain, and it was revealed that turnover of FlgM was increased in *flk* background due to FlgM secretion into periplasm where it is degraded, suggesting that Flk prevents premature secretion of the FlgM into periplasm, thus acting as a braking systems for the flagellar export system

(Aldridge *et al.*, 2006). Loss of only Flk does not show any phenotype related to motility, and *flk* gene is not located in the flagellar regulon, so the role of Flk in the wild-type cell is still unclear (Karlinsey *et al.*, 1997; Kutsukake, 1997).

1.3. Flagellar assembly

As described in Section 1.2, flagellar assembly is tightly coupled to the gene expression, and the monitoring system at the stage of hook completion allows cells to achieve efficient and economical filament formation. The sequence of events in flagellar assembly has been extensively studied in *Salmonella* and *E. coli* by studying partial structures of flagella from mutants defective in a certain flagellar gene (Kubori *et al.*, 1992; Suzuki and Komeda, 1981; Suzuki *et al.*, 1978). In general, assembly starts at the inner structure of the basal body then proceeds to the outer ones (Fig. 2.4). The first built structure is the MS ring and proximal rod, which is formed by a single protein FliF (Ueno *et al.*, 1992). The MS ring is the core structure of the rotor and is embedded in the cytoplasmic membrane. The C ring attaches on

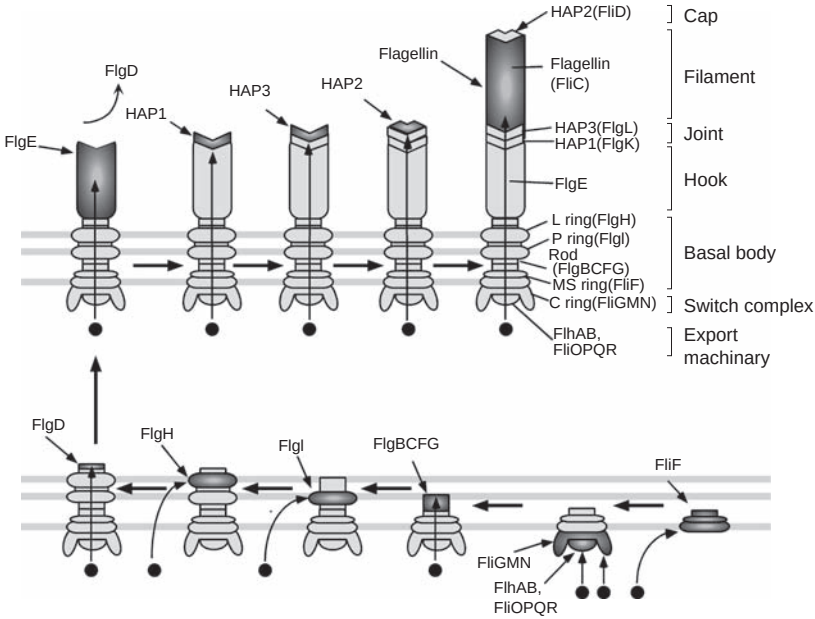

Figure 2.4 **Morphological assembly of bacterial flagellum. The model of pathway is created based on the assumption that the structure is built from a simple to complicated form. The flagellar morphogenesis is thought to begin with the formation of MS ring structure followed by the assembly of proteins for axial structures, each of which is secreted by the flagellum-specific export apparatus (except FlgA, FlgI, and FlgH).**

the cytoplasmic face of MS ring (Francis *et al.*, 1994). The C ring contains mostly two switch proteins FliM and FliN (Zhao *et al.*, 1996a,b), and is associated with MS ring via another switch/motor protein FliG, which probably contributes to a part of the face of MS ring (Thomas *et al.*, 2006). Assembly of these three proteins on the basal body requires the MS-ring platform, and mutations give rise to the nonflagellate phenotype. Inside the MS ring, there is the flagellum-specific export apparatus, visualized in freeze-fracture images as a protrusion inside the C ring (Katayama *et al.*, 1996). When the export apparatus is established in the flagellar base is still unclear. Details of the export apparatus are described in Section 2.2.

After the export apparatus is constructed, structural proteins for the basal body, expressed from class 2 operons, are secreted through the export apparatus in the order described below. First, the proximal rod, composed of FlgB, FlgC, and FlgF, is added on the MS ring, probably in this order (Homma *et al.*, 1990). FliE is needed for this assembly, joining FliF, and proximal rod as an adaptor (Minamino *et al.*, 2000b). Then the distal rod, made of FlgG, is assembled on the proximal rod. Formation of the rod requires FlgJ, which is exported to the periplasmic space via export apparatus and acts as a cap on the growing rod to facilitate the polymerization at the tip (Kubori *et al.*, 1992). FlgJ also has a muramidase activity at its C-terminal half, hydrolyzing the peptidoglycan adjacent to the MS ring to allow the rod to penetrate the peptidoglycan layer (Nambu *et al.*, 1999). Then the P ring (made of FlgI) is formed around the distal rod, followed by L-ring (FlgH) formation (Chevance *et al.*, 2007). FlgI and FlgH are not secreted through the export apparatus, but through the Sec pathway using a signal sequence at their N-termini (Homma *et al.*, 1987). P-ring formation requires the Dsb system, which is involved in intramolecular disulfide bond formation in the periplasm (Dailey and Berg, 1993). FlgI protein contains two cysteine residues important for protein stability (Hizukuri *et al.*, 2006). P-ring formation also requires the FlgA protein that acts as a periplasmic chaperone, assisting a polymerization reaction of FlgI into the P ring through FlgI–FlgI interaction (Nambu and Kutsukake, 2000). The hook assembles next, from about 120 copies of FlgE proteins at the distal end of the growing hook, with the aid of hook-capping protein FlgD. Hook elongation proceeds to the well-controlled length of 55 ± 6 nm by a sophisticated export switching mechanism (Hirano *et al.*, 1994). After hook reached to the defined length, FlgD dissociates from the tip of the hook, then replaced by the three HAPs, FlgK, FlgL, and FliD in this order (Homma and Iino, 1985). Addition of FlgK and FlgL is facilitated by the chaperone FlgN (Fraser *et al.*, 1999), whereas that of FliD is facilitated by another chaperone FliT (Bennett *et al.*, 2001). Finally, the FliC filament subunits (flagellin) are inserted at the distal end (Iino, 1969). FliD acts as a cap to facilitate the filament elongation by inserting each FliC subunit between the FlgL and FliD zones, with rotary cap mechanism revealed by

electron cryomicroscopic observation (Yonekura *et al.*, 2000). Mutants that lack FliD cannot polymerize the filament and excrete flagellin monomers into the culture (Homma *et al.*, 1984). However, when purified FliD is added to this mutant, flagellins stop leaking out and start polymerizing on the hook (Homma *et al.*, 1986). Using this system, growth rate of the filament was observed and revealed that initial growth rate is about 30 nm/min, which corresponds to one flagellin incorporated per second, suggesting that to reach the 10 μm long of the filament of wild-type cells, it takes several generations (Ikeda *et al.*, 1993).

Vibrio alginolyticus has a single polar flagellum, so components required for polar flagellum are localized to a single cell pole. The mechanism for directing the MS ring (or to initiate MS-ring assembly) at the pole has remained unknown, but recent studies revealed that two proteins, FlhF and FlhG, are somehow involved in the process (Kusumoto *et al.*, 2006). Almost all of the cells of an *flhF* null strain do not have a polar flagellum, whereas an *flhG* strain has multiple flagella at a pole. Overproduction of FlhF in the wild-type strain increased the number of polar flagella, whereas excess FlhG reduced it, indicating that these two proteins function in opposing ways. Although the *flhFG* double null strain also showed almost no flagella, a very small but significant fraction of the cells possesses several flagella at the lateral position (Kusumoto *et al.*, 2008). These results suggest that FlhF functions in polar location of the flagellum. This idea is supported by a study in *Pseudomonas putida*, possessing polar flagella, which showed that an *flhF* mutant exhibits a peritrichously flagellated phenotype (Pandza *et al.*, 2000).

FlhF and FlhG show similarity to FtsY and MinD, respectively. FtsY is a component of the prokaryotic SRP receptor (Luirink and Sinning, 2004) and MinD is a cell division inhibitor (Shapiro *et al.*, 2002). MinD shows a structural similarity to Ffh (Cordell and Lowe, 2001), which is a prokaryotic SRP that forms a complex with FtsY to function in a signal recognition targeting pathway for protein secretion at the membrane (Focia *et al.*, 2004). Therefore, FlhF may function together with FlhG in the same manner with FtsY/Ffh system to locate flagellar components, possibly the MS-ring protein FliF, to the cell pole. The direct interaction between FlhF and FlhG has been suggested (Kusumoto *et al.*, 2008). A recently reported crystal structure of FlhF from *Bacillus subtilis* revealed a dimer formation of FlhF and significant structural similarity of FlhF to FtsY/Ffh, supporting the idea described above (Bange *et al.*, 2007). However, many features of the polar localization mechanism remain unknown.

1.4. Regulation of rotation

Most flagellar motors are reversible rotary machines, able to rotate both clockwise (CW) and counterclockwise (CCW) (Silverman and Simon, 1974). Rotational switching completes very quickly, within only 1 ms

(Kudo *et al.*, 1990). Rotational direction is controlled by environmental stimuli, such as pH, temperature, and chemicals like sugars and amino acids. Methyl-accepting chemotaxis proteins (MCPs) sense these stimuli and transmit signals to the motor through a two-component phosphorelay signaling cascade (Fig. 2.5). When a repellent signal is sensed by the MCP, autophosphorylation activity of the CheA protein, associated with MCP on the cytoplasmic side, is activated and a histidine residue of CheA is phosphorylated. Then this phospho group is transferred to the Asp residue of the response regulator CheY. Phosphorylated CheY protein (CheY-P) then associated with the motor to trigger CW rotation. On the other hand, when an attractant signal is sensed by the MCP, autophosphorylation activity of CheA is repressed, so that the level of CheY-P decreases and the motor rotates in its default direction, CCW. The molecular mechanisms of MCP function and two-component signaling are reviewed elsewhere (Armitage, 1999; Parkinson *et al.*, 2005).

The target of CheY-P in the motor is the switch complex, composed of FliG, FliM, and FliN. As described above, FliG/FliM/FliN complex is also called ''the switch complex'' because mutations in these proteins cause defects in switching the CCW/CW rotation in response to tactic stimuli. FliM functions most directly in regulation of the switching frequency by binding to CheY-P (Welch *et al.*, 1993). This binding of CheY-P to FliM probably changes the FliG–FliM interaction, and causes movement of the C-terminal domain of FliG ($FliG_C$) that interacts with the stator protein MotA, thereby altering the rotor–stator interface to switch the direction of rotary motion.

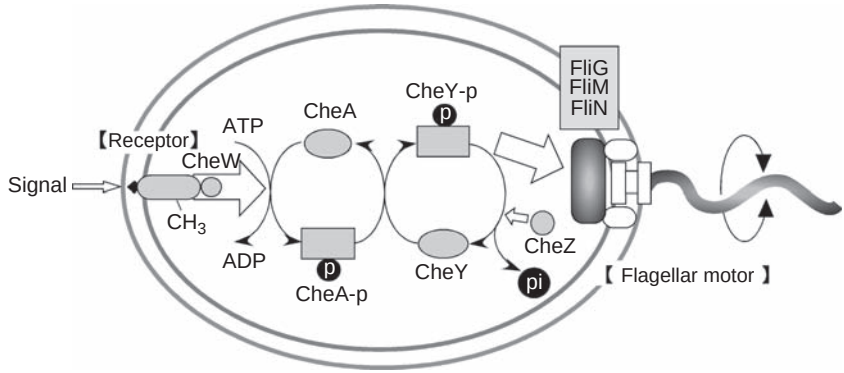

Figure 2.5 Schematic diagram of signal transduction of *Escherichia coli* chemotaxis. The chemoreceptors are embedded in the cytoplasmic membrane and localized at a pole. Chemotaxis substances or ligands bind to the receptor and the signals are transmitted into a cell and are transferred through the two-component phosphorelay system via the Che proteins. The phosphorylated CheY can bind to FliM and the direction of the motor rotation is changed.

Studies of intracellular level of CheY-P in a single cell that causes switching from CCW to CW revealed that switching is a highly cooperative event, showing a Hill coefficient of about 10, suggesting that chemotactic signal is amplified within the switch (Cluzel *et al.*, 2000). Fluorescence resonance energy transfer-based observation of CheY interaction with FliM by using CFP-FliM and CheY-YFP showed that binding of CheY-P to FliM is much less cooperative than motor switching (Hill coefficient of 1.7 ± 0.3) (Sourjik and Berg, 2002). This result was further supported by *in vitro* biochemical studies showing that CheY-P binding to the isolated intact switch complex was not cooperative (Hill coefficient is around 1) (Sagi *et al.*, 2003). These results indicate that the chemotactic signal is amplified within the switch, but subsequent to the CheY-P binding to FliM.

Some bacteria respond to tactic stimuli using modes, other than directional switching. *Rhodobacter sphaeroides* has a unidirectional flagellar motor that alternates between CW rotation and brief stops, during which the bacterium is reoriented by Brownian motion and changes in flagellar filament morphology (Armitage and Macnab, 1987). In the case of *Sinorhizobium meliloti*, the motor also rotates unidirectionally in the CW direction and swimming cells respond to tactic stimuli by modulating the flagellar rotary speed (Schmitt, 2002). The marine bacterium *V. alginolyticus* has dual flagellar systems, Na^+-driven polar flagellum (Pof) and H^+-driven lateral flagella (Laf), and their switching modes are different: the Laf motor rotates unidirectionally in CCW and responds to tactic signals by slowing down, whereas the Pof motor turns in both directions (Kojima *et al.*, 2007). In each case described, tactic signals are transmitted through the two-component signaling pathway, and CheY-P association to the motor modulates rotation.

2. Basal Structure of Flagella as Motor

2.1. Basal body

Structural features and the components of the basal body are described in Section 1.1. The supramolecular complex of the basal body is constructed by 7 kinds of proteins and ~130 molecules in total are assembled (Macnab, 2003). Aizawa *et al.* (1985) established a method to isolate the basal body of *Salmonella* with high yield and purity. Using this method, but greatly modified to allow C-ring isolation, the structure of the flagellar basal body and C ring of *Salmonella* had been investigated by the single particle analysis using negatively stained- or cryo-electron microscopy (Francis *et al.*, 1994). A resolution was obtained at 20 Å that is used for building the three-dimensional reconstitution

of images (Suzuki *et al.*, 2004; Thomas *et al.*, 2001, 2006). The flagellar basal body has a rotational symmetry with its axis in the center of the rod. The center of the rod is a hollow tube and the flagellar components required for axial structure are exported through this tube. The detailed single particle analysis of the MS ring revealed an interface between the MS ring and rod (Suzuki *et al.*, 2004). The MS ring looks like a cylinder mounted on two disks. Suzuki *et al.* (2004) reported that the MS-ring structure can be divided into five domains (C, P, S, M, and R), and discussed functions of each domain. The near-axial C and P domains are involved in the protein export and thought to change its conformation by the association with the export apparatus and open a channel through the protein. The C domain associates with the most proximal side of the rod and thereby the rod begins its assembly on the C domain. Although the S and M domains form the two disks characteristic of the MS ring, their functions are not clear. The R domain that forms cylinder-like part attaches to the outer face of the rod. It was speculated that the interaction between the rod and R domain is important for the rod–MS ring junction to release the twisting stress and symmetry mismatch. Thomas *et al.* (2006) has greatly improved resolution of images, by classifying particles according to size and applying the averaging procedures appropriate for each symmetry class. This improvement allows us to see for the first time the detailed feature of the C ring, not just a dumbbell-like structure. Their images revealed that the symmetry of individual M rings varies from 24-fold to 26-folds, whereas that of the C rings varies from 32-fold to 36-fold, with no apparent correlations between the symmetries of the two rings. The resolution of these improved EM images is now good enough to allow the crystal structures solved for the C-ring components to be docked into the map. The LP ring is an extraordinarily rigid structure and can maintain the ring morphology even under stringent condition such as 7.5 M urea (Akiba *et al.*, 1991). Single particle analysis revealed that the P ring looks like a dumbbell and seems to contact with a part of the rod, whereas the L ring seems not to contact the rod (Stallmeyer *et al.*, 1989).

MotX and MotY, which are required for the rotation of the polar flagellar motor of *V. alginolyticus*, are associated with the basal body and form an additional ring structure beneath the LP ring, termed T ring (Terashima *et al.*, 2006). Partial T-ring structures were observed in the Δ*motX* strain but not in the Δ*motY* and Δ*motX*Δ*motY* strains, suggesting that MotX associates with the basal body via MotY to form a complete T-ring structure. Stoichiometry of the MotX and MotY proteins in the T ring has not been determined yet. Further detailed observations of the T ring to reconstruct the three-dimensional images will be informative to understand their function.

2.2. Export apparatus

Most of the flagellar substructures are constructed beyond the cytoplasmic membrane. Therefore, protein components, synthesized in the cytoplasm, must be exported across the inner and outer membranes to be assembled at the appropriate final destinations. This is achieved by the flagellum-specific export apparatus that resides inside the MS-ring structure (Macnab, 2004). This system has a character in common with the needle complex that works for the secretion of virulence factors by pathogenic bacteria (Cornelis, 2006). Morphology of these two secretion machineries is quite similar to each other, and they are now classified in the type III export pathway (Hueck, 1998). The flagellum-specific export apparatus exports protein substrate in order without signal peptide cleavage. Most of the studies for the export apparatus have been carried out in *Salmonella*, and here we describe its general overview.

The core of the export apparatus is composed of six transmembrane proteins, FlhA, FlhB, FliO, FliP, FliQ, and FliR, that form an export channel complex inside the MS-ring structure. Three cytosolic proteins FliH, FliI, and FliJ are required for flagellum-specific export and interact with the channel, thereby contributing a part of the export apparatus. Recent study revealed that flagellar C-ring protein FliN is also involved in the export, so it is a part of the apparatus (Brown *et al.*, 2005; Gonzalez-Pedrajo *et al.*, 2006; McMurry *et al.*, 2006; Paul *et al.*, 2006). FlhA and FlhB have a large cytoplasmic domain at their C-termini, where soluble components interact with. The export apparatus (or a part of it) has been visualized as a protrusion inside the C ring, by the freeze-fracture image (Katayama *et al.*, 1996). However, only FliP and FliR have been detected in the basal body preparations so far (Fan *et al.*, 1997). FliI is an ATPase and its sequence shows similarity to the β subunit of the F_OF_1-ATPase, a rotary motor that drives chemical reaction of ATP synthesis (Fan and Macnab, 1996). Recently, crystal structure of FliI is solved at 2.4 Å, and revealed that its similarity is not only in the sequence (29% identity) but also in the structural level (Imada *et al.*, 2007). FliI is a member of the Walker-type ATPase family, and it is thought to form a ring-shaped hexamer for protein export (Claret *et al.*, 2003; Minamino *et al.*, 2006). These lines of evidence lead to an attractive model that FliI hexamer functions as a motor, unfolding and threading export substrates thought its central channel by cooperative conformational changes of subunits, just as speculated for AAA ATPase complexes. ATPase activity of FliI is negatively regulated by binding to FliH, in a complex of $FliH_2FliI_1$ stoichiometry (Minamino and Macnab, 2000a). FliH also binds to the hydrophobic patch of FliN, and their interaction would mediate efficient localization of FliI near the C-ring complex. FliJ is a general chaperone, preventing aggregation of export substrates presumably by interacting with them (Fraser *et al.*, 2003;

Minamino *et al.*, 2000a). Interactions among export components have been investigated by far-western method (affinity blotting), and it was found that cytosolic components interact with each other and probably forming FliH/FliI/FliJ complex in some point, and the cytoplasmic domain of membrane components FlhA and FlhB interacts with all soluble components (Minamino and Macnab, 2000b). Affinity blotting experiments also indicate that cytoplasmic domain of FlhA and FlhB interact with substrates, suggesting that these two proteins are involved in protein translocation. From these results, the outline of export is emerging: protein substrate is captured by FliH/FliI/FliJ complex without denaturation and transferred to the export apparatus. In the same time, FliI docks to the cytoplasmic face of the apparatus, forming hexameric ring structure that has an enhanced ATPase activity released from FliH inhibition. Then the substrates are exported through a central channel of apparatus, probably formed mainly by transmembrane segments (TMs) of FlhA and FlhB. After crossing the inner membrane, substrates are assembled at the appropriate position in ordered fashion, from the innermost structure to the external ones.

How is this ordered export achieved? As discussed in Section 1.2, coupling of flagellar gene expression to the stages of flagellar assembly makes it possible for the ordered export. But there is one more mechanism operating in the flagellum-specific export apparatus: the substrate-specificity switching (Kutsukake *et al.*, 1994). The apparatus has two export substrate-specificity states, the rod/hook type and the filament type (Minamino and Macnab, 1999). Therefore, proteins forming the rod and hook structures are exported prior to the proteins required for filament formation. When the hook structure reaches a certain length (ca 55 nm), FliK and FlhB sense this state, and the substrate specificity of the apparatus switches from the rod/hook type to the filament type, causing the export of a new substrate class (Ferris and Minamino, 2006; Moriya *et al.*, 2006; Shibata *et al.*, 2007; Waters *et al.*, 2007). In addition, this switching leads to FlgM export, followed by expression of the class 3 operons (Hughes *et al.*, 1993; Kutsukake, 1994). It is reported that this switching is irreversible (Minamino *et al.*, 1999).

2.3. Switch complex

The switch complex functions in the rotation/switching/assembly of the flagellum and is composed of the three kinds of proteins, FliG, FliM, and FliN (Fig. 2.6). Null mutants of each protein exhibit Fla^- phenotype (non-flagellate), and point mutations give rise to Fla^-, Che^- (defective in chemotaxis), and Mot^- (defective in motility) phenotypes (Yamaguchi *et al.*, 1986a, b). Stoichiometry of the FliG, FliM, and FliN in the C ring have been reported to be 26, 34, and more than 100 copies, respectively (Francis *et al.*, 1992; Suzuki *et al.*, 2004; Thomas *et al.*, 1999). Three-dimensional

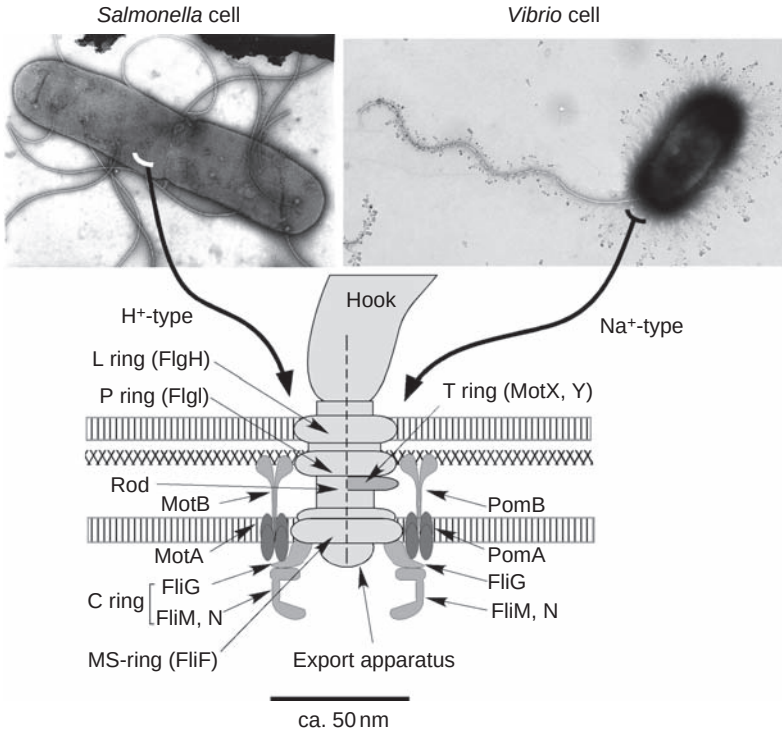

Figure 2.6 Cell body and flagellar basal structure of the proton- and sodium-driven type. The components emphasized by darker drawing are essential components for torque generation. The stator of flagellar motor consists of MotA and MotB of H^+-driven motor in *Escherichia coli* and of PomA and PomB of Na^+-driven motor in *Vibrio alginolyticus*. For the Na^+-driven motor, additional components of MotX and MotY, which form a T ring in the basal body, are also essential. Ion flow through MotAB or PomAB complex is believed to be coupled with torque generation by the interaction between the stator component of MotA or PomA and the rotor component of FliG. Electron micrograph of osmotically shocked *Salmonella* cell to visualize flagellar base is shown in left photograph. The flagellum of *V. alginolyticus* cell is observed and visualized by the electron microscopy in right photograph.

reconstructions from electron cryomicrographs of the rotor revealed that the C ring displays ~34-fold symmetry and the MS ring shows about 25-fold symmetry (Thomas *et al.*, 2006), and confirmed that most of the C-ring structure was composed of FliM and FliN. It was known that the FliF binds to FliG, and N-terminal 46 residues of FliG are required for the binding (Oosawa *et al.*, 1994). Recent studies revealed more detailed FliG–FliM interactions, and it will be discussed later (Brown *et al.*, 2007). In addition, spontaneous mutants of FliF–FliG fusion were found to be functional (Francis *et al.*, 1992). Therefore, the FliF:FliG ratio should be 1:1, and it is

consistent with FliG stoichiometry in C ring and the symmetry of MS ring as described earlier. By direct comparison of the ring structure made of FliF and FliF–FliG fusion protein obtained by electron cryomicroscopy and single-particle image revealed that a part of the FliG occupies the outer rim and face of the M ring, whereas the remaining part is likely a part of the C ring (Suzuki *et al.*, 2004). FliM interacts with FliG and FliN but not with FliF, and FliN does not interact with FliF (Oosawa *et al.*, 1994). Therefore, FliM and FliN are probably located at the central and bottom position of the C ring, respectively.

Structural studies of the switch proteins have been undertaken by using the thermophilic bacteria *Thermotoga maritima* as a protein source, and crystal structures of the functional domains have been determined (Fig. 2.7). For FliG, middle and C-terminal domains of the protein (residues 104–335, termed $FliG_{MC}$) correspond to two-third of the full-length protein (Brown *et al.*, 2002; Lloyd *et al.*, 1999). The middle domain (residues 115–190, termed $FliG_M$) has a conserved surface patch formed by the residues $EHPQ_{125–128}$ and R_{160} (the EHPQR motif), which is important for binding to FliM (Brown *et al.*, 2007). The $FliG_C$ (residues 198–335) has a conserved surface hydrophobic patch, which is also important for the binding to FliM (Brown *et al.*, 2007). A region near the C-terminus has five well-conserved charged residues that interact with those in the stator protein MotA, and electrostatic interaction of these charged residues at the rotor–stator interface is important for torque generation (Lloyd and Blair, 1997; Zhou *et al.*, 1998a). Structure showed that charged residues of FliG are clustered on the prominent ridge of $FliG_C$ where two subsets of the charged residues are aligned as a ''V''-like shape. $FliG_M$ is connected to the $FliG_C$ by an α-helix and short linker including well-conserved two consecutive Gly residues (termed Gly–Gly motif). This Gly–Gly motif seems to be involved in the motion of both domains, acting as a flexible hinge mediating relative movements of two connecting domains. These structural features of FliG suggest that FliG is likely to have two orientations that bring different subset of charged residues into alignment around the edge of the rotor, where they could interact sequentially with charged residues of the stator protein MotA. Therefore, such an arrangement of charged residues may be important for the switching of the rotational direction. Yeast two-hybrid method was used to investigate the interaction between switch proteins, and revealed two distinct binding sites for FliM in FliG: the EHPQR motif of the $FliG_M$ and the hydrophobic patch of the $FliG_C$ (Marykwas *et al.*, 1996). Consistent with this, tryptophan replacements in residues that participate in these binding sites influenced the binding to FliM and also the assembly of the flagellum (Brown *et al.*, 2007). The hydrophobic patch in $FliG_C$ is positioned adjacent to the Gly–Gly linker and opposite to charge-bearing ridge. Because the structure of the N-terminal domain has not been determined yet, it is not clear how FliG binds to FliF.

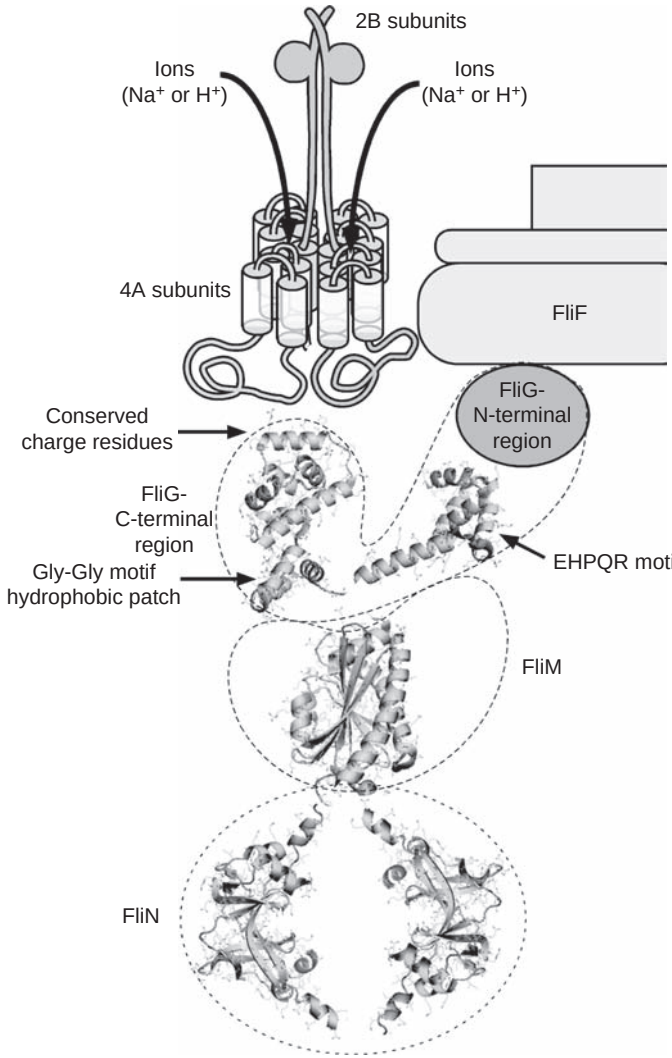

Figure 2.7 The structures of stator and rotor. The stator is formed by the $MotA_4MotB_2$ or $PomA_4PomB_2$ complex. The B subunit has a peptidoglycan-binding motif (protruded ball) and the A subunit has large cytoplasmic domain, containing the conserved charged residues important for flagellar rotation, between second and third transmembrane segments. The crystal structure of the FliG middle and the C-terminal domain, the FliM middle domain, and the two-third of FliN of *Thermatoga maritima* are shown using the PDB data, 1l kv, 2hp7, and 1yab, respectively. The C-terminal region of FliG has a ridge containing the important charged residues, which are believed to interact with the charged residues of the cytoplasmic domain of MotA, for the flagellar rotation. FliN is depicted as a homotetramer composed of dimer-of-dimers. FliG, FliM, and FliN form a switch complex. FliF forms the MS ring of the basal body.

However, as noted above, since FliF–FliG fusion protein is functional, the C-terminal end of FliF and N-terminal end of FliG are likely to be in proximity.

Crystal structure of the middle domain of FliM (residues 44–226, termed $FliM_M$) from *T. maritima*, which corresponds to two-third of the full-length protein, has been determined (Park *et al.*, 2006) (Fig. 2.7). FliM is involved in changing of the rotational direction triggered by the binding of CheY-P to FliM, a chemotactic signaling molecule (Sockett *et al.*, 1992; Welch *et al.*, 1993). The phosphorylation state of CheY is regulated by a kinase (CheA) and phosphatase (CheZ, CheC, or CheX), which are involved in chemotactic signaling pathway (Parkinson, 2003). The structure of FliM reveals structural similarity to these phosphatases. Disulfide cross-linking experiments using Cys-substituted FliM variants designed by using the structural information revealed the interface of FliM protein responsible for its self-association in the C-ring structure. Based on this arrangement of FliM subunits, about 33–35 copies of FliM subunits form a ring with a diameter of ~44 nm, consistent with its rotational symmetry (34-fold) in the C ring observed in electron cryomicroscopy (Thomas *et al.*, 2006, 1999). CheY-P binds to N-terminal portion of FliM, which is not present in the structure. Truncation of the N-terminal 43 residues is required for crystal growth of $FliM_M$. It is probably disordered when extracted from the C-ring structure. On the other hand, crystal structure of CheY protein in complex with FliM peptide including N-terminal 16 residues has been reported (Dyer and Dahlquist, 2006; Lee *et al.*, 2001). The CheY-FliM peptide structure revealed the allosteric communication between the phosphorylation site and the target-binding surface of CheY protein. The C-terminal part of FliM has been shown to be important for the binding to FliN (Marykwas *et al.*, 1996). A GGXG motif involved in the interaction with FliG exists in the opposite side of the FliN-binding region (Mathews *et al.*, 1998; Tang *et al.*, 1996; Toker and Macnab, 1997). However, weak electron density in this region discerns only the first two glycine residues.

The structure of FliN corresponding to the two-third of full-length protein (residues 68–154) from *T. maritima* (Brown *et al.*, 2005) has been determined. FliN, that mostly contributes to form the C-ring structure, is found to be a tightly intertwisted dimer composed mostly of β-sheet (Fig. 2.7). Structure also revealed a hydrophobic patch, formed by several well-conserved hydrophobic residues, on the surface of the FliN dimer. Mutations in these residues in the patch give rise to Fla^- or Che^- phenotype, indicating that it is important for the flagellar assembly and the switching. Motility of these mutants is partially restored by the overexpression of FliI and FliH (Paul *et al.*, 2006), soluble components of export apparatus, suggesting that FliN is involved in the secretion of flagellar proteins. This is not surprising, since a temperature-sensitive FliN mutant was unable to regrow flagellar filament after shearing it at the restrictive temperature

(Vogler *et al.*, 1991). FliN has been known to involve the export of filament subunits or capping proteins. In addition, FliN has a homology to the export apparatus for virulence factors of pathogenic bacteria (Tang *et al.*, 1995). Therefore, although FliN is involved in switching and motility, it is more directly involved in flagellar assembly, probably as a part of flagellum-specific export apparatus. Consistent with this idea, recent biochemical studies showed that FliN associates with FliH (McMurry *et al.*, 2006; Paul *et al.*, 2006), and a five-protein complex consisting of FliG, FliM, FliN, FliH, and FliI can be isolated (Gonzalez-Pedrajo *et al.*, 2006). These lines of evidence suggest that FliN in C ring provides a docking site for export substrate via FliH to efficiently deliver them to the apparatus, and FliN–FliH interaction involves the hydrophobic patch of FliN. Contribution of FliN to the rotational switching is also involved in the hydrophobic patch. Mutations giving Che^- phenotype are mapped around the hydrophobic patch, and defects could be partially rescued by overexpression of the CheY, suggesting that FliN may contribute to the binding site of CheY-P (Paul *et al.*, 2006). As describe earlier, FliN occupies most part of the C ring, and it is located at the bottom of the ring. Analytical ultracentrifugation of purified FliN of *T. maritima* showed that the FliN exists as a dimer in solution, and FliM and FliN together form the stable $FliM_1/FliN_4$ complex (Brown *et al.*, 2005). *E. coli* FliN exists as a stable homotetramer in solution. These results are consistent with the stoichiometry of FliM to FliN in the C ring. Targeted disulfide cross-linking studies of FliN suggested that FliN is organized in doughnut-shaped tetramers, whose shape is closely matched for the bottom of C ring in the reconstructed electron microscopic image (Paul and Blair, 2006).

2.4. Motor complex

The MotA/MotB or PomA/PomB complex that acts as the torque-generating unit exists in the cytoplasmic membrane and assembles around the rotor (Kojima and Blair, 2004a; Yorimitsu and Homma, 2001). MotA and MotB form the torque-generating unit of the H^+-driven flagellar motor, whereas PomA and PomB form that of the Na^+-driven flagellar motor of *Vibrio* spp. and are orthologues of MotA and MotB (Asai *et al.*, 1997; Dean *et al.*, 1984; Stader *et al.*, 1986) (Figs. 2.7 and 2.8). MotA and PomA have four TMs (Asai *et al.*, 1997; Zhou *et al.*, 1995). A large cytoplasmic loop between the second and third TMs contains conserved charged residues that have been shown to interact with the conserved charged residues in the rotor protein FliG, and their electrostatic interactions are important for torque generation (discussed also in Section 3.1; Lloyd and Blair, 1997; Zhou and Blair, 1997; Zhou *et al.*, 1998a) (Fig. 2.8). On the other hand, periplasmic loops between first and second TMs (loop1–2) and third and fourth TMs (loop3–4) are very short. MotB and

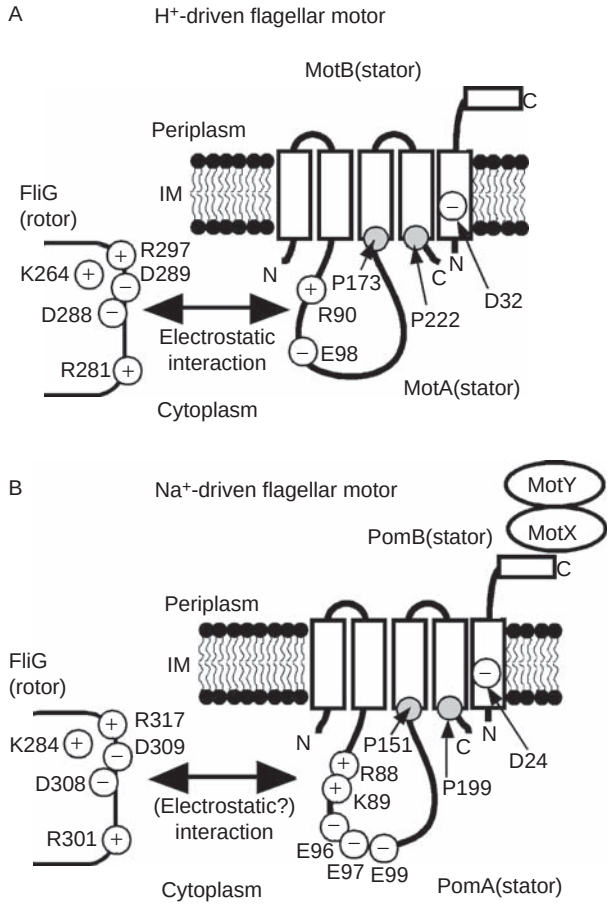

Figure 2.8 **Charged residues of the putative interaction surface between stator and rotor. The *Vibrio alginolyticus* PomA R88 and E96 correspond to R90 and E98 of the *Escherichia coli* MotA, and K284, R301, D308, D309, and R317 of *V. alginolyticus* FliG correspond to K264, R281, D288, D289, and R297 of *E. coli* FliG, respectively. The aspartic acid residue in B subunit (D32 in MotB and D24 in PomB) is believed to be an ion-binding site.**

PomB have a single TM at its N-terminus (Asai *et al*., 1997; Chun and Parkinson, 1988). This TM contains an absolutely conserved negatively charged residue (Asp32 in MotB of *E. coli* and Asp24 in PomB of *V. alginolyticus*), which is critical for motor rotation and predicted to be the ion-binding site in the stator complex (Zhou *et al*., 1998b). Most of MotB and PomB proteins are located in the periplasmic space. C-terminal portions of MotB and PomB contain the putative peptidoglycan-binding (PGB) motif that is well conserved among proteins such as OmpA and Pal,

which are outer membrane proteins that interact with the peptidoglycan layer noncovalently (De Mot and Vanderleyden, 1994; Koebnik, 1995). The MotA/MotB and PomA/PomB complexes are also called the stator, the nonrotating part of the motor. The stator complex forms a heterohexamer composed of four A subunits (MotA or PomA) and two B subunits (MotB or PomB) (Kojima and Blair, 2004b; Sato and Homma, 2000a,b; Yorimitsu *et al.*, 2004). The MotA/MotB stator functions as a H^+ channel and the PomA/PomB stator functions as an Na^+ channel (Blair and Berg, 1990; Sato and Homma, 2000a; Stolz and Berg, 1991).

Although structural information is critical to understand the mechanism for torque generation, currently there are no high-resolution structural data on the stator complex because its strongly hydrophobic nature hinders to obtain crystals. Instead, arrangements of the TMs of MotA and MotB from *E. coli* (18 segments total in a complex) have been investigated by systematic disulfide cross-linking studies. The results uncovered initial picture of the MotA/MotB stator complex: a symmetric dimer of MotB segments is at the center of the complex, and TMs of four MotA molecules are arranged around the MotB dimer (Braun and Blair, 2001; Braun *et al.*, 2004). Cys residues introduced in the third and fourth TMs (TM3 and TM4) of MotA can form disulfide bridges between those introduced in the single TM of MotB that contains the proton-accepting Asp residue, suggesting that proton-conducting channel is formed by these three segments. Arrangement of the MotB dimer that fits to the cross-linking results revealed that the critical Asp32 residues of two MotB molecules are positioned on the separate surface of the MotB dimer, so possibly there exist two proton-conducting channels in a $MotA_4/MotB_2$ stator complex. This arrangement seems to fit into the PomA/PomB Na^+-conducting stator complex: the TM3 of PomA positions very near the TM of PomB (Yakushi *et al.*, 2004). Phenamil, a potent inhibitor for eukaryotic epithelial sodium channel, also specifically inhibits the rotation of Na^+-driven motor (Atsumi *et al.*, 1990). Mutations that allow motor to rotate in the presence of phenamil (Kojima *et al.*, 1997) were mapped near the cytoplasmic face of the TM3 of PomA (D148Y) and TM of PomB (P16S) (Jaques *et al.*, 1999; Kojima *et al.*, 1999), and when replaced to Cys, these two residues can form a disulfide bridge (Yakushi *et al.*, 2004). These results suggest that residues in TM3 of PomA and TM of PomB (including critical Asp24) may participate in forming an Na^+-binding site near the cytoplasmic face. Systematic Cys replacement of the residues located in the periplasmic loops of PomA revealed that Pro172, which locate in the loop3–4, forms cross-linked dimer under the oxidation condition, so loop3–4 of two PomA molecules are positioned side by side in a PomA/PomB complex (Yorimitsu *et al.*, 2000).

The number of the stator complexes assembled around the rotor was measured by various methods. The stepwise increase of the rotation speed that was dependent on the expression of the stator proteins (Blair and Berg,

1988; Block and Berg, 1984) and the fluorescence intensity change of green fluorescent protein (GFP)-MotB measured by fluorescence recovery after photobleaching (FRAP) method indicate that at least 11 stator complexes are estimated in a single motor (Leake *et al.*, 2006; Reid *et al.*, 2006). The electron cryotomography of whole cells of *Treponema primitia* showed *in situ* structure of the complete flagellar motor at the 7 nm resolution (Murphy *et al.*, 2006). The image indicates that the stator assembly possessed 16-fold rotational symmetry, within the range of the stator number described above. Recently, the purified PomA/PomB complexes reconstituted into the proteoliposome have been observed by cryo-electron microscopy and rough image of stator was reported (Yonekura *et al.*, 2006). Rod-shaped objects protruded out from both sides of the lipid bilayer. Its diameter was ~20 Å, and length of a longer rod and a shorter rod were ~70 and 35 Å, respectively. The PomA/PomB complex with truncated C-terminus of PomB, which lacks PGB motif, was also observed, and the longer rod is found to be the C-terminal domain that contains the PGB motif.

3. Torque Generation

In this chapter, we overview the current knowledge of the mechanism of torque generation, based on genetic and biochemical studies. Many hypotheses of torque generation have been proposed, and were extensively reviewed elsewhere (Berg, 2003; Kojima and Blair, 2004a). It is noteworthy that some interesting motor models were recently published (Schmitt, 2003; Xing *et al.*, 2006).

3.1. Interaction between stator and rotor

It is believed that the rotational force of the flagellar motor is generated by the interaction between the cytoplasmic loop region of the stator component, MotA or PomA, and the C-terminal domain of the rotor component, FliG. The rotor–stator interaction is coupled to the H^+ or Na^+ flow through the stator powered by the electrochemical gradient across the cytoplasmic membrane. Domains of MotA (or PomA) and FliG responsible for the rotor–stator interaction contain the conserved charged residues important for the torque generation (Fig. 2.8) (Lloyd and Blair, 1997; Yorimitsu *et al.*, 2002; Zhou and Blair, 1997). In *E. coli* motor, they were Arg90 and Glu98 of MotA, and Lys264, Arg281, Asp288, Asp289, and Arg297 of FliG (Fig. 2.8A). No single residue is critical for rotation, but they function collectively. Charge neutralization or inversion of these residues disrupts motor rotation, but certain combinations of MotA mutations with FliG mutations show strong synergism (e.g., MotA-R90A and

FliG R281A) or suppression (e.g., MotA-R90E and FliG D289K), which suggests that the charged residues of MotA interact with those of FliG (Zhou *et al.*, 1998a). Therefore, such electrostatic interactions between rotor and stator are important for the torque generation. As discussed in Section 2.3, crystal structure of the $FliG_C$ revealed that these charged residues are clustered on the prominent ridge of the $FliG_C$, where two subsets of the charged residues (R281/D288/K264 and R281/D289/R297) are aligned as a ''V''-like shape (Lloyd *et al.*, 1999). Structure and genetic evidence lead to the rotational switching model that switching may result from distinct combination of electrostatic interactions between rotor and stator.

In the case of Na^+-driven motor of *V. alginolyticus*, these charged residues are also conserved in PomA and FliG (R88 and E96 of PomA and K284, R301, D308, D309, and R317 of FliG) (Fig. 2.8B). However, when these residues and neighboring additional three charges (K89, E97, and E99) of PomA were all neutralized, PomA was still functional (Yorimitsu *et al.*, 2002). Likewise, single or all possible combinations of charge-neutralizing mutations in five conserved charged residues did not affect the motility. Inversion of charge in PomA or FliG barely gave nonmotile or slow-motile phenotype (Yorimitsu *et al.*, 2002, 2003). These results suggest that Na^+-driven motor may require additional charged residues in PomA and/or FliG for complete electrostatic interaction(s). Alternatively, electrostatic interaction between rotor and stator are not important for the torque generation in *V. alginolyticus*. It was found that chimeric FliG protein consisting of the N-terminal two-third from *V. alginolyticus* and the C-terminal one-third from *E. coli* (termed $FliG^{VE}$) is functional in the *fliG* strain of *V. alginolyticus*, and its opposite variant of chimeric protein (N-terminal two-third from *E. coli* and C-terminal one-third from *V. alginolyticus*; $FliG^{EV}$) is functional in the *fliG* strain of *E. coli* (Yorimitsu *et al.*, 2003). Likewise, the MotA/MotB stator from *E. coli* is functional in the Δ*pomAB* strain of *V. alginolyticus* and its motor is driven by proton motive force (PMF) (Asai *et al.*, 2003). Chimeric protein PotB, consisted of the N-terminal TM of PomB from *V. alginolyticus* and the C-terminal periplasmic segment from *E. coli* MotB, is functional in the Δ*motAB* strain of *E. coli*, whose motor is driven by sodium motive force (Asai *et al.*, 2003) (Fig. 2.9A). These results indicate that certain parts of the motor responsible for rotation can be interchangeable between species, and general mechanism of the motor rotation is quite similar regardless of the coupling ion. To understand the role of charged residues in *V. alginolyticus* for motor rotation, conserved charged residues of *V. alginolyticus* with or without mutations were introduced into the hybrid *E. coli* motor composed of chimeric rotor ($FliG^{EV}$) and stator proteins (PomA/PotB), and Na^+-driven motility of the cells containing these motor proteins were investigated (Yakushi *et al.*, 2006). It was revealed that the charged residues in the

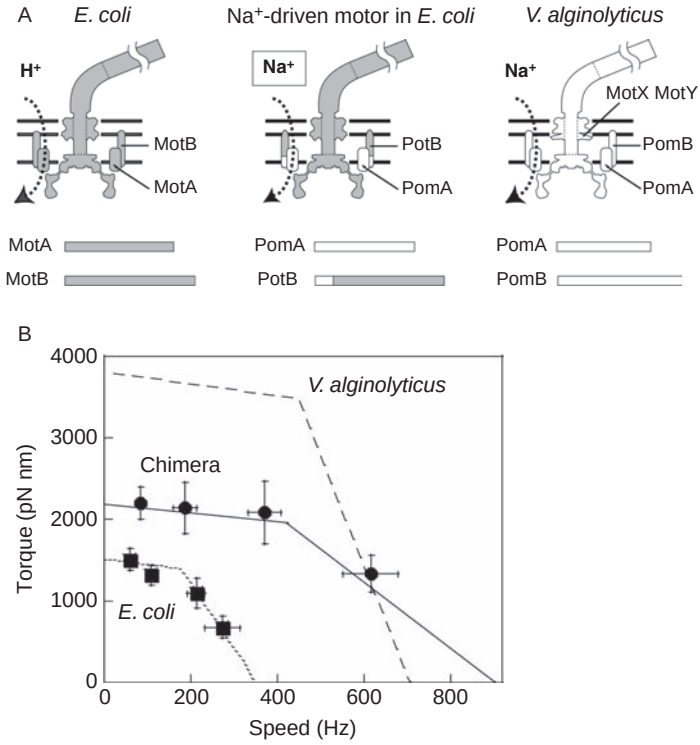

Figure 2.9 Hybrid and chimeric motors with the Na^+- and the H^+-driven components. (A) The gray and the open part show the regions of the H^+- (MotA or MotB) and the Na^+-driven components (PomA or PomB), respectively. The horizontal lines show the outer membrane, peptidoglycan layer, and the cytoplasmic membrane. (B) The torque–speed relationships of different flagellar motors. Measured speeds and estimated torques of chimeric motors are represented by circles, the H^+-driven *Escherichia coli* motor (squares) using filament drag coefficients (Inoue *et al.*, 2008). Dotted and dashed line are reported torque–speed relationships for H^+-driven *E. coli* motor (Chen and Berg, 2000b) and Na^+-driven *Vibrio alginolyticus* motor (Sowa *et al.*, 2003), respectively.

V. alginolyticus rotor and stator proteins were found to require for motor rotation when they were engineered in the *E. coli* motor, although the synergism and suppression in rotor–stator double mutants were weaker than those seen in *E. coli*. Therefore, basically rotor–stator interaction occurs in the *V. alginolyticus* motor in the same way as in *E. coli*, but the rotor–stator interface is more robust in *V. alginolyticus*. Additional charged residues of PomA may contribute such robustness (Obara *et al.*, 2008), but other factors, probably MotX and MotY, may enhance the motor function in *V. alginoltyticus*. The flagellar motor of *S. meliloti* rotates only CW direction, and its speed was modulated by the tactic stimuli (Gotz and Schmitt, 1987; Schmitt, 2002). Like *E. coli* and *V. alginolyticus*, electrostatic interactions

between conserved charged residues in rotor (R294 and E302 of FliG) and stator (R90, E98, and E150 of MotA) of *Sinorhizobium* are important for torque generation. Initially, it was expected that different charge distribution at the rotor–stator interface, due to the absence of several conserved charged residues in FliG (only two are conserved), might be the basis for the different modes of motor rotation. However, mutational analyses revealed that unlike *E. coli*, E150 is essential for torque generation, whereas R90 and E98 are crucial for chemotaxis-controlled modulation of rotation speed (Attmannspacher *et al.*, 2005). Therefore, it was proposed that MotA E150 interacts with FliG R294 to achieve fast rotation, but conformational changes in FliG triggered by CheY-P binding to FliM lead to the a new rotor–stator alignment that places E150 of MotA adjacent to D302 of FliG, so that electric repulsion between them might result in lower torque and slower rotation.

Biochemical analysis of the interaction between stator and rotor has not proceeded as compared to the genetic analysis. Only a study has been reported so far that demonstrated MotA–FliG or MotA–FliM interactions by pull-down assay (Tang *et al.*, 1996). Then what is the nature of torque generation? Although the structure of the stator complex has not been solved and physical property of the stator complex have been still unclear, systematic mutational studies indicated that MotB Asp32 of *E. coli*, which exists in the single TM of MotB, is the only protonatable residue in the motor proteins responsible for the flagellar rotation, suggesting that protonation of this critical aspartate in the stator complex triggers conformational changes in the stator complex that drive rotor (Zhou *et al.*, 1998b). To test this idea, protease susceptibility of MotA in complex with MotB was examined, and it was revealed that replacement of the critical aspartate (Asp32) of MotB to asparagine or any other small neutral amino acid caused a conformational change in MotA, that could be detected as a change of protease susceptibility (Kojima and Blair, 2001). MotA conformation is also restricted by the well-conserved prolines located at the cytoplasmic face of TM3 and 4 (Pro173 and Pro222 in *E. coli*). In a way that disrupts α-helix, forming β-turn, proline greatly affects secondary and tertiary structures of the protein. Mutations in Pro173 and Pro222 abolished or severely impaired motility, and mutant proteins exhibit strong dominant-negative effect on motility. Therefore, these residues might regulate the conformation of the MotA/MotB complex and/or control conformational changes (Braun *et al.*, 1999; Zhou and Blair, 1997).

3.2. Ion-binding site

As discussed in Section 3.1, an ion-binding site of the stator channel has been believed to be MotB D32 in *E. coli* and PomB D24 in *V. alginolyticus* (Yorimitsu and Homma, 2001). H^+ or Na^+ associates with the negatively

charged side chain of the acidic amino acid in the stator, although pK_a of carboxyl group in these residues in the physiological condition has not been measured yet. As described in Section 3.1, when the conserved acidic or basic amino acid residues in MotA, MotB, FliG, FliM, and FliN, those of which are important for torque generation, were replaced to Ala, all the mutants except D32A of MotB still retained motility (Zhou *et al.*, 1998b). Replacement of Asp at position 32 of MotB to various amino acids showed that all but glutamate at that position were nonfunctional. Therefore, D32 of MotB is likely to serve as the proton-binding site in the stator complex. Likewise, PomB D24 probably functions as the binding site for Na^+. It is noteworthy that an Na^+ binds to the functionally critical glutamate residue (E139) in the crystal of NtpK protein, the channel component of another Na^+-translocating rotary motor, V_OV_1-ATPase from *Enterococcus hirae* (Murata *et al.*, 2005). Recently determined crystal structures of Na^+-coupled transporters revealed that not a single but several side chains including backbone carbonyl group(s) participate in forming an Na^+-binding site (Hunte *et al.*, 2005; Yamashita *et al.*, 2005). Therefore, in the case of a PomA/PomB complex, there still may exist additional residues involved in formation of an Na^+-binding site, possibly including D148 of PomA and P16 of PomB, those of which affect phenamil resistance when mutated. Also, it is possible that charged residues at the channel entrance or exit or the main chain carbonyl group(s) of the hydrophobic residues lining in the channel may play important roles for the selective ion influx (Kojima *et al.*, 2000).

It has been known that cell growth and motility are still normal even if the MotA/MotB complex is overexpressed more than 50 times over the wild-type level, suggesting that overproduced complexes are inactive for proton traslocation (Wilson and Macnab, 1988, 1990). When the N-terminal 60 residues of MotB that includes its single TM was fused to the unrelated polypeptide, consisted of 50 residues encoded by a part of TetA (MotB60-TetA), its overproduction together with MotA impairs the cell growth (Stolz and Berg, 1991), and this growth impairment was abolished by the mutation in D32 of MotB (Zhou *et al.*, 1998b). These results led to the proposal that a part of the complex (possibly the periplasmic domain of MotB) blocks proton flow through the MotA/MotB channel making it inactive. This model is supported by the mutational study demonstrating that a deletion of the segment just C-terminal to the TM of MotB (Δ51–70) or substitution of the residues in that region (I58, Y61, F62, and P52/P65) causes a strong growth impairment when overproduced (Hosking *et al.*, 2006). Detailed analyses of this region brought a model that the segment (termed "plug") consists of an amphipathic α-helix and is inserted into the cell membrane parallel with its periplasmic face to interfere with channel formation. Interaction of a MotA/MotB complex with a flagellar basal body triggers movement of the plug from membrane and opening of the proton channel. Therefore, this plug may play a central role

in regulating the open-closed states of the stator channel to prevent premature proton flow.

3.3. Ion specificity

So far, two types of the motor classified by the coupling ion have been identified: the H^+-type and the Na^+-type. Most motile bacteria including *E. coli*, *S. typhimurium*, *B. subtilis*, *R. sphaeroides*, and *Pseudomonas aeruginosa* have H^+-driven motor and *V. alginolyticus* and alkalophilic *Bacillus* have Na^+-driven motor (Berry and Armitage, 1999; Doyle *et al.*, 2004; Imae and Atsumi, 1989; Yorimitsu and Homma, 2001). It seems that since *V. alginolyticus* lives in the sea where Na^+ is abundant, it may have evolved to acquire Na^+-conducting activity through the stator complex.

Which part of the stator proteins determines ion specificity? The H^+-driven stator of the *Rhodobacter sphearoides* is composed of MotA (RsMotA) and MotB (RsMotB), and RsMotA are found to be remarkably similar to the Na^+-driven stator of PomA from *V. alginolyticus* (Asai *et al.*, 1999; Shah and Sockett, 1995). Both of them are composed of 253 amino acids and their identity is more than 40% over their entire length. RsMotB has similarity only to the transmembrane region of PomB. When RsMotA was expressed in the *pomA* strain of *V. alginolyticus*, the motor was functional and driven by Na^+-motive force. On the other hand, expression of RsMotB together with RsMotA in the *pomB* strain of *V. alginolyticus*, cells are nonmotile (Asai *et al.*, 1999). Therefore, determinants of ion specificity of stator should exist in the PomB (and MotB). A series of chimeric proteins, consisting of N-terminal RsMotB and C-terminal PomB (termed MomB) (Asai *et al.*, 2000), was constructed. Some of the MomB constructs, whose entire TM was derived from RsMotB, functioned as Na^+-type stator when coexpressed with RsMotA in the Δ*pomAB* strain of *V. alginolyticus*. In this case, four proteins RsMotA, MomB, MotX, and MotY are involved in the Na^+-driven rotation. Interestingly, a MomB construct, whose junction is between F33 and V34 of PomB, functions better as Li^+-driven motor than as Na^+-driven motor. Later, it was found that a chimeric protein of PotB, a fusion of N-terminal TM of PomB and the C-terminal periplasmic segment of *E. coli* MotB, functions as an Na^+-type stator in *E. coli* only when coexpressed with PomA (Asai *et al.*, 2003). In this case, just two proteins PomA and PotB are required for Na^+-driven rotation (Fig. 2.9A). These lines of evidence indicate that cytoplasmic and transmembrane domains of PomA/PomB complex are sufficient for Na^+-driven motility, and periplasmic C-terminal part of B subunit (MotB or PomB) determines the requirement of MotX and MotY for function. Probably, the size of channel pore is varied in these chimeric stator complexes, altering the ion specificity. More precise descriptions of ion specificity in the stator will be provided by the high-resolution atomic model of the stator complex.

3.4. Assembly of functional motor

Whereas the assembly mechanism of the axial flagellar structure is now well understood (see Section 1.3), the mechanism of stator assembly is still not clear. Early experiments showed that controlled expression of *motA* or *motB* in their defective strains demonstrated stepwise restoration of the rotation rate with equal speed increment that saturated at eight steps, suggesting that eight independently functioning MotA/MotB stator units are incorporated into the wild-type motor (Blair and Berg, 1988; Block and Berg, 1984). Recent studies with higher resolution reported that as much as 11 stator units can be incorporated (Reid *et al.*, 2006). This number is in proximity to the observed particles that surround the rotor by freeze-fracture images (Khan *et al.*, 1988). MotB has a putative PGB motif that is well conserved among proteins such as OmpA and Pal, which are outer membrane proteins that interact with the peptidoglycan layer noncovalently (De Mot and Vanderleyden, 1994; Koebnik, 1995). The PGB motif of MotB is believed to associate with the peptidoglycan layer to anchor the MotA/MotB stator complex around the rotor. It is not clear how and when MotA/MotB stator complexes are targeted and anchored at the appropriate position around the rotor.

In *V. alginolyticus* and *V. parahaemolyticus*, MotX and MotY have been identified as essential components for the rotation of Na^+-driven polar flagellar motors (McCarter, 1994a,b; Okabe *et al.*, 2001; Okunishi *et al.*, 1996). As described in Section 2.1, they attach to the basal body to form a ring structure (termed T ring) that can be observed beneath the LP ring by electron microscopy (Terashima *et al.*, 2006). Biochemical studies have shown that MotX directly interacts with MotY, and affects membrane localization of the PomA/PomB complex and of the PomB alone, suggesting an interaction between MotX and PomB (Okabe *et al.*, 2005). In addition, when MotX or MotY is absent, GFP-fused PomA or GFP-fused PomB in complex with their partner subunit does not localize at the flagellated cell pole, suggesting that MotX and MotY in the T ring are involved in the incorporation of PomA/PomB complex into the flagellar motor (Terashima *et al.*, 2006). Like MotB and PomB, MotY possesses peptidoglycan-binding motif and a recently solved MotY structure showed remarkably similar structure to the Pal and RmpM (OmpA homologue), well-known peptidoglycan-binding protein (Kojima *et al.*, 2008). Detailed functions of MotX and MotY are still unclear, but they are speculated to be involved in ion specificity, or in extremely rapid rotation (1100 Hz) approximately four times faster than that of *E. coli* (300 Hz).

In *S. meliloti*, MotC and MotE have shown to be involved in the motility and regulation of the rotation speed of the flagllar motor (Eggenhofer *et al.*, 2004; Platzer *et al.*, 1997). MotC is the periplasmic protein and regulates the rotation speed by acting on MotB. MotE is the specific chaperone for MotC and controls the rotation speed indirectly by regulating amount of the

MotC proteins in periplasm. These proteins do not show similarity to MotX and MotY. In some bacteria, two kinds of stator might be assembled to a single flagellar base. *Pseudomonas aeruginosa*, which has a single polar flagellum, has dual sets of *motA* and *motB* genes, *motAB* and *motCD*, as well as another gene, *motY*. All these five genes contribute to H^+-driven motility (Doyle *et al.*, 2004). Function of MotA/MotB stator requires MotY, and these three proteins are important for the surface swarming. On the other hand, MotC/MotD does not require MotY for its function, and they are important for the swimming in liquid. Furthermore, noncognate pairs like MotA/MotD and MotB/MotC can work together to generate torque: mutants that contain *motA/motD* or *motB/motC* double mutations still retain motility. Therefore, *Pseudomonas* cells seem to choose two types of stators for motility depending on the surrounding environment (swimming or surface swarming) (Doyle *et al.*, 2004; Toutain *et al.*, 2005). Similarly, when swarming on the surface, *V. parahaemolyticus* as well as *V. alginolyticus* cells induced multiple lateral flagella that are driven by proton-type motor (Atsumi *et al.*, 1992; McCarter *et al.*, 1988). The stator for lateral flagellar motors contains LafT and LafU, orthologues of MotA and MotB, and somehow its function requires a second set of MotY, $MotY_L$ (Stewart and McCarter, 2003). The reason why $MotY_L$ is necessary for rotation of the lateral flagellar motor is not clear.

Another example is the motor of *B. subtilis*: it has an Na^+-driven MotP/MotS stator and a proton-driven MotA/MotB stator, but a single set of flagellar rotor proteins (Ito *et al.*, 2004). Like the hybrid stator of *P. aeruginosa*, hybrid stators like MotP/MotB and MotA/MotS are functional in *B. subtilis* and ion specificities of these motors depend on the B subunit (MotA/MotS for Na^+-type and MotP/MotB for H^+-type) (Ito *et al.*, 2005). These results are consistent with the observation of hybrid motors with chimeric proteins using stator proteins of *V. alginolyticus* and *R. sphaeroides*. Since cells carrying MotP/MotS and MotP/MotB stator can swim faster in liquid with high viscosity, MotP function is suggested to be important for the optimal function in elevated viscosity. In order to achieve optimal behavior in variable environments, these bacteria seem to evolve to use distinct sets of stator complexes or have additional components besides conventional stator proteins to fully exert motor rotation.

4. Molecular Physiology of Motor

4.1. Torque–speed relationship

To understand the mechanism of motor rotation, we need to know its basic properties: the power input and output, and their relationships. Measuring these properties of the motor involves technical difficulties, so

understanding of the motor physiology has been accompanied by technical development in the measurement system. Although the studies of power input for a single motor have still been hindered by such difficulties, one can measure the power output as the ''rotation'' by using a quite simple method that has been employed since the discovery of flagellar rotation. Cells are attached to a coverslip by a single flagellar filament and the rotation of each single motor is monitored by the resulting rotation of the cell body (Silverman and Simon, 1974). Such tethered cells rotate slowly (around 10 Hz) because of the large viscous load. Measurement of rotation of lightly loaded motors in swimming cells was achieved by a light scattering method under the microscope (Lowe *et al.*, 1987), and values obtained by these two measurements were used for the initial estimation of a torque–speed relationship, an essential feature that characterizes the flagellar motor. The results showed a linear relationships: that as the speed increases, the torque linearly decreases.

To cover a wide range of the speed by the measurement of a single motor, the electrorotation method was developed (Berg and Turner, 1993; Iwazawa *et al.*, 1993). In this technique, a tethered cell was spun under a rotating electric field that enabled motors to rotate up to several hundreds of Hertz. Measurement of the motor rotation has been carried out by this method, and revealed characteristic feature of the torque–speed relationships for the flagellar motor: for forward rotation, motor torque remained approximately constant up to speeds of about 60% of the zero-torque speed, then the torque dropped linearly with speed, crossed zero, and reached a minimum (Berg and Turner, 1993). In yet another approach, the cell body was fixed to the glass surface and a polystyrene bead was attached to a stub of one of its flagellar filaments (Ryu *et al.*, 2000). By using beads of different sizes and changing the viscosity of external medium, one can measure motor torque under a wide range of speeds. The results confirmed the previous measurement by electrorotation method, showing the essentially constant torque and then linear decline as the speed increases (Chen and Berg, 2000b). The latter method allows us to measure the rotation at various conditions, such as different temperatures and using D_2O instead of H_2O for the effect of solvent isotope (Chen and Berg, 2000a). The results showed that in the low-speed regime, torque was independent of temperature, and solvent isotope effects were relatively small.

In the high-speed regime, torque was strongly dependent on temperature, as seen by a downward shift in the ''knee'' value, the region of the transition from constant torque to declining torque, at lower temperature. Also, solvent isotope effects were large. These results were consistent with previous studies for artificially energized cells of *Streptococcus* (Khan and Berg, 1983; Manson *et al.*, 1980). Therefore, torque–speed relationship of the flagellar motor indicates that at low speeds, the motor operates near thermodynamic equilibrium, where rates of movement of the internal

mechanical components or translocation of protons are not rate-limiting, and that at high speeds, the rate-limiting step is proton transfer event, which results in the decline in torque at high speed. As discussed by Berry and Berg, a torque–speed relationship with this shape can be interpreted in the context of a simple three-state kinetic model and it suggests a rotation mechanism with a power stroke, in which motor rotation and dissipation of the energy available from proton transit occur synchronously (Berry and Berg, 1999). Fung and Berg (1995) found that when the motor operates in the low-speed regime near stall, its speed is proportional to the voltage applied across the inner cell membrane. Moreover, Gabel and Berg (2003) reported a linear relationship between speed (0–270 Hz) and PMF for light load on the motor. If we assume tightly coupled motor in which the translocation of a fixed number of protons drives each rotation, the linear speed–PMF relation is indicative of a simple voltage-gated proton channel.

Comparative studies have been reported for the Na^+-driven polar flagellar motor of *V. alginolyticus* (Sowa *et al.*, 2003). It has been shown that the torque–speed curve had the same shape as those of the wild-type *E. coli* motor and the hybrid motor with PomA/PotB chimeric stator in *E. coli* with full expression of the stator proteins: the torque is approximately constant (at ~2200 pN nm) from stall up to a ''knee'' speed of ~420 Hz, and then falls linearly with speed, extrapolating to zero torque at ~910 Hz (Inoue *et al.*, 2008) (Fig. 2.9B). The overall shape of the torque–speed curve is quite similar to the H^+-driven *E. coli* motor described earlier, but the effect of the concentrations of the coupling ion on torque–speed curves of *V. alginolyticus* was different from those of *E. coli*. The curves for *E. coli* did not change even when the external environment had a pH value in the range of 4.7–8.8. However, when external NaCl concentrations were changed, the generated torque was changed over a wide range of speeds for *Vibrio* motor. This difference seems to be derived from not the mechanism of flagellar motors but the cell homeostasis when the concentration of the external coupling ion is varied. The Na^+-driven motor is likely to generate torque using basically the same mechanism as the H^+-driven motor.

4.2. Steps in rotation of motor

The rotation of the motor occurs by a sequence of discrete molecular events, presumably including the stages of ion binding in the stator followed by conformational changes in the stator that drive the rotor. Therefore, one can imagine that the motor behaves like a stepping motor. Since the discovery of flagellar rotation, such a step has been investigated but until recently it has not clearly demonstrated. The difficulty in observing rotational steps is due to the presence of an elastic linkage, the hook, between the tethered filament and the cell body, which smoothes the observed

rotation, and is also due to multiple independently functioning torque-generating units (stator complexes) per motor. One way to avoid this difficulty is to examine variations in rotation period. Such a stochastic analysis by assuming that intervals between steps follow a Poisson distribution led to an estimation of about 400 steps per revolution (Samuel and Berg, 1995). A similar analysis was done with motors containing only one or a few torque-generating units, and showed that the individual units step independently (Samuel and Berg, 1996).

Recently, direct observation of steps in the motor has been achieved by making a motor rotate as slow as possible in the work of Sowa *et al* (2005). The hybrid *E. coli* motor equipped with chimeric Na^+-driven stator complex PomA/PotB was used under the expression control of inducible promoter. Therefore, it was able to establish a motor with a small initial number of stator units, possibly one, by growing cells with low inducer level. Furthermore, by using the Na^+-type motor, the rotation rate can be reduced by lowering external Na^+ concentration. Motor rotation was detected by back-focal-plane (BFP) interferometry of 500-nm diameter beads attached to spontaneously sticky flagellar filament stub or by high-speed video recording of 200-nm diameter fluorescent beads attached in the same way. By using these experimental setups, the stepping rotations were observed at speeds below 7 and 40 Hz in BFP and fluorescence experiments, respectively. Interestingly, both backward and forward steps were observed at all speeds in both experiments, with higher probability at lower speeds. In this experiment, a *cheY* strain was used so that motor never rotates CW, thus backward steps represent microscopic reversibility rather than motor switching. Similar steps have been detected in the ATP-driven molecular motors. The step size was analyzed from these observations, and it was revealed that there is a peak at 13.7° (26 per revolution) and −10.3° (35 per revolution) for forward and backward steps, respectively. Stepping motion in the ATP-driven molecular motors reflects both the discrete nature of the input energy and the periodicity of the ''track'' along which the motor runs (Mehta *et al.*, 1999; Schnitzer and Block, 1997; Yasuda *et al.*, 1998). Likewise, observation of 26 steps per revolution in the flagellar motor is consistent with the periodicity of the ring of FliG protein (see Section 2.3), suggesting that the motor steps along each FliG molecule in the rotor. Then how many ions can be translocated during one step? Because the simultaneous measurement of a single motor rotation and the ion translocation through the stator complex has not yet been established, we can only estimate it from the published parameters. It was reported that a wild-type *E. coli* cell with a PMF of about 150 mV drives a 1 μm bead with an estimated 280 pN nm per unit (Ryu *et al.*, 2000), suggesting that maximal step size for one ion in one unit would be 5° if all the input energy was consumed for the torque generation. Thus, there may be smaller substeps, or alternatively mechanical step may be coupled to

several ion translocations. As discussed in Section 2.4, the structural model for the stator complex proposed by the disulfide cross-linking study suggested two distinct channels per stator complex (Braun and Blair, 2001; Braun *et al.*, 2004), indicative of the latter possibility. In any case, the atomic model of the stator complex and establishment of simultaneous measurement system to investigate input–output relationships will be awaited for solving this problem.

4.3. Fluorescent imaging of motor

Recent development of single-molecule measurements of enzyme activities by using fluorescent microscopic methods makes it possible to reveal much about fundamental mechanisms of these protein machines. Toward the simultaneous measurement of the single motor rotation and ion flux through the stator complex, several attempts of fluorescent imaging of motor components have been undertaken. Our laboratory has used GFP for such an imaging *in vivo* (Fukuoka *et al.*, 2007, 2005). GFP was fused to the stator proteins, PomA and PomB of *V. alginolyticus*, and their behaviors *in vivo* were observed under the fluorescent microscope (Fukuoka *et al.*, 2005). By using this system, first, it was confirmed that GFP-PomA or GFP-PomB proteins were actually localized at the flagellated cell pole of *Vibrio*. Their polar localization requires the partner subunit (PomB or PomA) and the C-terminal domain of PomB that contains PGB motif required for anchoring the stator complexes to the motor. The polar localization of GFP-fused stator proteins was not observed in the absence of the polar flagellum. Finally, cells that express the PomA/GFP-PomB stator exhibited motility, although it was significantly reduced as compared with wild-type strain. Therefore, this is the initial success in imaging the functional stator proteins *in vivo*. Since the PomA/PomB stator complex assembles into the single polar flagellum of *Vibrio*, assembly of the stator complex at the flagellated cell pole can be observed as the polar localization of the GFP-fused stator proteins.

When we observed their behavior in the absence of Na^+, the coupling ion for polar flagellar motor of *Vibrio*, the GFP-fused stator proteins were not localized at the flagellated cell pole (Fukuoka *et al.*, submitted for publication). This effect appears to be Na^+-dependent and reversible, since addition of Na^+ in the medium restores the polar localization of the GFP-fused stators. The mutations of PomB D24, which is the binding site for Na^+, affected the localization. Therefore, stator assembly seems to be regulated by the energy source of the motor, the Na-motive force. This finding also suggested more dynamic behavior of the stator proteins than previously expected. These results are consistent with the previous reports

(Armitage and Evans, 1985; Evans and Armitage, 1985) and the recent report by Leake *et al.* (2006), demonstrating simultaneous measurement of the single motor rotation and the number and dynamics of GFP-fused MotB molecules in the motor in single molecule level by total internal reflection fluorescence (TIRF) microscopy. They tethered cells expressing GFP-MotB, and observed them under the TIRF or brightfield microscopy. TIRF images of tethered cells showed spots at the center of the cell rotation measured from brightfield images, indicating functional assembly of the stator consisting of GFP-MotB and MotA. Then they carried out stepwise photobleaching of single GFP-MotB in the motor. Counting fluorophores revealed that each motor contains around 22 copies of GFP-MotB, consistent with 11 stators reported by the recent resurrection experiment. They also reported by the analyses using FRAP and fluorescence loss in photobleaching methods that (1) there is a membrane pool of ~200 GFP-MotB molecules diffusing at $\sim 0.008\ \mu m^2\ s^{-1}$, and (2) turnover of GFP-MotB between the membrane pool and motor was observed with a rate constant of the order of $0.04\ s^{-1}$. Therefore, the static image of the "stator" is in need of change, and we need to understand its function under the consideration of more dynamic behavior. The stator complex appears to be transiently anchored around the rotor to generate torque, and rapidly exchanged when it worn or by responding to the change in energetic environment in the cell.

Fluorescent imaging of the rotor protein has also been attempted, and we were able to visualize functional GFP-FliG molecules in the center of the rotating tethered cell (Fukuoka *et al.*, 2007). We are expecting that appropriate combination of functional GFP-fused stator and rotor protein in the motor may enable us to carry out measurement of FRET between stator and rotor components to demonstrate real-time imaging of rotor–stator interaction *in vivo*.

Imaging of the energy input into the motor is another big challenge. Recently, using a fluorescent probe for Na^+, Sodium Green, intracellular Na^+ concentration in single *E. coli* cells has been measured (Lo *et al.*, 2006). This method requires low-light electron-multiplying charge-coupled device camera and laser fluorescence microscopy, and makes it possible to measure intracellular Na^+ of a series of 50 single cells, without any detectable effect on the flagellar motor. The values obtained are consistent with the ones measured by other methods. Likewise, fluorescence technique to measure membrane potential in single cell has been established by using the dye tetramethylrhodamine methyl ester (Lo *et al.*, 2007). These fluorescence techniques to measure input energy (membrane potential and ion gradient) together with the rotation analysis in the single molecule level finally open the new era for motor physiology that would make it possible to visualize input–output relationships in real time and *in vivo*.

5. Conclusion

In addition to the proton-driven motor, the Na^+-driven motor has been studied extensively and many important data have accumulated. Using these insights, a genetic manipulation of the Na^+-driven *E. coli* hybrid motor with chimeric stator led us to a recent breakthrough to observe directly the steps in rotation of a single motor, the basic process of the motor. From now on, we can expect to elucidate the rotation mechanism by discussing the input and output relations of the energy during a single step in a rotation. Moreover, the technology of single-molecule fluorescent observation has been introduced, and it will be able to visualize a dynamic interaction between rotor and stator. To understand the mechanism of energy conversion that changes the ion flux into the mechanical power, the crystal structures of the membrane motor proteins are also needed. We would like to learn the biological nature from the tiny nanomachine of the bacterial flagella.

REFERENCES

Aizawa, S., Dean, G. E., Jones, C. J., Macnab, R. M., and Yamaguchi, S. (1985). Purification and characterization of the flagellar hook-basal body complex of *Salmonella typhimurium*. *J. Bacteriol.* **161,** 836–849.

Akiba, T., Yoshimura, H., and Namba, K. (1991). Monolayer crystallization of flagellar L-P rings by sequential addition and depletion of lipid. *Science* **252,** 1544–1546.

Aldridge, P., Karlinsey, J. E., Becker, E., Chevance, F. F., and Hughes, K. T. (2006). Flk prevents premature secretion of the anti-sigma factor FlgM into the periplasm. *Mol. Microbiol.* **60,** 630–643.

Armitage, J. P. (1999). Bacterial tactic responses. *Adv. Microb. Physiol.* **41,** 229–289.

Armitage, J. P., and Evans, M. C. W. (1985). Control of the proton-motive force in *Rhodopseudomonas sphaeroides* in the light and dark and its effect on the initiation of flagellar rotation. *Biochimica Biophysica Acta* **806,** 42–45.

Armitage, J. P., and Macnab, R. M. (1987). Unidirectional, intermittent rotation of the flagellum of *Rhodobacter sphaeroides*. *J. Bacteriol.* **169,** 514–518.

Asai, Y., Kojima, S., Kato, H., Nishioka, N., Kawagishi, I., and Homma, M. (1997). Putative channel components for the fast-rotating sodium-driven flagellar motor of a marine bacterium. *J. Bacteriol.* **179,** 5104–5110.

Asai, Y., Kawagishi, I., Sockett, R. E., and Homma, M. (1999). Hybrid motor with H^+- and Na^+-driven components can rotate *Vibrio* polar flagella by using sodium ions. *J. Bacteriol.* **181,** 6332–6338.

Asai, Y., Kawagishi, I., Sockett, R. E., and Homma, M. (2000). Coupling ion specificity of chimeras between H^+- and Na^+-driven motor proteins, MotB and PomB, in *Vibrio* polar flagella. *EMBO J.* **19,** 3639–3648.

Asai, Y., Yakushi, T., Kawagishi, I., and Homma, M. (2003). Ion-coupling determinants of Na^+-driven and H^+-driven flagellar motors. *J. Mol. Biol.* **327,** 453–463.

Asakura, S. (1970). Polymerization of flagellin and polymorphism of flagella. *Adv. Biophys.* **1,** 99–155.

Atsumi, T., Sugiyama, S., Cragoe, E. J., Jr., and Imae, Y. (1990). Specific inhibition of the Na^+-driven flagellar motors of alkalophilic *Bacillus* strains by the amiloride analog phenamil. *J. Bacteriol.* **172,** 1634–1639.

Atsumi, T., McCarter, L., and Imae, Y. (1992). Polar and lateral flagellar motors of marine *Vibrio* are driven by different ion-motive forces. *Nature* **355,** 182–184.

Attmannspacher, U., Scharf, B., and Schmitt, R. (2005). Control of speed modulation (chemokinesis) in the unidirectional rotary motor of *Sinorhizobium meliloti*. *Mol. Microbiol.* **56,** 708–718.

Bange, G., Petzold, G., Wild, K., Parlitz, R. O., and Sinning, I. (2007). The crystal structure of the third signal-recognition particle GTPase FlhF reveals a homodimer with bound GTP. *Proc. Natl. Acad. Sci. USA* **104,** 13621–13625.

Bennett, J. C., Thomas, J., Fraser, G. M., and Hughes, C. (2001). Substrate complexes and domain organization of the *Salmonella* flagellar export chaperones FlgN and FliT. *Mol. Microbiol.* **39,** 781–791.

Berg, H. C. (2003). The rotary motor of bacterial flagella. *Annu. Rev. Biochem.* **72,** 19–54.

Berg, H. C., and Anderson, R. A. (1973). Bacteria swim by rotating their flagellar filaments. *Nature* **245,** 380–382.

Berg, H. C., and Turner, L. (1993). Torque generated by the flagellar motor of *Escherichia coli*. *Biophys. J.* **65,** 2201–2216.

Berry, R. M., and Armitage, J. P. (1999). The bacterial flagella motor. *Adv. Microb. Physiol.* **41,** 291–337.

Berry, R. M., and Berg, H. C. (1999). Torque generated by the flagellar motor of *Escherichia coli* while driven backward. *Biophys. J.* **76,** 580–587.

Blair, D. F., and Berg, H. C. (1988). Restoration of torque in defective flagellar motors. *Science* **242,** 1678–1681.

Blair, D. F., and Berg, H. C. (1990). The MotA protein of *E. coli* is a proton-conducting component of the flagellar motor. *Cell* **60,** 439–449.

Block, S. M., and Berg, H. C. (1984). Successive incorporation of force-generating units in the bacterial rotary motor. *Nature* **309,** 470–472.

Braun, T. F., and Blair, D. F. (2001). Targeted disulfide cross-linking of the MotB protein of *Escherichia coli*: Evidence for two H^+ channels in the stator complex. *Biochemistry* **40,** 13051–13059.

Braun, T. F., Poulson, S., Gully, J. B., Empey, J. C., Van Way, S., Putnam, A., and Blair, D. F. (1999). Function of proline residues of MotA in torque generation by the flagellar motor of *Escherichia coli*. *J. Bacteriol.* **181,** 3542–3551.

Braun, T. F., Al-Mawsawi, L. Q., Kojima, S., and Blair, D. F. (2004). Arrangement of core membrane segments in the MotA/MotB proton-channel complex of *Escherichia coli*. *Biochemistry* **43,** 35–45.

Brown, P. N., Hill, C. P., and Blair, D. F. (2002). Crystal structure of the middle and C-terminal domains of the flagellar rotor protein FliG. *EMBO J.* **21,** 3225–3234.

Brown, P. N., Mathews, M. A., Joss, L. A., Hill, C. P., and Blair, D. F. (2005). Crystal structure of the flagellar rotor protein FliN from *Thermotoga maritima*. *J. Bacteriol.* **187,** 2890–2902.

Brown, P. N., Terrazas, M., Paul, K., and Blair, D. F. (2007). Mutational analysis of the flagellar protein FliG: Sites of interaction with FliM and implications for organization of the switch complex. *J. Bacteriol.* **189,** 305–312.

Calladine, C. R. (1978). Change of wave form in bacterial flagella: The role of mechanics at the molecular level. *J. Mol. Biol.* **118,** 457–479.

Chen, X., and Berg, H. C. (2000a). Solvent-isotope and pH effects on flagellar rotation in *Escherichia coli*. *Biophys. J.* **78,** 2280–2284.

Chen, X., and Berg, H. C. (2000b). Torque-speed relationship of the flagellar rotary motor of *Escherichia coli*. *Biophys. J.* **78,** 1036–1041.

Chevance, F. F., Takahashi, N., Karlinsey, J. E., Gnerer, J., Hirano, T., Samudrala, R., Aizawa, S., and Hughes, K. T. (2007). The mechanism of outer membrane penetration by the eubacterial flagellum and implications for spirochete evolution. *Genes Dev.* **21,** 2326–2335.

Chilcott, G. S., and Hughes, K. T. (2000). Coupling of flagellar gene expression to flagellar assembly in *Salmonella enterica* serovar *typhimurium* and *Escherichia coli*. *Microbiol. Mol. Biol. Rev.* **64,** 694–708.

Chun, S. Y., and Parkinson, J. S. (1988). Bacterial motility: Membrane topology of the *Escherichia coli* MotB protein. *Science* **239,** 276–278.

Claret, L., Calder, S. R., Higgins, M., and Hughes, C. (2003). Oligomerization and activation of the FliI ATPase central to bacterial flagellum assembly. *Mol. Microbiol.* **48,** 1349–1355.

Cluzel, P., Surette, M., and Leibler, S. (2000). An ultrasensitive bacterial motor revealed by monitoring signaling proteins in single cells. *Science* **287,** 1652–1655.

Cordell, S. C., and Lowe, J. (2001). Crystal structure of the bacterial cell division regulator MinD. *FEBS Lett.* **492,** 160–165.

Cornelis, G. R. (2006). The type III secretion injectisome. *Nat. Rev. Microbiol.* **4,** 811–825.

Dailey, F. E., and Berg, H. C. (1993). Mutants in disulfide bond formation that disrupt flagellar assembly in *Escherichia coli*. *Proc. Natl. Acad. Sci. USA* **90,** 1043–1047.

De Mot, R., and Vanderleyden, J. (1994). The C-terminal sequence conservation between OmpA-related outer membrane proteins and MotB suggests a common function in both Gram-positive and Gram-negative bacteria, possibly in the interaction of these domains with peptidoglycan. *Mol. Microbiol.* **12,** 333–334.

Dean, G. D., Macnab, R. M., Stader, J., Matsumura, P., and Burks, C. (1984). Gene sequence and predicted amino acid sequence of the motA protein, a membrane-associated protein required for flagellar rotation in *Escherichia coli*. *J. Bacteriol.* **159,** 991–999.

Doyle, T. B., Hawkins, A. C., and McCarter, L. L. (2004). The complex flagellar torque generator of *Pseudomonas aeruginosa*. *J. Bacteriol.* **186,** 6341–6350.

Dyer, C. M., and Dahlquist, F. W. (2006). Switched or not? The structure of unphosphorylated CheY bound to the N-terminus of FliM. *J. Bacteriol.* **188,** 7354–7363.

Eggenhofer, E., Haslbeck, M., and Scharf, B. (2004). MotE serves as a new chaperone specific for the periplasmic motility protein, MotC, in *Sinorhizobium meliloti*. *Mol. Microbiol.* **52,** 701–712.

Evans, M. C. W., and Armitage, J. P. (1985). Initiation of flagellar rotation in *Rhodopsudomonas sphaeroides*. *FEBS Lett.* **186,** 93–97.

Fahrner, K. A., Block, S. M., Krishnaswamy, S., Parkinson, J. S., and Berg, H. C. (1994). A mutant hook-associated protein (HAP3) facilitates torsionally induced transformations of the flagellar filament of *Escherichia coli*. *J. Mol. Biol.* **238,** 173–186.

Fan, F., and Macnab, R. M. (1996). Enzymatic characterization of FliI—An ATPase involved in flagellar assembly in *Salmonella typhimurium*. *J. Biol. Chem.* **271,** 31981–31988.

Fan, F., Ohnishi, K., Francis, N. R., and Macnab, R. M. (1997). The FliP and FliR proteins of *Salmonella typhimurium*, putative components of the type III flagellar export apparatus, are located in the flagellar basal body. *Mol. Microbiol.* **26,** 1035–1046.

Ferris, H. U., and Minamino, T. (2006). Flipping the switch: Bringing order to flagellar assembly. *Trends Microbiol.* **14,** 519–526.

Focia, P. J., Shepotinovskaya, I. V., Seidler, J. A., and Freymann, D. M. (2004). Heterodimeric GTPase core of the SRP targeting complex. *Science* **303,** 373–377.

Francis, N. R., Irikura, V. M., Yamaguchi, S., DeRosier, D. J., and Macnab, R. M. (1992). Localization of the *Salmonella typhimurium* flagellar switch protein FliG to the cytoplasmic M-ring face of the basal body. *Proc. Natl. Acad. Sci. USA* **89,** 6304–6308.

Francis, N. R., Sosinsky, G. E., Thomas, D., and DeRosier, D. J. (1994). Isolation, characterization and structure of bacterial flagellar motors containing the switch complex. *J. Mol. Biol.* **235,** 1261–1270.

Fraser, G. M., Bennett, J. C., and Hughes, C. (1999). Substrate-specific binding of hook-associated proteins by FlgN and FliT, putative chaperones for flagellum assembly. *Mol. Microbiol.* **32,** 569–580.

Fraser, G. M., Gonzalez-Pedrajo, B., Tame, J. R., and Macnab, R. M. (2003). Interactions of FliJ with the *Salmonella* type III flagellar export apparatus. *J. Bacteriol.* **185,** 5546–5554.

Fukuoka, H., Yakushi, T., Kusumoto, A., and Homma, M. (2005). Assembly of motor proteins, PomA and PomB, in the Na^+-driven stator of the flagellar motor. *J. Mol. Biol.* **351,** 707–717.

Fukuoka, H., Sowa, Y., Kojima, S., Ishijima, A., and Homma, M. (2007). Visualization of functional rotor proteins of the bacterial flagellar motor in the cell membrane. *J. Mol. Biol.* **367,** 692–701.

Fung, D. C., and Berg, H. C. (1995). Powering the flagellar motor of *Escherichia coli* with an external voltage source. *Nature* **375,** 809–812.

Gabel, C. V., and Berg, H. C. (2003). The speed of the flagellar rotary motor of *Escherichia coli* varies linearly with protonmotive force. *Proc. Natl. Acad. Sci. USA* **100,** 8748–8751.

Gillen, K., and Hughes, K. T. (1991). Negative regulatory loci coupling flagellin synthesis to flagellar assembly in *Salmonella typhimurium*. *J. Bacteriol.* **173,** 2301–2310.

Gonzalez-Pedrajo, B., Minamino, T., Kihara, M., and Namba, K. (2006). Interactions between C ring proteins and export apparatus components: A possible mechanism for facilitating type III protein export. *Mol. Microbiol.* **60,** 984–998.

Gotz, R., and Schmitt, R. (1987). *Rhizobium meliloti* swims by unidirectional, intermittent rotation of right-handed flagellar helices. *J. Bacteriol.* **169,** 3146–3150.

Hirano, T., Yamaguchi, S., Oosawa, K., and Aizawa, S. I. (1994). Roles of FliK and FlhB in determination of flagellar hook length in *Salmonella typhimurium*. *J. Bacteriol.* **176,** 5439–5449.

Hizukuri, Y., Yakushi, T., Kawagishi, I., and Homma, M. (2006). Role of the intramolecular disulfide bond in FlgI, the flagellar P-ring component of *Escherichia coli*. *J. Bacteriol.* **188,** 4190–4197.

Homma, M., and Iino, T. (1985). Locations of hook-associated proteins in flagellar structures of *Salmonella typhimurium*. *J. Bacteriol.* **162,** 183–189.

Homma, M., Fujita, H., Yamaguchi, S., and Iino, T. (1984). Excretion of unassembled flagellin by *Salmonella typhimurium* mutants deficient in the hook-associated proteins. *J. Bacteriol.* **159,** 1056–1059.

Homma, M., Iino, T., Kutsukake, K., and Yamaguchi, S. (1986). *In vitro* reconstitution of flagellar filaments onto hooks of filamentless mutants of *Salmonella typhimurium* by addition of hook-associated proteins. *Proc. Natl. Acad. Sci. USA* **83,** 6169–6173.

Homma, M., Komeda, Y., Iino, T., and Macnab, R. M. (1987). The *flaFIX* gene product of *Salmonella typhimurium* is a flagellar basal body component with a signal peptide for export. *J. Bacteriol.* **169,** 1493–1498.

Homma, M., Kutsukake, K., Hasebe, M., Iino, T., and Macnab, R. M. (1990). FlgB, FlgC, FlgF and FlgG. A family of structurally related proteins in the flagellar basal body of *Salmonella typhimurium*. *J. Mol. Biol.* **211,** 465–477.

Hosking, E. R., Vogt, C., Bakker, E. P., and Manson, M. D. (2006). The *Escherichia coli* MotAB proton channel unplugged. *J. Mol. Biol.* **364,** 921–937.

Hueck, C. J. (1998). Type III protein secretion systems in bacterial pathogens of animals and plants. *Microbiol. Mol. Biol. Rev.* **62,** 379–433.

Hughes, K. T., Gillen, K. L., Semon, M. J., and Karlinsey, J. E. (1993). Sensing structural intermediates in bacterial flagellar assembly by export of a negative regulator. *Science* **262,** 1277–1280.

Hunte, C., Screpanti, E., Venturi, M., Rimon, A., Padan, E., and Michel, H. (2005). Structure of a Na^+/H^+ antiporter and insights into mechanism of action and regulation by pH. *Nature* **435,** 1197–1202.

Iino, T. (1969). Genetics and chemistry of bacterial flagella. *Bacteriol. Rev.* **33,** 454–475.

Ikeda, T., Asakura, S., and Kamiya, R. (1985). ''Cap'' on the tip of *Salmonella* flagella. *J. Mol. Biol.* **184,** 735–737.

Ikeda, T., Homma, M., Iino, T., Asakura, S., and Kamiya, R. (1987). Localization and stoichiometry of hook-associated proteins within *Salmonella typhimurium* flagella. *J. Bacteriol.* **169,** 1168–1173.

Ikeda, T., Yamaguchi, S., and Hotani, H. (1993). Flagellar growth in a filament-less *Salmonella* fliD mutant supplemented with purified hook-associated protein-2. *J. Biochem. (Tokyo)* **114,** 39–44.

Imada, K., Minamino, T., Tahara, A., and Namba, K. (2007). Structural similarity between the flagellar type III ATPase FliI and F_1-ATPase subunits. *Proc. Natl. Acad. Sci. USA* **104,** 485–490.

Imae, Y., and Atsumi, T. (1989). Na^+-driven bacterial flagellar motors. *J. Bioenerg. Biomembr.* **21,** 705–716.

Inoue, Y., Lo, C. J., Fukuoka, H., Takahashi, H., Sowa, Y., Pilizota, T., Wadhams, G. H., Homma, M., Berry, R. M., and Ishijima, A. (2008). Torque-speed relationships of Na^+-driven chimeric flagellar motors in *Escherichia coli*. *J. Mol. Biol.* **376,** 1251–1259.

Ito, M., Hicks, D. B., Henkin, T. M., Guffanti, A. A., Powers, B. D., Zvi, L., Uematsu, K., and Krulwich, T. A. (2004). MotPS is the stator-force generator for motility of alkaliphilic *Bacillus*, and its homologue is a second functional Mot in *Bacillus subtilis*. *Mol. Microbiol.* **53,** 1035–1049.

Ito, M., Terahara, N., Fujinami, S., and Krulwich, T. A. (2005). Properties of motility in *Bacillus subtilis* powered by the H^+-coupled MotAB flagellar stator, Na^+-coupled MotPS or hybrid stators MotAS or MotPB. *J. Mol. Biol.* **352,** 396–408.

Iwazawa, J., Imae, Y., and Kobayasi, S. (1993). Study of the torque of the bacterial flagellar motor using a rotating electric field. *Biophys. J.* **64,** 925–933.

Jaques, S., Kim, Y. K., and McCarter, L. L. (1999). Mutations conferring resistance to phenamil and amiloride, inhibitors of sodium-driven motility of *Vibrio parahaemolyticus*. *Proc. Natl. Acad. Sci. USA* **96,** 5740–5745.

Kamiya, R., and Asakura, S. (1976). Helical transformations of *Salmonella* flagella *in vitro*. *J. Mol. Biol.* **106,** 167–186.

Karlinsey, J. E., Pease, A. J., Winkler, M. E., Bailey, J. L., and Hughes, K. T. (1997). The *flk* gene of *Salmonella typhimurium* couples flagellar P- and L-ring assembly to flagellar morphogenesis. *J. Bacteriol.* **179,** 2389–2400.

Katayama, E., Shiraishi, T., Oosawa, K., Baba, N., and Aizawa, S. (1996). Geometry of the flagellar motor in the cytoplasmic membrane of *Salmonella typhimurium* as determined by stereo-photogrammetry of quick-freeze deep-etch replica images. *J. Mol. Biol.* **255,** 458–475.

Khan, S., and Berg, H. C. (1983). Isotope and thermal effects in chemiosmotic coupling to the flagellar motor of *Streptococcus*. *Cell* **32,** 913–919.

Khan, S., Dapice, M., and Reese, T. S. (1988). Effects of *mot* gene expression on the structure of the flagellar motor. *J. Mol. Biol.* **202,** 575–584.

Kobayashi, K., Saitoh, T., Shah, D. S., Ohnishi, K., Goodfellow, I. G., Sockett, R. E., and Aizawa, S. I. (2003). Purification and characterization of the flagellar basal body of *Rhodobacter sphaeroides*. *J. Bacteriol.* **185,** 5295–5300.

Koebnik, R. (1995). Proposal for a peptidoglycan-associating alpha-helical motif in the C-terminal regions of some bacterial cell-surface proteins. *Mol. Microbiol.* **16,** 1269–1270.

Kojima, S., and Blair, D. F. (2001). Conformational change in the stator of the bacterial flagellar motor. *Biochemistry* **40,** 13041–13050.

Kojima, S., and Blair, D. F. (2004a). The bacterial flagellar motor: Structure and function of a complex molecular machine. *Int. Rev. Cytol.* **233,** 93–134.

Kojima, S., and Blair, D. F. (2004b). Solubilization and purification of the MotA/MotB complex of *Escherichia coli*. *Biochemistry* **43,** 26–34.

Kojima, S., Atsumi, T., Muramoto, K., Kudo, S., Kawagishi, I., and Homma, M. (1997). *Vibrio alginolyticus* mutants resistant to phenamil, a specific inhibitor of the sodium-driven flagellar motor. *J. Mol. Biol.* **265,** 310–318.

Kojima, S., Asai, Y., Atsumi, T., Kawagishi, I., and Homma, M. (1999). Na^+-driven flagellar motor resistant to phenamil, an amiloride analog, caused by mutations in putative channel components. *J. Mol. Biol.* **285,** 1537–1547.

Kojima, S., Shoji, T., Asai, Y., Kawagishi, I., and Homma, M. (2000). A slow-motility phenotype caused by substitutions at residue Asp31 in the PomA channel component of a sodium-driven flagellar motor. *J. Bacteriol.* **182,** 3314–3318.

Kojima, M., Kubo, R., Yakushi, T., Homma, M., and Kawagishi, I. (2007). The bidirectional polar and unidirectional lateral flagellar motors of *Vibrio alginolyticus* are controlled by a single CheY species. *Mol. Microbiol.* **64,** 57–67.

Kojima, S., Shinohara, A., Terashima, H., Yakushi, T., Sakuma, M., Homma, M., Namba, K., and Imada, K. (2008). Insights into the stator assembly of the *Vibrio* flagellar motor from the crystal structure of MotY. *Proc. Natl. Acad. Sci. USA* **190,** 7696–7701.

Kubori, T., Shimamoto, N., Yamaguchi, S., Namba, K., and Aizawa, S. (1992). Morphological pathway of flagellar assembly in *Salmonella typhimurium*. *J. Mol. Biol.* **226,** 433–446.

Kudo, S., Magariyama, Y., and Aizawa, S.-I. (1990). Abrupt changes in flagellar rotation observed by laser dark-field microscopy. *Nature* **346,** 677–680.

Kusumoto, A., Kamisaka, K., Yakushi, T., Terashima, H., Shinohara, A., and Homma, M. (2006). Regulation of polar flagellar number by the *flhF* and *flhG* genes in *Vibrio alginolyticus*. *J. Biochem. (Tokyo)* **139,** 113–121.

Kusumoto, A., Shinohara, A., Terashima, H., Kojima, S., Yakushi, T., and Homma, M. (2008). Collaboration of FlhF and FlhG to regulate polar-flagella number and localization in *Vibrio alginolyticus*. *Microbiology* **154,** 1390–1399.

Kutsukake, K. (1994). Excretion of the anti-sigma factor through a flagellar substructure couples flagellar gene expression with flagellar assembly in *Salmonella typhimurium*. *Mol. Gen. Genet.* **243,** 605–612.

Kutsukake, K. (1997). Hook-length control of the export-switching machinery involves a double-locked gate in *Salmonella typhimurium* flagellar morphogenesis. *J. Bacteriol.* **179,** 1268–1273.

Kutsukake, K., and Iino, T. (1994). Role of the FliA-FlgM regulatory system on the transcriptional control of the flagellar regulon and flagellar formation in *Salmonella typhimurium*. *J. Bacteriol.* **176,** 3598–3605.

Kutsukake, K., Ohya, Y., and Iino, T. (1990). Transcriptional analysis of the flagellar regulon of *Salmonella typhimurium*. *J. Bacteriol.* **172,** 741–747.

Kutsukake, K., Minamino, T., and Yokoseki, T. (1994). Isolation and characterization of FliK-independent flagellation mutants from *Salmonella typhimurium*. *J. Bacteriol.* **176,** 7625–7629.

Leake, M. C., Chandler, J. H., Wadhams, G. H., Bai, F., Berry, R. M., and Armitage, J. P. (2006). Stoichiometry and turnover in single, functioning membrane protein complexes. *Nature* **443,** 355–358.

Lee, S. Y., Cho, H. S., Pelton, J. G., Yan, D., Henderson, R. K., King, D. S., Huang, L., Kustu, S., Berry, E. A., and Wemmer, D. E. (2001). Crystal structure of an activated response regulator bound to its target. *Nat. Struct. Biol.* **8,** 52–56.

Liu, X., and Matsumura, P. (1994). The FlhD/FlhC complex, a transcriptional activator of the *Escherichia coli* flagellar class II operons. *J. Bacteriol.* **176,** 7345–7351.

Lloyd, S. A., and Blair, D. F. (1997). Charged residues of the rotor protein FliG essential for torque generation in the flagellar motor of *Escherichia coli*. *J. Mol. Biol.* **266,** 733–744.

Lloyd, S. A., Tang, H., Wang, X., Billings, S., and Blair, D. F. (1996). Torque generation in the flagellar motor of *Escherichia coli*: Evidence of a direct role for FliG but not for FliM or FliN. *J. Bacteriol.* **178,** 223–231.

Lloyd, S. A., Whitby, F. G., Blair, D. F., and Hill, C. P. (1999). Structure of the C-terminal domain of FliG, a component of the rotor in the bacterial flagellar motor. *Nature* **400,** 472–475.

Lo, C. J., Leake, M. C., and Berry, R. M. (2006). Fluorescence measurement of intracellular sodium concentration in single *Escherichia coli* cells. *Biophys. J.* **90,** 357–365.

Lo, C. J., Leake, M. C., Pilizota, T., and Berry, R. M. (2007). Nonequivalence of membrane voltage and ion-gradient as driving forces for the bacterial flagellar motor at low load. *Biophys. J.* **93,** 294–302.

Lowe, G., Meister, M., and Berg, H. C. (1987). Rapid rotation of flagellar bundles in swimming bacteria. *Nature* **325,** 637–640.

Luirink, J., and Sinning, I. (2004). SRP-mediated protein targeting: Structure and function revisited. *Biochim. Biophys. Acta* **1694,** 17–35.

Macnab, R. M. (2003). How bacteria assemble flagella. *Annu. Rev. Microbiol.* **57,** 77–100.

Macnab, R. M. (2004). Type III flagellar protein export and flagellar assembly. *Biochim. Biophys. Acta* **1694,** 207–217.

Macnab, R. M., and Ornston, M. K. (1977). Normal-to-curly flagellar transitions and their role in bacterial tumbling. Stabilization of an alternative quaternary structure by mechanical force. *J. Mol. Biol.* **112,** 1–30.

Manson, M. D., Tedesco, P. M., and Berg, H. C. (1980). Energetics of flagellar rotation in bacteria. *J. Mol. Biol.* **138,** 541–561.

Marykwas, D. L., Schmidt, S. A., and Berg, H. C. (1996). Interacting components of the flagellar motor of *Escherichia coli* revealed by the two-hybrid system in yeast. *J. Mol. Biol.* **256,** 564–576.

Mathews, M. A., Tang, H. L., and Blair, D. F. (1998). Domain analysis of the FliM protein of *Escherichia coli*. *J. Bacteriol.* **180,** 5580–5590.

McCarter, L. L. (1994a). MotX, the channel component of the sodium-type flagellar motor. *J. Bacteriol.* **176,** 5988–5998.

McCarter, L. L. (1994b). MotY, a component of the sodium-type flagellar motor. *J. Bacteriol.* **176,** 4219–4225.

McCarter, L. L. (2001). Polar flagellar motility of the Vibrionaceae. *Microbiol. Mol. Biol. Rev.* **65,** 445–462.

McCarter, L. L. (2004). Dual flagellar systems enable motility under different circumstances. *J. Mol. Microbiol. Biotechnol.* **7,** 18–29.

McCarter, L., Hilmen, M., and Silverman, M. (1988). Flagellar dynamometer controls warmer cell differentiation of *V. parahaemolyticus*. *Cell* **54,** 345–351.

McMurry, J. L., Murphy, J. W., and Gonzalez-Pedrajo, B. (2006). The FliN-FliH interaction mediates localization of flagellar export ATPase FliI to the C ring complex. *Biochemistry* **45,** 11790–11798.

Mehta, A. D., Rock, R. S., Rief, M., Spudich, J. A., Mooseker, M. S., and Cheney, R. E. (1999). Myosin-V is a processive actin-based motor. *Nature* **400,** 590–593.

Mimori, Y., Yamashita, I., Murata, K., Fujiyoshi, Y., Yonekura, K., Toyoshima, C., and Namba, K. (1995). The structure of the R-type straight flagellar filament of *Salmonella* at 9 angstrom resolution by electron cryomicroscopy. *J. Mol. Biol.* **249,** 69–87.

Minamino, T., and Macnab, R. M. (1999). Components of the *Salmonella* flagellar export apparatus and classification of export substrates. *J. Bacteriol.* **181,** 1388–1394.

Minamino, T., and Macnab, R. M. (2000a). FliH, a soluble component of the type III flagellar export apparatus of Salmonella, forms a complex with FliI and inhibits its ATPase activity. *Mol. Microbiol.* **37,** 1494–1503.

Minamino, T., and Macnab, R. M. (2000b). Interactions among components of the *Salmonella* flagellar export apparatus and its substrates. *Mol. Microbiol.* **35,** 1052–1064.

Minamino, T., and Namba, K. (2004). Self-assembly and type III protein export of the bacterial flagellum. *J. Mol. Microbiol. Biotechnol.* **7,** 5–17.

Minamino, T., Doi, H., and Kutsukake, K. (1999). Substrate specificity switching of the flagellum-specific export apparatus during flagellar morphogenesis in *Salmonella typhimurium*. *Biosci. Biotechnol. Biochem.* **63,** 1301–1303.

Minamino, T., Chu, R., Yamaguchi, S., and Macnab, R. M. (2000a). Role of FliJ in flagellar protein export in *Salmonella*. *J. Bacteriol.* **182,** 4207–4215.

Minamino, T., Yamaguchi, S., and Macnab, R. M. (2000b). Interaction between FliE and FlgB, a proximal rod component of the flagellar basal body of *Salmonella*. *J. Bacteriol.* **182,** 3029–3036.

Minamino, T., Kazetani, K., Tahara, A., Suzuki, H., Furukawa, Y., Kihara, M., and Namba, K. (2006). Oligomerization of the bacterial flagellar ATPase FliI is controlled by its extreme N-terminal region. *J. Mol. Biol.* **360,** 510–519.

Morgan, D. G., Owen, C., Melanson, L. A., and Derosier, D. J. (1995). Structure of bacterial flagellar filaments at 11 angstrom resolution: Packing of the alpha-helices. *J. Mol. Biol.* **249,** 88–110.

Moriya, N., Minamino, T., Hughes, K. T., Macnab, R. M., and Namba, K. (2006). The type III flagellar export specificity switch is dependent on FliK ruler and a molecular clock. *J. Mol. Biol.* **359,** 466–477.

Murata, T., Yamato, I., Kakinuma, Y., Leslie, A. G., and Walker, J. E. (2005). Structure of the rotor of the V-Type Na^+-ATPase from *Enterococcus hirae*. *Science* **308,** 654–659.

Murphy, G. E., Leadbetter, J. R., and Jensen, G. J. (2006). *In situ* structure of the complete *Treponema primitia* flagellar motor. *Nature* **442,** 1062–1064.

Nambu, T., and Kutsukake, K. (2000). The *Salmonella* FlgA protein, a putativeve periplasmic chaperone essential for flagellar P ring formation. *Microbiology* **146,** 1171–1178.

Nambu, T., Minamino, T., Macnab, R. M., and Kutsukake, K. (1999). Peptidoglycan-hydrolyzing activity of the FlgJ protein, essential for flagellar rod formation in *Salmonella typhimurium*. *J. Bacteriol.* **181,** 1555–1561.

Obara, M., Yakushi, T., Kojima, S., and Homma, M. (2008). Roles of charged residues in the C-terminal region of PomA, a stator component of the Na^+-driven flagellar motor. *J. Bacteriol.* **190,** 3565–3571.

Ohnishi, K., Kusukake, K., Suzuki, H., and Iino, T. (1990). Gene FliA encodes an alternative sigma factor specific for flagellar operons in *Salmonella typhimurium*. *Mol. Gen. Genet.* **221,** 139–147.

Ohnishi, K., Kutsukake, K., Suzuki, H., and Iino, T. (1992). A novel transcriptional regulation mechanism in the flagellar regulon of *Salmonella typhimurium*—An anti-sigma factor inhibits the activity of the flagellum-specific sigma factor, sigmaF. *Mol. Microbiol.* **6,** 3149–3157.

Okabe, M., Yakushi, T., Asai, Y., and Homma, M. (2001). Cloning and characterization of *motX*, a *Vibrio alginolyticus* sodium-driven flagellar motor gene. *J. Biochem. (Tokyo)* **130,** 879–884.

Okabe, M., Yakushi, T., and Homma, M. (2005). Interactions of MotX with MotY and with the PomA/PomB sodium ion channel complex of the *Vibrio alginolyticus* polar flagellum. *J. Biol. Chem.* **280,** 25659–25664.

Okunishi, I., Kawagishi, I., and Homma, M. (1996). Cloning and characterization of *motY*, a gene coding for a component of the sodium-driven flagellar motor in *Vibrio alginolyticus*. *J. Bacteriol.* **178,** 2409–2415.

Oosawa, K., Ueno, T., and Aizawa, S. (1994). Overproduction of the bacterial flagellar switch proteins and their interactions with the MS ring complex *in vitro*. *J. Bacteriol.* **176,** 3683–3691.

Pandza, S., Baetens, M., Park, C. H., Au, T., Keyhan, M., and Matin, A. (2000). The G-protein FlhF has a role in polar flagellar placement and general stress response induction in *Pseudomonas putida*. *Mol. Microbiol.* **36,** 414–423.

Park, S. Y., Lowder, B., Bilwes, A. M., Blair, D. F., and Crane, B. R. (2006). Structure of FliM provides insight into assembly of the switch complex in the bacterial flagella motor. *Proc. Natl. Acad. Sci. USA* **103,** 11886–11891.

Parkinson, J. S. (2003). Bacterial chemotaxis: A new player in response regulator dephosphorylation. *J. Bacteriol.* **185,** 1492–1494.

Parkinson, J. S., Ames, P., and Studdert, C. A. (2005). Collaborative signaling by bacterial chemoreceptors. *Curr. Opin. Microbiol.* **8,** 116–121.

Paul, K., and Blair, D. F. (2006). Organization of FliN subunits in the flagellar motor of *Escherichia coli*. *J. Bacteriol.* **188,** 2502–2511.

Paul, K., Harmon, J. G., and Blair, D. F. (2006). Mutational analysis of the flagellar rotor protein FliN: Identification of surfaces important for flagellar assembly and switching. *J. Bacteriol.* **188,** 5240–5248.

Platzer, J., Sterr, W., Hausmann, M., and Schmitt, R. (1997). Three genes of a motility operon and their role in flagellar rotary speed variation in *Rhizobium meliloti*. *J. Bacteriol.* **179,** 6391–6399.

Pruss, B. M., and Matsumura, P. (1996). A regulator of the flagellar regulon of *Escherichia coli*, *flhD*, also affects cell division. *J. Bacteriol.* **178,** 668–674.

Pruss, B. M., and Matsumura, P. (1997). Cell cycle regulation of flagellar genes. *J. Bacteriol.* **179,** 5602–5604.

Reid, S. W., Leake, M. C., Chandler, J. H., Lo, C. J., Armitage, J. P., and Berry, R. M. (2006). The maximum number of torque-generating units in the flagellar motor of *Escherichia coli* is at least 11. *Proc. Natl. Acad. Sci. USA* **103,** 8066–8071.

Ryu, W. S., Berry, R. M., and Berg, H. C. (2000). Torque-generating units of the flagellar motor of *Escherichia coli* have a high duty ratio. *Nature* **403,** 444–447.

Sagi, Y., Khan, S., and Eisenbach, M. (2003). Binding of the chemotaxis response regulator CheY to the isolated, intact switch complex of the bacterial flagellar motor: Lack of cooperativity. *J. Biol. Chem.* **278,** 25867–25871.

Samatey, F. A., Imada, K., Nagashima, S., Vonderviszt, F., Kumasaka, T., Yamamoto, M., and Namba, K. (2001). Structure of the bacterial flagellar protofilament and implications for a switch for supercoiling. *Nature* **410,** 331–337.

Samatey, F. A., Matsunami, H., Imada, K., Nagashima, S., Shaikh, T. R., Thomas, D. R., Chen, J. Z., Derosier, D. J., Kitao, A., and Namba, K. (2004). Structure of the bacterial flagellar hook and implication for the molecular universal joint mechanism. *Nature* **431,** 1062–1068.

Samuel, A. D., and Berg, H. C. (1995). Fluctuation analysis of rotational speeds of the bacterial flagellar motor. *Proc. Natl. Acad. Sci. USA* **92,** 3502–3506.

Samuel, A. D., and Berg, H. C. (1996). Torque-generating units of the bacterial flagellar motor step independently. *Biophys. J.* **71,** 918–923.

Sato, K., and Homma, M. (2000a). Functional reconstitution of the Na^+-driven polar flagellar motor component of *Vibrio alginolyticus*. *J. Biol. Chem.* **275,** 5718–5722.

Sato, K., and Homma, M. (2000b). Multimeric structure of PomA, a component of the Na^+-driven polar flagellar motor of *Vibrio alginolyticus*. *J. Biol. Chem.* **275,** 20223–20228.

Schmitt, R. (2002). *Sinorhizobial* chemotaxis: A departure from the enterobacterial paradigm. *Microbiology* **148,** 627–631.

Schmitt, R. (2003). Helix rotation model of the flagellar rotary motor. *Biophys. J.* **85,** 843–852.

Schnitzer, M. J., and Block, S. M. (1997). Kinesin hydrolyses one ATP per 8-nm step. *Nature* **388,** 386–390.

Schoenhals, G. J., and Macnab, R. M. (1996). Physiological and biochemical analyses of FlgH, a lipoprotein forming the outer membrane L ring of the flagellar basal body of *Salmonella typhimurium*. *J. Bacteriol.* **178,** 4200–4207.

Shah, D. S., and Sockett, R. E. (1995). Analysis of the *motA* flagellar motor gene from *Rhodobacter sphaeroides*, a bacterium with a unidirectional, stop-start flagellum. *Mol. Microbiol.* **17,** 961–969.

Shapiro, L., McAdams, H. H., and Losick, R. (2002). Generating and exploiting polarity in bacteria. *Science* **298,** 1942–1946.

Shibata, S., Takahashi, N., Chevance, F. F., Karlinsey, J. E., Hughes, K. T., and Aizawa, S. (2007). FliK regulates flagellar hook length as an internal ruler. *Mol. Microbiol.* **64,** 1404–1415.

Silverman, M., and Simon, M. I. (1974). Flagellar rotation and the mechanism of bacterial motility. *Nature* **249,** 73–74.

Sockett, H., Yamaguchi, S., Kihara, M., Irikura, V., and Macnab, R. M. (1992). Molecular analysis of the flagellar switch protein FliM of *Salmonella typhimurium*. *J. Bacteriol.* **174,** 793–806.

Sourjik, V., and Berg, H. C. (2002). Binding of the *Escherichia coli* response regulator CheY to its target measured *in vivo* by fluorescence resonance energy transfer. *Proc. Natl. Acad. Sci. USA* **99,** 12669–12674.

Sowa, Y., Hotta, H., Homma, M., and Ishijima, A. (2003). Torque-speed relationship of the Na^+-driven flagellar motor of *Vibrio alginolyticus*. *J. Mol. Biol.* **327,** 1043–1051.

Sowa, Y., Rowe, A. D., Leake, M. C., Yakushi, T., Homma, M., Ishijima, A., and Berry, R. M. (2005). Direct observation of steps in rotation of the bacterial flagellar motor. *Nature* **437,** 916–919.

Stader, J., Matsumura, P., Vacante, D., Dean, G. E., and Macnab, R. M. (1986). Nucleotide sequence of the *Escherichia coli* MotB gene and site-limited incorporation of its product into the cytoplasmic membrane. *J. Bacteriol.* **166,** 244–252.

Stallmeyer, B. M. J., Aizawa, S., Macnab, R. M., and DeRosier, D. J. (1989). Image reconstruction of the flagellar basal body of *Salmonella typhimurium*. *J. Mol. Biol.* **205,** 519–528.

Stewart, B. J., and McCarter, L. L. (2003). Lateral flagellar gene system of *Vibrio parahaemolyticus*. *J. Bacteriol.* **185,** 4508–4518.

Stolz, B., and Berg, H. C. (1991). Evidence for interactions between MotA and MotB, torque-generating elements of the flagellar motor of *Escherichia coli*. *J. Bacteriol.* **173,** 7033–7037.

Suzuki, H., Yonekura, K., and Namba, K. (2004). Structure of the rotor of the bacterial flagellar motor revealed by electron cryomicroscopy and single-particle image analysis. *J. Mol. Biol.* **337,** 105–113.

Suzuki, T., and Komeda, Y. (1981). Incomplete flagellar structures in *Escherichia coli* mutants. *J. Bacteriol.* **145,** 1036–1041.

Suzuki, T., Iino, T., Horiguchi, T., and Yamaguchi, S. (1978). Incomplete flagellar structures in nonflagellate mutants of *Salmonella typhimurium*. *J. Bacteriol.* **133,** 904–915.

Tang, H., Billings, S., Wang, X., Sharp, L., and Blair, D. F. (1995). Regulated underexpression and overexpression of the FliN protein of *Escherichia coli* and evidence for an interaction between FliN and FliM in the flagellar motor. *J. Bacteriol.* **177,** 3496–3503.

Tang, H., Braun, T. F., and Blair, D. F. (1996). Motility protein complexes in the bacterial flagellar motor. *J. Mol. Biol.* **261,** 209–221.

Terashima, H., Fukuoka, H., Yakushi, T., Kojima, S., and Homma, M. (2006). The *Vibrio* motor proteins, MotX and MotY, are associated with the basal body of Na^+-driven flagella and required for stator formation. *Mol. Microbiol.* **62,** 1170–1180.

Thomas, D. R., Morgan, D. G., and DeRosier, D. J. (1999). Rotational symmetry of the C ring and a mechanism for the flagellar rotary motor. *Proc. Natl. Acad. Sci. USA* **96,** 10134–10139.

Thomas, D. R., Morgan, D. G., and DeRosier, D. J. (2001). Structures of bacterial flagellar motors from two FliF-FliG gene fusion mutants. *J. Bacteriol.* **183,** 6404–6412.

Thomas, D. R., Francis, N. R., Xu, C., and DeRosier, D. J. (2006). The three-dimensional structure of the flagellar rotor from a clockwise-locked mutant of *Salmonella enterica* serovar *Typhimurium*. *J. Bacteriol.* **188,** 7039–7048.

Toker, A. S., and Macnab, R. M. (1997). Distinct regions of bacterial flagellar switch protein FliM interact with FliG, FliN and CheY. *J. Mol. Biol.* **273,** 623–634.

Toutain, C. M., Zegans, M. E., and O'Toole, G. A. (2005). Evidence for two flagellar stators and their role in the motility of *Pseudomonas aeruginosa*. *J. Bacteriol.* **187,** 771–777.

Ueno, T., Oosawa, K., and Aizawa, S. (1992). M ring, S ring and proximal rod of the flagellar basal body of *Salmonella typhimurium* are composed of subunits of a single protein, FliF. *J. Mol. Biol.* **227,** 672–677.

Vogler, A. P., Homma, M., Irikura, V. M., and Macnab, R. M. (1991). *Salmonella typhimurium* mutants defective in flagellar filament regrowth and sequence similarity of FliI to F_OF_1, vacuolar, and archaebacterial ATPase subunits. *J. Bacteriol.* **173,** 3564–3572.

Waters, R. C., O'Toole, P. W., and Ryan, K. A. (2007). The FliK protein and flagellar hook-length control. *Protein Sci.* **16,** 769–780.

Welch, M., Oosawa, K., Aizawa, S. I., and Eisenbach, M. (1993). Phosphorylation-dependent binding of a signal molecule to the flagellar switch of bacteria. *Proc. Natl. Acad. Sci. USA* **90,** 8787–8791.

Wilson, M. L., and Macnab, R. M. (1988). Overproduction of the MotA protein of *Escherichia coli* and estimation of its wild-type level. *J. Bacteriol.* **170,** 588–597.

Wilson, M. L., and Macnab, R. M. (1990). Co-overproduction and localization of the *Escherichia coli* motility proteins MotA and MotB. *J. Bacteriol.* **172,** 3932–3939.

Wolfe, A. J., and Visick, K. L. (2008). Get the message out: Cyclic-di-GMP regulates multiple levels of flagellar-based motility. *J. Bacteriol.* **190,** 463–475.

Wu, J., and Newton, A. (1997). Regulation of the *Caulobacter* flagellar gene hierarchy; not just for motility. *Mol. Microbiol.* **24,** 233–239.

Xing, J., Bai, F., Berry, R., and Oster, G. (2006). Torque-speed relationship of the bacterial flagellar motor. *Proc. Natl. Acad. Sci. USA* **103,** 1260–1265.

Yakushi, T., Maki, S., and Homma, M. (2004). Interaction of PomB with the third transmembrane segment of PomA in the Na^+-driven polar flagellum of *Vibrio alginolyticus*. *J. Bacteriol.* **186,** 5281–5291.

Yakushi, T., Yang, J., Fukuoka, H., Homma, M., and Blair, D. F. (2006). Roles of charged residues of rotor and stator in flagellar rotation: Comparative study using H^+-driven and Na^+-driven motors in *Escherichia coli*. *J. Bacteriol.* **188,** 1466–1472.

Yamaguchi, S., Aizawa, S., Kihara, M., Isomura, M., Jones, C. J., and Macnab, R. M. (1986a). Genetic evidence for a switching and energy-transducing complex in the flagellar motor of *Salmonella typhimurium*. *J. Bacteriol.* **168,** 1172–1179.

Yamaguchi, S., Fujita, H., Ishihara, H., Aizawa, S., and Macnab, R. M. (1986b). Subdivision of flagellar genes of *Salmonella typhimurium* into regions responsible for assembly, rotation, and switching. *J. Bacteriol.* **166,** 187–193.

Yamashita, A., Singh, S. K., Kawate, T., Jin, Y., and Gouaux, E. (2005). Crystal structure of a bacterial homologue of Na^+/Cl^--dependent neurotransmitter transporters. *Nature* **437,** 215–223.

Yamashita, I., Hasegawa, K., Suzuki, H., Vonderviszt, F., Mimori-Kiyosue, Y., and Namba, K. (1998). Structure and switching of bacterial flagellar filaments studied by X-ray fiber diffraction. *Nat. Struct. Biol.* **5,** 125–132.

Yasuda, R., Noji, H., Kinosita, K., Jr., and Yoshida, M. (1998). F_1-ATPase is a highly efficient molecular motor that rotates with discrete 120 degree steps. *Cell* **93,** 1117–1124.

Yonekura, K., Maki, S., Morgan, D. G., DeRosier, D. J., Vonderviszt, F., Imada, K., and Namba, K. (2000). The bacterial flagellar cap as the rotary promoter of flagellin self-assembly. *Science* **290,** 2148–2152.

Yonekura, K., Maki-Yonekura, S., and Namba, K. (2003). Complete atomic model of the bacterial flagellar filament by electron cryomicroscopy. *Nature* **424,** 643–650.

Yonekura, K., Yakushi, T., Atsumi, T., Maki-Yonekura, S., Homma, M., and Namba, K. (2006). Electron cryomicroscopic visualization of PomA/B stator units of the sodium-driven flagellar motor in liposomes. *J. Mol. Biol.* **357,** 73–81.

Yorimitsu, T., and Homma, M. (2001). Na^+-driven flagellar motor of *Vibrio*. *Biochim. Biophys. Acta* **1505,** 82–93.

Yorimitsu, T., Asai, Y., Sato, K., and Homma, M. (2000). Intermolecular cross-linking between the periplasmic Loop3–4 regions of PomA, a component of the Na^+-driven flagellar motor of *Vibrio alginolyticus*. *J. Biol. Chem.* **275,** 31387–31391.

Yorimitsu, T., Sowa, Y., Ishijima, A., Yakushi, T., and Homma, M. (2002). The systematic substitutions around the conserved charged residues of the cytoplasmic loop of Na^+-driven flagellar motor component PomA. *J. Mol. Biol.* **320,** 403–413.

Yorimitsu, T., Mimaki, A., Yakushi, T., and Homma, M. (2003). The conserved charged residues of the C-terminal region of FliG, a rotor component of the Na^+-driven flagellar motor. *J. Mol. Biol.* **334,** 567–583.

Yorimitsu, T., Kojima, M., Yakushi, T., and Homma, M. (2004). Multimeric structure of the PomA/PomB channel complex in the Na^+-driven flagellar motor of *Vibrio alginolyticus*. *J. Biochem. (Tokyo)* **135,** 43–51.

Zhao, R., Amsler, C. D., Matsumura, P., and Khan, S. (1996a). FliG and FliM distribution in the *Salmonella typhimurium* cell and flagellar basal bodies. *J. Bacteriol.* **178,** 258–265.

Zhao, R., Pathak, N., Jaffe, H., Reese, T. S., and Khan, S. (1996b). FliN is a major structural protein of the C-ring in the *Salmonella typhimurium* flagellar basal body. *J. Mol. Biol.* **261,** 195–208.

Zhou, J., and Blair, D. F. (1997). Residues of the cytoplasmic domain of MotA essential for torque generation in the bacterial flagellar motor. *J. Mol. Biol.* **273,** 428–439.

Zhou, J., Fazzio, R. T., and Blair, D. F. (1995). Membrane topology of the MotA protein of *Escherichia coli*. *J. Mol. Biol.* **251,** 237–242.

Zhou, J., Lloyd, S. A., and Blair, D. F. (1998a). Electrostatic interactions between rotor and stator in the bacterial flagellar motor. *Proc. Natl. Acad. Sci. USA* **95,** 6436–6441.

Zhou, J., Sharp, L. L., Tang, H. L., Lloyd, S. A., Billings, S., Braun, T. F., and Blair, D. F. (1998b). Function of protonatable residues in the flagellar motor of *Escherichia coli*: A critical role for Asp 32 of MotB. *J. Bacteriol.* **180,** 2729–2735.

This page intentionally left blank

CHAPTER THREE

Programmed Cell Death in Plants: New Insights into Redox Regulation and the Role of Hydrogen Peroxide

Ilya Gadjev,[1,*] Julie M. Stone,[†] *and* Tsanko S. Gechev*

Contents

Abstract

Programmed cell death (PCD), the highly regulated dismantling of cells, is essential for plant growth and survival. PCD plays key roles in embryo development, formation and maturation of many cell types and tissues, and plant

[1] Present address: The John Bingham Laboratory, National Institute of Agricultural Botany, Cambridge CB3 0LE, United Kingdom
* Department of Plant Physiology and Plant Molecular Biology, University of Plovdiv, Plovdiv 4000, Bulgaria
[†] Department of Biochemistry and Center for Plant Science Innovation, University of Nebraska, Lincoln N230 Beadle Center, Lincoln, Nebraska 68588

International Review of Cell and Molecular Biology, Volume 270
ISSN 1937-6448, DOI: 10.1016/S1937-6448(08)01403-2

reaction/adaptation to environmental conditions. Reactive oxygen species (ROS) are not only toxic by products of aerobic metabolism with strictly controlled cellular levels, but they also function as signaling agents regulating many biological processes and producing pleiotropic effects. Over the last decade, ROS have become recognized as important modulators of plant PCD. Molecular genetic approaches using plant mutants and transcriptome studies related to ROS-mediated PCD have revealed a wide array of plant-specific cell death regulators and have contributed to unraveling the elaborate redox signaling network. This review summarizes the biological processes, in which plant PCD participates and discusses the signaling functions of ROS with emphasis on hydrogen peroxide.

Key Words: Programmed cell death, Reactive oxygen species, Hydrogen peroxide, Antioxidants, Plant development, Stress responses, Cell signaling.

1. Introduction

Programmed cell death (PCD) is an active, genetically controlled process leading to selective elimination of unwanted or damaged cells in eukaryotes. PCD is essential for growth and development of multicellular organisms as well as for proper response to environment (Gechev *et al.*, 2006; Lam, 2004). Coordination between cell death and proliferation, growth, and differentiation is of fundamental importance for the maintenance of tissue and organ homeostasis (Van Breusegem and Dat, 2006). Plant PCD is associated with a number of developmental processes including embryo formation, degeneration of the aleurone layer during monocot seed germination, differentiation of tracheary elements in water-conducting xylem tissues, formation of root aerenchyma and epidermal trichomes, anther tapetum degeneration, floral organ abscission, pollen self-incompatibility, remodeling of some types of leaf shape, and leaf senescence (Gechev *et al.*, 2006; Thomas and Franklin-Tong, 2004). PCD is also connected with plant immunity to biotrophic pathogens. In all these examples, PCD is essential or beneficial for plants. However, necrotrophic pathogens can cause disease by triggering PCD in healthy tissues (Coffeen and Wolpert, 2004; Navarre and Wolpert, 1999; Wang *et al.*, 1996b). Unwanted PCD can also be instigated by many abiotic factors like extreme temperatures, salinity, and pollutants (Koukalova *et al.*, 1997; Overmyer *et al.*, 2000; Swidzinski *et al.*, 2002).

Whereas PCD is well-studied in animals, our knowledge of the genetic mechanisms that regulate and execute plant cell death is limited. Recent biochemical and molecular genetic studies have revealed parts of the

complex plant cell death network and broadened our understanding of the machinery controlling cell death in plants. Hydrogen peroxide (H_2O_2) and other reactive oxygen species (ROS) have become recognized to be key modulators of PCD as well as many other biological processes such as growth, development, and stress adaptation (Gechev *et al.*, 2006). Although specific ROS receptors/sensors remain largely elusive, downstream components of H_2O_2 and ROS signal transduction networks controlling plant PCD have been identified, including protein kinases, protein phosphatases, and transcription factors. The majority of these are restricted to plants, with only a few genes having close homologues in animals. The notion that the plant cell death network is genetically different from the animal cell death machinery was further supported by identification of plant-specific proteases and nucleases involved in execution of some types of plant PCD. Thus, despite some functional similarities with animals and fungi, many aspects of the plant PCD gene network appear to be unique.

Hydrogen peroxide is produced in all cellular compartments as a result of reactions of energy transfer, electron leakage from saturated electron transport chains, and the activities of various oxidases and peroxidases (Apel and Hirt, 2004). Because of its low reactivity compared with other types of ROS, it has relatively long life, low toxicity, and ability to readily cross biological membranes. Thus, although the majority of hydrogen peroxide is generated in chloroplasts, peroxisomes, and the apoplast, it can quickly migrate into neighboring compartments to provoke a myriad of biological responses distant from the site of generation. Further complicating the picture are the interconversions and interactions between different types of ROS. A highly dynamic and redundant network of low molecular weight antioxidants, ROS-scavenging, and ROS-producing proteins adjusts ROS levels in different subcellular locations according to the cellular needs at that particular time (Gechev *et al.*, 2006; Mittler *et al.*, 2004). The consequent biological responses depend on the chemical identity of the ROS, its site of production, the timing and the intensity of the signal, the developmental stage of the plant, the plant stress history, and the interactions with other signaling agents. In particular, interactions between H_2O_2 and nitric oxide (NO) are of primary importance for the control and the realization of several types of cell death (Delledonne, 2005; Delledonne *et al.*, 2001; Zago *et al.*, 2006). Plant hormones and the link between ROS and lipid messengers are equally as important for tuning the cell death response (Gechev and Hille, 2005).

This chapter summarizes our current knowledge about plant PCD with respect to the biological processes associated with PCD and the cell death network. In the second part, we focus on hydrogen peroxide and other ROS as signaling molecules that modulate plant PCD and other plant processes, with emphasis on the factors that determine particular plant responses and discuss the emerging hydrogen peroxide cell death network.

2. PCD in Plants

All eukaryotes possess active genetic cell death programs that have become integral parts of their growth, development, and reactions with the environment (Lam, 2004). In plant biology the term ''programmed cell death'' is widely used to describe genetically controlled forms of cell death, which share common morphological and biochemical features with animal cell apoptosis, including shrinkage of the cytoplasm, condensation and aggregation of the chromatin, cleavage of the nuclear DNA into internucleosomal fragments, and formation of apoptotic bodies in some cases (Wang *et al.*, 1996b). These are active processes requiring ''*de novo*'' protein synthesis and are distinct from necrosis-cell death caused by extrinsic factors independent of specific genetic control and cellular activities (Van Breusegem and Dat, 2006).

Processes showing analogy to PCD in multicellular organisms have been described in prokaryotes (*Bacillus*, *Streptomyces*, *Myxobacteria*) and unicellular eukaryotes (Ameisen, 2002; Pennell and Lamb, 1997). Several unicellular species belonging to different branches of the eukaryote phylogenetic tree have been reported to exhibit apoptotic-like cell death programs (Ameisen, 2002). The controlled cell death in *Volvox* and *Marsilea* is thought to share similarities with PCD in both plants and animals (Pennell and Lamb, 1997). The common origin of *Dictyostelium*, green algae, ferns, plants, and animals suggests that the mechanisms of PCD are to a certain degree conserved throughout eukaryotes (Ameisen, 2002; Pennell and Lamb, 1997). The chains of events leading to controlled cellular death in different branches of Eukaryota not only share common elements in their executionary and regulatory systems but are also characterized by a variety of unique features typical of each eukaryotic group. Plant PCD differs morphologically and genetically from the suicidal mechanisms in fungi and animals. There are no universal hallmarks of plant cell death and no universal proteases dedicated to PCD analogous to the animal caspases.

The specific morphological attributes associated with plant PCD are in part limited by the prominent plant cell wall, which precludes engulfment of cell compartments by surrounding cells. Plant-specific organelles such as the vacuole and the chloroplasts are important to the plant cell death network and contribute to the unique aspects of plant PCD. In most manifestations of plant PCD, the *cell wall* remains after the decomposition of the protoplast and the reutilization of its components. The hypersensitive response (HR) to pathogens, for instance, is marked by destruction of the organelles, collapse of the plasma membrane, and its separation from the cell wall, which is left deformed after the leakage of the protoplast's contents into the apoplast (Gunawardena *et al.*, 2004; Lam, 2004; Lamb and Dixon, 1997). During tracheary elements differentiation, the cell wall not only remains but also

undergoes reinforcement and thickening that is coordinated with the vacuole swelling and rupture. Only the fragment of the primary cell walls located between adjacent tracheary elements is hydrolyzed to form a channel (Nakashima *et al.*, 2000). In contrast, there are examples of total lysis of the cell wall during the formation of aerenchyma and the remodeling of the leaf shape (Gunawardena *et al.*, 2004).

In recent years, a number of studies have outlined the importance of the *vacuole* in plant cell death. Vacuoles have emerged as crucial sources for factors that mediate cellular lysis in addition to being depots for a variety of metabolites, and functioning in defense and in recycling of cellular components. Collapse of the tonoplast and release of accumulated nucleases and proteases are considered common phenomena associated with the lytic events in all forms of PCD in plants, but a key role of the vacuole has been reported for the processes of tracheary elements differentiation, formation of lysigenous aerenchyma, leaf fenestration, elimination of the aleurone layer, senescence, interaction with mycotoxins, as well as in the HR (Gunawardena *et al.*, 2004; Hatsugai *et al.*, 2004; Kuroyanagi *et al.*, 2005; Lam, 2005; Obara *et al.*, 2001; Pennell and Lamb, 1997). The tonoplast invaginates, releases vesicles toward the interior of the vacuole, gradually fragments, and becomes difficult to distinguish in the early stages of the PCD associated with the remodeling of the lace plant leaf shape. These events are followed by changes in the nuclear morphology, chromatin condensation, and DNA fragmentation (Gunawardena *et al.*, 2004). Nuclear DNA cleavage has been observed before the vacuole collapse during the HR (Mittler *et al.*, 1997). Using the HR induced by TMV infection as a model, Hatsugai *et al.* (2004) have demonstrated that the previously characterized vacuole-localized protease vacuolar processing enzyme (VPE) is a fundamental mediator in plant PCD. VPE is a caspase-like cysteine protease that cleaves a peptide bond at the C-terminal side of asparagine and aspartate. The catalytic diads and the substrate pockets of VPE and caspase-1 are conserved but there is little overall similarity between the sequences of the two proteins (Hatsugai *et al.*, 2006). Of the four VPE genes in the genome of *Arabidopsis*, three (*αvpe*, *γvpe*, and *δvpe*) appear to contribute to different types of PCD in plants (Kuroyanagi *et al.*, 2005). Vacuoles also accumulate other important hydrolytic enzymes like the S1-type Zn^{2+}-dependent nuclease ZEN1 (*Zinnia* endonuclease-1), which has been found to be a major participant in nuclear DNA degradation during the developmental cell death associated with xylem formation (Ito and Fukuda, 2002; Kuriyama and Fukuda, 2002). Vacuoles in plants and lysosomes in animals play essential roles in *autophagy*, a conserved mechanism in all eukaryotes for degradation of cellular contents to recycle nutrients or break down damaged proteins or toxic material (Bassham, 2007). In plants, autophagy is important for nutrient remobilization during sugar and nitrogen starvation and leaf senescence, degradation of oxidized

proteins during oxidative stress, disposal of protein aggregates, and possibly even removal of damaged proteins and organelles during normal growth conditions as a housekeeping function (Bassham, 2007; Xiong *et al.*, 2007). Many types of plant PCD exhibit typical morphological features of autophagic cell death, including an increase in vacuole and cell size, uptake of organelles into the vacuole followed by organelle degradation, and eventual lysis of the vacuole resulting in cell death (Filonova *et al.*, 2000; Gaffal *et al.*, 2007). However, paradoxically autophagy is necessary to prevent excessive spreading of cell death during pathogen-triggered HR (Liu *et al.*, 2005). Silencing of BECLIN1 gene, required for autophagy, results in accelerated senescence and lesions expanded beyond the infection site of the pathogen (Liu *et al.*, 2005). Although the exact mechanism by which autophagy prevents the spread of cell death is still unknown, this reveals potentially antagonistic roles for autophagy with respect to HR-associated PCD.

Chloroplasts are important sources of signals that can initiate plant PCD. Examples of chloroplast-derived molecules involved in chloroplast-to-nucleus retrograde signaling and initiation of stress responses or PCD include hydrogen peroxide, singlet oxygen, and Mg-protoporphyrin IX (Koussevitzky *et al.*, 2007; Lee *et al.*, 2007; Liu *et al.*, 2007; Wagner *et al.*, 2004). Photosynthetic electron transport chains produce hydrogen peroxide and superoxide anion radicals, especially under conditions leading to over-energization of the electron transfer chains (Gechev *et al.*, 2006). Although excessive production of ROS is potentially dangerous, in this case the ability of oxygen to accept electrons prevents overreduction of the electron transport chains, thus minimizing the chance of singlet oxygen production. Many abiotic and biotic stress conditions inhibit carbon fixation reactions in the stroma, which in combination with the increased ROS production may lead to severe oxidative stress. During the tobacco HR, a mitogen-activated protein kinase (MAPK) cascade shuts down carbon fixation in chloroplasts, and hydrogen peroxide, generated by light in the chloroplasts, triggers PCD (Liu *et al.*, 2007). In another example, the conditional *flu* (*fluorescent*) mutant of *Arabidopsis thaliana*, defective in the negative feedback control of chlorophyll biosynthesis, accumulates the chlorophyll precursor protochlorophyllide. The protochlorophyllide is a potent photosensitizer and upon dark-to-light shift singlet oxygen ($^1O_2$) rapidly accumulates as a result of energy transfer from the excited protochlorophyllide to O_2 (Meskauskiene *et al.*, 2001). The biological effects of $^1O_2$ are due to switching on a genetic cell death program, not cytotoxicity, as evidenced by the identification of *EXECUTER1* and *EXECUTER2* genes involved in the relaying of the signal (Lee *et al.*, 2007; Wagner *et al.*, 2004). As $^1O_2$ is a very short-lived and reactive, it is possible that other messengers, most likely lipid-derived molecules, mediate the transmission of the signal to the nucleus. Singlet oxygen is detoxified by carotenoids located in the thylakoids. *Arabidopsis* mutants defective in carotenoid biosynthesis or treated

with the carotenoid biosynthetic inhibitor norflurason bleach and undergo cell death (Strand *et al.*, 2003). Norflurason-treated plants accumulate Mg-protoporphyrin IX, which may function as a signal released from the chloroplasts to repress nuclear-encoded genes in another retrograde chloroplast-to-nucleus signaling pathway (Strand *et al.*, 2003). The *gun* mutants with reduced Mg-protoporphyrin IX levels display increased tolerance to norflurason-induced cell death. Further studies suggest that the chloroplast-localized pentatricopeptide-repeat protein GUN1 and the Apetala2-type transcription factor ABI4 participate in the same signaling pathway (Koussevitzky *et al.*, 2007). The interaction between GUN1 and EXECUTER-regulated pathways remains unclear. A number of other studies on chloroplast-localized genes also support a critical role for the chloroplasts in plant PCD (Hu *et al.*, 1998; Ishikawa *et al.*, 2001, 2003; Seo *et al.*, 2000).

Chloroplast signals appear to coordinately regulate plant PCD with mitochondria. *Mitochondria* are prominent players in animal cell death. Many lethal agents targeted at them cause release of cytochrome *c* and other proapoptotic proteins, which can initiate caspase activation and apoptosis. In plants, mitochondria may not play such a universal role. Nevertheless, involvement of mitochondria and release of cytochrome *c* have been reported in different types of plant PCD like heat-shock induced cell death, cell death associated with formation of tracheary elements, or self-incompatibility (Balk *et al.*, 1999; Thomas and Franklin-Tong, 2004; Yu *et al.*, 2002).

Accelerated cell death2 (ACD2) is an *A. thaliana* chloroplast protein that modulates the amount of PCD triggered by *Pseudomonas syringae* and protoporphyrin IX treatment (Yao and Greenberg, 2006). Upon infection with avirulent bacterial pathogen, ACD2 redistributes in cells undergoing PCD and their neighboring cells from being primarily chloroplast localized to being more broadly localized in mitochondria and cytosol where the protein protects cells from mitochondrial H_2O_2-dependent PCD. Further substantiating the role of mitochondria in some forms of PCD, *acd2* mutant plants undergoing spontaneous cell death suffer a loss of mitochondrial membrane potential which appears to be a common event that precedes nuclear morphological changes during PCD induced by ceramides, protoporphyrin IX, and the HR elicitor AvrRpt2 (Yao *et al.*, 2004). The genetically controlled death of the tapetal cells shows morphological and biochemical similarities to apoptosis like nuclear shrinkage, chromatin condensation, nuclear DNA fragmentation, and release of cytochrome *c* from mitochondria (Balk *et al.*, 2003). ROS and the open state of the mitochondrial permeability pores are necessary for the development of salt stress-induced PCD in tobacco protoplasts (Lin *et al.*, 2006). An Mg^{2+}-dependent DNase with a potential role in plant PCD is localized in the mitochondrial intermembrane space (Balk *et al.*, 2003). H_2O_2 burst in

mitochondria was detected also in victorin-induced PCD in oat, and the possible involvement of H_2O_2 was suggested by delaying the cell death with scavengers such as catalase and *N*-acetyl-L-cysteine (Yao *et al.*, 2002). Finally, mitochondria-associated hexokinases appear to play an important role in the regulation of plant PCD, similar to their function in the control of apoptotic cell death in animals (Kim *et al.*, 2006b).

2.1. Role of PCD in plant biology: Biological processes and functions associated with PCD

PCD is indispensable for plant survival and development. It accompanies various processes starting as early as embryogenesis. PCD can be observed in the tissues of germinating seeds, in the root cap, during the formation of aerenchyma, during the differentiation of tracheary elements, in various tissues of the reproductive organs, during leaf shape remodeling, some types of trichome development, and leaf senescence (Fig. 3.1). PCD can also be observed during interactions with biotrophic and necrotrophic plant pathogens and as a result of exposure to unfavorable abiotic factors. Here we summarize examples of developmental and environmentally related PCD. Whereas PCD can be found during both plant and animal embryogenesis or formation of body shape, most of the above-listed processes are specific to plants and reflect unique aspects of plant architecture and physiology.

2.1.1. Developmental PCD

Developmental PCD is a terminal stage of plant cell differentiation. In some cases, the dead cells play specific functions (e.g., tracheary elements, fiber cells, trichomes), in other cases, cells must die to form organs with proper functions or shapes (e.g., unisexual reproductive organs in dicots, leaf shape in some plants, aerenchyma tissue), or cells die because they accomplished their function and/or are no longer required (e.g., petals and nectaries in some flowers after pollination, leaf senescence, Fig. 3.1).

The life cycle of terrestrial plants and some algae alternates between haploid gametophyte and diploid sporophyte phases. In flowering plants, the sporophyte phase begins with the formation of a diploid zygote and persists through development of the embryo and the adult plant with its flowers. The gametophyte phase, produced by meiosis from the sporophyte, is limited only to small reproductive structures in the flowers—male gametophyte (microgametophyte) in the pollen grains and female gametophyte (megagametophyte) in the ovules.

Developmental PCD occurs in various tissues of *reproductive organs* and in some cases, the organs themselves undergo abscission (Fig. 3.1) (Rogers, 2006). By removing the organs and tissues that are no longer necessary, the plant preserves its energy resources, eliminates possible entry sites for pathogens,

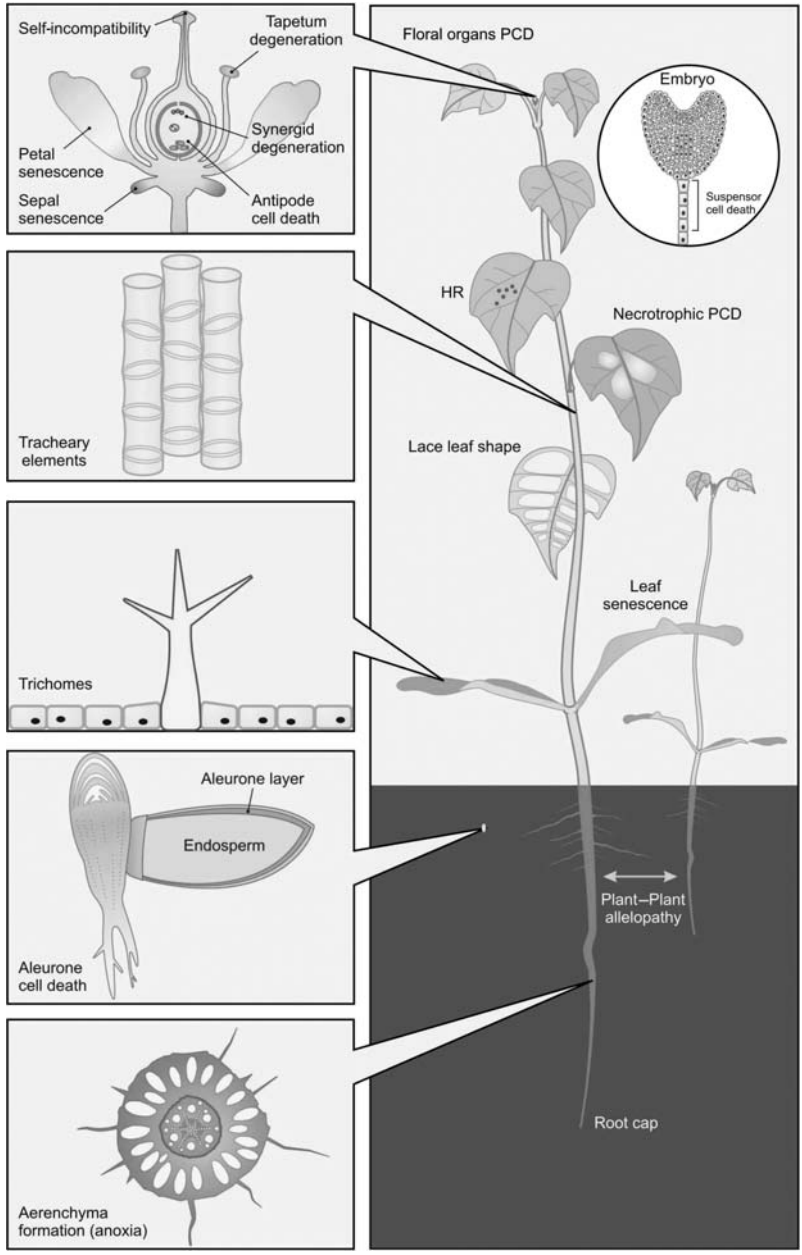

Figure 3.1 Examples of programmed cell death (PCD) in plant development and in response to environmental fluctuations. PCD occurs during embryogenesis (suspensor elimination), tapetum degeneration, pollen self-incompatibility, organ senescence (petals, sepals, leaves), formation of lace leaf shape, synergid and antipode cell death in the female gametophyte, tracheary element differentiation, some types of trichome maturation, cell death of the aleurone layer in germinating monocot seeds, aerenchyma formation under oxygen deprivation (anoxia), cell death of root cap cells, cell death during allelopathic plant–plant interactions, and plant attack by necrotrophic or hypersensitive response (HR)-triggering pathogens.

and excludes competition of nonpollinated flowers for pollinators. After having accomplished their role, *sepals* and *petals* may senesce and either abscise or remain *in situ*, protecting the initial growth of the ovule. Pollination is often accompanied by increased levels of ethylene, a major signal for the petal senescence, especially in the long-lived flowers like orchids. In short-lived flowers, senescence can be controlled independently from pollination and is modulated by other hormones (Rogers, 2006). Petal cells in tobacco are histologically homogenous and their senescence follows an acropetal gradient, culminating in death of the entire corolla at the last stages of the process (Della Mea *et al.*, 2007). Senescence and PCD of corolla are characterized by gradual decrease in chlorophyll, activation of proteases, DNA laddering, nuclear blebbing, rupture of the tonoplast membrane, pigment depletion and modification of the cell walls.

The *Digitalis purpurea floral nectary* tissue undergoes PCD with hallmarks including increased vacuolization, progressive incorporation of plasmatic components into the vacuole reminiscent of autophagy, degradation of the plastids and the nucleus with gradual disappearance of chromatin, loss of tonoplast integrity, and subsequent autolysis of the remaining cellular content (Gaffal *et al.*, 2007). In contrast, the neighboring phloem cells of the nectary remain intact beyond the secretory phase. Abortion of *stamen* or *carpel primordia* is a form of developmental PCD utilized to produce unisexual flowers. In maize, the abortion of stamen primordia in female flowers begins near the apex of the primordium and then spreads basipetally, forming an abrupt border with the living cells adjasent to the base of the primordium (Calderon-Urrea and Dellaporta, 1999; Gunawardena *et al.*, 2004).

The haploid female gametophyte (megagametophyte) develops in the diploid tissues of the ovule, either a structure enclosed within the ovary of the gynoecium in flowering plants or naked and not hemmed in a carpel in gymnosperms (Yadegari and Drews, 2004). The nucellus, located in the middle of the ovule inside the integuments, is functually equivalent to the megasporangium. The megasporocyte in the immature ovules undergoes sporogenesis through meiosis to produce one surviving haploid megaspore and three other haploid cells that eventually die in a programmed manner (Coimbra *et al.*, 2007). After fertilization, the nucellus, surrounding the embryo, usually starts functioning as a nutritive tissue—perisperm. However, at later stages, *nucellus* degenerates in a PCD fashion (Dominguez *et al.*, 2001). In wheat grains, the process is characterized with internucleosomal cleavage of the nuclear DNA, fragmentation of the cytoplasm, vacuolization of the nuclear envelope, degradation of the organelles, and disruption of the plasma membrane (Dominguez *et al.*, 2001).

The megaspore, enveloped by the nucellus, undergoes mitotic cycles and develops into the haploid megagametophyte (embryo sac), which in most flowering plants (more than 70% of all species) consists of seven cells,

one of them with two nuclei (Yadegari and Drews, 2004). The cells at the micropylar end differentiate into the egg cell and the two synergid cells. The chalazal cells develop into the three antipodal cells. The large central cell of the embryo sac contains two polar nuclei (Yadegari and Drews, 2004). The *synergid cells*, producing signals that attract and guide the growth of the pollen tube, eventually degenerate in a programmed manner (Christensen *et al.*, 2002; Punwani *et al.*, 2007). In some plants, synergid cell death is the final step of the megagametogenesis developmental program, whereas in other species, synergid cell death occurs only after pollination (Yadegari and Drews, 2004). In *Arabidopsis*, cell death is triggered after direct contact with the pollen tube (Sandaklie-Nikolova *et al.*, 2007). The synergid cell death requires mitochondrial J-domain-containing protein GFA2, orthologue of the yeast mitochondrial chaperone Mdj1p (Christensen *et al.*, 2002). The three *antipodal cells* on the opposite end of the ovule in *Arabidopsis* undergo cell death immediately before fertilization. In contrast, in maize and other grasses the antipodal cells proliferate into as many as 100 cells in the mature embryo sac (Yadegari and Drews, 2004).

PCD is observed also in the much larger female gametophyte of gymnosperms (He and Kermode, 2003a,b). The megagametophyte is a living tissue in mature seeds of white spruce but undergoes PCD after germination. This PCD is characterized by vacuolization, nuclear fragmentation, internucleosomal cleavage, and activation of serine and cysteine proteases (He and Kermode, 2003a,b).

During the late developmental stages of male sexual organs, *tapetum* cells must degenerate in order to release pollen. The tapetum degeneration is believed to be executed via PCD with such hallmarks as loss of mitochondrial membrane integrity, vacuolization, nuclear blebbing, and DNA fragmentation (Rogers, 2006). Tapetum degeneration retardation (*tdr*) gene plays a key role in this type of PCD with likely targets a cysteine protease and a protease inhibitor (Li *et al.*, 2006).

Self-incompatibility is a plant-specific mechanism to prevent inbreeding by rejection of incompatible pollen. Self-incompatibility in *Papaver* is associated with activation of a Ca^{2+} signaling cascade followed by release of cytochrome *c* from mitochondria into the cytosol and caspase-3-like enzyme activity (Bosch and Franklin-Tong, 2007; Thomas and Franklin-Tong, 2004). The process is mediated by the activity of MAPK signaling cascade (Li *et al.*, 2006). These events trigger actin depolimerization essential for the cell death (Thomas *et al.*, 2006).

During pollination, the pollen tube enters the female gametophyte through the micropyle of the ovule and releases its contents including the two male gametes. In a process unique to flowering plants, one of the sperm cells migrates to the egg cell and the other one fertilizes the binuclear central cell to form a triploid *endosperm* (Yadegari and Drews, 2004). Later the endosperm, functioning as a storage tissue, undergoes PCD mediated by

ethylene and abscisic acid and accompanied by an increase in nuclease activity and DNA laddering (Young and Gallie, 2000). Nonfertilized *ovules* are also eliminated by a type of PCD (Sun *et al.*, 2004). The endosperm is surrounded by a single cell thick aleurone layer. During seed germination, the plant embryo produces gibberellic acid (GA) triggering the *aleurone* cells to release α-amylase, which in turn hydrolyzes and mobilizes starch from the endosperm in the seeds providing the embryo with energy. The aleurone cells are eliminated by PCD when the germination is completed. The cytoplasm and the nucleus shrink accompanied by nuclear DNA fragmentation into oligonucleosome fragments. ROS and GA play central roles in the control and execution of aleurone PCD (Fath *et al.*, 2001; Yadegari and Drews, 2004). GA represses transcription of antioxidant enzymes [i.e., catalase, ascorbate peroxidase (APX), and superoxide dismutase (SOD)], leading to the dramatic increase in ROS responsible for the cell death (Fath *et al.*, 2002). GA-stimulated repression of antioxidant enzymes and enhanced ROS production is realized through destruction of DELLA proteins (Achard et al., 2008). DELLA proteins are positive regulators of antioxidant enzymes gene expression, thus alleviating stress and delaying H_2O_2-induced PCD. At the same time, DELLA - reduced ROS production represses root growth in *Arabidopsis* (Achard et al., 2008). A nuclear-localized GA-induced nuclease was found to be active just prior to the appearance of DNA laddering in wheat aleurone cells undergoing PCD (Dominguez *et al.*, 2004).

The division of the *zygote* into two cells, apical and basal, is a crucial moment in plant morphogenesis that sets the polar pattern in plant development. The fate of the two cells is tightly coordinated and leads to the formation of an embryo (from the apical cell) and a *suspensor* (from the basal cell). The suspensor channels growth factors to the embryo for a short time and is subsequently eliminated by genetically controlled cell death exhibiting similarities with apoptotic cell death in animals (Bozhkov *et al.*, 2005a).

Postembryonic development is also dependent on PCD. The lateral *root cap cells* are constantly eliminated as a result of well-documented genetically regulated cell death associated with H_2O_2 accumulation, not simply by the abrasive influence of the soil (Pennell and Lamb, 1997; Van Breusegem and Dat, 2006).

A well-characterized model system for the study of plant PCD is the development of *tracheary elements* in the xylem of vascular plants (Kuriyama and Fukuda, 2002). The differentiation of mesophyll into xylem in *Zinnia elegans* cell cultures is connected with accumulation of nucleases and proteases in the vacuole and with reticulation of the cell walls. The swelling of the vacuole is followed by its destruction and by fragmentation of the organelle and nuclear DNA in the course of the ongoing autolysis. Brassinosteroids and ROS play key roles in the initiation of the terminal stages of tracheary elements differentiation including the autolytic program. Some

apoptotic morphologies are not observed and the process shares many analogies with autophagic cell death associated with microtubule rearrangement (Lam, 2005; Obara *et al.*, 2001). A similar scenario occurs in other forms of developmental cell death—aerenchyma formation in the root and the senescence-associated cell death (Lam, 2004).

The programmed elimination of cells plays a crucial role in the sculpting of the plant body. PCD participates in the developmental remodeling of *lace leaf shape*, which can be seen as a process analogous to the elimination of the interdigital tissue during digit formation in the vertebrate limb (Gunawardena *et al.*, 2004). While in many species, the pinnately or palmately dissected leaf shape is achieved through localized growth suppression or stimulation in early leaf morphogenesis, the complex leaf shapes of some monocots arise solely through localized developmental cell death in the early stages of leaf expansion (Gunawardena *et al.*, 2004). In the lace plant (*Aponogeton madagascariensis*), the fenestrated leaf shape appears as a result of a cytologically well-characterized PCD, which initiates with tonoplast rupture and nuclear DNA cleavage. Cell shrinkage and nuclear and organellar degradation are observed in the later stages of the process (Gunawardena *et al.*, 2004). This type of developmental cell death resembles to a certain degree the formation of tracheary elements.

Trichomes of many plant species are dead in their fully differentiated stage. The trichome development follows a switch from mitosis to endoreduplication, cell branching, expansion, and eventual cell death preceded by a burst in hydrogen peroxide (Hulskamp, 2004). These processes are interconnected as misexpression of the cyclin-dependent kinase inhibitor. ICK1/KRP1 reduces the endoreduplication and cell size and induces cell death (Schnittger *et al.*, 2003). Enhanced hydrogen peroxide levels are observed in trichomes of knockout plants of succinic semialdehyde dehydrogenase, a key enzyme of γ-aminobutyrate metabolic pathway (Bouche *et al.*, 2003). These plants are more sensitive to UV and heat stress and their trichomes rapidly undergo cell death when transferred to elevated light intensities supplemented with UV radiation.

Plant *senescence* describes the spectrum of terminal events in plant vegetative and reproductive development connected with active turnover and reutilization of cellular material from tissues and organs to be eliminated eventually followed by cell death (Pennell and Lamb, 1997). Senescence of leaves and other organs is dependent on genetic and hormonal control. Analysis of various mutants and senescence-regulated genes revealed a highly complex molecular regulatory network in which receptors, transcription regulators, and metabolism regulators coordinate this process at molecular, cellular, organellar, and organismal levels (Lim *et al.*, 2007). Both internal (plant hormones) and external factors (abiotic or biotic stresses) can modulate plant senescence. Ethylene is an important regulator of this process, as indicated by delayed leaf senescence in experiments using

ethylene antagonists (compounds blocking its synthesis and perception) and mutants defective in ethylene biosynthetic or signaling pathways. Ethylene stimulates the expression of senescence-associated genes (in *Arabidopsis*: *SAGs*, *s*enescence-*a*ssociated *g*enes; in tomato: *SENUs*, *sen*escence-*u*pregulated genes) encoding proteins such as cysteine proteases, RNases, and a glutamine synthetase (Della Mea *et al.*, 2007). However, transgenic plants constitutively overproducing ethylene do not exhibit premature senescence, indicating that other signals in combination with ethylene are required to initiate the process (Lim *et al.*, 2007). Polyamines are involved in the control of apoptosis in animals and PCD in plants where they influence senescence of different organs (Della Mea *et al.*, 2007). ROS like superoxide radicals and hydrogen peroxide are also key coordinators of senescence (del Rio *et al.*, 2006). In contrast to ethylene, cytokinins are known as negative regulators of senescence (Lim *et al.*, 2007). However, both ethylene and cytokinin signals appear to be transmitted through classic two-component relay systems. Cytokinins are perceived by three receptors that transfer the signal to histidine phosphotransfer proteins which in turn translocate to the nucleus and relay the signal to response regulator proteins that either induce or repress the expression of cytokinin-regulated genes. Arabidopsis cytokinin receptor histidine kinase 3 (AHK3) transmits the cytokinin signal to positively control leaf longevity (Kim *et al.*, 2006a). Missense mutation or overexpression of AHK3 leads to delayed senescence, while loss-of-function mutation leads to accelerated senescence symptoms. The cytokinin signal is relayed via the response regulator ARR2 leading to suppression of nuclease, protease, and lipase SAGs (Kim *et al.*, 2006a). Interestingly, high concentrations of cytokinins induce PCD with typical apoptotic features in both *Arabidopsis* and *Daucus carota*, including chromatin condensation, DNA laddering, and release of cytochrome *c* from mitochondria (Carimi *et al.*, 2003). The biological relevance of this phenomenon remains unclear.

Reverse genetics studies identified a number of transcription factors that are positive regulators of leaf senescence. *WRKY53*, belonging to the plant-specfic WRKY family of transcription factors, is highly induced at the early stages of leaf senescence but its expression decreases at the later stages coinciding with the cell death symptoms, suggesting that it may play a regulatory role and govern the global transcriptional reprogramming during senescence (Hinderhofer and Zentgraf, 2001). Indeed, null mutants of *WRKY53* display delayed leaf senescence, whereas *WRKY53* overexpression accelerated the process (Miao *et al.*, 2004). Interestingly, WRKY53 interacts with the jasmonic acid-inducible protein ESR/ESP, and the two proteins mutually antagonize each other (Miao and Zentgraf, 2007). In addition to WRKY53, transcription factors from the NAC family have been identified as positive regulators of leaf senescence in *Arabidopsis* (Lim *et al.*, 2007). Knockout *AtNAP* mutants exhibit significantly delayed leaf senescence (Guo and Gan, 2006).

2.1.2. PCD in the interactions between plants and the environment

A number of plant adaptation processes, including the HR to pathogens, some plant–plant allelopathic interactions, and aerenchyma formation in response to oxygen deprivation, require PCD. In contrast, many unfavorable abiotic stress factors as well as necrotrophic pathogens trigger unwanted PCD. Thus, PCD both serves as a positive and negative aspects of plant adaptation to the environment.

2.1.2.1. Interactions with pathogens The invasion of an avirulent pathogen leads to a localized *HR*, characterized by rapid collapse of the tissue at the immediate and surrounding regions of the site of infection, and formation of dry lesions clearly distinguishable from the surrounding healthy tissue (Lam, 2004). In this way, HR protects plants from potential propagation and development of the pathogen. This localized response is frequently associated with the establishment of *systemic acquired resistance*, manifested in distant organs, and accompanied by the induction of pathogenesis-related genes, the synthesis of secondary metabolites with protective functions, and cell wall reinforcement (Dangl and Jones, 2001).

Clear evidence for the genetic control of HR-associated cell death comes from identification of mutant *Arabidopsis*, maize, and tomato plants that spontaneously undergo HR-like cell death in absence of pathogen attack (Overmyer *et al.*, 2000). Some of these ''initiation'' mutants exhibit localized lesions typical of the HR, whereas the cell death in other ''propagation'' mutants is massive. The existence of these two classes of mutants reflects the complexity of the genetic control and indicates that genetically distinct processes are responsible for the different stages during HR lesion formation—the initiation and the confinement of the cell death (Overmyer *et al.*, 2000). HR is a type of PCD showing some similarities to apoptosis (Lam, 2004). The process starts with rapid ion fluxes through the plasma membrane and a burst of H_2O_2 and superoxide anion radicals, leading to increased cytosolic Ca^{2+} levels, activated protein kinase cascades, global transcriptional reprogramming, and rapid cell death. The oxidative burst is biphasic where the first wave is shorter, having signaling functions, and the second phase is longer with sustained ROS production that initiates PCD (Lamb and Dixon, 1997). Key generators of ROS in *Arabidopsis* are the apoplastic peroxidases and the membrane-localized NADPH oxidases, composed of AtrbohD- and AtrbohF-encoded subunits (Bindschedler *et al.*, 2006; Torres *et al.*, 2002). Hydrogen peroxide produced by these enzymes is essential not only for PCD in cells surrounding the invading pathogen but also for prevention of cell death in neighboring cells and tissues (Torres *et al.*, 2005). The HR is characterized by nuclear DNA cleavage, rapid cytoskeletal reorganization, and organelle dismantling. The caspase-like protease γVPE emerged as an important executor in this type of cell death. Vacuolar processing enzyme (VPE) is synthesized

as an inactive larger precursor, which after processing is transported to and subsequently fully activated in the vacuole (Hatsugai *et al.*, 2004; Kuroyanagi *et al.*, 2005). In *Arabidopsis*, the cells undergoing PCD during the HR condense and shrink resembling apoptotic bodies (Lam, 2004; Pennell and Lamb, 1997). In addition to ROS, HR-associated cell death is modulated by different phytohormones. Pharmacological and genetic experiments showed the importance of salicylic acid (SA) in a number of HR systems. It has been proposed that depending on its concentration, SA stimulates or suppresses PCD thus contributing to the establishment of the boundary between the lesion and the living tissue (Alvarez, 2000). The interaction based on a feedback control between the levels of ROS and SA as well as the balance between the intracellular NO and H_2O_2 are of primary importance (Delledonne *et al.*, 2001; Zago *et al.*, 2006; Zaninotto *et al.*, 2006). Recently, processes similar to autophagy in animals have been shown to act as negative regulators of the HR-associated cell death by inhibiting the growth of the lesions in the healthy tissue through possible prevention of the effect of the progressing cell death signal (Patel *et al.*, 2006). A model has been proposed which suggests that in response to pathogen recognition, autophagy-associated genes are upregulated leading to the formation of autophagosomes in the healthy cells adjacent to the HR PCD. These autophagosomes can sequester VPE pre- and proproteins that will be degraded after the fusion with the vacuole, thus preventing its dismantling and the development of PCD (Liu *et al.*, 2005; Patel *et al.*, 2006; Seay and Dinesh-Kumar, 2005).

Necrotrophic fungi secrete so-called *host-selective toxins* to trigger cell death in the host plant to feed on the dead tissue (Stone *et al.*, 2000; Wang *et al.*, 1996a). Examples of such phytotoxic molecules are the AAL-toxin and fumonisin B1, synthesized by *Alternaria alternata* f. sp. *lycopersici* and *Fusarium verticillioides* (formerly *moniliforme*), respectively. The two toxins share similar chemical structures and act as sphingosine analogues to inhibit ceramide synthase, a key enzyme in sphingosine metabolism, leading to decreased levels of complex ceramides, increased levels of their precursors, and eventual cell death (Gechev *et al.*, 2004; Spassieva *et al.*, 2002). The cell death induced by AAL-toxin and fumonisin B1 is the end result of active, genetically controlled processes showing morphological and biochemical analogies to animal apoptosis, including nuclear condensation, DNA fragmentation, and requiring *de novo* protein synthesis (Asai *et al.*, 2000; Stone *et al.*, 2000; Wang *et al.*, 1996a). The process is accompanied by oxidative burst and is regulated by ROS (Gechev *et al.*, 2004). The caspase-like VPE is a key regulator of fumonisin-induced cell death in *A. thaliana* (Kuroyanagi *et al.*, 2005). Victorin, another host-selective toxin produced by *Cochliobolus victoriae*, triggers PCD in oat (Navarre and Wolpert, 1999). Victorin-induced PCD displays morphological and biochemical hallmarks of animal apoptosis, including chromatin condensation, DNA laddering, and cell shrinkage (Coffeen and Wolpert, 2004). Victorin binds to and inhibits

mitochondrial glycine decarboxylase complex, resulting in changes of mitochondrial potential with a concomitant H_2O_2 burst (Yao *et al.*, 2002). Calcium fluctuations, ethylene, and subtilisin-like serine proteases with caspase-like activity seem to play role in victorin-induced cell death (Coffeen and Wolpert, 2004). Recently, screening for victorin-insensitive mutants in *Arabidopsis* identified thioredoxin h5 (ATTRX5, coiled-coil nucleotide-binding site leucine-rich repeat protein) as required for the cell death (Sweat and Wolpert, 2007). Victorin responses seem specific for ATTRX5 as the closely related ATTRX3 only partially compensates for the loss of function (Sweat and Wolpert, 2007). Interestingly, ATTRX5 is highly induced by AAL-toxin- and H_2O_2-dependent cell death (Gechev and Hille, 2005; Gechev et al., 2004).

2.1.2.2. Plant–plant allelopathic interactions PCD plays a role in some interesting types of allelopathic plant–plant interactions (Bais *et al.*, 2003). *Centaurea maculosa* displaces native species from their habitat by secreting the phytotoxin catechin into the soil. The catechin triggers H_2O_2 accumulation in root meristems of neighboring species, activates a Ca^{2+}-dependent signaling cascade, transcriptome reprogramming, and eventually cell death (Bais *et al.*, 2003).

2.1.2.3. Plant PCD triggered by abiotic factors Many abiotic stress factors, including pollutants, UV-light, salinity, and extreme temperatures, can result in oxidative stress and subsequently ROS-dependent PCD. *Ozone* (O_3) is an important air pollutant, a potent toxin, and component of the photochemical smog in urban areas (Overmyer *et al.*, 2003). O_3 enters the apoplast where it elicits generation of ROS, mainly hydrogen peroxide (Pellinen *et al.*, 2002). The ROS burst is biphasic with a smaller peak at 4 h and a larger peak at 16 h, similar to what is seen with pathogen attack (Mahalingam *et al.*, 2006). This is accompanied by a burst of NO at 9 h. These ROS and reactive nitrogen species (RNS) act not simply as destructive toxic agents but also as signals unlocking the PCD program (Overmyer *et al.*, 2003). Hallmarks of O_3-induced cell death include intensive ion fluxes across membranes, shrinkage of the nuclei, chromatin condensation, nuclear DNA fragmentation, lesion formation, induction of pathogenesis-related genes, and reinforcement of the cell wall (Overmyer *et al.*, 2005). These reactions are dependent on *de novo* transcription and protein synthesis, ATPase, kinase, and caspase-like proteolytic activities, and are modulated by ethylene and SA levels (Overmyer *et al.*, 2005; Sandermann, 2004).

Other pollutants like *heavy metals* can also initiate H_2O_2-induced PCD. Cadmium initiates an oxidative burst and eventual cell death in tobacco (Garnier *et al.*, 2006). The oxidative burst is observed in three waves localized mainly to the apoplast and mitochondria. Calcium release from

internal pools leads to NADPH oxidase-dependent hydrogen peroxide accumulation preceding the cell death. Membrane peroxidation and mitochondrial superoxide radical production are also essential for cadmium-induced cell death (Garnier *et al.*, 2006). Distinct MAPKs are activated in response to cadmium or copper-induced heavy metal stress (Jonak *et al.*, 2004). Other heavy metals like aluminum or mercury can also cause perturbations in redox homeostasis and ROS-dependent cell death (Ortega-Villasante *et al.*, 2007; Pan *et al.*, 2001).

Exposure of plants to *high light* intensities and/or *UV-light* can result in activation of PCD (Davison *et al.*, 2002; Danon *et al.*, 2004). Overexpression of β-carotene hydroxylase, an enzyme in the zeaxanthin biosynthetic pathway, enhances high light-induced cell death in *Arabidopsis* (Davison *et al.*, 2002). UV-C overexposure triggers a rapid burst of ROS followed by loss of mitochondrial membrane potential and cell death (Gao *et al.*, 2008). The cell death can be retarded by antioxidants (ascorbic acid), inhibitors of photosynthetic electron transport (DCMU), inhibitors of mitochondrial permeability transition pores (cyclosporin), or caspase inhibitors (Danon *et al.*, 2004; Gao *et al.*, 2008). The burst of hydrogen peroxide and superoxide radicals is followed by induction of metacaspase 8 (AtMC8), which is involved in mediating UV-C and ROS-induced cell death (He *et al.*, 2008).

Salt stress causes PCD with hallmarks of TUNEL staining and DNA laddering in different plant species (Huh *et al.*, 2002; Lin *et al.*, 2006). In *Arabidopsis*, salt stress induces PCD in primary roots of both wild-type and *s*alt *o*verly *s*ensitive (*sos1*) mutant seedlings. However, whereas wild-type plants survived salt stress levels due to formation of secondary roots from the shoot/root transition zone, *sos1* mutants failed to do so and died (Huh *et al.*, 2002). Salt stress-induced PCD in rice root tip cells and tobacco protoplasts is associated with disturbed Ca^{2+}, K^+, and H^+ ion equilibrium and increased production of hydrogen peroxide (Huh *et al.*, 2002; Shabala *et al.*, 2007). High H_2O_2 level together with the open state of the mitochondrial permeability pores are compulsory for the realization of the cell death program, showing direct analogies with apoptosis in animals (Lin *et al.*, 2006). Interestingly, expression of animal antiapoptotic gene CED-9 in tobacco maintains K^+ homeostasis and protects from salt- and oxidative stress-induced cell death (Shabala *et al.*, 2007).

Exposure to *heat shock* can lead to PCD in a number of species, including *Arabidopsis* and tobacco (Swidzinski *et al.*, 2002). Heat shock leads to a burst of H_2O_2, which in turn leads to cytochrome *c* release from mitochondria followed by activation of proteases with caspase-3-like and proteasome activities (Coffeen and Wolpert, 2004; Vacca *et al.*, 2007). The ROS scavenging enzymes catalase and SOD or specific caspase-3 inhibitors block the activation of caspase-3-like activities and cell death (Vacca *et al.*, 2007). The Arabidopsis Bax-1 inhibitor protein seems to be a negative regulator of heat-shock induced cell death (Watanabe and Lam, 2006).

Low temperature induces cell death in tobacco BY-2 cells with typical PCD hallmarks as chromatin condensation and DNA laddering (Koukalova *et al.*, 1997). Such cell culture retained 11% living cells even after prolonged cold treatment. Although the mechanism of cold-induced PCD is not clear, heterologous overexpression of the animal antiapoptotic genes *bcl-x*L and *ced-9* improves the tolerance to low-temperature-induced necrotic lesions in tomato (Xu *et al.*, 2004), supporting functional conservation of PCD components between plants and animals.

Formation of lysigenous aerenchyma tissue in response to labored gas exchange and *hypoxia* occurs in a number of species, including *Arabidopsis* and maize (Kuriyama and Fukuda, 2002; Muhlenbock *et al.*, 2007; Pennell and Lamb, 1997). Typical for this tissue, the intercellular spaces filled with air to facilitate gas exchange and oxygen transfer, appear as a result of PCD. Protein phosphorylation and Ca^{2+} fluxes, disruption of cytoplasmic streaming, and tonoplast rupture that releases vacuolar lytic enzymes are among the first processes observed during this type of PCD, followed by shrinkage of the nucleus, chromatin condensation, nuclear DNA fragmentation, and decomposition of the organelles and the cell wall (Gunawardena *et al.*, 2001). In *Arabidopsis*, aerenchyma formation under hypoxic conditions is associated with ethylene and hydrogen peroxide production (Muhlenbock *et al.*, 2007). The cell death regulator *L*ESION *S*TIMULATING *D*ISEASE1 (LSD1) negatively regulates ethylene and hydrogen peroxide production as well as PCD, as evidenced by increased ACC (ethylene precursors) and H_2O_2 levels and two-fold greater aerenchyma formation in *lsd1* mutants. At the same time, in absence of functional LSD1, ethylene- and hydrogen peroxide-dependent PCD during hypoxia is positively regulated by *E*NHANCED *D*ISEASE *S*USCEPTIBILITY1 (EDS1) and *P*HYTO*A*LEXIN *D*EFICIENT4 (PAD4) defense regulators (Muhlenbock *et al.*, 2007).

2.2. Plant cell death machinery: Plant-specific regulators, transcription factors, proteases, and nucleases

In the last few years, numerous studies identified different components of the versatile plant cell death network. Despite this progress, the cell death pathways in plants still remain enigmatic with most of the genes and proteins involved yet to be discovered or, for most of the identified players, yet to be placed in a specific position within the complex network. For example, there are no core universal regulators and executioners of plant PCD analogous to the members of the animal Ced-9/Bcl-2, Ced-4/APAF1, and caspase families (Lam, 2004). From the emerging picture, it is becoming increasingly clear that most of the genes involved in the regulation of plant PCD are specific to the plant kingdom and this is most likely a reflection of the specific morphology and physiology of plants. Nevertheless, there are structural and functional similarities underlined by the ability of some

animal or yeast pro- and antiapoptotic proteins to function as cell death regulators in plants (Lam, 2004). Expression of the proapoptotic Bcl-2 member Bax induces PCD in plants, whereas the antiapoptotic protein Bcl-xL or its *C. elegans* homologue Ced-9 suppresses pathogen-induced cell death (Dickman *et al.*, 2001; Kawai-Yamada *et al.*, 2001; Lacomme and Santa Cruz, 1999; Lam, 2004; Xu *et al.*, 2004). Research data suggest connection between the function of Bcl-xL/Ced-9 and redox homeostasis. Transgenic plants expressing the protein accumulate anthocyanins and exhibit better resistance to UV irradiation, paraquat treatment, TMV infection, salt-stress, low-temperature exposure, and wounding (Mitsuhara *et al.*, 1999; Qiao *et al.*, 2002; Xu *et al.*, 2004). As previously mentioned, the expression of CED-9 conferred increased salt and oxidative stress tolerance to *Nicotiana benthamiana* plants by altering ion flux patterns across plasma membrane (Shabala *et al.*, 2007). The inhibitor of Bax-induced PCD—Bax Inhibitor 1 (BI-1)—functions as cell death suppressor in fungi, plants, and animals. This is a transmembrane protein with predominant localization to the endoplasmatic reticulum (ER). AtBI-1 has been found to modulate ER stress-mediated PCD associated with accumulation of H_2O_2 in *Arabidopsis* (Watanabe and Lam, 2008). The *BAP1* and *BAP2* genes of *Arabidopsis* together with their partner *BON1* function as general inhibitors of PCD in plants and yeast, induced by various stimuli including ROS (Yang et al., 2007).

Many of the newly identified genes are presumably involved in modulating the initial signaling events. These include genes that modulate the intensity of the cell death stimulus, participate in the interaction with other signaling molecules, or perceive the cell death signal, thus playing roles as receptors. Other genes relay and amplify the cell death signal by MAPK- or Ca^{2+}/Calmodulin (CAM)-dependent cascades, ultimately regulating cell death-specific transcription factors to govern the global transcriptional reprogramming observed during cell death. Finally, as a result of this reprogramming, sets of genes including proteases and nucleases orchestrate the orderly executed cell suicide and remobilization of resources. Interestingly, as it is with animal caspases, some of these plant proteases may not be simple executioners of cell death but are also involved in regulating the initial steps of the process by proteolytically activating pro-death factors or degrading antiapoptotic proteins.

Alterations in *ion fluxes* are one of the primary events of PCD initiation. The *Arabidopsis* lesion mimic mutant gene *hlm1* and its barley homologue *nec1* encode cyclic nucleotide-gated channels (CNGC) (Balague *et al.*, 2003; Rostoks *et al.*, 2006). The *Arabidopsis* CNGC4 is permeable to both K^+ and Na^+ and is activated by both cGMP and cAMP. The gene is induced by pathogens and is believed to be involved in the HR (Balague *et al.*, 2003). Hydrogen peroxide-induced oscillations in Ca^{2+} ions are essential signals for many biological responses, including stomatal closure, stress adaptation, and several types of PCD (Allen *et al.*, 2001; Lecourieux

et al., 2002; Pei *et al.*, 2000; Rentel *et al.*, 2004). It appears that the Ca^{2+} signature is quite specific for the different responses; increased cytosolic Ca^{2+} can be short-lived or sustained and oscillations may vary in amplitude and phase. Other cyclic nucleotide-gated channels, CNGC1 and CNGC2, also known as DND1 and DND2, respectively, are also induced by pathogens and conduct Ca^{2+} into cells during HR, but have opposite phenotypes to *hlm1* and *nec1* when mutated (Ali *et al.*, 2007; Clough *et al.*, 2000). The Ca^{2+} wave induces a burst of NO essential for PCD. Interestingly, *dnd1* plants retain characteristic responses to avirulent pathogens and are resistant against a broad spectrum of virulent pathogens (Yu *et al.*, 1998). Targets of Ca^{2+} can be Ca^{2+}/CAM-binding proteins, Ca^{2+}-dependent protein kinases, various EF-hand containing proteins (e.g., NADPH oxidase related to the oxidative burst), and also proteins without EF-hands (Lecourieux *et al.*, 2006). The plant-specific MLO family transmembrane proteins posess CAM-binding domains. Mutations in *mlo* gene of barley lead to spontaneous cell death without any obvious inducing signals (lesion mimic mutants of the initiation type) and enhanced disease resistance to powdery mildew (Kim *et al.*, 2002). However, the powdery mildew-resistant plants are more susceptible to necrotrophic pathogens that utilize PCD to feed on dead tissues (Jarosch *et al.*, 1999).

Hydrogen peroxide-induced *Ca^{2+} oscillations* can in turn amplify ROS signals by activating the CAM-binding protein NAD kinase and EF-hand motif-containing NADPH oxidase (Harding *et al.*, 1997; Lecourieux *et al.*, 2006). Both H_2O_2 and $NO^{\bullet}$ orchestrate pathogen-induced PCD (Delledonne, 2005; Delledonne *et al.*, 2001). Ca^{2+} can also induce $NO^{\bullet}$ essential for pathogen-induced cell death (Lamotte *et al.*, 2004). Indeed, plant $NO^{\bullet}$ synthase contains CAM-binding motif and both Ca^{2+} and CAM are required for its full activation (Guo *et al.*, 2003). In turn, $NO^{\bullet}$ participates in Ca^{2+} release, thus amplifying the initial signal (Lamotte *et al.*, 2004). Plant genes involved in Ca^{2+} responses and modulation of H_2O_2 or $NO^{\bullet}$ levels are important determinants of PCD. More on these genes, particularly on the antioxidant gene network, will be discussed in Section 3.

Plant hormones like ethylene, brassinosteroids, and cytokinins together with other signaling molecules regulate PCD in a complex manner. Studying the genetic components of the hormone pathways identified plant-specific receptors and other proteins that are involved in various types of PCD. Brassinosteroids are plant hormones that regulate growth and development (Vert and Chory, 2006). In *Arabidopsis*, they are perceived outside the cell by two receptor-like protein kinases BRI1 and BAK1 (Gendron and Wang, 2007). The group of receptor-like kinases in plants has expanded and diversified to more than 600 members in *Arabidopsis* and 1000 in rice to regulate various aspects of development and stress responses (Morillo and Tax, 2006). Interestingly, BAK1 can also contain the spread of pathogen-induced PCD and this function can be uncoupled from brassinosteroid

regulation of plant development (Kemmerling *et al.*, 2007). *Bak1* mutants show enhanced production of hydrogen peroxide and spreading necrosis upon infection with necrotrophic fungal pathogens, while brassinosteroid-insensitive and -deficient mutants do not exhibit increased sensitivity and spreading lesions in response to such pathogens (Kemmerling *et al.*, 2007). BAK1 can also physically associate with the flagellin receptor-like protein kinase FLS2 to regulate plant immunity (Chinchilla *et al.*, 2007). *Bak1* mutants challenged with the bacterial flagellin-derived peptide elicitor do not mount an H_2O_2 burst and flagellin-dependent stress responses (Chinchilla *et al.*, 2007). Thus, BAK1 has multiple roles in plant growth, development, and cell death.

Cytokinins are also plant-specific hormones involved in plant growth and development (Sakakibara, 2006). As discussed earlier, cytokinins negatively regulate leaf senescence-associated PCD in *Arabidopsis* and AHK3 is the receptor involved in perception of the signal (Kim *et al.*, 2006b).

Other specific plant cell death regulators are revealed by identification and cloning of genes responsible for lesion-mimic mutants *acd1*, *acd2*, *acd5*, *acd6*, and *acd11*. While ACD1 and ACD2 are connected to chlorophyll catabolism, ACD5 and ACD11 are related to lipid metabolism (Brodersen *et al.*, 2002; Liang *et al.*, 2003; Tanaka *et al.*, 2003). As indicated earlier, ACD2 may not only be involved in chlorophyll metabolism but also shields chloroplasts and mitochondria from excess ROS production (Yao and Greenberg, 2006). The earlier-mentioned chloroplast proteins EXECUTER1 and EXECUTER2 are also restricted to plants.

Cell death signals are relayed by a complex network of Ca^{2+} and MAPK cascades to activate PCD transcriptional reprogramming via cell death-specific *transcription factors*. LOL1 and LSD1 are positive and negative regulators of superoxide-induced cell death, respectively, acting as a molecular rheostat to control PCD in *Arabidopsis* (Dietrich *et al.*, 1997; Epple *et al.*, 2003). The negative cell death regulator LSD1 retains the basic leucine zipper transcription factor AtbZIP10 in the cytosol, thus preventing it from initiating PCD transcriptional reprogramming (Kaminaka *et al.*, 2006). The phenotype of *lsd1* mutants is uncontrolled, spreading cell death, initiated by $O_2^{\bullet -}$ (Jabs *et al.*, 1996). Interestingly, a triple mutant between *lsd1* and two ROS-generating NADPH oxidase subunit homologues, *atrbohD* and *atrbohF*, showed uncontrolled cell death even under growth conditions that normally repress *lsd1* cell death (Torres *et al.*, 2005). The *lsd1* phenotype was restored by overexpression of *AtrbohD*, demonstrating that $O_2^{\bullet -}$ produced by NADPH oxidase and its subsequent dismutation to H_2O_2 is somehow able to antagonize the $O_2^{\bullet -}$-induced cell death in the neighboring cells (Torres *et al.*, 2005). AtMYB30 is another positive regulator of pathogen-induced PCD and has an important role in disease resistance (Vailleau *et al.*, 2002). Silencing of AtMYB30 strongly inhibits HR-like cell death in response to avirulent pathogens, which corresponds with decreased defense gene expression and decreased resistance to

virulent pathogens. Targets of MYB30 are genes from the acyl-CoA elongase complex and the action of MYB30 seems to modulate very-long-chain fatty acid content (Raffaele et al., 2008). Another transcriptional regulator, AtSPL14, suppresses fumonisin B1-induced cell death when misregulated (Stone *et al.*, 2005).

WRKY is a large plant-specific family of transcription factors that governs transcriptional reprogramming during pathogen responses and developmental processes such as leaf senescence and some types of trichome development/maturation (Eulgem and Somssich, 2007). Members of the WRKY family are highly upregulated during abiotic and biotic stresses. Transcriptome analysis of PCD induced by hydrogen peroxide, superoxide anion radicals, and singlet oxygen identified WRKY75 as commonly induced by all three types of ROS (Gadjev *et al.*, 2006). WRKY53 is induced during senescence-associated PCD, and functional studies with knockouts and WRKY53-overexpressing plants confirmed its role in leaf senescence (Miao and Zentgraf, 2007).

The global transcriptional reprogramming results in a complete switch to a cell death program in which sets of proteases and nucleases play roles in the orderly destruction of the plant cell (Lam, 2004, 2005). Plant proteases can be involved in both the regulatory and the executionary phases of cell death, as is the case with caspases in animal apoptosis. *Caspases*, a family of cysteine proteases highly conserved from nematodes to humans, are the core signaling and execution proteases in animals (Chichkova *et al.*, 2004; He *et al.*, 2008). They are normally expressed in a dormant form and/or are localized in an isolated cellular compartment, which allows them to play the role of major regulatory switches initiating the irreversible processes of controlled cell death (Lam, 2004, 2005). In plants, both cysteine and serine protease activities have been reported to be important factors in the attainment of ROS-driven PCD (Levine *et al.*, 1996). Inhibitors of cysteine proteases have been shown as an agent suppressing the HR induced by pathogens and ROS (Solomon *et al.*, 1999). Other pharmacological studies with inhibitors of the total caspase activity and with specific inhibitors of different initiator and effector animal caspases revealed the presence of caspase-like activities in the plant cell (Chichkova *et al.*, 2004; Danon *et al.*, 2004; Urquhart *et al.*, 2007). The plant-specific vacuolar protease VPE, structurally unrelated to caspases, possesses caspase-like activity essential for PCD induced by fumonisin B1 or during HR (Hatsugai *et al.*, 2004; Kuroyanagi *et al.*, 2005). However, direct structural orthologues of canonical caspases have not been found in plants. The absence of these key regulators from the sequenced plant genomes together with the fact that apparently most instances of plant PCD are associated with the induction of caspase-like activities imply that alternative mechanisms must control PCD in plants (Lam, 2004; Sanmartin *et al.*, 2005). This role may be served by the caspase-like vacuole processing enzymes and/or the more distantly related metacaspases, which are also

found in *Protozoa*, *Fungi*, and *Chromista* (Vercammen *et al.*, 2007). Caspases, metacaspases, and paracaspases (found in *Animalia*) are seen as phylogenetically equidistant from each other (Vercammen *et al.*, 2007). The three groups share the caspase-specific catalytic diad of histidine and cysteine but the overall sequence similarity among the representatives of these three major branches is very low (Bozhkov *et al.*, 2005b). Paracaspase activity has not been implicated in the execution of cell death, but metacaspases have been found to play an important role in ROS-induced PCD in yeast and plants (Madeo *et al.*, 2002; Suarez *et al.*, 2004; Vercammen *et al.*, 2007). Plant metacaspases have been classified as type I and type II based on their sequence and structural features. *Arabidopsis* contains three type I (*AtMCP1a-1c*) and six type II (*AtMCP2a-2f*) metacaspases (Sanmartin *et al.*, 2005; Vercammen *et al.*, 2007). Metacaspases do not have caspase activities; instead, these cysteine-dependent proteases cleave their substrates after arginine and lysine and can be inhibited by the serine protease inhibitor Serpin1 (Vercammen *et al.*, 2004, 2006). It has been demonstrated that a type II metacaspase from *Picea abies*, mcII-Pa, is essential for PCD during somatic embryogenesis (Bozhkov *et al.*, 2005b). This cysteine-dependent arginine-specific protease translocates from cytoplasm to nuclei in terminally differentiated suspensor cells, destined for elimination, where it colocalizes with the nuclear pore complex and chromatin and participates in the nuclear envelope disassembly and the DNA fragmentation. Recently, *Arabidopsis* metacaspase 8 (AtMC8) has been implicated in cell death induced by UV-C, H_2O_2, and paraquat (He *et al.*, 2008). Overexpressing AtMC8 enhances PCD, while knocking out the gene retards the cell death symptoms.

Not only cysteine but also serine-dependent protease activities participate in plant PCD. Serine proteases with specificity to aspartate have been reported to be associated with the control of cell death in *Avena sativa* (Coffeen and Wolpert, 2004). A nuclear-localized serine protease and a Ca^{2+} /Mg^{2+} nuclease were recently isolated from wheat grain nucellar cells undergoing PCD (Dominguez and Cejudo, 2006).

Proteases are not simply executioners but also important regulators of the initial events in the PCD signaling cascade. This is underlined best by studying the complex role of the proteasome and the COP signalosome in cell death. Plant proteasomes degrade specific substrates targeted by ubiquitination via a series of reactions catalyzed by ubiquitin-activating (E1), conjugating (E2), and ligating (E3) enzymes (Smalle and Vierstra, 2004). The COP9 signalosome is a multiprotein complex interacting with and regulating E3 ubiquitin ligases, thus influencing the specificity of protein degradation (Serino and Deng, 2003). This is one of the many cases when an important complex is first discovered in *Arabidopsis* and later reported in other kingdoms. Proteasome-dependent proteolytic degradation is involved in myriad of plant processes related to development, hormone signaling,

stress responses, and cell death (Chini *et al.*, 2007; Moon *et al.*, 2004; Tan *et al.*, 2007). Proteasomal degradation has a dual role in PCD, as different proapoptotic or negative cell death regulators can be degraded by this proteolytic complex in particular types of cell death. This may explain why proteasome function is required for some types of PCD (e.g., cell death induced by heat shock in tobacco), while in other cases, inhibition of proteasome function triggers cell death accompanied by cytochrome *c* release from mitochondria and caspase-like activities (Kim *et al.*, 2003; Vacca *et al.*, 2007). Interestingly, manipulation of tomato ubiquitin-proteasome system by the E3 ubiquitin ligase from the bacterial pathogen *P. syringae* can suppress immunity-associated cell death (Janjusevic *et al.*, 2006).

Induction of nucleases and nuclear fragmentation are common events in PCD (Dominguez *et al.*, 2004; Zaina *et al.*, 2003). A 40 kD Zn^{2+}-dependent S1 type endonuclease 1 named ZEN1 (*Zinnia* endonuclease-1) is responsible for nuclear DNA degradation (Ito and Fukuda, 2002). Silencing of *ZEN1* suppressed the degradation of nuclear DNA in tracheary elements undergoing PCD but did not affect vacuole collapse in *Zinnia* cell suspension culture. BFN1 – a nuclease showing similarities to ZEN1 – has been associated with senescence, abscission and programmed cell death-related processes in plants (Farage-Barhom et al., 2008; Pérez-Amador *et al.*, 2000).

3. Hydrogen Peroxide and Other ROS as Signals Modulating Plant PCD

3.1. Production and removal of ROS

ROS are produced in plants and other aerobic organisms as a result of O_2 reduction during a number of normal metabolic processes. These harmful and highly reactive intermediates of O_2 reduction can damage biological molecules and structures and have been considered by many as unwelcome by-products of metabolism (Gechev *et al.*, 2006; Moller *et al.*, 2007). Plants initially developed an antioxidant system composed of antioxidant enzymes and small antioxidant molecules as a means of protection against excessive ROS production. The evolution of this antioxidant system into an elaborate network of ROS-producing and -detoxifying enzymes permitted ROS to be co-opted as signaling molecules that regulate various cellular processes, including growth, development, stress adaptation, and cell death. To modulate so many and such diverse processes, the biological response to altered ROS levels needs to be very specific. The specificity of the biological response to altered ROS levels depends on the type of ROS, the intensity of the signal, and the sites of ROS production. These multiple factors, provided by the ROS network, interact with other factors such as plant

developmental stage, previous stress encounters, plant hormones, RNS, and lipid messengers to determine the final outcome of ROS signaling.

The most important types of ROS are superoxide ($O_2^{\bullet -}$) and hydroxyl ($HO^{\bullet}$) radicals, hydrogen peroxide (H_2O_2), and singlet oxygen ($^1O_2$), reviewed in a number of recent articles (Apel and Hirt, 2004; Gechev *et al.*, 2006; Moller *et al.*, 2007). Their biochemical properties together with those of the most important RNS are summarized in Table 3.1. Hydrogen peroxide is perhaps the most prominent signaling molecule characterized by its relative stability and significant mobility. The half-life of H_2O_2 is 1 ms, the longest of all ROS types. In contrast, $O_2^{\bullet -}$ and $^1O_2$ have much shorter half-lives of about 1–4 μs and $HO^{\bullet}$ has an extremely short half-life of only 1 ns (Gechev *et al.*, 2006; Moller *et al.*, 2007). The reactivity and half-lives of different ROS are linked with their mobility in the cell: H_2O_2 can migrate from the sites of its synthesis to adjacent compartments and even neighboring cells, while the highly destructive $HO^{\bullet}$ reacts with any biomolecule it contacts and is therefore not very mobile (Bienert *et al.*, 2006, 2007; Henzler and Steudle, 2000). $O_2^{\bullet -}$ can inactivate important metabolic enzymes containing Fe-S clusters to alter enzyme activities (Halliwell, 2006; Van Breusegem *et al.*, 2001). Its protonated form, $HO_2^{\bullet}$, is found mainly in acidic cellular environments. It can cross biological membranes and initiate lipid oxidation by extracting protons from polyunsaturated fatty acids. In most biological systems, $O_2^{\bullet -}$ is rapidly converted to H_2O_2 by the enzyme SOD (Halliwell, 2006). H_2O_2 can inactivate enzymes by oxidizing their thiol groups (Halliwell, 2006). The destructive properties of $O_2^{\bullet -}$ and H_2O_2 are more prominent when they interact in the presence of metal ions to form $HO^{\bullet}$ during the so-called Haber-Weiss reaction (Kehrer, 2000). Because $HO^{\bullet}$ is highly reactive, cells do not possess enzymatic mechanisms for $HO^{\bullet}$ detoxification and rely on mechanisms that prevent its formation. These mechanisms include elimination of $O_2^{\bullet -}$ and H_2O_2 and/or sequestering Fe^{3+}/Cu^{2+} metal ions that catalyze the Haber-Weiss reaction with metal-binding proteins, such as ferritins or metallothioneins (Hintze and Theil, 2006; Mittler *et al.*, 2004). In addition to reacting with H_2O_2 and forming $HO^{\bullet}$, $O_2^{\bullet -}$ can react with $NO^{\bullet}$ to form peroxynitrite ($ONOO^-$). Peroxynitrite is rapidly protonated to peroxynitrous acid (ONOOH), which is a powerful oxidizing agent. It can damage all biomolecules and initiate reactions leading to formation of several other destructive radical- and nonradical reactive species (Halliwell, 2006). $^1O_2$ is a nonradical ROS produced by spin reversal of one electron of the ground state triplet oxygen ($^3O_2$) (Laloi *et al.*, 2006). Such spin reversals occur under input of energy and are most often caused by reaction with the highly energized triplet-state chlorophyll (Laloi *et al.*, 2006). If not quenched by carotenoids, $^1O_2$ can in turn transfer its energy to other molecules and damage them, like the rapid peroxidation of polyunsaturated fatty acids (Halliwell, 2006). As other types of ROS, $^1O_2$ can have either

Table 3.1 Most important reactive oxygen species (ROS) and reactive nitrogen species (RNS), their properties and scavengers

Type of ROS	Half-life and mobility	Mode of action	Main scavengers	References
Superoxide radical ($O_2^{\bullet -}$)	1 μs, 30 nm	Reacts with double bond-containing compounds, Fe–S clusters of proteins; reacts with $NO^{\bullet}$ to form $ONOO^-$	Superoxide dismutases (SOD)	Halliwell, 2006; Moller *et al.*, 2007
Hydrogen peroxide (H_2O_2)	1 ms, 1 μm	Oxidizes proteins (cysteine residues); reacts with $O_2^{\bullet -}$ in a Fe-catalyzed reaction to form $HO^{\bullet}$	Catalases, various peroxidases, peroxiredoxins, flavonoids	Halliwell, 2006; Moller *et al.*, 2007
Hydroxyl radical ($HO^{\bullet}$)	1 ns, 1 nm	Extremely reactive with proteins, DNA, lipids, and other biomolecules	Flavonoids, prevention of $HO^{\bullet}$ formation by sequestering Fe	Gechev *et al.*, 2006; Halliwell, 2006; Moller *et al.*, 2007
Singlet oxygen ($^1O_2$)	1 μs, 30 nm	Directly oxidizes proteins, polyunsaturated fatty acids, DNA	Carotenoids, α-tocopherol	Gechev *et al.*, 2006; Halliwell, 2006; Moller *et al.*, 2007
Nitric oxide ($NO^{\bullet}$)	Limited due to reactivity	Nitrosylates proteins via S-nitrosothiols	Hemoglobins, glutathione	Halliwell, 2006; Neill *et al.*, 2008
Peroxynitrite ($ONOO^-$)	Not determined	Very reactive with lipids, DNA and proteins		Moller *et al.*, 2007; Neill *et al.*, 2008

signaling or cytotoxic effects depending on the endogenous levels accumulated (Przybyla *et al.*, 2008).

ROS and RNS are produced by multiple sources during a variety of cellular processes at different sites in all cellular compartments (Fig. 3.2) (Gechev *et al.*, 2006). In general, ROS are maintained at constant basal levels in healthy cells, but their levels transiently or persistently increase under different stress conditions or upon developmental signals.

H_2O_2 is synthesized mainly in chloroplasts, peroxisomes, and glyoxysomes but also in the apoplast, cytosol, mitochondria, endomembrane system, and nucleus (Ashtamker *et al.*, 2007; Gechev *et al.*, 2006). Chloroplasts are a major site of ROS generation in plants (Asada, 2006). Photosynthetic electron transfer chains produce $O_2^{\bullet -}$, especially under conditions leading to overenergization of the electron transfer chains (Dat *et al.*, 2000). $O_2^{\bullet -}$ is formed by electron leakage from Fe-S centers of photosystem I, reduced ferredoxin (Mehler reaction), or the acceptor side of photosystem II to O_2 and is then quickly metabolized to H_2O_2 by SOD. Although excessive production of ROS is dangerous, in this case the ability of oxygen to accept electrons prevents overreduction of the electron transport chains, thus minimizing the chance of $^1O_2$ accumulation (Dat *et al.*, 2000). $^1O_2$ is produced by energy transfer to $^3O_2$ from the excited triplet state chlorophyll in photosystem II, especially under high light intensities (Laloi *et al.*, 2006). Carotenoids can quench $^1O_2$ directly, a role which is shared with tocopherols or prevent $^1O_2$ formation by quenching the excited triplet state chlorophyll (Asada, 2006). Peroxisomes and glyoxysomes are other major sites of H_2O_2 generation during photorespiration and fatty acid oxidation, respectively (del Rio *et al.*, 2006). Photorespiration is a complex process tightly linked to photosynthesis. Under conditions that impair CO_2 fixation in chloroplasts, the ribulose-1,5-bisphosphate carboxylase oxygenase activity increases and the produced glycolate moves to peroxisomes, where it is oxidized by glycolate oxidase forming H_2O_2. Fatty acid oxidation in glyoxysomes of germinating seeds generates H_2O_2 as a by-product of the acyl-CoA-oxidase enzyme activity. Mitochondrial respiration is another process leading to H_2O_2 and $O_2^{\bullet -}$ formation (Moller, 2001). The main sources of ROS production in mitochondria are NADH dehydrogenase, ubiquinone radical, and complex III (Moller, 2001). Although mitochondrial ROS production is much lower compared to chloroplasts (no $^1O_2$ production, lack of light energy-absorbing chlorophyll pigments), mitochondrial ROS are important regulators of a number of cellular processes, including stress adaptation and PCD (Robson and Vanlerberghe, 2002). The estimated H_2O_2 production in mitochondria may be 20 times slower than in chloroplasts, at least in C_3 plants (Foyer and Noctor, 2003). Plasma membrane-bound NAD(P)H oxidases as well as cell wall-associated extracellular peroxidases are the main H_2O_2- and $O_2^{\bullet -}$-producing enzymes in the apoplast (Bindschedler *et al.*, 2006; Choi *et al.*, 2007; Sagi and Fluhr,

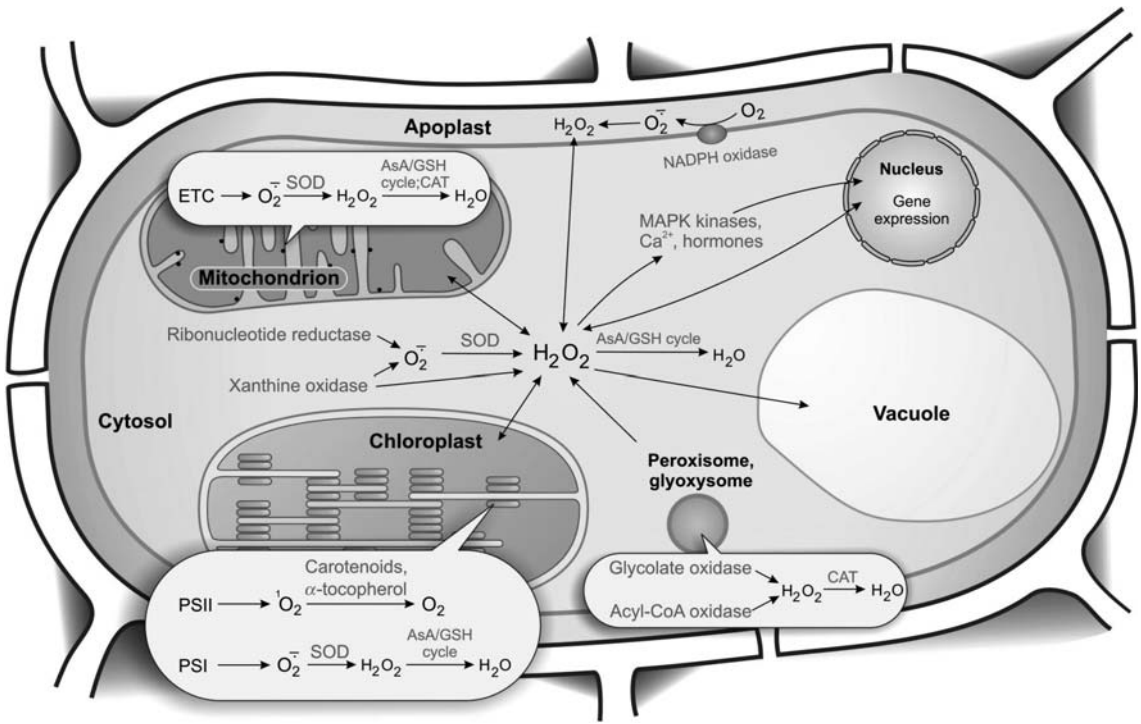

Figure 3.2 Production and metabolic fate of various ROS (hydrogen peroxide, superoxide anion radical, singlet oxygen) in different cellular compartments. Major enzymes and nonenzymatic components involved in ROS homeostasis are indicated. Plants have many different sources of ROS and have evolved elaborate mechanisms to scavenge and utilize the various forms of ROS. Abbreviations are as follows: ROS, reactive oxygen species; PSI, photosystem I; PSII, photosystem II; ETC, electron transport chain; SOD, superoxide dismutase; CAT, catalase; AsA/GSH, ascorbic acid/glutathione.

2006). These enzymes are regulated by various developmental and environmental stimuli. Most notably, ROS produced by them participate in the so-called oxidative burst observed as a part of the pathogen-induced HR but also regulate cell growth, development, and cell death (Foreman *et al.*, 2003; Gapper and Dolan, 2006; Laloi *et al.*, 2006; Sagi and Fluhr, 2006; Torres *et al.*, 2002). $O_2^{\bullet -}$ and H_2O_2 are produced also by xanthine oxidase during purine catabolism, ribonucleotide reductase during deoxyribonucleotide synthesis, and various other oxidases induced by biotic and abiotic stresses. The nucleus has also recently been reported as a site of H_2O_2 production (Ashtamker *et al.*, 2007). Studies on cryptogein-induced ROS production during cell death of *Nicotiana tabacum* BY-2 suspension cells with Amplex Red/Amplex Ultra Red reagents, which report real time H_2O_2 accumulation, revealed that internal signals develop more rapidly than the external apoplastic signals. Using 2′,7′-dichlorofluorescein diacetate as a fluorescent probe, subcellular accumulation of H_2O_2 was first detected in the nucleus and then, after a short delay, in the endomembrane system and cytoplasm (Ashtamker *et al.*, 2007). The authors report that even isolated nuclei are capable of producing H_2O_2 in a calcium-dependent manner.

Balancing H_2O_2 and other ROS levels is essential to ensure an accurate execution of their signaling functions and to prevent their toxicity. Therefore, plants have evolved an elaborate antioxidant system, consisting of enzymes and nonenzymatic antioxidants, which together with the ROS-producing enzymes maintain ROS homeostasis in all cellular compartments and adjust ROS levels according to the cellular need at a particular time (Table 3.2) (Mittler *et al.*, 2004). SODs are the only plant enzymes capable of scavenging $O_2^{\bullet -}$, while H_2O_2 can be catabolized directly by catalases or with the aid of various reductants by APXs, peroxiredoxins, glutathione peroxidases (GPX), and the heterogenous group of guaiacol peroxidases (Dat *et al.*, 2000). Nonenzymatic antioxidants also contribute to ROS homeostasis, with ascorbate, glutathione, tocopherol, and carotenoids as the most abundant water- and lipid-soluble antioxidants (Table 3.3) (Dellapenna and Pogson, 2006). As catalase degrades H_2O_2 without any reducing power, this enzyme provides plants with an energy-efficient way to remove H_2O_2. However, catalase is active only at relatively high H_2O_2 concentrations. Lower H_2O_2 levels are eliminated by APX and other peroxidases with the aid of various reductants like ascorbate and glutathione. Whereas some of the ROS network enzymes such as SOD, catalase, and APX are entirely dedicated to ROS homeostasis, others like guaiacol peroxidases, thioredoxins, ferritins, and glutathione-*S*-transferases are involved also in various other processes related to control of development, redox regulation of target proteins, and detoxification reactions. Some of the ROS-associated enzymes, like guaiacol peroxidases, thioredoxins, glutaredoxins, and glutathione-*S*-transferases, have evolved into very large

Table 3.2 Most important plant enzymes and antioxidants involved in reactive oxygen species (ROS) and reactive nitrogen species (RNS) homeostasis

Enzyme/antioxidant	Function	Localization	References
NADPH oxidases	Generate ROS ($O_2^{\bullet -}$ and eventually H_2O_2). Localized production of ROS by NADPH oxidases is involved in plant growth and pathogen-induced cell death	pm	Gechev *et al.*, 2006
Guaiacol peroxidases (POX)	Detoxify H_2O_2 with various substrates as reductants; can also produce ROS ($O_2^{\bullet -}$, $HO^{\bullet}$, $HOO^{\bullet -}$). Involved in lignin biosynthesis, hormone metabolism, cross-linking of cell wall polymers, pathogen defense, plant development, senescence, and symbiotic interactions	cw, vac, cyt, mit	Bindschedler *et al.*, 2006; Passardi *et al.*, 2004; Prasad *et al.*, 1995
Glycolate oxidase	Generates significant amounts of H_2O_2 during conversion of photorespiratory glycolate to glyoxylate	per	Dat *et al.*, 2000
Acyl-CoA-oxidase	Produces H_2O_2 during fatty acids oxidation in glyoxysomes	gly	Dat *et al.*, 2000
Ribonucleotide reductase	Involved in DNA synthesis. Generates $O_2^{\bullet -}$ as by-product in cytosol	cyt	Fontecave *et al.*, 1987
Xanthine oxidase	Generates H_2O_2 as by-product from purine catabolism	cyt	Dat *et al.*, 2000
Nitric oxide synthase/ nitric oxide associated	Involved in production of $NO^{\bullet}$	cyt, myt, chl	Neill *et al.*, 2008
Nitrate reductase	Converts nitrate to nitrite. Produces $NO^{\bullet}$	cyt	Neill *et al.*, 2008

(*continued*)

Table 3.2 (*continued*)

Enzyme/antioxidant	Function	Localization	References
Superoxide dismutase (SOD)	Dismutation of $O_2^{\bullet -}$; leads to H_2O_2 formation	chl, cyt, mit, per	Mittler *et al.*, 2004
Catalase	Detoxifies H_2O_2; no reductant required	per, gly, mit	Dat *et al.*, 2000
Ascorbate peroxidase (APX)	Detoxifies H_2O_2 with ascorbate as reductant	chl, cyt, per, mit	Asada, 2006
Monodehydroascorbate reductase (MDHAR)	Reduces monodehydroascorbate radicals with NAD(P)H as reductant	chl, mit, cyt	Mittler *et al.*, 2004
Dehydroascorbate reductase (DHAR)	Reduces dehydroascorbate radicals with GSH as reductant	chl, mit, cyt	Mittler *et al.*, 2004
Glutathione reductase (GR)	Reduces oxidized glutathione with NADPH as reductant	chl, mit, per, cyt	Mittler *et al.*, 2004
Glutathione peroxidases (GPX)	Detoxify H_2O_2 and lipid hydroperoxides with GSH as reductant	chl, cyt, mit, er	Mittler *et al.*, 2004
Glutathione-*S*-transferases (GST)	Detoxification reactions (glutathionation); can detoxify lipid hydroperoxides and exhibit DHAR activity; and can act as noncatalytic carriers that facilitate the distribution and transport of various biomolecules	cyt, chl, mit, nuc, apo	Moons, 2005
Peroxiredoxins (Prx)	Thiol-containing peroxidases, detoxify H_2O_2	chl, mit, nuc	Mittler *et al.*, 2004
Thioredoxins (Trx)	Redox-control of enzymes and transcription factors, electron donor to Prx and GPX	chl, cyt, mit, nuc	Mittler *et al.*, 2004
Glutaredoxins (Grx)	Deglutathionilation, redox-control of enzymes and transcription factors, electron donor to DHA and Prx. Protection against oxidative damage, reacts with $NO^{\bullet}$, and regulation of plant development	chl, cyt, mit, plasmalemma, er	Rouhier *et al.*, 2004

Ferritin	Binds iron, thus sequestering it in a bioavailable, nontoxic form and preventing formation of $HO^{\bullet}$. Iron homeostasis	chl, mit	Hintze and Theil, 2006
Alternative oxidases (AOX)	Channel electrons from electron transfer chains of mitochondria and chloroplasts directly to oxygen, thus minimizing $O_2^{\bullet -}$ production under conditions that favor electron transport chain overenergization. The chloroplastic AOX homologue immutants also participates in carotenoid biosynthesis	chl, mit	Mittler *et al.*, 2004
Ascorbate	Substrate for APX. Detoxifies H_2O_2	chl, cyt, mit, per, vac, apo	Asada, 2006
Glutathione	Substrate for various peroxidases, glutathione transferases, and glutathione reductases. Detoxifies H_2O_2, other hydroperoxides, and toxic compounds	chl, cyt, mit, per, vac, apo	Dat *et al.*, 2000
α-Tocopherol	Protects membrane lipids from peroxidation, detoxifies lipid peroxides, and quenches $^1O_2$	Membranes	Dellapenna and Pogson, 2006
Carotenoids	Quench $^1O_2$. Photosystem assembly, key components of the light harvesting complex, precursors of ABA	chl, chromo-, elaio-, and amyloplasts	Dellapenna and Pogson, 2006
Flavonoids	Can directly scavenge H_2O_2 and $HO^{\bullet}$	Vac	Edreva, 2005; Gould *et al.*, 2002
Hemoglobins	Involved in $NO^{\bullet}$ scavenging	Cyt	Neill *et al.*, 2008

The abbreviations are chl, chloroplasts; cyt, cytosol; myt, mitochondria; nuc, nucleus; er, endoplasmatic reticulum; vac, vacuole; per, peroxisomes; gly, glyoxysomes; cw, cell wall; apo, apoplast.

Table 3.3 Plant-specific proteins involved in H_2O_2 network and PCD

Gene/protein	Function	References
BAK1	LRR protein kinase, coreceptor with FLS2 for brassinosteroid signaling and cell death; BAK1 has also brassinoid-independent role in PCD. *Bak1* mutants challenged with flagellin do not mount H_2O_2 burst but when challenged with necrotrophic pathogens have enhanced production of ROS and PCD	Chinchilla *et al.*, 2007; Kemmerling *et al.*, 2007
AtPep1	Upregulated by H_2O_2. AtPep1 can induce H_2O_2 synthesis and defense gene expression as well as its own precursor gene	Huffaker and Ryan, 2007; Huffaker *et al.*, 2006
LCB1	Subunit of serine palmitoyltransferase, mutants fail to generate ROS, and execute PCD after FB1 treatment	Shi *et al.*, 2007
LOH2	*Loh2* mutants exhibit perturbations in sphingolipid biosynthesis, accumulation of H_2O_2 and PCD upon AAL-toxin treatment	Gechev *et al.*, 2004
ACD2	Protects from PCD that requires early oxidative burst in mitochondria	Yao and Greenberg, 2006
ANP1	H_2O_2-inducible MAPKKK, activates Arabidopsis kinases MPK3 and MPK6 and eventually transcription of GST6 and HSP18.2. Overexpression of ANP1 induces multiple stress tolerance	Kovtun *et al.*, 2000
OXI1	H_2O_2 inducible, needed for full activation of MPK3 and MPK6 and normal root hair growth	Rentel *et al.*, 2004
OMTK1	MAPKKK in alfalfa specific to H_2O_2, activates downstream MAP kinase MMK3 to channel the H_2O_2 cell death signal	Nakagami *et al.*, 2004
AtNDK1	Interacts with Arabidopsis catalases; overexpression leads to increased resistance to paraquat and ability to eliminate H_2O_2	Fukamatsu *et al.*, 2003
NDPK2	Reduces accumulation of H_2O_2, enhances abiotic and oxidative stress tolerance	Moon *et al.*, 2003
GSTs	Marker for H_2O_2 accumulation; various roles in protection against abiotic and oxidative stress tolerance	Gechev *et al.*, 2006; Kovtun *et al.*, 2000

HSPs	Marker for H_2O_2; protective role against stress; possible role as H_2O_2 sensor	Kovtun *et al.*, 2000; Miller and Mittler, 2006
Thioredoxin h5 ATTRX5	Participates in H_2O_2 homeostasis. Required for victorin-induced PCD	Sweat and Wolpert, 2007
LSD1	Negative regulator of ROS-induced cell death. Mutations lead to increase in H_2O_2 and ethylene production and enhanced hypoxia-induced PCD during lysigenous aerenchyma formation	Dietrich *et al.*, 1997; Muhlenbock *et al.*, 2007
LOL1	Positive regulator of ROS-induced cell death; antagonizes LSD1	Epple *et al.*, 2003
WRKY53	WRKY53 can be induced by H_2O_2 and can regulate its own expression in a negative feed back loop. Involved in senescence-induced cell death	Miao *et al.*, 2004
Zat12	Induced by H_2O_2 and other ROS. ZAT12 overexpressors have elevated levels of oxidative stress-related transcripts, while ZAT12-deficient plants are more sensitive to H_2O_2-induced cell death	Davletova *et al.*, 2005b
AtMC8	Protease mediating UV and H_2O_2-induced cell death. Overexpression of MC8 enhances, while knockout reduces, H_2O_2-dependent cell death in protoplasts	He *et al.*, 2008
Proteasome subunits	Many proteasome components upregulated during H_2O_2-induced PCD. Involved in several types of cell death	Kim *et al.*, 2003; Vacca *et al.*, 2007; Vandenabeele *et al.*, 2004
ZEN1	Nuclease involved in nuclear DNA fragmentation during PCD in tracheary elements differentiation	Ito and Fukuda, 2002

multigene families with diverse functions to facilitate the adaptation of the photosynthesizing organisms to terrestrial life in elevated oxygen concentrations and different stressful environments (Meyer *et al.*, 2005; Moons, 2005; Passardi *et al.*, 2004; Prasad *et al.*, 1995; Rouhier *et al.*, 2004). These and other antioxidant enzymes together with the ROS-producing enzymes compose a highly sophisticated and redundant network, which in *A. thaliana* consists of at least 289 genes (Table 3.2) (Gechev *et al.*, 2006).

All cellular compartments that produce ROS, including chloroplasts, mitochondria, peroxisomes, and the cytosol, are well-equipped with antioxidant enzymes and antioxidants (Fig. 3.2, Table 3.2). ROS are normally scavenged at the sites of their production by the local antioxidant systems. However, when the local antioxidant capacity cannot cope with the ROS generation levels (e.g., during high ROS production under stress or reduced antioxidant enzyme activities upon developmental signals), H_2O_2 can leak from those compartments into the cytosol and other compartments. As a next line of defense, plants may have evolved mechanisms to deal with excess H_2O_2 by transporting and detoxifying it in vacuoles (Gould *et al.*, 2002). Vacuoles are very rich in flavonoids, powerful antioxidants that can scavenge hydrogen peroxide, singlet oxygen, superoxide, hydroxyl, peroxyl radicals, and peroxynitrite (Edreva, 2005; Tsuda *et al.*, 2000). They also contain high levels of ascorbate, glutathione, and peroxidases localized at the tonoplast inner surface (Gould *et al.*, 2002).

3.2. Biological functions modulated by ROS: Plant growth, development, stress responses, and PCD

Hydrogen peroxide modulates a number of biological functions including seed dormancy, pollen tube and root hair growth and elongation, tuber development in potato, numerous stress responses, and PCD (Gechev *et al.*, 2006; Kim *et al.*, 2007; Oracz *et al.*, 2007).

Inability of mature seeds to germinate under favorable conditions, referred to as seed dormancy, is an important adaptive phenomenon enabling seeds to delay germination until conditions are more appropriate for seedling growth (Oracz *et al.*, 2007). Breaking dormancy in most species occurs during storage in dry conditions or during imbibition at low temperature (stratification). Releasing seed dormancy in sunflower is associated with marked production of H_2O_2 and $O_2^{\bullet -}$ in cells of embryonic axes (Oracz *et al.*, 2007). Moreover, treating seeds with ROS-generating herbicide paraquat was able to release the dormancy, and specific embryo proteins became oxidized.

ROS generated by NADPH oxidases are involved in pollen tube growth. Transgenic tobacco plants with antisense constructs to silence pollen-specific NADPH oxidase by decreasing specific mRNA levels displayed inhibited pollen tube growth (Potocky *et al.*, 2007). Normal growth

of the pollen tube was restored by exogenous application of H_2O_2. Genetic evidence for the role of ROS in plant growth is provided by the double mutant of two *Arabidopsis* NADPH oxidase homologues, *atrbohD* and *atrbohF*, which not only has decreased ROS accumulation after pathogen challenge but also has reduced ABA-mediated seed germination and root elongation inhibition (Kwak *et al.*, 2003; Torres *et al.*, 2002). Furthermore, studies on the *atrbohC* mutant revealed that it has low ROS levels and defective root hair growth (Foreman *et al.*, 2003). Consistent with these findings, knockout mutation of the *A. thaliana* serine/threonine kinase *oxi1* results in reduced root hair growth (Rentel *et al.*, 2004). H_2O_2 production may have, on the other hand, an inhibitory effect on growth, as suggested by the inhibition of auxin responses by ANP1, the MAPK kinase kinase that relays the H_2O_2 signal in *A. thaliana* (Kovtun *et al.*, 2000). The balance between $O_2^{\bullet -}$ and H_2O_2 is also believed to regulate plant growth and tuber development in potato (Kim *et al.*, 2007).

Hydrogen peroxide is an important modulator of plant stress responses. Significant increases in endogenous H_2O_2 levels are observed during a number of adverse environmental conditions as a result of increased ROS production and/or impaired ROS detoxification (Dat *et al.*, 2000; Mittler *et al.*, 2004). Extreme temperatures, drought, UV and high light intensities, and many pollutants can cause oxidative stress and cell death (Dat *et al.*, 2000; Gechev *et al.*, 2004). In addition, H_2O_2 is a secondary messenger during wounding responses and various biotic interactions (Bais *et al.*, 2003; Orozco-Cardenas *et al.*, 2001). Redox changes are sensed by the plant cell as a ''warning'' message, and depending on the situation, genetic programs leading to stress acclimation or PCD are switched on (Gechev *et al.*, 2002). Small transient increases in H_2O_2 serve as signals triggering stress acclimation against subsequent more severe abiotic or oxidative stress. Protective roles for H_2O_2 have been demonstrated against chilling, salt, high light, heat, and oxidative stress (Karpinski *et al.*, 1999; Lopez-Delgado *et al.*, 1998). H_2O_2-induced acclimation can be very durable; for example, the tolerance to high temperature lasts more than a month after the initial H_2O_2 treatment (Lopez-Delgado *et al.*, 1998). H_2O_2 can initiate acclimation not only in local leaves but also in distant nonacclimated leaves, a process referred to as systemic acquired acclimation (Karpinski *et al.*, 1999). H_2O_2 is also involved in initiating cell death-protective responses in the neighboring cells that surround the sites of the HR to pathogens and triggers systemic acquired resistance in distant tissues (Alvarez *et al.*, 1998; Torres *et al.*, 2005). Consistent with its signaling role, H_2O_2 can alter resistance against a number of pathogens (Chamnongpol *et al.*, 1998). H_2O_2-induced stress tolerance can be explained by activation of defense mechanisms such as antioxidant enzymes, MAPKs, stress-specific transcription factors, dehydrins, low-temperature-induced, heat-shock, and pathogenesis-related proteins (Gechev *et al.*, 2002; Karpinski *et al.*, 1999; Moon *et al.*, 2003; Vranova

et al., 2002). Genes involved in both induction and maintenance of stress acclimation are part of these defense mechanisms (Charng *et al.*, 2006).

H_2O_2-induced cell death is implicated in a number of developmental processes and stress responses. These include the already mentioned aleurone cell death, lysigenous aerenchyma formation, tracheary elements maturation, trichome development, formation of lace leaf shape, organ senescence, plant–plant allelopathic interactions, the HR to pathogens, and some types of necrotrophic cell death (Fig. 3.1). Thus, paradoxically, H_2O_2-induced cell death is essential for plant growth, development, and proper responses to the environment (Gechev *et al.*, 2006). At the same time, cell death can be an unwanted event during many unfavorable environmental conditions, including heat, cold, salt and xenobiotic stresses, and compatible or disease-causing plant–pathogen interactions (Koukalova *et al.*, 1997; Swidzinski *et al.*, 2002).

PCD can be initiated also by other types of ROS, including singlet oxygen and superoxide radicals (Dat *et al.*, 2003; Op den Camp *et al.*, 2003; Vranova *et al.*, 2002). In addition, $HO^{\bullet}$-initiated lipid peroxidation is a rich source of oxidized lipids that can trigger PCD on their own or in concert with other ROS (Montillet *et al.*, 2005; Mueller, 2004). Singlet oxygen-induced enzymatic lipid peroxidation, however, is likely a part of stress response pathway rather than a cell death or growth inhibition pathway as double *flu/aos* mutants, producing singlet oxygen but with compromised jasmonate biosynthesis, have the same growth inhibition and cell death as the single *flu* mutant (Przybyla *et al.*, 2008).

3.3. Specificity of ROS signals: How different responses like stress acclimation or PCD are achieved?

One of the intriguing questions is how H_2O_2 and other ROS, being such simple molecules, can regulate so many different processes in different cell types and organs at different developmental stages. It is now accepted that the biological outcome of ROS signaling depends on multiple factors including ROS chemical identity and sites of production, duration and intensity of the signal (Gechev *et al.*, 2006; Queval *et al.*, 2007), developmental stage of the plant, previous stress encounters, and interaction with other signaling molecules such as NO, lipid messengers, and plant hormones (Kwak *et al.*, 2006; Zaninotto *et al.*, 2006). H_2O_2 is the most prominent ROS signal. In recent years, a number of microarray- or AFLP-based studies identified many genes that respond to elevated H_2O_2 levels (Desikan *et al.*, 2001; Gechev *et al.*, 2005; Levine *et al.*, 1994; Vandenabeele *et al.*, 2003, 2004; Vanderauwera *et al.*, 2005). In addition, mutants presumably involved in H_2O_2 signaling were identified (Table 3.3). Signaling properties and distinct transcriptional responses were also confirmed for the other ROS (Demidchik *et al.*, 2003; Op den Camp *et al.*,

2003; Vranova *et al.*, 2002). Comparing the transcriptional responses to different ROS, specific transcription footprints for $O_2^{\bullet -}$, $^1O_2$, and H_2O_2 have been identified (Gadjev *et al.*, 2006). This specificity can be determined by promoter modules specific for the various types of ROS (Shao *et al.*, 2007).

The fate of the ROS signaling is to a large extent related to the chemical properties of different ROS and their doses (Gechev *et al.*, 2002; Op den Camp *et al.*, 2003; Vranova *et al.*, 2002). In general, low doses of $O_2^{\bullet -}$ and H_2O_2 protect against oxidative and abiotic stress, while high doses trigger cell death (Gechev *et al.*, 2002; Vranova *et al.*, 2002). This cell death is genetically programmed, although extremely high doses of ROS can cause necrosis (Laloi *et al.*, 2006; Montillet *et al.*, 2005; Van Breusegem and Dat, 2006).

The site of ROS production is of particular importance to the biological outcome of the initial signal (Carol *et al.*, 2005; Mullineaux *et al.*, 2006). Localized production of $O_2^{\bullet -}$ by NADPH oxidase in the root hair tip triggers Ca^{2+} peaks at the hair tip necessary for the root hair growth (Foreman *et al.*, 2003). This spatial regulation of NADPH oxidase activity is regulated by the Rho-like GTPases (Carol *et al.*, 2005). These GTPases also control tracheary element differentiation through localized ROS production (Nakanomyo *et al.*, 2002).

Although H_2O_2 is relatively mobile, there may be "hot spots" of hydrogen peroxide within the cell. Similar hot spots are even more likely to occur for the other, less mobile, types of ROS: $^1O_2$, $O_2^{\bullet -}$, and especially $HO^{\bullet}$. In contrast with others, H_2O_2 can migrate quite a distance from the site of its production and even cross biological membranes through specialized aquaporins (Bienert *et al.*, 2006, 2007; Henzler and Steudle, 2000). This transport is another way of adjusting the local concentration of H_2O_2, modulating the biological effect. Example of cross-compartment communication associated with H_2O_2 mobility is the increased levels of H_2O_2 produced in cytosol in the absence of the cytosolic APX, which leads to inhibition of chloroplastic APX and collapse of the chloroplastic antioxidant system (Davletova *et al.*, 2005a). It has also been shown that peroxisomal catalase can act as a sink for H_2O_2 produced in peroxisomes or elsewhere (Willekens *et al.*, 1997).

3.4. Hydrogen peroxide signaling network: Perception, transduction, and transcription factors

In recent years, a variety of forward and reverse genetics studies revealed a number of components in the H_2O_2 signaling network, including protein kinases, protein phosphatases, and ROS-responsive transcription factors (Table 3.3). Among these genes, many are involved in the generation of H_2O_2 and are required for PCD and other biological responses (e.g., NADPH oxidases, extracellular peroxidases), whereas others are involved

in the modulation of H_2O_2 and other ROS levels (e.g., catalase, APXs, and other antioxidant enzymes, Table 3.2).

One of the earliest events that follow elevation in H_2O_2 levels is alteration in sodium, potassium, and calcium ion fluxes discussed earlier. The transient Ca^{2+} oscillations are stress-specific and can lead to various downstream effects through the numerous Ca^{2+}-interacting proteins, including calmodulins and calcium-dependent protein kinases or/and over-amplification of the H_2O_2 signal. In addition to calcium-dependent protein kinases, a vast network of MAPKs is involved in relaying the H_2O_2 signal. With its 20 MAPKs, 10 MAPK kinases and 60 MAPK kinase kinases in *Arabidopsis*, the versatile MAPK network offers many convergence and divergence points for different stress signals (Ichimura *et al.*, 2002). MAPK kinase cascades mediate PCD triggered by pathogens or chloroplast-derived H_2O_2 (Asai *et al.*, 2002; Liu *et al.*, 2007). The MAPK kinase kinase MEKK1 is regulated by different stresses and H_2O_2 in a proteasome-dependent manner (Nakagami *et al.*, 2006). It activates the downstream MAPK MPK4. Compromising MEKK1 results in impaired H_2O_2-induction of MPK4. Surprisingly, MEKK1 can interact directly with WRKY53, transcription factor involved in senescence-induced PCD, thus bypassing downstream kinases (Miao *et al.*, 2007). The H_2O_2-inducible MAPK kinase kinase ANP1 activates two downstream MAPKs, AtMPK3 and AtMPK6, to eventually regulate gene expression of specific H_2O_2-inducible transcripts (Kovtun *et al.*, 2000). Two of the upregulated genes, GST6 and HSP18.2, as well as the whole heat-shock regulon are both reliable markers for H_2O_2 production and protectors against abiotic and oxidative stress (Gechev and Hille, 2005; Vanderauwera *et al.*, 2005). In addition, heat-shock proteins have been implicated as possible H_2O_2 sensors (Miller and Mittler, 2006). Overexpression of ANP1 in transgenic plants resulted in increased tolerance to heat shock, freezing, and salt stress (Kovtun *et al.*, 2000). The serine/threonine kinase OXI1 (*oxi*dative signal-inducible *1*) is another essential component of the H_2O_2 signaling network in *A. thaliana* (Rentel *et al.*, 2004). It is inducible by abiotic stress and H_2O_2. OXI1 activity is required for full activation of AtMPK3 and AtMPK6. *Oxi1* mutants have abnormal root hair growth and enhanced susceptibility to pathogen infection, demonstrating once more the importance of ROS in plant development and stress responses (Rentel *et al.*, 2004). Another H_2O_2-inducible kinase is OMTK1 in alfalfa (Nakagami *et al.*, 2004). In contrast to OXI1, OMTK1 is specific to H_2O_2. OMTK1 activates MMK3, downstream MAPK that can also be activated by ethylene and elicitors (Nakagami *et al.*, 2004).

Nucleotide diphosphate kinases are other components of the H_2O_2 signaling network. *Arabidopsis NUCLEOTIDE DIPHOSPHATE KINASE2* (*NDK2*) is also inducible by H_2O_2 and its overexpression reduces the accumulation of H_2O_2 and enhances tolerance to cold, salt,

and oxidative stresses (Moon *et al.*, 2003). *Arabidopsis* NDK1 interacts with the three *A. thaliana* catalases; its overexpression results in enhanced ability to detoxify H_2O_2 and resistance to paraquat (Fukamatsu *et al.*, 2003).

The H_2O_2 gene network eventually transmits the signal to ROS-specific transcription factors. Some of these are the previously described zinc finger proteins LSD1 and LOL1, negative and positive regulators of ROS-induced cell death, the senescence-specific WRKY53, and the ROS-inducible WRKY75 and heat-shock transcription factors (Table 3.3) (Dietrich *et al.*, 1997; Epple *et al.*, 2003; Gechev *et al.*, 2005; Miao *et al.*, 2004; Vanderauwera *et al.*, 2005). Two other zinc finger transcription factors, Zat11 and Zat12, are induced by H_2O_2 and other ROS (Gadjev *et al.*, 2006). Overexpressing Zat12 results in elevated transcript levels of oxidative- and light stress-responsive transcripts, while compromising Zat12 results in increased sensitivity to H_2O_2-induced oxidative stress (Rizhsky *et al.*, 2004; Davletova *et al.*, 2005b).

Transcriptional reprogramming resulting from the activation of cell death-specific factors eventually leads to activation of execution components of the H_2O_2 cell death network (Table 3.3). Among these are various proteases (AtMC8, proteasome pathway) and nucleases (ZEN1) that take part in the orderly dismantling of the plant cell.

3.5. ROS interaction with other signaling molecules modulates plant PCD

Interaction with other signaling molecules such as $NO^{\bullet}$, lipid messengers, or plant hormones determines the outcome or fine-tune the biological response to altered ROS levels (Kwak *et al.*, 2006; Zaninotto *et al.*, 2006). $NO^{\bullet}$ itself controls growth and development in a complex manner through modulation of Ca^{2+}, calcium-dependent protein kinases, cGMP, and MAPKs (Neill *et al.*, 2008). For example, $NO^{\bullet}$ interacts with H_2O_2 and $O_2^{\bullet -}$ to regulate cell death during HR (Delledonne *et al.*, 2001). It has been proposed that ROS are key mediators in channeling $NO^{\bullet}$ into the death pathway. *Arabidopsis* overexpressing the H_2O_2-detoxifying enzyme thylakoid APX has increased resistance toward NO-induced cell death (Murgia *et al.*, 2004).

Lipid-derived messengers also interplay with ROS to modulate PCD. Sphingolipids are bioactive lipids that regulate plant growth and PCD (Liang *et al.*, 2003). Fumonisin B1 and AAL-toxin inhibit ceramide synthase, resulting in accumulation of free sphingoid bases and depletion of complex ceramides, followed by H_2O_2 accumulation and subsequent cell death (Gechev *et al.*, 2004). The resistance to the two toxins in tomato and *Arabidopsis* is controlled by genes most likely parts of the ceramide synthase (Brandwagt *et al.*, 2000; Gechev *et al.*, 2004). The accumulation of free sphingoid bases seems to be crucial for triggering PCD as inhibiting serine

palmitoyl transferase (SPT), enzyme that catalyzes the first, rate-limiting step of sphingolipid biosynthesis, results in reduced cell death symptoms (Spassieva *et al.*, 2002). A recently isolated mutant of long-chain base 1 (LCB1), component of SPT, was indeed compromised in accumulation of sphingoid bases in response to FB1, ROS burst, and cell death (Shi *et al.*, 2007). Supporting this scenario, direct feeding with sphingoid bases was able to induce ROS accumulation and cell death. Hydroxylation of sphingoid long chain bases is also related to plant growth and cell death, as *Arabidopsis* compromised simultaneously in the two long-chain-base hydroxylase genes *Sphingoid Base Hydroxylase1* and *Sphingoid Base Hydroxylase2* exhibit dwarfism and PCD (Chen *et al.*, 2008). The interplay between sphingolipids and ROS during cell death was further substantiated by isolation of mutants more tolerant to fungal toxin- and ROS-induced cell death (Gechev *et al.*, 2008; Gechev and Hille, 2005; Stone *et al.*, 2000).

Other lipids capable of modulating H_2O_2-induced cell death are oxylipins and phospholipids (Loeffler *et al.*, 2005; Meijer and Munnik, 2003). The oxylipin phytoprostane B1, for example, can trigger detoxification and defense responses, and plants primed with phytoprostane B1 are more tolerant to oxidative stress-induced cell death (Loeffler *et al.*, 2005). H_2O_2 can activate phospholipase D in *Arabidopsis* and the released phosphatidic acid can inhibit H_2O_2-induced cell death (Zhang *et al.*, 2003). Plants with compromised phospholipase D are unable to release phosphatidic acid and are more susceptible to H_2O_2-induced cell death.

H_2O_2-induced cell death and stress responses are influenced by a variety of plant hormones. H_2O_2 is in complex interaction with a number of plant hormones to regulate PCD. Ethylene and SA are positive regulators of several types of H_2O_2-induced cell death, including PCD during lysigenous aerenchyma formation and the HR (Muhlenbock *et al.*, 2007; Wang *et al.*, 2002). Abiotic, biotic, and oxidative stress can stimulate ethylene biosynthesis through activation of ACC synthase and ACC oxidase; in turn, the elevated levels of both ethylene and SA can overamplify the H_2O_2 signal (Wang *et al.*, 2002). Interactions of ethylene and H_2O_2 are not confined to regulation of cell death. These two signaling molecules, together with ABA, have recently been reported to regulate stomatal closure in *Arabidopsis* (Desikan *et al.*, 2005). Ethylene and ROS are also positive regulators of leaf senescence (Lim *et al.*, 2007). Jasmonic acid, on the other hand, is a negative regulator of leaf senescence. The jasmonate-inducible protein ESR/ESP interacts in an antagonistic fashion with the senescence-specific, H_2O_2-inducible transcription factor WRKY53 (Miao and Zentgraf, 2007). GA is stimulating H_2O_2 burst through inhibition of antioxidant enzymes to trigger H_2O_2-dependent cell death in aleurone layer of monocots (Fath *et al.*, 2001). Small polypeptide hormones, including systemin and the recently identified AtPep1, can stimulate H_2O_2 synthesis and activate defense gene expression in *Arabidopsis* (Huffaker and Ryan, 2007; Huffaker *et al.*, 2006;

Orozco-Cardenas *et al.*, 2001). AtPep1 itself is regulated by H_2O_2 and can induce its own precursor gene *propep1*, suggesting a possible amplification of the H_2O_2 signal (Huffaker *et al.*, 2006). PROPEP1 and PROPEP2 are elevated during H_2O_2 and AAL-toxin-induced cell death (Gechev *et al.*, 2004; Huffaker *et al.*, 2006).

4. Concluding Remarks

We have reviewed the latest body of literature related to ROS-mediated PCD in plants. Given the intensive interest in this area of research, as it relates to both general aspects of plant development and responses to abiotic and biotic stress, we were unable to include all of the vast information currently available and apologize for omission of relevant citations. Further characterization of the genes identified and their physiological functions in different aspects of plant development and response to environmental fluctuations will help to delineate the intricate network and elucidate the detailed mechanisms of specific checks and balances determined by levels and localization of various forms of ROS in all aspects of plant growth and development.

ACKNOWLEDGMENTS

Authors thank Viktor Ivanov for artwork. This work was supported by grants from NATO (CBP.EAP.CLG9827280) to JMS, NSF of Bulgaria Genomics programme (G5), International Atomic Energy Agency (Contract 13220) and Swiss National Science Foundation (Scientific Cooperation between Eastern Europe and Switzerland program, Project IB73A0-110774) to TG.

REFERENCES

Achard, P., Renou, J. P., Berthomé, R., Harberd, N. P., and Genschik, P. (2008) Plant DELLAs restrain growth and promote survival of adversity by reducing the levels of reactive oxygen species. *Curr. Biol.* **18**, 656-660.

Ali, R., Ma, W., Lemtiri-Chlieh, F., Tsaltas, D., Leng, Q., von Bodman, S., and Berkowitz, G. A. (2007). Death don't have no mercy and neither does calcium: *Arabidopsis* CYCLIC NUCLEOTIDE GATED CHANNEL2 and innate immunity. *Plant Cell* **19,** 1081–1095.

Allen, G. J., Chu, S. P., Harrington, C. L., Schumacher, K., Hoffman, T., Tang, Y. Y., Grill, E., and Schroeder, J. I. (2001). A defined range of guard cell calcium oscillation parameters encodes stomatal movements. *Nature* **411,** 1053–1057.

Alvarez, M. E. (2000). Salicylic acid in the machinery of hypersensitive cell death and disease resistance. *Plant Mol. Biol.* **44,** 429–442.

Alvarez, M. E., Pennell, R. I., Meijer, P. J., Ishikawa, A., Dixon, R. A., and Lamb, C. (1998). Reactive oxygen intermediates mediate a systemic signal network in the establishment of plant immunity. *Cell* **92,** 773–784.

Ameisen, J. C. (2002). On the origin, evolution, and nature of programmed cell death: A timeline of four billion years. *Cell Death Differ.* **9,** 367–393.

Apel, K., and Hirt, H. (2004). Reactive oxygen species: Metabolism, oxidative stress, and signal transduction. *Annu. Rev. Plant Biol.* **55,** 373–399.

Asada, K. (2006). Production and scavenging of reactive oxygen species in chloroplasts and their functions. *Plant Physiol.* **141,** 391–396.

Asai, T., Stone, J. M., Heard, J. E., Kovtun, Y., Yorgey, P., Sheen, J., and Ausubel, F. M. (2000). Fumonisin B1-induced cell death in *Arabidopsis* protoplasts requires jasmonate-, ethylene-, and salicylate-dependent signaling pathways. *Plant Cell* **12,** 1823–1835.

Asai, T., Tena, G., Plotnikova, J., Willmann, M. R., Chiu, W. L., Gomez-Gomez, L., Boller, T., Ausubel, F. M., and Sheen, J. (2002). MAP kinase signalling cascade in *Arabidopsis* innate immunity. *Nature* **415,** 977–983.

Ashtamker, C., Kiss, V., Sagi, M., Davydov, O., and Fluhr, R. (2007). Diverse subcellular locations of cryptogein-induced reactive oxygen species production in tobacco bright yellow-2 cells. *Plant Physiol.* **143,** 1817–1826.

Bais, H. P., Vepachedu, R., Gilroy, S., Callaway, R. M., and Vivanco, J. M. (2003). Allelopathy and exotic plant invasion: From molecules and genes to species interactions. *Science* **301,** 1377–1380.

Balague, C., Lin, B. Q., Alcon, C., Flottes, G., Malmstrom, S., Kohler, C., Neuhaus, G., Pelletier, G., Gaymard, F., and Roby, D. (2003). HLM1, an essential signaling component in the hypersensitive response, is a member of the cyclic nucleotide-gated channel ion channel family. *Plant Cell* **15,** 365–379.

Balk, J., Leaver, C. J., and Mccabe, P. F. (1999). Translocation of cytochrome c from the mitochondria to the cytosol occurs during heat-induced programmed cell death in cucumber plants. *FEBS Lett.* **463,** 151–154.

Balk, J., Chew, S. K., Leaver, C. J., and Mccabe, P. F. (2003). The intermembrane space of plant mitochondria contains a DNase activity that may be involved in programmed cell death. *Plant J.* **34,** 573–583.

Bassham, D. C. (2007). Plant autophagy-more than a starvation response. *Curr. Opin. Plant Biol.* **10,** 587–593.

Bienert, G. P., Schjoerring, J. K., and Jahn, T. P. (2006). Membrane transport of hydrogen peroxide. *Biochim. Biophys. Acta* **1758,** 994–1003.

Bienert, G. P., Moller, A. L. B., Kristiansen, K. A., Schulz, A., Moller, I. M., Schjoerring, J. K., and Jahn, T. P. (2007). Specific aquaporins facilitate the diffusion of hydrogen peroxide across membranes. *J. Biol. Chem.* **282,** 1183–1192.

Bindschedler, L. V., Dewdney, J., Blee, K. A., Stone, J. M., Asai, T., Plotnikov, J., Denoux, C., Hayes, T., Gerrish, C., Davies, D. R., Ausubel, F. M., and Paul Bolwell, G. (2006). Peroxidase-dependent apoplastic oxidative burst in *Arabidopsis* required for pathogen resistance. *Plant J.* **47,** 851–863.

Bosch, M., and Franklin-Tong, N. (2007). Temporal ans spatial activation of caspase-like enzymes induced by self-incompatibility in papaver pollen. *Proc. Natl. Acad. Sci. USA* **104,** 18327–18332.

Bouche, N., Fait, A., Bouchez, D., Moller, S. G., and Fromm, H. (2003). Mitochondrial succinic-semialdehyde dehydrogenase of the gamma-aminobutyrate shunt is required to restrict levels of reactive oxygen intermediates in plants. *Proc. Natl. Acad. Sci. USA* **100,** 6843–6848.

Bozhkov, P. V., Filonova, L. H., and Suarez, M. F. (2005a). Programmed cell death in plant embryogenesis. *Curr. Top. Dev. Biol.* **67,** 135–179.

Bozhkov, P. V., Suarez, M. F., Filonova, L. H., Daniel, G., Zamyatnin, A. A., Rodriguez-Nieto, S., Zhivotovsky, B., and Smertenko, A. (2005b). Cysteine protease mcll-Pa executes programmed cell death during plant embryogenesis. *Proc. Natl. Acad. Sci. USA* **102,** 14463–14468.

Brandwagt, B. F., Mesbah, L. A., Takken, F. L. W., Laurent, P. L., Kneppers, T. J. A., Hille, J., and Nijkamp, H. J. J. (2000). A longevity assurance gene homolog of tomato mediates resistance to *Alternaria alternata* f. sp *lycopersici* toxins and fumonisin B-1. *Proc. Natl. Acad. Sci. USA* **97,** 4961–4966.

Brodersen, P., Petersen, M., Pike, H. M., Olszak, B., Skov, S., Odum, N., Jorgensen, L. B., Brown, R. E., and Mundy, J. (2002). Knockout of *Arabidopsis* accelerated-cell-death11 encoding a sphingosine transfer protein causes activation of programmed cell death and defense. *Genes Dev.* **16,** 490–502.

Calderon-Urrea, A., and Dellaporta, S. L. (1999). Cell death and cell protection genes determine the fate of pistils in maize. *Development* **126,** 435–441.

Carimi, F., Zottini, M., Formentin, E., Terzi, M., and Lo Schiavo, F. (2003). Cytokinins: New apoptotic inducers in plants. *Planta* **216,** 413–421.

Carol, R. J., Takeda, S., Linstead, P., Durrant, M. C., Kakesova, H., Derbyshire, P., Drea, S., Zarsky, V., and Dolan, L. (2005). A RhoGDP dissociation inhibitor spatially regulates growth in root hair cells. *Nature* **438,** 1013–1016.

Chamnongpol, S., Willekens, H., Moeder, W., Langebartels, C., Sandermann, H., Van Montagu, A., Inzé, D., and Van Camp, W. (1998). Defense activation and enhanced pathogen tolerance induced by H_2O_2 in transgenic tobacco. *Proc. Natl. Acad. Sci. USA* **95,** 5818–5823.

Charng, Y. Y., Liu, H. C., Liu, N. Y., Hsu, F. C., and Ko, S. S. (2006). *Arabidopsis* Hsa32, a novel heat shock protein, is essential for acquired thermotolerance during long recovery after acclimation. *Plant Physiol.* **140,** 1297–1305.

Chen. M., Markham, J. E., Dietrich, C. R., Jaworski, J. G. and Cahoon, E. B. (2008) Sphingolipid long-chain base hydroxylation is important for growth and regulation of sphingolipid content and composition in *Arabidopsis*. *Plant Cell* **20,** 1862-1878.

Chichkova, N. V., Kim, S. H., Titova, E. S., Kalkum, M., Morozov, V. S., Rubtsov, Y. P., Kalinina, N. O., Taliansky, M. E., and Vartapetian, A. B. (2004). A plant caspase-like protease activated during the hypersensitive response. *Plant Cell* **16,** 157–171.

Chinchilla, D., Zipfel, C., Robatzek, S., Kemmerling, B., Nurnberger, T., Jones, J. D. G., Felix, G., and Boller, T. (2007). A flagellin-induced complex of the receptor FLS2 and BAK1 initiates plant defence. *Nature* **448,** 497–500.

Chini, A., Fonseca, S., Fernandez, G., Adie, B., Chico, J. M., Lorenzo, O., Garcia-Casado, G., Lopez-Vidriero, I., Lozano, F. M., Ponce, M. R., Micol, J. L., and Solano, R. (2007). The JAZ family of repressors is the missing link in jasmonate signalling. *Nature* **448,** 666–671.

Choi, H. W., Kim, Y. J., Lee, S. C., Hong, J. K., and Hwang, B. K. (2007). Hydrogen peroxide generation by the pepper extracellular peroxidase $CaPO_2$ activates local and systemic cell death and defense response to bacterial pathogens. *Plant Physiol.* **145,** 890–904.

Christensen, C. A., Gorsich, S. W., Brown, R. H., Jones, L. G., Brown, J., Shaw, J. M., and Drews, G. N. (2002). Mitochondrial GFA2 is required for synergid cell death in *Arabidopsis*. *Plant Cell* **14,** 2215–2232.

Clough, S. J., Fengler, K. A., Yu, I. C., Lippok, B., Smith, R. K., and Bent, A. F. (2000). The *Arabidopsis* dnd1 "defense, no death" gene encodes a mutated cyclic nucleotide-gated ion channel. *Proc. Natl. Acad. Sci. USA* **97,** 9323–9328.

Coffeen, W. C., and Wolpert, T. J. (2004). Purification and characterization of serine proteases that exhibit caspase-like activity and are associated with programmed cell death in *Avena sativa*. *Plant Cell* **16,** 857–873.

Coimbra, S., Almeida, J., Junqueira, V., Costa, M. L., and Pereira, L. G. (2007). Arabinogalactan proteins as molecular markers in *Arabidopsis thaliana* sexual reproduction. *J. Exp. Bot.* **58,** 4027–4035.

Dangl, J. L., and Jones, J. D. G. (2001). Plant pathogens and integrated defence responses to infection. *Nature* **411,** 826–833.

Danon, A., Rotari, V. I., Gordon, A., Mailhac, N., and Gallois, P. (2004). Ultraviolet-C overexposure induces programmed cell death in *Arabidopsis*, which is mediated by caspase-like activities and which can be suppressed by caspase inhibitors, p35 and Defender against Apoptotic Death. *J. Biol. Chem.* **279,** 779–787.

Dat, J., Vandenabeele, S., Vranova, E., Van Montagu, M., Inzé, D., and Van Breusegem, F. (2000). Dual action of the active oxygen species during plant stress responses. *Cell. Mol. Life Sci.* **57,** 779–795.

Dat, J. F., Pellinen, R., Beeckman, T., van de Cotte, B., Langebartels, C., Kangasjarvi, J., Inzé, D., and Van Breusegem, F. (2003). Changes in hydrogen peroxide homeostasis trigger an active cell death process in tobacco. *Plant J.* **33,** 621–632.

Davison, P. A., Hunter, C. N., and Horton, P. (2002). Overexpression of beta-carotene hydroxylase enhances stress tolerance in Arabidopsis. *Nature* **418,** 203–206.

Davletova, S., Rizhsky, L., Liang, H. J., Zhong, S. Q., Oliver, D. J., Coutu, J., Shulaev, V., Schlauch, K., and Mittler, R. (2005a). Cytosolic ascorbate peroxidase 1 is a central component of the reactive oxygen gene network of *Arabidopsis*. *Plant Cell* **17,** 268–281.

Davletova, S., Schlauch, K., Coutu, J., and Mittler, R. (2005b). The zinc-finger protein Zat12 plays a central role in reactive oxygen and abiotic stress signaling in *Arabidopsis*. *Plant Physiol.* **139,** 847–856.

del Rio, L. A., Sandalio, L. M., Corpas, F. J., and Barroso, J. B. (2006). Reactive oxygen species and reactive nitrogen species in peroxisomes. Production, scavenging, and role in cell signaling. *Plant Physiol.* **141,** 330–335.

Della Mea, M., De Filippis, F., Genovesi, V., Fracassini, D. S., and Del Duca, S. (2007). The acropetal wave of developmental cell death of tobacco corolla is preceded by activation of transglutaminase in different cell compartments. *Plant Physiol.* **144,** 1211–1222.

Dellapenna, D., and Pogson, B. J. (2006). Vitamin synthesis in plants: Tocopherols and carotenoids. *Annu. Rev. Plant Biol.* **57,** 711–738.

Delledonne, M. (2005). NO news is good news for plants. *Curr. Opin. Plant Biol.* **8,** 390–396.

Delledonne, M., Zeier, J., Marocco, A., and Lamb, C. (2001). Signal interactions between nitric oxide and reactive oxygen intermediates in the plant hypersensitive disease resistance response. *Proc. Natl. Acad. Sci. USA* **98,** 13454–13459.

Demidchik, V., Shabala, S. N., Coutts, K. B., Tester, M. A., and Davies, J. M. (2003). Free oxygen radicals regulate plasma membrane Ca^{2+} and K^{+}-permeable channels in plant root cells. *J. Cell Sci.* **116,** 81–88.

Desikan, R., Mackerness, S. A. H., Hancock, J. T., and Neill, S. J. (2001). Regulation of the *Arabidopsis* transcriptome by oxidative stress. *Plant Physiol.* **127,** 159–172.

Desikan, R., Hancock, J. T., Bright, J., Harrison, J., Weir, L., Hooley, R., and Neill, S. J. (2005). A role for ETR1 in hydrogen peroxide signaling in stomatal guard cells. *Plant Physiol.* **137,** 831–834.

Dickman, M. B., Park, Y. K., Oltersdorf, T., Li, W., Clemente, T., and French, R. (2001). Abrogation of disease development in plants expressing animal antiapoptotic genes. *Proc. Natl. Acad. Sci. USA* **98,** 6957–6962.

Dietrich, R. A., Richberg, M. H., Schmidt, R., Dean, C., and Dangl, J. L. (1997). A novel zinc finger protein is encoded by the arabidopsis LSD1 gene and functions as a negative regulator of plant cell death. *Cell* **88,** 685–694.

Dominguez, F., and Cejudo, F. J. (2006). Identification of a nuclear-localized nuclease from wheat cells undergoing programmed cell death that is able to trigger DNA fragmentation and apoptotic morphology on nuclei from human cells. *Biochem. J.* **397,** 529–536.

Dominguez, F., Moreno, J., and Cejudo, F. J. (2001). The nucellus degenerates by a process of programmed cell death during the early stages of wheat grain development. *Planta* **213,** 352–360.

Dominguez, F., Moreno, J., and Cejudo, F. J. (2004). A gibberellin-induced nuclease is localized in the nucleus of wheat aleurone cells undergoing programmed cell death. *J. Biol. Chem.* **279,** 11530–11536.

Edreva, A. (2005). The importance of non-photosynthetic pigments and cinnamic acid derivatives in photoprotection. *Agric. Ecosyst. Environ.* **106,** 135–146.

Epple, P., Mack, A. A., Morris, V. R. F., and Dangl, J. L. (2003). Antagonistic control of oxidative stress-induced cell death in *Arabidopsis* by two related, plant-specific zinc finger proteins. *Proc. Natl. Acad. Sci. USA* **100,** 6831–6836.

Eulgem, T., and Somssich, I. E. (2007). Networks of WRKY transcription factors in defense signaling. *Curr. Opin. Plant Biol.* **10,** 366–371.

Farage-Barhom, S., Burd, S., Sonego, L., Perl-Treves, R., and Lers, A. (2008). Expression analysis of the BFN1 nuclease gene promoter during senescence, abscission, and programmed cell death-related processes. *J. Exp. Bot.* **59,** 3247-58.

Fath, A., Bethke, P. C., and Jones, R. L. (2001). Enzymes that scavenge reactive oxygen species are down-regulation prior to gibberellic acid-induced programmed cell death in barley aleurone. *Plant Physiol.* **126,** 156–166.

Fath, A., Bethke, P., Beligni, V., and Jones, R. (2002). Active oxygen and cell death in cereal aleurone cells. *J. Exp. Bot.* **53,** 1273–1282.

Filonova, L. H., Bozhkov, P. V., Brukhin, V. B., Daniel, G., Zhivotovsky, B., and von Arnold, S. (2000). Two waves of programmed cell death occur during formation and development of somatic embryos in the gymnosperm, Norway spruce. *J. Cell Sci.* **113,** 4399–4411.

Fontecave, M., Graslund, A., and Reichard, P. (1987). The function of superoxide-dismutase during the enzymatic formation of the free-radical of ribonucleotide reductase. *J. Biol. Chem.* **262,** 12332–12336.

Foreman, J., Demidchik, V., Bothwell, J. H. F., Mylona, P., Miedema, H., Torres, M. A., Linstead, P., Costa, S., Brownlee, C., Jones, J. D. G., Davies, J. M., and Dolan, L. (2003). Reactive oxygen species produced by NADPH oxidase regulate plant cell growth. *Nature* **422,** 442–446.

Foyer, C. H., and Noctor, G. (2003). Redox sensing and signalling associated with reactive oxygen in chloroplasts, peroxisomes and mitochondria. *Physiol. Plant.* **119,** 335–364.

Fukamatsu, Y., Yabe, N., and Hasunuma, K. (2003). *Arabidopsis* NDK1 is a component of ROS signaling by interacting with three catalases. *Plant Cell Physiol.* **44,** 982–989.

Gadjev, I., Vanderauwera, S., Gechev, T., Laloi, C., Minkov, I., Shulaev, V., Apel, K., Inzé, D., Mittler, R., and Van Breusegem, F. (2006). Transcriptomic footprints disclose specificity of reactive oxygen species signaling in *Arabidopsis*. *Plant Physiol.* **141,** 434–445.

Gaffal, K. P., Friedrichs, G. J., and El Gammal, S. (2007). Ultrastructural evidence for a dual function of the phloem and programmed cell death in the floral nectary of *Digitalis purpurea*. *Ann. Bot.* **99,** 593–607.

Gao, C., Xing, D., Li, L., and Zhang, L. (2008). Implication of reactive oxygen species and mitochondrial dysfunction in the early stages of plant programmed cell death induced by ultraviolet-C overexposure. *Planta* **227,** 755–767.

Gapper, C., and Dolan, L. (2006). Control of plant development by reactive oxygen species. *Plant Physiol.* **141,** 341–345.

Garnier, L., Simon-Plas, F., Thuleau, P., Agnel, J. P., Blein, J. P., Ranjeva, R., and Montillet, J. L. (2006). Cadmium affects tobacco cells by a series of three waves of

reactive oxygen species that contribute to cytotoxicity. *Plant Cell Environ.* **29,** 1956–1969.

Gechev, T., Gadjev, I., Van Breusegem, F., Inzé, D., Dukiandjiev, S., Toneva, V., and Minkov, I. (2002). Hydrogen peroxide protects tobacco from oxidative stress by inducing a set of antioxidant enzymes. *Cell. Mol. Life Sci.* **59,** 708–714.

Gechev, T. S., and Hille, J. (2005). Hydrogen peroxide as a signal controlling plant programmed cell death. *J. Cell Biol.* **168,** 17–20.

Gechev, T. S., Gadjev, I. Z., and Hille, J. (2004). An extensive microarray analysis of AAL-toxin-induced cell death in *Arabidopsis thaliana* brings new insights into the complexity of programmed cell death in plants. *Cell. Mol. Life Sci.* **61,** 1185–1197.

Gechev, T. S., Minkov, I. N., and Hille, J. (2005). Hydrogen peroxide-induced cell death in *Arabidopsis*: Transcriptional and mutant analysis reveals a role of an oxoglutarate-dependent dioxygenase gene in the cell death process. *IUBMB Life* **57,** 181–188.

Gechev, T. S., Van Breusegem, F., Stone, J. M., Denev, I., and Laloi, C. (2006). Reactive oxygen species as signals that modulate plant stress responses and programmed cell death. *Bioessays* **28,** 1091–1101.

Gechev, T. S., Ferwerda, M. A., Mehterov, N., Laloi, C., Qureshi, M. K., and Hille, J. (2008). *Arabidopsis* AAL-toxin-resistant mutant *atr1* shows enhanced tolerance to programmed cell death induced by reactive oxygen species. *Biochem. Biophys. Res. Commun.* **375**, 639–644.

Gendron, J. M., and Wang, Z. Y. (2007). Multiple mechanisms modulate brassinosteroid signaling. *Curr. Opin. Plant Biol.* **10,** 436–441.

Gould, K. S., McKelvie, J., and Markham, K. R. (2002). Do anthocyanins function as antioxidants in leaves? Imaging of H_2O_2 in red and green leaves after mechanical injury. *Plant Cell Environ.* **25,** 1261–1269.

Gunawardena, A. H. L. A., Pearce, D. M. E., Jackson, M. B., Hawes, C. R., and Evans, D. E. (2001). Rapid changes in cell wall pectic polysaccharides are closely associated with early stages of aerenchyma formation, a spatially localized form of programmed cell death in roots of maize (*Zea mays* L.) promoted by ethylene. *Plant Cell Environ.* **24,** 1369–1375.

Gunawardena, A. H. L. A., Greenwood, J. S., and Dengler, N. G. (2004). Programmed cell death remodels lace plant leaf shape during development. *Plant Cell* **16,** 60–73.

Guo, F. Q., Okamoto, M., and Crawford, N. M. (2003). Identification of a plant nitric oxide synthase gene involved in hormonal signaling. *Science* **302,** 100–103.

Guo, Y. F., and Gan, S. S. (2006). AtNAP, a NAC family transcription factor, has an important role in leaf senescence. *Plant J.* **46,** 601–612.

Halliwell, B. (2006). Reactive species and antioxidants. Redox biology is a fundamental theme of aerobic life. *Plant Physiol.* **141,** 312–322.

Harding, S. A., Oh, S. H., and Roberts, D. M. (1997). Transgenic tobacco expressing a foreign calmodulin gene shows an enhanced production of active oxygen species. *EMBO J.* **16,** 1137–1144.

Hatsugai, N., Kuroyanagi, M., Yamada, K., Meshi, T., Tsuda, S., Kondo, M., Nishimura, M., and Hara-Nishimura, I. (2004). A plant vacuolar protease, VPE, mediates virus-induced hypersensitive cell death. *Science* **305,** 855–858.

Hatsugai, N., Kuroyanagi, M., Nishimura, M., and Hara-Nishimura, I. (2006). A cellular suicide strategy of plants: Vacuole-mediated cell death. *Apoptosis* **11,** 905–911.

He, R., Drury, G. E., Rotari, V. I., Gordon, A., Willer, M., Tabasum, F., Woltering, E. J., and Gallois, P. (2008). Metacaspase-8 modulates programmed cell death induced by UV and H_2O_2 in *Arabidopsis*. *J. Biol. Chem.* **283,** 774–783.

He, X., and Kermode, A. R. (2003a). Nuclease activities and DNA fragmentation during programmed cell death of megagametophyte cells of white spruce (*Picea glauca*) seeds. *Plant Mol. Biol.* **51,** 509–521.

He, X., and Kermode, A. R. (2003b). Proteases associated with programmed cell death of megagametophyte cells after germination of white spruce (*Picea glauca*) seeds. *Plant Mol. Biol.* **52,** 729–744.

Henzler, T., and Steudle, E. (2000). Transport and metabolic degradation of hydrogen peroxide in Chara corallina: Model calculations and measurements with the pressure probe suggest transport of H_2O_2 across water channels. *J. Exp. Bot.* **51,** 2053–2066.

Hinderhofer, K., and Zentgraf, U. (2001). Identification of a transcription factor specifically expressed at the onset of leaf senescence. *Planta* **213,** 469–473.

Hintze, K. J., and Theil, E. C. (2006). Cellular regulation and molecular interactions of the ferritins. *Cell. Mol. Life Sci.* **63,** 591–600.

Hu, G. S., Yalpani, N., Briggs, S. P., and Johal, G. S. (1998). A porphyrin pathway impairment is responsible for the phenotype of a dominant disease lesion mimic mutant of maize. *Plant Cell* **10,** 1095–1105.

Huffaker, A., and Ryan, C. A. (2007). Endogenous peptide defense signals in *Arabidopsis* differentially amplify signaling for the innate immune response. *Proc. Natl. Acad. Sci. USA* **104,** 10732–10736.

Huffaker, A., Pearce, G., and Ryan, C. A. (2006). An endogenous peptide signal in *Arabidopsis* activates components of the innate immune response. *Proc. Natl. Acad. Sci. USA* **103,** 10098–100103.

Huh, G. H., Damsz, B., Matsumoto, T. K., Reddy, M. P., Rus, A. M., Ibeas, J. I., Narasimhan, M. L., Bressan, R. A., and Hasegawa, P. M. (2002). Salt causes ion disequilibrium-induced programmed cell death in yeast and plants. *Plant J.* **29,** 649–659.

Hulskamp, M. (2004). Plant trichomes: A model for cell differentiation. *Nat. Rev. Mol. Cell Biol.* **5,** 471–480.

Ichimura, K., Shinozaki, K., Tena, G., Sheen, J., Henry, Y., Champion, A., Kreis, M., Zhang, S. Q., Hirt, H., Wilson, C., Heberle-Bors, E., Ellis, B. E., *et al.* (2002). Mitogen-activated protein kinase cascades in plants: A new nomenclature. *Trends Plant Sci.* **7,** 301–308.

Ishikawa, A., Okamoto, H., Iwasaki, Y., and Asahi, T. (2001). A deficiency of coproporphyrinogen III oxidase causes lesion formation in *Arabidopsis*. *Plant J.* **27,** 89–99.

Ishikawa, A., Tanaka, H., Nakai, M., and Asahi, T. (2003). Deletion of a chaperonin 60 beta gene leads to cell death in the *Arabidopsis* lesion initiation 1 mutant. *Plant Cell Physiol.* **44,** 255–261.

Ito, J., and Fukuda, H. (2002). ZEN1 is a key enzyme in the degradation of nuclear DNA during programmed cell death of tracheary elements. *Plant Cell* **14,** 3201–3211.

Jabs, T., Dietrich, R. A., and Dangl, J. L. (1996). Initiation of runaway cell death in an *Arabidopsis* mutant by extracellular superoxide. *Science* **273,** 1853–1856.

Janjusevic, R., Abramovitch, R. B., Martin, G. B., and Stebbins, C. E. (2006). A bacterial inhibitor of host programmed cell death defenses is an E3 ubiquitin ligase. *Science* **311,** 222–226.

Jarosch, B., Kogel, K. H., and Schaffrath, U. (1999). The ambivalence of the barley Mlo locus: Mutations conferring resistance against powdery mildew (*Blumeria graminis f. sp, hordei*) enhance susceptibility to the rice blast fungus *Magnaporthe grisea*. *Mol. Plant Microbe Interact.* **12,** 508–514.

Jonak, C., Nakagami, H., and Hirt, H. (2004). Heavy metal stress. Activation of distinct mitogen-activated protein kinase pathways by copper and cadmium. *Plant Physiol.* **136,** 3276–3283.

Kaminaka, H., Nake, C., Epple, P., Dittgen, J., Schutze, K., Chaban, C., Holt, B. F., Merkle, T., Schafer, E., Harter, K., and Dangl, J. L. (2006). bZIP10-LSD1 antagonism modulates basal defense and cell death in *Arabidopsis* following infection. *EMBO J.* **25,** 4400–4411.

Karpinski, S., Reynolds, H., Karpinska, B., Wingsle, G., Creissen, G., and Mullineaux, P. (1999). Systemic signaling and acclimation in response to excess excitation energy in *Arabidopsis*. *Science* **284,** 654–657.

Kawai-Yamada, M., Jin, L., Yoshinaga, K., Hirata, A., and Uchimiya, H. (2001). Mammalian Bax-induced plant cell death can be down-regulated by overexpression of *Arabidopsis Bax Inhibitor-1* (*AtBI-1*). *Proc. Natl. Acad. Sci. USA* **98,** 12295–12300.

Kehrer, J. P. (2000). The Haber-Weiss reaction and mechanisms of toxicity. *Toxicology* **149,** 43–50.

Kemmerling, B., Schwedt, A., Rodriguez, P., Mazzotta, S., Frank, M., Qamar, S. A., Mengiste, T., Betsuyaku, S., Parker, J. E., Mussig, C., Thomma, B. P., Albrecht, C., *et al.* (2007). The BRI1-associated kinase 1, BAK1, has a brassinolide-independent role in plant cell-death control. *Curr. Biol.* **17,** 1116–1122.

Kim, H. J., Ryu, H., Hong, S. H., Woo, H. R., Lim, P. O., Lee, I. C., Sheen, J., Nam, H. G., and Hwang, I. (2006a). Cytokinin-mediated control of leaf longevity by AHK3 through phosphorylation of ARR2 in *Arabidopsis*. *Proc. Natl. Acad. Sci. USA* **103,** 814–819.

Kim, M., Lim, J. H., Ahn, C. S., Park, K., Kim, G. T., Kim, W. T., and Pai, H. S. (2006b). Mitochondria-associated hexokinases play a role in the control of programmed cell death in *Nicotiana benthamiana*. *Plant Cell* **18,** 2341–2355.

Kim, M., Ahn, J. W., Jin, U. H., Choi, D., Paek, K. H., and Pai, H. S. (2003). Activation of the programmed cell death pathway by inhibition of proteasome function in plants. *J. Biol. Chem.* **278,** 19406–19415.

Kim, M. C., Panstruga, R., Elliott, C., Muller, J., Devoto, A., Yoon, H. W., Park, H. C., Cho, M. J., and Schulze-Lefert, P. (2002). Calmodulin interacts with MLO protein to regulate defence against mildew in barley. *Nature* **416,** 447–450.

Kim, M. S., Kim, H. S., Kim, Y. S., Baek, K. H., Oh, H. W., Hahn, K. W., Bae, R. N., Lee, I. J., Joung, H., and Jeon, J. H. (2007). Superoxide anion regulates plant growth and tuber development of potato. *Plant Cell Rep.* **26,** 1717–1725.

Koukalova, B., Kovarik, A., Fajkus, J., and Siroky, J. (1997). Chromatin fragmentation associated with apoptotic changes in tobacco cells exposed to cold stress. *FEBS Lett.* **414,** 289–292.

Koussevitzky, S., Nott, A., Mockler, T. C., Hong, F., Sachetto-Martins, G., Surpin, M., Lim, I. J., Mittler, R., and Chory, J. (2007). Signals from chloroplasts converge to regulate nuclear gene expression. *Science* **316,** 715–719.

Kovtun, Y., Chiu, W. L., Tena, G., and Sheen, J. (2000). Functional analysis of oxidative stress-activated mitogen-activated protein kinase cascade in plants. *Proc. Natl. Acad. Sci. USA* **97,** 2940–2945.

Kuriyama, H., and Fukuda, H. (2002). Developmental programmed cell death in plants. *Curr. Opin. Plant Biol.* **5,** 568–573.

Kuroyanagi, M., Yamada, K., Hatsugai, N., Kondo, M., Nishimura, M., and Hara-Nishimura, I. (2005). Vacuolar processing enzyme is essential for mycotoxin-induced cell death in *Arabidopsis thaliana*. *J. Biol. Chem.* **280,** 32914–32920.

Kwak, J. M., Mori, I. C., Pei, Z. M., Leonhardt, N., Torres, M. A., Dangl, J. L., Bloom, R. E., Bodde, S., Jones, J. D. G., and Schroeder, J. I. (2003). NADPH oxidase AtrbohD and AtrbohF genes function in ROS-dependent ABA signaling in *Arabidopsis*. *EMBO J.* **22,** 2623–2633.

Kwak, J. M., Nguyen, V., and Schroeder, J. I. (2006). The role of reactive oxygen species in hormonal responses. *Plant Physiol.* **141,** 323–329.

Lacomme, C., and Santa Cruz, S. (1999). Bax-induced cell death in tobacco is similar to the hypersensitive response. *Proc. Natl. Acad. Sci. USA* **96,** 7956–7961.

Laloi, C., Przybyla, D., and Apel, K. (2006). A genetic approach towards elucidating the biological activity of different reactive oxygen species in *Arabidopsis thaliana*. *J. Exp. Bot.* **57,** 1719–1724.

Lam, E. (2004). Controlled cell death, plant survival and development. *Nat. Rev. Mol. Cell Biol.* **5,** 305–315.

Lam, E. (2005). Vacuolar proteases livening up programmed cell death. *Trends Cell Biol.* **15,** 124–127.

Lamb, C., and Dixon, R. A. (1997). The oxidative burst in plant disease resistance. *Annu. Rev. Plant Physiol. Plant Mol. Biol.* **48,** 251–275.

Lamotte, O., Gould, K., Lecourieux, D., Sequeira-Legrand, A., Lebrun-Garcia, A., Durner, J., Pugin, A., and Wendehenne, D. (2004). Analysis of nitric oxide signaling functions in tobacco cells challenged by the elicitor cryptogein. *Plant Physiol.* **135,** 516–529.

Lecourieux, D., Mazars, C., Pauly, N., Ranjeva, R., and Pugin, A. (2002). Analysis and effects of cytosolic free calcium increases in response to elicitors in *Nicotiana plumbaginifolia* cells. *Plant Cell* **14,** 2627–2641.

Lecourieux, D., Raneva, R., and Pugin, A. (2006). Calcium in plant defence-signalling pathways. *New Phytol.* **171,** 249–269.

Lee, K. P., Kim, C., Landgraf, F., and Apel, K. (2007). EXECUTER1- and EXECUTER2-dependent transfer of stress-related signals from the plastid to the nucleus of *Arabidopsis thaliana*. *Proc. Natl. Acad. Sci. USA* **104,** 10270–10275.

Levine, A., Tenhaken, R., Dixon, R., and Lamb, C. (1994). H_2O_2 from the oxidative burst orchestrates the plant hypersensitive disease resistance response. *Cell* **79,** 583–593.

Levine, A., Pennell, R. I., Alvarez, M. E., Palmer, R., and Lamb, C. (1996). Calcium-mediated apoptosis in a plant hypersensitive disease resistance response. *Curr. Biol.* **6,** 427–437.

Li, N., Zhang, D. S., Liu, H. S., Yin, C. S., Li, X. X., Liang, W. Q., Yuan, Z., Xu, B., Chu, H. W., Wang, J., Wen, T. Q., Huang, H., *et al.* (2006). The rice tapetum degeneration retardation gene is required for tapetum degradation and anther development. *Plant Cell* **18,** 2999–3014.

Liang, H., Yao, N., Song, L. T., Luo, S., Lu, H., and Greenberg, L. T. (2003). Ceramides modulate programmed cell death in plants. *Genes Dev.* **17,** 2636–2641.

Lim, P. O., Kim, H. J., and Nam, H. G. (2007). Leaf senescence. *Annu. Rev. Plant Biol.* **58,** 115–136.

Lin, J. S., Wang, Y., and Wang, G. X. (2006). Salt stress-induced programmed cell death in tobacco protoplasts is mediated by reactive oxygen species and mitochondrial permeability transition pore status. *J. Plant Physiol.* **163,** 731–739.

Liu, Y., Schiff, M., Czymmek, K., Talloczy, Z., Levine, B., and Dinesh-Kumar, S. P. (2005). Autophagy regulates programmed cell death during the plant innate immune response. *Cell* **121,** 567–577.

Liu, Y. D., Ren, D. T., Pike, S., Pallardy, S., Gassmann, W., and Zhang, S. Q. (2007). Chloroplast-generated reactive oxygen species are involved in hypersensitive response-like cell death mediated by a mitogen-activated protein kinase cascade. *Plant J.* **51,** 941–954.

Loeffler, C., Berger, S., Guy, A., Durand, T., Bringmann, G., Dreyer, M., von Rad, U., Durner, J., and Mueller, M. J. (2005). B-1-phytoprostanes trigger plant defense and detoxification responses. *Plant Physiol.* **137,** 328–340.

Lopez-Delgado, H., Dat, J., Foyer, C. H., and Scott, I. M. (1998). Induction of thermotolerance in potato microplants by acetylsalicylic acid and H_2O_2. *J. Exp. Bot.* **49,** 713–720.

Madeo, F., Herker, E., Maldener, C., Wissing, S., Lachelt, S., Herian, M., Fehr, M., Lauber, K., Sigrist, S. J., Wesselborg, S., and Frohlich, K. U. (2002). A caspase-related protease regulates apoptosis in yeast. *Mol. Cell* **9,** 911–917.

Mahalingam, R., Jambunathan, N., Gunjan, S. K., Faustin, E., Weng, H., and Ayoubi, P. (2006). Analysis of oxidative signalling induced by ozone in *Arabidopsis thaliana*. *Plant Cell Environ.* **29,** 1357–1371.

Meijer, H. J. G., and Munnik, T. (2003). Phospholipid-based signaling in plants. *Annu. Rev. Plant Biol.* **54,** 265–306.

Meskauskiene, R., Nater, M., Goslings, D., Kessler, F., den Camp, R. O., and Apel, K. (2001). FLU: A negative regulator of chlorophyll biosynthesis in *Arabidopsis thaliana*. *Proc. Natl. Acad. Sci. USA* **98,** 12826–12831.

Meyer, Y., Reichheld, J. P., and Vignols, F. (2005). Thioredoxins in *Arabidopsis* and other plants. *Photosynth. Res.* **86,** 419–433.

Miao, Y., and Zentgraf, U. (2007). The antagonist function of Arabidopsis WRKY53 and ESR/ESP in leaf senescence is modulated by the jasmonic and salicylic acid equilibrium. *Plant Cell* **19,** 819–830.

Miao, Y., Laun, T., Zimmermann, P., and Zentgraf, U. (2004). Targets of the WRKY53 transcription factor and its role during leaf senescence in *Arabidopsis*. *Plant Mol. Biol.* **55,** 853–867.

Miao, Y., Laun, T. M., Smykowski, A., and Zentgraf, U. (2007). Arabidopsis MEKK1 can take a short cut: It can directly interact with senescence-related WRKY53 transcription factor on the protein level and can bind to its promoter. *Plant Mol. Biol.* **65,** 63–76.

Miller, G., and Mittler, R. (2006). Could heat shock transcription factors function as hydrogen peroxide sensors in plants. *Ann. Bot.* **98,** 279–288.

Mitsuhara, I., Malik, K. A., Miura, M., and Ohashi, Y. (1999). Animal cell-death suppressors Bcl-x(L) and Ced-9 inhibit cell death in tobacco plants. *Curr. Biol.* **9,** 775–778.

Mittler, R., Simon, L., and Lam, E. (1997). Pathogen-induced programmed cell death in tobacco. *J. Cell Sci.* **110,** 1333–1344.

Mittler, R., Vanderauwera, S., Gollery, M., and Van Breusegem, F. (2004). Reactive oxygen gene network of plants. *Trends Plant Sci.* **9,** 490–498.

Moller, I. M. (2001). Plant mitochondria and oxidative stress: Electron transport, NADPH turnover, and metabolism of reactive oxygen species. *Annu. Rev. Plant Physiol. Plant Mol. Biol.* **52,** 561–591.

Moller, I. M., Jensen, P. E., and Hansson, A. (2007). Oxidative modifications to cellular components in plants. *Annu. Rev. Plant Biol.* **58,** 459–481.

Montillet, J. L., Chamnongpol, S., Rusterucci, C., Dat, J., van de Cotte, B., Agnel, J. P., Battesti, C., Inzé, D., Van Breusegem, F., and Triantaphylides, C. (2005). Fatty acid hydroperoxides and H_2O_2 in the execution of hypersensitive cell death in tobacco leaves. *Plant Physiol.* **138,** 1516–1526.

Moon, H., Lee, B., Choi, G., Shin, S., Prasad, D. T., Lee, O., Kwak, S. S., Kim, D. H., Nam, J., Bahk, J., Hong, J. C., Lee, S. Y., *et al.* (2003). NDP kinase 2 interacts with two oxidative stress-activated MAPKs to regulate cellular redox state and enhances multiple stress tolerance in transgenic plants. *Proc. Natl. Acad. Sci. USA* **100,** 358–363.

Moon, J., Parry, G., and Estelle, M. (2004). The ubiquitin-proteasome pathway and plant development. *Plant Cell* **16,** 3181–3195.

Moons, A. (2005). Regulatory and functional interactions of plant growth regulators and plant glutathione S-transferases (GSTS). *Plant Horm.* **72,** 155–202.

Morillo, S. A., and Tax, F. E. (2006). Functional analysis of receptor-like kinases in monocots and dicots. *Curr. Opin. Plant Biol.* **9,** 460–469.

Mueller, M. J. (2004). Archetype signals in plants: The phytoprostanes. *Curr. Opin. Plant Biol.* **7,** 441–448.

Muhlenbock, P., Plaszczyca, M., Plaszczyca, M., Mellerowicz, E., and Karpinski, S. (2007). Lysigenous aerenchyma formation in *Arabidopsis* is controlled by lesion simulating disease1. *Plant Cell* **19,** 3819–3830.

Mullineaux, P., Karpinski, S., and Baker, N. (2006). Spatial dependence for hydrogen peroxide-directed signaling in light-stressed plants. *Plant Physiol.* **141,** 346–350.

Murgia, I., Tarantino, D., Vannini, C., Bracale, M., Carravieri, S., and Soave, C. (2004). *Arabidopsis thaliana* plants overexpressing thylakoidal ascorbate peroxidase show increased

resistance to paraquat-induced photooxidative stress and to nitric oxide-induced cell death. *Plant J.* **38,** 940–953.

Nakagami, H., Kiegerl, S., and Hirt, H. (2004). OMTK1, a novel MAPKKK, channels oxidative stress signaling through direct MAPK interaction. *J. Biol. Chem.* **279,** 26959–26966.

Nakagami, H., Soukupova, H., Schikora, A., Zarsky, V., and Hirt, H. (2006). A mitogen-activated protein kinase kinase kinase mediates reactive oxygen species homeostasis in *Arabidopsis*. *J. Biol. Chem.* **281,** 38697–38704.

Nakanomyo, I., Kost, B., Chua, N. H., and Fukuda, H. (2002). Preferential and asymmetrical accumulation of a Rac small GTPase mRNA in differentiating xylem cells of *Zinnia elegans*. *Plant Cell Physiol.* **43,** 1484–1492.

Nakashima, J., Takabe, K., Fujita, M., and Fukuda, H. (2000). Autolysis during *in vitro* tracheary element differentiation: Formation and location of the perforation. *Plant Cell Physiol.* **41,** 1267–1271.

Navarre, D. A., and Wolpert, T. J. (1999). Victorin induction of an apoptotic/senescence-like response in oats. *Plant Cell* **11,** 237–249.

Neill, S. J., Bright, J., Desikan, R., Hancock, J. T., Harrison, J., and Wilson, I. (2008). Nitric oxide evolution and perception. *J. Exp. Bot.* **59,** 25–35.

Obara, K., Kuriyama, H., and Fukuda, H. (2001). Direct evidence of active and rapid nuclear degradation triggered by vacuole rupture during programmed cell death in Zinnia. *Plant Physiol.* **125,** 615–626.

Op Den Camp, R. G. L., Przybyla, D., Ochsenbein, C., Laloi, C., Kim, C. H., Danon, A., Wagner, D., Hideg, E., Gobel, C., Feussner, I., Nater, M., and Apel, K. (2003). Rapid induction of distinct stress responses after the release of singlet oxygen in *Arabidopsis*. *Plant Cell* **15,** 2320–2332.

Oracz, K., Bouteau, H. E. M., Farrant, J. M., Cooper, K., Belghazi, M., Job, C., Job, D., Corbineau, F., and Bailly, C. (2007). ROS production and protein oxidation as a novel mechanism for seed dormancy alleviation. *Plant J.* **50,** 452–465.

Orozco-Cardenas, M. L., Narvaez-Vasquez, J., and Ryan, C. A. (2001). Hydrogen peroxide acts as a second messenger for the induction of defense genes in tomato plants in response to wounding, systemin, and methyl jasmonate. *Plant Cell* **13,** 179–191.

Ortega-Villasante, C., Hernandez, L. E., Rellan-Alvarez, R., Del Campo, F. F., and Carpena-Ruiz, R. O. (2007). Rapid alteration of cellular redox homeostasis upon exposure to cadmium and mercury in alfalfa seedlings. *New Phytol.* **176,** 96–107.

Overmyer, K., Tuominen, H., Kettunen, R., Betz, C., Langebartels, C., Sandermann, H., and Kangasjarvi, J. (2000). Ozone-sensitive *Arabidopsis* rcd1 mutant reveals opposite roles for ethylene and jasmonate signaling pathways in regulating superoxide-dependent cell death. *Plant Cell* **12,** 1849–1862.

Overmyer, K., Brosche, M., and Kangasjarvi, J. (2003). Reactive oxygen species and hormonal control of cell death. *Trends Plant Sci.* **8,** 335–342.

Overmyer, K., Brosche, M., Pellinen, R., Kuittinen, T., Tuominen, H., Ahlfors, R., Keinanen, M., Saarma, M., Scheel, D., and Kangasjarvi, J. (2005). Ozone-induced programmed cell death in the *Arabidopsis* radical-induced cell death1 mutant. *Plant Physiol.* **137,** 1092–1104.

Pan, J. W., Zhu, M. Y., and Chen, H. (2001). Aluminum-induced cell death in root-tip cells of barley. *Environ. Exp. Bot.* **46,** 71–79.

Passardi, F., Penel, C., and Dunand, C. (2004). Performing the paradoxical: How plant peroxidases modify the cell wall. *Trends Plant Sci.* **9,** 534–540.

Patel, S., Caplan, J., and Dinesh-Kumar, S. P. (2006). Autophagy in the control of programmed cell death. *Curr. Opin. Plant Biol.* **9,** 391–396.

Pei, Z. M., Murata, Y., Benning, G., Thomine, S., Klusener, B., Allen, G. J., Grill, E., and Schroeder, J. I. (2000). Calcium channels activated by hydrogen peroxide mediate abscisic acid signalling in guard cells. *Nature* **406,** 731–734.

Pellinen, R. I., Korhonen, M. S., Tauriainen, A. A., Palva, E. T., and Kangasjarvi, J. (2002). Hydrogen peroxide activates cell death and defense gene expression in birch. *Plant Physiol.* **130,** 549–560.

Pennell, R. I., and Lamb, C. (1997). Programmed cell death in plants. *Plant Cell* **9,** 1157–1168.

Pérez-Amador, M. A., Abler, M. L., De Rocher, E. J., Thompson, D. M., van Hoof, A., LeBrasseur, N. D., Lers, A., and Green, P. J. (2000). Identification of BFN1, a bifunctional nuclease induced during leaf and stem senescence in *Arabidopsis*. *Plant Physiol.* **122,** 169–180.

Potocky, M., Jones, M. A., Bezvoda, R., Smirnoff, N., and Zarsky, V. (2007). Reactive oxygen species produced by NADPH oxidase are involved in pollen tube growth. *New Phytol.* **174,** 742–751.

Prasad, T. K., Anderson, M. D., and Stewart, C. R. (1995). Localization and characterization of peroxidases in the mitochondria of chilling-acclimated maize seedlings. *Plant Physiol.* **108,** 1597–1605.

Przybyla, D., Göbel, C., Imboden, A., Feussner, I., Hamberg, M., and Apel, K. (2008). Enzymatic, but not non-enzymatic $^1O_2$-mediated peroxidation of polyunsaturated fatty acids forms part of the EXECUTER1-dependent stress response program in the *flu* mutant of *Arabidopsis thaliana*. *Plant J.* **54**(2), 236–248.

Punwani, J. A., Rabiger, D. S., and Drews, G. N. (2007). MYB98 positively regulates a battery of synergid-expressed genes encoding filiform apparatus localized proteins. *Plant Cell* **19,** 2557–2568.

Qiao, J., Mitsuhara, I., Yazaki, Y., Sakano, K., Gotoh, Y., and Miura, M. (2002). Enhanced resistance to salt, cold and wound stresses by overproduction of animal cell death suppressors Bcl-xL and Ced-9 in tobacco cells—their possible contribution through improved function of organella. *Plant Cell Physiol.* **43,** 992–1005.

Queval, G., Issakidis-Bourguet, E., Hoeberichts, F. A., Vandorpe, M., Gakiere, B., Vanacker, H., Miginiac-Maslow, M., Van Breusegem, F., and Noctor, G. (2007). Conditional oxidative stress responses in the *Arabidopsis* photorespiratory mutant cat2 demonstrate that redox state is a key modulator of daylength-dependent gene expression, and define photoperiod as a crucial factor in the regulation of H_2O_2-induced cell death. *Plant J.* **52,** 640–657.

Raffaele, S., Vailleau, F., Léger, A., Joubès, J., Miersch, O., Huard, C., Blée, E., Mongrand, S., Domergue, F., and Roby, D. (2008). A MYB transcription factor regulates very-long-chain fatty acid biosynthesis for activation of the hypersensitive cell death response in *Arabidopsis*. *Plant Cell* **20,** 752-767.

Rentel, M. C., Lecourieux, D., Ouaked, F., Usher, S. L., Petersen, L., Okamoto, H., Knight, H., Peck, S. C., Grierson, C. S., Hirt, H., and Knight, M. R. (2004). OXI1 kinase is necessary for oxidative burst-mediated signalling in *Arabidopsis*. *Nature* **427,** 858–861.

Rizhsky, L., Davletova, S., Liang, H. J., and Mittler, R. (2004). The zinc finger protein Zat12 is required for cytosolic ascorbate peroxidase 1 expression during oxidative stress in *Arabidopsis*. *J. Biol. Chem.* **279,** 11736–11743.

Robson, C. A., and Vanlerberghe, G. C. (2002). Transgenic plant cells lacking mitochondrial alternative oxidase have increased susceptibility to mitochondria-dependent and -independent pathways of programmed cell death. *Plant Physiol.* **129,** 1908–1920.

Rogers, H. J. (2006). Programmed cell death in floral organs: How and why do flowers die? *Ann. Bot.* **97,** 309–315.

Rostoks, N., Schmierer, D., Mudie, S., Drader, T., Brueggeman, R., Caldwell, D. G., Waugh, R., and Kleinhofs, A. (2006). Barley necrotic locus nec1 encodes the cyclic nucleotide-gated ion channel 4 homologous to the *Arabidopsis* HLM1. *Mol. Genet. Genomics* **275,** 159–168.

Rouhier, N., Gelhaye, E., and Jacquot, J. P. (2004). Plant glutaredoxins: Still mysterious reducing systems. *Cell. Mol. Life Sci.* **61,** 1266–1277.

Sagi, M., and Fluhr, R. (2006). Production of reactive oxygen species by plant NADPH oxidases. *Plant Physiol.* **141,** 336–340.

Sakakibara, H. (2006). Cytokinins: Activity, biosynthesis, and translocation. *Annu. Rev. Plant Biol.* **57,** 431–449.

Sandaklie-Nikolova, L., Palanivelu, R., King, E. J., Copenhaver, G. P., and Drews, G. N. (2007). Synergid cell death in *Arabidopsis* is triggered following direct interaction with the pollen tube. *Plant Physiol.* **144,** 1753–1762.

Sandermann, H. (2004). Molecular ecotoxicology of plants. *Trends Plant Sci.* **9,** 406–413.

Sanmartin, M., Jaroszewski, L., Raikhel, N. V., and Rojo, E. (2005). Caspases. Regulating death since the origin of life. *Plant Physiol.* **137,** 841–847.

Schnittger, A., Weinl, C., Bouyer, D., Schobinger, U., and Hulskamp, M. (2003). Misexpression of the cyclin-dependent kinase inhibitor ICK1/KRP1 in single-celled *Arabidopsis* trichomes reduces endoreduplication and cell size and induces cell death. *Plant Cell* **15,** 303–315.

Seay, M. D., and Dinesh-Kumar, S. P. (2005). Life after death: Are autophagy genes involved in cell death and survival during plant innate immune responses? *Autophagy* **1,** 185–186.

Seo, S., Okamoto, M., Iwai, T., Iwano, M., Fukui, K., Isogai, A., Nakajima, N., and Ohashi, Y. (2000). Reduced levels of chloroplast FtsH protein in tobacco mosaic virus-infected tobacco leaves accelerate the hypersensitive reaction. *Plant Cell* **12,** 917–932.

Serino, G., and Deng, X. W. (2003). THE COP9 signalosome: Regulating plant development through the control of proteolysis. *Annu. Rev. Plant Biol.* **54,** 165–182.

Shabala, S. N., Cuin, T. A., Prismall, L., and Nemchinov, L. G. (2007). Expression of animal CED-9 anti-apoptotic gene in tobacco modifies plasma membrane ion fluxes in response to salinity and oxidative stress. *Planta* **227,** 189–197.

Shao, N., Krieger-Liszkay, A., Schroda, M., and Beck, C. F. (2007). A reporter system for the individual detection of hydrogen peroxide and singlet oxygen: Its use for the assay of reactive oxygen species produced *in vivo*. *Plant J.* **50,** 475–487.

Shi, L., Bielawski, J., Mu, J., Dong, H., Teng, C., Zhang, J., Yang, X., Tomishige, N., Hanada, K., Hannun, Y. A., and Zuo, J. (2007). Involvement of sphingoid bases in mediating reactive oxygen intermediate production and programmed cell death in *Arabidopsis*. *Cell Res.* **17,** 1030–1040.

Smalle, J., and Vierstra, R. D. (2004). The ubiquitin 26S proteasome proteolytic pathway. *Annu. Rev. Plant Biol.* **55,** 555–590.

Solomon, M., Belenghi, B., Delledonne, M., Menachem, E., Levine, A. (1999) The involvement of cysteine proteases and protease inhibitor genes in the regulation of programmed cell death in plants. *Plant Cell* **11,** 431-44.

Spassieva, S. D., Markham, J. E., and Hille, J. (2002). The plant disease resistance gene Asc-1 prevents disruption of sphingolipid metabolism during AAL-toxin-induced programmed cell death. *Plant J.* **32,** 561–572.

Stone, J. M., Heard, J. E., Asai, T., and Ausubel, F. M. (2000). Simulation of fungal-mediated cell death by fumonisin B1 and selection of fumonisin B1-resistant (fbr) *Arabidopsis* mutants. *Plant Cell* **12,** 1811–1822.

Stone, J. M., Liang, X., Nekl, E. R., and Stiers, J. J. (2005). *Arabidopsis* AtSPL14, a plant-specific SBP-domain transcription factor, participates in plant development and sensitivity to fumonisin B1. *Plant J.* **41,** 744–754.

Strand, A., Asami, T., Alonso, J., Ecker, J. R., and Chory, J. (2003). Chloroplast to nucleus communication triggered by accumulation of Mg-protoporphyrinIX. *Nature* **421,** 79–83.

Suarez, M. F., Filonova, L. H., Smertenko, A., Savenkov, E. I., Clapham, D. H., von Arnold, S., Zhivotovsky, B., and Bozhkov, P. V. (2004). Metacaspase-dependent programmed cell death is essential for plant embryogenesis. *Curr. Biol.* **14,** R339–R340.

Sun, K., Hunt, K., and Hauser, B. A. (2004). Ovule abortion in *Arabidopsis* triggered by stress. *Plant Physiol.* **135,** 2358–2367.

Sweat, T. A., and Wolpert, T. J. (2007). Thioredoxin h5 is required for victorin sensitivity mediated by a CC-NBS-LRR gene in *Arabidopsis*. *Plant Cell* **19,** 673–687.

Swidzinski, J. A., Sweetlove, L. J., and Leaver, C. J. (2002). A custom microarray analysis of gene expression during programmed cell death in *Arabidopsis thaliana*. *Plant J.* **30,** 431–446.

Tan, X., Calderon-Villalobos, L. I. A., Sharon, M., Zheng, C. X., Robinson, C. V., Estelle, M., and Zheng, N. (2007). Mechanism of auxin perception by the TIR1 ubiquitin ligase. *Nature* **446,** 640–645.

Tanaka, R., Hirashima, M., Satoh, S., and Tanaka, A. (2003). The Arabidopsis-accelerated cell death gene ACD1 is involved in oxygenation of pheophorbide a: Inhibition of the pheophorbide a oxygenase activity does not lead to the "Stay-Green" phenotype in *Arabidopsis*. *Plant Cell Physiol.* **44,** 1266–1274.

Thomas, S. G., and Franklin-Tong, V. E. (2004). Self-incompatibility triggers programmed cell death in Papaver pollen. *Nature* **429,** 305–309.

Thomas, S. G., Huang, S. J., Li, S. T., Staiger, C. J., and Franklin-Tong, V. E. (2006). Actin depolymerization is sufficient to induce programmed cell death in self-incompatible pollen. *J. Cell Biol.* **174,** 221–229.

Torres, M. A., Dangl, J. L., and Jones, J. D. G. (2002). Arabidopsis gp91(phox) homologues AtrbohD and AtrbohF are required for accumulation of reactive oxygen intermediates in the plant defense response. *Proc. Natl. Acad. Sci. USA* **99,** 517–522.

Torres, M. A., Jones, J. D. G., and Dangl, J. L. (2005). Pathogen-induced, NADPH oxidase-derived reactive oxygen intermediates suppress spread of cell death in *Arabidopsis thaliana*. *Nat. Genet.* **37,** 1130–1134.

Tsuda, T., Kato, Y., and Osawa, T. (2000). Mechanism for the peroxynitrite scavenging activity by anthocyanins. *FEBS Lett.* **484,** 207–210.

Urquhart, W., Gunawardena, A. H., Moeder, W., Ali, R., Berkowitz, G. A., and Yoshioka, K. (2007). The chimeric cyclic nucleotide-gated ion channel ATCNGC11/12 constitutively induces programmed cell death in a Ca^{2+} dependent manner. *Plant Mol. Biol.* **65,** 747–761.

Vacca, R. A., Valenti, D., Bobba, A., de Pinto, M. C., Merafina, R. S., De Gara, L., Passarella, S., and Marra, E. (2007). Proteasome function is required for activation of programmed cell death in heat shocked tobacco Bright-Yellow 2 cells. *FEBS Lett.* **581,** 917–922.

Vailleau, F., Daniel, X., Tronchet, M., Montillet, J. L., Triantaphylides, C., and Roby, D. (2002). A R2R3-MYB gene, AtMYB30, acts as a positive regulator of the hypersensitive cell death program in plants in response to pathogen attack. *Proc. Natl. Acad. Sci. USA* **99,** 10179–10184.

Van Breusegem, F., and Dat, J. (2006). Reactive oxygen species in plant cell death. *Plant Physiol.* **141,** 384–390.

Van Breusegem, F., Vranova, E., Dat, J. F., and Inzé, D. (2001). The role of active oxygen species in plant signal transduction. *Plant Sci.* **161,** 405–414.

Vandenabeele, S., Van Der Kelen, K., Dat, J., Gadjev, I., Boonefaes, T., Morsa, S., Rottiers, P., Slooten, L., Van Montagu, M., Zabeau, M., Inzé, D., and Van Breusegem, F. (2003). A comprehensive analysis of hydrogen peroxide-induced gene expression in tobacco. *Proc. Natl. Acad. Sci. USA* **100,** 16113–16118.

Vandenabeele, S., Vanderauwera, S., Vuylsteke, M., Rombauts, S., Langebartels, C., Seidlitz, H. K., Zabeau, M., Van Montagu, M., Inzé, D., and Van Breusegem, F.

(2004). Catalase deficiency drastically affects gene expression induced by high light in *Arabidopsis thaliana*. *Plant J.* **39,** 45–58.

Vanderauwera, S., Zimmermann, P., Rombauts, S., Vandenabeele, S., Langebartels, C., Gruissem, W., Inzé, D., and Van Breusegem, F. (2005). Genome-wide analysis of hydrogen peroxide-regulated gene expression in *Arabidopsis* reveals a high light-induced transcriptional cluster involved in anthocyanin biosynthesis. *Plant Physiol.* **139,** 806–821.

Vercammen, D., van de Cotte, B., De Jaeger, G., Eeckhout, D., Casteels, P., Vandepoele, K., Vandenberghe, I., Van Beeumen, J., Inzé, D., and Van Breusegem, F. (2004). Type II metacaspases Atmc4 and Atmc9 of *Arabidopsis thaliana* cleave substrates after arginine and lysine. *J. Biol. Chem.* **279,** 45329–45336.

Vercammen, D., Belenghi, B., van de Cotte, B., Beunens, T., Gavigan, J. A., De Rycke, R., Brackenier, A., Inzé, D., Harris, J. L., and Van Breusegem, F. (2006). Serpin1 of *Arabidopsis thaliana* is a suicide inhibitor for metacaspase 9. *J. Mol. Biol.* **364,** 625–636.

Vercammen, D., Declercq, W., Vandenabeele, P., and Van Breusegem, F. (2007). Are metacaspases caspases. *J. Cell Biol.* **179,** 375–380.

Vert, G., and Chory, J. (2006). Downstream nuclear events in brassinosteroid signalling. *Nature* **441,** 96–100.

Vranova, E., Atichartpongkul, S., Villarroel, R., Van Montagu, M., Inzé, D., and Van Camp, W. (2002). Comprehensive analysis of gene expression in *Nicotiana tabacum* leaves acclimated to oxidative stress. *Proc. Natl. Acad. Sci. USA* **99,** 10870–10875.

Wagner, D., Przybyla, D., Camp, R. O. D., Kim, C., Landgraf, F., Lee, K. P., Wursch, M., Laloi, C., Nater, M., Hideg, E., and Apel, K. (2004). The genetic basis of singlet oxygen-induced stress responses of *Arabidopsis thaliana*. *Science* **306,** 1183–1185.

Wang, H., Jones, C., CiacciZanella, J., Holt, T., Gilchrist, D. G., and Dickman, M. B. (1996a). Fumonisins and *Alternaria alternata lycopersici* toxins: Sphinganine analog mycotoxins induce apoptosis in monkey kidney cells. *Proc. Natl. Acad. Sci. USA* **93,** 3461–3465.

Wang, H., Li, J., Bostock, R. M., and Gilchrist, D. G. (1996b). Apoptosis: A functional paradigm for programmed plant cell death induced by a host-selective phytotoxin and invoked during development. *Plant Cell* **8,** 375–391.

Wang, K. L. C., Li, H., and Ecker, J. R. (2002). Ethylene biosynthesis and signaling networks. *Plant Cell* **14,** S131–S151.

Watanabe, N., and Lam, E. (2006). *Arabidopsis* Bax inhibitor-1 functions as an attenuator of biotic and abiotic types of cell death. *Plant J.* **45,** 884–894.

Watanabe, N., and Lam, E. (2008). BAX inhibitor-1 modulates endoplasmic reticulum stress-mediated programmed cell death in *Arabidopsis*. *J. Biol. Chem.* **283,** 3200–3210.

Willekens, H., Chamnongpol, S., Davey, M., Schraudner, M., Langebartels, C., VanMontagu, M., Inze, D., and VanCamp, W. (1997). Catalase is a sink for H_2O_2 and is indispensable for stress defence in C-3 plants. *EMBO J.* **16,** 4806–4816.

Xiong, Y., Contento, A. L., Nguyen, P. Q., and Bassham, D. C. (2007). Degradation of oxidized proteins by autophagy during oxidative stress in *Arabidopsis*. *Plant Physiol.* **143,** 291–299.

Xu, P., Rogers, S. J., and Roossinck, M. J. (2004). Expression of antiapoptotic genes bcl-xL and ced-9 in tomato enhances tolerance to viral-induced necrosis and abiotic stress. *Proc. Natl. Acad. Sci. USA* **101,** 15805–15810.

Yadegari, R., and Drews, G. N. (2004). Female gametophyte development. *Plant Cell* **16,** S133–S141.

Yang, H., Yang, S., Li, Y., and Hua, J. (2007). The Arabidopsis BAP1 and BAP2 genes are general inhibitors of programmed cell death. *Plant Physiol.* **145**, 135–146.

Yao, N., and Greenberg, J. T. (2006). *Arabidopsis* accelerated cell death2 modulates programmed cell death. *Plant Cell* **18,** 397–411.

Yao, N., Tada, Y., Sakamoto, M., Nakayashiki, H., Park, P., Tosa, Y., and Mayama, S. (2002). Mitochondrial oxidative burst involved in apoptotic response in oats. *Plant J.* **30,** 567–579.

Yao, N., Eisfelder, B. J., Marvin, J., and Greenberg, J. T. (2004). The mitochondrion—an organelle commonly involved in programmed cell death in *Arabidopsis thaliana*. *Plant J.* **40,** 596–610.

Young, T. E., and Gallie, D. R. (2000). Programmed cell death during endosperm development. *Plant Mol. Biol.* **44,** 283–301.

Yu, I. C., Parker, J., and Bent, A. F. (1998). Gene-for-gene disease resistance without the hypersensitive response in *Arabidopsis* dnd1 mutant. *Proc. Natl. Acad. Sci. USA* **95,** 7819–7824.

Yu, X. H., Perdue, T. D., Heimer, Y. M., and Jones, A. M. (2002). Mitochondrial involvement in tracheary element programmed cell death. *Cell Death Differ.* **9,** 189–198.

Zago, E., Morsa, S., Dat, J., Alard, P., Ferrarini, A., Inzé, D., and Delledonne, M. (2006). Nitric oxide- and hydrogen peroxide-responsive gene regulation during cell death induction in tobacco. *Plant Physiol.* **141,** 401–411.

Zaina, G., Morassutti, C., De Amicis, F., Fogher, C., and Marchetti, S. (2003). Endonuclease genes up-regulated in tissues undergoing programmed cell death are expressed during male gametogenesis in barley. *Gene* **315,** 43–50.

Zaninotto, F., Camera, S. L., Polverari, A., and Delledonne, M. (2006). Cross talk between reactive nitrogen and oxygen species during the hypersensitive disease resistance response. *Plant Physiol.* **141,** 379–383.

Zhang, W. H., Wang, C. X., Qin, C. B., Wood, T., Olafsdottir, G., Welti, R., and Wang, X. M. (2003). The oleate-stimulated phospholipase D, PLD delta, and phosphatidic acid decrease H_2O_2-induced cell death in arabidopsis. *Plant Cell* **15,** 2285–2295.

CHAPTER FOUR

Protein Trafficking in Polarized Cells

Amy Duffield,*,† Michael J. Caplan,* *and* Theodore R. Muth‡

Contents

Abstract

Epithelial cells line the lumens of organs and thus constitute the interface between the body's interior and exterior surfaces. This position endows these cells with the important task of regulating what enters and what is exported from the body. In order to accomplish this function, epithelia must have structurally and functionally distinct membrane surfaces: the apical surface exposed to the lumen, and the basolateral surface in contact with the laterally adjacent epithelial cells, and the connective tissue and capillary network below the epithelia. The specific lipid and protein contents of the apical and basolateral membrane surfaces are determined by a number of sorting and retention mechanisms. Many of these sorting and retention mechanisms are shared with other polarized cell types including neurons and certain cells of the immune system. This chapter focuses on recent advances in understanding how these various mechanisms facilitate the generation, maintenance, and dynamic regulation of protein and lipid trafficking within epithelial cells.

* Department of Cellular and Molecular Physiology, Yale University School of Medicine, New Haven, Connecticut 06520
† Department of Pathology, Johns Hopkins Medical Institutions, Baltimore, Maryland 21287
‡ Department of Biology, Brooklyn College, City University of New York, Brooklyn, New York 11210

International Review of Cell and Molecular Biology, Volume 270
ISSN 1937-6448, DOI: 10.1016/S1937-6448(08)01404-4

Key Words: Epithelia, Polarity, Trafficking, Sorting determinants, Membrane targetting.

1. Introduction

The intracellular transport of proteins is vital to the function of cells, and defective protein transport and distribution have been linked to a number of human diseases (Choudhury *et al.*, 1997; Di Pietro and Dell'Angelica, 2005; Hoeller *et al.*, 2005; Howell *et al.*, 2006; Kim and Arvan, 1998; Thomas *et al.*, 1992). While the importance of appropriate intracellular trafficking is appreciated, the mechanisms that regulate trafficking have not been fully characterized. The trafficking information that directs the transport of membrane proteins can be found on their intracellular, extracellular, and transmembrane domains. These trafficking signals interact with other proteins or lipids that carry out the sorting process. A large number of proteins that may participate in protein sorting have been identified; however, the interplay between these proteins is complex and not fully understood.

Membrane proteins can traffic to a number of different sites within the cell. Proteins may sort to intracellular compartments, such as endosomes, lysosomes, or secretory vesicles, and can also be delivered to the cell surface. In epithelial cells, the plasma membrane is divided into two distinct domains, the apical and basolateral surfaces, and the cell must be able to target proteins to the correct surface. The apical domain typically faces the lumen of a tubular or ductal tissue, and thus is in communication with the ''outside'' of the body, whereas the basolateral domain contacts the extracellular fluid compartment (Fig. 4.1). These domains are separated by tight junctions, and proteins present in one domain cannot freely diffuse to the other domain (Yeaman *et al.*, 1999). Appropriate physiological responses to stimuli often demand that proteins be either internalized from or inserted into the plasma membrane. Furthermore, these regulated trafficking events frequently require proteins to be inserted into or removed exclusively from either the basolateral or the apical domain; thus, epithelial cells have developed a number of mechanisms that regulate polarized sorting. Other cell types, including neurons and immune cells, also exhibit polarized protein sorting, but the mechanisms involved in these fascinating processes are beyond the scope of this chapter (see excellent reviews by Groc and Choquet, 2006; Kim and Sheng, 2004; Lai and Jan, 2006; Taner *et al.*, 2004).

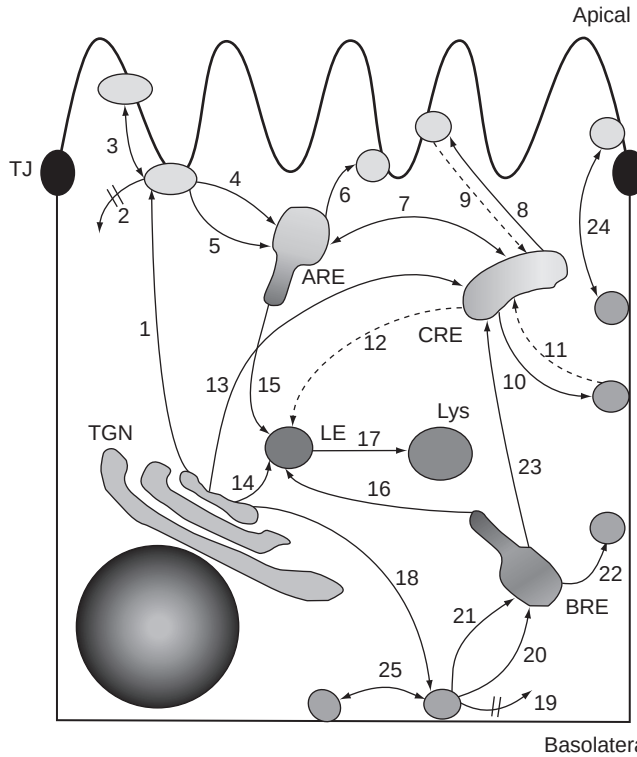

Figure 4.1 This figure illustrates the major trafficking routes within polarized epithelia. Newly synthesized membrane proteins progress through the endoplasmic reticulum and Golgi complex. In the TGN, the proteins are packaged into vesicles, and these vesicles may be delivered directly to the apical or basolateral plasma membrane. These membrane proteins may then follow a number of intracellular sorting pathways. Pathways 1 and 18 depict proteins that are delivered directly to the apical or basolateral membrane, respectively (Mostov *et al.*, 2003). These proteins may by retained at the membrane through interactions with other proteins, pathways 2 and 19 (Harris and Lim, 2001; Murshid and Presley, 2004; Zimmermann, 2006), or be endocytosed via either a clathrin-independent mechanism, pathways 4 and 20 (Alfalah *et al.*, 2005; Cheng *et al.*, 2006; Johannes and Lamaze, 2002; Laude and Prior, 2004; Stan, 2005), or a clathrin-dependent mechanism, pathways 5 and 21 (Cheng and Walz, 2007; Sorkin, 2004) to recycling endosomes. It is possible that some proteins are endocytosed and returned to their original membrane domain without fusing with recycling endosomes, pathways 3 and 25 (Rea *et al.*, 2004; Sheff *et al.*, 1999). Proteins that pass through apical or basolateral recycling endosomes can be returned to their orginal membrane domain, paths 6 or 22 (Hao and Maxfield, 2000), LEs, paths 15 and 16 (Luzio *et al.*, 2001; Rodriguez-Boulan *et al.*, 2004), or the CRE, pathways 7 and 23 (Hao and Maxfield, 2000). Proteins can also be delivered directly to the CRE directly from the TGN to the CRE, pathway 13 (Ang *et al.*, 2004) or to LEs, pathway 14 (Ang *et al.*, 2004; Bomsel *et al.*, 1999; Bonifacino and Traub, 2003). Proteins in the CRE can sort either to the apical or basolateral surface, pathways 8 and 10 (Ang *et al.*, 2004; Sheff *et al.*, 2002; Thompson *et al.*, 2007). Proteins in the LE can also move into Lys, path 17 (Luzio *et al.*, 2001; Russell *et al.*, 2006; van der Goot and

2. Exocytosis, Endocytosis, and Sorting Pathways

Membrane proteins may be targeted to their ultimate destination immediately after synthesis and passage through the trans-Golgi network (TGN), or they may reach their final destination via a more circuitous route that can involve transcytosis between surface plasma membrane domains and passage through endosomal compartments (Fig. 4.2). Proteins that begin the sorting process in the TGN are loaded into a vesicle, and delivered to the plasma membrane or an intracellular compartment (Mostov *et al.*, 2003). Recently, the importance of recycling endosomes as an intermediate step between the TGN and the basolateral surface has been established (Ang *et al.*, 2004). The localization of the adaptor protein-1B (AP-1B) clathrin adaptor complex to recycling endosomes, along with the transient localization of the vesicular stomatitis glycoproteins (VSV-G), which is dependent on the AP-1B complex for proper targeting, to the recycling endosomes, shows that at least some cargo molecules do not pass directly from the TGN to the basolateral membrane. This work suggests the significance of recycling endosomes in protein sorting during secretion and endocytosis.

When vesicles reach the plasma membrane, they must dock and fuse with the lipid bilayer. The plasmalemma, or target membrane, contains transmembrane proteins called target soluble *N*-ethylmaleimide-sensitive factor attachment protein receptors (t-SNARES), such as SNAP25 and syntaxin (Hong, 2005; Snyder *et al.*, 2006; Ungermann and Langosch, 2005; Waters and Hughson, 2000). A vesicle that is approaching the target membrane contains transmembrane proteins that are referred to as v-SNAREs, such as VAMP. The vesicle and target membrane SNAREs associate with one another to create a four helix bundle, and the formation of this complex is regulated by several proteins, including munc18/nSec1 (Fisher *et al.*, 2001). This tethering event is likely facilitated by members of the Rab family of small GTPase proteins (Sutton *et al.*, 1998; Waters and Hughson, 2000). After the vesicles are docked, the membranes must fuse, and this fusion event is mediated by various proteins and lipids (Murthy and De Camilli, 2003). The ATPase *N*-ethylmaleimide-sensitive factor (NSF) then assists in the disassembly and recycling of the SNARE complex proteins (Sollner *et al.*, 1993). Vesicle

Gruenberg, 2006. Movement directly between the apical and bsaolateral domains is carried out by transcytosis, pathway 24 (Hoessli *et al.*, 2004; Fuchs and Ellinger, 2004; Kobayashi *et al.*, 2002; Rojas and Apodaca, 2002). Dotted lines indicate possible routes for intracellular trafficking that have not yet been conclusively established, pathways 9, 11 and 12 (Hoekstra *et al.*, 2004). The apical membrane is represented by a thicker line than the basolateral membrane. TGN, trans-Golgi network; TJ, tight junction; ASE, apical sorting endosome; BSE, basolateral sorting endosome; LE, late endosome; Lys, lysosome; CRE, common recycling endosome.

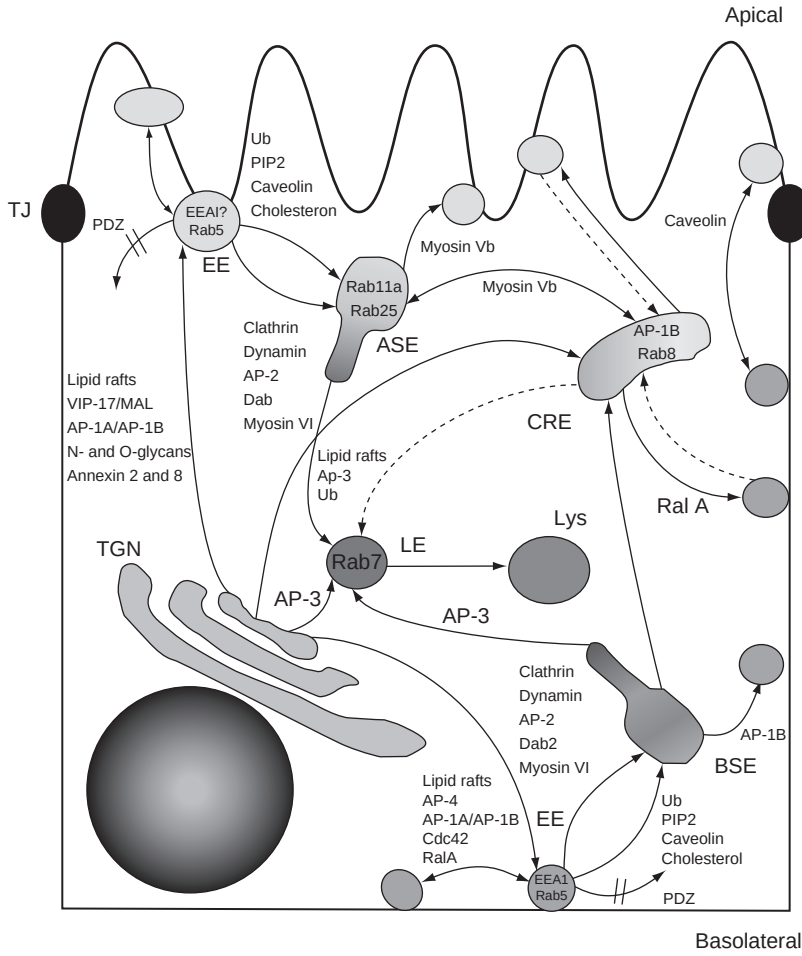

Figure 4.2 This figure shows the major trafficking pathways illustrated in Fig. 4.1, and indicates a number of important proteins, lipid components, and glycosyl chains that have a role in carrying out and regulating these pathways. Refer to the text for greater detail and references. Of necessity, this figure does not include many other factors that have important roles in trafficking, but whose complete description was beyond the scope of this chapter.

docking and fusion machinery is similar in both constitutive and regulated exocytosis (Fujita *et al.*, 2007; Rickman *et al.*, 2007).

Proteins that arrive at the plasma membrane may be retained at the membrane via interactions with the cytoskeleton and other proteins associated with the cytoskeleton (Harris and Lim, 2001; Murshid and Presley, 2004; Zimmermann, 2006). Many plasma membrane proteins that are not anchored into place by the cytoskeleton undergo relatively rapid endocytosis

and postendocytic sorting (Bomberger *et al.*, 2005; Bomsel *et al.*, 1989; Cottrell *et al.*, 2007).

Endocytosis can occur through either a clathrin-mediated or a clathrin-independent process. Clathrin-independent uptake may occur via caveolae or other membrane microdomains. Caveolae are small flask-shaped plasma membrane invaginations that contain the protein caveolin-1. They are relatively static structures, but a number of factors can stimulate caveolae uptake, creating caveosomes (Mukherjee *et al.*, 2006; Parton *et al.*, 1994; Pelkmans and Helenius, 2002; Thomsen *et al.*, 2002). The uptake of caveosomes is likely to be similar to clathrin-mediated endocytosis because caveolae are enriched in proteins that function in membrane docking and fusion events (Oh *et al.*, 1998; Schnitzer *et al.*, 1995). Caveolae may be a subgroup in a broader class of membrane microdomains that are involved in facilitating endocytic events (Alfalah *et al.*, 2005; Cheng *et al.*, 2006; Johannes and Lamaze, 2002; Laude and Prior, 2004; Stan, 2005). Microdomains form when a distinct set of lipids and proteins partition within the plane of the membrane, creating discrete regions within the plasmalemma. Membrane proteins associated with different microdomains may demonstrate various levels of endocytic activity, and some membrane microdomains may in fact facilitate clathrin-mediated endocytosis (Sandvig *et al.*, 1989; Torgersen *et al.*, 2001).

Clathrin-mediated endocytosis is a well-characterized process (Cheng and Walz, 2007; Sorkin, 2004). There are several stages in clathrin-dependent endocytosis including cargo selection, formation of the clathrin-coated pit, clathrin-coated vesicle scission, and vesicle uncoating. Cargo selection is primarily performed by APs that link clathrin and cargo proteins, such as clathrin AP-2. Clathrin gathered by APs then self-assembles into cage-like structures, deforming the overlying membrane and creating clathrin-coated pits (Kirchhausen, 2000). AP-2 also interacts with inositol polyphosphates, such as phosphatidylinositol 4,5 bisphosphate, which may serve to concentrate on the various participants in clathrin-mediated endocytosis at the plasma membrane (Haucke, 2005; Jost *et al.*, 1998; Lafer, 2002). Several clathrin-binding proteins, including Eps15, seem to provide a link between clathrin-coated vesicles and the actin cytoskeleton (Duncan *et al.*, 2001; Kalthoff *et al.*, 2002; Toshima *et al.*, 2005, 2007). Finally, clathrin-coated pits pinch off from the plasma membrane, in a process that is initiated by the GTPase dynamin (Takei *et al.*, 1995).

Current data suggest that most endocytosed material is initially found in early endosomes regardless of whether the vesicles are internalized via clathrin-dependent or clathrin-independent endocytosis (Johannes and Lamaze, 2002; Naslavsky *et al.*, 2004). Early endosomes contain various proteins that participate in vesicle formation and fusion (Folsch, 2005; Saraste and Goud, 2007). These proteins include the GTPase Rab5, the Rab5 effector protein endosome antigen 1 (EEA1), several other Rabs including Rab4, Rab22 and

Rab21, and SNARES such as syntaxin 13 (McBride *et al.*, 1999; Simpson *et al.*, 2004; Wilson *et al.*, 2000). After endocytosis, primary endosomes may return immediately to the surface without passing through intermediate compartments (Rea *et al.*, 2004). Alternatively, a primary endosome may fuse with other newly formed endosomes and existing endosomes to form a sorting endosome. Rabs, EEA1 and SNARES, as well as patches of phosphatidyl inositol 3-phosphate are required for these fusion events (Murray and Backer, 2005; Tuma *et al.*, 2001).

The sorting endsome is a peripherally located compartment with an internal pH of ~6, and is relatively short-lived (Maxfield and McGraw, 2004). As the sorting endosome matures, its lumen is acidified by the V-type ATPase, and the decreasing pH dissociates any bound ligand that has been internalized with its receptor. Tubules that pinch off of the acidifying sorting endosome may either return to the plasma membrane directly and rapidly with a $t_{1/2}$ of about 2 min, or may traffic to a longer-lived common recycling endosome (CRE) (Hao and Maxfield, 2000).

The CRE consists of tubular organelles that are closely associated with microtubules. Accordingly, the CRE is often located close to the microtubule organizing center, but it may also be dispersed throughout the cytoplasm (Hoekstra *et al.*, 2004). This compartment sorts proteins to the appropriate cell surface or intracellular compartments, and transit through the CRE is somewhat slower than transit through sorting endosomes. The transferrin receptor, for instance, traffics through the CRE and is returned to the apical membrane with a $t_{1/2}$ of about 10 min (Futter *et al.*, 1998; Sheff *et al.*, 2002; Thompson *et al.*, 2007). The CRE appears to be important for sorting to both the apical and basolateral membranes, and experiments have demonstrated that passage through an intermediate recycling endosome is crucial for the delivery of vesicles containing vesicular stomatitis virus G protein to both the basolateral and apical membranes (Ang *et al.*, 2004).

While endocytosed proteins may return to the surface from which they originated, they can also be delivered to the opposite cell surface in a process called transcytosis (Fuchs and Ellinger, 2004; Rojas and Apodaca, 2002). Transcytosis can occur from the apical to basolateral membrane as with cubulin and megalin, basolateral to apical membrane as with secretory immunoglobulin A and polymeric immunoglobulin receptor, or back and forth between these membranes as with the neonatal Fc receptor (Kobayashi *et al.*, 2002). Transcytosis of vesicles can occur directly from one membrane domain to another without passage through intervening compartments. This rapid transcytosis occurs in endothelial cells, and is thought to be mediated by caveolae (Hoessli *et al.*, 2004; Schubert *et al.*, 2001). Transcytosed proteins may also move through intermediate compartments, including sorting endosomes and the CRE, during passage through polarized cells (Leyt *et al.*, 2007; Tuma and Hubbard, 2003).

Some proteins that are internalized from the cell surface, such as low-density lipoprotein (LDL), are routed from the sorting endosome into the late endosomal compartment (Rodriguez-Boulan *et al.*, 2004). Proteins that are sorted to late endosomes may move directly from the TGN to this intracellular compartment, or they may traffic to the late endosome only after initial delivery to the plasma membrane or sorting endosomes (Ang *et al.*, 2004; Bonifacino and Traub, 2003). Late endosomes have a significantly lower lumenal pH than early endosomes, and a different protein composition. Morphologically, late endosomes are less tubular and more spherical than early endosomes, and contain an elaborate system of internal membranes. There are two current models describing the formation of late endosomes, although neither has been experimentally proven (Gruenberg and Stenmark, 2004; van der Goot and Gruenberg, 2006). The maturation model proposes that early endosomes acidify and lose a subset of their resident proteins through the gradual loss of recycling tubules. The stable compartment model proposes that the proteins destined for the cell surface or the CRE segregate entirely from proteins destined for the late endosome, and that these two compartments then undergo fission to form two distinct new vesicles. Regardless of the model, once the appropriate subset of proteins and lipids is routed from early endosomes back to the plasma membrane, the proteins and lipid that will ultimately traffic to the late endosomes are contained in a compartment referred to as a multivesicular endosome or multivesicular body (MVB). This compartment is transported along microtubules until its fusion with late endosomes (Bomsel *et al.*, 1990). The late endosome is not a sorting ''dead end.'' It participates in protein and lipid trafficking, and late endosomal proteins may be directed from this compartment not only to lysosomes but also to the Golgi or cell surface (Russell *et al.*, 2006; van der Goot and Gruenberg, 2006). Proteins that move from late endosomes to lysosomes do so through the fusion of late endosomes with existing lysosomes (Luzio *et al.*, 2001).

It is important to note that primarily ''forward'' motion of vesicles has been discussed here, but that retrograde transport, for instance, trafficking from endosomes to the TGN, occurs and is crucial for cell function (for reviews of retrograde trafficking, see Bard and Malhotra, 2006; Spooner *et al.*, 2006; Ungar *et al.*, 2006; Watson and Spooner, 2006).

3. Apical Sorting

3.1. Apical sorting signals

How are proteins routed to the apical membrane? As demonstrated in Fig. 4.1, proteins destined for the apical membrane may be directly targeted to this location, or they may be sorted via a more indirect transcytotic route

(Nichols *et al.*, 2001; Polishchuk *et al.*, 2004; Sabharanjak *et al.*, 2002). Apical sorting determinants are frequently located in a protein's transmembrane or extracellular domain (see Table 4.1).

Transmembrane sorting signals frequently facilitate apical sorting by determining their parent proteins' inclusion in a specific membrane microdomain. For experimental purposes, membrane microdomains can be operationally differentiated from one another by their insolubility in various detergents. Lipid rafts are one of the best characterized microdomains, and are defined by their insolubility in cold Triton X-100 (Brown, 2006; Chang *et al.*, 2006; Delacour *et al.*, 2006; Salaun *et al.*, 2004). Rafts are thought to form initially in the Golgi complex. Most lipid raft-containing vesicles bud from the TGN and traffic to the apical membrane (Brown *et al.*, 1989; Lafont *et al.*, 1999; Lisanti *et al.*, 1989; Paladino *et al.*, 2004). Thus, a protein's inclusion in a lipid raft frequently facilitates its delivery to the apical surface (Simons and Ikonen, 2000). The lipid raft protein VIP17/MAL1 may either escort its associated proteins to the apical membrane, or it may retain associated proteins within the apical membrane, although its precise mechanism of action is not clear (Brown, 2006; Kamsteeg *et al.*, 2007; Puertollano *et al.*, 1999; Ramnarayanan *et al.*, 2007; Tall *et al.*, 2003). Glycosylphosphatidylinositol (GPI) is also incorporated into lipid rafts; therefore, proteins that are covalently linked to GPI tend to accumulate at the apical plasma membrane as well (Brown and London, 1998; Simons and Ikonen, 2000). A small subset of GPI-anchored proteins is localized to the basolateral membrane, and the basolateral plasmalemma also contains some lipid raft microdomains. It is, however, possible that apical lipid rafts and basolateral lipid rafts actually represent two different membrane microdomains (Brown, 2006; Brugger *et al.*, 2004; Cheng *et al.*, 2006; Paladino *et al.*, 2004). Additionally, there is recent evidence indicating the importance of phosphatidylinositol-3,4,5-triphosphate in the generation of basolateral plasma membranes in Madin-Darby canine kidney (MDCK) cells (Gassama-Diagne *et al.*, 2006). Normally, phosphatidylinositol-3,4,5-triphosphate is restricted to the basolateral domain of epithelia; however, when artificially inserted into the apical membrane phosphatidylinositol-3,4,5-triphosphate triggered the formation of basolateral-like domains protruding above the existing apical surface. These basolateral-like domains rapidly begin to collect proteins known to reside in basolateral membrane domains, suggesting a role for phosphatidylinositol-3,4,5-triphosphate in promoting the correct targeting to and/or retention of proteins at the basolateral surface (Gassama-Diagne *et al.*, 2006).

The mechanism by which lipid rafts promote apical sorting is not yet fully elucidated. Lipid rafts may "float" their resident proteins directly to the apical membrane, but incorporation in a raft is not sufficient to ensure that a GPI-anchored protein is stabilized in the apical membrane (Langhorst *et al.*, 2005; Paladino *et al.*, 2004; Rodriguez-Boulan *et al.*, 2004; Schuck and Simons, 2006). Recent work has demonstrated that oligomerization of

Table 4.1 Sorting motifs

	Signal	Examples	Comments
Apical (signals are extracellular, transmembrane, or cytoplasmic)	Lipid rafts	Hemagglutinin (rafts), placental alkaline phosphatase (GPI-linked)	The lipid raft protein VIP17/MAL may participate; GPI-anchored proteins are often included in lipid rafts
	Glycosylation	Nerve growth factor receptor p75	N-linked or O-linked
	Cytoplasmic sequences	Megalin, rhodopsin, GAT3	Sequences are of variable length and composition
Basolateral (signals are cytoplasmic)	Complex	Poly-Ig receptor, neural cell adhesion molecule epidermal growth factor receptor, GAT2	Tend to be cytoplasmic
	NPXY	LDL receptor	Typically more active in enhancing endocytosis than BL sorting
	Dihydrophobic -LL- -II- -LI- -IL-	Fc receptor myosin heavy chain class II invariant chain	May be subdivided into [DE]XXX[LI] and DXXLL families; see "endosomal/lysosomal" below
	YXXØ	LDL receptor, H,K-ATPase β-subunit	AP-1 & AP-4 have been associated with basolateral sorting

Endosomal/ lysosomal (signals are cytoplasmic)	NPXY	LDL receptor, megalin, integrin β-1, APP	May be colinear with basolateral sorting motif
	Dihydrophobic [DE]XXX[LI]	Tyrosinase, TRP-1, CD4, GLUT-4, invariant chain[44]	Sorting to specialized intracellular vesicles: late endosomes, lysosomes, melanosomes, regulated storage vesicles
	DXXLL	CI-MPR, CD-MPR	Cycling between TGN and endosomes
	YXXØ	Lamp-1, Lamp-2, Lamp-3 (CD63), transferrin receptor	Sorting to specialized intracellular vesicles: late endosomes, lysosomes, melanosomes, regulated storage vesicles
	Acidic clusters	Furin, PC7, CPD	Often contain sites for phosphoylation by CKII
	Ubiquitin	EGF, ENaC	Ubiquitination is posttranslational; involved in regulated protein turnover

EGF, epithelial growth factor; GPI, glycosylphosphatidylinositol; LDL, low-density lipoprotein; TGN, trans-Golgi network.
Apical, basolateral, and endosomal/lysosomal sorting motifs are summarized. Proteins that stabilize other proteins at either the apical or basolateral membrane are not included in this table.

some lipid raft proteins during transit through the Golgi seems to promote apical delivery of these membrane microdomains, and that GPI-anchored lipid raft proteins which are localized to the basolateral membrane tend not to oligomerize. These data suggest that both lipid raft inclusion and protein–protein interactions are required for apical membrane delivery. An alternative model has also been proposed in which GPI-anchored proteins initially delivered to the cells' lateral membranes are internalized by a clathrin-independent pathway, and redistributed to the apical membrane (Nyasae *et al.*, 2003; Polishchuk *et al.*, 2004).

Glycosylation is an extracellular protein modification that tends to favor apical sorting of soluble and membrane proteins. Both N- and O-glycosylation have been shown to promote the apical delivery of proteins (Naim *et al.*, 1999; Potter *et al.*, 2004; Scheiffele and Fullekrug, 2000; Scheiffele *et al.*, 1995; Wagner *et al.*, 1995; Yeaman *et al.*, 1997). Apical sorting information encoded through N-glycosylation is robust and can override basolateral sorting information that is present in a protein's cytoplasmic tail (Potter *et al.*, 2004). The mechanism for apical delivery of glycosylated proteins has not yet been determined. It has been proposed that glycosylated proteins resident in lipid rafts may be cross-linked by lectins, which functionally oligomerize these proteins and enhance their apical delivery much in the way that protein–protein interactions enhance apical localization (Fullekrug and Simons, 2004). It is not, however, necessary that apically localized N-glycosylated proteins be incorporated within a lipid raft, because N-glycans can direct a protein to the apical membrane even if this protein is not resident in a raft. Recent work also suggests that terminal glycosylation, rather than core glycosylation, of N-glycans seems to be important for apical sorting (Potter *et al.*, 2004; Vagin *et al.*, 2004). Despite the tendency for glycosylation to drive apical sorting, it is clear that by no means do all glycosylated proteins ultimately localize to the apical membrane. In fact, the protein population of the basolateral plasma membrane is replete with glycoproteins, demonstrating that the mere presence of glycosyl residues is not in itself sufficient to specify apical targeting.

Several cytoplasmic apical sorting signals have also been identified (Dunbar *et al.*, 2000; Muth *et al.*, 1998). They range from short sequences of a few amino acids to amino acid stretches of up to 30 residues, and the molecular machinery that interacts with these specific signals is only beginning to be determined (Inukai *et al.*, 2004; Takeda *et al.*, 2003).

3.2. Apical sorting machinery

There are several proteins that seem to be associated with the apical delivery of vesicles, including the annexins, myosins, various PDZ domain-containing apical scaffolding proteins, the cytoskeleton, and SNARES (Altschuler *et al.*, 2003; Jacob *et al.*, 2003). Annexin II is an actin- and

phospholipid-binding protein that has been associated with exocytosis, endocytosis, and other membrane fission events. It is present in a subset of lipid raft-containing vesicles that traffic to the apical membrane along actin filaments, and disruption of annexin II decreases the apical delivery of proteins that reside in annexin II-positive vesicles (Danielsen and Hansen, 2006; Delacour and Jacob, 2006; Jacob *et al.*, 2004). The translocation of annexin II to the apical membrane seems to be dependent on it complexing with S100A10, which enhances its phospholipid binding, and phosphorylation of tyrosine 23 (Deora *et al.*, 2004; Isacke *et al.*, 1986; Thiel *et al.*, 1992). The precise mechanism of action of annexin II remains unknown, although it has been postulated that this protein acts as an adaptor between apically directed vesicles and actin filaments. Another annexin, annexin XIIIb, has also been implicated in the apical delivery of both hemagglutinin and the ubiquitin protein ligase Nedd4 (Lafont *et al.*, 1998; Noda *et al.*, 2001; Plant *et al.*, 2000).

Current data suggest that three myosins, myosin Ia, II, and myosin Vb, may also be involved in apical trafficking (Au *et al.*, 2007; Chan *et al.*, 2005; Fath, 2006; Frank *et al.*, 2004). Myosin Ia is localized to the apical microvillar comparment in adult *Drosophila melanogaster* gut and is present in the same apically directed vesicles that contain annexin II (Jacob *et al.*, 2003; Morgan *et al.*, 1995). Myosin Vb is localized to the apical recycling system in polarized cells, and it facilitates the exit of proteins from apical recycling endosomes, although these proteins may then be transported to either the apical or basolateral plasmalemma (Lapierre *et al.*, 2001). This myosin is not, however, involved in direct transport to the apical membrane from the TGN.

PDZ proteins that are resident in the apical membrane may participate in the apical localization of their interaction partners (Lamprecht and Seidler, 2006; Zimmermann, 2006). PDZ refers to the proteins Postsynaptic Density protein 95, Drosophila *D*isks Large and *Z*ona Occludens-1, all of which contain a specific sequence, called a PDZ domain, which interacts with a five amino acid consensus sequence in the carboxy terminus of associated proteins. Many PDZ proteins also contain other domains that facilitate various protein–protein interactions, such an SH3 or PH domain. Thus, many PDZ proteins are able to participate in the formation of a web of associated proteins. The PDZ proteins NHERF-1, NHERF-2, and PDZK1 are all resident in the plasma membrane, and have been shown to promote the apical retention of some of their interaction partners. In the apical brush-border membrane of renal proximal tubule cells, the apical localization of type II Na^+-dependent phosphate cotransporter (NaPi-IIa) is maintained in part through its interaction with NHERF-1 and PDZK1, and the apical localization of a Na^+/H^+ proton exchanger (NHE3) is maintained in part through its interaction with NHERF-2 (Capuano *et al.*, 2005, 2007; Donowitz and Li, 2007; Lee-Kwon *et al.*, 2003; Shenolikar *et al.*, 2002; Tandon *et al.*, 2007; Yun *et al.*, 2002). It is not currently known

whether PDZ domain proteins assist in the actual sorting of their associated proteins, stabilize their interaction partners in the apical plasma membrane, or perform both functions. As will be discussed below, PDZ proteins are also present at the basolateral membrane; hence, merely containing a PDZ consensus sequence will not necessarily result in a protein's delivery to the apical membrane.

Many of the proteins that participate in apical sorting interact with the cytoskeleton, including annexins and myosins. Recent experiments have demonstrated that at least one subset of apically directed vesicles rides actin filaments to the apical membrane, and the motor protein responsible for vesicle trafficking along the actin tracts is myosin 1a (Jacob *et al.*, 2003; Mazzochi *et al.*, 2006). There is, however, another subset of apically directed vesicles that is delivered to the apical membrane via an actin-independent pathway, thus actin cannot be wholly responsible for the delivery of all apical membrane proteins (Delacour *et al.*, 2006; Fath *et al.*, 2005; Jacob *et al.*, 2003).

Actin dynamics have been well characterized in at least one case of regulated exocytosis. Parietal cells in the stomach undergo a massive exocytosis of intracellular vesicles that fuse with the apical membrane when these cells are stimulated by gastric secretagogues. Studies of parietal cells have demonstrated that most actin in both resting and activated cells is in the filamentous state, and activation does not stimulate a rapid exchange between monomeric and filamentous actin (Yao and Forte, 2003). Thus, it appears that upon activation, existing microfilaments are simply rearranged to facilitate trafficking of exocytic vesicles to the apical membrane.

Actin is also involved in endocytosis from the apical membrane. Actin dynamics at the apical plasma membrane may be mediated by the small GTPase ADP-ribosylation factor 6 (ARF6), which stimulates clathrin-mediated endocytosis at the apical plasmalemma (Mostov *et al.*, 2000). Current data suggest that ARF6 enhances endocytosis through direct action in the clathrin-coated pits and by modifying actin dynamics in the subapical actin pool (Altschuler *et al.*, 1999).

Microtubules are also believed to participate in many, if not most, intracellular trafficking events, including apical sorting (Delacour *et al.*, 2006; Musch, 2004). In epithelial cells, microtubules tend to orient along an apical–basolateral axis, with their plus-ends directed toward the basolateral plasmalemma, suggesting that these cytoskeletal elements participate in the development and maintenance of polarity (Bacallao *et al.*, 1989; Bre *et al.*, 1990). Disruption of microtubules impairs both apical and basolateral transport (Breitfeld *et al.*, 1990; Hunziker *et al.*, 1990; Lafont *et al.*, 1994; Leung *et al.*, 2000; Pous *et al.*, 1998). Microtubules may belong to either a class of dynamically unstable microtubules or a class of stable microtubules. The population of unstable microtubules seems to mediate protein transport to the plasma membrane, as well as transcytosis of membrane proteins to the apical plasmalemma. The population of stable microtubules, however,

seems to mediate transport of membrane proteins to the basolateral plasmalemma, suggesting that different classes of microtubules are responsible for different sorting pathways (Lafont *et al.*, 1994; Pous *et al.*, 1998).

Syntaxins, or t-SNARES, may also play a role in the localization of membrane proteins. The t-SNARE syntaxin 3 is localized to the apical membrane MDCK cells, whereas syntaxin 4 is localized to the basolateral membrane in the same cell line (Low *et al.*, 1996). Interestingly, it was recently found that syntaxin 3 is concentrated in lipid rafts, which could conceivably facilitate the apical localization of this syntaxin, although these experiments were preformed in RBL mast cells which are not polarized (Pombo *et al.*, 2003). Thus, vesicles that contain v-SNARES that interact specifically with syntaxin 3 are more likely to fuse with the apical membrane; however, the candidate v-SNARES have not yet been identified.

4. Basolateral Sorting

4.1. Basolateral sorting signals

Basolateral sorting signals are relatively well defined when compared to the motley assortment of apical sorting signals discussed previously (Table 4.1). Basolateral sorting signals are typically short sequences that are found in the cytoplasmic tails of proteins. They include NPXY motifs, dihydrophobic-based sorting signals, and tyrosine-based YXXØ motifs. Dihydrophobic motifs contain -LL-, -II-, or another combination of two hydrophobic amino acids. Tyrosine-based motifs are defined by a four amino acid sequence YXXØ, where X can be any amino acid and Ø is an amino acid with a bulky hydrophobic side chain (Bonifacino and Dell'Angelica, 1999; Yeaman *et al.*, 1999). There are also a number of longer and more complicated basolateral sorting signals, including sequences found within the poly-Ig receptor, neural cell adhesion molecule epidermal growth factor receptor, and transferrin receptor polypeptides (Yeaman *et al.*, 1999). Additionally, some of the mechanisms that promote the apical localization of proteins can also participate in the basolateral localization of proteins, including localization of proteins into specific membrane domains and interaction with PDZ proteins.

The NPXY sorting signal is both a basolateral sorting signal and an endocytosis motif. In most proteins, the NPXY motif functions only to enhance endocytosis. In some proteins, however, this motif can facilitate the basolateral accumulation of proteins, although a few proteins that contain an NPXY motif do accumulate at the apical membrane (Takeda *et al.*, 2003; Yeaman *et al.*, 1999). The recognition proteins for the NPXY motif remain somewhat elusive, although the proteins AP-2 and disabled-2 (Dab2) are postulated to decode the sorting information contained within the NPXY motif (Boll *et al.*, 2002; Bonifacino and Traub, 2003).

Dileucine-like motifs also function as both basolateral sorting determinants and as mediators of internalization. These motifs are separated into two classes, the DXXLL and the [DE]XXX[LI] motifs. Although proteins in both classes are frequently localized to the basolateral membrane, the sorting information found in these two classes of dihydrophobic motifs is ultimately decoded by different sets of molecular machinery (Bonifacino and Traub, 2003; Campo *et al.*, 2005; Derby and Gleeson, 2007). The DXXLL basolateral sorting motifs interact with Golgi-localized, gamma-ear-containing, ARF-binding proteins or GGAs (Bonifacino and Traub, 2003). GGAs are a recently described class of proteins that act as ARF-dependent clathrin adaptors (Boman *et al.*, 2000). They are found in both the TGN and endosomes, and mediate the transport of cargo between these two compartments (Bonifacino and Traub, 2003; Dell'Angelica *et al.*, 2000). GGAs are recruited to membranes through their association with ARFs . ARFs are members of the Ras superfamily, and participate in vesicle formation through the recruitment of lipid-modifying enzymes and clathrin APs to the membrane (Bonifacino, 2004). Thus, GGAs and clathrin AP-1 may be recruited to the same membrane region by ARFs, and recent data have demonstrated that the GGAs and AP-1 work together to sort cargo proteins to the basolateral membrane (Doray *et al.*, 2002).

[DE]XXX[LI] dihydrophobic motifs affect intracellular targeting through their interactions with clathrin adaptor complexes (Hofmann *et al.*, 1999; Honing *et al.*, 1998). Tyrosine-based motifs also interact with the clathrin adaptor complexes. Depending on the composition and context of a given dihyrophobic or tyrosine-based motif, the motif may interact with various APs, allowing a single class of sorting motifs to exert diverse effects upon the intracellular trafficking of proteins. Thus, the [DE]XXX[LI] and YXXØ motifs can serve as basolateral sorting signals, internalization signals, and lysosomal sorting signals (Hirst and Robinson, 1998). These cytoplasmic sequences may function only as basolateral sorting signals, as with the vesicular stomatitis virus G protein YXXØ motif (Thomas *et al.*, 1993). The [DE]XXX[LI] and YXXØ motifs can also function solely as internalization signals, like the membrane-proximal motif in the LDL receptor YXXØ motif (Matter *et al.*, 1992). However, both classes of motifs frequently function as colinear internalization and basolateral sorting signals, as with the tyrosine-based motif in the H,K-ATPase β-subunit (Courtois-Coutry *et al.*, 1997; Roush *et al.*, 1998).

4.2. Basolateral sorting machinery

The clathrin APs that decode the information present in NPXY, [DE]XXX[LI], and YXXØ motifs are heterotetrameric complexes that link clathrin to membrane proteins (Maldonado-Baez and Wendland, 2006; McNiven and Thompson, 2006; Wolfe and Trejo, 2007). The ability of the [DE]XXX[LI]

and YXXØ sorting motifs to interact with different members of the clathrin AP family allows these short amino acid sequences to affect many aspects of their resident proteins' intracellular trafficking.

The AP-1 complex has been implicated in retrograde and anterograde trafficking to and from the Golgi, as well as in postendocytic recyling (Gan *et al.*, 2002; Hinners and Tooze, 2003). This complex is primarily localized to clathrin-coated structures of the TGN, TGN-derived clathrin-coated vesicles, and immature secretory granules (Boehm and Bonifacino, 2002). The AP-1 complex is composed of the γ, $\sigma 1$, $\beta 1$, and $\mu 1$ subunits (Hinners and Tooze, 2003). The $\beta 1$ subunit interacts with [DE]XXX[LI] motifs, and the $\mu 1$ subunit interacts with both [DE]XXX[LI] and tyrosine-based motifs (Bonifacino and Dell'Angelica, 1999; Bonifacino and Traub, 2003).

There are two distinct subtypes of AP-1: AP-1A and AP1B. These complexes contain a $\mu 1$A subunit or a $\mu 1$B subunit, respectively. The $\mu 1$A subunit is ubiquitous, whereas the $\mu 1$B subunit is found only in specific epithelial cells (Ohno *et al.*, 1999; Rodionov and Bakke, 1998). The $\mu 1$B protein is particularly interesting because it is expressed in MDCK cells but is not expressed in LLC-PK_1 cells (Ohno *et al.*, 1999). The transfection of $\mu 1$B into LLC-PK_1 cells redirects a subset of proteins that is typically expressed at the apical membrane to the basolateral membrane (Folsch *et al.*, 1999). Thus, AP-1B appears to be involved in and required for the sorting of at least some of its associated proteins to the basolateral plasmalemma. The expression of AP-1B is neither, however, required for the basolateral sorting of all proteins that contain a tyrosine-based motif, nor does it necessarily result in the basolateral localization of associated proteins (Duffield *et al.*, 2004).

The AP-2 complex is ubiquitously expressed and is found at the plasma membrane (Lafer, 2002). This complex links cargo proteins with the clathrin coat, mediating the endocytosis of its cargo, although $\mu 2$-independent clathrin-mediated endocytosis may also occur (Boehm and Bonifacino, 2002; Nesterov *et al.*, 1999). The AP-2 complex is composed of α, $\sigma 2$, $\beta 2$, and $\mu 2$ subunits. The $\beta 2$ subunit contains the complex's clathrin-binding site and interacts with [DE]XXX[LI] motifs (Kirchhausen, 1999; Lafer, 2002). The $\mu 2$ subunit is responsible for cargo selection via its interaction with NPXY, [DE]XXX[LI] and tyrosine-based motifs (Rodionov and Bakke, 1998). The AP-2 complex stimulates endocytosis through its association with both a variety of other proteins and with inositol phospholipids (Diril *et al.*, 2006; Lafer, 2002; Schmidt *et al.*, 2006).

AP-3 facilitates the delivery of cargo proteins to lysosomes or related organelles, including melanosomes, platelet dense granules, and Weibel-Palade bodies. It is composed of the $\beta 3$, δ, σ, and $\mu 3$ subunits (Starcevic *et al.*, 2002). The μ-subunits mediate the interaction between AP-3 and both [DE]XXX[LI] and tyrosine-based motifs (Bonifacino and Traub, 2003). Definitive localization of AP-3 has been complicated by a number

of factors; however, it has been localized to both the TGN and transferrin-positive endosomes, which are likely to be early or recycling endosomes (Danglot and Galli, 2007; Starcevic *et al.*, 2002). AP-3 may also escort proteins into the lysosomal compartment directly from the TGN (Starcevic *et al.*, 2002). Other data, however, suggest that AP-3 participates in postendocytic sorting by trafficking its cargo to lysosomes via interactions in early or recycling endosomes (Shim and Lee, 2005; Starcevic *et al.*, 2002).

AP-4 is a recently identified member of the clathrin adaptor family. It is not as well characterized as the other clathrin adaptor complexes, although it may be involved in sorting to the basolateral membrane (Barois and Bakke, 2005; Rodriguez-Boulan *et al.*, 2005; Simmen *et al.*, 2002). Tyrosine-based motifs interact with the μ-subunit of the AP-4 clathrin adaptor complexes (Simmen *et al.*, 2002).

4.3. Other basolateral sorting proteins

Much like apical sorting, the basolateral localization of membrane proteins can be affected by both PDZ protein interactions and interactions with the cytoskeleton. PDZ proteins influence the basolateral localization of the LET-23 epithelial growth factor receptor (EGFR) of *Caenorhabditis elegans*, which is localized to the basolateral membrane in vulval precursor cells via its interaction with the PDZ complex Lin-10-Lin-2-Lin-7 (Kaech *et al.*, 1998).

One particularly notable protein that can interact with a PDZ domain and is associated with basolateral sorting is the small Rho GTPase Cdc42 (Wells *et al.*, 2006). When Cdc42 function is disrupted via the expression of a dominant negative Cdc42 construct, the basolateral protein VSV G is missorted to the apical membrane. The expression of dominant-negative Cdc42 appears to prevent basolateral recycling from endosomes, and also alters both cell shape and membrane polarity (Kroschewski *et al.*, 1999).

Cdc42 can affect membrane polarity and basolateral sorting in various ways, including the regulation of actin and microtubule dynamics, exit of proteins from the TGN, and targeting of exocytic vesicles. Cdc42 and other Rho family GTPases, including Rac1 and RhoA, associate with cytoskeletal elements to induce polarization by regulating cytoskeletal dynamics (Bader *et al.*, 2004; Fukata *et al.*, 2003). In particular, activation of Cdc42 and Rac1, acting with the proteins PAK and stathmin, may facilitate the stabilization of microtubles, which is suggestive of a function in basolateral sorting given the potential role for stable microtubles in the postendocytic basolateral distribution of membrane proteins (Daub *et al.*, 2001). Cdc42, RhoA, and Rac1 are also involved in the formation of actin structures that are capable of enhancing or inhibiting exocytosis (Bader *et al.*, 2004).

Cdc42 also seems to be responsible for the exit of vesicles bound for the basolateral membrane from the TGN. A subpopulation of Cdc42 is localized to the Golgi apparatus, and its localization to the Golgi is dependent on

ARF, a small GTP-binding protein that is also involved in vesicle formation (Erickson *et al.*, 1996). Previous work has demonstrated that the Golgi colocalizes with and is surrounded by a pool of actin filaments, and actin filaments have been found to associate with Golgi membranes (Musch *et al.*, 2001). Disruption of Cdc42 function disrupts the organization of this actin pool, hampers the basolateral trafficking of LDL receptor, and stimulates the apical delivery of the apical marker p75 (Musch *et al.*, 2001). These data suggest that Cdc42 can affect not only microtubule dynamics but also microfilament dynamics, and that Cdc42 participates not only in postendocytic sorting to the basolateral membrane but also in direct delivery of proteins to the basolateral plasmalemma.

Cdc42 also participates in the sorting of vesicles to the basolateral membrane by assisting in the creation of tight junctions and providing localized targets for vesicles in transit. Both of these pathways are mediated by members of the Par protein family. In order to initiate both Par pathways, an unknown signal is presumed to activate guanine nucleotide exchange factors, which in turn activates Cdc42 (Macara, 2004). The activated Cdc42 then interacts with the PDZ and CRIB domains of Par6 in the Par6–atypical protein kinase C (Par6–aPKC) complex, and the resulting conformational change in Par6 triggers the activation of aPKC (Garrard *et al.*, 2003). The Par6–aPKC complex is localized near the zonula adherens (Hurd *et al.*, 2003). Par3, which may act as a scaffolding protein, competes with the mammalian Lethal giant larvae (mLgl) protein to join the Par6–aPKC complex, resulting in the formation of either a Par3–Par6–aPKC complex or an mLgl–Par6–aPKC complex. The Par3–Par6–aPKC complex promotes formation of tight junctions, which are necessary for the cell to become and remain polarized, although it is not clear whether Cdc42 activity is required for the formation of tight junctions (Gao *et al.*, 2002; Suzuki *et al.*, 2001; Yamanaka *et al.*, 2001). The Par6–aPKC–mLgl complex promotes basolateral sorting by phosphorylating mLgl, and releasing the phosphorylated mLgl from the Par6–aPKC complex. The phosphorylated mLgl migrates into the basolateral membrane, where it promotes vesicle docking at the basolateral plasmalemma, perhaps by working in concert with the basolateral t-SNARE syntaxin 4 (Yamanaka *et al.*, 2003). Members of the cadherin family of membrane proteins participate in these processes by forming calcium-dependent homophilic interactions at points of contact between neighboring cells. E-cadherin is a member of the cadherin family that is expressed in epithelial cells, and the formation of tight junctions is dependent on E-cadherin at least in part because of its ability to activate the small GTPases, Rac1, and Cdc42. Interestingly, recent work has demonstrated that in MDCK cells the role of E-cadherin is essential for the formation of tight junctions, but not their maintenance (Capaldo and Macara, 2007). This suggests that the role of E-cadherin may be as a scaffold for the recruitment of additional junctional components, such as α-catenin,

and that after this initial role in establishing the junctional complexes, E-cadherin is no longer required to maintain junctional integrity.

Work from a number of labs has recently described the role of the tumor suppressor kinase LKB1 and the AMP activated protein kinase (AMPK) in protein trafficking. LKB1 and AMP facilitate the formation of tight junctions. Early in the process of tight junction formation, the LKB1-specific AP STRAD activates LKB1 and directs its movement from the cytoplasm into the cell nucleus (Baas *et al.*, 2003). Interestingly, the activation of LKB1 in epithelial cells results in the formation of an apical brush border as well as functional sorting of proteins to apical and basolateral surfaces in the absence of junctional cell–cell contacts (Baas *et al.*, 2004). AMP-activated protein kinase, which has a role in regulation of the cellular energy status by monitoring the ratio of AMP/ATP, is activated via phosphorylation by LKB1 (Lee *et al.*, 2007; Mirouse *et al.*, 2007; Zhang *et al.*, 2006; Zheng and Cantley, 2007). The assembly of tight junctions is regulated by AMPK in MDCK cells in a calcium-inducible manner, and this mechanism is likely to involve mTOR (mammalian target of rapamycin), as treatment of cells with rapamycin was shown to limit the junctional formation defects caused by the elimination of AMPK activity (Zhang *et al.*, 2006). Work in *Drosophila* supports the role of LKB1 in epithelial polarity and points to other downstream targets that are likely to be critical components of the pathway leading up to junctional formation and the establishment of epithelial polarity (Lee *et al.*, 2007; Mirouse *et al.*, 2007). These studies suggest that the tumor-suppressing properties of LKB1 are likely to be associated with the ability of LKB1 to promote cell–cell junction formation and the functional differentiation associated with correctly polarized epithelial cells.

Another protein that interacts with Cdc42, albeit indirectly, and enhances the delivery of membrane proteins to the basolateral plasmalemma is RalA. RalA is a small GTPase in the Ras superfamily that is present on the plasma membrane and in intracellular vesicles (Shipitsin and Feig, 2004). RalA's interaction partners suggest that it is involved in endocytosis or other membrane dynamics. These interaction partners include actin-binding proteins, ARF, and RalBP1/RLIP. RalBP1/RLIP is a Cdc42 guanine nucleotidase activating, or GAP, protein, and also complexes with several proteins involved in endocytosis, such as AP-2, epsin, and eps15 (Jullien-Flores *et al.*, 2000; Morinaka *et al.*, 1999; Ohta *et al.*, 1999). Disruption of RalA has been shown to disrupt basolateral sorting of the EGFR receptor as well as other proteins that are resident in the basolateral membrane of MDCK cells. Current data suggest that RalA directs basolateral sorting by interacting with Sec5, a crucial protein required for assembly of the exocyst complex (Balakireva *et al.*, 2006; Moskalenko *et al.*, 2002). In mammalian cells, the exocyst complex is involved in the delivery of vesicles from the TGN to the basolateral membrane. Thus, RalA may direct basolateral

sorting via several pathways. The closely related protein RalB does not appear to direct basolateral sorting (Shipitsin and Feig, 2004).

5. Endosomal and Lysosomal Sorting Signals

Endosomal and lysosomal sorting signals typically consist of short cytoplasmic sequences of amino acids, much like the basolateral sorting signals (see Table 4.1). As noted previously, many classes of basolateral sorting motifs are also endosomal or lysosomal sorting determinants, including NPXY, YXXØ, and [DE]XXX[LI] motifs. Endocytosis and targeting to intracellular compartments is mediated by clathrin APs. Clathrin AP-mediated endocytosis of a given protein may also be enhanced by an AP, CD63, that links cargo to AP-2 and AP-3, resulting in the increased localization of the cargo to a late endosomal compartment (Duffield *et al.*, 2003).

The sorting of some membrane proteins to intracellular vesicles is mediated by ubiquitination (Katzmann and Wendland, 2005; Miranda and Sorkin, 2007; Purdy and Russell, 2007). Ubiquitin is a 76 amino acid peptide that can form covalent bonds with other proteins. These bonds are formed between the carboxy terminus of ubiquitin and the amino groups of other proteins. Ubiquitin most frequently conjugates with the ε-amino group of lysine, but can also conjugate with a protein's amino terminus, and proteins can be either monoubiquitinated or polyubiquitinated. Polyubiquitination occurs when ubiquitin binds to other ubiquitin residues that are already conjugated to a protein, forming chains of ubiquitin. Ubiquitin can be appended to other ubiquitin molecules at lysines 29, 48, and 63, and the localization of these chains may have different consequences for their host protein (Hicke and Dunn, 2003).

Ubiquitination can affect the fate of a protein as it prepares to exit the biosynthetic pathway. This modification facilitates the sorting of proteins directly from the TGN to vacuoles in yeast and late endsomes in mammalian cells, but it is not yet clear whether the proteins are mono- or polyubiquitinated (Hicke and Dunn, 2003; Katzmann and Wendland, 2005; Keleman *et al.*, 2002). At least one ubiquitin protein ligase, hPOSH, is present in the Golgi, and ubiquitinates the HIV protein Gag. Ubiquitination of Gag is required for its targeting from the TGN to late endosomes (Alroy *et al.*, 2005).

Ubiquitination also enhances the internalization of proteins from the plasma membrane. It has been demonstrated that when proteins which are stably resident in the plasma membrane are ubiquitinated, these proteins will undergo endocytosis (Purdy and Russell, 2007). Monoubiquitination is sufficient to provoke endocytosis, but diubiquitination, with the ubiquitin–ubiquitin bond formed at Lys63, has been shown to enhance endocytosis to

a greater extent than monoubiquitination. Longer ubiquitin tails may further augment endocytosis (Haririnia *et al.*, 2007; Kawadler and Yang, 2006; Liu *et al.*, 2007).

The endocytosis signal of ubiquitin is not a short linear sequence, as is seen with the NPXY and YXXØ motifs, and is instead composed of hydrophobic patches that are centered around isoleucine 44 and phenylalanine 4 (Shih *et al.*, 2000). Recognition of ubiquitinated proteins is performed by ubiquitin-binding molecules, which contain ubiquitin associated (UAB) or ubiquitin-interacting motifs (UIM), and bind directly to isoleucine 44 of ubiquitin. The association may be further augmented by other protein–protein interactions (Shih *et al.*, 2000). The proteins epsin and eps15 contain UIM (Bonifacino and Traub, 2003). Epsin also contains a phosphatidylinositol 4,5 bisphosphate-binding site, as well as sites for interaction with AP-2, clathrin, and eps15 (Bonifacino and Traub, 2003). These proteins and lipids all participate in clathrin-mediated endocytosis, suggesting that ubiquitinated cargo is internalized via clathrin-mediated endocytosis; however, clathrin is not required for ubiquitin-associated endocytosis (Shih *et al.*, 2000). In fact, recent data suggest that when epsin is recruited to clathrin-coated pits, it no longer associates with ubiquitinated proteins (Chen and De Camilli, 2005). The precise mechanism of ubiquitin-mediated endocytosis thus remains unclear (Hurley and Emr, 2006; Miranda and Sorkin, 2007).

Ubiquitin may also provide sorting information after a protein's internalization. Ubiquitin can direct its associated proteins to enter MVBs, and from there the protein may be targeted for degradation (Katzmann *et al.*, 2002). In particular, ubiquitination plays a role in downregulating surface expression of EGFR (Katzmann *et al.*, 2002). The internalization and ubiquitination signals may act in concert, as they do with a G protein-coupled receptor in yeast, or ubiquitination may act only as a MVB sorting motif (Hicke and Dunn, 2003). For example, the human β-adrenergic G protein-coupled receptor is internalized via an ubiquitin-independent mechanism, but relies on ubiquitination for its transport to the lysosome and its subsequent degradation (Shenoy and Lefkowitz, 2003).

Transport of ubiquitinated cargo to the late endosome or lysosome is mediated by UIM-containing proteins, including Hrs/Vps27 and STAM/Hse (Hicke and Dunn, 2003). Hrs/Vps27 and STAM/Hse bind to both one another and to ubiquitinated cargo. Hrs/Vps27 binds clathrin, and may serve to link ubiquitinated proteins to clathrin-mediated endosomal sorting pathways (Raiborg *et al.*, 2002). Hrs/Vps27 and STAM/Hse also have an affinity for lipids that are enriched in MVBs, such as phosphatidylinositol-3-phosphate, and this affinity may facilitate the trafficking of associated ubiquitinated proteins to MVBs (Hicke and Dunn, 2003).

Much in the way that lipid affinity may help Hrs/Vps27 and STAM/Hse traffic its cargo to intracellular compartments, localization to lipid rafts may

also promote trafficking to late endosomes. Recent data demonstrate that GPI-anchored, raft-associated proteins may be preferentially trafficked to the late endosomal or lysosomal compartment, and that decreased raft association tends to favor localization to the recycling endosome (Fivaz *et al.*, 2002). Thus, both lipid and protein components of intracellular membrane participate in trafficking to intracellular vesicles.

6. Conclusion

The steady progress toward understanding how epithelia establish and maintain their structural and functional polarity, while significant, has yet to fully describe the mediators and mechanisms of this essential and dynamic process. The clear connection between breakdowns in proper surface membrane and compartmental protein targeting and human disease underscores the need for further studies. Our current understanding of epithelial polarity relies on evidence from relatively few proteins and it is unclear whether the routes, sorting determinants, and regulation observed in the targeting of these ''model'' proteins can be broadly applied to other proteins and in other cell types. Exisiting models cannot yet adequately explain the mechanisms that govern how the cellular sorting machinery can effectively recognize the variety of cargoes and ensure their delivery, stabilization, and recycling from the numerous subcellular destinations. Moreover, the trafficking models developed from work in tissue culture cell lines may not reliably hold for cells in complex organ tissues that may experience changing environmental conditions. It is therefore important that technological advances in cellular imaging and transgenic organisms be applied to the close scrutiny of protein sorting in epithelia, ideally in as natural environments as possible.

REFERENCES

Alfalah, M., Wetzel, G., Fischer, I., Busche, R., Sterchi, E. E., Zimmer, K., Sallmann, H. P., and Naim, H. Y. (2005). A novel type of detergent-resistant membranes may contribute to an early protein sorting event in epithelial cells. *J. Biol. Chem.* **280**(52), 42636–42643.

Alroy, I., Tuvia, S., Greener, T., Gordon, D., Barr, H. M., Taglicht, D., Mandil-Levin, R., Ben-Avraham, D., Konforty, D., Nir, A., Levius, O., Bicoviski, V., *et al.* (2005). The trans-Golgi network-associated human ubiquitin-protein ligase POSH is essential for HIV type 1 production. *Proc. Natl. Acad. Sci. USA* **102**(5), 1478–1483.

Altschuler, Y., Hodson, C., and Milgram, S. L. (2003). The apical compartment: Trafficking pathways, regulators and scaffolding proteins. *Curr. Opin. Cell Biol.* **15**(4), 423–429.

Altschuler, Y., Liu, S.-H., Katz, L., Tang, K., Hardy, S., Brodsky, F., Apodaca, G., and Mostov, K. (1999). ADP-ribosylation factor 6 and endocytosis at the apical surface of Madin-Darby canine kidney cells. *J. Cell Biol.* **147**(1), 7–12.

Ang, A. L., Taguchi, T., Francis, S., Folsch, H., Murrells, L. J., Pypaert, M., Warren, G., and Mellman, I. (2004). Recycling endosomes can serve as intermediates during transport from the Golgi to the plasma membrane of MDCK cells. *J. Cell Biol.* **167**(3), 531–543.

Au, J. S. Y., Puri, C., Ihrke, G., Kendrick-Jones, J., and Buss, F. (2007). Myosin VI is required for sorting of AP-1B-dependent cargo to the basolateral domain in polarized MDCK cells. *J. Cell Biol.* **177**(1), 103–114.

Baas, A. F., Boudeau, J., Sapkota, G. P., Smit, L., Medema, R., Morrice, N. A., Alessi, D. R., and Clevers, H. C. (2003). Activation of the tumour suppressor kinase LKB1 by the STE20-like pseudokinase STRAD. *EMBO J.* **22**(12), 3062–3072.

Baas, A. F., Kuipers, J., van der Wel, N. N., Batlle, E., Koerten, H. K., Peters, P. J., and Clevers, H. C. (2004). Complete polarization of single intestinal epithelial cells upon activation of LKB1 by STRAD. *Cell* **116**(3), 457–466.

Bacallao, R., Antony, C., Dotti, C., Karsenti, E., Stelzer, E. H. K., and Simons, K. (1989). The subcellular organization of Madin-Darby canine kidney cells during the formation of a polarized epithelium. *J. Cell Biol.* **109**(6I), 2817–2832.

Bader, M. F., Doussau, F., Chasserot-Golaz, S., Vitale, N., and Gasman, S. (2004). Coupling actin and membrane dynamics during calcium-regulated exocytosis: A role for Rho and ARF GTPases. *Biochim. Biophys. Acta Mol. Cell Res.* **1742**(1–3), 37–49, Sp. Iss. SI.

Balakireva, M., Rosse, C., Langevin, J., Chien, Y. C., Gho, M., Gonzy-Treboul, G., Voegeling-Lemaire, S., Aresta, S., Lepesant, J. A., Bellaiche, Y., White, M., and Camonis, J. (2006). The Ral/exocyst effector complex counters c-Jun N-terminal kinase-dependent apoptosis in Drosophila melanogaster. *Mol. Cell. Biol.* **26**(23), 8953–8963.

Bard, F., and Malhotra, V. (2006). The formation of TGN-to-plasma-membrane transport carriers. *Annu. Rev. Cell Dev. Biol.* **22,** 439–455.

Barois, N., and Bakke, O. (2005). The adaptor protein AP-4 as a component of the clathrin coat machinery: A morphological study. *Biochem. J.* **385**(Part 2), 503–510.

Boehm, M., and Bonifacino, J. S. (2002). Genetic analyses of adaptin function from yeast to mammals. *Gene* **286**(2), 175–186.

Boll, W., Rapoport, I., Brunner, C., Modis, Y., Prehn, S., and Kirchhausen, T. (2002). The μ2 subunit of the clathrin adaptor AP-2 binds to FDNPVY and yppØ sorting signals at distinct sites. *Traffic* **3**(8), 590–600.

Boman, A. L., Zhang, C., Zhu, X., and Kahn, R. A. (2000). A family of ADP-ribosylation factor effectors that can alter membrane transport through the trans-Golgi. *Mol. Biol. Cell* **11**(4), 1241–1255.

Bomberger, J. M., Parameswaran, N., Hall, C. S., Aiyar, N., and Spielman, W. S. (2005). Novel function for receptor activity-modifying proteins (RAMPs) in post-endocytic receptor trafficking. *J. Biol. Chem.* **280**(10), 9297–9307.

Bomsel, M., Prydz, K., Parton, R. G., Gruenberg, J., and Simons, K. (1989). Endocytosis in filter-grown Madin-Darby canine kidney cells. *J. Cell Biol.* **109**(6), 3243–3258.

Bomsel, M., Parton, R., Kuznetsov, S. A., Schroer, T. A., and Gruenberg, J. (1990). Microtubule- and motor-dependent fusion *in vitro* between apical and basolateral endocytic vesicles from MDCK cells. *Cell* **62**(4), 719–731.

Bonifacino, J. S. (2004). The GGA proteins: Adaptors on the move. *Nat. Rev. Mol. Cell Biol.* **5**(1), 23–32.

Bonifacino, J. S., and Dell'Angelica, E. C. (1999). Molecular bases for the recognition of tyrosine-based sorting signals. *J. Cell Biol.* **145**(5), 923–926.

Bonifacino, J. S., and Traub, L. M. (2003). Signals for sorting of transmembrane proteins to endosomes and lysosomes. *Annu. Rev. Biochem.* **72,** 395–447.

Bre, M., Pepperkok, R., Hill, A., Levilliers, N., Ansorge, W., Stelzer, E., and Karsenti, E. (1990). Regulation of microtubule dynamics and nucleation during polarization in MDCK-II cells. *J. Cell Biol.* **111**(6), 3013–3021.

Breitfeld, P. P., Mckinnon, W. C., and Mostov, K. E. (1990). Effect of nocodazole on vesicular traffic to the apical and basolateral surfaces of polarized MDCK cells. *J. Cell Biol.* **111**(6), 2365–2373.

Brown, D. A. (2006). Lipid rafts, detergent-resistant membranes, and raft targeting signals. *Physiology* **21,** 430–439.

Brown, D. A., and London, E. (1998). Functions of lipid rafts in biological membranes. *Annu. Rev. Cell Dev. Biol.* **14,** 111–136.

Brown, D. A., Crise, B., and Rose, J. (1989). Mechanism of membrane anchoring affects polarized expression of 2 proteins in MDCK cells. *Science* **245**(4925), 1499–1501.

Brugger, B., Graham, C., Leibrecht, I., Mombelli, E., Jen, A., Wieland, F., and Morris, R. (2004). The membrane domains occupied by glycosylphosphatidylinositol-anchored prion protein and Thy-1 differ in lipid composition. *J. Biol. Chem.* **279**(9), 7530–7536.

Capaldo, C. T., and Macara, I. G. (2007). Depletion of E-cadherin disrupts establishment but not maintenance of cell junctions in Madin-Darby canine kidney epithelial cells. *Mol. Biol. Cell* **18**(1), 189–200.

Campo, C., Mason, A., Maouyo, D., Olsen, O., Yoo, D., and Welling, P. A. (2005). Molecular mechanisms of membrane polarity in renal epithelial cells. *Rev. Physiol. Biochem. Pharmacol.* **153,** 47–99.

Capuano, P., Bacic, D., Roos, M., Gisler, S. M., Biber, J., Kaissling, B., Weinman, E. J., Wagner, C. A., and Murer, H. (2005). Defective coupling of apical PTH receptors to phospholipase c and loss of PTH induced internalization of NaPI-IIa in NHERF1 knock out mice. *Nephrol. Dial. Transplant.* **20**(Suppl. 5), V187–V188.

Capuano, P., Bacic, D., Roos, M., Gisler, S. M., Stange, G., Biber, J., Kaissling, B., Weinman, E. J., Shenolikar, S., Wagner, C. A., and Murer, H. (2007). Defective coupling of apical PTH receptors to phospholipase C prevents internalization of the Na^+-phosphate cotransporter NaPi-IIa in Nherf1-deficient mice. *Am. J. Phys. -Cell Phys.* **292**(2), C927–C934.

Chan, W., Calderon, G., Swift, A. L., Moseley, J., Li, S. H., Hosoya, H., Arias, I. M., and Ortiz, D. F. (2005). Myosin II regulatory light chain is required for trafficking of bile salt export protein to the apical membrane in Madin-Darby canine kidney cells. *J. Biol. Chem.* **280**(25), 23741–23747.

Chang, T. Y., Chang, C. C. Y., Ohgami, N., and Yamauchi, Y. (2006). Cholesterol sensing, trafficking, and esterification. *Annu. Rev. Cell Dev. Biol.* **22,** 129–157.

Chen, H., and De Camilli, P. (2005). The association of epsin with ubiquitinated cargo along the endocytic pathway is negatively regulated by its interaction with clathrin. *Proc. Natl. Acad. Sci. USA* **102**(8), 2766–2771.

Cheng, Y., and Walz, T. (2007). Reconstructing the endocytotic machinery. *Methods Cell Biol.* **79,** 463–487.

Cheng, Z., Singh, R. D., Marks, D. L., and Pagano, R. E. (2006). Membrane microdomains, caveolae, and caveolar endocytosis of sphingolipids. *Mol. Membr. Biol.* **23**(1), 101–110.

Choudhury, P., Liu, Y., Bick, R. J., and Sifers, R. N. (1997). Intracellular association between UDP-glucose: Glycoprotein glucosyltransferase and an incompletely folded variant of α1-antitrypsin. *J. Biol. Chem.* **272**(20), 13446–13451.

Cottrell, G. S., Padilla, B., Pikios, S., Roosterman, D., Steinhoff, M., Grady, E. F., and Bunnett, N. W. (2007). Post-endocytic sorting of calcitonin receptor-like receptor and receptor activity-modifying protein 1. *J. Biol. Chem.* **282**(16), 12260–12271.

Courtois-Coutry, N., Roush, D., Rajendran, V., McCarthy, J. B., Geibel, J., Kashgarian, M., and Caplan, M. J. (1997). A tyrosine-based signal targets H/K-ATPase to a regulated compartment and is required for the cessation of gastric acid secretion. *Cell* **90**(3), 501–510.

Danglot, L., and Galli, T. (2007). What is the function of neuronal AP-3? *Mol. Biol. Cell* **99** (7), 349–361.

Danielsen, E. M., and Hansen, G. H. (2006). Lipid raft organization and function in brush borders of epithelial cells. *Mol. Membr. Biol.* **23**(1), 71–79.

Daub, H., Gevaert, K., Vandekerckhove, J., Sobel, A., and Hall, A. (2001). Rac/Cdc42 and p65PAK regulate the microtubule-destabilizing protein stathmin through phosphorylation at serine 16. *J. Biol. Chem.* **276**(3), 1677–1680.

Delacour, D., and Jacob, R. (2006). Apical protein transport. *Cell. Mol. Life Sci.* **63**(21), 2491–2505.

Delacour, D., Cramm-Behrens, C. I., Drobecq, H., Le Bivic, A., Naim, H. Y., and Jacob, R. (2006). Requirement for galectin-3 in apical protein sorting. *Curr. Biol.* **16** (4), 408–414.

Dell'Angelica, E. C., Puertollano, R., Mullins, C., Aguilar, R. C., Vargas, J. D., Hartnell, L. M., and Bonifacino, J. S. (2000). GGAs: A family of ADP ribosylation factor-binding proteins related to adaptors and associated with the Golgi complex. *J. Cell Biol.* **149**(1), 81–93.

Deora, A. B., Kreitzer, G., Jacovina, A. T., and Hajjar, K. A. (2004). An annexin 2 phosphorylation switch mediates p11-dependent translocation of annexin 2 to the cell surface. *J. Biol. Chem.* **279**(42), 43411–43418.

Derby, M. C., and Gleeson, P. A. (2007). New insights into membrane trafficking and protein sorting. *Int. Rev. Cytol.—A Survey of Cell Biol.* **261,** 47.

Di Pietro, S. M., and Dell'Angelica, E. C. (2005). The cell biology of Hermansky-Pudlak syndrome: Recent advances. *Traffic* **6**(7), 525–533.

Diril, M. K., Wienisch, M., Jung, N., Klingauf, J., and Haucke, V. (2006). Stonin 2 is an AP-2-dependent endocytic sorting adaptor for synaptotagmin internalization and recycling. *Dev. Cell* **10**(2), 233–244.

Donowitz, M., and Li, X. H. (2007). Regulatory binding partners and complexes of NHE3. *Physiol. Rev.* **87**(3), 825–872.

Doray, B., Ghosh, P., Griffith, J., Geuze, H. J., and Kornfeld, S. (2002). Cooperation of GGAs and AP-1 in packaging MPRs at the trans-Golgi network. *Science* **297**(5587), 1700–1703.

Duffield, A., Kamsteeg, E. J., Brown, A. N., Pagel, P., and Caplan, M. J. (2003). The tetraspanin CD63 enhances the internalization of the H,K-ATPase beta-subunit. *Proc. Natl. Acad. Sci. USA* **100**(26), 15560–15565.

Duffield, A., Folsch, H., Mellman, I., and Caplan, M. J. (2004). Sorting of H,K-ATPase beta-subunit in MDCK and LLC-PK1 cells is independent of μ 1B adaptin expression. *Traffic* **5**(6), 449–461.

Dunbar, L. A., Aronson, P., and Caplan, M. J. (2000). A transmembrane segment determines the steady-state localization of an ion-transporting adenosine triphosphatase. *J. Cell Biol.* **148**(4), 769–778.

Duncan, M. C., Cope, M. J. T. V., Goode, B. L., Wendland, B., and Drubin, D. G. (2001). Yeast Eps15-like endocytic protein, Pan1p, activates the Arp2/3 complex. *Nat. Cell Biol.* **3**(7), 687–690.

Erickson, J. W., Zhang, C. J., Kahn, R. A., Evans, T., and Cerione, R. A. (1996). Mammalian Cdc42 is a brefeldin A-sensitive component of the Golgi apparatus. *J. Biol. Chem.* **271**(43), 26850–26854.

Fath, K. R. (2006). Roles of the actin cytoskeleton and myosins in the endomembrane system. *Adv. Mol. Cell Biol.* **37,** 119–134.

Fisher, R. J., Pevsner, J., and Burgoyne, R. D. (2001). Control of fusion pore during exocytosis by Munc18. *Science* **291**(5505), 875–878.

Fivaz, M., Vilbois, F., Thurnheer, S., Pasquali, C., Abrami, L., Bickel, P. E., Parton, R. G., and van der Goot, F. G. (2002). Differential sorting and fate of endocytosed GPI-anchored proteins. *EMBO J.* **21**(15), 3989–4000.

Folsch, H. (2005). The building blocks for basolateral vesicles in polarized epithelial cells. *Trends Cell Biol.* **15**(4), 222–228.

Folsch, H., Ohno, H., Bonifacino, J. S., and Mellman, I. (1999). A novel clathrin adaptor complex mediates basolateral targeting in polarized epithelial cells. *Cell* **99**(2), 189–198.

Frank, D. J., Noguchi, T., and Miller, K. G. (2004). Myosin VI: A structural role in actin organization important for protein and organelle localization and trafficking. *Curr. Opin. Cell Biol.* **16**(2), 189–194.

Fuchs, R., and Ellinger, I. (2004). Endocytic and transcytotic processes in villous syncytiotrophoblast: Role in nutrient transport to the human fetus. *Traffic* **5**(10), 725–738.

Fujita, Y., Xu, A., Xie, L., Arunachalam, L., Chou, T., Jiang, T., Chiew, S., Kourtesis, J., Wang, L., Gaisano, H. Y., and Sugita, S. (2007). $Ca2^{+}$-dependent activator protein for secretion 1 is critical for constitutive and regulated exocytosis but not for loading of transmitters into dense core vesicles. *J. Biol. Chem.* **282**(29), 21392–21403.

Fukata, M., Nakagawa, M., and Kaibuchi, K. (2003). Roles of Rho-family GTPases in cell polarisation and directional migration. *Curr. Opin. Cell Biol.* **15**(5), 590–597.

Fullekrug, J., and Simons, K. (2004). Lipid rafts and apical membrane traffic. *Gastroenteropancreatic Neuroendocrine Tumor Disease: Molecular and Cell Biological Aspects* **1014,** 164–169.

Futter, C. E., Gibson, A., Allchin, E. H., Maxwell, S., Ruddock, L. J., Odorizzi, G., *et al.* (1998). In polarized MDCK cells basolateral vesicles arise from clathrin-γ- adaptin-coated domains on endosomal tubules. *J. Cell Biol.* **141**(3), 611–623.

Gan, Y. B., McGraw, T. E., and Rodriguez-Boulan, E. (2002). The epithelial-specific adaptor AP1B mediates post-endocytic recycling to the basolateral membrane. *Nat. Cell Biol.* **4**(8), 605–609.

Gao, L., Joberty, G., and Macara, I. G. (2002). Assembly of epithelial tight is negatively regulated by junctions. *Curr. Biol.* **12**(3), 221–225.

Garrard, S. M., Capaldo, C. T., Gao, L., Rosen, M. K., Macara, I. G., and Tomchick, D. R. (2003). Structure of Cdc42 in a complex with the GTPase-binding domain of the cell polarity protein. *EMBO J.* **22**(5), 1125–1133.

Gassama-Diagne, A., Yu, W., ter Beest, M., Martin-Belmonte, F., Kierbel, A., Engel, J., and Mostov, K. (2006). Phosphatidylinositol-3,4,5-trisphosphate regulates the formation of the basolateral plasma membrane in epithelial cells. *Nat. Cell Biol.* **8**(9), 963–U64.

Groc, L., and Choquet, D. (2006). AMPA and NMDA glutamate receptor trafficking: Multiple roads for reaching and leaving the synapse. *Cell Tissue Res.* **326**(2), 423–438.

Gruenberg, J., and Stenmark, H. (2004). The biogenesis of multivesicular endosomes. *Nat. Rev. Mol. Cell Biol.* **5**(4), 317–323.

Hao, M., and Maxfield, F. R. (2000). Characterization of rapid membrane internalization and recycling. *J. Biol. Chem.* **275**(20), 15279–15286.

Haririnia, A., D'Onofrio, M., and Fushman, D. (2007). Mapping the interactions between Lys48 and Lys63-linked di-ubiquitins and a ubiquitin-interacting motif of S5a. *J. Mol. Biol.* **368**(3), 753–766.

Harris, B. Z., and Lim, W. A. (2001). Mechanisma and role of PDZ domains in signaling complex assembly. *J. Cell Sci.* **114**(18), 3219–3231.

Haucke, V. (2005). Phosphoinositide regulation of clathrin-mediated endocytosis. *Biochem. Soc. Trans.* **33**(6), 1285–1289.

Hicke, L., and Dunn, R. (2003). Regulation of membrane protein transport by ubiquitin and ubiquitin-binding proteins. *Annu. Rev. Cell Dev. Biol.* **19,** 141–172.

Hinners, I., and Tooze, S. A. (2003). Changing directions: Clathrin-mediated transport between the Golgi and endosomes. *J. Cell Sci.* **116**(5), 763–771.

Hirst, J., and Robinson, M. S. (1998). Clathrin and adaptors. *Biochim. Biophys. Acta Mol. Cell Res.* **1404**(1–2), 173–193.

Hoekstra, D., Tyteca, D., and van IJzendoorn, S. C. D. (2004). The subapical compartment: A traffic center in membrane polarity development. *J. Cell Sci.* **117**(11), 2183–2192.

Hoeller, D., Volarevic, S., and Dikic, I. (2005). Compartmentalization of growth factor receptor signalling. *Curr. Opin. Cell Biol.* **17**(2), 107–111.

Hoessli, D. C., Semac, I., Iqbal, A., Nasir-ud-Din, A., and Borisch, B. (2004). Glycosphingolipid clusters as organizers of plasma membrane rafts and caveolate. *Curr. Org. Chem.* **8**(5), 439–452.

Hofmann, M. W., Honing, S., Rodionov, D., Dobberstein, B., von Figura, K., and Bakke, O. (1999). The leucine-based sorting motifs in the cytoplasmic domain of the invariant chain are recognized by the clathrin adaptors AP1 and AP2 and their medium chains. *J. Biol. Chem.* **274**(51), 36153–36158.

Hong, W. (2005). SNAREs and traffic. *Biochim. Biophys. Acta* **1744**(3), 493–517.

Honing, S., Sandoval, I. V., and von Figura, K. (1998). A di-leucine-based motif in the cytoplasmic tail of LIMP-II and tyrosinase mediates selective binding of AP-3. *EMBO J.* **17**(5), 1304–1314.

Howell, G. J., Holloway, Z. G., Cobbold, C., Monaco, A. P., and Ponnambalam, S. (2006). Cell biology of membrane trafficking in human disease. *Int. Rev. Cytol.* **252,** 1–69.

Hunziker, W., Male, P., and Mellman, I. (1990). Differential microtubule requirements for transcytosis in MDCK cells. *EMBO J.* **9**(11), 3515–3525.

Hurd, T. W., Gao, L., Roh, M. H., Macara, I. G., and Margolis, B. (2003). Direct interaction of two polarity complexes implicated in epithelial tight junction assembly. *Nat. Cell Biol.* **5**(2), 137–142.

Hurley, J. H., and Emr, S. D. (2006). The ESCRT complexes: Structure and mechanism of a membrane-trafficking network. *Annu. Rev. Biophys. Biomol. Struct.* **35,** 277–298.

Inukai, K., Shewan, A. M., Pascoe, W. S., Katayama, S., James, D. E., and Oka, Y. (2004). Carboxy terminus of glucose transporter 3 contains an apical membrane targeting domain. *Mol. Endocrinol.* **18**(2), 339–349.

Isacke, C. M., Trowbridge, I. S., and Hunter, T. (1986). Modulation of p36 phosphorylation in human-cells—Studies using anti-p36 monoclonal-antibodies. *Mol. Cell. Biol.* **6**(7), 2745–2751.

Jacob, R., Heine, M., Alfalah, M., and Naim, H. Y. (2003). Distinct cytoskeletal tracks direct individual vesicle populations to the apical membrane of epithelial cells. *Curr. Biol.* **13**(7), 607–612.

Jacob, R., Heine, M., Eikemeyer, J., Frerker, N., Zimmer, K. P., Rescher, U., Gerke, V., and Naim, H. Y. (2004). Annexin II is required for apical transport in polarized epithelial cells. *J. Biol. Chem.* **279**(5), 3680–3684.

Johannes, L., and Lamaze, C. (2002). Clathrin-dependent or not: Is it still the question? *Traffic* **3**(7), 443–451.

Jost, M., Simpson, F., Kavran, J. M., Lemmon, M. A., and Schmid, S. L. (1998). Phosphatidylinositol-4,5-bisphosphate is required for endocytic coated vesicle formation. *Curr. Biol.* **8**(25), 1399–1402.

Jullien-Flores, V., Mahe, Y., Mirey, G., Leprince, C., Meunier-Bisceuil, B., Sorkin, A., and Camonis, J. H. (2000). RLIP76, an effector of the GTPase Ral, interacts with the AP2 complex: Involvement of the Ral pathway in receptor endocytosis. *J. Cell Sci.* **113**(16), 2837–2844.

Kaech, S. M., Whitfield, C. W., and Kim, S. K. (1998). The LIN-2/LIN-7/LIN-10 complex mediates basolateral membrane localization of the C-elegans EGF receptor LET-23 in vulval epithelial cells. *Cell* **94**(6), 761–771.

Kalthoff, C., Alves, J., Urbanke, C., Knorr, R., and Ungewickell, E. J. (2002). Unusual structural organization of the endocytic proteins AP180 and epsin 1. *J. Biol. Chem.* **277**(10), 8209–8216.

Kamsteeg, E. J., Duffield, A. S., Konings, I. B. M., Spencer, J., Pagel, P., Deen, P. M. T., and Caplan, M. J. (2007). MAL decreases the internalization of the aquaporin-2 water channel. *Proc. Natl. Acad. Sci. USA* **104**(42), 16696–16701.

Katzmann, D. J., and Wendland, B. (2005). Analysis of ubiquitin-dependent protein sorting within the endocytic pathway in *Saccharomyces cerevisiae*. *Methods Enzymol.* **399**(Part B), 192–211.

Katzmann, D. J., Odorizzi, G., and Emr, S. D. (2002). Receptor downregulation and multivesicular-body sorting. *Nat. Rev. Mol. Cell Biol.* **3**(12), 893–905.

Keleman, K., Rajagopalan, S., Cleppien, D., Teis, D., Paiha, K., Huber, L. A., Technau, G. M., and Dickson, B. J. (2002). Comm sorts Robo to control axon guidance at the Drosophila midline. *Cell* **110**(4), 415–427.

Kim, P. S., and Arvan, P. (1998). Endocrinopathies in the family of endoplasmic reticulum (ER) storage diseases: Disorders of protein trafficking and the role of ER molecular chaperones. *Endocr. Rev.* **19**(2), 173–202.

Kim, E., and Sheng, M. (2004). PDZ domain proteins of synapses. *Nat. Rev. Neurosci.* **5**(10), 771–781.

Kirchhausen, T. (2000). Clathrin. *Annu. Rev. Biochem.* **69,** 699–727.

Kirchhausen, T. (1999). Adaptors for clathrin-mediated traffic. *Annu. Rev. Cell Dev. Biol.* **15,** 705-.

Kobayashi, N., Suzuki, Y., Tsuge, T., Okumura, K., Ra, C., and Tomino, Y. (2002). FcRn-mediated transcytosis of immunoglobulin G in human renal proximal tubular epithelial cells. *Am. J. Physiol. Ren. Physiol.* **282**(2 51–2), F358–F365.

Kroschewski, R., Hall, A., and Mellman, I. (1999). Cdc42 controls secretory and endocytic transport to the basolateral plasma membrane of MDCK cells. *Nat. Cell Biol.* **1**(1), 8–13.

Kawadler, H., and Yang, X. L. (2006). Lys63-linked polyubiquitin chains—Linking more than just ubiquitin. *Cancer Biol. Ther.* **5**(10), 1273–1274.

Lafer, E. M. (2002). Clathrin—Protein interactions. *Traffic* **3**(8), 513–520.

Lafont, F., Burkhardt, J. K., and Simons, K. (1994). Involvement of microtubule motors in basolateral and apical transport in kidney-cells. *Nature* **372**(6508), 801–803.

Lafont, F., Lecat, S., Verkade, P., and Simons, K. (1998). Annexin XIIIb associates with lipid microdomains to function in apical delivery. *J. Cell Biol.* **142**(6), 1413–1427.

Lafont, F., Verkade, P., Galli, T., Wimmer, C., Louvard, D., and Simons, K. (1999). Raft association of SNAP receptors acting in apical trafficking in Madin-Darby canine kidney cells. *Proc. Natl. Acad. Sci. USA* **96**(7), 3734–3738.

Lai, H. C., and Jan, L. Y. (2006). The distribution and targeting of neuronal voltage-gated ion channels. *Nat. Rev. Neurosci.* **7**(7), 548–562.

Lamprecht, G., and Seidler, U. (2006). The emerging role of PDZ adapter proteins for regulation of intestinal ion transport. *Am. J. Physiol.-Gastrointest. Liver Physiol.* **291**(5), G766–G777.

Langhorst, M. F., Reuter, A., and Stuermer, C. A. O. (2005). Scaffolding microdomains and beyond: The function of reggie/flotillin proteins. *Cell. Mol. Life Sci.* **62**(19–20), 2228–2240.

Lapierre, L. A., Kumar, R., Hales, C. M., Navarre, J., Bhartur, S. G., Burnette, J. O., Provance, D. W., Mercer, J. A., Bahler, M., and Goldenring, J. R. (2001). Myosin Vb is associated with plasma membrane recycling systems. *Mol. Biol. Cell* **12**(6), 1843–1857.

Laude, A. J., and Prior, I. A. (2004). Plasma membrane microdomains: Organization, function and trafficking (review). *Mol. Membr. Biol.* **21**(3), 193–205.

Lee, J. H., Koh, H., Kim, M., Kim, Y., Lee, S. Y., Karess, R. E., Lee, S. H., Shong, M., Kim, J. M., Kim, J., and Chung, J. K. (2007). Energy-dependent regulation of cell structure by AMP-activated protein kinase. *Nature* **447**(7147), 1017–1020.

Lee-Kwon, W., Kawano, K., Choi, J. W., Kim, J. H., and Donowitz, M. (2003). Lysophosphatidic acid stimulates brush border Na^+/H^+ exchanger 3 (NHE3) activity by increasing its exocytosis by an NHE3 kinase A regulatory protein-dependent mechanism. *J. Biol. Chem.* **278**(19), 16494–16501.

Leung, S. M., Ruiz, W. G., and Apodaca, G. (2000). Sorting of membrane and fluid at the apical pole of polarized Madin-Darby canine kidney cells. *Mol. Biol. Cell* **11**(6), 2131.

Leyt, J., Melamed-Book, N., Vaerman, J., Cohen, S., Weiss, A. M., and Aroeti, B. (2007). Cholesterol-sensitive modulation of transcytosis. *Mol. Biol. Cell* **18**(6), 2057–2071.

Lisanti, M. P., Caras, I. W., Davitz, M. A., and Rodriguez-Boulan, E. (1989). A glycophospholipid membrane anchor acts as an apical targeting signal in polarized epithelial-cells. *J. Cell Biol.* **109**(5), 2145–2156.

Liu, K., Hua, Z. L., Nepute, J. A., and Graham, T. R. (2007). Yeast P4-ATPases Drs2p and Dnf1p are essential cargos of the NPFXD/Sla1p endocytic pathway. *Mol. Biol. Cell* **18**(2), 487–500.

Low, S. H., Chapin, S. J., Weimbs, T., Komuves, L. G., Bennett, M. K., and Mostov, K. E. (1996). Differential localization of syntaxin isoforms in polarized Madin-Darby canine kidney cells. *Mol. Biol. Cell* **7**(12), 2007–2018.

Luzio, J. P., Mullock, B. M., Pryor, P. R., Lindsay, M. R., James, D. E., and Piper, R. C. (2001). Relationship between endosomes and lysosomes. *Biochem. Soc. Trans.* **29**(Part 4), 476–480.

Macara, A. G. (2004). Par proteins: Partners in polarization. *Curr. Biol.* **14**(4), R160–R162.

Maldonado-Baez, L., and Wendland, B. (2006). Endocytic adaptors: Recruiters, coordinators and regulators. *Trends Cell Biol.* **16**(10), 505–513.

Matter, K., Hunziker, W., and Mellman, I. (1992). Basolateral sorting of LDL receptor in MDCK cells—The cytoplasmic domain contains 2 tyrosine-dependent targeting determinants. *Cell* **71**(5), 741–753.

Maxfield, F. R., and McGraw, T. E. (2004). Endocytic recycling. *Nat. Rev. Mol. Cell Biol.* **5**(2), 121–132.

Mazzochi, C., Benos, D. J., and Smith, P. R. (2006). Interaction of epithelial ion channels with the actin-based cytoskeleton. *Am. J. Physiol.-Ren. Physiol.* **291**(6), F1113–F1122.

McBride, H. M., Rybin, V., Murphy, C., Giner, A., Teasdale, R., and Zerial, M. (1999). Oligomeric complexes link Rab5 effectors with NSF and drive membrane fusion via interactions between EEA1 and syntaxin 13. *Cell* **98**(3), 377–386.

McNiven, M. A., and Thompson, H. M. (2006). Vesicle formation at the plasma membrane and trans-Golgi network: The same but different. *Science* **313**(5793), 1591–1594.

Miranda, M., and Sorkin, A. (2007). Regulation of receptors and transporters by ubiquitination: New insights into surprisingly similar mechanisms. *Mol. Interv.* **7**(3), 157–167.

Mirouse, V., Swick, L. L., Kazgan, N., St Johnston, D., and Brenman, J. E. (2007). LKB1 and AMPK maintain epithelial cell polarity under energetic stress. *J. Cell Biol.* **177**(3), 387–392.

Morgan, N. S., Heintzelman, M. B., and Mooseker, M. S. (1995). Characterization of myosin-Ia and Myosin-Ib, 2 unconventional myosins associated with the drosophila brush-border cytoskeleton. *Dev. Biol.* **172**(1), 51–71.

Morinaka, K., Koyama, S., Nakashima, S., Hinoi, T., Okawa, K., Iwamatsu, A., and Kikuchi, A. (1999). Epsin binds to the EH domain of POB1 and regulates receptor-mediated endocytosis. *Oncogene* **18**(43), 5915–5922.

Moskalenko, S., Henry, D. O., Rosse, C., Mirey, G., Camonis, J. H., and White, M. A. (2002). The exocyst is a Ral effector complex. *Nat. Cell Biol.* **4**(1), 66–72.

Mostov, K. E., Verges, M., and Altschuler, Y. (2000). Membrane traffic in polarized epithelial cells. *Curr. Opin. Cell Biol.* **12**(4), 483–490.

Mostov, K. E., Su, T., and ter Beest, M. (2003). Polarized epithelial membrane traffic: Conservation and plasticity. *Nat. Cell Biol.* **5**(4), 287–293.

Mukherjee, S., Tessema, M., and Wandinger-Ness, A. (2006). Vesicular trafficking of tyrosine kinase receptors and associated proteins in the regulation of signaling and vascular function. *Circ. Res.* **98**(6), 743–756.

Murray, J. T., and Backer, J. M. (2005). Analysis of hVps34/hVps15 interactions with Rab5 *in vivo* and *in vitro*. *Methods Enzymol.* **403,** 789–799.

Murshid, A., and Presley, J. F. (2004). ER-to-golgi transport and cytoskeletal interactions in animal cells. *Cell. Mol. Life Sci.* **61**(2), 133–145.

Murthy, V. N., and De Camilli, P. (2003). Cell biology of the presynaptic terminal. *Annu. Rev. Neurosci.* **26,** 701–728.

Musch, A. (2004). Microtubule organization and function in epithelial cells. *Traffic* **5**(1), 1–9.
Musch, A., Cohen, D., Kreitzer, G., and Rodriguez-Boulan, E. (2001). cdc42 regulates the exit of apical and basolateral proteins from the trans-Golgi network. *EMBO J.* **20**(9), 2171–2179.
Muth, T. R., Ahn, J., and Caplan, M. J. (1998). Identification of sorting determinants in the C-terminal cytoplasmic tails of the gamma-aminobutyric acid transporters GAT-2 and GAT-3. *J. Biol. Chem.* **273**(40), 25616–25627.
Naim, H. Y., Joberty, G., Alfalah, M., and Jacob, R. (1999). Temporal association of the N- and O-linked glycosylation events and their implication in the polarized sorting of intestinal brush border sucrase-isomaltase, aminopeptidase N, and dipeptidyl peptidase IV. *J. Biol. Chem.* **274**(25), 17961–17967.
Naslavsky, N., Weigert, R., and Donaldson, J. G. (2004). Characterization of a nonclathrin endocytic pathway: Membrane cargo and lipid requirements. *Mol. Biol. Cell* **15**(8), 3542–3552.
Nesterov, A., Carter, R. E., Sorkina, T., Gill, G. N., and Sorkin, A. (1999). Inhibition of the receptor-binding function of clathrin adaptor protein AP-2 by dominant-negative mutant μ2 subunit and its effects on endocytosis. *EMBO J.* **18**(9), 2489–2499.
Nichols, B. J., Kenworthy, A. K., Polishchuk, R. S., Lodge, R., Roberts, T. H., Hirschberg, K., *et al.* (2001). Rapid cycling of lipid raft markers between the cell surface and Golgi complex. *J. Cell Biol.* **152**(3), 529–541.
Noda, Y., Okada, Y., Saito, N., Setou, M., Xu, Y., Zhang, Z. Z., and Hirokawa, N. (2001). KIFC3, a microtubule minus end-directed motor for the apical transport of annexin XIIIb-associated Triton-insoluble membranes. *J. Cell Biol.* **155**(1), 77–88.
Nyasae, L. K., Hubbard, A. L., and Tuma, P. L. (2003). Transcytotic efflux from early endosomes is dependent on cholesterol and glycosphingolipids in polarized hepatic cells. *Mol. Biol. Cell* **14**(7), 2689–2705.
Oh, P., McIntosh, D. P., and Schnitzer, J. E. (1998). Dynamin at the neck of caveolae mediates their budding to form transport vesicles by GTP-driven fission from the plasma membrane of endothelium. *J. Cell Biol.* **141**(1), 101–114.
Ohno, H., Tomemori, T., Nakatsu, F., Okazaki, Y., Aguilar, R. C., Foelsch, H., Mellman, I., Saito, T., Shirasawa, T., and Bonifacino, J. S. (1999). μ 1B, a novel adaptor medium chain expressed in polarized epithelial cells. *FEBS Lett.* **449**(2–3), 215–220.
Ohta, Y., Suzuki, N., Nakamura, S., Hartwig, J. H., and Stossel, T. P. (1999). The small GTPase RalA targets filamin to induce filopodia. *Proc. Natl. Acad. Sci. USA* **96**(5), 2122–2128.
Paladino, S., Sarnataro, D., Pillich, R., Tivodar, S., Nitsch, L., and Zurzolo, C. (2004). Protein oligomerization modulates raft partitioning and apical sorting of GPI-anchored proteins. *J. Cell Biol.* **167**(4), 699–709.
Parton, R. G., Joggerst, B., and Simons, K. (1994). Regulated internalization of caveolae. *J. Cell Biol.* **127**(5), 1199–1215.
Pelkmans, L., and Helenius, A. (2002). Endocytosis via caveolae. *Traffic* **3**(5), 311–320.
Plant, P. J., Lafont, F., Lecat, S., Verkade, P., Simons, K., and Rotin, D. (2000). Apical membrane targeting of Nedd4 is mediated by an association of its C2 domain with annexin XIIIb. *J. Cell Biol.* **149**(7), 1473–1483.
Polishchuk, R., Di Pentima, A., and Lippincott-Schwartz, J. (2004). Delivery of raft-associated, GPI-anchored proteins to the apical surface of polarized MDCK cells by a transcytotic pathway. *Nat. Cell Biol.* **6**(4), 297–307.
Pombo, I., Rivera, J., and Blank, U. (2003). Munc18–2/syntaxin3 complexes are spatially separated from syntaxin3-containing SNARE complexes. *FEBS Lett.* **550**(1–3), 144–148.
Potter, B. A., Ihrke, G., Bruns, J. R., Weixel, K. M., and Weisz, O. A. (2004). Specific N-glycans direct apical delivery of transmembrane, but not soluble or glycosylphosphatidylinositol-anchored forms of endolyn in Madin-Darby canine kidney cells. *Mol. Biol. Cell* **15**(3), 1407–1416.

Pous, C., Chabin, K., Drechou, A., Barbot, L., Phung-Koskas, T., Settegrana, C., Bourguet-Kondracki, M. L., Maurice, M., Cassio, D., Guyot, M., and Durand, G. (1998). Functional specialization of stable and dynamic microtubules in protein traffic in WIF-B cells. *J. Cell Biol.* **142**(1), 153–165.

Puertollano, R., Martin-Belmonte, F., Millan, J., de Marco, M. D., Albar, J. P., Kremer, L., and Alonso, M. A. (1999). The MAL proteolipid is necessary for normal apical transport and accurate sorting of the influenza virus hemagglutinin in Madin-Darby canine kidney cells. *J. Cell Biol.* **145**(1), 141–151.

Purdy, G. E., and Russell, D. G. (2007). Ubiquitin trafficking to the lysosome—Keeping the house tidy and getting rid of unwanted guests. *Autophagy* **3**(4), 399–401.

Raiborg, C., Bache, K. G., Gillooly, D. J., Madshush, I. H., Stang, E., and Stenmark, H. (2002). Hrs sorts ubiquitinated proteins into clathrin-coated microdomains of early endosomes. *Nat. Cell Biol.* **4**(5), 394–398.

Ramnarayanan, S. P., Cheng, C. A., Bastaki, M., and Tuma, P. L. (2007). Exogenous MAL reroutes selected hepatic apical proteins into the direct pathway in WIF-B cells. *Mol. Biol. Cell* **18**(7), 2707–2715.

Rea, R., Li, J., Dharia, A., Levitan, E. S., Sterling, P., and Kramer, R. H. (2004). Streamlined synaptic vesicle cycle in cone photoreceptor terminals. *Neuron* **41**(5), 755–766.

Rickman, C., Medine, C. N., Bergmann, A., and Duncan, R. R. (2007). Functionally and spatially distinct modes of munc18-syntaxin 1 interaction. *J. Biol. Chem.* **282**(16), 12097–12103.

Rodionov, D. G., and Bakke, O. (1998). Medium chains of adaptor complexes AP-1 and AP-2 recognize leucine-based sorting signals from the invariant chain. *J. Biol. Chem.* **273** (11), 6005–6008.

Rodriguez-Boulan, E., Musch, A., and Le Bivic, A. (2004). Epithelial trafficking: New routes to familiar places. *Curr. Opin. Cell Biol.* **16**(4), 436–442.

Rodriguez-Boulan, E., Geri, K., and Musch, A. (2005). Organization of vesicular trafficking in epithelia. *Nat. Rev. Mol. Cell Biol.* **6**(3), 233–247.

Rojas, R., and Apodaca, G. (2002). Immunoglobulin transport across polarized epithelial cells. *Nat. Rev. Mol. Cell Biol.* **3**(12), 944–955.

Roush, D. L., Gottardi, C. J., Naim, H. Y., Roth, M. G., and Caplan, M. J. (1998). Tyrosine-based membrane protein sorting signals are differentially interpreted by polarized Madin-Darby canine kidney and LLC-PK1 epithelial cells. *J. Biol. Chem.* **273**(41), 26862–26869.

Russell, M. R. G., Nickerson, D. P., and Odorizzi, G. (2006). Molecular mechanisms of late endosome morphology, identity and sorting. *Curr. Opin. Cell Biol.* **18**(4), 422–428.

Sabharanjak, S., Sharma, P., Parton, R. G., and Mayor, S. (2002). GPI-anchored proteins are delivered to recycling endosomes via a distinct cdc42-regulated clathrin-independent pinocytic pathway. *Dev. Cell* **2**(4), 411–423.

Salaun, C., James, D. J., and Chamberlain, L. H. (2004). Lipid rafts and the regulation of exocytosis. *Traffic* **5**(4), 255–264.

Sandvig, K., Olsnes, S., Brown, J. E., Petersen, O. W., and Van Deurs, B. (1989). Endocytosis from coated pits of shiga toxin: A glycolipid-binding protein from shigella dysenteriae 1. *J. Cell Biol.* **108**(4), 1331–1343.

Saraste, J., and Goud, B. (2007). Functional symmetry of endomembranes. *Mol. Biol. Cell* **18**(4), 1430–1436.

Scheiffele, P., and Fullekrug, J. (2000). Glycosylation and protein transport. *Mol. Trafficking* **36,** 27–35.

Scheiffele, P., Peranen, J., and Simons, K. (1995). N-Glycans as apical sorting signals in epithelial-cells. *Nature* **378**(6552), 96–98.

Schmidt, U., Briese, S., Leicht, K., Schurmann, A., Joost, H. G., and Al-Hasani, H. (2006). Endocytosis of the glucose transporter GLUT8 is mediated by interaction of a dileucine motif with the beta 2-adaptin subunit of the AP-2 adaptor complex. *J. Cell Sci.* **119**(11), 2321–2331.

Schnitzer, J. E., Liu, J., and Oh, P. (1995). Endothelial caveolae have the molecular transport machinery for vesicle budding, docking, and fusion including VAMP, NSF, SNAP, annexins, and GTPases. *J. Biol. Chem.* **270**(24), 14399–14404.

Schubert, W., Frank, P. G., Razani, B., Park, D. S., Chow, C., and Lisanti, M. P. (2001). Caveolae-deficient endothelial cells show defects in the uptake and transport of albumin *in vivo*. *J. Biol. Chem.* **276**(52), 48619–48622.

Schuck, S., and Simons, K. (2006). Controversy fuels trafficking of GPI-anchored proteins. *J. Cell Biol.* **172**(7), 963–965.

Sheff, D., Pelletier, L., O'Connell, C. B., Warren, G., and Mellman, I. (2002). Transferrin receptor recycling in the absence of perinuclear recycling endosomes. *J. Cell Biol.* **156**(5), 797–804.

Shenolikar, S., Voltz, J. W., Minkoff, C. M., Wade, J. B., and Weinman, E. J. (2002). Targeted disruption of the mouse NHERF-1 gene promotes internalization of proximal tubule sodium-phosphate cotransporter type IIa and renal phosphate wasting. *Proc. Natl. Acad. Sci. USA* **99**(17), 11470–11475.

Shenoy, S. K., and Lefkowitz, R. J. (2003). Trafficking patterns of beta-arrestin and G protein-coupled receptors determined by the kinetics of beta-arrestin deubiquitination. *J. Biol. Chem.* **278**(16), 14498–14506.

Shih, S. C., Sloper-Mould, K. E., and Hicke, L. (2000). Monoubiquitin carries a novel internalization signal that is appended to activated receptors. *EMBO J.* **19**(2), 187–198.

Shim, J., and Lee, J. (2005). The AP-3 clathrin-associated complex is essential for embryonic and larval development in *Caenorhabditis elegans*. *Mol. Cells* **19**(3), 452–457.

Shipitsin, M., and Feig, L. A. (2004). RalA but not RalB enhances polarized delivery of membrane proteins to the basolateral surface of epithelial cells. *Mol. Cell. Biol.* **24**(13), 5746–5756.

Simmen, T., Honing, S., Icking, A., Tikkanen, R., and Hunziker, W. (2002). AP-4 binds basolateral signals and participates in basolateral sorting in epithelial MDCK cells. *Nat. Cell Biol.* **4**(2), 154–159.

Simons, K., and Ikonen, E. (2000). Cell biology—How cells handle cholesterol. *Science* **290** (5497), 1721–1726.

Simpson, J. C., Griffiths, G., Wessling-Resnick, M., Fransen, J. A. M., Bennett, H., and Jones, A. T. (2004). A role for the small GTPase Rab21 in the early endocytic pathway. *J. Cell Sci.* **117**(26), 6297–6311.

Snyder, D. A., Kelly, M. L., and Woodbury, D. J. (2006). SNARE complex regulation by phosphorylation. *Cell Biochem. Biophys.* **45**(1), 111–123.

Sollner, T., Bennett, M. K., Whiteheart, S. W., Scheller, R. H., and Rothman, J. E. (1993). A protein assembly-disassembly pathway *in vitro* that may correspond to sequential steps of synaptic vesicle docking, activation, and fusion. *Cell* **75**(3), 409–418.

Sorkin, A. (2004). Cargo recognition during clathrin-mediated endocytosis: A team effort. *Curr. Opin. Cell Biol.* **16**(4), 392–399.

Spooner, R. A., Smith, D. C., Easton, A. J., Roberts, L. M., and Lord, J. M. (2006). Retrograde transport pathways utilised by viruses and protein toxins. *Virol. J.* **3**.

Stan, R. V. (2005). Structure of caveolae. *Biochim. Biophys. Acta—Mol. Cell Res.* **1746**(3), 334–348.

Starcevic, M., Nazarian, R., and Dell'Angelica, E. C. (2002). The molecular machinery for the biogenesis of lysosome-related organelles: Lessons from Hermansky-Pudlak syndrome. *Semin. Cell Dev. Biol.* **13**(4), 271–278.

Sutton, R. B., Fasshauer, D., Jahn, R., and Brunger, A. T. (1998). Crystal structure of a SNARE complex involved in synaptic exocytosis at 2.4 A resolution. *Nature* **395**(6700), 347–353.

Suzuki, A., Yamanaka, T., Hirose, T., Manabe, N., Mizuno, K., Shimizu, M., Akimoto, K., Izumi, Y., Ohnishi, T., and Ohno, S. (2001). Atypical protein kinase C is involved in the evolutionarily conserved PAR protein complex and plays a critical role in establishing epithelia-specific junctional structures. *J. Cell Biol.* **152**(6), 1183–1196.

Takeda, T., Yamazaki, H., and Farquhar, M. G. (2003). Identification of an apical sorting determinant in the cytoplasmic tail of megalin. *Am. J. Physiol.-Cell Physiol.* **284**(5), C1105–C1113.

Takei, K., McPherson, P. S., Schmid, S. L., and De Camilli, P. (1995). Tubular membrane invaginations coated by dynamin rings are induced by GTP-γS in nerve terminals. *Nature* **374**(6518), 186–190.

Tall, R. D., Alonso, M. A., and Roth, M. G. (2003). Features of influenza HA required for apical sorting differ from those required for association with DRMs or MAL. *Traffic* **4**(12), 838–849.

Tandon, C., De Lisle, R. C., Boulatnikov, I., and Naik, P. K. (2007). Interaction of carboxyl-terminal peptides of cytosolic-tail of apactin with PDZ domains of NHERF/EBP50 and PDZK-1/CAP70. *Mol. Cell. Biochem.* **302**(1–2), 157–167.

Taner, S. B., Onfelt, B., Pirinen, N. J., McCann, F. E., Magee, A. I., and Davis, D. M. (2004). Control of immune responses by trafficking cell surface proteins, vesicles and lipid rafts to and from the immunological synapse. *Traffic* **5**(9), 651–661.

Thiel, C., Osborn, M., and Gerke, V. (1992). The tight association of the tyrosine kinase substrate annexin II with the submembranous cytoskeleton depends on intact p11-binding and Ca-2+-binding sites. *J. Cell Sci.* **103**(Part 3), 733–742.

Thomas, P. J., Shenbagamurthi, P., Sondek, J., Hullihen, J. M., and Pedersen, P. L. (1992). The cystic fibrosis transmembrane conductance regulator. Effects of the most common cystic fibrosis-causing mutation on the secondary structure and stability of a synthetic peptide. *J. Biol. Chem.* **267**(9), 5727–5730.

Thomas, D. C., Brewer, C. B., and Roth, M. G. (1993). Vesicular stomatitis-virus glycoprotein contains a dominant cytoplasmic basolateral sorting signal critically dependent upon a tyrosine. *J. Biol. Chem.* **268**(5), 3313–3320.

Thompson, A., Nessler, R., Wisco, D., Anderson, E., Winckler, B., and Sheff, D. (2007). Recycling endosomes of polarized epithelial cells actively sort apical and basolateral cargos into separate subdomains. *Mol. Biol. Cell* **18**(7), 2687–2697.

Thomsen, P., Roepstorff, K., Stahlhut, M., and Van Deurs, B. (2002). Caveolae are highly immobile plasma membrane microdomains, which are not involved in constitutive endocytic trafficking. *Mol. Biol. Cell* **13**(1), 238–250.

Torgersen, M. L., Skretting, G., Van Deurs, B., and Sandvig, K. (2001). Internalization of cholera toxin by different endocytic mechanisms. *J. Cell Sci.* **114**(20), 3737–3747.

Toshima, J., Toshima, J. Y., Duncan, M. C., Cope, M. J. T. V., Sun, Y., Martin, A. C., Anderson, S., Yates, J. R., III, Mizuno, K., and Drubin, D. G. (2007). Negative regulation of yeast Eps15-like Arp2/3 complex activator, Pan1p, by the Hip1R-related protein, Sla2p, during endocytosis. *Mol. Biol. Cell* **18**(2), 658–668.

Toshima, J., Toshima, J. Y., Martin, A. C., and Drubin, D. G. (2005). Phosphoregulation of Arp2/3-dependent actin assembly during receptor-mediated endocytosis. *Nat. Cell Biol.* **7**(3), 246–254.

Tuma, P. L., and Hubbard, A. L. (2003). Transcytosis: Crossing cellular barriers. *Physiol. Rev.* **83**(3), 871–932.

Tuma, P. L., Nyasae, L. K., Backer, J. M., and Hubbard, A. L. (2001). Vps34p differentially regulates endocytosis from the apical and basolateral domains in polarized hepatic cells. *J. Cell Biol.* **154**(6), 1197–1208.

Ungar, D., Oka, T., Krieger, M., and Hughson, F. M. (2006). Retrograde transport on the COG railway. *Trends Cell Biol.* **16**(2), 113–120.

Ungermann, C., and Langosch, D. (2005). Functions of SNAREs in intracellular membrane fusion and lipid bilayer mixing. *J. Cell Sci.* **118**(17), 3819–3828.

Vagin, O., Turdikulova, S., and Sachs, G. (2004). The H,K-ATPase beta subunit as a model to study the role of N-glycosylation in membrane trafficking and apical sorting. *J. Biol. Chem.* **279**(37), 39026–39034.

van der Goot, F. G., and Gruenberg, J. (2006). Intra-endosomal membrane traffic. *Trends Cell Biol.* **16**(10), 514–521.

Wagner, M., Morgans, C., and Kochbrandt, C. (1995). The oligosaccharides have an essential but indirect role in sorting gp80 (clusterin, trpm-2) to the apical surface of MDCK cells. *Eur. J. Cell Biol.* **67**(1), 84–88.

Waters, M. G., and Hughson, F. M. (2000). Membrane tethering and fusion in the secretory and endocytic pathways. *Traffic* **1**(8), 588–597.

Watson, P., and Spooner, R. A. (2006). Toxin entry and trafficking in mammalian cells. *Adv. Drug Deliv. Rev.* **58**(15), 1581–1596.

Wells, C. D., Fawcett, J. P., Traweger, A., Yamanaka, Y., Goudreault, M., Elder, K., Kulkarni, S., Gish, G., Virag, C., Lim, C., Colwill, K., Starostine, A., *et al.* (2006). A Rich1/Amot complex regulates the Cdc42 GTPase and apical-polarity proteins in epithelial cells. *Cell* **125**(3), 535–548.

Wilson, J. M., De Hoop, M., Zorzi, N., Toh, B., Dotti, C. G., and Parton, R. G. (2000). EEA1, a tethering protein of the early sorting endosome, shows a polarized distribution in hippocampal neurons, epithelial cells, and fibroblasts. *Mol. Biol. Cell* **11**(8), 2657–2671.

Wolfe, B. L., and Trejo, J. (2007). Clathrin-dependent mechanisms of G protein-coupled receptor endocytosis. *Traffic* **8**(5), 462–470.

Yamanaka, T., Horikoshi, Y., Suzuki, A., Sugiyama, Y., Kitamura, K., Maniwa, R., Nagai, Y., Yamashita, A., Hirose, T., Ishikawa, H., and Ohno, S. (2001). PAR-6 regulates aPKC activity in a novel way and mediates cell-cell contact-induced formation of the epithelial junctional complex. *Genes Cells* **6**(8), 721–731.

Yamanaka, T., Horikoshi, Y., Sugiyama, Y., Ishiyama, C., Suzuki, A., Hirose, T., Iwamatsu, A., Shinohara, A., and Ohno, S. (2003). Mammalian LgI forms a protein complex with PAR-6 and aPKC independently of PAR-3 to regulate epithelial cell polarity. *Curr. Biol.* **13**(9), 734–743.

Yao, X. B., and Forte, J. G. (2003). Cell biology of acid secretion by the parietal cell. *Annu. Rev. Physiol.* **65,** 103–131.

Yeaman, C., Grindstaff, K. K., and Nelson, W. J. (1999). New perspectives on mechanisms involved in generating epithelial cell polarity. *Physiol. Rev.* **79**(1), 73–98.

Yeaman, C., LeGall, A. H., Baldwin, A. N., Monlauzeur, L., LeBivic, A., and Rodriguez-Boulan, E. (1997). The O-glycosylated stalk domain is required for apical sorting of neurotrophin receptors in polarized MDCK cells. *J. Cell Biol.* **139**(4), 929–940.

Yun, C. C., Chen, Y. P., and Lang, F. (2002). Glucocorticoid activation of Na^+/H^+ exchanger isoform 3 revisited—The roles of SGX1 and NHERF2. *J. Biol. Chem.* **277**(10), 7676–7683.

Zhang, L., Li, J., Young, L. H., and Caplan, M. J. (2006). AMP-activated protein kinase regulates the assembly of epithelial tight junctions. *Proc. Natl. Acad. Sci. USA* **103**(46), 17272–17277.

Zheng, B., and Cantley, L. C. (2007). Regulation of epithelial tight junction assembly and disassembly by AMP-activated protein kinase. *Proc. Natl. Acad. Sci. USA* **104**(3), 819–822.

Zimmermann, P. (2006). The prevalence and significance of PDZ domain-phosphoinositide interactions. *Biochim. Biophys. Acta – Mol. Cell Biol. Lipids* **1761**(8), 947–956.

This page intentionally left blank

CHAPTER FIVE

Chick Embryo Chorioallantoic Membrane as a Useful Tool to Study Angiogenesis

Domenico Ribatti*

Contents

Abstract

The chick embryo chorioallantoic membrane (CAM) is an extraembryonic membrane mediating gas and nutrient exchanges until hatching. Since it has a dense capillary network, it has been commonly used *in vivo* to study both angiogenesis and antiangiogenesis in response to normal tissues and cells, to tumor bioptic specimens and cells, or to soluble factors. During the last 8 years, this assay has been used in over 550 published works. This chapter summarizes current knowledge about the embryological origin of the CAM, morphology of its blood and lymphatic vessels, the use of CAM in the study of tumor

* Department of Human Anatomy and Histology, University of Bari Medical School, I-70124 Bari, Italy.
e-mail: ribatti@anatomia.uniba.it

International Review of Cell and Molecular Biology, Volume 270
ISSN 1937-6448, DOI: 10.1016/S1937-6448(08)01405-6

angiogenesis and metastasis, angiogenic and antiangiogenic substances. The angiogenic response of CAM to multiple myeloma and neuroblastoma cells and bioptic specimens and their responses to antiangiogenic molecules and the role played by fibroblast growth factor-2 in CAM vascularization have been analyzed in detail. Finally, advantages and limitations of CAM as an experimental model to study angiogenesis and antiangiogenesis are discussed.

Key Words: Angiogenesis, Antiangiogenesis, Chorioallantoic membrane, Fibroblast growth factor-2, Intussusceptive growth, Multiple myeloma, Neuroblastoma, Tumor growth.

1. Introduction

As pointed out by Auerbach in (1991), ''Perhaps the most consistent limitation to progress in angiogenesis research has been the availability of simple, reliable, reproducible, quantitative assays of the angiogenesis response.'' *In vitro* angiogenesis assays, based on endothelial cell (EC) cultures or tissue explant, focus on isolated EC functions (e.g., EC proliferation, migration, or invasion) and do not examine the coordination of cell functions required for a successful angiogenic response (Auerbach *et al.*, 2000; Jain *et al.*, 1997).

In contrast, *in vivo* angiogenesis assays examine the entire spectrum of molecular and cellular processes. However, these *in vivo* assays are not only expensive and technically difficult to perform but also require substantial amounts of test compound and most rely on selective morphometric analysis for quantification (Auerbach *et al.*, 2000; Jain *et al.*, 1997). Because of these limitations, current drug development strategies for identification and testing angiogenesis inhibitors depend principally on the use of *in vitro* systems.

Although *in vitro* angiogenesis assays have been useful for identification of potential molecular targets to block EC responses and preliminary screening of novel pharmacological agents, they frequently cannot be correlated with *in vivo* angiogenesis measurements. This is most likely the result of the complex and multiple cellular mechanisms evoked during new blood vessel formation *in vivo*.

Currently, novel angiogenesis-targeted therapies lack *in vivo* screening models suitable for objective, quantitative preclinical testing, making it difficult to obtain a dose-response analysis and estimate therapeutic doses before initiating clinical trials.The development of inhibitors of angiogenesis relies on a range of preclinical assays that mimic various steps of the angiogenic cascade. Knowledge of the mechanism of action of the tested compound will dictate the choice of assay. Alternatively, the behavior of the compound in different assays may indicate the mechanism of action.

Ideally, assays of angiogenesis should be easy, reproducible, quantitative, cost-effective, and permit rapid analysis. A typical analysis of antiangiogenic activity is done than one assay, beginning with the more elementary assays *in vitro* that will provide easy, rapid, and affordable data. *In vitro* assays cannot be considered conclusive; however, the activity of a compound must be confirmed in other assays of increasing complexity, including *in vivo* assays of angiogenesis, angiogenic-dependent tumor growth, and metastasis. *In vivo* assays are usually unsuitable for the quantitative screening of a large number of compounds, as they are often complex, expensive, and may require specific surgical skills. Nonetheless, they are always required to confirm ultimately the activity of a potential drug.

The classical assays for studying angiogenesis *in vivo* include the hamster check pouch, the rabbit ear chamber, the rodent dorsal skin and air sac, the iris and avascular cornea of the rodent eye (Ribatti and Vacca, 1999), and the chick embryo chorioallantoic membrane (CAM). Several models have been introduced, including subcutaneous implantation in rodents of various three-dimensional substrates, including a polymer sponge (Andrade *et al.*, 1987), Matrigel, a laminin-rich mixture of basement membrane components (Passaniti *et al.*, 1992), and a polyvinyl alcohol foam disc covered on both sides with a Millipore filter (disc angiogenesis system) (Fajardo *et al.*, 1998). Finally, zebra fish (*Danio rerio*) embryos may represent a suitable model to study the mechanisms of angiogenesis and angiosuppression during development (Nicoli *et al.*, 2007).

2. Chorioallantoic Membrane and Its Embryological Origin

The CAM of the developing chick embryo is an extraembryonic membrane mediating gas and nutrient exchanges until hatching. Since the CAM has a very dense capillary network, it is commonly used to study *in vivo* both angiogenesis and antiangiogenesis in response to different factors. During 2000–2007, over 550 publications have used the chick embryo CAM as a model system to study angiogenesis and antiangiogenesis (NCBI, Pub Med). The CAM, particularly, that of the White Leghorn is the most widely used. The CAM of the Japanese quail has also been used. The quail-derived endothelium expresses a unique marker which can be identified using the QH1 antibody.

Chick embryo development lasts 21 days before hatching. The allantois of the chick embryo appears at about 3.5 days of incubation as an evagination from the ventral wall of the endodermal hind gut. During the fourth day, it pushes out of the body of the embryo into the extraembryonic coelom. Its proximal portion lies parallel and just caudal to the yolk sac.

When the distal portion grows clear of the embryo it becomes enlarged. The narrow proximal portion is known as the allantoic stalk, the enlarged distal portion as the allantoic vesicle. Fluid accumulation distends the allantois so that its terminal portion resembles a balloon in entire embryos.

The allantoic vesicle enlarges very rapidly from day 4 to day 10 of incubation. In this process, the mesodermal layer of the allantois becomes fused with the adjacent mesodermal layer of the chorion to form the CAM. A double layer of mesoderm is thus created, its chorionic component is somatic mesoderm and its allantoic component is splanchnic mesoderm. In this double layer, an extremely rich vascular network develops and is connected with the embryonic circulation by the allantoic arteries and veins. Immature blood vessels, lacking a complete basal lamina and smooth muscle cells, scattered in the mesoderm grow very rapidly until day 8 and give rise to a capillary plexus, which comes to be intimately associated with the overlying chorionic epithelial cells and mediates gas exchange with the outer environment. At day 14, the capillary plexus is located at the surface of the ectoderm adjacent to the shell membrane. Rapid capillary proliferation continues until day 11; thereafter, the EC mitotic index declines rapidly, and the vascular system attains its final arrangement on day 18, just before hatching (Ausprunk *et al.*, 1974).

The umbilical artery after emerging from the embryonic adnominal wall, branches into two primary chorioallantoic artery, and the CAM is drained by a single chorioallantoic vein. Fuchs and Lindenbaum (1988) described six or seven generations of branches of the allantoic artery. The first five or six are located in a plane parallel to the CAM surface and deep to the vein, which has a similar distribution (Fig. 5.1). The fifth and sixth generations of blood vessels change direction, passing almost vertically in the two-dimensional capillary plexus.

This circulation and the position of the allantois immediately subjacent to the porous shell, confer a respiratory function on the highly vascularized CAM. In addition to the respiratory interchange of oxygen and carbon dioxide, the allantois also serves as a reservoir for the waste products excreted by the embryo, mostly urea at first and chiefly uric acid, later. CAM is also involved in mobilization of calcium from the shell to start bone mineralization.

2.1. Morphology of chorioallantoic membrane blood and lymphatic vessels

On day 4, all CAM vessels have the appearance of undifferentiated capillaries. Their walls consist of a single layer of ECs lacking a basal lamina (Ausprunk *et al.*, 1974). By day 8, the CAM displays small thin-walled capillaries with a lumenal diameter of 10–15 μm beneath the chorionic epithelium and other vessels with a diameter of 10–115 μm in the

mesodermal layer, whose walls have a layer of mesenchymal cells surrounding the endothelium and are completely wrapped by a basal lamina together with the ECs (Ausprunk *et al.*, 1974).

On days 10–12, the capillaries resemble those in the 8-day membrane and are now near the surface of the chorionic epithelium. The mesodermal vessels are now distinct arterioles and venules. In addition to the endothelium, the walls of arterioles (10- to 85-μm diameter) contain one or two layers of mesenchymal cells and increased amounts of connective tissue surrounding them. Venules (10- to 115-μm diameter) are surrounded by an incomplete investment of mesenchymal cells and connective tissue has also accumulated within their walls. The mesenchymal cells are presumed to be developing smooth muscle cells and the walls of CAM arterioles also develop a distinct adventitia containing fibroblast-like cells (Ausprunk *et al.*, 1974).

Between days 4 and 8, the ECs form punctuate junctional appositions and a few plasmalemmal vesicles are observed (Shumko *et al.*, 1988). Between days 9 and 13, the arteriolar endothelium displays more extensive junctional complexes with multiple membrane contact points (Shumko *et al.*, 1988). In contrast to the arterioles, endothelial junctional appositions of the CAM venules remains punctuate (Shumko *et al.*, 1988). Between days 14 and 18, these appositions remain as simple punctuate configurations (Shumko *et al.*, 1988). The venules possess multiple sites of interendothelial contact with areas of junctional dilations, while the arterioles display complex interdigitating cell junctions (Shumko *et al.*, 1988).

The extracellular matrix of the CAM modifies its composition in terms of expression of fibronectin, laminin, collagen type IV, and distribution of specific glycosaminoglycans, favoring the angiogenic process that occurs in the space between the chorionic epithelium and the mesodermal blood vessels (Ausprunk, 1986; Ribatti *et al.*, 1998a).

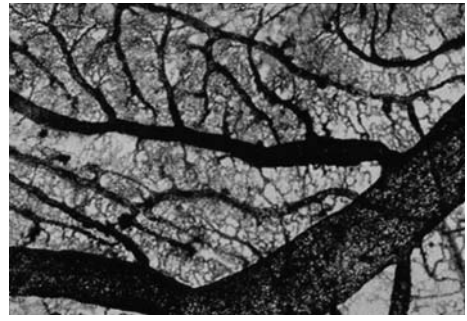

Figure 5.1 **A macroscopic picture of the chorioallantoic membrane (CAM) vascular tree after intravenous India ink injection at 14 day of incubation. Note the extreme complexity of the vascular architecture. Original magnification, $\times 160$.**

Fibronectin appears in the extracellular matrix beneath the chorion at early stages of development when the subepithelial capillary plexus is not yet formed and it may promote the migration of ECs merging by sprouting from the mesodermal blood vessels (Ribatti *et al.*, 1998). Moreover, fibronectin overexpression in extracellular matrix parallels the vasoproliferative processes induced by angiogenic stimuli in the CAM (Ribatti *et al.*, 1997a). Accordingly, a close relationship *in vivo* between fibronectin overexpression and angiogenesis has been demonstrated by others (Risau and Lemmon, 1988; Sariola *et al.*, 1984). Laminin immunoreactivity is present during all stages of vessel formation in CAM development (Ribatti *et al.*, 1998) in keeping with its role in the early formation and later differentiation of the subendothelial basement membrane (Risau and Lemmon, 1988).

Type IV collagen appears in the late stages of CAM vascular development concomitantly with the terminal differentiation of ECs and maturation of basement membrane (Ribatti *et al.*, 1998). It results in progressively slower microvascular EC proliferation and correlates with the formation of a lumen, gradual reduction in endothelial migration, establishment of cell polarity and acquisition of a differentiated endothelial phenotype (Form *et al.*, 1986; Nicosia and Madri, 1987).

Ausprunk (1986) demonstrated that hyaluronic acid plays a crucial role in the formation, alignment, or migration of the capillary plexus of the CAM, while heparan sulfate, chondroitin sulfate, and dermatan sulfate are important in the differentiation and development of arterial and venous vessels of the CAM CAM arterioles and venules are accompanied by a pair of interconnected lymphatics. Veins are also associated with lymphatics and larger veins are surrounded by a lymphatic plexus (Oh *et al.*, 1987). Lymph is drained by trunks of the umbilical stalk into the coccygeal lymphatics and the lymph hearts of the embryo (Wilting *et al.*, 1999). In ultrathin sections the endothelium of the CAM lymphatic capillaries has no basal lamina and an extremely thin endothelial lining (Oh *et al.*, 1997). The lymphatic ECs of the differentiated CAM specifically express vascular endothelial growth factor receptor-3 (VEGFR-3) whereas expression of VEGFR-2 is found in both its blood vascular and its lymphatic ECs (Wilting *et al.*, 1996). The ligand of VEGFR-3, VEGF-C, is expressed ubiquitously in the allantoic bud, and later predominantly in the allantoic epithelium and the wall of larger blood vessels (Papoutsi *et al.*, 2001). The lymphatics of the CAM are located immediately adjacent to the larger blood vessels and the expression of VEGF-C in the blood vascular wall serves for the patterning of lymphatics. The application of VEGF-C on the differentiated CAM induces development of lymphatics, which are derived by proliferation of the preexisting lymphatics (Oh *et al.*, 1997). The homeobox gene Prox-1, which is specifically expressed in lymphatics, has been demonstrated in the CAM (Papoutsi *et al.*, 2001).

2.2. A single blood sinus or a capillary plexus beneath the chorionic epithelium?

Fulleborn (1895) described a ''great blood sinus interrupted by strands of tissue.'' Other authors (Mc Cormick *et al.*, 1984; Narbaitz, 1977; Schoefl, 1984) maintain that there is a vascular sinus and that the CAM vascular bed is a single flat sinus, interrupted by a series of gaps. When the sinus comes close to the CAM surface, the architecture of the chorionic epithelium changes from that of a double layer of flat cells to an intricate arrangement of highly differentiated cells, such as the sinus-covering cells (Narbaitz, 1977), which are adapted for gas exchange, and villus-cavity cells, which are thought to be involved in the absorption of calcium from the eggshell (Coleman and Terepka, 1972). In the chick CAM therefore active migration of the chorionic epithelium rather than ECs is apparently involved and the intraepithelial positioning of the vascular sinus is largely due to growth and differentiation of the chorionic epithelium.

Other authors have identified a capillary plexus formed during the early stages of incubation, and eventually intimately associated with the overlying chorionic epithelial cells (Ausprunk *et al.*, 1974; Burton and Palmer, 1989; Danchakoff, 1917; Fanczi and Feher, 1979; Moscona, 1959; Ribatti *et al.*, 1998a). Danchakoff (1917) described a multitude of sprouts arising from the mesenchymal blood vessels and invading the chorionic epithelium, resulting in a well-perfused capillary meshwork (Fig. 5.2). Burton and Palmer (1989)

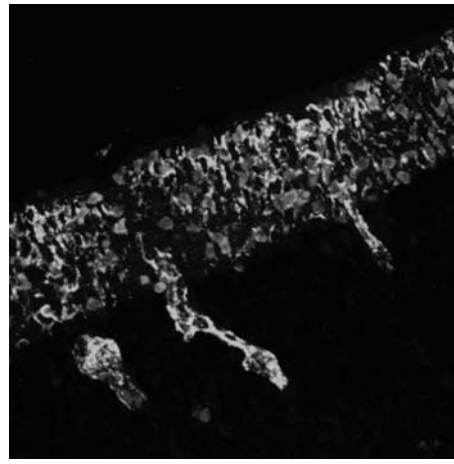

Figure 5.2 **A confocal laser scanner microscopy picture obtained by using an antibody antifactor VIII to detect endothelial cells and showing three sprouts arising from the chorioallantoic membrane (CAM) mesenchymal blood vessels and invading the chorionic epithelium, resulting in a capillary meshwork. Original magnification, ×160.**

reported that short vascular buds invaded the mesenchyme at day 6 from the arterial and venous sides, culminating in capillary plexus formation. The presence of a complete basement membrane and the lack of phagocytic cells intermingled with the ECs provide the main morphological evidence of the existence of a capillary plexus.

2.3. The chorioallantoic membrane vascular growth

A widely accepted view is that blood vessels arise through two mechanisms during development, vasculogenesis and angiogenesis (Risau, 1997). Vasculogenesis entails the direct formation of blood vessels by differentiation of angioblastic precursor cells *in situ*, while angiogenesis (''sprouting angiogenesis'') entails new vessel formation from preexisting vessels, capillaries, and postcapillary venules.

Intussusceptive microvascular growth (IMG) (''intussusception or non-sprouting angiogenesis'') is a new concept of microvascular growth relevant for many vascular systems, which constitutes an additional and alternative mechanism to endothelial sprouting (Patan *et al.*, 1992). The first reports on IMG were published by Burri *et al.* who investigated the lung vasculature in postnatal rats (Burri and Tarek, 1990; Caduff *et al.*, 1986) and postulated that the capillary network primarily increased its complexity and vascular surface by insertion of a multitude of transcapillary pillars, a process they called ''intussusception'' (meaning ''in-itself growth''). They described four consecutive steps in pillar formation: creation of a zone of contact between opposite capillary walls; reorganization of the intercellular junctions of the endothelium with central perforation of the endothelial bilayer; formation of an interstitial pillar core; subsequent invasion of the pillar by cytoplasmic extensions of myofibroblasts and pericytes, and by collagen fibrils. Lastly, the pillars are thought to increase in diameter and become a capillary mesh.

Patan *et al.* (1993) observed the same morphological transformation during IMG in the CAM. Pillar formation in the CAM occurs both as transcapillary interconnection of opposite capillary walls and folding of the capillary wall into the lumen, followed by progressive thinning of the meso-like fold resulting in pillar separation (Patan *et al.*, 1996). In addition, tissue pillars can arise by capillary fusion. The walls of neighboring vessels running in parallel fuse at several places, and give rise to one or more tissue pillars (Patan *et al.*, 1996).

We have demonstrated that after recombinant human erythropoietin stimulation, the generation of new blood vessels in the CAM occurred more frequently following an IMG mechanism (Crivellato *et al.*, 2004). This response is peculiar of erythropoietin, because it is abolished when an erythropoietin-blocking antibody was coadministered with erythropoietin.

According to Schlatter *et al.* (1997), CAM vascularization undergoes three phases of development with both sprouting and IMG: in the early

phase (days 5–7), multiple capillary sprouts invade the mesenchyme, fuse and form the primary capillary plexus. During the second (intermediate phase) (days 8–12), sprouts are no longer present since they have been replaced by tissue pillars, with a maximal frequency at day 11. During the late phase (day 13 and older), the growing pillars increase in size to form intercapillary meshes more than 2.5 μm in diameter.

An extensive morphometric investigation by De Fouw *et al.* (1989) has shown rapid extension of the CAM surface from 6 cm^2 at day 6 to 65 cm^2 at day 14. During this period, the number of feed vessels increased (2.5- and 5-fold for precapillary and postcapillary vessels), predominantly due to growth and remodeling after day 10. Rizzo and De Fouw (1993) found 50% of ECs thinning out from day 10 to day 14 of incubation.

The CAM endothelium exhibits an intrinsically high mitotic rate (thymidine labeling index 23% for 5 h thymidine exposure) until day 10 (Ausprunk *et al.*, 1974). At day 11, this falls to 2% and remains low throughout the remaining incubation period. Investigation of the presence of bromodeoxyuridine-labeled ECs in the growing CAM from day 6 to day 15 by Kurz *et al.* (1995) revealed a significant (>50%) loss of proliferative activity at day 10 (intermediate phase) in comparison with day 6 (sprouting phase). After day 10, proliferative activity decreased further, and at days 14 and 15 (late phase), dividing cells were less than 10% of the value of day 6.

The ultrastructural alterations associated with the focal microvascular histodifferentiation are in line with the changes in the vascular pattern. Small differences between CAM arterioles, capillaries, and venules are noted during the early phase. During the intermediate phase, the interstitial perivascular spaces increase their collagen content and cell volume density. During the late phase, a circular tunic containing layers of presumptive smooth muscle cells surrounds the endothelium of the arterioles and not that of the venules. Their morphology is thus distinct (Shumko *et al.*, 1988).

3. Use of Chorioallantoic Membranes in the Study of Angiogenesis

The first evidence of the tumor-induced angiogenesis *in vivo* by using the CAM assay dated 1913 (Ribatti, 2004). The CAM has long been a favored system for the study of tumor angiogenesis and metastasis (Auerbach *et al.*, 1976; Dagg *et al.*, 1956; Quigley and Armstrong, 1998), because at this stage the chick's immunocompetent system is not fully developed and the conditions for rejection have not been established (Leene *et al.*, 1973). As other vertebrates, chickens are protected by a dual immune system composed of B and T cells, controlling the antibody and cell-mediated immunity, respectively. The B cells are differentiated in the bursa of Fabricius, the

organ equivalent to the bone marrow in mammals, whereas T cells are differentiated in the thymus (Davison, 2003; Funk and Thompson, 1996). Until day 10, the chick embryo immune system is not completely developed. The presence of T cells can be first detected at day 11 and of B cells at day 12 (Janse and Jeurissen, 1991). After day 15, the B cell repertory begins to diversify and by day 18 chicken embryos become immunocompetent.

All studies of mammalian neoplasms in the CAM have utilized solid tumors and cell suspensions derived from solid tumors (Tables 5.1 and 5.2). Compared with mammals' models, where tumor growth often takes between 3 and 6 weeks, assays using chick embryos are faster. Between 2 and 5 days after tumor cell inoculation, the tumor xenografts become visible and are supplied with vessels of CAM origin. Tumors grafted onto the CAM remain nonvascularized for a couple of days, after which they can be penetrated by new blood vessels and begin a phase of rapid growth. Tumor cells can be identified in the CAM, as well as in the internal organs of the embryo, such as lungs, liver, and brain (Bobek *et al.*, 2004; Gordon and Qigley, 1986).

Walker 256 carcinoma specimens implanted on the CAM do not exceed a mean diameter of 0.93 ± 0.29 mm during the prevascular phase ($\sim$72 h). Rapid growth begins 24 h after vascularization and tumors reach a mean diameter of 8.0 ± 2.5 mm by 7 days (Knighton *et al.*, 1977). When tumor grafts of increasing size (from 1 mm to 4 mm) are implanted on the 9-day CAM, grafts larger than 1 mm undergo necrosis and autolysis during the 72-h prevascular phase. They shrink rapidly until the onset of vascularization, when rapid growth resumes (Knighton *et al.*, 1977).

Ausprunk *et al.* (1977) compared the behavior of tumor grafts to grafts of normal adult and embryo tissues. In tumor tissue, preexisting blood vessels

Table 5.1 Angiogenic response induced by tumors implanted onto the chorioallantoic membrane (CAM)

Tumor	Authors
Adenocarcinoma of the endometrium	Palczak and Splawinski (1989)
B-cell non-Hodgkin's lymphoma	Ribatti *et al.* (1990)
Glioblastoma	Klagsbrun *et al.* (1976)
Head and neck squamous cell carcinoma	Petruzzelli *et al.* (1993)
Hepatocellular carcinoma	Marzullo *et al.* (1998)
Lipoma	Lucarelli *et al.* (1999)
Melanoma	Auerbach *et al.* (1976)
Meningioma	Klagsbrun *et al.* (1976)
Neuroblastoma	Ribatti *et al.* (2002)
Walker 256 carcinoma	Klagsbrun *et al.* (1976)

Table 5.2 Angiogenic response induced by tumor cells implanted onto the chorioallantoic membrane (CAM)

Tumor cells	Authors
B-16 melanoma cells	Takigawa *et al.* (1990)
Endothelial cells isolated from patients with multiple myeloma	Vacca *et al.* (2003)
Lymphoblastoid cells	Vacca *et al.* (1998)
Mammary tumor cells transfected with vascular endothelial growth factor	Ribatti *et al.* (2001b)
Neuroblastoma	Ribatti *et al.* (2002)
Plasma cells isolated from patients with multiple myeloma	Ribatti *et al.* (2003)
Walker carcinoma 256 cells	Klagsbrun *et al.* (1976)

in the tumor graft disintegrated within 24 h after implantation, and revascularization occurred by penetration of proliferating host vessels into the tumor tissue. By contrast, preexisting vessels did not disintegrate in the embryo graft and anastomosed to the host vessels with almost no neovascularization. In adult tissues, preexisting graft vessels disintegrated (although this process was slower than in tumor vessels) and did not stimulate capillary proliferation in the host. Lastly, tumor vessels did not reattach to those of the host.

Hagedorn *et al.* (2005) have developed a glioblastoma multiforme tumor progression model on the CAM. They demonstrated that avascular tumors formed within 2 days, than progressed through VEGFR-2-dependent angiogenesis, associated with hemorrhage, necrosis, and peritumoral edema. Blocking of VEGFR-2 and platelet-derived growth factor receptor (PDGFR) signaling pathways by using small-molecule receptor tyrosine kinase inhibitors abrogated tumor development. Moreover, gene regulation during the angiogenic switch was analyzed by oligonucleotide microarrays, permitting identification of regulated genes whose functions are associated mainly with tumor vascularization and growth.

3.1. Angiogenesis and antiangiogenesis in multiple myeloma

In patients with monoclonal gammopathy of undetermined significance (MGUS) and multiple myeloma (MM), angiogenesis correlates with plasma cell growth (S-phase fraction) (Vacca *et al.*, 1994). Moreover, angiogenesis is paralleled by an increased angiogenic ability of bone marrow plasma cell conditioned medium of patients with active MM as compared with those

with nonactive MM and MGUS, and partly dependent fibroblast growth factor-2 (FGF-2) production (Vacca *et al.*, 1999a).

Plasma cell conditioned media were tested to their ability to induce angiogenesis in the CAM (Vacca *et al.*, 1999a). The conditioned medium of 77% patients with active MM induced an angiogenic response; by contrast, only 33% and 20% of conditioned medium from patients with nonactive MM and MGUS, respectively, induced the response. Anti-FGF-2 antibody partly inhibited conditioned medium angiogenic response. In another work, we have attempted a fine characterization of the angiogenic response induced by plasma cells obtained from patients with active MM, as compared to those obtained from patients with nonactive MM and MGUS, respectively, in the CAM assay. To this purpose, we have investigated about the time course of the angiogenic response induced by gelatin sponges soaked with the cell suspensions and implanted on the CAM surface from day 8 to day 12 of incubation by evaluating the number of vessels, of the vessel bifurcation and the intervascular distance at 24, 48, 72, and 96 h, respectively, after the implants (Ribatti *et al.*, 2003). Results demonstrated that plasma cell suspensions obtained from patients with active MM induce a vasoproliferative response, significantly higher as compared to that induced by cell suspensions obtained from patients with nonactive MM and MGUS, respectively. These responses are a function of the day of implantation (Fig. 5.3). In fact, implants made from day 8 to day 10 are strongly angiogenic, while those made from day 11 to day 12 do not. This finding might depend on the fact that CAM endothelium exhibits an intrinsically high mitotic rate until day 10 (Ausprunk *et al.*, 1974). Thereafter, the endothelial mitotic index declines rapidly, and the vascular system attains

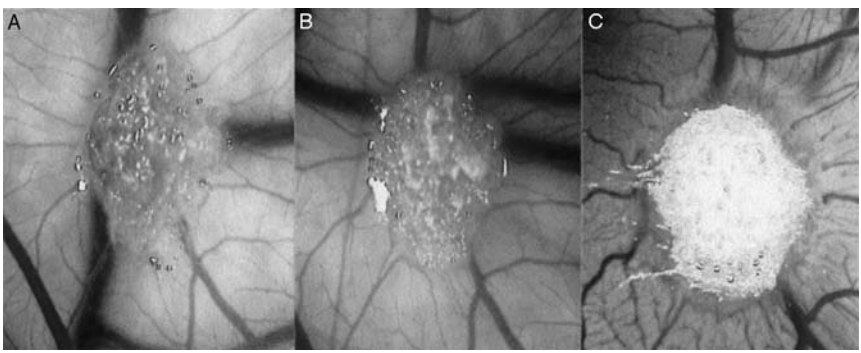

Figure 5.3 Time course of the macroscopic appearance of chorioallantoic membrane (CAM) implanted at day 8 (in A) loaded with 18,000 plasma cells of a patient with active multiple myeloma (MM). Note that, whereas on day 9 (in B) no vascular reaction is detectable, on day 12 (in C) numerous allantoic vessels develop radially toward the implant in a "spoked-wheel" pattern. Original magnification, ×50. Reproduced with permission from Ribatti *et al.* (2003).

its final arrangement on day 18, just before hatching (Ausprunk *et al.*, 1974). Consequently, cell suspensions implanted on the CAM of successively older embryos are not able to induce a vasoproliferative response in parallel with the reduced rates of growth of CAM's ECs.

More recently, we have isolated ECs from bone marrow of patients with MM (MMEC) (Vacca *et al.*, 2003). They show intrinsic angiogenic ability, because they rapidly form a capillary network *in vitro*, and extrinsic ability, because they generate numerous new vessels *in vivo* in the CAM assay (Vacca *et al.*, 2003). We have attempted a fine characterization of the angiogenic response induced by MMEC, as compared with MGUSEC in the CAM assay, by investigating the effects of MMEC and MGUSEC on the expression of endogenous levels in the CAM of VEGF, FGF-2, angiopoietin-1 (Ang-1), hypoxia-inducible factor-1α (HIF-1α), and endostatin by reverse transcriptase-polymerase chain reaction (RT-PCR) (Mangieri *et al.*, 2008). RT-PCR demonstrated that the expression of endostatin mRNA detected in MM-treated CAM was significantly lower respect to control CAM. These data suggest that angiogenic switch in MM may involve loss of an endogenous angiogenesis inhibitor, such as endostatin.

Recently, we have demonstrated that zoledronic acid exerted an antiangiogenic activity in MMEC mediated by abrogation of their VEGF/VEGF receptor-2 (VEGFR-2) autocrine loop and gene modulation of other angiogenic targets (Scavelli *et al.*, 2007). Moreover, in the CAM assay, zoledronic acid 10 μM and 30 μM was added to the MMEC-conditioned medium and a significant reduction in the angiogenic response was found. These data suggest that zoledronic acid has an antiangiogenic effect in MM which may be involved in an indirect antitumor activity.

3.2. Angiogenesis and antiangiogenesis in human neuroblastoma

Neuroblastoma is the most frequently occurring solid tumor in children. Several recent studies implicate angiogenesis in the regulation of neuroblastoma growth and inhibition of angiogenesis is a promising approach in the treatment of this tumor (Ribatti and Ponzoni, 2008).

In a paper published in 1998, we investigated two human neuroblastoma cell lines, LAN-5 and GI-LI-N, for their capacity to induce angiogenesis in the CAM assay (Ribatti *et al.*, 1998b) and demonstrated that conditioned medium from both cells lines, LAN-5 cells more than GI-LI-N ones, induced angiogenesis.

The role that the oncogene MYCN plays in the regulation of angiogenesis in neuroblastoma remains controversial. With the aim to better elucidate this matter, we tested fresh biopsy samples from patients with MYCN amplified and with MYCN nonamplified tumors for their angiogenic capacity by using the CAM assay (Ribatti *et al.*, 2002). Moreover,

conditioned medium obtained from five different human neuroblastoma cell lines MYCN amplified and nonamplified and bioptic fragments obtained from xenografts derived from four neuroblastoma cell lines injected in nude mice were assayed for their angiogenic potential. Results clearly demonstrated that MYCN amplification parallel angiogenesis in neuroblastoma. When fresh biopsy samples from patients, conditioned medium derived from neuroblastoma cells lines and bioptic fragments derived from xenografts of the same cell lines injected in nude mice were tested, the response was univocal: the angiogenic response was significantly higher in the MYCN-amplified specimens as compared to nonamplified ones (Ribatti *et al.*, 2002).

In 2001, we studied the effects of the synthetic retinoid fenretinide (HPR) *in vivo* by using the CAM assay (Ribatti *et al.*, 2001a). Results showed that HPR inhibited VEGF- and FGF-2-induced angiogenesis in the CAM assay. A significant antiangiogenic potential of HPR has been observed also in neuroblastoma biopsies-induced angiogenesis *in vivo* in the CAM assay. Finally, immunohistochemistry experiments performed in the CAM assay demonstrated that endothelial staining of both VEGFR-2 and FGF-2-receptor-2 (FGF-2-R-2) was reduced after implantation of HPR-loaded sponges, as compared to controls. These data suggest that HPR exerts its antiangiogenic activity through both a direct effect on EC proliferative activity and an inhibitory effect on the responsivity of the ECs to the proliferative stimuli mediated by angiogenic growth factors.

We have investigated the antiangiogenic activity of interferon gamma (IFN-γ) by using an experimental model in which IFN-γ gene transfer clampens the tumorigenic and angiogenic activity of ACN neuroblastoma cell line in immunodeficient mice (Ribatti *et al.*, 2006b). We demonstrated that ACN/IFN-γ xenografts had less *in vivo* angiogenic potential than the vector-transfected ACN/neo, when grafted onto the CAM (Fig. 5.4).

In another study, we evaluated the synergistic antiangiogenic effect of low dose of vinblastine and rapamycin in neuroblastoma (Marimpietri *et al.*, 2005, 2007). The angiogenic responses induced by neuroblastoma cell-derived conditioned medium, neuroblastoma tumor xenografts and human neuroblastoma biopsy specimens were inhibited in the CAM assay by each drug and more significantly by their combination. The observation that these well-known drugs displays synergistic effects as antiangiogenics when administered frequently at very low dose may be of significance in the designing of new ways of treating neuroblastoma.

Bortezomib is a selective and reversible inhibitor of the 26S proteasome that shows potent antitumor activity *in vitro* and *in vivo* against several human cancers of adulthood. No data are available on bortezomib activity against human neuroblastoma and we demonstrated that bortezomib inhibited angiogenesis in CAM stimulated by conditioned medium from

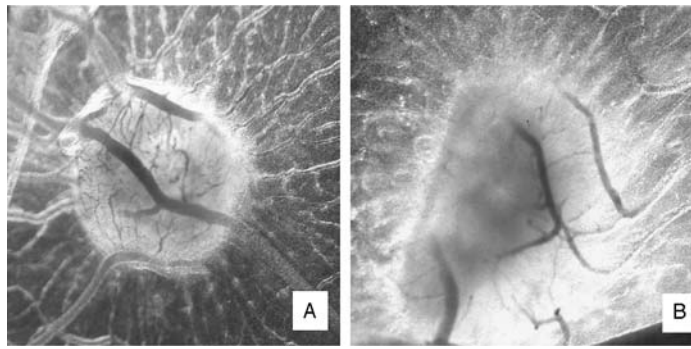

Figure 5.4 In (A), a 12-day-old chorioallantoic membrane (CAM) incubated on day 8 for 4 days with bioptic specimens of ACN/neo tumor xenograft, showing numerous blood vessels around the graft. In (B), a 12-day-old CAM incubated on day 8 for 4 days with bioptic specimen of (ACN/IFN-γ) tumor xenograft, showing few vessels around the graft. Original magnification, $\times$50. Reproduced with permission from Ribatti *et al.* (2006b).

neuroblastoma cell lines, by neuroblastoma xenografts, and by primary neuroblastoma biopsy specimens (Brignole *et al.*, 2006).

The therapeutic efficacy of cancer active-targeting using doxorubicin (DOX)-loaded immunoliposomes was evaluated with the CAM model (Pastorino *et al.*, 2006). The DOX-loaded liposomes were coupled either to monoclonal antibodies-targeting tumor cells (anti-GD2) or to NGR peptides that target tumor vessels. The antiangiogenic effects of these formulations were tested on xenografts derived from neuroblastoma cell lines grown on the CAM surface. When anti-GD2 or NGR liposomes were administered separately, 50–60% of vessel growth inhibition was achieved, whereas administering a combination of both types of liposomes increased vessel growth inhibition to 90%. The higher efficiency of the combined treatment was further validated in tumor-bearing mice.

3.3. Tumor metastasis

Other studies using the tumor cell/CAM model have focused on the invasion of the chorionic epithelium and the blood vessels by tumor cells (Armstrong *et al.*, 1982; Kim *et al.*, 1998; Scher *et al.*, 1976), that is, the metastatic potency of tumors (Dagg *et al.*, 1956). The cells invade the chorionic epithelium and the mesenchymal connective tissue below, where they find in the form of a dense bed of blood vessels that is the target for intravasation.

In the CAM, the vast majority of injected cells (generally $>$ 80%) survive in the microcirculation and have successfully extravasated by 1–3 days later. Most of the extravasated cancer cells migrate through the mesenchyme and

attach to arterioles, rather than venules or lymphatics and preferentially migrate to the vicinity of preexisting vessels (Koop *et al.*, 1994). Metastasis results from release of tumor cells from the intravasated tissue and their transport to distant organs, where the tumor cells arrest and extravasate. Tumor cells that have metastasized to distant site of the CAM are indicators of intravasation.

The advantages of the CAM model as an alternative experimental animal model of metastasis include (a) the chick embryo is naturally immunodeficient and can accept cancer cells regardless of their origin without specific or nonspecific immune response; (b) the changes in morphology of cancer cells arrested in the CAM microcirculation can be readily observed by *in vivo* microscopy (Chambers *et al.*, 1992); and (c) in contrast to standard mouse models, most cancer cells arrested in the CAM microcirculation survive without significant cell damage, and a large number of them complete extravasation (Chambers *et al.*, 1992).

3.4. Other applications

A variety of growth factors and normal cells have been reported to induce CAM angiogenesis (Tables 5.3 and 5.4). In studies of angiogenesis inhibitors (Table 5.5), on the contrary, there are two approaches which differ in the target vessels, that is, those which examine the response in the rapidly growing CAM and those that evaluate the inhibition of growth induced by an angiogenic cytokine, such as FGF-2.

The test substance is soaked in inert synthetic polymers laid upon the CAM: Elvax 40 (ethylene-vinyl acetate copolymer) and hydron (a poly-2-hydroxyethil-methacrylate polymer) are commonly used. The two polymers were first described and validated by Langer and Folkman (1976): both provided to be biologically inert when implanted onto the CAM and both were found to polymerize in the presence of the test substance, allowing its sustained release during the assay. However, hydron requires the test substance to be added to a solution of hydron and ethanol. When the test pellets are vacuum-dried, ethanol is removed leaving a solid pellet that contains the test substance. If the test material is not compatible with ethanol, Elvax can be used instead. Elvax is dissolved in methylene chloride before the test material is suspended/dissolved in the polymer, after which methylene chloride is removed by vacuum-drying. A more sustained release can be achieved by ''sandwiching'' the test substance between two Elvax layers. The polymers cause the substance to be released at constant rates (nanograms to micrograms) around-the-clock.

Methylcellulose discs are more widely used and are prepared usually as a final concentration of 1% solution of methylcellulose and then the agent of interest is added to the solution. The discs can be sterilized using UV light and subsequently they are placed onto the CAM surface. The release of the

Table 5.3 Stimulators of angiogenesis tested in the chorioallantoic membrane (CAM) assay

Substance	Authors
Adenosindiphosphate	Fraser *et al.* (1979)
Adenosine	Dusseau *et al.* (1986)
Amyloid beta	Boscolo *et al.* (2007)
Angiogenin	Fett *et al.* (1985)
C-C chemokine I-309	Bernardini *et al.* (2000)
C-C chemokine 11 (eotaxin)	Salcedo *et al.* (2002)
C-C chemokine CCL15	Hwang *et al.* (2004)
C-C chemokine CCL23	Hwang *et al.* (2005)
Copper	Mc Auslan *et al.* (1983)
C-X-CL1/macrophage inflammatory protein-2 (MIP-2)	Scapini *et al.* (2004)
DMR-Gremlin	Stabile *et al.* (2007)
Epidermal growth factor	Stewart *et al.* (1989)
Erythropoietin	Ribatti *et al.* (1999c)
Fibrin	Barnhill and Ryan (1983)
Fibrin degradation products	Thompson *et al.* (1985)
Fibroblast growth factor-2	Ribatti *et al.* (1995)
Heparin	Ribatti *et al.* (1987)
Histamine	Thompson and Brown (1987)
Hyaluronic acid (degradation products)	West *et al.* (1985)
Leptin	Ribatti *et al.* (2001c)
Lipoprotein-A	Ribatti *et al.* (1998c)
Monocyte chemoattractant protein-1 (MCP-1)	Hong *et al.* (2005)
Osteocalcin	Cantatore *et al.* (2005)
Osteogenic protein-1	Ramoshebi and Ripamonti (2000)
Osteopontin	Leali *et al.* (2003)
Placental growth factor-1	Ziche *et al.* (1997)
Platelet-derived growth factor	Wilting *et al.* (1992)
Phorbol esters	Morris *et al.* (1988)
Prostaglandin E2	Form and Auerbach (1983)
Transforming growth factor beta	Yang and Moses (1990)
Tumor necrosis factor alpha	Olivo *et al.* (1992)
Urotensin-II	Spinazzi *et al.* (2006)
Vascular endothelial growth factor	Wilting *et al.* (1993)

agent is slow and minimal reaction to control discs was reported. Agarose discs and Millipore discs soaked in the solution under investigation have been used.

Table 5.4 Angiogenic response induced by cells implanted onto the chorioallantoic membrane (CAM)

Cells	Authors
Basophils	De Paulis *et al.* (2006)
Chinese hamster ovary cells transfected with endothelin-1	Cruz *et al.* (2001)
Dendritic cells	Riboldi *et al.* (2005)
Endothelial cells transfected with fibroblast growth factor-2	Ribatti *et al.* (1997b)
Eosinophils	Puxeddu *et al.* (2005)
Lymphocytes	Ribatti *et al.* (1991)
Macrophages	Leibovich *et al.* (1987)
Mast cells	Ribatti *et al.* (2001d)
Neutrophils	Ardi *et al.* (2007)

Wilting *et al.* (1991, 1992) used cultured coverslide glasses (Thermanox) 4–5 mm on diameter, on which 5 μl of several angiogenic factors were placed. Glasses were turned over and placed onto the CAM on day 9 of incubation, and the angiogenic response was evaluated 96 h later. Alternatively, when testing a fluid substance, the latter is inoculated (20–50 μl) directly into the cavity of the allantoic vesicle so that its activity reaches the whole vascular area in a uniform manner (Gualandris *et al.*, 1996; Ribatti *et al.*, 1987). Another method has been proposed by Nguyen *et al.* (1994): a collagen gel is conjugated with the testing substance and placed between two pieces of mesh (bottom layer 4 × 4 mm, upper layer 2 × 2 mm). The resulting ''sandwich'' is then placed on the CAM on day 8 of incubation.

We have developed a new method for the quantitation of angiogenesis and antiangiogenesis in the CAM (Ribatti *et al.*, 2006a). Gelatin sponges treated with a stimulator or an inhibitor of blood vessel formation are implanted on growing CAM on day 8. Blood vessels, growing vertically into the sponge and at the boundary between sponge and surrounding mesenchyme, are counted morphometrically on day 12. The newly formed blood vessels grow perpendicularly to the plane of the CAM inside the sponge, which does not contain preexisting vessels.

The gelatin sponge is also suitable for the delivery of tumor cell suspensions, as well as of any other cell type, onto the CAM surface and the evaluation of their angiogenic potential (Ribatti *et al.*, 1997b, 1999a; Vacca *et al.*, 1999a). As compared with the application of large amounts of a recombinant angiogenic cytokine in a single bolus, the use of cell implants that overexpress angiogenic cytokines allows the continuous delivery of growth factors, which is produced by a limited number of cells (as low as

Table 5.5 Angiogenesis inhibitors tested in the chorioallantoic membrane (CAM) assay

Substances	Authors
Adiponectin	Brakenhielm *et al.* (2004)
Alpha(v)-beta 3/alpha(v)-beta 5 integrin antagonist	Belvisi *et al.* (2005)
Amiloride	Knoll *et al.* (1999)
Aminopeptidase-N antagonists	Bhagwat *et al.* (2001)
Angioinhibins	Ingber *et al.* (1990)
Angiostatin	O'Reilly *et al.* (1994)
Angiotensinogen	Brand *et al.* (2007)
Antibody anti-fibroblast growth factor-2	Ribatti *et al.* (1995)
Antibody anti-vascular endothelial growth factor	Vitaliti *et al.* (2000)
Aplidine	Taraboletti *et al.* (2004)
Ascorbic acid	Ashino *et al.* (2003)
Bleomycin	Oikawa *et al.* (1990a)
Beta cyclodextrintetradecasulfate (TDS)+ angiostatic steroids	Folkman *et al.* (1989)
Bortezomib	Roccaro *et al.* (2006)
Capsaicin	Min *et al.* (2004)
Cartilage	Eisenstein *et al.* (1975)
Chemically sulfated *Escherichia coli* K5 polysaccharide derivatives	Presta *et al.* (2005)
Chondrocyte-derived inhibitor	Eisenstein *et al.* (1975)
Cyclooxygenase inhibitor	Jung *et al.* (2007)
Cyclosporin	Iurlaro *et al.* (1998)
Eponeomycin	Oikawa *et al.* (1993a)
Fenretinide	Ribatti *et al.* (2001a)
Ghrelin	Conconi *et al.* (2004)
Heparanase	Sasisekharon *et al.* (1994)
Heparin or heparin fragments + cortisone	Folkman *et al.* (1983
Heparin + 11-hydrocortisone or 17-hydroxyprogesterone	Crum *et al.* (1985)
Heparin substitutes	Folkman *et al.* (1989)
Herbamycin	Oikawa *et al.* (1989a)
Inhibitors of basement membrane biosynthesis	Maragoudakis *et al.* (1988a)
Integrin alpha(v)beta3 antagonist	Friedlander *et al.* (1995)
Integrin alpha(v)beta5/alpha(v)beta3 antagonists	Kumar *et al.* (2001)
Interleukin-12	Airoldi *et al.* (2007)
Interleukin-27	Shimizu *et al.* (2006)
Low molecular weight undersulfated glycol-split heparin	Casu *et al.* (2004)

(*continued*)

Table 5.5 (*continued*)

Substances	Authors
Methylene blue	Zacharakis *et al.* (2006)
Methyltransferase inhibitors	Hellebrekers *et al.* (2006)
Myo-inositol trispyrophosphate	Sihn *et al.* (2007)
Neridronate	Ribatti *et al.* (2007)
NGR-SL-Doxorubicin	Pastorino *et al.* (2006)
Nitric oxide endogenous	Pipili-Synetos *et al.* (1995)
Opioid peptides	Dai *et al.* (2008)
Pentosan polysulfate	Rusnati *et al.* (2001)
Pentraxin PTX3	Rusnati *et al.* (2004)
Phenethyl isothiocyanate	Xiao and Singh (2007)
Phorbol esters	Morris *et al.* (1988)
Platelet factor 4	Maione *et al.* (1990)
Proline analogues	Ingber and Folkman (1988)
Protamine	Taylor and Folkman (1982)
Protein kinase C	Tsopanoglou, *et al.* (1993)
Purine analogues	Presta *et al.* (1999)
Radicicol	Oikawa *et al.* (1993b)
RDG-peptidomimetic	Urbinati *et al.* (2005)
Resveratrol	Mousa *et al.* (2005)
Retinoids	Oikawa *et al.* (1989b)
Ruthenium red-based compound (NAMI-A)	Vacca *et al.* (2002)
Somatostatin	Woltering *et al.* (1991)
Squalamine	Sills *et al.* (1998)
Staurosporine	Oikawa *et al.* (1992)
Suramin	Danesi *et al.* (1993)
Suramin + angiostatic steroids	Wilks *et al.* (1991)
TAU 1120	Nozaki *et al.* (1993)
Thymidine phosphorylase inhibitors	Liekens *et al.* (2004)
Vinblastine	Vacca *et al.* (1999b)
Vinblastine + rapamycin	Marimpietri *et al.* (2005)
Vitamin D3 analogues	Oikawa *et al.* (1990b)
Zoledronic acid	Scavelli *et al.* (2007)

10,000–20,000 cells per implant), thus mimicking more closely the initial stages of tumor angiogenesis and metastasis. Cells that overexpress FGF-2 and secrete ~2–3 pg of FGF-2 throughout the experimental period exert a proangiogenic response when applied onto the CAM that is similar to the one elicited by 1 μg of recombinant cytokine (Ribatti *et al.*, 2001b).

Many techniques can be applied within the constraints of paraffin and plastic embedding, including histochemistry and immunohistochemistry.

Electron microscopy can also be used in combination with light microscopy. Moreover, unfixed sponges can be utilized for chemical studies, such as the determination of DNA, protein, and collagen content, as well as for RT-PCR analysis of gene expression by infiltrating cells, including ECs.

An angiogenic response occurs 72–96 h after stimulation in the form of an increased vessel density around the implant, with the vessels radially converging toward the center-like spokes in a wheel (Ribatti *et al.*, 1995). Conversely, when an angiostatic compound is tested, the vessels become less dense around the implant after 72–96 h, and eventually disappear (Iurlaro *et al.*, 1998; Minischetti *et al.*, 2000; Ribatti *et al.*, 1995; Vacca *et al.*, 1999b). When the substance is inoculated into the cavity of allantoic vesicle, the angiogenic or antiangiogenic response affects the CAM vessels as a whole.

3.4.1. *In ovo* and *ex ovo* methods

Fertilized White Leghorn chicken eggs staged according to Hamburger and Hamilton (1951) are placed in an incubator as soon as embryogenesis starts and are kept under constant humidity at 37 °C. On day 3, a square window is opened in the shell after removal of 2–3 ml of albumen to detach the CAM from the shell itself and the underlying CAM vessels are disclosed (Fig. 5.5). The window is sealed with a glass and incubation goes on until the day of experiment. This technique may preserve a more physiological environment; however, it limits the area for use and observation.

The embryo and its extraembryonic membranes are transferred to a Petri dish on day 3 or day 4 of incubation and CAM develops at the top as a flat membrane and reaches the edge of the dish to provide a two-dimensional monolayer onto which multiple grafts can be placed (Auerbach *et al.*, 1974). Because the entire membrane can be seen, rather than just a small portion through the shell window, multiple grafts can be placed on each CAM and photographs can be taken to document vascular changes over time.

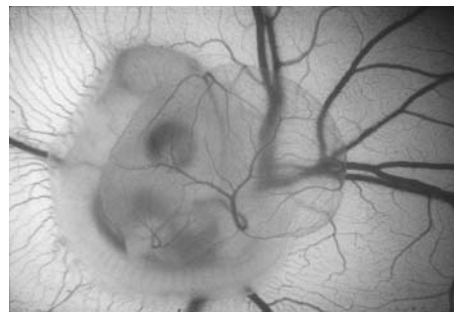

Figure 5.5 Allantoic sac of a 5-day embryo showing *in ovo* distribution pattern of allantoic vessels. Original magnification, ×25.

Subsequently, several modifications of this method have been described. Other types of containers used include plastic slings, plastic weigh boats, foam cups, and plastic dishes. Dugan and coworkers (1981) used an inert plastic container equipped with a ''parafilm'' ring (4–5 cm inside depth) to provide support for the embryo and its membranes. Advantages include somewhat longer viability and lower costs, though these are offset by the difficulty of monitoring angiogenesis during incubation and by the fact that one cannot obtain two-dimensional photographs suitable for image analysis.

Survival rate of eggs cultured *ex ovo* is the major success-limiting step in this technique. In the original description of embryos cultured in Petri dishes, there was a 50% loss in the first 3 days after cracking, with 80% of those which survive to day 7 continuing at least day 16 (Auerbach *et al.*, 1974). Subsequently, improved survival rates were reported by the same laboratory, with 87% of the embryos surviving removing of the shell, and 68% alive on day 4 (Crum *et al.*, 1985). *Ex ovo* method may be preferred to the *in vivo* method because (a) it allows the quantification of the response over a wider area of the CAM; (b) large number of samples can be tested at any one time; (c) the time required for a response to occur is shorter (2–3 days).A variant of the *ex ovo* method is based on the vertical growth of new vessels into a collagen gel containing the test sample sandwiched between two parallel nylon meshes. New vessels grow vertically into the gel and the nylon meshes align the capillaries for rapid counting (Nguyen *et al.*, 1994).

3.4.2. Methods of quantifying the angiogenic response

Several methods of quantifying the CAM angiogenic response have been developed. Quantitation of angiogenesis was initially done by scoring the extent of vascularization on a graded scale of 0–4. Serial dilution assays were developed to score the number of positives at any particular dilution using four eggs per assay point. With dilution of the test sample and reduction in its concentration, the number of positives gradually decreases until an end point (0/4) is reached (Folkman, 1974).

Another method considers changes in the distribution and density of CAM vessels next to the implant which are evaluated *in vivo* by means of a stereomicroscope at regular intervals following the graft procedure. The score is 0 when no changes can be seen; it is +1 when few neovessels converge toward the implant, and +2 when a considerable change in the number and distribution of the converging neovessels is observed (Knighton *et al.*, 1977).

The vasoproliferative response may be graded as a vascular index derived from photographic reconstructions. All converging neovessels contained inside a 1 mm-diameter ring superimposed on the CAM are counted: the ring is drawn around the implant in such a way that it forms an angle of less than 45° with respect to a straight line drawn from the implant's

center. Vessels branching dichotomically outside the ring are counted as 2, while those branching inside the ring are counted as 1 (Dusseau *et al.*, 1986).

Folkman and Cotran (1976) measured the degree of vasoproliferative response, as evaluated under the stereomicroscope, by an arbitrary 0–5 scale. Zero describes a condition of the vascular network that shows no change from the time of grafting; +1 marks a slight increase in the vessel density associated with occasional changes in the course of vessels converging toward the implant; +2, +3, +4, and +5, respectively, indicate a progressive increase in vessel density associated with more pronounced changes in their course, while a +5 score also highlights strong hyperemia. A coefficient describing the degree of angiogenesis can also be derived from the ratio of the calculated value to the highest attainable value. Therefore, the lowest coefficient is 0 and the highest is 1.

Strick *et al.* (1991) calculated the length of the vessels and expressed it in terms of index density, that is, the vessel density relative to a fractional image area of the vasculature. Nguyen *et al.* (1994) expressed the vasoproliferative response after 72–216 h as a percentage of the squares in the upper mesh occupied by neovessels. The effect of the inhibitory substances (placed on the bottom mesh) is quantified by calculating the inhibition of the vasoproliferative response induced by an angiogenic factor.

Use of a numerical grading scale allows calculation of a coefficient of angiogenesis (Vu *et al.*, 1985). Semiautomated image analysis techniques have also been developed (Voss *et al.*, 1984). Also, fractal analysis has been used for evaluating the changes of CAM vasculature (Kirchner *et al.*, 1996). The alterations in the branching pattern measured by fractal dimension and vessel density by grid intersection were evaluated to define the response to FGF-2 and to angiostatin (Parson-Wingerter *et al.*, 1998).

Quantitative evaluation of vessel density can be obtained by applying morphometric and planimetric methods to histologic observations of CAM specimens fixed at regular intervals after implantation. The number of vessels is evaluated as the total number of vessels present in six randomly chosen microscopic fields. Vessel density is evaluated by a planimetric method (Elias and Hyde, 1983), which utilizes a square reticule placed in the eyepiece of a photomicroscope. Six randomly chosen fields per section are observed and the total number of intersection points occupied by transversally sectioned vessels is counted. Vessel density equals this total number, expressed as a percent value of all intersection points. Evaluation of the number and the density of vessels should be made by two independent observers and processed statistically.

The uptake of ^{3}H thymidine into the whole CAM was evaluated using both autoradiography and scintillation counting and the rate of uptake was shown to be directly proportional to the concentration applied to the surface (Thompson *et al.*, 1985). Angiogenesis was related to the total hemoglobin content which was proportional to the rate of ^{3}H thymidine uptake.

3.5. Limitations of the chorioallantoic membrane assay

The main limitation of CAM assays is the nonspecific inflammatory reactions that may develop as a result of grafting, and induce a secondary vasoproliferative response, so quantification of the primary response is difficult (Jakob *et al.*, 1978; Spanel-Burowski *et al.*, 1988). Inflammatory angiogenesis in which infiltrating macrophages or other leukocytes are the source of angiogenic factors cannot be distinguished from direct angiogenic activity of the test material without a detailed histological study of multiple positive and negative controls. Investigation of histological CAM sections would help to detect the presence of a perivascular inflammatory infiltrate, together with a hyperplastic reaction, if any, of the chorionic epithelium. In an extensive series of experiments by Jakob *et al.* (1978), a variety of carrier vehicle alone (Millipore filters, fiber glass discs, discs of filter paper, agarose, and polyacrylamide gels), as well as natural egg components (eggshell membrane, coagulated albumin, and coagulated yolk) produced a number of inflammatory reactions. Cortisone or angiostatic steroids have been included in the experimental protocol to prevent nonspecific inflammatory reactions.

However, a nonspecific inflammatory response is much less likely when the test material is grafted as soon as the CAM begins to develop while the host's immune system is relatively immature (Leene *et al.*, 1973). There are two more drawbacks to the CAM assay: first, the test material is placed on existing vessels, and newly formed blood vessels grow within the CAM mesenchyme. Real neovascularization can hardly be distinguished from a falsely increased vascular density due to rearrangement of existing vessels that follows contraction of the membrane (Knighton *et al.*, 1991). In the rabbit of murine cornea assay, the presence of blood vessels that penetrate from the limbus into the avascular stroma of the cornea can be unambiguosly interpreted as an index of angiogenic response.

Second, timing of the CAM angiogenic response is essential. Many studies determine angiogenesis after 24 h, when there is no angiogenesis, but only vasodilation. Measurements of vessel density are really measurements of visible vessel density, and vasodilation and neovascularization are not readily distinguishable. This drawback can be overcome by using sequential photography to document new vessel formation.

Saline solutions should be avoided, in that hyperosmotic effect of crystal salts may damage the chorion epithelium and induce fibroblast proliferation (Wilting *et al.* 1991). This implies that the substance should be used at concentrations of picograms to milligrams: higher concentrations would indeed cause the hyperosmotic effect (Wilting *et al.*, 1992). The CAM is also extremely sensitive to modification by environmental factors, such as changes in oxygen tension, which make the sealing of the opening in the shell critical, pH, osmolarity, and the amount of keratinization (Auerbach *et al.*, 2000).

4. Role of FGF-2 in Chorioallantoic Membrane Vascularization

To evaluate the presence of a FGF-2-like molecule in CAM and in chorioallatoic fluid (CAF), different amounts of CAM extracts and CAF samples obtained from embryos at days 8, 10, 14, and 18, respectively, of incubation were assayed for their ability to stimulate plasminogen activator production in GM 7373 ECs. Both CAM and CAF samples induce an increase in GM 7373 cell-associated plasminogen activator activity in a dose-dependent manner (Ribatti *et al.*, 1995). The potency of the different samples in stimulating plasminogen activator production in GM7373 ECs differs as a function of the age of the embryo, suggesting that the amounts of plasminogen activator-inducing activity present in CAM and CAF may vary during embryonic development (Ribatti *et al.*, 1995). To confirm the presence of FGF-2 in CAM and CAF, samples were assayed for their ability to interact with heparin and to cross-react with neutralizing polyclonal antihuman FGF-2 antibody. In a first experiment, CAM extracts obtained from a 14-day embryo were run through a heparin–Sepharose column or were incubated with neutralizing polyclonal antihuman FGF-2 antibody or with nonimmune rabbit serum. Then the plasminogen activator-inducing activity of these samples was evaluated on GM 7373 ECs. The plasminogen activator-inducing activity of CAM extract is retained by the heparin–Sepharose column and it is specifically neutralized by an anti-FGF-2 antibody, while nonimmune rabbit serum was uneffective, thus identifying this activity as a FGF-2-like activity (Ribatti *et al.*, 1995). In another set of experiments, an aliquot of CAF was obtained from different embryos and loaded onto a heparin–Sepharose column. Fractions were collected and assayed for their ability to stimulate plasminogen activator production in GM 7373 ECs. Most of the plasminogen activator-inducing activity present in CAF binds to the resin and is eluted with the 2 M NaCl wash. Moreover, preincubation of this fraction with neutralizing anti-FGF-2 antibody completely abolish its plasminogen activator-inducing activity (Ribatti *et al.*, 1995). Aliquots of CAM and CAF obtained from a 14-day embryo were partially purified on heparin–Sepharose columns and probed in a Western blot with the affinity-purified antihuman FGF-2 antibody, recognizing a heparin-binding Mr 16,000 protein in both samples (Ribatti *et al.*, 1995). We have also quantified the temporal changes of FGF-2 in CAM and CAF during embryonic development, evaluating the amount of total plasminogen activator-inducing activity present in the crude CAM extracts and CAF samples obtained from chick embryos between day 6 and day 18 of incubation. The levels of FGF-2 in CAM and CAF vary significantly during embryonic development, maximal concentrations being observed between

day 10 and day 14 of incubation, when the vascular density of the CAM also reaches its maximum. The absolute concentrations of FGF-2 appear to be much higher in CAM than in CAF (Ribatti *et al.*, 1995).

In a series of experiments performed *in vivo* FGF-2 or anti-FGF-2 antibody were adsorbed on methylcellulose discs and applied on the top of the CAM of embryos at day 8 of incubation. Application of FGF-2 led to a positive angiogenic response in 85% of the animals, consisting of a spoke-wheel vascular pattern around the implant (Ribatti *et al.*, 1995). Under light microscopy, blood vessels, predominantly capillaries, with a narrow lumen, were distributed in the upper portion of the CAM and their number was increased, while the intermediate mesenchyme contained numerous fibroblasts (Ribatti *et al.*, 1995). In keeping with the capacity to exert a mitogenic activity for a variety of cell types of mesodermal and neuroectodermal origin, FGF-2 induces also fibroblast cell proliferation and hyperplasia of the chorionic epithelium. At ultastructural level, small vascular tubes with a very narrow lumen, located beneath the chorion, were recognizable. Application of anti-FGF-2 antibody on the surface of the CAM resulted in a significant antiangiogenic effect in 75% of the embryos (Ribatti *et al.*, 1995). An avascular zone free of vessels could be evidenced beneath the implant after intravascular injection of India ink. Microscopically, few blood vessels were still recognizable beneath the implant. Also, no blood vessels were detectable in the intermediate mesenchyme where fibroblasts were less numerous than in control embryos. Quantitation of the angiogenic response performed at day 12 of incubation by using a morphometric method confirmed the morphological observations. When FGF-2 was applied on the surface of the CAM, the microvessel density was 3.3 times higher than in control embryos. Conversely, application of anti-FGF-2 antibody resulted in 3 times reduction in the microvessel density (Ribatti *et al.*, 1995).

These findings indicate that endogenous FGF-2 is intrinsically involved in CAM vascularization on the basis of the evidence that FGF-2 is present in elevated amounts in the CAM from day 6 to day 18 of incubation, maximal concentrations being observed between day 10 and day 14. Apparently, this observation does not fully agree with the time course of the vasoproliferative processes taking place in the CAM. Ausprunk *et al.* (1974) have shown that CAM ECs have a labeling index of ~23% before day 11 of incubation; this index decreases to 2.8% thereafter. Nevertheless, in agreement with the kinetics of expression of CAM FGF-2, vascular density of the membrane continues to increase until days 12–14, when it reaches a plateau (Maragoudakis *et al.*, 1988b). This apparent discrepancy can be explained by considering that vascular sprouting may occur through migration and redistribution of existing ECs, in the absence of cell proliferation (Sholley *et al.*, 1984). Interestingly, FGF-2 can induce capillary EC *in vitro* to invade a three-dimensional collagen matrix and to form capillary-like tubules,

without cell proliferation, but dependent on cell movement and protease production (Montesano *et al.*, 1986). Thus, it is possible to hypothesize that endogenous chick FGF-2 may play a rate-limiting role in CAM vascularization by affecting not only the proliferation of ECs but also their migration, redistribution, and invasive behavior.

Our *in situ* hybridization data strongly suggest that the action of FGF-2 during this process occurs in two steps: at early stages of development the major source of FGF-2 is chorionic epithelial cells. Even though FGF-2 is devoid of a signal sequence for secretion (Abraham *et al.*, 1986), an alternative mechanism of exocytosis of FGF-2 has been proposed (Mignatti *et al.*, 1991, 1992).

Limited amounts of FGF-2 can be released from cellular sites of synthesis and then sequestered in the extracellular matrix. Dissociation of extracellular FGF-2 from the matrix and binding to surface receptors follows (Moscatelli, 1992) and triggers a paracrine loop of stimulation. Thus, FGF-2 released by chorionic epithelial cells may induce an angiogenic response in undifferentiated vessels in the CAM mesoderm by stimulating EC proliferation, movement, and protease production (Montesano *et al.*, 1986). At later stages, FGF-2 mRNA expression predominates in ECs forming the capillary plexus, suggesting that FGF-2 plays an autocrine role in further development of the endothelium.

When mouse aortic ECs stably transfected with a retroviral expression vector harboring a human FGF-2 cDNA were injected twice into the allantoic sac of the chick embryo at days 8 and 9, significant modifications of the developing vasculature of the CAM were observed: blood vessels with an irregular course and frequently branching were present 4 days later. In contrast, blood vessels run straight and interdigitate regularly in the CAM of embryos injected with parental cells or vehicle (Gualandris *et al.*, 1996). Intravenous injection of India ink revealed the presence of ink-filled enlarged hemangioma-like scattered within the blood vessel network of transfected cell-treated CAM (Gualandris *et al.*, 1996; Ribatti *et al.*, 1999a). These lesions are characterized by enlarged blood-filled sacs lined by a thin EC monolayer. Careful examination of serial sections showed no sign of thrombotic and/or hemorrhagic lesions. India ink was evident within the ECs-lined enlarged cavernae and the surrounding small blood vessels, but was undetectable in the stroma. Transfected ECs treated for 3 h with mitomycin before injection into the allantoic sac were still able to induce a vasoproliferative response and the formation of hemangiomas (Ribatti *et al.*, 1999a). In contrast, fixation of the cells with glutaraldehyde completely abolished their angiogenic and hemangioma-inducing activity. These data indicate that the injection of live, nonproliferating FGF-2-transfected ECs is sufficient to induce the observed modification of the CAM vasculature that are therefore due to alterations of the behavior of the ECs at the host. When transfected ECs were injected twice into the

allantoic sac together with neutralizing anti-FGF-2 polyclonal antibody, this latter had no effects on the modification of CAM vasculature induced by transfected ECs (Ribatti *et al.*, 1999a).These data suggest that the angiogenic and hemangioma-inducing activity exerted by the transfected ECs injected into the allantoic sac may not depend on the release of FGF-2 into the allantoic fluid.

To evaluate whether the angiogenic activity of transfected ECs is due to diffusible factor(s), we assessed the activity of serum-free transfected cell conditioned medium. The concentrated conditioned medium was adsorbed into a gelatin sponge and applied on the top of the CAM. Live transfected ECs were delivered onto the CAM under the same experimental condition as positive controls (Ribatti *et al.*, 1999a). After 4 days, macroscopic observation of the CAM showed that the sponges treated with transfected ECs or with their concentrated conditioned medium were surrounded by numerous allantoic vessels which developed radially toward the implant in a ''spoked wheel'' pattern. Scattered hemangiomas were recognizable in close proximity to the sponge (Fig. 5.6). Also in this condition, the angiogenic activity of transfected ECs was not affected when cells were applied onto the CAM together with neutralizing anti-FGF-2 antibody. The data further indicate that the transfected ECs release an angiogenic activity distinct from FGF-2.

The CAM may represent an *in vivo* system to assess the hypothesis that exogenous urokinase plasminogen activator may affect neovascularization via an endogenous FGF-2-dependent mechanism of action. Suspensions of urokinase plasminogen activator overexpressing ECs or parental ECs were delivered on the top of day 8 CAM by using a gelatin sponge implant (Ribatti *et al.*, 1999b). Macroscopic observation of the CAM at day 12 showed that the gelatin sponges adsorbed with urokinase plasminogen activator-transfected ECs were surrounded by allantoic vessels that

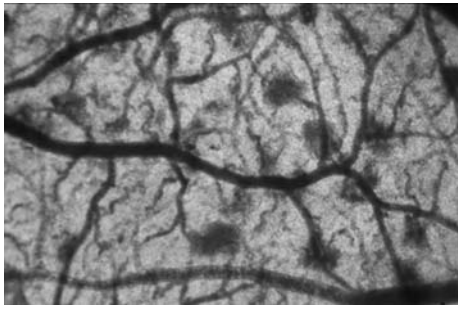

Figure 5.6 **Alterations of the chorioallantoic membrane (CAM) vasculature after implantation of a gelatin sponge adsorbed with fibroblast growth factor-2 (FGF-2)-transfected endothelial cells-conditioned medium. The CAM vasculature was visualized after 4 days by intravenous injection of India ink. Note numerous hemangiomas intermingled between allantoic vessels. Original magnification, ×200.**

developed radially toward the implant in a ''spoked-wheel'' pattern. The allantoic vessels were less numerous in the specimens treated with parental ECs, whereas no vascular reaction was detectable around the sponges treated with vehicle only (Ribatti *et al.*, 1999b). At the microscopic level, a highly vascularized tissue was recognizable among the trabeculae of urokinase plasminogen activator overexpressing ECs-treated sponges. The tissue consisted of newly formed blood vessels growing perpendicularly to the plane of the CAM and of infiltrating fibroblasts within an abundant network of collagen fibers. The vessels were less numerous in the parental ECs-treated sponges and were absent among trabeculae of implants treated with vehicle (Ribatti *et al.*, 1999b). A higher microvessel density was detectable within the sponges treated with urokinase plasminogen activator-transfected ECs that in those treated with parental ECs or vehicle, when the angiogenic response was quantified by a morphometric method (Ribatti *et al.*, 1999b). To assess whether the stronger angiogenic response elicited by urokinase plasminogen activator-overexpressing ECs was due to an increased mobilization of endogenous FGF-2, these cells were added to the CAM in the presence of anti-FGF-2 antibody. Anti-FGF-2 antibody reduced the angiogenic response elicited by urokinase plasminogen activator-overexpressing ECs to value similar to those measured in control ECs-treated CAM (Ribatti *et al.*, 1999b). It is interesting to note that urokinase plasminogen activator-overexpressing ECs added with anti-FGF-2 antibody retain a limited angiogenic activity that is more potent than that exerted by parental (Neo 2) cells tested under the same experimental conditions. This suggests that released urokinase plasminogen activator may induce the mobilization of endogenous angiogenic factor other than FGF-2 and/or that urokinase plasminogen activator may *per se* elicit a limited angiogenic response.

To confirm this hypothesis, the angiogenic activity of purified human urokinase plasminogen activator was evaluated and it exerted a dose-dependent angiogenic response in the CAM (Ribatti *et al.*, 1999b). Furthermore, we compared the angiogenic activity of enzymatically active and inactive human urokinase plasminogen activator. For this purpose, purified human urokinase plasminogen activator was preincubated with the serine protease inhibitor phenylmethylsulsonyl fluoride (PMSF), an irreversible urokinase plasminogen activator inhibitor, or vehicle. After incubation, urokinase plasminogen activator samples were dialyzed extensively to remove free PMSF and their angiogenic activity was evaluated in the CAM. Preincubation of urokinase plasminogen activator with 1-mM PMSF significantly inhibits the angiogenic activity of the enzyme. Moreover, the angiogenic activity was reduced significantly by anti-FGF-2 antibody (Ribatti *et al.*, 1999b). These data indicate that purified urokinase plasminogen activator exerts an FGF-2-dependent angiogenic activity in the CAM and that this effect depends, at least in part, on a catalytic activity of the enzyme.

To further substantiate this hypothesis, we compared the angiogenic activity of purified human urokinase plasminogen activator to that exerted by human ATF, lacking enzymatic activity. Human ATF was ineffective when assayed for its angiogenic capacity in the CAM. The inability of ATF to induce angiogenesis in the CAM indicates that the proteolytic activity of urokinase plasminogen activator is of pivotal importance in mediating its angiogenic capacity *in vivo* (Ribatti *et al.*, 1999b).

By utilizing the CAM assay, we have shown that anti-FGF-2 antibody reduces significantly the angiogenic activity exerted by urokinase plasminogen activator-overexpressing cells and purified human urokinase plasminogen activator, thus implicating extracellular endogenous FGF-2 in the growth of newly formed blood vessels stimulated by urokinase plasminogen activator. However, the incapacity of anti-FGF-2 antibody to fully suppress the angiogenic ability of purified urokinase plasminogen activator and urokinase plasminogen activator-overexpressing ECs suggests that more factors besides FGF-2 might be implicated in protease-triggered CAM neovascularization.

It is interesting to note that both urokinase plasminogen activator-overexpressing ECs and purified human urokinase plasminogen activator exert an angiogenic response in the CAM that is less potent than that exerted by exogenous FGF-2, suggesting that the levels of endogenous angiogenic growth factors available to the protease action may represent a limiting factor in this experimental system. In conclusion, our findings demonstrate that urokinase plasminogen activator-overexpressing ECs and purified urokinase plasminogen activator exert a potent angiogenic effect on the CAM which depends on the catalytic activity of the enzyme and is reversed by neutralizing anti-FGF-2 antibody.

We have compared the angiogenic activity of FGF-2- or VEGF-transfected cells adsorbed onto gelatin sponges and applied on top of the CAM (Ribatti *et al.*, 2001b). Both cell lines induced a comparable vasoproliferative response, as demonstrated by the appearance of similar number of blood vessels within the sponge (Fig. 5.7). Electron microscopy demonstrated that VEGF-overexpressing cells modified the phenotype of the endothelium of the CAM blood capillaries. In fact, the endothelium lining 30% of these vessels showed segmental attenuations was frequently interrupted and became fenestrated, mimicking what is observed in tumor vasculature (Ribatti *et al.*, 2001b).

5. Concluding Remarks

In vivo angiogenesis assays have resulted in important progress in elucidating the mechanisms of action of several angiogenic factors and inhibitors. It is reasonable to reserve the term ''angiogenic factor'' for substances that

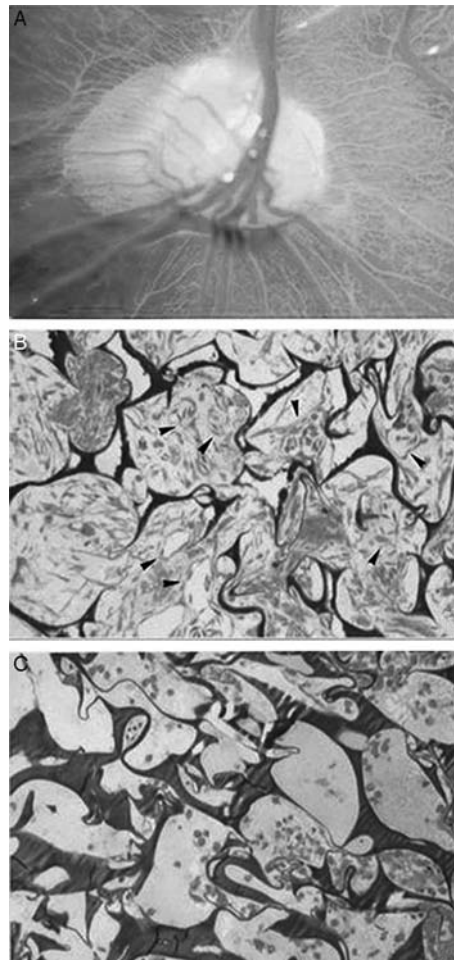

Figure 5.7 Effect of vascular endothelial growth factor (VEGF)-transfected cell on chorioallantoic membrane (CAM) neovascularization. In (A), macroscopic observation of the CAM, on day 12, showing the gelatin sponge surrounded by allantoic vessels that develop radially toward the implant in a "spoked-wheel" pattern. In (B), histologic analysis of the CAM grafted with VEGF-transfected cells. A highly vascularized tissue is recognizable among the sponge trabeculae, consisting of newly formed blood vessels (arrowheads). The vessels are absent in the sponges treated with the medium alone (in C). Original magnification, A, ×50; B, C, ×400. Reproduced with permission from Ribatti *et al.* (2001b).

produce new capillary growth in an *in vivo* assay.One of the most important technical problems faced by us in the study of angiogenesis and antiangiogenesis is the difficulty of obtaining meaningful assessment of efficacy. *In vivo* angiogenesis assays, such as those performed in the chick CAM, have resulted in important progress in elucidating the mechanisms of action of several

Table 5.6 Advantages and limitations of the *in ovo* and *ex ovo* methods

In ovo
Advantages
– The source of calcium for building skeletal elements is kept
– Normal development of the embryo
– High embryo survival rate
– Easy methodology
– Sterility is not required
– Embryos can reach hatching
Limitations
– Small surface is exposed
– Difficult monitoring
– Risk of angiogenesis induced by eggshell pieces
Ex ovo
Advantages
– Large CAM area available for testing
– Direct visualization of the entire CAM
– Evaluation of several samples in one single embryo
– Easy grafting and monitoring of excised tissues
– No eggshell failing on CAM
– Easy access to CAM vasculature
– Possibility of transillumination
Limitations
– Difficult methodology
– Low embryo survival rate
– Do not reflect physiological conditions
– Embryo cannot reach hatching

angiogenic factors and inhibitors. The main advantages of the *in vivo* assays are their low cost, simplicity, reproducibility, and reliability (Table 5.6). On the contrary, there are only very few restrictions to use CAM (Table 5.6), essentially due to (a) nonspecific inflammatory reactions that may develop with an attending secondary stimulation of angiogenesis and, (b) preexisting vessels may be present, which make it hard to distinguish the extent of angiogenesis and antiangiogenesis. In view of these limitations, two different assays should ideally be performed in parallel to confirm the angiogenic or antiangiogenic activity of test substances.

ACKNOWLEDGMENTS

This work was supported by grants from Associazione Italiana per la Ricerca sul Cancro (Local Funds) Milan; Ministero dell'Università e della Ricerca Scientifica (PRIN 2005 and FIRB 2001), Rome, Italy.

REFERENCES

Abraham, J. A., Mergia, A., Whang, J. L., Tumolo, A., Friedman, J., Hjerrild, J., Gospodarowicz, D., and Fiddes, J. (1986). Nucleotide sequence of a bovine clone encoding the angiogenic protein basic fibroblast growth factor. *Science* **233,** 545–548.

Airoldi, I., Di Carlo, E., Cocco, C., Taverniti, G., D'Antuono, T., Ognio, E., Watanabe, M., Ribatti, D., and Pistoia, V. (2007). Endogenous IL-12 triggers an anti-angiogenic program in melanoma cells. *Proc. Natl. Acad. Sci. USA* **104,** 3996–4001.

Andrade, S. P., Fan, T. P. D., and Lewis, G. P. (1987). Quantitative *in vivo* studies on angiogenesis in a rat sponge model. *Br. J. Exp. Pathol.* **68,** 755–766.

Ardi, V. C., Kupriyanova, T. A., Deryugina, E. I., and Quigley, J. P. (2007). Human neutrophils uniquely release TIMP-free MMP-9 to provide a potents catalytic stimulator of angiogenesis. *Proc. Natl. Acad. Sci. USA* **104,** 20262–20267.

Armstrong, P. B., Quigley, J. P., and Sidebottom, E. (1982). Transepithelial invasion and intramesenchymal infiltration of the chick embryo chorioallantois by tumor cell lines. *Cancer Res.* **42,** 1826–1837.

Ashino, H., Shimamura, M., Nakajima, H., Donbou, M., Kawanaka, S., Oikawa, T., Iwaguchi, T., and Kawashima, S. (2003). Novel function of ascorbic acid as angiostatic factor. *Angiogenesis* **6,** 259–269.

Auerbach, R., Kubai, L., Knighton, D., and Folkman, J. (1974). A simple procedure for the long-term cultivation of chicken embryos. *Dev. Biol.* **41,** 391–394.

Auerbach, R., Kubai, L., and Sidky, Y. (1976). Angiogenesis induction by tumors, embryonic tissues, and lymphocytes. *Cancer Res.* **36,** 3435–3440.

Auerbach, R., Auerbach, W., and Polakowski, I. (1991). Assays for angiogenesis: A review. *Pharmacol. Ther.* **51,** 1–11.

Auerbach, R., Akhtar, N., Lewis, R. L., and Shinners, B. L. (2000). Angiogenesis assays: Problems and pittfals. *Cancer Met. Rev.* **19,** 167–172.

Ausprunk, D. H. (1986). Distribution of hyaluronic acid and sulfated glycosaminoglycans during blood vessel development in the chick chorioallantoic membrane. *Am. J. Anat.* **177,** 313–331.

Ausprunk, D. H., Knighton, D. R., and Folkman, J. (1974). Differentiation of the vascular endothelium in the chick chorioallantois: A structural and autoradiographic study. *Dev. Biol.* **38,** 237–247.

Ausprunk, D. H., Knighton, D., and Folkman, J. (1977). Vascularization of normal and neoplastic tissues grafted to the chick chorioallantois. *Am. J. Pathol.* **79,** 597–618.

Barnhill, R. L., and Ryan, T. J. (1983). Biochemical modulation of angiogenesis in the chorioallantoic membrane of the chick embryo. *J. Invest. Dermatol.* **81,** 485–488.

Belvisi, L., Riccioni, T., Marcellini, M., Vesci, L., Chiarucci, I., Efrati, D., Potenza, D., Scolastico, C., Manzoni, L., Lombardo, K., Stasi, M. A., Orlandi, A., *et al.* (2005). Biological and molecular properties of a new alpha(v)beta3/alpha(v)beta5 integrin antagonist. *Mol. Cancer Ther.* **4,** 1670–1680.

Bernardini, G., Spinetti, G., Ribatti, D., Camarda, G., Morbidelli, L., Ziche, M., Santoni, A., Capogrossi, M. C., and Napolitano, M. (2000). I-309 binds to and activates endothelial cell functions and acts as an angiogenic molecule *in vivo*. *Blood* **96,** 4039–4045.

Bhagwat, S. V., Ladhdenranta, J., Giordano, R., Arap, W., Pasqualini, R., and Shapiro, L. H. (2001). CD13/APN is activated by angiogenic signals and is essential for capillary tube formation. *Blood* **97,** 652–659.

Bobek, V., Plachy, J., Pinterova, D., Kolostova, K., Boubelik, M., Jiang, P., Yang, M., and Hoffman, R. M. (2004). Development of a green fluorescent protein metastatic-cancer chick-embryo drug-screen model. *Clin. Exp. Metastasis* **21,** 347–352.

Boscolo, E., Folin, M., Grandi, G., Mangieri, D., Longo, V., Scienza, R., Zampieri, P., Conconi, M. T., Parnigotto, P. P., and Ribatti, D. (2007). Beta amyloid angiogenic activity *in vitro* and *in vivo*. *Int. J. Mol. Med.* **19,** 581–587.

Brakenhielm, E., Veitonmaki, N., Cao, R., Kihara, S., Matsuzawa, Y., Zhivotovsky, B., Funahashi, T., and Cao, Y. (2004). Adiponectin-induced antiangiogenesis and antitumor activity involve caspase-mediated endothelial cell apotosis. *Proc. Natl. Acad. Sci. USA* **101,** 2476–2481.

Brand, M., Lamandé, N., Larger, E., Corvol, P., and Gasc, J. M. (2007). Angiotensinogen impairs angiogenesis in the chick chorioallantoic membrane. *J. Mol. Med.* **85,** 451–460.

Brignole, C., Marimpietri, D., Pastorino, F., Nico, B., Di Paolo, D., Cioni, M., Piccardi, F., Cilli, M., Pezzolo, A., Corrias, M. V., Pistoia, V., Ribatti, D., *et al.* (2006). Effect of bortezomib on human neuroblastoma cell growth, apoptosis, and angiogenesis. *J. Natl. Cancer Inst.* **98,** 1142–1157.

Burri, P. H., and Tarek, M. R. (1990). A novel mechanism of capillary growth in the rat pulmonary microcirculation. *Anat. Rec.* **228,** 35–45.

Burton, G. J., and Palmer, M. E. (1989). The chorioallantoic capillary plexus of the chicken egg: A microvascular corrosion casting study. *Scanning Microsc.* **3,** 549–558.

Caduff, J. H., Fischer, L. C., and Burri, P. H. (1986). Scanning electron microscopic study of the developing microvasculature in the postnatal rat lung. *Anat. Rec.* **216,** 154–164.

Cantatore, F. P., Crivellato, E., Nico, B., and Ribatti, D. (2005). Osteocalcin is angiogenic *in vivo*. *Cell Biol. Int.* **29,** 583–585.

Casu, B., Guerrini, M., Guglieri, S., Naggi, A., Perez, M., Torri, G., Cassinelli, G., Ribatti, D., Carminati, P., Giannini, G., Penco, S., Pisano, C., *et al.* (2004). Under-sulfated and glycol-split heparins endowed with antiangiogenic activity. *J. Med. Chem.* **47,** 838–848.

Chambers, A. F., Schmidt, E. E., Mac Donald, I. C., Morris, V. L., and Groom, A. C. (1992). Early steps in hematogenous metastasis of B16F1 melanoma cells in the chick embryo studied by high-resolution intravital videomicroscopy. *J. Natl. Cancer Inst.* **84,** 797–803.

Coleman, J. R., and Terepka, A. R. (1972). Fine structural changes associated with the onset of calcium, sodium and water transport by the chick chorioallantoic membrane. *J. Membrane Biol.* **7,** 111–127.

Conconi, M. T., Nico, B., Guidolin, D., Baiguera, S., Spinazzi, R., Rebuffat, P., Malendowicz, L. K., Vacca, A., Carraro, G., Parnigotto, P. P., Nussdorfer, G. G., and Ribatti, D. (2004). Ghrelin inhibits FGF-2-mediated angiogenesis *in vitro* and *in vivo*. *Peptides* **25,** 2179–2185.

Crivellato, E., Nico, B., Vacca, A., Djonov, V., Presta, M., and Ribatti, D. (2004). Reccombinant human erythropoietin induces intussusceptive microvascular growth *in vivo*. *Leukemia* **18,** 331–336.

Crum, R., Szabo, W., and Folkman, J. (1985). A new class of steroids inhibits angiogenesis in the presence of heparin. *Science* **230,** 1375–1378.

Cruz, A., Parnot, C., Ribatti, D., Corvol, P., and Gasc, J. M. (2001). Endothelin-1, a regulator of angiogenesis in the chick chorioallantoic membrane. *J. Vasc. Res.* **38,** 536–545.

Dagg, C. P., Karnofsky, D. A., and Roddy, J. (1956). Growth of transplantable human tumors in the chick embryo and hatched chick. *Cancer Res.* **16,** 589–594.

Dai, X., Cui, S. G., Wang, T., Liu, Q., Song, H. J., and Wang, R. (2008). Endogenous opioid peptides, endomorphin-1 and deltorphin I, stimulate angiogenesis in the CAM assay. *Eur. J. Pharmacol.* **579,** 269–275.

Danchakoff, V. (1917). The position of the respiratory vascular net in the allantois of the chick. *Am. J. Anat.* **21,** 407–419.

Danesi, R., Del Bianchi, S., Soldani, P., Campagni, A., La Rocca, R. V., Meyers, C. E., Paparelli, A., and Del Tacca, M. (1993). Suramin inhibits bFGF-induced endothelial cell proliferation and angiogenesis in the chick chorioallantoic membrane. *Br. J. Cancer* **68,** 932–938.

Davison, T. F. (2003). The immunologists' debt to the chicken. *Br. Poult. Sci.* **44,** 6–21.

De Fouw, D. O., Rizzo, V. J., Steinfeld, R., and Feinberg, R. N. (1989). Mapping of the microcirculation in the chick chorioallantoic membrane during normal angiogenesis. *Microvasc. Res.* **38,** 136–147.

De Paulis, A., Prevete, N., Fiorentino, I., Rossi, F. W., Staibano, S., Montuori, N., Ragno, P., Longobardi, A., Liccardo, B., Genovese, A., Ribatti, D., Walls, A. F., *et al.* (2006). Expression and function of the vascular endothelial growth factors and their receptors in human basophils. *J. Immunol.* **177,** 7322–7331.

Dugan, J. D., Jr, Lawton, M. T., Glaser, B., and Brem, H. (1981). A new technique for explantation and *in vitro* cultivation of chicken embryos. *Anat. Rec.* **229,** 125–128.

Dusseau, J. W., Hutchins, P. M., and Malbasa, D. S. (1986). Stimulation of angiogenesis by adenosine on the chick chorioallantoic membrane. *Circ. Res.* **59,** 163–170.

Eisenstein, R., Kuettner, K. E., Neopolitan, C., Sobel, L. W., and Sorgente, N. (1975). The resistance of certain tissues to invasion. III. Cartilage extracts inhibit the growth of fibroblasts and endothelial cells in culture. *Am. J. Pathol.* **87,** 337–348.

Elias, H., and Hyde, D. M. (1983). Stereological measurements of isotropic structures. *In* "A Guide to Practical Stereology" (H. Elias and D. M. Hyde, eds.), pp. 25–44. Karger, Basel.

Fajardo, L. F., Kowalski, J., Kwan, H. H., Prionas, S. D., and Allison, A. C. (1998). The disc angiogenesis system. *Lab. Invest.* **58,** 718–724.

Fanczi, T., and Feher, S. (1979). Ultrastructural studies of chicken embryo CAM during incubation. *Anat. Histol. Embryol.* **8,** 151–159.

Fett, J. W., Strydom, D. J., Lobb, R. R., Alderman, E. M., Bethune, J. L., Riordan, J. F., and Vallee, B. L. (1985). Isolation and characterization of angiogenin, an angiogenic protein from human carcinoma cells. *Biochemistry* **24,** 5480–5486.

Folkman, J. (1974). Proceedings: Tumor angiogenesis factor. *Cancer Res.* **34,** 2109–2113.

Folkman, J., and Cotran, R. (1976). Relation of vascular proliferation to tumor growth. *Int. Rev. Exp. Pathol.* **16,** 207–248.

Folkman, J., Langer, R., Linhardt, R. J., Haudenschild, C., and Taylor, S. (1983). Angiogenesis inhibition and tumor regression caused by heparin or a heparin fragment in the presence of cortisone. *Science* **221,** 719–725.

Folkman, J., Weisz, P. B., Joullic, M. M., Li, W. W., and Ewing, R. (1989). Control of angiogenesis with synthetic heparin substitutes. *Science* **243,** 1490–1493.

Form, D. M., and Auerbach, R. (1983). PGE_2 and angiogenesis. *Proc. Soc. Exp. Biol. Med.* **172,** 214–218.

Form, D. M., Pratt, B. M., and Madri, J. A. (1986). Endothelial cell proliferation during angiogenesis. *In vitro* modulation by basement membrane components. *Lab. Invest.* **55,** 521–530.

Fraser, R. A., Ellis, M., and Stalker, A. L. (1979). Experimental angiogenesis in the chorioallantoic membrane. *In* "Current Advances in Basic and Clinical Microcirculation," (D. H. Lewis, ed.), pp. 25–26. *Bibl. Anat.* **18**, 25–26.

Friedlander, M., Brooks, P. C., Shaffer, R. W., Kincaid, C. M., Varner, J. A., and Cheresh, D. A. (1995). Definition of two distinct angiogenic pathways by distinct αv integrins. *Science* **270,** 1500–1502.

Fuchs, A., and Lindenbaum, E. S. (1988). The two- and three-dimensional structure of the microcirculation of the chick chorioallantoic membrane. *Acta Anat.* **131,** 271–275.

Fulleborn, F. (1895). Beitrage zur Entwicklung der Allantois der Vogel. Inaugural Dissertation, Berlin.

Funk, P. E., and Thompson, C. B. (1996). Current concepts in chicken B cell development. *Curr. Top. Microbiol. Immunol.* **212,** 17–28.

Gordon, J. R., and Qigley, J. P. (1986). Early spontaneous metastasis in the human epidermoid carcinoma Hep3/chick embryo model: Contribution of incidental colonization. *Int. J. Cancer* **38,** 437–444.

Gualandris, A., Rusnati, M., Belleri, M., Nelli, E. E., Bastaki, M., Molinari-Tosatti, M. P., Bonardi, F., Parolini, S., Albini, A., Morbidelli, L., Ziche, M., Corallini, A., *et al.* (1996). Basic fibroblast growth factor overexpression in endothelial cells: An autocrine mechanism for angiogenesis and angioproliferative diseases. *Cell Growth Diff.* **7,** 147–160.

Hagedorn, M., Javerzat, S., Gilges, D., Meyre, A., de Lafarge, B., Eichmann, A., and Bikfalvi, A. (2005). Accessing key step of human tumor progression *in vivo* by using an avian embryo model. *Proc. Natl. Acad. Sci. USA* **102,** 1643–1648.

Hamburger, V., and Hamilton, H. L. (1951). A series of normal stages in development of the chick embryo. *J. Morphol.* **88,** 49–92.

Hellebrekers, D. M., Jair, K. W., Viré, E., Eguchi, S., Hoebers, N. T., Fraga, M. F., Esteller, M., Fuks, F., Baylin, S. B., van Engeland, M., and Griffioen, A. W. (2006). Angiostatic activity of DNA methyltransferase inhibitors. *Mol. Cancer Ther.* **5,** 467–475.

Hong, K. H., Ryu, J., and Han, K. H. (2005). Monocyte chemoattractant protein-1-induced angiogenesis is mediated by vascular endothelial growth factor-A. *Blood* **105,** 1405–1407.

Hwang, J., Kim, C. W., Son, K. N., Han, K. Y., Lee, K. H., Kleinman, H. K., Ko, J., Na, D. S., Kwon, B. S., Gho, Y. S., and Kim, J. (2004). Angiogenic activity of human CC chemokine CCL15 *in vitro* and *in vivo*. *FEBS Lett.* **570,** 47–51.

Hwang, J., Son, K. H., Kim, C. W., Ko, J., Na, D. S., Kwon, B. S., Gho, Y. S., and Kim, J. (2005). Human CC chemokine CCL23, a ligand for CCR1, induces endothelial cell migration and promotes angiogenesis. *Cytokine* **30,** 254–263.

Ingber, D., and Folkman, J. (1988). Inhibition of angiogenesis through modulation of collagen metabolism. *Lab. Invest.* **59,** 44–51.

Ingber, D., Fujita, T., Kishomoto, S., Kanamaru, T., Sudo, K., Brem, H., and Folkman, J. (1990). Angioinhibins: Synthetic analogues of fumagillin which inhibit angiogenesis and suppress tumor growth. *Nature* **348,** 555–557.

Iurlaro, M., Vacca, A., Minischetti, M., Ribatti, D., Pellegrino, A., Sardanelli, A., Giacchetta, F., and Dammacco, F. (1998). Antiangiogenesis by cyclosporine. *Exp. Hematol.* **26,** 1215–1222.

Jain, R. K., Schlengerm, K., Hockel, M., and Yuan, F. (1997). Quantitative angiogenesis assays: Progress and problems. *Nat. Med.* **3,** 203–208.

Jakob, W., Jentzsch, K. D., Manersberger, B., and Heider, G. (1978). The chick chorioallantoic membrane as a bioassay for angiogenesis factors: Reaction induced by carrier materials. *Exp. Pathol.* **15,** 241–249.

Janse, E. M., and Jeurissen, S. H. (1991). Ontogeny and function of two non-lymphoid cell populations in the chicken embryo. *Immunobiology* **182,** 472–481.

Jung, H. J., Shimm, J. S., Suh, Y. G., Kim, Y. M., Ono, M., and Kwon, H. J. (2007). Potent inhibition of *in vivo* angiogenesis and tumor growth by a novel cyclooxygenase-2 inhibitor, enoic acanthoic acid. *Cancer Sci.* **98,** 1943–1948.

Kim, J., Yu, W., Kowalski, K., and Ossowski, L. (1998). Requirement for specific proteases in cancer cell intravasation as revealed by a novel semiquantitative PCR-based assay. *Cell* **94,** 353–362.

Kirchner, L. M., Schmidt, S. P., and Gruber, B. S. (1996). Quantitation of angiogenesis in the chick chorioallantoic membrane model using fractal analysis. *Microvasc. Res.* **51,** 1–14.

Klagsbrun, M., Knighton, D., and Folkman, J. (1976). Tumor angiogenesis activity in cells grown in tissue culture. *Cancer Res.* **36,** 110–114.

Knighton, D. R., Ausprunk, D., Tapper, D., and Folkman, J. (1977). Avascular and vascular phases of tumour growth in the chick embryo. *Br. J. Cancer* **35,** 347–356.

Knighton, D. R., Fiegel, V. D., and Phillips, G. D. (1991). The assays for angiogenesis. *Prog. Clin. Biol. Res.* **365,** 291–299.

Knoll, A., Schmidt, S., Chapman, M., Wiley, D., Bulgrin, J., Blank, J., and Krichner, L. (1999). A comparison of two controlled-release delivery systems for the delivery of amiloride to control angiogenesis. *Microvasc. Res.* **58,** 1–9.

Koop, S., Khokha, R., Schmidt, E. E., Mac Donald, I. C., Morris, V. L., Chambers, A. F., and Groom, A. C. (1994). Overexpression of metalloproteinase inhibitor in B16F10 cells does not affect extravasation but reduced tumor growth. *Cancer Res.* **54,** 4791–4797.

Kumar, C. C., Malkowski, M., Yin, Z., Tanghetti, E., Yaremko, B., Varner, J. A., Liu, M. H., Smith, E. M., and Neustadt, B. (2001). Inhibition of angiogenesis and tumor growth by SCH221153, a dual $\alpha v\beta 3$ and $\alpha v\beta 5$ integrin receptor antagonist. *Cancer Res.* **61,** 2232–2238.

Kurz, H., Ambrosy, S., Wilting, J., Marme, D., and Christ, B. (1995). Proliferation pattern of capillary endothelial cells in chorioallantoic membrane development indicates local growth control, which is counteracted by vascular endothelial growth factor application. *Dev. Dyn.* **203,** 174–186.

Langer, R., and Folkman, J. (1976). Polymers for sustained release of proteins and other macromolecules. *Nature* **263,** 797–800.

Leali, D., Dell'Era, P., Stabile, H., Sennino, B., Chambers, A. F., Naldini, A., Sozzani, S., Nico, B., Ribatti, D., and Presta, M. (2003). Osteopontin (Eta-1) and fibroblast growth factor-2 cross-talk in angiogenesis. *J. Immunol.* **171,** 1085–1093.

Leene, W., Duyzings, M. J. M., and Von Steeg, C. (1973). Lymphoid stem cell identification in the developing thymus and bursa of Fabricius of the chick. *Z. Zellforsch.* **136,** 521–533.

Leibovich, S., Polverini, P. J., Shepard, H. M., Wiseman, D. M., Shively, V., and Nusier, N. (1987). Macrophage-induced angiogenesis is mediated by TNF-alpha. *Nature* **329,** 630–632.

Liekens, S., Hernandez, A. I., Ribatti, D., De Clercq, E., Camarasa, M. J., Pérez-Pérez, M. J., and Balzarini, J. (2004). The nucleoside derivative 5'-O-trytyl-inosine (KIN59) suppresses thymidine phosphorylase-triggered angiogenesis via a noncompetitive mechanism of action. *J. Biol. Chem.* **279,** 29598–29605.

Lucarelli, E., Sangiorgi, L., Benassi, S., Donati, D., Gobbi, G. A., Picci, P., Vacca, A., and Ribatti, D. (1999). Angiogenesis in lipoma. An experimental study in the chick embryo chorioallantoic membrane. *Int. J. Mol. Med.* **4,** 593–596.

Maione, T. E., Gray, G. S., Petro, J., Hunt, A. J., Donner, A. L., Bauer, S. I., Carson, H. F., and Sharpe, R. J. (1990). Inhibition of angiogenesis by recombinant human platelet factor-4 and related peptides. *Science* **247,** 77–79.

Mangieri, D., Nico, B., Benagiano, V., De Giorgis, M., Vacca, A., and Ribatti, D. (2008). Angiogenic activity of multiple myeloma endothelial cells *in vivo* in the chick embryo chorioallantoic membrane assay is associated to a down-regulation in the expression of endogenous endostatin. *J. Cell Mol. Med.* **12,** 1023–1028.

Maragoudakis, M. E., Sarmonka, M., and Panoutscacopoulou, M. (1988a). Inhibition of basement membrane biosynthesis prevents angiogenesis. *J. Pharmacol. Exp. Ther.* **244,** 729–733.

Maragoudakis, M. E., Panoutsacopoulou, M., and Sarmonika, M. (1988b). Rate of basement membrane biosynthesis as an index of angiogenesis. *Tissue Cell* **20,** 531–539.

Marimpietri, D., Nico, B., Vacca, A., Mangieri, D., Catarsim, P., Ponzoni, M., and Ribatti, D. (2005). Synergistic inhibition of human neuroblastoma-related angiogenesis by vinblastine and rapamycin. *Oncogene* **24,** 6785–6795.

Marimpietri, D., Brignole, C., Nico, B., Pastorino, F., Pezzolo, A., Piccardi, F., Cilli, M., Di Paolo, D., Pagnan, G., Longo, L., Perri, P., Ribatti, D., *et al.* (2007). Combined therapeutic effects of vinblastine and rapamycin on human neuroblastoma growth, apoptosis, and angiogenesis. *Clin. Cancer Res.* **13,** 3977–3988.

Marzullo, A., Vacca, A., Roncali, L., Pollice, L., and Ribatti, D. (1998). Angiogenesis in hepatocellular carcinoma. An experimental study in the chick embryo chorioallantoic membrane. *Int. J. Oncol.* **13,** 17–21.

Mc Auslan, B. R., Reilly, W. G., Hannan, G. N., and Gole, G. A. (1983). Angiogenic factors and their assay. Activity of formylmethyonil leucyl phenylalanine, adenosine diphosphate, heparin, copper and bovine endothelium stimulating factor. *Microvasc. Res.* **26,** 323–338.

Mc Cormick, J. F., Nassauer, J., Bielunas, J., and Leighton, J. (1984). Anatomy of the chick chorioallantois membrane relevant to its use as a substrate in bioassy systems. *Scan. Elect. Microsc.* **4,** 2023–2030.

Mignatti, P., Morimoto, T., and Rifkin, D. B. (1991). Basic fibroblast growth factor released by single isolated cells stimulates their migration in an autocrine manner. *Proc. Natl. Acad. Sci. USA* **88,** 11007–11011.

Mignatti, P., Morimoto, T., and Rifkin, D. B. (1992). Basic fibroblast growth factor, a protein devoid of secretory signal sequence, is released by cells via a pathway independent of the endoplasmic reticulum-Golgi complex. *J. Cell. Physiol.* **151,** 81–93.

Min, J. K., Han, K. Y., Kim, E. C., Kim, Y. M., Lee, S. W., Kim, O. H., Kim, K. W., Gho, Y. S., and Kwon, Y. G. (2004). Capsaicin inhibits *in vitro* and *in vivo* angiogenesis. *Cancer Res.* **64,** 644–651.

Minischetti, M., Vacca, A., Ribatti, D., Iurlaro, M., Ria, R., Pellegrino, A., Gasparini, G., and Dammacco, F. (2000). TNP-470 and recombinant human interferon-α2a inhibit angiogenesis synergistically. *Br. J. Haematol.* **109,** 829–837.

Montesano, R., Vassalli, J. D., Baird, A., Guillemin, R., and Orci, L. (1986). Basic fibroblast growth factor induces angiogenesis *in vitro*. *Proc. Natl. Acad. Sci. USA* **83,** 7297–7301.

Morris, P. B., Hidat, T., Blackshear, P. J., Klintworth, G. K., and Swain, J. L. (1988). Tumor promoting phorbol esters induced angiogenesis *in vivo*. *Am. J. Physiol.* **254,** C318–322.

Moscatelli, D. (1992). Basic fibroblast growth factor (bFGF) dissociates rapidly from heparan sulfates but slowly from receptors. Implications for mechanisms of bFGF release from pericellular matrix. *J. Biol. Chem.* **267,** 25803–25809.

Moscona, A. (1959). Squamous metaplasia and keratinization of chorionic epithelium of the chick embryo in egg and culture. *Dev. Biol.* **1,** 1–23.

Mousa, S. S., Mousa, S. S., and Mousa, S. A. (2005). Effect of resveratrol on angiogenesis and platelet/fibrin-accelerated tumor growth in the chick chorioallantoic membrane model. *Nutr. Cancer* **52,** 59–65.

Narbaitz, R. (1977). Structure of intra-chorionic blood sinus in the chick embryo. *J. Anat.* **124,** 347–354.

Nguyen, D., Shing, Y., and Folkman, J. (1994). Quantitation of angiogenesis and antiangiogenesis in the chick embryo chorioallantoic membrane. *Microvasc. Res.* **47,** 31–40.

Nicoli, S., Ribatti, D., Cotelli, F., and Presta, M. (2007). Mammalian tumor xenografts induce neovascularization in zebrafish embryos. *Cancer Res.* **67,** 2927–2931.

Nicosia, R. F., and Madri, J. A. (1987). The microvascular extracellular matrix. Developmental changes during angiogenesis in the aortic ring-plasma clot model. *Am. J. Pathol.* **128,** 78–90.

Nozaki, Y., Hida, T., Iinuma, S., Ishii, T., Sudo, K., Muroi, M., and Kanamaru, T. (1993). Tau-1120, a new anthracycline with potent angiostatic activity. *J. Antibiot.* **46,** 569–579.

O'Reilly, M. S., Holmgren, L., Shing, Y., Chen, C., Rosenthal, R. A., Moses, M., Lane, W. S., Cao, Y., Sage, E. H., and Folkman, J. (1994). Angiostatin: A novel angiogenesis inhibitor that mediates the suppression of metastases by a Lewis lung carcinoma. *Cell* **79,** 315–328.

Oh, S. J., Jeltsch, M. M., Birkenhager, R., McCarthy, J. E. G., Weich, H. A., Christ, B., Alitalo, K., and Wilting, J. (1997). VEGF and VEGF-C: Specific induction of angiogenesis and lymphangiogenesis in the differentiated avian chorioallantoic membrane. *Dev. Biol.* **188,** 96–109.

Oikawa, T., Hirotani, K., Shimamura, M., Ashino-Fuse, H., and Iwaguchi, T. (1989a). Powerful antiangiogenic activity of herbamycin (named angiostatic antibiotic). *J. Antibiot.* **42,** 1202–1204.

Oikawa, T., Hirotani, K., Nakamura, O., Shudo, K., Hiragun, A., and Iwaguchi, T. (1989b). A highly potent antiangiogenic activity of retinoids. *Cancer Lett.* **48,** 157–162.

Oikawa, T., Hirotani, K., Ogasawara, H., Katayama, T., Ashino-Fuse, H., Shimamura, M., Iwaguchi, T., and Nakamura, O. (1990a). Inhibition of angiogenesis by bleomycin and its copper complex. *Chem. Pharm. Bull.* **38,** 1790–1792.

Oikawa, T., Hirotani, K., Ogasawara, H., Katayama, T., Nakamura, O., Iwaguchi, T., and Hiragun, A. (1990b). Inhibition of angiogenesis by vitamin D3 analogues. *Eur. J. Pharmacol.* **178,** 247–250.

Oikawa, T., Shimamura, M., and Ashino, H. (1992). Inhibition of angiogenesis by staurosporine, a potent protein kinase inhibitor. *J. Antibiot.* **45,** 1155–1160.

Oikawa, T., Haegawa, M., Shimamura, M., Ashini, H., Murota, S., and Morita, I. (1993a). Eponeomycin, a novel antibiotic, is a high powerful angiogenesis inhibitor. *Biochem. Biophys. Res. Commun.* **181,** 1070–1076.

Oikawa, T., Ito, H., Ashino, H., Toi, M., Tomigaga, T., Morita, I., and Murota, S. (1993b). Radicilor, a microbial cell differentiation modulator, inhibits *in vivo* angiogenesis. *Eur. J. Pharmacol.* **241,** 221–227.

Olivo, M., Bhardwaj, R., Schulze-Osthof, K., Sorg, G., Jurgen-Jacob, H., and Flamme, J. (1992). A comparative study on the effects of tumor necrosis factor alpha (TNF-α), human angiogenic factor (h-AF) and basic fibroblast growth factor (bFGF) on the chorioallantoic membrane of the chick embryo. *Anat. Rec.* **234,** 105–115.

Palczak, R., and Splawinski, J. (1989). Angiogenic activity and neovascularization in adenocarcinoma of the endometrium. *Int. J. Gynecol. Obstet.* **29,** 343–357.

Papoutsi, M., Tomarev, S. I., Eichmann, A., Prols, F., Christ, B., and Wilting, J. (2001). Endogenous origin of the lymphatics in the avian chorioallantoic membrane. *Dev. Dyn.* **222,** 238–251.

Parson-Wingerter, P., Lwai, B., Yang, M. C., Elliott, K. E., Milaninia, A., Redlitz, A., Clark, J. I., and Sage, E. H. (1998). A novel assay of angiogenesis in the quail chorioallantoic membrane. Stimulation of bFGF and inhibition by angiostatin according to fractal dimension and grid interaction. *Microvasc. Res.* **55,** 201–214.

Passaniti, A., Taylor, R. M., Pili, R., Guo, Y., Long, P. V., Haney, J. A., Pauly, R. R., Grant, D. S., and Martin, G. R. (1992). A simple, quantitative method for expressing angiogenesis and antiangiogenic agents using reconstituted basement membrane, heparin, and fibroblast growth factor. *Lab. Invest.* **67,** 519–528.

Pastorino, F., Brignole, C., Di Paolo, D., Nico, B., Pezzolo, A., Marimpietri, D., Pagnan, G., Piccardi, F., Cilli, M., Longhi, R., Ribatti, D., Corti, A., *et al.* (2006). Targeting liposomal chemotherapy via both tumor cell-specific and tumor-vasculature-specific ligands potentiates therapeutic efficacy. *Cancer Res.* **66,** 10073–10082.

Patan, S., Alvarez, M. J., Schitt, N. Y. J. C., and Burri, P. H. (1992). Intussusceptive microvascular growth: A common alternative to capillary sprouting. *Arch. Histol. Cytol.* **55,** 65–75.

Patan, S., Haenni, B., and Burri, P. H. (1993). Evidence for intussusceptive capillary growth in the chicken chorio-allantoic membrane (CAM). *Anat. Embryol.* **187,** 121–130.

Patan, S., Haenni, B., and Burri, P. H. (1996). Implementation of intussusceptive microvascular growth in chicken chorioallantoic membrane (CAM). 1. Pillar formation by folding of the capillary wall. *Microvasc. Res.* **51,** 80–98.

Petruzzelli, G. J., Johnson, J. T., Snyderman, C. H., and Myers, E. N. (1993). Angiogenesis induced by head and neck squamous cell carcinoma xenografts in the chick embryo chorioallantoic membrane model. *Ann. Otol. Rhinol. Laryngol.* **102,** 215–221.

Pipili-Synetos, E., Papageorgiou, A., Sakkoula, E., Sotiropoulou, G., Fotsis, T., Karakiulakis, G., and Maragoudakis, M. E. (1995). Inhibition of angiogenesis, tumor growth and metastasis by the NO-releasing vasodilators, isosorbide mononitrate and dimitrate. *Br. J. Pharmacol.* **116,** 1829–1834.

Presta, M., Rusnati, M., Belleri, M., Morbidelli, L., Ziche, M., and Ribatti, D. (1999). Purine analogue 6-methylmercaptopurine riboside inhibits early and late phase of the angiogenic process. *Cancer Res.* **59,** 2417–2424.

Presta, M., Oreste, P., Zoppetti, G., Belleri, M., Tanghetti, E., Leali, D., Urbinati, C., Bugatti, A., Ronca, R., Nicoli, S., Moroni, E., Stabile, H., *et al.* (2005). Antiangiogenic activity of semisynthetic biotecnological heparins: Low-molecular-weight-sulfated Escherichia coli K5 polysaccharide derivatives as fibroblast growth factor antagonists. *Arterioscler. Thromb. Vasc. Biol.* **25,** 71–76.

Puxeddu, I., Alian, A., Piliponsky, A. M., Ribatti, D., Panet, A., and Levi-Schaffer, F. (2005). Human peripheral blood eosinophils induce angiogenesis. *Int. J. Biochem. Cell Biol.* **37,** 628–636.

Quigley, J. P., and Armstrong, P. B. (1998). Tumor cell intravasation *alu*-citated: The chick embryo opens the window. *Cell* **94,** 281–284.

Ramoshebi, L. N., and Ripamonti, U. (2000). Osteogenic protein-1, a bone morphogenetic protein, induces angiogenesis in the chick chorioallantoic membrane and synergizes with basic fibroblast growth factor and transforming growth factor-β1. *Anat. Rec.* **259,** 97–107.

Ribatti, D. (2004). The first evidence of the tumor-induced angiogenesis *in vivo* by using the chorioallantoic membrane assay. *Leukemia* **18,** 1350–1351.

Ribatti, D., and Ponzoni, M. (2008). Angiogenesis in malignant and non-malignant pediatric tumors. *In* "Antiangiogenic Agents an Cancer Therapy," (B. A. Teicher and L. M. Ellis, eds.), pp. 475–486. Humana Press, Totowa, NJ, USA.

Ribatti, D., and Vacca, A. (1999). Models for studying angiogenesis *in vivo*. *Int. J. Biol. Markers* **14,** 207–213.

Ribatti, D., Roncali, L., Nico, B., and Bertossi, M. (1987). Effects of exogenous heparin on the vasculogenesis of the chorioallantoic membrane. *Acta Anat.* **130,** 257–263.

Ribatti, D., Vacca, A., Bertossi, M., De Benedictis, G., Roncali, L., and Dammacco, F. (1990). Angiogenesis induced by B-cell non-Hodgkin's lymphomas. Lack of correlation with tumor malignancy and immunologic phenotype. *Anticancer Res.* **10,** 401–406.

Ribatti, D., Loria, M. P., and Tursi, A. (1991). Lymphocyte-induced angiogenesis. A morphometric study in the chick embryo chorioallantoic membrane. *Acta Anat.* **142,** 334–338.

Ribatti, D., Urbinati, C., Nico, B., Rusnati, M., Roncali, L., and Presta, M. (1995). Endogenous basic fibroblast growth factor is implicated in the vascularization of the chick embryo chorioallantoic membrane. *Dev. Biol.* **170,** 39–49.

Ribatti, D., Vacca, A., Costantino, F., Minischetti, M., Locci, P., Becchetti, E., Roncali, L., and Dammacco, F. (1997a). Exogenous heparin induces fibronectin overexpression parallel to angiogenesis in the extracellular matrix of the chick embryo chorioallantoic membrane. *Tissue Cell* **29,** 131–136.

Ribatti, D., Gualandris, A., Bastaki, M., Vacca, A., Iurlaro, M., Roncali, L., and Presta, M. (1997b). New model for the study of angiogenesis and antiangiogenesis in the chick embryo chorioallantoic membrane: The gelatin sponge/chorioallantoic membrane assay. *J. Vasc. Res.* **34,** 455–463.

Ribatti, D., Bertossi, M., Nico, B., Vacca, A., Ria, R., Riva, A., Roncali, L., and Presta, M. (1998a). Role of basic fibroblast growth factor in the formation of the capillary plexus in

the chick embryo chorioallantoic membrane. An *in situ* hybridization, immunohistochemical and ultrastructural study. *J. Submicrosc. Cytol. Pathol.* **30,** 127–136.

Ribatti, D., Alessandri, G., Vacca, A., Iurlaro, M., and Ponzoni, M. (1998b). Human neuroblastoma cells produce extracellular matrix-degrading enzymes, induce endothelial cell proliferation and are angiogenic *in vivo*. *Int. J. Cancer* **77,** 449–454.

Ribatti, D., Vacca, A., Giacchetta, F., Anichini, M., Roncali, L., and Dammacco, F. (1998c). Lipoprotein(a) induces angiogenesis on the chick embryo chorioallantoic membrane. *Eur. J. Clin. Invest.* **28,** 533–537.

Ribatti, D., Gualandris, A., Belleri, M., Massardi, L., Nico, B., Rusnati, M., Dell'Era, P., Vacca, A., Roncali, L., and Presta, M. (1999a). Angiogenesis and hemangioma formation in the chick embryo chorioallantoic membrane by fibroblast growth factor-2 (FGF-2) overexpressing endothelial cells. *J. Pathol.* **18,** 590–599.

Ribatti, D., Leali, D., Vacca, A., Giuliani, R., Gualandris, R., Roncali, L., Nolli, M. L., and Presta, M. (1999b). *In vivo* angiogenic activity of urokinase: Role of endogenous fibroblast growth factor-2. *J. Cell Sci.* **112,** 4213–4221.

Ribatti, D., Presta, M., Vacca, A., Ria, R., Giuliani, R., Dell'Era, P., Nico, B., Roncali, L., and Dammacco, F. (1999c). Human erythropoietin induces a pro-angiogenic phenotype in cultured endothelial cells and stimulates neovascularization *in vivo*. *Blood* **93,** 2627–2636.

Ribatti, D., Alessandri, G., Baronio, M., Raffaghello, L., Cosimo, E., Marimpietri, D., Montaldo, P. G., De Falco, G., Caruso, A., Vacca, A., and Ponzoni, M. (2001a). Inhibition of neuroblastoma-induced angiogenesis by fenretinide. *Int. J. Cancer* **94,** 314–321.

Ribatti, D., Nico, B., Morbidelli, L., Donnini, S., Ziche, M., Vacca, A., Roncali, L., and Presta, M. (2001b). Cell-mediated delivery of fibroblast growth factor-2 and vascular endothelial growth factor onto the chick chorioallantoic membrane: Endothelial fenestrations and angiogenesis. *J. Vasc. Res.* **38,** 536–545.

Ribatti, D., Nico, B., Belloni, A. S., Vacca, A., Roncali, L., and Nussdorfer, G. G. (2001c). Angiogenic activity of leptin in the chick embryo chorioallantoic membrane is in part mediated by endogenous fibroblast growth factor-2. *Int. J. Mol. Med.* **8,** 265–268.

Ribatti, D., Crivellato, E., Candussio, L., Nico, B., Vacca, A., and Dammacco, F. (2001d). Mast cells and their secretory granules are angiogenic in the chick embryo chorioallantoic membrane. *Clin. Exp. Allergy* **31,** 602–608.

Ribatti, D., Raffaghello, L., Pastorino, F., Nico, B., Brignole, C., Vacca, A., and Ponzoni, M. (2002). *In vivo* angiogenic activity of neuroblastoma cells correlates with MYCN oncogene overexpression. *Int. J. Cancer* **102,** 351–354.

Ribatti, D., De Falco, G., Nico, B., Ria, R., Crivellato, E., and Vacca, A. (2003). *In vivo* time-course of the angiogenic response induced by multiple myeloma plasma cells in the chick embryo chorioallantoic membrane. *J. Anat.* **203,** 323–328.

Ribatti, D., Nico, B., Vacca, A., and Presta, M. (2006a). The gelatin sponge-chorioallantoic membrane assay. *Nat. Protoc.* **1,** 85-91.

Ribatti, D., Nico, B., Pezzolo, A., Vacca, A., Meazza, R., Cinti, R., Carlini, B., Parodi, F., Pistoia, V., and Corrias, M. V. (2006b). Angiogenesis in a human neuroblastoma xenograft model: Mechanisms and inhibition by tumor-derived interferon-gamma. *Br. J. Cancer* **94,** 1845–1852.

Ribatti, D., Nico, B., Mangieri, D., Maruotti, N., Longo, V., Vacca, A., and Cantatore, F. P. (2007). Neridronate inhibits angiogenesis *in vitro* and *in vivo*. *Clin. Rheumatol.* **26,** 1094–1098.

Riboldi, E., Musso, T., Moroni, E., Urbinati, C., Bernasconi, S., Rusnati, M., Adorini, L., Presta, M., and Sozzani, S. (2005). Cutting edge: Proangiogenic properties of alternatively activated dendritic cells. *J. Immunol.* **175,** 2788–2792.

Risau, W. (1997). Mechanisms of angiogenesis. *Nature* **386,** 671–674.

Risau, W., and Lemmon, V. (1988). Changes in the vascular extracellular matrix during embryonic vasculogenesis and angiogenesis. *Dev. Biol.* **125,** 441–450.

Rizzo, V., and De Fouw, D. O. (1993). Macromolecular selectivity of chick chorioallantoic membrane microvessels during normal angiogenesis and endothelial differentiation. *Tissue Cell* **25,** 847–856.

Roccaro, A. M., Hideshima, T., Raje, N., Kumar, S., Ishitsuka, K., Yasui, H., Shiraishi, N., Ribatti, D., Nico, B., Vacca, A., Dammacco, F., Richardson, P. G., *et al.* (2006). Bortezomib mediates antiangiogenesis in multiple myeloma via direct and indirect effects on endothelial cells. *Cancer Res.* **66,** 184–191.

Rusnati, M., Urbinati, C., Caputo, A., Possati, L., Lortat-Jacob, H., Giacca, M., Ribatti, D., and Presta, M. (2001). Pentosan polysulfate as an inhibitor of extracellular HIV-1 Tat. *J. Biol. Chem.* **276,** 22420–22425.

Rusnati, M., Camozzi, M., Moroni, E., Bottazzi, B., Peri, G., Indraccolo, S., Amadori, A., Mantovani, A., and Presta, M. (2004). Selective recognition of fibroblast growth factor-2 by the long pentraxin PTX3 inhibits angiogenesis. *Blood* **104,** 92–99.

Salcedo, R., Young, H. A., Fonce, M. L., Ward, J. M., Kleinman, H. K., Murphy, W. J., and Oppenheim, J. J. (2002). Eotaxin (CCL11) induces *in vivo* angiogenic responses by human $CCR3^+$ endothelial cells. *J. Immunol.* **166,** 7571–7578.

Sariola, H., Kuusela, P., and Ekblom, P. (1984). Cellular origin of fibronectin in interspecies hybrid kidneys. *J. Cell Biol.* **99,** 2099–2107.

Sasisekharon, R., Moses, M. A., Nugent, M. A., Cooney, C. L., and Langer, R. (1994). Heparinase inhibits neovascularization. *Proc. Natl. Acad. Sci. USA* **91,** 1524–1528.

Scapini, P., Morini, M., Tecchio, C., Minghelli, S., Di Carlo, E., Tanghetti, E., Albini, A., Lowell, C., Berton, G., Noonan, D. M., and Cassatella, M. A. (2004). CXCL1/macrophage inflammatory protein-2-induced angiogenesis *in vivo* is mediated by neutrophil-derived vascular endothelial growth factor-A. *J. Immunol.* **172,** 5034–5040.

Scavelli, C., Di Pietro, G., Cirulli, T., Coluccia, M., Boccarelli, A., Giannini, T., Mangialardi, R., Bertieri, R., Coluccia, A. M. L., Ribatti, D., Dammacco, F., and Vacca, A. (2007). Zoledronic acid affects over-angiogenesis phenotype of endothelial cells in patients with multiple myeloma. *Mol. Cancer Ther.* **6,** 3256–3262.

Scher, C. D., Haudenschild, C., and Klagsbrun, M. (1976). The chick chorioallantoic membrane as a model system for the study of tissue invasion by viral transformed cells. *Cell* **8,** 373–382.

Schlatter, P., Konig, M. F., Karlsson, L. M., and Burri, P. H. (1997). Quantitative study of intussusceptive capillary growth in the chorioallantoic membrane (CAM) of the chicken embryo. *Microvasc. Res.* **54,** 65–73.

Schoefl, G. L. (1984). Positioning of the respiratory sinus in the chick chorio-allantois. *In* "Progress in Microcirculation Research" (F. C. Courtice, D. G. Garlick, and M. A. Perry, eds.), pp. 54–58. Committee in Postgraduate Medical Education, Sidney.

Shimizu, M., Shimamura, M., Owaki, T., Asakawa, M., Fujita, K., Kudo, M., Iwakuram, Y., Takeda, Y., Luster, A. D., Mizuguch, J., and Yoshimoto, T. (2006). Antiangiogenic and antitumor activity of IL-27. *J. Immunol.* **176,** 7317–7324.

Sholley, M. M., Ferguson, G. P., Seibel, H. R., Montour, J. L., and Wilson, J. D. (1984). Mechanisms of neovascularization. Vascular sprouting can occur without proliferation of endothelial cells. *Lab. Invest.* **51,** 624–634.

Shumko, J. Z., De Fouw, D. O., and Feinberg, R. N. (1988). Vascular histodifferentiation in the chick chorioallantoic membrane: A morphometric study. *Anat. Rec.* **220,** 179–189.

Sihn, G., Walter, T., Klein, J. C., Queguiner, I., Iwao, H., Nicolau, C., Lehn, J. M., Corvol, P., and Gasc, J. M. (2007). Anti-angiogenic properties of myo-inositol trispyrophosphate *in ovo* and growth reduction of implanted glioma. *FEBS Lett.* **581,** 962–966.

Sills, A. K., Williams, J. I., Tyler, B. M., Epstein, D. S., Sipos, E. P., Davis, J. D., McLane, M. P., Pitchford, S., Cheshire, K., Gannon, F. H., Kinney, W. A., Chao, T. L., *et al.* (1998). Squalamine inhibits angiogenesis and solid tumor growth *in vivo* and perturbs embryonic vasculature. *Cancer Res.* **58,** 2784–2792.

Spanel-Burowski, K., Schnapper, U., and Heymer, B. (1988). The chick chorioallantoic membrane assay in the assessment of angiogenic factors. *Biomed Res.* **9,** 253–260.

Spinazzi, R., Albertin, G., Nico, B., Guidolin, D., Di Liddo, R., Rossi, G. P., Ribatti, D., and Nussdorfer, G. G. (2006). Urotensin II ans its receptor (UT-R) are expressed in rat brain endothelial cells, and urotensin II via UT-R stimulates angiogenesis *in vivo* and *in vitro*. *Int. J. Mol. Med.* **18,** 1107–1112.

Stabile, H., Mitola, S., Moroni, E., Belleri, M., Nicoli, S., Coltrini, D., Peri, F., Pessi, A., Orsatti, L., Talamo, F., Castronovo, V., Waltregny, D., *et al.* (2007). Bone morphogenetic protein antagonist Dmr/gremlin is a novel proangiogenic factor. *Blood* **109,** 1834–1840.

Stewart, R., Nelson, J., and Wilson, D. J. (1989). Epidermal growth factor promotes chick embryo angiogenesis. *Cell Biol. Int. Rep.* **13,** 957–965.

Strick, D. M., Waycaster, R. L., Montani, J., Gay, W. J., and Adair, T. H. (1991). Morphometric measurements of the chorioallantoic membrane vascularity: Effects of hypoxia and hyperoxia. *Am. J. Physiol.* **29,** H1385–H1389.

Takigawa, M., Enomoto, M., Nishida, Y., Pan, H. O., Kinishita, A., and Suzuki, F. (1990). Tumor angiogenesis and polyamines, α-difluoromethylornithine, an irreversible inhibitor of ornithine decarboxylase, inhibit B16 melanoma-induced angiogenesis *in ovo* and the proliferation of vascular endothelial cells *in vitro*. *Cancer Res.* **50,** 4131–4138.

Taraboletti, G., Poli, M., Dossi, R., Manenti, L., Borsotti, P., Faircloth, G. T., Broggini, M., D'Incalci, M., Ribatti, D., and Giavazzi, R. (2004). Antiangiogenic activity of aplidine, a new agent of marine origin. *Br. J. Cancer* **90,** 2418–2424.

Taylor, S., and Folkman, J. (1982). Protamine is an inhibitor of angiogenesis. *Nature* **297,** 307–312.

Thompson, W. D., and Brown, F. I. (1987). Quantitation of histamine-induced angiogenesis in the chick chorioallantoic membrane, mode of histamine is indirect. *Int. J. Microcirc. Clin. Exp.* **6,** 343–357.

Thompson, W. D., Campbell, R., and Evans, T. (1985). Fibrin degradation and angiogenesis, quantitative analysis of the angiogenic response in the chick chorioallantoic membrane. *J. Pathol.* **145,** 27–32.

Tsopanoglou, N. E., Pipili-Synetos, E., and Maragoudakis, M. E. (1993). Protein kinase C involvment in the regulation of angiogenesis. *J. Vasc. Res.* **30,** 202–208.

Urbinati, C., Mitola, S., Tanghetti, E., Kumar, C., Waltenberger, J., Ribatti, D., Presta, M., and Rusnati, M. (2005). Integrin alphavbeta3 as a target for blocking HIV-1 Tat-induced cell activation *in vitro* and angiogenesis *in vivo*. *Arterioscler. Thromb. Vasc. Biol.* **25,** 2315–2320.

Vacca, A., Ribatti, D., Roncali, L., Ranieri, G., Serio, G., Silvestris, F., and Dammacco, F. (1994). Bone marrow angiogenesis and progression in multiple myeloma. *Br. J. Haematol.* **87,** 503–508.

Vacca, A., Ribatti, D., Iurlaro, M., Albini, A., Minischetti, M., Bussolino, F., Pellegrino, A., Ria, R., Rusnati, M., Presta, M., Vincenti, V., Persico, M. G., *et al.* (1998). Human lymphoblastoid cells produce extracellular matrix-degrading enzymes and induce endothelial cell proliferation, migration, morphogenesis, and angiogenesis. *Int. J. Clin. Lab. Res.* **28,** 55–68.

Vacca, A., Ribatti, D., Presta, M., Minischetti, M., Iurlaro, M., Ria, R., Albini, A., Bussolino, F., and Dammacco, F. (1999a). Bone marrow neovascularization, plasma cell angiogenic potential, and matrix metalloproteinase-2 secretion parallel progression of human multiple myeloma. *Blood* **93,** 3064–3073.

Vacca, A., Iurlaro, M., Ribatti, D., Minischetti, M., Nico, B., Ria, R., Pellegrino, A., and Dammacco, F. (1999b). Antiangiogenesis is produced by nontoxic doses of vinblastine. *Blood* **94,** 4143–4155.

Vacca, A., Bruno, M., Boccarelli, A., Coluccia, M., Ribatti, D., Bergamo, A., Sartor, L., and Sava, G. (2002). Inhibition of endothelial cell functions and of angiogenesis by the metastasis inhibitor NAMI-A. *Br. J. Cancer* **86,** 993–998.

Vacca, A., Ria, R., Semeraro, F., Merchionne, F., Coluccia, M., Boccarelli, A., Scavelli, C., Nico, B., Gernone, A., Batelli, F., Tabilio, A., Gudolin, D., *et al.* (2003). Endothelial cells in the bone marrow of multiple myeloma. *Blood* **102,** 3340–3348.

Vitaliti, A., Wittmer, M., Steiner, R., Wyder, L., Neri, D., and Klemenz, R. (2000). Inhibition of tumor angiogenesis by a single-chain antibody directed against vascular endothelial growth factor. *Cancer Res.* **60,** 4311–4314.

Voss, K., Jacob, W., and Roth, K. (1984). A new image analysis method for the quantitation of neovascularization. *Exp. Pathol.* **26,** 155–161.

Vu, M. T., Smith, C. F., Burger, P. C., and Klintworth, G. K. (1985). An evaluation of methods to quantitate the chick chorioallantoic membrane assay in angiogenesis. *Lab. Invest.* **53,** 499–508.

West, D. C., Hampson, I. N., Arnold, F., and Kumar, S. (1985). Angiogenesis induced by degradation products of hyaluronic acid. *Science* **228,** 1324–1326.

Wilks, J. W., Scott, P. A., Vrba, L. K., and Cocuzza, J. B. (1991). Inhibition of angiogenesis with combination treatments of angiostatic steroids and suramin. *Int. J. Radiol.* **60,** 73–77.

Wilting, J., Christ, B., and Bokeloh, M. (1991). A modified chorioallantoic membrane (CAM) assay for qualitative and quantitative study of growth factors. Studies on the effects of carriers, PBS, angiogenin and bFGF. *Anat. Embryol.* **183,** 259–271.

Wilting, J., Christ, B., and Weich, H. A. (1992). The effects of growth factors on day 13 chorioallantoic membrane (CAM): A study of VEGF165 and PDGF-BB. *Anat. Embryol.* **186,** 251–257.

Wilting, J., Christ, B., Bokeloh, M., and Wiech, H. A. (1993). *In vivo* effects of vascular endothelial growth factor on the chicken chorioallantoic membrane. *Cell Tissue Res.* **274,** 163–172.

Wilting, J., Birkenhager, R., Eichmann, A., Kurz, H., Martony-Baron, G., Marmé, D., Mc Carthy, J. E. G., Christ, B., and Weich, H. A. (1996). VEGF121 induces proliferation of vascular endothelial cells and expression of flk-1 without affecting lymphatic vessels of the chorioallantoic membrane. *Dev. Biol.* **176,** 76–85.

Wilting, J., Neeff, H., and Christ, B. (1999). Embryonic lymphangiogenesis. *Cell Tissue Res.* **297,** 1–11.

Woltering, E. A., Barrie, R., O'Dorisio, T. M., Arce, D., Ure, T., Cramer, A., Holmes, D., Robertson, J., and Fassier, J. (1991). Somatostatin analogues inhibit angiogenesis in the chick chorioallantoic membrane. *J. Surg. Res.* **50,** 245–251.

Xiao, D., and Singh, S. V. (2007). Phenethyl isothiocyanate inhibits angiogenesis *in vitro* and *ex vivo*. *Cancer Res.* **67,** 2239–2246.

Yang, E. Y., and Moses, H. L. (1990). Transforming growth factor-β 1-induced changes in cell migration, proliferation, and angiogenesis in the chicken chorioallantoic membrane. *J. Cell Biol.* **111,** 731–741.

Zacharakis, N., Tone, P., Flordellis, C. S., Maragoudakis, M. E., and Tsopanoglou, N. E. (2006). Methylene blue inhibits angiogenesis in chick chorioallantoic membrane through a nitric oxide-independent mechanism. *J. Cell. Mol. Med.* **10,** 493–498.

Ziche, M., Maglione, D., Ribatti, D., Morbielli, L., Lago, C. T., Battisti, M., Paoletti, I., Barra, A., Tucci, M., Parise, G., Vincenti, V., Granger, H. J., *et al.* (1997). Placenta growth factor-1 is chemotactic, mitogenic, and angiogenic. *Lab. Invest.* **76,** 517–531.

CHAPTER SIX

Molecular and Cellular Biology of Synucleins

Andrei Surguchov*,†

Contents

* Retinal Biology Research Laboratory, VA Medical Center, Kansas City, Missouri 64128
† Kansas University Medical Center, Kansas City, Kansas, Missouri 66148

International Review of Cell and Molecular Biology, Volume 270
ISSN 1937-6448, DOI: 10.1016/S1937-6448(08)01406-8

Abstract

Synucleins are small, soluble proteins expressed primarily in neural tissues and certain tumors. The family includes three known proteins: α-synuclein, β-synuclein, and γ-synuclein. A typical structural feature of synucleins is the presence of a repetitive, degenerative AA motif KTKEGV throughout the first 87 residues and acidic stretches within the C-terminal region. Members of the synuclein family are natively unfolded proteins that are characterized by a high net charge and low hydropathy. The synuclein family recently came into the spotlight when one of its members, α-synuclein, was linked both genetically and neuropathologically to Parkinson's disease. It has a role in other neurodegenerative diseases, such as dementia with Lewy bodies, multiple system atrophy, neurodegeneration with brain iron accumulation type 1, and Alzheimer's disease. Interestingly, another member of the family, β-synuclein, possesses antagonistic properties to α-synuclein. The third member of the family, γ-synuclein, is implicated in different types of cancer, some neurodegenerative diseases and ocular pathology. The involvement of synuclein proteins in the etiology of common human diseases has raised exciting questions and is currently the subject of intense investigation.

Key Words: Synucleins, Protein aggregation, Chaperones, Parkinson's disease, Neurodegenerative diseases, Breast cancer, Proteasomes.

Abbreviations

AA	amino acid
Aab	autoantibody
Ab	antibody
AD	Alzheimer's disease
AFM	atomic force microscopy
ATS	acidic tail of α-synuclein
CNS	central nervous system
CSF	cerebrospinal fluid
CSPα	cysteine-string protein-α
DA	dopamine

DAN	dopaminergic neurons
DAT	dopamine transporter
DLB	dementia with Lewy bodies
ER	endoplasmic reticulum
FA	fatty acid
GCI	glial cytoplasmic inclusions
GRKs	G–protein-coupled receptor kinases
Hsp	heat-shock proteins
IHC	immunohistochemistry
IPL	inner plexiform layer
KO	knockout
LB	Lewy bodies
LN	Lewy neurites
NMR	nuclear magnetic resonance
MPP^+	1-methyl-4-phenylpyridinium
MSA	multiple system atrophy
NAC	non-Aβ-component of AD amyloid
NACP	non-Aβ-component precursor of AD amyloid
NDD	neurodegenerative disease
NFL	neurofiber layer
PD	Parkinson's disease
PLD	phospholipase D
PTM	posttranslational modifications
RGC	retinal ganglion cells
ROS	reactive oxygen species
SNARE	soluble *N*-ethylmaleimide-sensitive factor attachment protein receptor
SNc	substantia nigra pars compacta
SNP	single-nucleotide polymorphism
Tg	transgenic
TH	tyrosine hydroxylase
5′-UTR	5′-untranslated region
VMAT2	vesicular monoamine transporter protein
wt	wild type

1. Introduction

The last 20 years of studying synucleins were full of exciting findings, fascinating hypotheses, and controversial data. Amazingly, these 20 years can be logically subdivided into two decades: the first one started after the cloning and identification of the first synuclein by Maroteaux *et al.* (1988). The second decade began after the publication of genetic data by

Polymeropoulos *et al.* (1997) and Krüger *et al.* (1998) showing that α-synuclein is genetically linked to Parkinson's disease (PD).

The most amazing and striking contradictions in the study of synucleins concern their normal physiological functions. The majority of papers devoted to synucleins begins with the sentence: ''The normal function of α-synuclein remains unknown.'' After this statement, however, the authors usually specify several possible functions and a list of processes in which synucleins are involved, for example, synaptic plasticity, maintenance of the synaptic vesicle pool, regulation of dopamine (DA) biosynthesis and homeostasis, chaperone activity, regulation of proteasome activity, transcriptional modulation, and so on. Is it then possible to say that the function of this protein is truly unknown, when this protein affects a dozen of different processes and is implicated in several cellular pathways? During these last years, it clearly became evident that the main function of α-synuclein is related with the maintenance of synaptic vesicle pools and that it also plays a role in several other cellular processes. A recent emerging function of α-synuclein that is not yet completely understood is connected with its ability to form ion channels in synaptic membranes in response to an action potential. The channel formation may be a part of the normal function of α-synuclein that could result in the modulation of ion movements related to the process of depolarization/repolarization. Being a multifunctional protein, α-synuclein is implicated in many cellular processes and sorting out primary events from secondary or tertiary ones, has been difficult.

There are at least two structural features of α-synuclein and other members of the synuclein family that makes their study challenging. One of them is their easily changeable conformation, which is altered considerably upon lipid binding and interaction with other ligands (Perrin *et al.*, 2000, 2001). The second feature is the existence of many molecular isoforms of synucleins generated as a result of different posttranslational modifications (PTM), alternative splicing, truncation, aggregation states, and binding to other proteins and ligands. These isoforms may have different features including conformation and localization. Thus, synucleins have ''chameleon'' features and the transition from one form to another changes their properties. These alterations depend on the physiological conditions of the cells and tissues where synucleins are expressed.

The synuclein family attracts researchers with different backgrounds and diverse interests. While pragmatic scientists study these proteins because of their connection to severe human diseases, more romantic researchers are excited by their involvement in bird songs learning (George *et al.*, 1995).

1.1. Discovery of the first synuclein

Twenty years ago, Maroteaux *et al.* (1988) were screening an expression library by an antiserum against cholinergic vesicles and isolated a cDNA clone encoding a 143-amino acid (AA) neuron-specific protein from the

electric lobe of Pacific electric ray *Torpedo californica*. Because of its localization to the nuclear envelope of neurons and to the presynaptic nerve terminals, this protein was named synuclein. Some investigators consider *Torpedo* synuclein to be an α-isoform (Lotharius and Brundin, 2002a; Recchia *et al.*, 2004), probably because its length is more similar to the length of α-synuclein. However, based on the AA sequence, it can be currently assigned to γ-synuclein (Fig. 6.1). The longer size of this *T. californica* synuclein is explained by the insertion of a repeat after residue 24. The original *Torpedo* clone was used to screen a rat brain cDNA library. A highly homologous cDNA clone (85% homology) encoding 140 AAs was

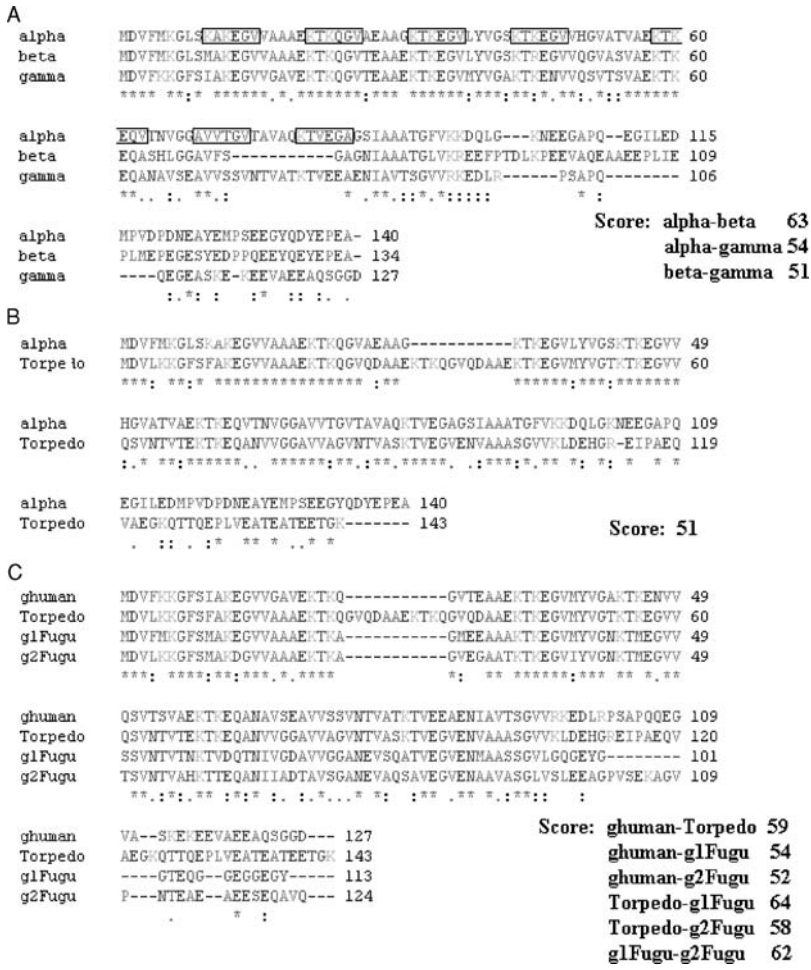

Figure 6.1 Human α-, β-, and γ-synucleins and synuclein from *Torpedo californica* and Fugu are aligned with ClustalW program. (A) Alignment of human α-, β-, and γ-synucleins. Repeats are shown in brackets. (B) Alignment of human α-synuclein with *Torpedo* synuclein. (C) Alignment of human γ-synuclein with *Torpedo* and Fugu synuclein.

isolated from this rat cDNA library and considered a rat orthologue of synuclein (Maroteaux *et al.*, 1988), while currently it can be assigned to α-synuclein. The authors drew a conclusion that the gene was specifically expressed in the central nervous system (CNS) of *Torpedo* and rat, and that its immunoreactivity is localized in the presynaptic nerve terminals and the nucleus. The predicted protein contained an 11-AA fragment that is repeated 7 times, followed by a 40–50 residue acidic tail (Figs. 6.1 and 6.2).

Although the authors of this first article about synucleins did not possess sophisticated methods of genomics and proteomics, the major conclusions from their results were correct and proved by other investigators. This includes the synuclein's localization to the presynaptic nerve terminals and nucleus, affinity of synuclein for membranes, inability to fold into a molecule capable of catalytic function, axonal transport of synuclein to the nerve terminals, the existence of several forms of synuclein with different molecular mass, and association of synuclein with synaptic vesicles. The Maroteaux's hypotheses about the role of synuclein in trafficking and the regulation of gene expression also deserve appreciation since these hypotheses were only based on the logic analysis of the synuclein structure and some indirect data. The idea put forth in one of the concluding sentences of this pioneering work may be considered as a program for many investigators who currently work in the synuclein project: ''One of the most interesting roles of the proteins may be to coordinate nuclear and synaptic events.''

A remarkable feature of the synucleins is that the majority of data about these proteins concerns their role in different types of pathology, while less is known about their functions in normal cells and tissues.

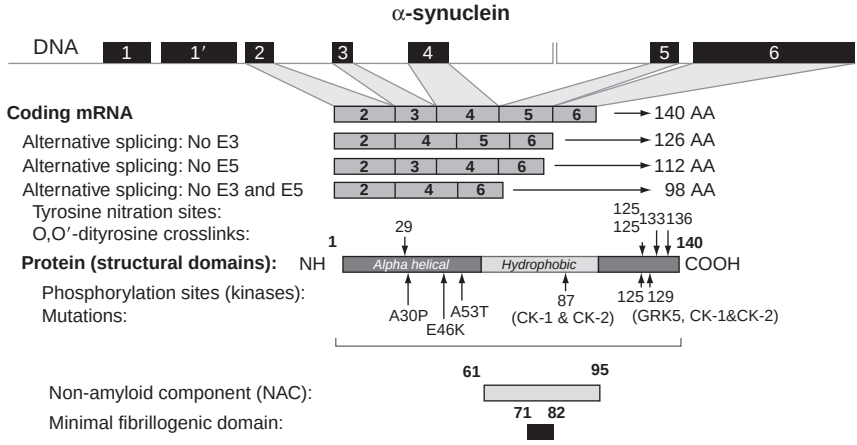

Figure 6.2 α-Synuclein gene, alternative RNA transcripts, and functional domains of α-synuclein. PTMs and AA substitutions as a result of mutations are shown in the central part of the scheme (modified from Dickson, 2001).

1.2. First 10 years after the discovery

After the publication of Maroteaux *et al.* (1988), a period of relatively low interest to synucleins continued for about 10 years. Nevertheless, during this decade, several important observations were made.

1. The detection of the non-Aβ-component of Alzheimer's disease (AD) amyloid (NAC) fragment corresponding to the central part of α-synuclein (AA 61–95, Fig. 6.2) in amyloid plaques was the first demonstration of the association between α-synuclein and neurodegenerative diseases (NDDs) (Uéda *et al.*, 1993, on Section 2.2.1.8, page 253).
2. Later, a 14-kDa phosphoneuroprotein (PNP14) found in rat and bovine was identified as a new member of the synuclein family (Nakajo *et al.*, 1993; Shibayama-Imazu *et al.*, 1993; Tobe *et al.*, 1992). Non-Aβ-component precursor of AD amyloid (NACP) and the human orthologue of the PNP14 were identified as two distinct synucleins and termed α-synuclein and β-synuclein, respectively (Fig. 6.1A) (Jakes *et al.*, 1994).
3. α-Synuclein was identified as a major component of proteinaceous inclusions, Lewy bodies (LB) and Lewy neurites (LN), (Figs. 6.3 and 6.4), the

```
Human     MDVFMKGLSKAKEGVVAAAEKTKQGVAEAAGKTKEGVLYVGSKTKEGVVHGVATVAEKTK 60
rat       MDVFMKGLSKAKEGVVAAAEKTKQGVAEAAGKTKEGVLYVGSKTKEGVVHGVTTVAEKTK 60
mouse     MDVFMKGLSKAKEGVVAAAEKTKQGVAEAAGKTKEGVLYVGSKTKEGVVHGVTTVAEKTK 60
Bovine    MDVFMKGLSKAKEGVVAAAEKTKQGVAEAAGKTKEGVLYVGSKTKEGVVHGVTTVAEKTK 60
Gallus    MDVFMKGLNKAKEGVVAAAEKTKQGVAEAAGKTKEGVLYVGSKTKEGVVHGVTTVAEKTK 60
Serinus   MDVFMKGLSKAKEGVVAAAEKTKQGVAEAAGKTKEGVLYVGSKTKEGVVHGVTTVAEKTK 60
Xenopus   MDVFKKGFSMAKEGVVAAAEKTKQGVTEAAEKTKEGVMYVGAKTKEGVVHSVSTVAEKTK 60
          **** **:. ****************:*** :*****:***::*******.*:*******

Human     EQVTNVGGAVVTGVTAVAQKTVEGAGSIAAATGFVKKDQLGK-NEEGAPQEGILED--MP 117
rat       EQVTNVGGAVVTGVTAVAQKTVEGAGNIAAATGFVKKDQMGK-GEEGYPQEGILED--MP 117
mouse     EQVTNVGGAVVTGVTAVAQKTVEGAGNIAAATGFVKKDQMGK-GEEGYPQEGILED--MP 117
Bovine    EQVTNVGEAVVTGVTAVAQKTVEGAGSIAAATGFGKKDHMGK-GEEGASQEGILED--MP 117
Gallus    EQVSNVGGAVVTGVTAVAQKTVEGAGNIAAATGLVKKDQLAKQNEEGFLQEGMVNNTDIP 120
Serinus   EQVSNVGGAVVTGVTAVAQKTVEGAGNIAAATGLVKKDQLAKQNEEGFLQEGMVNNTGAA 120
Xenopus   EQANVVGGAVVSGVNQVASKTVEGTENIVGTTGLVKKEDLHP----GQPEEPAAEE---- 112
          **.. ** ***:**. **.*****: .*..:**: **:.:      *  :*   ::

Human     VDPDNEAYEMPSEEGYQDYEPEA 140
rat       VDPSSEAYEMPSEEGYQDYEPEA 140
mouse     VDPGSEAYEMPSEEGYQDYEPEA 140
Bovine    VDPDNEAYEMPSEEGYQDYEPEA 140
Gallus    VDPENEAYEMPPEEEYQDYEPEA 143
Serinus   VDPDNEAYEMPPEEEYQDYEPEA 143
Xenopus   -EPAVEATESTEQVGDGEN---- 130
           :*  ** * . :    :
```

Figure 6.3 Alignment of α-synuclein from seven vertebrate species with the program ClustalW.

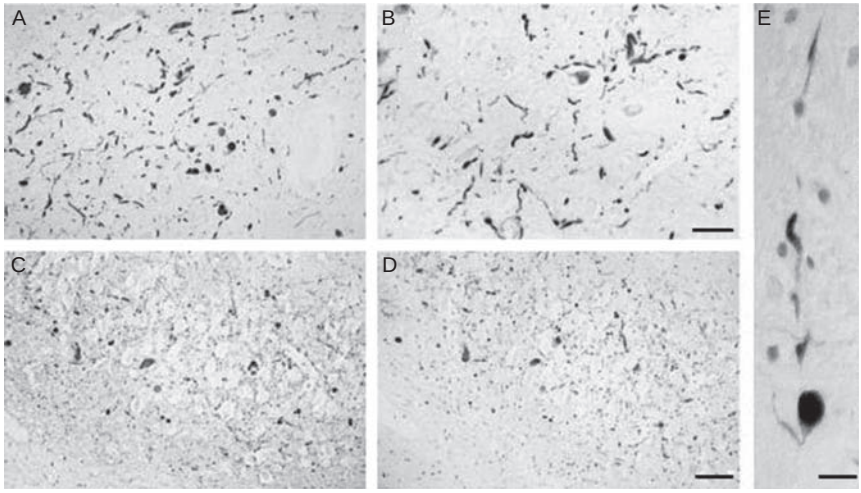

Figure 6.4 Tissue from patients with DLB immunostained for α-synuclein. (A and B) α-Synuclein-positive LB and LN in SNc stained with different Abs: PER1 (A) or PER2 (B). [Scale bar = 100 μm (in B for A and B).] (C and D) α-Synuclein-positive LN in hippocampus stained with Abs: PER1 (C) or PER2 (D). [Scale bar = 80 μm (in D for C and D).] (E) α-Synuclein-positive intraneuritic LB and LN in SNc stained with PER2. (Scale bar = 40 μm.) (From Spillantini *et al.*, 1998a.)

characteristic lesions in brains of patients with PD and dementia with Lewy bodies (DLB) (Arima *et al.*, 1998; Forno, L. S. (1996); Spillantini *et al.*, 1997, 1998a). Importantly, this localization was observed both in familial and sporadic cases of PD, which are not associated with α-synuclein mutations. α-Synuclein is also implicated in the pathogenesis of multiple system atrophy (MSA) (Arima *et al.*, 1998; Spillantini *et al.*, 1998b; Tu *et al.*, 1998), amyotrophic lateral sclerosis (ALS) (Mezey *et al.*, 1998), neurodegeneration with brain iron accumulation, type 1 (NBIA1) (Saito *et al.*, 2000; Wakabayashi *et al.*, 2000b), and Down's syndrome (Lippa *et al.*, 1999). The accumulation of α- and β-synucleins was also found in brain neurons and glial cells in lysosomal storage disease and peroxisomal disease, for example, adreno-leukodystrophy (Suzuki *et al.*, 2007). LB are present in patients with Gaucher disease, which is a lipid storage disease caused by a deficiency of the lysosomal enzyme glucocerebrosidase (Wong *et al.*, 2004). Several NDDs involving α-synuclein deposition are collectively known as ''synucleinopathy disorders'' (Galvin *et al.*, 2001a; Martí *et al.*, 2003).

4. Finally, a third member of the synuclein family has been identified in mammalian species (Fig. 6.1A) independently in several laboratories and termed breast cancer specific gene 1 (Ji *et al.*, 1997), persyn (Buchman *et al.*, 1998a), γ-synuclein (Lavedan *et al.*, 1998b), or synoretin

(Surguchov *et al.*, 1999). Finally, the name "γ-synuclein" became generally accepted for the purpose of consistency. γ-Synuclein is involved in several forms of cancer, some NDDs, and ocular pathology (Duda *et al.*, 1999; Galvin *et al.*, 2000; Jia *et al.*, 1999; Maurage *et al.*, 2003; Surguchov *et al.*, 2001a, 2005).

1.3. Second birth of synucleins: Prime time for α-synuclein

An important milestone in synuclein studies came 10 years after the first publication when two missense mutations in α-synuclein were found to be genetically linked to PD. Thus, 1997–1998 became the years signifying the second birth of synucleins. These findings have focused a great deal of interest on this protein family. Polymeropoulos *et al.* (1997) reported that a point mutation $G^{209}A$ corresponding to an AA substitution $Ala^{53}Tre$ ($A^{53}T$) in α-synuclein (Fig. 6.2) was genetically linked to early-onset, autosomal dominant familial PD. Although the mutation was found only in a small population, the high penetrance of this mutation made the finding very important. The significance of this finding was confirmed by identifying full-length α-synuclein as a major component in LB from postmortem brains of sporadic PD patients (Spillantini *et al.*, 1997). Description of a second linked point mutation $G^{88}C$ corresponding to a substitution $Ala^{30}Pro$ ($A^{30}P$) (Fig. 6.2) in rare cases of familial PD followed in 1998 (Krüger *et al.*, 1998). This finding confirmed the linkage of α-synuclein to PD. Later, the third point mutation $Glu^{46}Lys$ ($E^{46}K$) (Fig. 6.2) was detected in a Spanish kindred with familial PD (Zarranz *et al.*, 2004). Finally, the duplication and multiplication events in the gene encoding α-synuclein have been associated with rare inherited forms of autosomal dominant PD (Chartier-Harlin *et al.*, 2004; Ibáñez *et al.*, 2004; Nishioka *et al.*, 2006; Singleton *et al.*, 2003).

Thus, either point mutations or higher gene dosage of wild type (wt)-α-synuclein causes this disease. The data with gene duplication and triplication suggests a direct relation between α-synuclein gene dosage and disease progression. These findings provided strong evidence that α-synuclein plays a key role in the pathogenesis of PD, despite of a low frequency of mutations in its gene among PD patients. However, the studies of mutant forms of α-synuclein helped researchers to better understand molecular and cellular mechanisms underlying the wt-protein role in sporadic forms of diseases.

Another observation indicating the role of α-synuclein in PD pathogenesis is its deposition in LB in the pathological hallmark of PD/DLB disease. In addition to PD patients, α-synuclein depositions may be present in patients with other NDDs, which are collectively known as "synucleinopathy disorders." Currently two opinions exist explaining the role of α-synuclein in diseases. One group of researchers consider that α-synuclein

is involved in diseases through a gain of toxic function (Cookson and van der Brug, 2007; Galvin *et al.*, 1999, 2001a), whereas the other group presents the results supporting the opinion that their implication in pathology is due to a loss of defensive properties (Alves da Costa *et al.*, 2000; Manning-Boğ *et al.*, 2003). Whatever point of view is correct, α-synuclein is the predominant protein in LB in sporadic and familial cases of PD that is actively sequestered into these proteinaceous inclusions (Baba *et al.*, 1998; Mezey *et al.*, 1998; Spillantini *et al.*, 1997).

2. Synuclein Family: How and Why Proteins Form Families

Members of the synuclein family exist only in vertebrate and do not have ancestors or precursors in prokaryotic organisms. Although some similarity in AA sequence of α-synuclein with other proteins exists, for example, with the class-A2 lipid-binding domains of the apolipoproteins (Clayton and George, 1998; George, 2002), chaperone 14-3-3 (Ostrerova *et al.*, 1999), or small heat-shock proteins (Hsp) (Kim *et al.*, 2004), it can be found only in relatively short AA sequences and hardly can be considered as a proof of a common ancestor(s) for these proteins. The similarity of C-terminal region of α-synuclein to some chaperones may be responsible for its protective functions.

Thus, synucleins are different from the majority of other eukaryotic proteins that have been either inherited from prokaryotic precursors without drastic changes in biochemical function, but recruited for novel roles in the eukaryotic cells, or evolved due to extensive structural modifications (Aravind *et al.*, 2006). Therefore, they may be considered as molecular innovations of eukaryotes. The majority of such new eukaryotic proteins are α-helical and metal-supported structures, whereas synucleins are naturally unfolded proteins. The first synuclein precursor most probably appeared at the onset of eukaryotic evolution when the development of new forms of eukaryotes required sophisticated regulation of CNS functioning related to fundamental processes of synaptic transmission and plasticity.

The majority of proteins are organized hierarchically into families and superfamilies, reflecting an ancient and continuing process of gene duplication and divergence. Different members of a family are often characteristic of different tissues of the body, where they perform analogous but distinctive tasks. Each family in the course of evolution has evolved from a single ancestral gene by a process of duplication and divergence (Alberts *et al.*, 2002; Taylor and Raes, 2004). The creation of new genes by diversification and specialization of existing genes has been crucial for the evolution of multicellular organisms. The evolution of three members of

the synuclein family may be described as follows. A chromosome that contained one copy of synuclein ancestor gave rise, through an error of DNA replication, to a chromosome containing two copies of the ancestor synuclein gene in tandem. After mutations in a duplicated gene and recombination, a new member of the family located in a different chromosome. Then the ancestor synuclein gene underwent other mutations, duplication, and recombination once again giving rise to the third member of the synuclein family. Different properties of the members of the family and different pattern of tissue-specific expression ensure higher flexibility and adaptive capabilities for multicellular organisms.

An interesting hypothesis explains the existence of two proteins with similar sequences, but antagonistic properties, that is α- and β-synucleins by their role as a driving force for synaptic evolution. Fujita *et al.* (2006) assume that these two proteins function as chaperone and antichaperone. While antichaperone synuclein provokes stress-induced diverse responses, the chaperone may provide buffering for them, allowing accumulation of nonlethal phenotypic variations in synapses. Thus, dual synuclein system may cope with forthcoming stresses in the brain by stimulating adaptive evolution. The failure to regulate this process due to mutations, environmental risk factors, etc. may result in imperfect adaptability against stresses, leading to NDDs.

The only one exception from the rule ''three synucleins in each vertebrate'' is the pufferfish *Fugu rubripes*, which has four synuclein genes in its genome, α-, β-, and two γ-synucleins (γ1 and γ2) (Fig. 6.1C). They are expressed in the brain, range from 113 to 127 AA in length and share many of the characteristics of human synucleins. The existence of four genes may be explained by the duplication of the whole genome that took place 230 million years ago and the subsequent loss of duplicated genes. Interestingly, Fugu α-, γ1-, and γ2-synucleins have a higher propensity to fibrillate compared with human α-synuclein, whereas β-synuclein is unable to form fibrils (Yoshida *et al.*, 2006).

2.1. Synuclein genes

2.1.1. Human synuclein genes

The human α-, β-, and γ-synuclein genes map to chromosome 4q21.3-q22 (Campion *et al.*, 1995; Chen *et al.*, 1995; Shibasaki *et al.*, 1995), 5q35 (Spillantini *et al.*, 1995), and 10q23 (Lavedan *et al.*, 1998a,b; Ninkina *et al.*, 1998), respectively. The α-synuclein gene is organized as seven exons, five of which are protein-coding, whereas the β-synuclein gene has six exons (five protein-coding) and the γ-synuclein gene has five protein-coding exons (Lavedan, 1998). The size of exons range from 42 to 1110 base pairs. The translation start codon ATG is encoded by exon 2 and the stop codon TAA is encoded by exon 6. The NAC fragment is encoded by exon 4. Exon 1 has different splicing sites, producing different 5′-untranslated sequences in the cDNAs. The overall

organization of these genes is very well conserved (Figs. 6.1 and 6.2). The 5′-untranslated region (5′-UTR) of the α-synuclein gene contains an exon with two alternative spliced sites, which could be considered as two adjacent exons (exons 1 and 2) (Fig. 6.2). Alternative splicing has also been observed for exons 4 and 6 of the α-synuclein gene (Campion *et al.*, 1995; Uéda *et al.*, 1994).

The predominant isoform of α-synuclein in humans is composed of 140 AA. The second isoform, α-synuclein-126, is produced by an inframe deletion of exon 3 (AAs 41–54), while the third isoform, α-synuclein-112, by an inframe deletion of exon 5 (AAs 103–130) (Beyer, 2006) (Fig. 6.2). The transcript for α-synuclein-140 is the most abundant, followed by α-synuclein-112 and α-synuclein-126.

Recently, a new brain-specific splice variant α-synuclein-98 was identified (Beyer *et al.*, 2007), which lacks both exon 3 and 5 (Fig. 6.2). This isoform has a varying expression level in different areas of fetal adult brain with the highest expression in the adult temporal and parietal cortices and the fetal parietal cortex. α-Synuclein-98 is overexpressed in the frontal cortices of LB diseases and AD brains and supposedly possesses very high amyloidogenic properties (Beyer *et al.*, 2007).

2.1.2. High level of synuclein conservation in vertebrates

Across mammalian species in the evolutionary ladder, α-synuclein protein is highly conserved, even though synucleinopathy develops selectively in humans. From an evolutionary standpoint, the α-synuclein gene is an example of remarkable adaptation, since in many vertebrate species, position 53 in encoded protein is occupied by threonine (Fig. 6.5), whereas in Old World monkeys and humans, alanine is located in this position. Back position to a threonine in the human protein ($A^{53}T$ mutation) causes PD. Apparently the majority of vertebrate may tolerate threonine in position 53. Similarly to human gene, alternative splicing was described for rat α-synuclein. The three rat cDNAs, SYN1, SYN2, and SYN3, appear to be splice variants of the same gene (Maroteaux and Scheller, 1991; Maroteaux *et al.*, 1988) with the most homology to human α-synuclein. So far, no splice variant has been described for the β- and γ-synuclein genes.

Comparison of AA sequence of the α-synuclein from several species of mammals and birds shows substitutions in only 4 positions out of the first 84 residues in N-terminal part of the protein (Fig. 6.5, the first 6 lines). Only the human α-synuclein mRNA contains an IRE-like sequence in its 5′-UTR. Generation of the human α-synuclein transcript requires RNA splicing out of an intron that precisely interrupts the canonical S1-CAGUG3′ motif of the predicted 5′-UTR stem loop. Thus, it is possible that a unique role for α-synuclein in presynaptic redox and iron metabolism rapidly evolved in primates with selection for RNA splicing that favored a gain of posttranscriptional regulation for α-synuclein protein production.

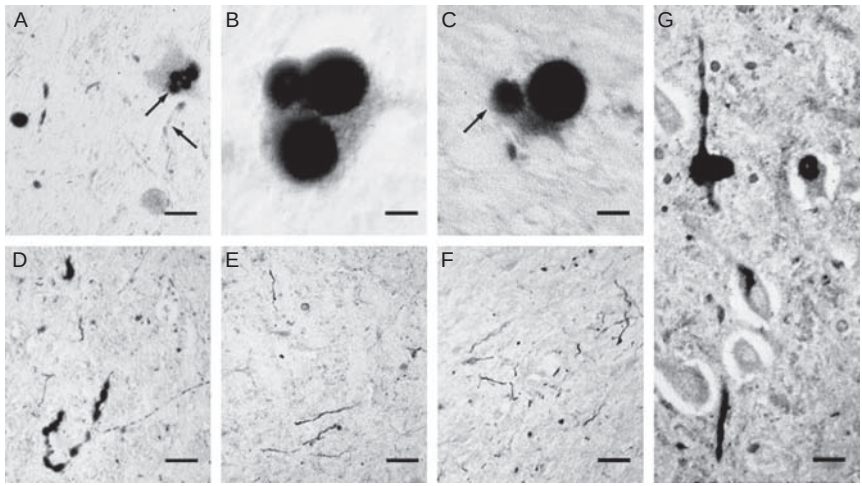

Figure 6.5 SNc from patients with PD (A–F) and cingulate cortex from a patient with DLB (G) immunostained for α-synuclein and ubiquitin (blue). (A) Nerve cell with four LB, three of which are double-stained for α-synuclein and ubiquitin, whereas one is immunoreactive only for α-synuclein (arrow). An LN neurite is stained only for α-synuclein (arrow) (scale bar = 30 μm). (B) Nerve cell with three LB that are double-stained for α-synuclein and ubiquitin. The halo of each LB is strongly immunoreactive for ubiquitin, whereas both the core and the halo of each LB are immunoreactive for α-synuclein (scale bar = 10 μm). (C) Nerve cell with two LB, one of which is double-stained for α-synuclein and ubiquitin, whereas one is immunoreactive only for α-synuclein (arrow) (scale bar = 13 μm). (D) LN double-stained for α-synuclein and ubiquitin (scale bar = 90 μm). (E and F) LN stained for α-synuclein by using Ab PER1 (E) and PER2 (F) (scale bar = 100 μm). (G) Intraneuronal and intraneuritic LB and LN double-stained for α-synuclein and ubiquitin. (Scale bar = 18 μm.) (From Spillantini *et al.*, 1998a.)

High level of conservation among vertebrates and absence of orthologues or homologues in invertebrate suggests that it is not essential for synaptic transmission per se, but may be evolved to perform an important function specific to vertebrates. Such function could be connected with a role in synaptic plasticity or another function of CNS existing only in vertebrates. This conclusion is supported by the relatively late translocation of α-synuclein into presynaptic terminals during synaptogenesis, after functional synapses have been established (Withers *et al.*, 1997).

2.1.3. Regulation of synuclein expression

2.1.3.1. α-synuclein α-Synuclein is a protein that is expressed abundantly and developmentally regulated in the CNS. In the rodent CNS, mRNA expression levels begin to rise at late embryonic stages and reach a peak in the first weeks of postnatal life, after which mRNA level begins to go down (Kholodilov *et al.*, 1999; Petersen *et al.*, 1999). Various stimuli and regulatory elements have been shown to regulate α-synuclein level in adult rodents *in vivo* (Kholodilov *et al.*, 1999; Manning-Boğ *et al.*, 2002; Vila *et al.*, 2000).

α-Synuclein is upregulated by growth factors, for example, nerve growth factor (NGF) and basic fibroblast growth factor (bFGF) (Clough and Stefanis, 2007), and by DA (Gómez-Santos *et al.*, 2005). This pathway involves JNK and p38 that might act through *cis*-elements in intron 1 of the gene and may be regulated by C/EBP*β*. The response elements for MAP/ERK pathway (NGF-RE1 and NGF-RE2), including a putative promoter, lie within intron 1. The PI3 kinase pathway is also involved in α-synuclein regulation; however, response elements for this pathway are located outside of intron 1. Most of the attention regarding the promoter region of α-synuclein has been focused on the NACP-Rep1 region located upstream of the start site (Section 2.1.5, page 240).

2.1.3.2. β-synuclein The promoter organization and transcriptional regulation of *β*-synuclein have not been studied in detail. However, the data on tissue distribution of α-, *β*-, and *γ*-synucleins suggests that the patterns of α- and *β*-synucleins are similar, whereas *γ*-synuclein has different pattern of expression and regulation.

2.1.3.3. γ-synuclein *γ*-Synuclein is almost absent in normal or benign breast lesions, but expressed at an extremely high level in the vast majority of the advanced staged breast carcinomas and ovarian cancer (Ji *et al.*, 1997; Lavedan, 1998). The abnormal expression of *γ*-synuclein in breast cancer cells is regulated by multiple transcriptional mechanisms.

Lu *et al.* (2001) isolated a 2195-bp fragment of human *γ*-synuclein gene containing 1 kb of 5′-flanking region, exon 1, and intron 1. By analyzing the promoter activity and the methylation status of the exon 1 region, the authors demonstrated that intron 1 plays a critical role in the control of *γ*-synuclein gene transcription through *cis*-regulatory sequences that affect *γ*-synuclein transcription in cell type-specific and cell type-nonspecific manners. Furthermore, the activator protein-1 (AP-1) is involved in *γ*-synuclein transcription in breast cancer cells through its binding to an AP-1 site (TGACTCA) in the intron 1. Importantly, the exon 1 region of *γ*-synuclein gene contains a CpG island that is unmethylated in *γ*-synuclein positive cells but methylated in *γ*-synuclein negative cells. Thus, transcription activators and repressors that interact with the *cis*-regulatory sequences present in the intron 1 contribute to the tissue-specific expression of *γ*-synuclein. Demethylation of exon 1 is an important factor responsible for the aberrant expression of *γ*-synuclein in breast carcinomas.

Further studies showed the existence of two closely located AP1-binding sites in the first intron of the *γ*-synuclein gene. Mutation of either AP1 motif in the *γ*-synuclein promoter reduces the promoter activity. 12-*O*-tetradecanoylphorbol-13-acetate increases *γ*-synuclein mRNA expression through the intronic AP1 sites. Inhibition of *γ*-synuclein expression by

blocking AP1 transactivation caused cell growth inhibition similar to the effect of γ-synuclein antisense mRNA (Lu *et al.*, 2002).

The 5′-flanking region of γ-synuclein provides the basal transcriptional activity without cell type specificity. A critical promoter element involved in abnormal expression of γ-synuclein is located in the first exon. The cell type specificity of transcription is affected through intronic *cis*-regulatory sequences. AP1 domains in the first intron play an important role in control of γ-synuclein transcription (Lu *et al.*, 2006). Cytokine oncostatin M affects γ-synuclein transcription presumably through the intronic AP1 sites. These studies demonstrate that AP1 is a key positive regulator in γ-synuclein transcription in breast cancer cells through specific interaction with two closely located AP1 sites residing in the first intron of the gene.

2.1.4. Mutations in synuclein genes

2.1.4.1. α-synuclein gene Some data about mutations in α-synuclein gene are already discussed in the Chapter I, C. The roles of $A^{53}T$ and $A^{30}P$ substitution have been extensively investigated both *in vitro* and *in vivo* and have provided important insights into the pathogenic pathways underlying the mechanism of PD. $A^{53}T$ mutation accelerates fibril formation relative to both wt- and $A^{30}P$ substitution. The effect of the $A^{30}P$ mutation on filament assembly is less evident. In different studies, this effect was either small (Narhi *et al.*, 1999) or absent (Serpell *et al.*, 2000). Interestingly, $A^{30}P$, but not $A^{53}T$, substitution reduces the level of α-synuclein binding to brain vesicles (Jensen *et al.*, 1998). Patients harboring the $A^{53}T$ mutation exhibit neuronal death, gliosis, and extensive LN in other parts of the brain including the cortex and hippocampus (Spira *et al.*, 2001). The $E^{46}K$ mutation significantly increases binding of α-synuclein to negatively charged liposomes and enhances the rate of filament assembly to similar level as the $A^{53}T$ mutation (Choi *et al.*, 2004; Greenbaum *et al.*, 2005).

The finding of the role of duplication/triplication of α-synuclein in PD (Chapter I, C) was essential for the understanding of its pathogenesis. Importantly, an increase of blood α-synuclein was detected in patients with gene triplication (Miller *et al.*, 2004). Patients with synuclein gene di/triplication often display prominent extranigral pathology, typical of DLB (Miller *et al.*, 2004; Singleton *et al.*, 2003).

Recently, Ahn *et al.* (2008) described α-synuclein gene duplication in sporadic (without positive family history) PD patients among Korean population. Although the frequency of such duplication was as low as 0.23% (2 of 869 patients with sporadic PD), these results further confirm the existence of direct cause-and-effect correlation between α-synuclein expression level and PD risk. Low penetrance, clinical heterogeneity, and normal DA transporter imaging in asymptomatic carriers suggest the role of

other genetic modifiers or environmental factors in the pathogenesis of PD due to α-synuclein gene duplication described by Ahn *et al.*

2.1.4.2. β-synuclein genes Two AA alterations in a conserved regions of β-synuclein genes in unrelated DLB patients are described, that is a valine to methionine substitution at codon 70 ($V^{70}M$) and a proline to histidine substitution at codon 123 ($P^{123}H$) (Ohtake *et al.*, 2004). Cosegregation analysis of an extended pedigree segregating the $P^{123}H$ β-synuclein alteration suggests that it is a dominant trait with reduced penetrance or a risk factor polymorphism. Histopathology and immunohistochemistry (IHC) analysis of index case brain sections revealed widespread LB pathology and α-synuclein aggregation without evidence of β-synuclein aggregation (Ohtake *et al.*, 2004). The authors draw a conclusion that mutations in the β-synuclein gene may predispose to DLB.

2.1.5. Polymorphisms in synuclein genes

A dinucleotide repeat polymorphic marker (REP1) with allele-length variability has been mapped to 8 kb upstream of the transcription start site in α-synuclein gene. Several studies observed an association of REP1 of the α-synuclein gene promoter with PD susceptibility (Tan *et al.*, 2004). However, other investigations did not confirm this association (Parsian *et al.*, 1998; Spadafora *et al.*, 2003). Thus, most probably, the length of tandem repeats in this region is associated with the risk of developing PD in some, but not all, populations. Recently, Maraganore *et al.* (2006) showed an association of the allele-length variability in the REP1 with PD susceptibility. Genotypes that included the 263 bp allele were associated with an increased risk for PD, whereas genotypes that included the 259 bp allele were associated with a reduced risk for PD. On the other hand, dinucleotide repeat sequence genotypes had no effect on the age at onset of PD overall ($p = 0.55$) (Maraganore *et al.*, 2006).

α-Synuclein gene expression varies significantly over a threefold range across the different REP1alleles, suggesting that the association of specific genotypes with an increased risk for PD may result from an increase in α-synuclein mRNA transcription (Chiba-Falek and Nussbaum, 2001; Chiba-Falek *et al.*, 2003). The recent finding of α-synuclein gene triplication as a rare cause of PD (Singleton *et al.*, 2003) suggests that polymorphism within the gene promoter may confer susceptibility via the same mechanism of gene overexpression. These results are in a good agreement with the results obtained in a yeast model, where a twofold difference in expression of the α-synuclein gene was sufficient to cause a catastrophic change in α-synuclein localization and resulted in the formation of cytoplasmic inclusions and cell death (Outeiro and Lindquist, 2003). The correlation between gene dosage and PD suggests that pharmacological manipulations

affecting α-synuclein expression level might be considered as therapeutic or preventive strategies.

In addition to polymorphisms in the promoter region of α-synuclein gene, an increased risk for idiopathic PD is also associated with polymorphisms in other in noncoding and coding regions of α-synuclein gene. Mueller *et al.* (2005) analyzed more than 50 single-nucleotide polymorphisms (SNPs) across the α-synuclein gene and found a strong association of a haplotype block including exons 5 and 6 as well as 5′-UTR with PD. SNP rs356219 in the 3′-region of α-synuclein gene has a significant effect on mRNA level in substantia nigra pars compacta (SNc) and cerebellum, while ''protective'' genotype 259/259 of the PD-associated promoter repeat NACP-Rep1 is associated with lower protein levels in blood than genotypes 261/261, 259/261, and 259/263. Thus, α-synuclein levels are influenced by genetic variability in the promoter and 3′-region of the α-synuclein gene (Fuchs *et al.*, 2007).

Variable poly-T sequence in intron 2 in the vicinity of exon 3 of the human gene may be represented by three different alleles (Beyer *et al.*, 2007). The level of expression of α-synuclein-126 mRNA, an isoform lacking exon 3, depended on the length of poly-T stretch. The shortest poly-T stretch (5T) was associated with the lowest level of α-synuclein expression, while 12T poly-T stretch ensured the highest level of expression. The most frequent 7T allele was associated with the medium level of expression (Beyer *et al.*, 2007). Since this polymorphism is related to the expression of α-synuclein-126 mRNA, lacking exon 3, it is possible that the length of poly-T stretch affects the efficiency of the exon 3 splicing. Frieling *et al.* (2007) described a decreased α-synuclein expression in patients with anorexia nervosa, which was associated with a DNA hypermethylation of the α-synuclein promoter. These results suggest that α-synuclein may be also implicated in eating disorders.

A possible association of two SNPs in β-synuclein gene with PD was analyzed by Brighina *et al.* (2007). One of them located in promoter region of the gene was associated with a delayed age at onset of PD in women. Therefore, the β-synuclein locus, though not a susceptibility gene for PD, might modify the age at onset of PD. Since this polymorphism is located in 5′-region, it is tempting to speculate that a differential regulation of β-synuclein gene transcription upon interaction with estrogens might account for the association of polymorphic variant with age at onset in women only. Two linked polymorphisms in the coding region of the γ-synuclein gene were detected, both in mRNA and exons III and IV of the gene (Ninkina *et al.*, 1998).

2.2. Synuclein proteins

2.2.1. Structural properties

α-Synuclein has a much larger Stokes radius (34 Å) but sedimented more slowly (s20, w = 1.7S) than globular proteins of similar M_r, indicating that the native protein is elongated, rather than globular (Weinreb *et al.*, 1996). According to MALDI-TOF, its molecular mass is 14,463, which is close to molecular mass predicted from AA sequence. However, the mobility of α-synuclein in electrophoresis in polyacrylamide gel in the presence of sodium dodecylsulphate corresponds to the apparent mass of ~19 kDa, which can be attributed to the abnormally low binding to SDS of the unfolded and acidic C-terminal fragment and partially to PTMs.

Analysis of α-synuclein by circular dichroism, ultraviolet, and Fourier transformed infrared spectroscopy confirmed its natively unfolded (random coil) secondary structure in aqueous solution (Uversky *et al.*, 2002; Weinreb *et al.*, 1996). The central hydrophobic region of α-synuclein is critical for β-sheet formation (Lin *et al.*, 2006). Both $A^{53}T$ and $A^{30}P$ mutants undergo self-association more readily than the wt, that is, at lower protein concentration and more rapidly (Li *et al.*, 2001). According to far-ultraviolet circular dichroism method, at neutral pH and physiological conditions, all three synucleins show spectra typical of an essentially unfolded polypeptide chain, but adopted identical partially folded conformations under conditions of acidic pH or high temperature (Li *et al.*, 2002).

While β-synuclein exhibits the properties of a typical random coil, α and γ-synucleins are slightly more compact and structured (Uversky *et al.*, 2002). Structurally, α-, β-, and γ-synucleins share a common design composed of three modular protein domains providing thereby an amphiphilic triblock polypeptide: (1) Over half of the synuclein molecule comprises a highly conserved N-terminal lipid-binding α-helix (residues 7–87) with high content of basic residues. Positively charged N-terminal part contains recurring 11 residue sequence that includes 7 imperfectly repeated hexamer (KTKEGV) motifs. This region is very similar in all three members of the synuclein family (Fig. 6.1). (2) A variable internal hydrophobic NAC domain (residues 61–95) comprises the highly hydrophobic NAC domain, which is essential for α-synuclein aggregation and by itself can readily form amyloid fibrils (Giasson *et al.*, 2001; Yoshimoto *et al.*, 1995). Partial deletion of the NAC region in β-synuclein made this protein nonamyloidogenic (Figs. 6.1 and 6.2). (3) The less-conserved C-terminal region of α-synuclein (residues 96–140) is characterized by a high content of acidic stretches residues (Fig. 6.1). This C-terminal part regulates amyloid aggregation and is located on the fibril surface. Residues 109–140 are organized as a tandem repeat of 16 residues that constitutes specific binding sites for Ca^{2+}, Cu^{2+}, and other cations (Hoyer *et al.*, 2004). This part is relatively resistant to proteolytic degradation.

The strong fibrillation propensity of α-synuclein is not shared by β- or γ-synuclein. β-Synuclein does not aggregate at all, while γ-synuclein can form amyloid fibrils at much higher concentrations and at a slower rate than α-synuclein. In addition, both β- and γ-synucleins inhibit α-synuclein fibrillation *in vitro* (Uversky *et al.*, 2002). The structure of α-synuclein allows the molecule to exist either in a poorly structured conformation or as an α-helix in the presence of phospholipids (Chandra *et al.*, 2003; Perrin *et al.*, 2000), suggesting highly dynamic changes depending upon the local cellular milieu. According to recent nuclear magnetic resonance (NMR) studies, the lipid-binding domain is composed of two α-helices when bound to phospholipids or synthetic membranes (Ulmer and Bax, 2005; Ulmer *et al.*, 2005).

Amphipathic N-terminal region of α-synuclein bears some similarity in AA sequence to the lipid-binding class A apolipoproteins A2 and C1–3 involved in lipid transport (Davidson *et al.*, 1998). Like α-synuclein, apolipoproteins have a highly unordered structure in the absence of lipids and adopt an α-helical structure upon lipid binding (Morrisett *et al.*, 1977). Another similarity between synucleins and apolipoproteins is that both groups of proteins are prone to form amyloid due to their unfolded structure (Hatters and Howlett, 2002). Apolipoproteins interact and may colocalize with amyloid and, similar to α-synuclein, are the components of AD plaques and LBs (Spillantini *et al.*, 1997).

NMR and X-ray crystallography studies of synuclein fibrils are limited because amyloid fibrils are insoluble and noncrystalline. However, the structure of α-synuclein fibrils can be studied by solid-state NMR spectroscopy (Heise *et al.*, 2005; Kloepper *et al.*, 2007a). This method shows that α-synuclein fibrils have weak cross-polarization signals at room temperature due to the local molecular dynamics. Low temperature enhances signal intensities while retaining high resolution (Kloepper *et al.*, 2007a). Dried samples of α-synuclein fibrils yield spectra with similar chemical shifts relative to those of hydrated fibrils, suggesting that an atomic-resolution structure is unaltered upon dehydration (Kloepper *et al.*, 2007b). At the same time, spectral sensitivity is enhanced for dehydrated samples because of the larger quantity of dried protein packed into NMR rotor. Therefore, water is nonessential to the core structure of α-synuclein fibrils.

2.2.1.1. α-synuclein α-Synuclein is an abundant acidic neuronal protein that is composed of 140 AAs in human and rodents (Fig. 6.1), and 143 in *S. canaria* (Jakes *et al.*, 1994; Spillantini *et al.*, 1997, 1998a). It has been estimated to account for as much as 0.1% of the protein in the homogenate (Shibayama-Imazu *et al.*, 1993) or 1% of the total protein in soluble cytosolic brain fractions (Iwai *et al.*, 1995). α-Synuclein is extremely heat-resistant and natively unfolded. The human and rodent sequences are 95.3% identical. One of the only six AA differences is at position 53, which is

normally an alanine in humans and threonine in rodents. Interestingly, it is the same substitution, Ala-53-Thr, that was observed in some familial cases of PD (Fig. 6.5) (Polymeropoulos *et al.*, 1997). The mouse and rat α-synuclein proteins differ by a single AA at position 121. The synuclein orthologue in zebra finches-synelfin protein is 86.7% and 85.3% identical to the human and rodent α-synucleins, respectively. The amphipathic N-terminal and the hydrophobic NAC regions are highly conserved between species, whereas the C-terminal region is highly variable in size and sequence (Davidson *et al.*, 1998; George, 2002).

2.2.1.2. β-synuclein *β*-Synuclein proteins are 134 AAs long and are the most conserved of the synuclein proteins (Fig. 6.1). Importantly, they lack 11 AAs in the region corresponding to the NAC35 peptide found in plaques of AD patients, which extends from residues 61 to 95 of α-synuclein. Mouse and rat *β*-synuclein proteins are identical and share 97.8% identity with the human *β*-synuclein. The bovine PNP14 is 97% and 98.5% identical to the human and rodent *β*-synuclein. *β*-Synuclein is phosphorylated in the rat brain, presumably by the Ca^{2+} calmodulin protein kinase II (Nakajo *et al.*, 1993). A possible phosphorylation site is the serine residue at position 118, which is conserved throughout species in the *β*-synuclein sequence but not in the α- or *γ*-synuclein.

2.2.1.3. γ-synuclein The *γ*-synuclein protein is the least conserved of the synuclein proteins. The human *γ*-synuclein is 127 AAs long (Fig. 6.1), and is 87.7% and 83.8% identical to the mouse and rat proteins, respectively, which are 4 AAs shorter. As for the α- and *β*-synuclein proteins, the region of highest homology is the N-terminal region. The Torpedo synuclein protein identified as the first synuclein by Matoteaux *et al.* (1988) is 143 AAs long, including a central fragment KTKQGVQDAAE absent in the other synuclein proteins (Fig. 6.1B). This fragment, however, may be a result of cloning artifact (Yoshida *et al.*, 2006). Besides this duplication, the Torpedo synuclein is 75.3% identical to the N-terminal portion of the human *γ*-synuclein. The last 35 AAs have little homology with the human or rodent *γ*-synucleins.

Despite a strong sequence similarity between the amyloid-forming regions of α- and *γ*-synucleins, human *γ*-synuclein has only a weak propensity to form amyloid fibrils (Biere *et al.*, 2000; Giasson *et al.*, 2001; Serpell *et al.*, 2000). *γ*-Synuclein has an increased α-helical propensity in the amyloid-forming region that is critical for α-synuclein fibrillation, suggesting that increased structural stability in this region may protect against *γ*-synuclein aggregation. Despite a similar AA sequence, there are significant differences in secondary structure between α- and *γ*-synucleins. One possible explanation for this is that disordered regions simply evolve faster than folded regions due to their reduced tertiary contacts (Marsh *et al.*,

2006). γ-Synuclein is colocalized with neurofilaments in the axons (Ninkina *et al.*, 2003) and affects neurofilament network integrity, probably by increasing the susceptibility of neurofilament-H to calcium-dependent proteases (Buchman *et al.*, 1998b).

2.2.1.4. Synucleins are natively unfolded proteins Synucleins have little or no ordered structure under physiological conditions mainly because of the electrostatic repulsion between the net negative charges and low intrinsic hydrophobicity. Natively unfolded proteins are characterized by a unique combination of low overall hydrophobicity and large net charge (Uversky *et al.*, 2000, 2001b; Weinreb *et al.*, 1996). At the same time, fibrillar and some prefibrillar oligomeric forms of this protein are highly structured (Conway *et al.*, 2000a,b; Li *et al.*, 2001; Volles *et al.*, 2001). Unfolded proteins, under conditions of extreme pH values or elevated temperature, can be transformed into more compact, structured conformations when the net electrostatic repulsion is reduced by the binding of oppositely charged ions (Uversky *et al.*, 2001b).

2.2.1.5. Lipid and membrane binding Monomeric α-synuclein exists in equilibrium between free and plasma membrane or vesicle-bound states (McLean *et al.*, 2000). The amount of membrane-bound α-synuclein was calculated to be 15% (Lee *et al.*, 2002a). Both overexpression of α-synuclein and its depletion are accompanied by alterations in membrane properties, including fluidity and fatty acid (FA) uptake (Castagnet *et al.*, 2005; Golovko *et al.*, 2005; Sharon *et al.*, 2001).

Due to its structural features and homology to FA-binding protein, α-synuclein is able to bind FA and participate in FA metabolism and transport (Sharon *et al.*, 2001). This α-synuclein property may be important for the fulfillment of its synaptic functions since FA are highly enriched in synaptic vesicles. α-Synuclein can transfer FA from the aqueous environment to sites of synaptic vesicle formation, for example, early endosomes or other intracellular destinations. Cells that either overexpress or entirely lack α-synuclein have an altered FA composition compared to the normal cells (Sharon *et al.*, 2003). A disruption of FA uptake and trafficking was detected *in vivo* in astrocytes from α-synuclein gene-ablated mice (Castagnet *et al.*, 2005). However, the analysis of *in vitro* interactions of α-synuclein with FA using NMR spectroscopy and electron microscopy suggests that α-synuclein is unlikely an intracellular FA carrier (Lücke *et al.*, 2006).

α-Synuclein could also modulate the turnover of polyunsaturated FA acyl groups, which have been implicated in clathrin-mediated endocytosis. After binding to synthetic vesicles containing polyunsaturated FA acyl groups, α-synuclein multimerizes and adopts a β-rich structure (Perrin *et al.*, 2001). By binding to synaptic vesicles and stabilizing their lipid and protein fine structure, α-synuclein may tune neurotransmission, regulate

synaptic vesicle recycling at the nerve terminal, and transfer FA to membrane compartments where vesicles are formed (Chandra *et al.*, 2005; Nuscher *et al.*, 2004). In lipidosis, α-synuclein and sometimes β-synuclein accumulate in neurons and glial cells in places of lipid storage (Suzuki *et al.*, 2007).

2.2.1.6. Mechanism of α-synuclein aggregation, fibrillation, and toxicity A natively unfolded protein, α-synuclein, can adopt different conformational states and different aggregated morphologies, including small aggregates, oligomers, spherical and linear protofibrils, and fibrils. The aggregation process initially forms oligomeric species that are relatively soluble; these oligomers might then self-assemble into fibrillar structures that are insoluble (Conway *et al.*, 1998; Giasson *et al.*, 1999). The small oligomeric aggregates and prefibrillar oligomers rather than the mature fibrils have been shown to be particularly toxic (Emadi *et al.*, 2007; Lashuel *et al.*, 2002; Takeda *et al.*, 2006; Volles and Lansbury, 2003). Another viewpoint suggests that protofibrils and/or protofibril rings are actually the pathogenic species, whereas fibrils are innocuous (or less toxic) (Bucciantini *et al.*, 2002; El-Agnaf *et al.*, 2003, 2004). The cellular membranes are the primary targets injured by protofibrils (Furukawa *et al.*, 2006). Several mechanisms for α-synuclein aggregation have been proposed, that is those involving the ubiquitin proteasome system (UPS) and oxidative stress have gained the most prominence now.

Aggregated α-synuclein can undergo sequestration and form proteinaceous inclusions [LBs in PD, glial cytoplasmic inclusions (GCI) in MSA], the role of which in the pathogenesis of NDDs is a matter of discussion. According to one point of view, neurons with LB are more compromised and the presence of inclusion bodies leads to cell dysfunction and death (Beyer and Ariza, 2007; Lu *et al.*, 2005). As an example of a negative role of LB in neurons, Lu *et al.* (2005) report that LB-positive DA neurons are sicker than their LB-negative counterparts. Alternatively, these inclusions may protect the cell from toxicity of soluble misfolded proteins (Tompkins *et al.*, 1997). It is also possible that LB formation is an epiphenomenon, induced by neuronal death. Finally, it is possible that LB are inert product.

Wt-α-synuclein and its mutated forms ($A^{53}T$ and $A^{30}P$) produce different amyloid fibrils in the course of self-aggregation (Wood *et al.*, 1999). Several differences in the aggregation behavior of the PD-linked mutants and the wt-protein have been documented. Monomeric α-synuclein aggregates *in vitro* are able to form stable fibrils via a metastable oligomeric (i.e., protofibril) state (Volles and Lansbury, 2002). The protofibrillization rate of $A^{53}T$ and $A^{30}P$ mutants is higher than that of wt- protein; the fibrillation rate is lower in $A^{30}P$ and higher in $A^{53}T$ (Conway *et al.*, 2000a,b). α-Synuclein is more fibrillogenic than β- and γ-synucleins and

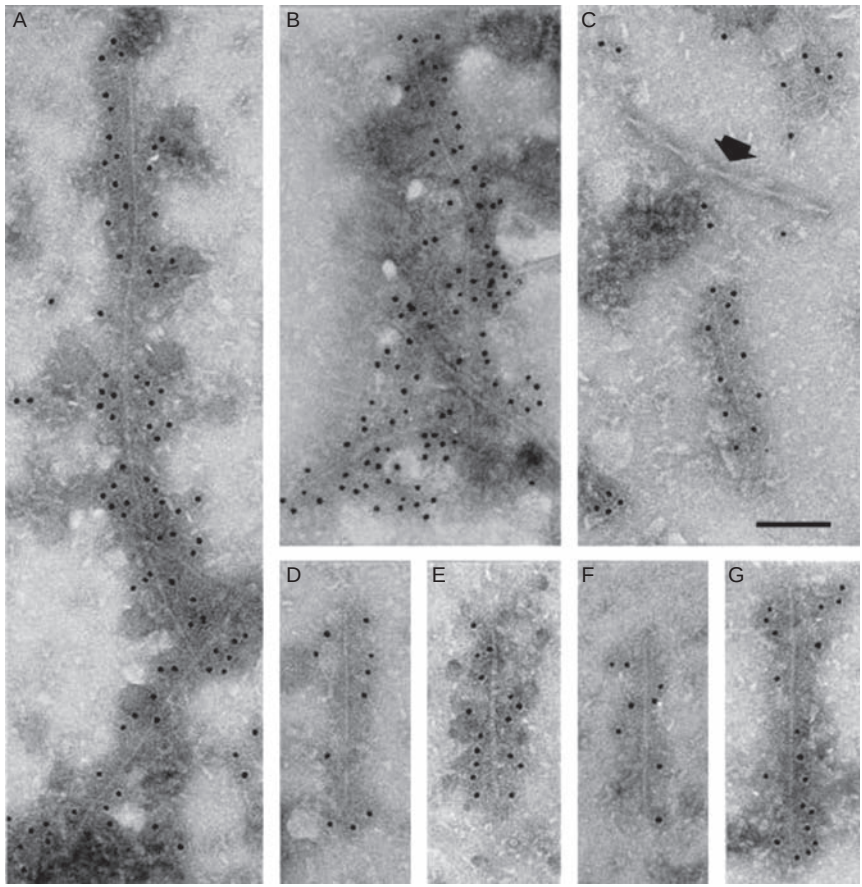

Figure 6.6 Filaments from cingulate cortex of patients with DLB labeled with anti-α-synuclein Ab. The gold particles conjugated to the second Ab appear as black dots. (A and B) Small clumps of labeled α-synuclein filaments. (C) A labeled α-synuclein filament and an unlabeled paired helical filament (arrow). The labeled filaments have various morphologies, including 5-nm filament (D); 10-nm filament with dark stain-penetrated center line (E); twisted filament showing alternating width (F); 10-nm filament with slender 5-nm extensions at ends (G, also C). [Scale bar = 100 nm (C).]

cannot cross-seed its homologues; β- and γ-synucleins inhibit α-synuclein fibril formation (Biere *et al.*, 2000; Uversky *et al.*, 2002).

Analysis of synuclein aggregation and fibrilization. Filaments containing α-synuclein as a major component can be detected in the brain of patients with NDDs by immunolabeling with anti-α-synuclein antibody (Ab) with the subsequent treatment by gold particles conjugated to the second Ab (Fig. 6.6). These filaments are 50–700 nm long and have various

morphologies, including a 5-nm straight filament and 10-nm filaments both straight and twisted (Spillantini *et al.*, 1998a).

α-Synuclein amyloid fibrils can be detected by fluorescence emission of specific fluorescent probes. The benzothiazole dye Thioflavin T and sulfonated azo dye Congo Red or its derivatives are most commonly used (Naiki *et al.*, 1989). Recently, a new fluorescent probes with higher emission intensity and selectivity to aggregated α-synuclein were developed suitable for detection of fibrillar α-synuclein (Volkova *et al.*, 2007). The study of full-length α-synuclein fibrillation by atomic force microscopy (AFM) demonstrated initial formation of protofilaments, two of which interact to form a protofibrils and two protofibrils assemble into mature fibrils (Khurana *et al.*, 2003).

Sequence determinants for fibrillogenesis of α-synuclein. A key role in the process of α-synuclein fibrillation is played by a 35-AA fragment that comprises the hydrophobic core of the protein (Iwai *et al.*, 1995), originally isolated from brain tissue of AD patients (Uéda *et al.*, 1993). However, the study of fibril structures by physicochemical methods demonstrated that the core region of α-synuclein involved in the fibril core is approximately two times longer (Heise *et al.*, 2005; Zibaee *et al.*, 2007). Qin *et al.* (2007) digested α-synuclein fibrils by trypsin and endoproteinase GluC and analyzed the morphology of the fibril remnants. They also used N- and C-terminal truncated forms of α-synuclein for fibril formation and investigation of their structure by AFM. The results allowed to identify α-synuclein region located between AA 32 and 102 that is involved in the assembly of the *β*-rich core of the protofilaments. The two terminal regions did not participate in the assembly of the protofilament core, but play a role in the interactions between protofilaments necessary for fibril maturation.

Zibaee *et al.* (2007) investigated the importance of different determinants in synuclein molecule for amyloid fibrillogenesis and confirmed previously published data (Biere *et al.*, 2000; Giasson *et al.*, 2001; Serpell *et al.*, 2000; Uversky *et al.*, 2002) about lower fibrillogenic propensity of *β*-synuclein compared to α-synuclein. They found that the deletion of AA residues 73–83 from α-synuclein did not abolish filament formation. Interestingly, a chimera composed of *β*-synuclein with α-synuclein (73–83) inserted had significantly lower fibrillogenic propensity than the wt-α-synuclein. Therefore, the presence of AA residues 73–83 in α-synuclein is not sufficient to explain the difference in fibrillogenic propensity between α- and *β*-synucleins. Deletion of AA residues 71–82 from α-synuclein abolished fibril assembly pointing to the important role of $V^{71}T^{72}$ in α-synuclein assembly into fibrils. Corresponding position in *β*-synuclein is occupied by $F^{71}S^{72}$ and in *γ*-synuclein by $V^{71}S^{72}$. Another important region of α-synuclein for fibril assembly is located near AA 45–46. Analysis of fibrillogenesis of different chimeras shows that the presence of the C-terminal region of *β*-synuclein affects the lag time, but is not sufficient to account for

the low fibrillogenic propensity of β-synuclein. These results suggest the existence of a correlation between fibrillogenic propensity and overall AA composition (Zibaee *et al.*, 2007). In other studies, the importance of AA residues 61–95 and 27–58 in α-synuclein aggregation was found (Tartaglia *et al.*, 2005). The filament morphologies of α-synuclein mutants and chimeras were different depending on AA sequence.

A central hydrophobic region of α-synuclein facilitates self-association and aggregation. The C-terminal tail of α-synuclein, on the other hand, inhibits aggregation, and a truncated form of the molecule is more aggregation-prone. Both the $A^{53}T$ (Conway *et al.*, 1998) and the $E^{46}K$ (Greenbaum *et al.*, 2005), but not the $A^{30}P$ mutation, significantly promotes protofibril formation. α-Synucleinopathic lesions contain a large amount of phosphorylated α-synuclein. Furthermore, phosphorylation of α-synuclein at Ser^{129} promotes fibril formation *in vitro* (Fujiwara *et al.*, 2002). When α-synuclein is overexpressed, most of the proteins end up as cytoplasmic inclusions rather than making their way to the cell membrane. Two distinct types of aggregates are observed, first the large juxtanuclear inclusion bodies (containing α-synuclein fibrils) and the other smaller, nonfibrillar spherical α-synuclein aggregates that are scattered throughout the cytoplasm (Lee and Lee, 2002).

2.2.1.7. α-synuclein forms pore-like structure or ion channels Detergent-resistant α-synuclein oligomers are a consistent pathological hallmark of PD and other α-synucleinopathies (Campbell *et al.*, 2001; Pountney *et al.*, 2004). Annular α-synuclein oligomer formation immediately precedes filament growth. *In vitro*, α-synuclein oligomers may acquire spherical, chain-like, or annular morphologies depending on the condition of incubation and the presence of mutations (Conway *et al.*, 2000b; Ding *et al.*, 2002; Lashuel *et al.*, 2002). Mutant α-synuclein $A^{30}P$ and $A^{53}T$ have an increased propensity to form annular oligomers, which topologically resemble bacterial pore-forming toxins. They are able to disrupt lipid bilayers (Jo *et al.*, 2002) and increase the permeability of lipid membranes and can be released from pathological inclusion bodies (Ding *et al.*, 2002; Lashuel *et al.*, 2002; Pountney *et al.*, 2004; Volles *et al.*, 2001).

α-Synuclein is able to form discrete annular oligomeric species in the presence of divalent cations, the size of which depends on the nature of the cation (Lowe *et al.*, 2004). Cobalt (II) and calcium (II) give frequent annular oligomers, 70–90 nm in diameter with calcium (II) and 22–30 nm in diameter with cobalt (II). Copper (II), iron (III), and nickel (II) yield 0.8–4 nm spherical particles, similar to α-synuclein incubated without metal ions. Magnesium (II), cadmium (II), and zinc (II) give larger, 5–8 nm spherical oligomers. In the absence of metal ions, annular oligomers ranging 45–90 nm in diameter are observed after 10 days incubation of α-synuclein lacking the C-terminal 15 AAs. After 3 weeks of incubation, short branched structures emerge in the samples and if the incubation continued

for an additional 2–3 months, extended filaments are formed. Truncated α-synuclein (1–125), lacking the C-terminal 15 AAs, did not form annular oligomers upon calcium addition, indicating the involvement of the calcium-binding domain in the formation of such oligomers (Lowe *et al.*, 2004).

α-Synuclein protofibrils permeabilize synthetic vesicles and form pore-like assemblies on the surface of brain-derived vesicles (Rochet *et al.*, 2004. DA reacts with α-synuclein to form a covalent adduct that slows the conversion of protofibrils to fibrils. This finding suggests that cytosolic DA in dopaminergic neurons (DAN) promotes the accumulation of toxic α-synuclein protofibrils, which might explain why these neurons are most vulnerable to degeneration in PD.

Helical α-synuclein can form highly conductive ion channels (Zakharov *et al.*, 2007). α-Synuclein binding to membranes containing anionic lipid is driven by electrostatic interactions between the basic ($pI = 9.7$) N-terminal segment of the protein and the negatively charged membrane surface. Furthermore, monomeric wt-α-synuclein and two mutants, $A^{53}T$ and $E^{46}K$, but not $A^{30}P$, can form ion channels in planar bilayer membranes containing anionic and curvature-inducing lipids. A trans-negative potential is required for channel activity, suggesting that *in vivo* α-synuclein may form active channels only in membranes that have been depolarized. Thus, intracellular, helical α-synuclein may form ion channels in synaptic membranes in response to an action potential. Channel formation may be a part of the normal function of α-synuclein that could result in modulation of ion movements related to the process of depolarization/repolarization. α-Synuclein forms ion channels with well-defined conductance in membranes containing 25–50% anionic lipid and 50% phosphatidyl-ethanolamine, which is present in neuronal membranes. Hypothetically, secreted extracellular α-synuclein could also form helical channels and induce cytotoxicity by dissipating the potential across the plasma membrane. Channels formed by extracellular α-synuclein could target either neuronal or glial cells containing phosphatidylethanolamine in their plasma membrane, inducing neurodegeneration or glial activation.

2.2.1.8. Posttranslational modifications PTMs may regulate normal synuclein functions, fulfill a role of switch from normal to pathological functions, and direct synucleins to different cellular compartments. Furthermore, PTMs of α-synuclein could promote the formation of LB and other inclusions. Analysis of the chemical composition of LB from patients has uncovered different forms of modified α-synuclein, including phosphorylated, nitrated, and mono-, di-, or tri-ubiquitinated forms of α-synuclein (Fujiwara *et al.*, 2002; Giasson *et al.*, 2000; Tofaris *et al.*, 2003).

Phosphorylation. Phosphorylation of α-synuclein at C-terminal residues, including Tyr^{125} and Ser^{129}, by several kinases appears to regulate synaptic function, ability to bind synaptic vesicles, and regulate protein–protein

interactions (Ellis *et al.*, 2001; Nakamura *et al.*, 2002; Okochi *et al.*, 2000). Extensive α-synuclein phosphorylation is also an important pathogenic event and may be a prerequisite for LB formation (Liu *et al.*, 2007). Most of the α-synuclein accumulated in LBs in brains with synucleinopathy is phosphorylated at Ser^{129} (Fujiwara *et al.*, 2002; Kahle *et al.*, 2002; Okochi *et al.*, 2000). Only 4% of normal soluble α-synuclein is phosphorylated, whereas in brain of patients with synucleinopathies, more than 90% of insoluble α-synuclein is phosphorylated (Chen and Feany, 2005; Liu *et al.*, 2007). Blocking phosphorylation by replacement of Ser^{129} on alanine reduces inclusion formation in neuronal cell cultures overexpressing α-synuclein (Lee *et al.*, 2004; Smith *et al.*, 2005). Furthermore, the phosphorylation of α-synuclein at Ser^{129} promotes fibril formation *in vitro* (Saito *et al.*, 2003).

All three members of the synuclein family can be phosphorylated by G–protein-coupled receptor kinases (GRKs) (Pronin *et al.*, 2000). GRK2 preferentially phosphorylates the α- and β-isoforms, whereas GRK5 uses preferentially α-synuclein as a substrate. GRK-mediated phosphorylation of synucleins is activated by factors that stimulate receptor phosphorylation, such as lipids (all GRKs) and Gβγ subunits (GRK2/3), suggesting that G–protein-coupled receptor activation may regulate synuclein phosphorylation. α-Synuclein is the best substrate for all GRKs, whereas γ-synucleins are phosphorylated significantly slower. Other kinases can also phosphorylate synucleins, for example, casein kinases 1 and 2 (CK1 and CK2) phosphorylate α-synuclein, while CK2 can effectively phosphorylate γ-synuclein but not β-synuclein. GRKs phosphorylate a single site in the C-tail of synucleins (Ser^{129} in α-, Ser^{118} in β-, and Ser^{124} in γ-synuclein) (Pronin *et al.*, 2000).

Takahashi *et al.* (2007) used tetracycline-off (TetOff)-inducible transfectant of neuronal lineage overexpressing human wt-α-synuclein to study oxidative stress-induced phosphorylation. $FeCl_2$ exposure of such transfectants promoted accumulation of Ser^{129}-phosphorylated monomers. This accumulation was accompanied by α-synuclein truncation, oligomerization, and formation of inclusions.

Nitration. The C-terminus of α-synuclein contains three Tyr residues in an Asp- and Glu-rich environment that can be nitrated. Moreover, Tyr residues may be oxidized to form dityrosine that cross-links the protein to form SDS and urea-stable dimers and oligomers (Souza *et al.*, 2000a). Monoclonal Abs were raised that recognize nitrated α-synuclein or nitrated and oxidized α-synuclein (Duda *et al.*, 2002; Giasson *et al.*, 2000).

Ubiquitination. Early immunocytochemical studies of LB and other intracellular protein inclusions showed that they are ubiquitinated. Later the target for ubiquitination was identified as α-synuclein in depositions of patients with PD, DLB, and MSA (Fig. 6.4) (Fujiwara *et al.*, 2002; Hasegawa *et al.*, 2002; Spillantini *et al.*, 1998a,b; Takeda *et al.*, 1998). The ubiquitin Ab stains mostly

the halo of the LB, while α-synuclein Ab stains both the halo and the core (Fig. 6.4A–C) (Spillantini *et al.*, 1998a). α-Synuclein is a substrate for mono-, di-, and tri- rather than polyubiquitination. Interestingly, accumulation of ubiquitinated α-synuclein is not invariably associated with significant impairment of proteasome function (Tofaris *et al.*, 2003). Ubiquitination of α-synuclein is not required for inclusion formation and the assembly of α-synuclein into fibrillar aggregates may precede their ubiquitination in α-synucleinopathies (Sampathu *et al.*, 2003). Protein-sequence analysis revealed that Lys^{21}, Lys^{23}, Lys^{32}, and Lys^{34} within the repeats in the N-terminal half (Figs. 6.1 and 6.2) are liable to ubiquitination *in vitro* (Nonaka *et al.*, 2005). $A^{53}T$ and $A^{30}P$ mutations and phosphorylation of α-synuclein at Ser^{129} had no significant effect on ubiquitination. Interestingly, assembled, filamentous α-synuclein is less ubiquitinated than the soluble form and the major ubiquitination sites in filamentous α-synuclein are different compared with the soluble protein and are localized to Lys^{6}, Lys^{10}, and Lys^{12} (Nonaka *et al.*, 2005).

Sumoylation. Small ubiquitin-like modifiers (SUMO) display similarities to ubiquitin. Diglycine motifs at the C-terminus are responsible for the formation of an isopeptide bond between a SUMO glycine and a target substrate glycine. For α-synuclein, a sumoylated species has M_r 36 kDa that is modified primarily by SUMO1, and to a lesser extent, by SUMO2 and SUMO3 (Dorval and Fraser, 2006). Lys^{102} is one sumoylation target in α-synuclein that contributes to this process, while other targets are lysine residues dispersed within the protein sequence.

O-Glycosylation. Shimura *et al.* (2001) identified 22-KDa glycosylated form of α-synuclein (alphaSp22) in a protein complex present in a normal human brain and containing E3 ubiquitin ligase and ubiquitin-conjugating enzyme (UbcH7). In an *in vitro* ubiquitination assay, alphaSp22 could be modified by parkin into polyubiquitinated, high M_r species (Shimura *et al.*, 2001). β-Synuclein can also contain β-N-acetylglucosamine linked to hydroxyls of serines or threonines (*O*-GlcNAc) according to proteomic analysis (Cole and Hart, 2001).

Cross-linking by tissue transglutaminase. Tissue transglutaminase catalyzes α-synuclein cross-linking, leading to the formation of high M_r aggregates both *in vitro* and in cellular models (Jensen *et al.*, 1995; Junn *et al.*, 2003). The formation of these aggregates was enhanced in the presence of the calcium ionophore A23187 and prevented by the inhibitor cystamine. IHC studies on postmortem brain tissue revealed the presence of tissue transglutaminase-catalyzed (γ-glutamyl) lysine cross-links in the halo of LBs in PD and DLB, colocalized with α-synuclein (Junn *et al.*, 2003).

Modification of α-synuclein by acrolein. Shamoto-Nagai *et al.* (2007) described a new form of α-synuclein PTM in the DA neurons of the SNc of PD

patients. This PTM is a modification by acrolein, an aldehyde product of lipid peroxidation. Modification of α-synuclein by acrolein enhances its oligomerization. In addition, acrolein inhibits 20S proteasome activity. Thus, acrolein may initiate vicious cycle of modification and aggregation of α-synuclein and impair proteolysis system causing neuronal death in PD and other NDDs.

Methionine oxidation. Since α-synuclein lacks Trp and Cys residues, its mild oxidation *in vitro* with H_2O_2 selectively converts all four methionine residues to the corresponding sulfoxides. Interestingly, the fibrillation of α-synuclein at physiological pH is completely inhibited by methionine oxidation. Furthermore, the Met-oxidized protein also inhibits fibrillation of unmodified α-synuclein. However, the presence of metals can completely overcome the inhibition of fibrillation of the Met-oxidized α-synuclein (Glaser *et al.*, 2005). Since α-synuclein oligomers may be cytotoxic, it is evident that both oxidative stress and environmental metal pollution may play a role in the aggregation of α-synuclein due to these mechanisms. In brain cells, the level of Met-oxidized α-synuclein may be controlled by methionine sulfoxide reductase and by proteasomes.

Truncated forms of synuclein. In 1993, Uéda and coauthors described relatively short peptides corresponding to the central part of α-synuclein molecule (Fig. 6.2, Chapter I, B) and showed that such peptides are associated with AD brain amyloid. Two peptides isolated after formic acid, CNBr, and protease treatment of AD brain amyloid are termed NAC. They were shown to correspond to residues 61–80 and 81–95 localized in the middle of a larger precursor termed NACP. The cDNA for NACP was subsequently cloned by PCR and cDNA library screening (Uéda *et al.*, 1993) and found to be a human homologue of the Torpedo ray synuclein. NAC peptide has a strong tendency to form a β-sheet configuration like β-amyloid. NAC may therefore be a comparatively protease-resistant core of the protein that is prone to aggregation (El-Agnaf *et al.*, 1998a,b; Iwai *et al.*, 1995).

The importance of the truncated forms of synucleins became evident when a high proportion of such species was found in protein deposits and inclusions (Baba *et al.*, 1998; Campbell *et al.*, 2001; Liu *et al.*, 2005a) and when their role as inducers of full-length α-synuclein aggregation was found (Crowther *et al.*, 1998; Li *et al.*, 2005; Serpell *et al.*, 2000; Withers *et al.*, 1997). Truncation of the C-terminus removes α-synuclein charge repulsion and thereby strongly enhances aggregation (Murray *et al.*, 2003).

The expression of mutant human α-synuclein is associated with higher cellular accumulation of truncated forms. Coexpression of truncated α-synuclein with full-length protein increases cell vulnerability to oxidative stress in dopaminergic SH-SY5Y cells (Liu *et al.*, 2005a). These results point to the role of truncated α-synuclein species in the formation of aggregates of disease-linked full-length α-synuclein.

α-*Synuclein cleavage.* The caspase-like activity of the 20 S proteasome produces truncated fragments similar to those found in patients and animal models from degradation of unstructured α-synuclein. According to one model, incomplete degradation of α-synuclein, especially under overloaded proteasome capacity, produces highly amyloidogenic fragments that rapidly induce the aggregation of full-length protein (Liu *et al.*, 2005a). These aggregates in turn reduce proteasome activity, leading to further accumulation of fragmented and full-length α-synuclein, creating a vicious cycle of cytotoxicity. The data suggests a precipitating role of truncated synucleins in PD pathogenesis and demonstrates that the proteasome can produce truncated species via the degradation of α-synuclein not bound to membranes. The issue about the role of proteasomes in α-synuclein degradation is controversial with some publications confirming the importance of proteasome in this process (Tofaris *et al.*, 2001) and others contradict this data (Paxinou *et al.*, 2001).

Proteolytic cleavage of α-synuclein can also be catalyzed my matrix metalloproteinases (MMPs), which are activated by oxidative stress. Most efficiently α-synuclein is cleaved by MMP-3, generating a 6.5 kDa major fragment; however, other enzymes were also active in the digestion, that is MMP-14, MMP-2, MMP-1, and MMP-9. α-Synuclein is gradually broken down by MMP-3 from its C-terminal end in positions $Ala^{78}\downarrow Gln^{79}$, $Gln^{79}\downarrow Lys^{80}$, $Ala^{91}\downarrow Thr^{92}$, and $Gly^{93}\downarrow Phe^{94}$ (Sung *et al.*, 2005). In addition to MMPs and proteasomes, α-synuclein may be degraded by catepsin D, lysosomal proteases that may play a role in producing truncated α-synuclein for oligomer assembly (Takahashi *et al.*, 2007).

Serine protease neurosin (kallikrein-6) degrades α-synuclein and colocalizes with pathological inclusions, that is LB and GCI. Upon cellular stress, neurosin is released from mitochondria to the cytosol, which resulted in the increase of degraded α-synuclein species. Downregulation of neurosin causes accumulation of α-synuclein in cultured cells (Iwata *et al.*, 2003).

2.2.1.9. Synuclein endo- and exocytosis When recombinant α-synuclein is added to the culture medium, it is transported into the intracellular cytoplasm, inducing death of H19–7 cells (Sung *et al.*, 2001). On the other hand, when α-synuclein is transiently expressed in dopaminergic neuroblastoma SK-N-BE cells, it is secreted into extracellular space (Sung *et al.*, 2005). The data about secretion of α-synuclein from cells explain its presence in human plasma (El-Agnaf *et al.*, 2003), cerebrospinal fluid (CSF) (Borghi *et al.*, 2000), extracellular LBs (Spillantini and Goedert, 2000), postsynaptic areas, and synaptic clefts (Lücking and Brice, 2000), and detection of its 61–95 fragment (NAC) in extracellular deposits in the brain of AD patients (Iwai *et al.*, 1995; Uéda *et al.*, 1993). Moreover, another member of the synuclein family, γ-synuclein, is overexpressed in infiltrating breast carcinoma (Jia *et al.*, 1999) (Chapter IV, B).

2.2.2. Proteins interacting with α-synuclein

Consistent with having chaperone function, the synucleins are known to participate in a large number of interactions. Numerous proteins have been identified that interact with α-synuclein (Dev *et al.*, 2003; Woods *et al.*, 2007; Zhou *et al.*, 2004), so here we will mention only those that possess important effect on synuclein structure or functions. In addition to proteins binding to soluble α-synuclein, more than 70 proteins have been identified that become sequestered in LB where α-synuclein is a major component (Wakabayashi *et al.*, 2007). Recently, Woods *et al.* (2007) devised a novel bacteriophage display screen to identify protein-binding partners of helical α-synuclein. The authors have identified 20 proteins with roles in diverse cellular processes related to membrane trafficking, ion channel modulation, redox metabolism, and gene regulation.

2.2.2.1. Synphilin There are several forms of synphilin originating from the *SNCAIP* gene with different exon organization and initial reading frame. Synphilin-1 is present in LB and may enhance the ability of α-synuclein to aggregate and form intracellular inclusions (Engelender *et al.*, 1999; Eyal *et al.*, 2006). The two proteins were found to interact *in vivo* and, when coexpressed, caused the formation of eosinophilic cytoplasmatic inclusions (Engelender *et al.*, 1999). Synphilin-1 is ubiquitinated by the E3 ubiquitin ligase SIAH, which is present in LB of PD patients. When synphilin-1 and SIAH are coexpressed in cells and proteasomal function is inhibited, ubiquitinated synphilin-1 inclusions are found in the majority of the cells (Liani *et al.*, 2004). Recently identified new synphilin isoforms, synphilin-1A is toxic to neurons and aggregation prone and recruits both α-synuclein and synphilin-1 into inclusions (Szargel *et al.*, 2007).

2.2.2.2. β- and γ-synucleins Both *β*- and *γ*-synucleins bind to α-synuclein and may inhibit α-synuclein fibril formation (Hashimoto *et al.*, 2001; Park and Lansbury, 2003). Complete inhibition of α-synuclein fibrillation was observed at 4:1 molar excess of *β*- and *γ*-synucleins (Uversky *et al.*, 2002).

2.2.2.3. Tubulin For the first time, colocalization of one of the synuclein members with tubulin was described in 1999. A filamentous form of *γ*-synuclein was colocalized with tubulovesicular structures along microtubules suggesting that *γ*-synuclein participates in vesicular trafficking (Surguchov *et al.*, 1999).

Later Alim *et al.* (2001) identified tubulin as one of the α-synuclein-binding/associated proteins. Furthermore, α-synuclein was copurified with microtubules. Double-labeling immunofluorescence revealed that tubulin colocalized with α-synuclein-positive pathological structures such as LBs,

LN in PD and DLB, and GCIs in MSA. Tubulin initiates the polymerization of α-synuclein, resulting in the formation of α-synuclein fibrils. Some epigenetic elements (e.g., drugs, chemicals, additives in food, or environmental toxins) may affect the assembly/disassembly equilibrium of microtubules. Thus produced abnormally increased free tubulin may trigger α-synuclein fibril formation. If so, those microtubule-disrupting elements can be risk factors for α-synuclein-associated degenerative diseases.

2.2.2.4. Cysteine-string protein-α α-Synuclein interacts with cysteine-string protein-α (CSPα), a synaptic vesicle protein possessing a cochaperone activity. After such interaction, α-synuclein binds to phospholipids and cooperates with *N*-ethylmaleimide sensitive factor (Bonini and Giasson, 2005; Chandra *et al.*, 2005). This interaction on the presynaptic membrane interface may play a protective role for the nerve terminals against different injuries. According to recent studies, α-synuclein's interaction with CSPα may play a key role in synaptic function.

2.2.2.5. 14-3-3 High-molecular-weight complexes immunoreactive for both α-synuclein and 14-3-3 have been detected in the SNc of PD patients (Xu *et al.*, 2002). This, together with the presence of 14-3-3 proteins in LB, may suggest an attempt of these molecular chaperones to sequester aberrant forms of α-synuclein in diseased nigral neurons.

2.2.2.6. Rab α-Synuclein interactions with members of the Rab family are not surprising because of their association with synapse and synaptic vesicles. Pull-down experiments have shown that α-synuclein from the mutant human $A^{30}P$ transgenic (Tg) mice interacts with Rab3a, Rab5, and Rab8 (Dalfó *et al.*, 2004). Rab3a has also been shown to bind α-synuclein in human samples of MSA (Dalfó and Ferrer, 2005). Rab3 binding to α-synuclein mediated by rabphilin is an early event preceding inclusion body formation. This interaction was not found in a normal brain, while in MSA, this binding has been shown in GCI-rich cerebellum and pons as well as in cerebral cortex.

2.2.2.7. Agrin Agrin binds to α-synuclein, inducing conformational changes, and enhances in3olubility of α-synuclein. Furthermore, agrin accelerates the formation of protofibrils by α-synuclein and decreases the half-time of fibril formation. Thus, agrin may contribute to the etiology of PD by modulating the aggregation state of α-synuclein in DAN (Liu *et al.*, 2005c).

2.2.2.8. Histones Association of α-synuclein with histones in the nucleus affects their acetylation and promotes neurotoxicity (Goers *et al.*, 2003; Kontopoulos *et al.*, 2006).

2.2.2.9. Chaperones α-Synuclein interacts with several chaperones, including Hsp27, Hsp70, Hsp90, and αB-crystallin (Outeiro *et al.*, 2006), and is colocalized with them in LB. The interaction of α-synuclein with Hsp-70 and endogenous C-terminus of Hsp70-interacting protein may play an important role in the fate of α-synuclein in a cell. C-terminus of Hsp70-interacting protein is a dual-function protein being a cochaperone and E3 ubiquitin ligase. Importantly, the C-terminus of Hsp70-interacting protein can mediate α-synuclein degradation by two discrete mechanisms, proteasomal or lysosomal degradation pathways. The C-terminus of Hsp70-interacting protein also plays a role in α-synuclein aggregation and is colocalized with α-synuclein and Hsp70 in LB (Shin *et al.*, 2005).

2.2.2.10. Tau α-Synuclein interacts with tau and induces its fibrilization. Alternatively, both tau and α-synuclein synergistically effect the polymerization of each other into fibrillar amyloid lesions (Giasson *et al.*, 2003b). It is possible that a limited amount of amyloidogenic α-synuclein fibrils can serve as seeds to initiate tau fibrillization. The initiation step most likely involves the formation of amyloid-like α-synuclein polymers. Another explanation of these results is that α-synuclein may act as a pathological chaperone for tau fibrilization.

3. Synuclein Functions

The physiological role of α-synuclein is debated. While its aggregation is considered linked to neuropathology, its normal major function may be related to fundamental processes of synaptic transmission and plasticity. In addition to this, major function α-synuclein is implicated in other physiological processes.

3.1. Synaptic maintenance

The high concentration of synucleins in presynaptic terminals and a growing body of experimental evidence obtained by different approaches suggests that they play a major role in the maintenance of synaptic vesicle pools and maintenance of presynaptic function (Cabin *et al.*, 2002; Chandra *et al.*, 2004; Murphy *et al.*, 2000), activity-dependent DA release (Abeliovich *et al.*, 2000; Perez *et al.*, 2002), and as a chaperone for the assembly of soluble *N*-ethylmaleimide-sensitive factor attachment protein receptor (SNARE) complexes that drive vesicle fusion with plasma membrane (Chandra *et al.*, 2005).

α-Synuclein might be an important presynaptic regulator of the vesicle cycle, involved in synaptic vesicle recycling. α-Synuclein can bind both

brain-derived and synthetic phospholipid vesicles via its N-terminal conserved repeat region. This binding induces a dramatic alteration in α-synuclein secondary structure from ''unfolded'' to α-helical (Davidson *et al.*, 1998; Jensen *et al.*, 1998). Vesicle binding is greatly enhanced by acidic phospholipids such as phosphatidic acid, but not by neutral phospholipids such as phosphatidylcholine (Davidson *et al.*, 1998). Because of α-synuclein's ability to interact with lipids and their association with synaptic vesicles, it has been suggested that synucleins might be involved in intracellular vesicular trafficking (Lavedan, 1998).

A recent study by Larsen *et al.* (2006) confirms the role of α-synuclein in the regulation of DA release. The authors used stable phosphatidyl choline 12 cell lines that expressed relatively low nontoxic level of wt- or $A^{30}P$ α-synuclein. This level of α-synuclein did not affect cell morphology and viability, but reduced stimulation-dependent DA release. These results are complementary to the increase in evoked DA found in α-synuclein knockout (KO) mice by Abeliovich *et al.* (2000). In further experiments, Larsen *et al.* (2006) investigated the mechanism of the regulation of DA release by α-synuclein. They found that α-synuclein inhibits ''priming,'' a reaction that transfers morphologically docked vesicles to a fusion-competent state. This causes SNAREpin formation. When SNAREpin assembly achieves a critical state, it becomes able to catalyze bilayer mixing, but is frozen by regulatory factors that preclude membrane fusion until Ca^{2+} entry (Jahn and Scheller, 2006).

3.2. Inhibition of phospholipase D and kinase activity

α-Synuclein has a high affinity for acidic phospholipids such as phosphatidic acid and acts as a feedback regulator of phosphatidic acid synthesis by inhibiting phospholipase D (PLD)2 (Davidson *et al.*, 1998). *β*- and *γ*-Synucleins as well as mutant $A^{30}P$ and $A^{53}T$ α-synuclein are also effective inhibitors of PLD2 (Payton *et al.*, 2004). Interestingly, this function of α-synuclein is modulated by phosphorylation, catalyzed by intracellular kinases. Phosphorylation of α-synuclein by GRKs reduces phospholipid binding and decreases the level of PLD2 inhibition by α-synuclein (Pronin *et al.*, 2000). PLD2 inhibition by α-synuclein is mediated by a lipid-stabilized α-helical structure in exon 4 as well as by residues within exon 6 (Payton *et al.*, 2004). Both α- and *β*-synucleins are also selective inhibitors of another form of phospholipase, PLD1 (Ahn *et al.*, 2002; Jenco *et al.*, 1998). Inhibition of PLD by synucleins may be important because PLD activity is increased in the brain of patients with NDDs.

For studying the effect of α-synuclein on PLD activity, stable clones of human embryonic kidney-293 cells overexpressing wt-α-synuclein and two mutant forms ($A^{53}T$ and $A^{30}P$) were generated (Ahn *et al.*, 2002). The comparison of PLD activity in these clones after stimulation of PLD by

pervanadate or phorbol 12-myristate 13-acetate showed that both activators stimulated PLD activity less in wt, $A^{30}P$, or $A^{53}T$ α-synuclein cell lines than in the control cell line.

Globular α-synuclein oligomers significantly inhibit *in vitro* autophosphorylation of p21-activated kinase (PAK4) compared to treatment with monomeric α-synuclein or β-synuclein. In $A^{30}P$ Tg mice, a significant decline in phosphorylation of LIM kinase 1, a physiological substrate of PAK4, was found. Thus, suppression of PAK activity may represent a downstream mechanism for oligomeric α-synuclein and a potential therapeutic target in PD (Danzer *et al.*, 2007).

3.3. Regulation of proteasomal function

The proteasomes play an important role in both inclusion body formation and DAN death. Proteasomal inhibition may have an impact on the DAN that seems to be particularly vulnerable to the stress of unfolded proteins (Lindersson *et al.*, 2004; Petrucelli *et al.*, 2002). Recent studies indicate that synucleins regulate proteasomal function. Three members of the synuclein family possess different effects on proteasomes and for α-synuclein, the effect depends on the level of its aggregation.

α-Synuclein especially in aggregated form displays a strong inhibitory activity toward the proteasome *in vitro* (Petrucelli *et al.*, 2002; Tanaka *et al.*, 2001). Aggregated but not monomeric α-synuclein binds efficiently to the 20 S proteasome part of the 26 S proteasome. The proteasome binding results in an efficient and selective noncompetitive inhibition of the chymotrypsin-like proteasomal activity of the 20 S proteolytic particles (Lindersson *et al.*, 2004). Aggregated α-synuclein inhibits 26 S proteasomal activity with an IC50 $\sim$ 1 nM that is more than 1000-fold lower than that of monomeric α-synuclein (16 μM) (Snyder *et al.*, 2005). Monomeric α- and β-synucleins inhibit the 20 S and 26 S proteasomal activities only weakly, but monomeric γ-synuclein strongly inhibits ubiquitin-independent proteolysis. The IC50 of monomeric γ-synuclein for the 20 S proteolysis is 400 nM (Snyder *et al.*, 2005). Thus, the α- and β-synucleins regulate proteasomal function and β-synuclein acts as a negative regulator of α-synuclein.

3.4. Synucleins as chaperones

All three members of the synuclein family possess chaperonic activity both *in vitro* and *in vivo* (Ahn *et al.*, 2006; Souza *et al.*, 2000b). α-Synuclein inhibits the aggregation of model substrates and protects the catalytic activity of alcohol dehydrogenase and rhodanese during heat stress, as well as esterases. In addition, α-synuclein suppresses the aggregation of reduced/denatured lysozyme on the refolding pathway. Deletion of the C-terminal regions abolishes chaperone activity, although largely unstructured

conformations are maintained (Ahn *et al.*, 2006; Kim *et al.*, 2002; Park *et al.*, 2002a,b,c).

Interestingly, the N-terminal part of α-synuclein shares 40% AA homology with molecular chaperone 14-3-3 (Ostrerova *et al.*, 1999), suggesting that the two proteins could subserve the same function. α-Synuclein interacts with 14-3-3 (Ostrerova *et al.*, 1999), and the interaction between the two proteins produces a 54–83 kDa protein complex in PD brain, which is selectively increased in SNc (Xu *et al.*, 2002). Thus, α-synuclein may sequester 14-3-3, leading to a reduction in the amount of 14-3-3 protein available to inhibit apoptosis and rendering the cells more susceptible to cellular stresses (Xu *et al.*, 2002). Both 14-3-3 and α-synuclein bind to tyrosine hydroxylase (TH), the rate-limiting enzyme in catecholamine synthesis (Chapter V,C), with divergent consequences: activity is stimulated by 14-3-3 but inhibited by α-synuclein (Jenco *et al.*, 1998). *β*- and *γ*-Synucleins protect cultured ocular cells from the accumulation of mutant aggregation prone opsin, which occurs in retinitis pigmentosa (Surgucheva *et al.*, 2005) being potential candidates for gene therapy of this ocular disease.

3.5. Protective effect of synucleins

Although in many studies, overexpression of α-synuclein caused toxic effect, under certain conditions, α-synuclein as well as two other members of the family may be protective. The precise proapoptotic versus antiapoptotic roles in specific types of neurons remain to be delineated more clearly. The effect may depend on the level of Tg synuclein expression, types of cells, the presence of chaperones, and low M_r substance, for example DA and other factors. For example, mice with Tg expression of wt- and mutant human α-synuclein developed neurodegeneration with age with partial penetrance, whereas Tg expression of the murine gene does not result in neurodegeneration (Chandra *et al.*, 2005). Even overexpression of human α-synuclein had been shown to protect against paraquat-induced neurodegeneration (Manning-Boğ *et al.*, 2003).

α-Synuclein delivered by protein transduction using the TAT sequence was also shown to be protective against oxidative stress and other cellular injuries (Albani *et al.*, 2004; Choi *et al.*, 2006). In both cases above, α-synuclein's protective effect may result from its ability to activate Hsp70 and the structural similarity between α-synuclein and small Hsp (Kim *et al.*, 2004). Therefore, there is an apparent dissociation between α-synuclein deposition and neurodegeneration, and this suggests that its involvement in human neurodegenerative processes may arise not only from a gain of toxic function but perhaps also from a loss of protective function.

Südhof and coworkers have been studying synaptic vesicle protein, CSPα, which contains a DNA-J domain characteristic of Hsp40 chaperones

(Chandra *et al.*, 2005). CSPα-deficient mice develop an age-dependent, progressive and fatal sensorimotor disorder, with degeneration of neuromuscular junctions and Calyx synapses with death at 2 months of age (Fernández-Chacón *et al.*, 2004). CSPα acts as a presynaptic chaperone that maintains continued synaptic function. Interestingly, Tg α-synuclein prevents this lethal neurodegeneration of CSPα-deficient mice and rescues their motor impairment phenotype. Expectedly, the CSPα-deficient phenotype is exacerbated in a background of α/β-synuclein double KO. α-Synuclein does not, however, function as a cochaperone of CSPα. The two proteins do not interact with each other and α-synuclein does not stimulate Hsc70 activity like CSPα. α-Synuclein may therefore not functionally replace CSPα-deficiency, but may rescue the detrimental consequence of the deficiency in a cell autonomous manner. This rescue activity apparently requires the membrane-bound form of α-synuclein, and is lost in the $A^{30}P$ mutant that is deficient in phospholipids binding. These findings highlighted a potential dual role of α-synuclein in neurodegeneration (Chandra *et al.*, 2005).

α-Synuclein silencing by antisense oligonucleotides in primary cultures of cerebellar granule cells may cause widespread death of neurons (Monti *et al.*, 2007). Therefore, α-synuclein represents prosurvival functions and its normal expression is essential for the viability of primary neurons. Treatment of these neurons by a neurotoxin 6-hydroxydopamine caused a reduction of α-synuclein and neuronal death. In addition, 6-hydroxydopamine reduced α-synuclein synthesis and stimulated its monoubiquitination and nuclear translocation (Monti *et al.*, 2007). Nuclear targeting of α-synuclein has been recently demonstrated to promote toxicity by direct binding to histones and inhibition of histone H3 acetylation. Importantly, α-synuclein toxicity can be reversed by histone deacetylase inhibitors, suggesting that these inhibitors are potential therapies for synucleinopathies (Kontopoulos *et al.*, 2006).

Wt-α-synuclein, but not its mutant forms ($A^{53}T$, $A^{30}P$), protects CNS dopaminergic cells from toxin 1-methyl-4-phenylpyridinium (MPP^+). However, no protective effect was found against 6-hydroxydopamine, H_2O_2, or β-amyloid peptide (Jensen *et al.*, 2003). Protection from MPP^+ was directly correlated with the preservation of mitochondrial function. The authors consider α-synuclein as a neuroprotectant, preventing mitochondrial dysfunction.

In a series of publications, Alves da Costa and coworkers used TSM1 neurons stably overexpressing wt-α-synuclein or $A^{53}T$ mutant form (Alves da Costa *et al.*, 2000, 2002, 2003). In the early article (2000), the authors showed that under basal conditions, caspase activity was reduced in wt-α-synuclein-expressing cells compared to neurons expressing the mutant protein. This inhibitory control of the caspase response was abolished by $A^{53}T$ mutation. Thus, the wt-α-synuclein exerted an antiapoptotic effect in neurons that was abolished by the $A^{53}T$ mutation.

Later Alves da Costa *et al.* (2002) demonstrated that α-synuclein induced reduction of caspase 3 immunoreactivity and activity was accompanied by lower DNA fragmentation, reduced number of dUTP nick end labeling (TUNEL)-positive neurons, and diminished p53 expression. Antiapoptotic function of α-synuclein is not expressed in neurons treated with 6OHDA. The authors speculated that the 6OHDA abolished the antiapoptotic phenotype by triggering α-synuclein aggregation. These antiapoptotic properties of α-synuclein can be restored by another member of the family, *β*-synuclein (Alves da Costa *et al.*, 2003). Thus, α-synuclein can display a physiological antiapoptotic phenotype abolished in the pathology. Among possible cellular mechanisms underlying the antiapoptotic function of α-synuclein, the authors discuss its chaperoning activity that can be realized during the interaction of α-synuclein with cellular intermediates of the apoptotic pathways (Alves da Costa *et al.*, 2000). α-Synuclein protective properties can be abolished or reversed as a result of a mutation, aggregation, or PTMs.

Since α-synuclein aggregates present in axonal terminals precede the formation of LB in DLB (Marui *et al.*, 2002), some investigators assume that LB are formed by an aggresome-related process as a general cytoprotective measure, in which smaller α-synuclein aggregates are sequestered from the neuronal periphery by active retrograde transport on microtubules (McNaught *et al.*, 2002). Presynaptic terminals in neurons are the loci of α-synuclein aggregate formation (Kramer and Schulz-Schaeffer, 2007).

3.6. Axonal transport

The knowledge of the mechanism of α-synuclein axonal transport is important for the understanding why it accumulates as protein deposits in synucleinopathies. The failure of axonal transport has been implicated in the development of several NDDs.

Transfected rat cortical neurons can be used as a model to investigate α-synuclein axonal transport (Saha *et al.*, 2004). α-Synuclein is actively transported from its site of synthesis in the cell body along axons to synaptic termini. Metabolic labeling of neuronal proteins in the rat optic nerve has shown that most α-synuclein (76%) moves in the slow component of axonal transport (Jensen *et al.*, 1998, 1999; Utton *et al.*, 2002). A proportion of α-synuclein also binds to vesicles and is moved in the fast component of axonal transport. Binding of $A^{30}P$ α-synuclein to vesicles is reduced compared with the wt-protein, suggesting that this mutation might compromise the fast axonal transport of α-synuclein (Jensen *et al.*, 1998; Jo *et al.*, 2002). It is conceivable that defective α-synuclein transport could lead to less α-synuclein exiting from the cell body along the axon and effectively cause local overexpression of α-synuclein in the perikaryon. Such overexpression might alter the normal cellular localization of α-synuclein and

affect its folding and/or association with other proteins, and increase its local concentration leading to its accumulation as LB. Phosphorylation of serine residues in α-synuclein diminishes its affinity for vesicles (Okochi *et al.*, 2000; Pronin *et al.*, 2000), suggesting that phosphorylation state of α-synuclein might regulate its axonal transport. Tyrosine phosphorylation (Ellis *et al.*, 2001; Nakamura *et al.*, 2002) may also affect α-synuclein axonal transport (Saha *et al.*, 2004). Mutant forms of α-synuclein, either associated with PD ($A^{30}P$ or $A^{53}T$) or mimicking defined serine, but not tyrosine phosphorylation states exhibit reduced axonal transport in cultured neurons (Saha *et al.*, 2004). Furthermore, transfection of $A^{30}P$, but not wt-, α-synuclein results in accumulation of the protein proximal to the cell body. These results suggest that the reduced axonal transport exhibited by the PD-associated α-synuclein mutants might contribute to perikaryal accumulation of α-synuclein and hence LB formation and neuritic abnormalities in diseased brain.

A possible mechanism for the reduced rates of transport of $A^{30}P$ α-synuclein at early time points might be related to the inhibition of its interaction with lipid membranes and vesicles. This in turn might slow the rate at which α-synuclein associates with components involved in neuronal transport (Jensen *et al.*, 1998; Jo *et al.*, 2002; Perrin *et al.*, 2000). However, another group did not detect any effects on slow axonal transport in peripheral nerves of Tg mice expressing human $A^{30}P$ α-synuclein (Li *et al.*, 2004a). The rate of association and/or dissociation of α-synuclein with the motor and/or accessory proteins involved in its initial transport may be a crucial rate-determining step in its axonal transport (Saha *et al.*, 2004).

Transport of α-synuclein depends on an intact microtubule, but not actin-cytoskeleton. α-Synuclein moves at overall slow rates of transport and nocodazole inhibits α-synuclein axonal transport (Utton *et al.*, 2005). Particulate structures containing α-synuclein travel rapidly when moving along axons but spend the majority of the time paused. These structures have similar characteristics to those previously observed for neurofilaments. The motile particles containing α-synuclein colocalize with the fast-transporting molecular motor kinesin-1 in neurons. This data suggests that α-synuclein transport in neurons may involve both kinesin and dynein motor proteins. Although both tau and α-synuclein are most probably transported through fast motors, there are clear differences between the mechanisms of their interactions with such motors, with tau being capable of directly binding to kinesin-1, whereas α-synuclein requires other accessory proteins to form a motile complex. Thus, the overall slow rate of axonal transport of α-synuclein may be mediated through fast transport motors, including kinesin and dynein. Abnormal axonal transport rates of α-synuclein, such as may occur in NDD, could result in the formation of intracellular aggregates and eventual cell death in affected neurons.

3.7. Synucleins in drug and alcohol addiction

α-Synuclein gene maps to a quantitative trait locus for alcohol preference, and expression of α-synuclein in different brain areas is increased in rats whose alcohol preference is inbred (Liang *et al.*, 2003). The differential regulation of rat α-synuclein gene expression contributes to alcohol preference. The α--synuclein gene is expressed at higher levels in alcohol-naive, inbred alcohol-preferring (iP) rats than in alcohol-nonpreferring (iNP) rats (Liang and Carr, 2006). The differential expression of α-synuclein observed between the iP and iNP strains may be mediated by polymorphic site located downstream of the gene in the 3′-UTR. An SNP in position +679 of the UTR differentially affects the half-life of iP mRNA compared with iNP mRNA. Recently, evidence has been presented that α-synuclein levels are elevated in midbrain DAN of chronic cocaine abusers (Mash *et al.*, 2003). Interestingly, an increased expression of α-synuclein mRNA in patients with alcoholism has been detected, which correlates to craving in addicted patients with alcoholism (Bönsch *et al.*, 2004).

α-Synuclein mRNA is increased in alcohol-dependent patients within withdrawal state. This increase is associated with craving, especially obsessive craving. Recent analysis of two polymorphic repeats within the α-synuclein gene showed highly significant frequency of longer alleles of NACP-REP1 in alcohol-dependent patients compared with healthy controls (Bönsch *et al.*, 2005). Furthermore, these lengths significantly correlate with levels of expressed α-synuclein mRNA. Overall this data suggests that synucleins may be implicated in the development of different forms of addiction. These studies point to a novel approach for a genetic determination of craving, a key factor in the genesis and maintenance not only of alcoholism but also of addiction in general. In a screening for genes differentially expressed after high-dose cocaine exposure, Brenz Verca *et al.* (2003) found γ-synuclein as a major upregulated candidate in the tegmentum (7.16 times upregulation), while α-synuclein upregulation was more modest (1.96–3.5 in different brain regions).

3.8. Synucleins in song learning

George *et al.* (1995) identified synuclein homologue in zebra finches *Taeniopygia guttata* and called it synelfin. Using confocal immunofluorescence microscopy, the authors detected synelfin immunoreactivity in presynaptic terminals. Its expression is increased early in this critical period in a brain nucleus specifically implicated in song learning, lateral MAN. Thus, synelfin may serve a novel function critical to the regulation of vertebrate neural plasticity (Jin and Clayton, 1997).

3.9. Models organisms and systems used to investigate synuclein functions

The complexity of disease etiology of genes in mammalian systems often necessitates the use of simpler model systems for their studies, the advantages of which are established methods of genetic manipulation (Lee and Price, 2001). The disadvantage of such model systems, for example, yeast and *Drosophila*, is the lack of endogenous α-synuclein. Therefore, these organisms may be deficient in the machinery that normally limits the tendency of this protein to aggregate *in vivo*.

In the majority of cases, the model organisms are used to overexpress α-synuclein and its mutant forms and to compare the effect of overexpression on different physiological functions. The results of such experiments demonstrate that whatever is the model organism, the excess accumulation of α-synuclein leads to cellular toxicity (Klucken *et al.*, 2004; Lee and Trojanowski, 2006; Moore *et al.*, 2005). In general, the results obtained with these Tg animals are in agreement with the data obtained with cell cultures demonstrating that α-synuclein overexpression is obviously detrimental (Kirik *et al.*, 2002; Outeiro *et al.*, 2006). One of the examples of successful application of model systems is the findings in yeast, *Drosophila*, and *Caenorhabditis elegans* that α-synuclein accumulation specifically inhibits endoplasmic reticulum (ER) to Golgi vesicular traffic. Below are other examples of the successful applications of model systems in synuclein studies.

3.9.1. Yeast model

The use of yeast allowed identification of flavonoids as potential drugs for the treatment of synucleinopathies (Griffioen *et al.*, 2006). Furthermore, catechins from the bioactive green tea extracts possess protective effects against α-synuclein toxicity (Ono and Yamada, 2006; Williams *et al.*, 2007).

α-Synuclein expressed in yeast is targeted to the plasma membrane, and can form cytoplasmic inclusions, as it does when expressed in mammalian cells. The expression of α-synuclein in yeast affects vesicular trafficking (particularly endocytosis), inhibits PLD, and causes the formation of lipid droplets. A screen for genes that if mutated are lethal only when expressed together with overexpressed α-synuclein revealed genes encoding components of the vesicular trafficking machinery (Outeiro and Lindquist, 2003; Willingham *et al.*, 2003). In other studies, α-synuclein impaired proteasome-mediated protein degradation, altered proteasome composition, and reduced the ability of yeast cells to withstand stationary phase aging (Chen *et al.*, 2005; Sharma *et al.*, 2006).

Recently, an interesting approach to determine synuclein toxicity in yeast was used by Volles and Lansbury (2007). These authors screened a library of random point mutants to find variants with different phenotypes.

Screening of 59 synuclein mutants *in vitro* allowed to find two double-point mutants that fibrillized slowly relative to wt, $A^{30}P$, and $A^{53}T$ α-synucleins. No correlation between the yeast toxicity and fibrillization rate was found, suggesting that fibrillization is not necessary for synuclein-induced toxicity. Furthermore, β-synuclein was of intermediate toxicity to yeast and γ-synuclein was nontoxic. In a second screen, 25 nontoxic α-synuclein sequence variants were isolated, most of which contained a mutation to either proline or glutamic acid that caused a defect in membrane binding. The authors hypothesize that yeast toxicity is caused by synuclein binding directly to membranes at levels sufficient to nonspecifically disrupt homeostasis.

3.9.2. *Drosophila* as a model

α-Synuclein is toxic to DAN when expressed in *Drosophila* (Feany and Bender, 2000). Overexpression of α-synuclein caused an adult-onset, selective loss of DAN associated with progressive motor dysfunction and with the presence of filamentous intraneuronal inclusions containing α-synuclein (Auluck *et al.*, 2002, 2005; Dawson *et al.*, 2002). Hsp70 had a dramatic rescue effect to maintain dopaminergic neural numbers and prevent the degeneration of DAN (Auluck *et al.*, 2002; Bonini, 2002), suggesting a potential therapeutic approach to enhance neuron survival in PD.

Another protein that has a protective effect against α-synuclein toxicity in *Drosophila* model is Rab1 (Auluck *et al.*, 2002). Rab1 coexpression rescued TH-positive neuron loss, and suppression of α-synuclein toxicity by Rab1 is as efficient as that of Hsp70 (Auluck *et al.*, 2002; Cooper *et al.*, 2006).

3.9.3. *C. elegans* as a model

The Tg worms that overexpressed wt- or mutant human α-synuclein in DAN exhibited accumulation of α-synuclein in the cell bodies and neurites of DAN (Kuwahara *et al.*, 2006). Importantly, Tg worms expressing $A^{30}P$ or $A^{53}T$ α-synuclein showed lower neuronal DA and failure in modulation of locomotory rate in response to food, a function attributed to DAN. These Tg worms also exhibited neuron-specific dysfunction caused by accumulation of α-synuclein, but not β-synuclein. A strong rescue effect of DAN loss by Rab 1 again was observed, which is comparable to torsin A (Cao *et al.*, 2005).

3.9.4. Mice and rats overexpressing human α-synuclein

Overexpression of human wt-, mutant $A^{53}T$, $A^{30}P$, or truncated α-synuclein in mice results in variable neuropathological and behavioral phenotypes, and expression level varies in the range of 0.5- to 30-fold compared with endogenous α-synuclein. The most significant phenotypic alterations are consistently observed in the highest expressing lines, regardless of the

promoter used to drive the transgene. This supports the idea that expression level plays a significant role in the disease progression and manifestation (Fleming *et al.*, 2005).

α-Synuclein under the control of the human PDGF-β promoter, which targets expression to the SNc, exhibited a considerable loss of dopaminergic terminals in the striatum and a decrease in motor performance (Masliah *et al.*, 2000) as well as reduced neurogenesis and lysosomal pathology (Rockenstein *et al.*, 2005; Winner *et al.*, 2007). In mice overexpressing $A^{53}T$ mutant driven by the *Thy*1 promoter, α-synuclein was expressed in nonnigral tissues, especially the spinal cord. Such expression caused denervation of neuromuscular junctions, subsequent degeneration of motor axons, and severe locomotor deficits (van der Putten *et al.*, 2000). Tg mice overexpressing the $A^{30}P$ α-synuclein driven by the *Thy*1 promoter also develop many of the properties of the LB disease, for example, resistance to proteinase K, neuritic pathology, and formation of α-synuclein inclusions (Neumann *et al.*, 2002). Finally, Tg mice overexpressing *Thy*1-driven wt-α-synuclein showed more chronic and age-progressive phenotypes. They revealed reduced hind limb stepping early on and significantly increased slipping in a beam walking test (Fleming *et al.*, 2004).

Overexpression of wt- and mutant α-synuclein under prion protein promoter caused its expression in SNc (Giasson *et al.*, 2002; Lee *et al.*, 2002b). Despite aberrant accumulation of α-synuclein in the midbrain, nigral DAN did not display any neuropathological abnormalities. Mice overexpressing $A^{53}T$ α-synuclein, but not the wt- or $A^{30}P$ protein, exhibited age-dependent motor impairments associated with neuropathology in spinal cord and other nonnigral brain regions. This pathology was accompanied by axonal degeneration of motor neurons.

Rat TH promoter ensures the accumulation of α-synuclein within DAN bodies (Matsuoka *et al.*, 2001). Two lines overexpressing $A^{53}T$ or $A^{30}P$ α-synuclein in the SNc did not display LB, nigral cell loss, reductions in striatal DA, or behavioral impairment (Matsuoka *et al.*, 2001). However, overexpression of α-synuclein containing both the $A^{53}T$ and $A^{30}P$ mutations resulted in impaired locomotor activity, reductions in striatal DA, and morphological abnormalities in nigral axons (Richfield *et al.*, 2002). In addition, Tg mice with such double-mutant α-synuclein expressed strong sensitization to the DA neurotoxic effects of the pesticides paraquat and maneb (Thiruchelvam *et al.*, 2004). Furthermore, combining two mutations ($A^{30}P$ and $A^{53}T$) in one protein did not increase neurotoxicity of α-synuclein. Adeno- or lentiviral-mediated models have been used to analyze the effect of α-synuclein in the SNc rat neurons. In these studies, overexpression of either wt- or mutant protein led to cellular and axonal pathology associated with loss of nigral neurons, decrease in striatal DA levels, and significant motor impairment but no fibrillar inclusions (Kirik *et al.*, 2002; Lo Bianco *et al.*, 2002).

An inventive approach to overexpress α-synuclein using its own promoter is to use 145 kB P1 artificial chromosome containing the entire human gene including 34 kB of upstream sequences (Gispert *et al.*, 2003). This upstream region contains all currently known regulatory elements for this gene (Touchman *et al.*, 2001). The use of artificial chromosome in Tg mice ensured whole-brain overexpression levels comparable with the level of expression of $A^{53}T$ α-synuclein under PrP promoter. However, in PAC mice, fewer neurons with somal α-synuclein accumulation were observed (Gispert *et al.*, 2003).

Another pioneering approach in mouse Tg models was crossbreeding of different mouse lines to detect genes modifying toxic effect of α-synuclein. A Tg mouse line with PDGFβ-driven expression of α-synuclein was crossbred with a double-mutant amyloid precursor protein mouse line with high plaque load (Masliah *et al.*, 2001). In such bigenic mice, the rotarod deficit develops at younger age and was accompanied by a higher amount of α-synuclein-positive inclusions. Surprisingly, breeding of Tg mice with $A^{53}T$-α-synuclein driven by PrP promoter with parkin KOs did not cause an aggravation of α-synuclein phenotype (von Coelln *et al.*, 2006). When a mouse line expressing wt- human α-synuclein driven by PDGFβ promoter was crossbred with another Tg line expressing β-synuclein driven by *Thy1* promoter, a significant reduction of the number of α-synuclein inclusions and improvement of locomotor function were observed (Hashimoto *et al.*, 2001).

Thus, Tg mouse studies suggest that α-synuclein is important for axonal and synaptic integrity, but surprisingly catechol-aminergic neurons are not particularly sensitive to mutant α-synuclein. α-Synuclein Tg mice fail to display any significant DA neuron abnormalities, particularly in comparison with pathological changes observed in *Drosophila* DA neurons and the DA-dependent α-synuclein toxicity seen in human neuronal cell cultures (Kahle, 2007; Xu *et al.*, 2002). These results may be explained by higher resistance of murine cells to mutant forms of α-synuclein.

3.9.5. Mammalian cell cultures

Overexpression of α-synuclein in human dopaminergic SH-SY5Y cells caused its aggregation. The aggregates were immunopositive for ubiquitin, nitrotyrosine, and dityrosine and also contained γ-tubulin and chaperones. They formed aggresome-like intracellular structures and after reactive oxygen species (ROS) exposure, caspase 3 was activated in such cells. Ferric iron played a key role in the aggregation of α-synuclein and the authors assumed that the aggregate formation was protective against various cellular insults including oxidative stress (Furukawa *et al.*, 2006; Takeda *et al.*, 2006).

Overexpression of $A^{53}T$ α-synuclein using adeno-associated virus (AAV) leads to the formation of distorted neurites, intraneuritic swellings, and

granular perikaryal deposits in cultured neurons. These cell culture models may correspond to an early phase of PD reflecting pathological neuritic alterations before significant neuronal cell loss occurs (Zach *et al.*, 2007).

A promising approach was recently used by Schneider *et al.* (2007) who overexpressed wt, $A^{53}T$, and $A^{30}P$ isoforms of α-synuclein in expanded populations of fetal cortical progenitors. The expressed α-synuclein was localized in the nucleus and around microvesicles. Only mutant $A^{53}T$ protein was acutely toxic, pointing to a high vulnerability of such progenitor cells to this mutation. Constitutive overexpression of wt-α-synuclein impaired the innate ability of progenitors to switch toward gliogenesis at later passages. When α-synuclein was overexpressed in terminally differentiated neuroectodermal cultures derived from human embryonic stem cells, it induced acute cytotoxicity and specifically reduced the number of neurons expressing TH or γ-aminobutiric acid. Thus, α-synuclein overexpression in neural embryonic cells causes a pattern of degeneration that is similar to some features of PD.

4. Localization of Synucleins

4.1. Intracellular localization

In early studies, it was established that α-synuclein localizes mostly in the cytosol and synaptic terminals (George *et al.*, 1995; Iwai *et al.*, 1995; Jakes *et al.*, 1994; Maroteaux *et al.*, 1988; Murphy *et al.*, 2000; Withers *et al.*, 1997). β-Synuclein shows a nearly identical subcellular localization, as it is also enriched in presynaptic nerve terminals and displays extensive colocalization in both mouse and human brain (Clayton and George, 1998). α-Synuclein can be detected in nerve terminals and in different subcellular fractions as well as in CSF, blood plasma, platelets, and lymphocytes. While α-synuclein is abundant in nerve terminals during adulthood, it has been found in the perikarya during development (Galvin *et al.*, 2001b). This change in intracellular localization suggests that α-synuclein function may evolve as neural differentiation and maturation progress.

4.1.1. α-synuclein nuclear localization

The indication about possible nuclear localization of synucleins appeared in the very first article about these proteins (Maroteaux *et al.*, 1988). In some later publications, the nuclear localization was criticized as an artifact of using for staining of nonpurified synuclein antiserum and synuclein was detected mostly in cytoplasm (Bennett, 2005; Iwai *et al.*, 1995). Nevertheless in several later studies, synucleins were detected in the nuclei (Schneider *et al.*, 2007; Yu *et al.*, 2007). The contradiction between these results might be explained by the fact that synucleins may have dynamic localization and

some triggers, for example stress can cause translocation of synucleins from the cytoplasm to the nucleus (Surgucheva *et al.*, 2006).

Nuclear translocation of α-synuclein is induced by monoubiquitination (Monti *et al.*, 2007) and oxidative stress (Sangchot *et al.*, 2002; Xu *et al.*, 2006). Another member of the synuclein family, γ-synuclein, also exhibits nucleocytoplasmic shuttling in response to stress. In photoreceptor cell culture 661W, most of γ-synuclein is present in the cytoplasm and perinuclear area in the form of particles (dots). However, under stress conditions, a translocation of γ-synuclein to the nucleus occurs (Fig. 6.7) (Surgucheva *et al.*, 2006), which may be connected with its role in the

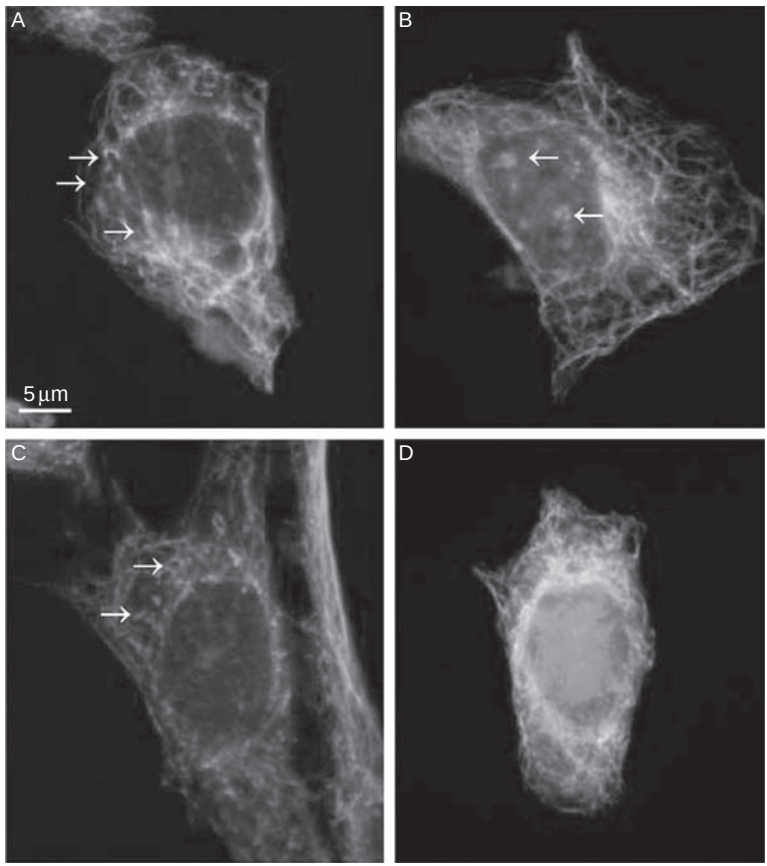

Figure 6.7 Immunolocalization of γ-synuclein in photoreceptor cells 661W. (A–D) Localization of γ-synuclein (black) and α-tubulin (gray). (A, C) Control cells; (B, D) cells incubated at 42 °C. γ-Synuclein localizes in the cytoplasm and perinuclear area in the form of dots or particles (arrows) under normal conditions (A, C) and is partially relocated to the nucleus at elevated temperature (B, D). (From Surgucheva *et al.*, 2006.)

regulation of transcription (Surgucheva *et al.*, 2003). γ-Synuclein can also be translocated by cytokinesis to the midbody, the cytoplasmic bridge linking the two daughter cells (Surgucheva *et al.*, 2006).

In a recent publication, Schneider *et al.* (2007) confirmed the nuclear localization of α-synuclein in progenitors derived from the human fetal cortex. Kontopoulos *et al.* (2006) reported about α-synuclein immunoreactivity in the nuclei of transiently transfected SH-SY5Y cells and also found endogenous α-synuclein in the nuclei of DAN in wt-mice. Importantly, α-synuclein promotes neurotoxicity when targeted to the nucleus. Conversely, sequestering α-synuclein in the cytoplasm does not yield significant toxicity.

4.1.2. α-Synuclein and mitochondria

Mitochondria play a pivotal role in neuronal cell survival or death because they are regulators of both energy metabolism and apoptotic pathways. It is well established that oxidative stress in the mitochondria is associated with the pathogenesis of NDDs and aging. However, a possible role of α-synuclein in this process came in the focus of investigation only recently. Currently, controversial results exist about the interrelationship between α-synuclein and mitochondria. Some group of investigators explain the effect of α-synuclein on mitochondrial functions as secondary, while others assume that α-synuclein exerts its effect on mitochondrial functions being a component of mitochondrial membrane.

α-Synuclein KO mice display resistance to MPTP-induced degeneration of DAN, and this resistance appears to result from an inability of the toxin to inhibit complex I (Dauer *et al.*, 2002). Furthermore, the mice with overexpression of α-synuclein treated with MPTP have significantly greater mitochondrial abnormalities than those seen in either of the saline-treated controls or the MPTP-treated wt-mice (Song *et al.*, 2004). Moreover, there is evidence that overexpression of α-synuclein impairs mitochondrial function, produces morphological changes in mitochondria, and promotes oxidative stress (Hsu *et al.*, 2000). Orth *et al.* (2004) demonstrated the fall in mitochondrial membrane potential in cells overexpressing wt- or $A^{53}T$ α-synuclein. Phosphatidyl choline 12 cells inducibly expressing α-synuclein show mitochondrial depolarization and induction of mitochondria-dependent cell death (Smith *et al.*, 2005; Tanaka *et al.*, 2001).

Although these studies are consistent with each other and with the concepts about a role of mitochondria in synuclein toxicity, the problem in interpreting them is that there is little evidence that α-synuclein affects mitochondria directly. However, recent studies demonstrate that α-synuclein may be a component of the outer mitochondrial membrane. Tg mice overexpressing $A^{53}T$ synuclein develop mitochondrial pathology. Mitochondrial complex IV activity was reduced and mitochondrial DNA was

damaged. Subsets of mitochondria contained human α-synuclein and were shrunken, swollen, or vacuolated (Martin *et al.*, 2006a).

A physical link between α-synuclein and mitochondria was also found by Li *et al.* (2007).These investigators detected α-synuclein in the fraction of purified mitochondria. As shown by confocal microscopy, α-synuclein colocalizes with subunit IV of cytochrome oxidase (COX IV). Beal (2004) put forward a hypothesis that α-synuclein could be transported into mitochondria through translocation mechanisms.

4.2. Extracellular localization

Synucleins do not have signal peptides or ER targeting signal sequences and for a long time, they were considered as exclusively intracellular proteins. However, a growing number of experimental data indicated that they can be secreted from cells and be present in CSF, blood plasma, platelets, and lymphocytes.

4.2.1. Presence in CSF and plasma

Full-length α-synuclein was identified in CSF suggesting that it can be released by neurons in the extracellular space. Since the amount of α-synuclein in CSF does not significantly vary in PD and normal cases, α-synuclein is not considered a peripheral marker of PD (Borghi *et al.*, 2000). Later El-Agnaf *et al.* (2003) detected α-synuclein in conditioned culture media from human neuroblastoma cells, as well as in human CSF and blood plasma. Therefore, cells normally secrete α-synuclein into media, both *in vitro* and *in vivo*. Later the same group developed ELISA method that detects only oligomeric "soluble aggregates" of α-synuclein and found significantly elevated levels of oligomeric forms of α-synuclein in plasma samples from PD patients compared with controls (El-Agnaf *et al.*, 2006). This approach may offer new opportunities for developing diagnostic tests for PD and related diseases. The method can also be used for testing therapeutic agents aimed at preventing or reversing the aggregation of α-synuclein.

4.2.2. Presence in platelets and lymphocytes

Hashimoto *et al.* (1997) studied the patterns of α- and β-synuclein expression in a megakaryocyte-platelet system. In this hematopoietic cell line, α-synuclein expression was upregulated during megakaryocytic differentiation, while β-synuclein was downregulated. The authors concluded that α-synuclein but not β-synuclein was abundantly expressed in platelets. Later Park and coauthors (2002) showed that α-synuclein may function as a specific negative regulator of α-granule release in platelets. Platelets contain full-length α-synuclein, its 6 and 12 kDa fragments, as well as γ-synuclein. However, the levels of both proteins in PD patients and normal controls were not different, indicating that they are not suitable

peripheral diagnostic markers for PD (Li *et al.*, 2002). Altered expression of α-synuclein in peripheral lymphocytes may induce apoptosis in PD patients (Kim *et al.*, 2004).

4.3. Synucleins in ocular tissues

The first synuclein from retina cDNA library was cloned by yeast two-hybrid system and initially called synoretin. Its coexpression with different *trans*-activator proteins demonstrated that it activated some signaling pathways presumably by binding to a transcription factor (Surguchov *et al.*, 1999). More detailed analysis demonstrated that this was a bovine orthologue of γ-synuclein (Surguchov *et al.*, 2001a) and in further publications, the authors switched to more conventional nomenclature.

Later two other members of the synuclein family were detected in the retina (Surguchov *et al.*, 2001a). The majority of α-synuclein is localized in the inner plexiform layer (IPL); while β-synuclein is present in the IPL and the inner nuclear layer and γ-synuclein in retinal ganglion cells (RGC) and the neurofiber layer (NFL). α-Synuclein is also present in the outer segments of photoreceptors and in their axon terminals (cone pedicles and rod spherules) in the outer plexiform layer of the retina. α-Synuclein is found in rod and cone bipolar cells, as well as in GABAergic and glycinergic amacrines, distributing along a complex plexus throughout the IPL (Martínez-Navarrete *et al.*, 2007). γ-Synuclein is the second largest RGC cluster after tubulin (Farkas *et al.*, 2004). Due to such specific localization, γ-synuclein may be considered as a marker of RGC (Surgucheva *et al.*, 2008). Synuclein ocular pathology was found in some eyes diseases and NDDs (Chapter V, H).

5. Synuclein Pathophysiology

α-Synuclein toxicity may be expressed through several different mechanisms, which sometimes are interconnected. Although not certain, the prevailing thought is that protein aggregation, especially the formation of small oligomeric species, is important in pathogenesis. This hypothesis is difficult to accurately test, since there is currently no established method to selectively remove partially aggregated synuclein. Other mechanisms consider formation of pore forming structures that cause the rupture of cellular membranes and neurotransmitter leakage, inhibition of axonal transport and protein turnover via the ubiquitin-proteasomal or chaperone-mediated autophagic systems, ER trafficking deficit, and damage to mitochondria. In addition to aggregation, several other mechanisms may switch α-synuclein into vicious molecule, for example the presence of a pathologic mutation, oxidative and nitrosative stress, phosphorylation, and other PTMs.

Mitochondrial and proteasomal dysfunction as well as DA can influence aggregation and folding of α-synuclein into a variety of forms including protofibrils, fibrils, and filaments. The processing of α-synuclein and cleavage at its C- terminus by ''synucleinases'' (Li *et al.*, 2005) correlate with disease severity and with its propensity to oligomerize. It appears that the protofibrils and oligomeric species are the most toxic forms, and the generation and stabilization of these forms by mutation or cellular milieu may be a central pathological mechanism.

A very different aspect of α-synuclein toxicity is related to its effect on membrane traffic. Recent reports indicate that mutant or simply overexpressed α-synuclein could cause damage by interfering with particular steps of neuronal membrane traffic. α-Synuclein selectively blocks ER-to-Golgi transport, thus causing ER stress (Cooper *et al.*, 2006; Ogburn and Figueiredo-Pereira, 2006).

5.1. Synuclein aggregation and its toxicity

5.1.1. Aggregation of α-synuclein in the brain

The conversion of α-synuclein from soluble monomers to aggregated, insoluble forms in the brain is a key event in the pathogenesis of PD and related NDDs. Development of synucleinopathies appears to be linked to processes that increase the rate at which α-synuclein forms toxic aggregates. These processes include elevation of protein concentration (via increased expression or reduced degradation) and formation of altered forms of α-synuclein (mutant, truncated, or chemically modified).

α-Synuclein accumulates in hallmark inclusions in neurons, such as LB and LN in PD (Forno, L. S. (1996); Krüger *et al.*, 1998; Mezey *et al.*, 1998; Polymeropoulos *et al.*, 1997) and DLB (Spillantini *et al.*, 1998b). Aggregates of α-synuclein are also present in brain of 60–70% of AD cases (Hamilton, 2000; Mukaetova-Ladinska *et al.*, 2000). Furthermore, α-synuclein is associated with pathological lesions in other NDDs, sometimes involving non-neuronal cells, such as the GCIs found in MSA (Arima *et al.*, 1998; Wakabayashi *et al.*, 1998).

5.1.2. Factors affecting synuclein aggregation and toxicity

Aggregation of α-synuclein and filament formation can be induced by mono- and polyvalent ions, elevated temperature, small amines, heparin and other glycosaminoglycans, oxidative and nitrative stresses, and different environmental insults (Bennett, 2005; Hoyer *et al.*, 2002; Uversky *et al.*, 2001a).

Transition metals differentially affect the level of α-synuclein aggregation, for example iron promotes and magnesium inhibits aggregation (Golts *et al.*, 2002). The apparent affinity of α-synuclein for magnesium is strong enough to allow interaction of α-synuclein with magnesium in living cells,

where the average intracellular concentration of magnesium is about 0.5 mM. This suggests that this interaction could have physiological significance. Although the concentration of free iron in the cell is lower (<1.5 μM), which is below the affinity of α-synuclein for iron (173 μM) determined *in vitro*, α-synuclein interacts with iron in the living cell. It is possible that cofactors increase the affinity of α-synuclein for iron sufficient to allow a physiological interaction (Golts *et al.*, 2002). Although binding of magnesium appears to introduce a conformation that promotes binding of iron, this same conformational change inhibits aggregation of α-synuclein. This data suggests that magnesium either changes the conformation of α-synuclein to one that resists aggregation or induces dimerization to a structure that resists aggregation.

5.1.3. Role of DA in synuclein aggregation and toxicity

Metabolism of DA and α-synuclein are tightly interrelated. For example, DA modulate α-synuclein aggregation, while α-synuclein regulates DA biosynthesis, storage, and release. Both DA and α-synuclein are involved in synaptic vehicles recycling and priming. The interaction of α-synuclein with DA may explain high susceptibility of DAN to α-synuclein expression. DA can bind to the α-synuclein monomer and alter the kinetics of its aggregation. The DA-α-synuclein adducts stabilize toxic protofibrils and inhibits fibrillation (Conway *et al.*, 2001; Rochet *et al.*, 2004; Moussa *et al.*, 2007). $A^{53}T$ mutation drastically increases the propensity of α-synuclein to aggregate in the presence of DA, thereby contributing to PD pathogenesis.

On the other hand, α-synuclein overexpression may regulate DA biosynthesis, acting on several enzymes that play different roles in this process. The activity of TH, the enzyme catalyzing the rate-limiting step in the biosynthesis of catecholamines, is negatively modulated by α-synuclein either interacting directly with the enzyme (Perez *et al.*, 2002) or decreasing its gene expression (Baptista *et al.*, 2003). These results point to a key role for α-synuclein in the regulation of DA synthesis. A loss in α-synuclein function consequent to its aggregation or decreased expression, as occurs in PD, may selectively disrupt DA homeostasis and negatively affect DAN survival (Perez *et al.*, 2002).

α-Synuclein can also directly couple to the carboxyl tail of the dopamine transporter (DAT). The α-synuclein–DAT protein complex formation accelerates DAT-mediated cellular DA uptake and DA-induced cellular apoptosis. Parkin, an E2-dependent E3 protein ubiquitin ligase associated with recessive early onset PD, exerts a protective effect against DA-induced α-synuclein-dependent cell toxicity. Parkin impairs the α-synuclein/DAT coupling by interacting with the C-terminus of the DAT and blocks the α-synuclein-induced enhancement in both DAT cell surface expression and DAT-mediated DA uptake (Moszczynska *et al.*, 2007). α-Synuclein modulates DAT function, and disruption of this modulatory process may cause

an increased reuptake of high levels of intracellular DA by DAT, leading to neurotoxicity (Sidhu *et al.*, 2004).

Defects in synaptic vesicle recycling could play a pathogenic role in the development of PD. In this case, α-synuclein role in the disease mechanism may be connected with regulation of vesicle recycling via its inhibition of PLD2 and/or its ability to bind FAs. Since DA is a highly cytotoxic neurotransmitter, its improper sequestration could potentially lead to DA-dependent DAN neurodegeneration.

Mutant α-synuclein may increase levels of cytoplasmic DA and may be important for DA storage (Lotharius and Brundin, 2002b). Lentivirus-mediated overexpression of $A^{53}T$ α-synuclein led to a decrease in the levels of vesicular monoamine transporter protein (VMAT2), reduced DA release in response to high potassium stimulation, and enhanced release in response to amphetamine (Lotharius *et al.*, 2002). Mutant cells also exhibited higher levels of cytoplasmic DA and increased production of superoxide radicals. These results suggest that $A^{53}T$ α-synuclein may cause impaired vesicular DA storage, culminating in cytosolic DA accumulation, and oxidative stress. Apoptosis induced in mesencephalic neurons by overexpression of $A^{53}T$ α-synuclein can be blocked by depleting cells of intracellular DA. Thus, the expression of the pathogenic properties of mutant α-synuclein may depend on DA (Xu *et al.*, 2002).

α-Synuclein can affect intracellular DA by other mechanisms, for example, through interactions with proteins that regulate DA synthesis and uptake. For example, binding of α-synuclein to the DAT enhances extracellular DA uptake by increasing the number of functional transporters at the cell surface (Lee *et al.*, 2001). Importantly, α-synuclein direct binding to TH inhibits its enzymatic activity (Perez *et al.*, 2002).

Although DA itself may not be toxic at physiologically relevant doses, DA metabolites may play a role in α-synuclein aggregation (Galvin, 2006). Overexpression of α-synuclein mutants could disrupt the ATP-dependent vesicular proton gradient, diminish pH of chromaffin vesicles, and lead to increased cytosolic species of catecholamines. Interestingly, wt-α-synuclein is significantly less potent in diminishing vesicular pH than either $A^{30}P$ or $A^{53}T$ mutants (Mosharov *et al.*, 2006). DA synthesized in the cytoplasm is taken up into synaptic vesicles via VMAT2 transporter, and it is presumably much more stable in these vesicles. The inhibition of ER-Golgi transport could result in an inhibition of delivery of VMAT2 to the synapses and accumulation of cytosolic DA that might be neurotoxic when metabolized. As DA helps stabilize protofibril formation by forming a DA-α-synuclein adduct, this may well cause a vicious circle where DA and α-synuclein enhance each others' toxicity. α-Synuclein also regulates catecholamine release from the synaptic vesicles, and its overexpression suppresses a vesicle ''priming'' step after secretory vesicle trafficking to docking sites, but before vesicle membrane fusion (Larsen *et al.*, 2006).

5.1.3.1. α-Synuclein, DA, and oxidative stress One of the possible mechanisms of PD is connected with the accumulation of toxic DA derivatives, causing oxidative stress and death of DAN (Lotharius *et al.*, 1999). In the presence of molecular oxygen, DA can undergo spontaneous autoxidation, generating toxic DA-quinones, superoxide free radicals, and H_2O_2 (Graham *et al.*, 1978). Oxidized catechols interact with α-synuclein AA sequence ^{125}YEMPS^{129} and the cleavage of this C-terminal fragment deprives the ability of oxidized catechols to inhibit α-synuclein aggregation (Mazzulli *et al.*, 2007). Thus, inappropriate C-terminal cleavage of α-synuclein, which occurs in PD brains, may cause its accelerated aggregation, inclusion formation, and dopaminergic neurodegeneration. Decline of intracellular catechol level may have similar consequences.

The metabolism of DA in nigral neurons produces ROS and other highly reactive chemical species that can cause oxidative stress, mitochondrial dysfunction, and cell death. Overexpression of α-synuclein, especially its mutant forms, increases the vulnerability of neurons to DA-induced cell death through an excessive generation of intracellular ROS (Junn and Mouradian, 2002). The dopaminergic specificity of α-synuclein neurotoxicity is related to endogenous DA production and ROS generation, because inhibition of DA synthesis by TH inhibitor α-methyl-*p*-tyrosine prevents α-synuclein-induced apoptosis in cultured DAN (Xu *et al.*, 2002). Oxidants may cause α-synuclein aggregation and initiate formation of toxic intermediate oligomers (Goldberg and Lansbury, 2000).

5.2. α-synuclein and microglia

Astrocytes do not synthesize α-synuclein, but take up α-synuclein produced and released by nerve cells (Braak *et al.*, 2007; Mori *et al.*, 2002; Tanji *et al.*, 2001). It is conceivable that the secretion of α-synuclein from neurons and absorption by glial cells is accompanied by some degree of its modifications, for example change of conformation or PTMs. In MSA, α-synuclein inclusions in the form of filamentary aggregates of about 25 nm in diameter are found most commonly in glia of oligodendrocytic origin (Tu *et al.*, 1998; Wakabayashi *et al.*, 1998).

5.2.1. Microglia activation

One of the important features of several NDDs is the accumulation of activated microglia (Croisier *et al.*, 2005). Microglia are the resident immune cells in the brain and activation links inflammation and neurodegeneration in PD (Hirsch *et al.*, 2003, Kim and Joh, 2006). α-Synuclein could activate microglia through a direct interaction or indirectly. Treatment of different cell cultures with exogenous α-synuclein or overexpression of α-synuclein in MN9D cell line causes microglial activation (Su *et al.*, 2007; Zhang *et al.*, 2005). These results are in a good agreement with the data demonstrating the

role of α-synuclein in microglial inflammation in SNc (Croisier *et al.*, 2005; Kim and Joh, 2006). Recent data suggest that α-synuclein-mediated microglial activation occurs through the class B scavenger receptor CD36 and downstream kinases (Su *et al.*, 2007). *In vivo* α-synuclein may exert this effect after its release from cells via ER/Golgi-independent exocytosis (Lee *et al.*, 2005b). Interestingly, another protein implicated in NDDs, amyloid β, also activates microglia through CD36 receptor (El Khoury *et al.*, 2003).

5.2.2. α-synuclein-containing inclusions in glial cells

α-Synuclein-immunoreactive inclusions in glial cells have received much less attention than similar inclusions in neurons. In the majority of studies on glia, the abnormal protein aggregation is detected in oligodendroglial cells (Braak *et al.*, 2007; Wakabayashi *et al.*, 2000a).

Oligodendroglial cytoplasmic inclusions of α-synuclein are diagnostic for MSA (Arima *et al.*, 1998; Spillantini *et al.*, 1998b; Wakabayashi *et al.*, 1998). α-Synuclein accumulation and aggregation in oligodendroglia may be explained by its impaired degradation or selective upregulation in glial cells (Miller *et al.*, 2005). An alternative explanation is the accumulation in glial cells of α-synuclein released by dying neurons (Wakabayashi and Takahashi, 2006; Wenning and Jellinger, 2005).

When α-synuclein is expressed in Tg mice driven by oligodendrocyte-specific myelin proteolipid protein promoter (PLP promoter), it is accumulated in the form of half-moon shaped and triangular inclusions similar to inclusions in MSA patients (Lantos, 1998). CNP-promoter (2′,3′-cyclic nucleotide 3′-phosphodiesterase)-driven α-synuclein expression causes neurodegeneration after administration of oxidized stress (Stefanova *et al.*, 2005) or upon aging (Yazawa *et al.*, 2005). However, in this Tg model, no GCI have been observed (Giasson *et al.*, 2003a).

Oligodendroglial overexpression of α-synuclein may induce neuroinflamation and neurodegeneration in MSA. Neuropathological studies have demonstrated an association of microglial activation and oligodendroglial α-synuclein burden in specific neuroanatomic systems affected in MSA. Aggregated α-synuclein, released or secreted from dying oligodendroglia, may induce microglial activation and thereby enhance the rate of neurodegeneration in MSA (Stefanova *et al.*, 2007).

5.3. Overlapping pathways in several human diseases

The most frequent sporadic forms of AD and PD are associated with an abnormal accumulation of Aβ and α-synuclein, respectively (Spillantini *et al.*, 1997; Takeda *et al.*, 1998). Human cases with clinical and neuropathological features of both AD and PD raise the possibility that these diseases involve overlapping pathways. Approximately 25% of patients with AD develop features of PD (Galasko *et al.*, 1994), and α-synuclein-

immunoreactive LB-like inclusions develop in many cases of sporadic AD and familial AD, as well as in Down syndrome (Hamilton, 2000; Lippa *et al.*, 1999). Moreover, LB in addition to α-synuclein usually contain APP (Arai *et al.*, 1991). The possible pathogenic interactions between Aβ and α-synuclein suggest that drugs aimed at blocking the accumulation of α-synuclein or Aβ α-synuclein might benefit a broader spectrum of NDDs than previously anticipated.

α-Synuclein is also expressed in differentiating brain tumors as well as various peripheral cancers and is involved in the regulation of tumor differentiation (Bruening *et al.*, 2000; Fung *et al.*, 2003; Kawashima *et al.*, 2000). Recent studies demonstrated that α-synuclein, but not β-synuclein, stimulates differentiation of osteosarcoma cells (Fujita *et al.*, 2007). α-Synuclein downregulates proteasome activity, which is regulated by alteration of PKC signaling activity and autophagy-lysosomal pathway. The mechanism of α-synuclein regulation of tumor differentiation overlaps that of neurological effects of α-synuclein (Fujita *et al.*, 2007).

5.4. β- and γ-synucleins in NDDs

5.4.1. β-synuclein

β-Synuclein plays a dual role in the neurodegeneration. Beneficial effects of β-synuclein are described in Chapter VII, A1. It has been reported that in addition to α-synuclein-containing LBs and LNs, the development of PD and DLB is accompanied by the appearance of nonfilamentous β-synuclein-positive aggregates in axon terminals of the hippocampus (Galvin *et al.*, 1999). This implicates β-synuclein, in addition to α-synuclein, in the progression of PD and DLB.

β-Synuclein pathology was also detected in a rare disease, neurodegeneration with brain iron accumulation, type 1 characterized clinically by Parkinsonism, cognitive impairment, and pseudobulbar features. β-Synuclein immunoreactivity was detected in spheroids but not in LB-like or glial inclusions in the brains of such patients (Galvin *et al.*, 2000). Pathological role of β-synuclein in NDDs may be associated with its ability to stimulate Aβ-aggregation *in vitro* (Jensen *et al.*, 1997) and with its possible autoimmunity that might play an inflammatory role in the pathogenesis of neurodegeneration (Mor *et al.*, 2003).

5.4.2. γ-synuclein

γ-Synuclein-positive inclusions have been found in axon terminals of the hippocampus (Galvin *et al.*, 1999). γ-Synuclein immunoreactivity was also detected in spheroids but not in LB-like or glial inclusions (Galvin *et al.*, 2000). The role of γ-synuclein in glaucoma and other ocular pathology is discussed in the Chapter V, H.

5.5. γ-synuclein in cancer

γ-Synuclein was initially identified as breast cancer-specific gene 1 because of its high expression in some forms of breast cancer (Ji *et al.*, 1997). Later the involvement of γ-synuclein in ovarian, liver, bladder cancer, and pancreatic adenocarcinoma was demonstrated (Iwaki *et al.*, 2004; Lavedan *et al.*, 1998b; Li *et al.*, 2004b; Ninkina *et al.*, 1998; Zhao *et al.*, 2006). Since expression level of γ-synuclein is well correlated with the metastatic lesions, the conclusion is drawn that γ-synuclein regulates tumor invasiveness and metastasis (Jia *et al.*, 1999; Liu *et al.*, 2005b). γ-Synuclein stimulates cell proliferation by increasing estrogen receptor-mediated signaling in breast cancer cells (Jiang *et al.*, 2003). In a later publication, Jiang *et al.* (2004) showed the role of a chaperone activity of γ-synuclein in the Hsp-based multiprotein chaperone complex for stimulation of estrogen receptor-α signaling.

Further studies showed that γ-synuclein interacts with a mitotic spindle checkpoint protein, BubR1, reducing checkpoint function and tumor progression (Gupta *et al.*, 2003; Inaba *et al.*, 2005). γ-Synuclein strongly stimulates the ligand-dependent transcriptional activity of estrogen receptor-α in breast cancer cells. The aberrant expression of γ-synuclein and BubR1-mediated interference with the spindle assembly checkpoint complex together may play an inhibitory role to the action of antimicrotubule drugs.

A strong correlation between γ-synuclein expression and metastasis is observed regardless of the cancer type (Liu *et al.*, 2005b). The aberrant expression of γ-synuclein and BubR1-mediated interference with the spindle assembly checkpoint complex together may play an inhibitory role to the action of antimicrotubule drugs (Fung *et al.*, 2003; Zhou *et al.*, 2006).

To determine if γ-synuclein is a biomarker for prognosis of breast cancer, Guo *et al.* (2007) generated a panel of monoclonal antibodies (mAbs) against γ-synuclein and correlated γ-synuclein expression in clinical breast cancer specimens with clinical outcome. Expression of γ-synuclein was strongly correlated with the stage, lymph node involvement, metastasis, tumor size, and Her-2 status. According to Cox multivariate analysis, γ-synuclein has independent prognostic significance above and beyond conventional variables (Guo *et al.*, 2007; Wu *et al.*, 2007). The authors conclude that γ-synuclein is a new unfavorable prognostic marker for breast cancer progression and a potential target for breast cancer treatment. Other investigators found that expression of γ-synuclein was associated with tumor grade but not with clinical outcome of patients with breast cancer (Martin *et al.*, 2006b).

Further evaluation of the prognostic power of γ-synuclein may provide information as to the drug resistance status of tumors and influence the clinical management and therapeutic approaches for cancer patients.

γ-Synuclein was also tested as a diagnostic tool and possible target in hepatocellular carcinomas (Zhao *et al.*, 2006). γ-Synuclein expression in primary tumors is a strong indicator of distant metastasis. Demethylation of γ-synuclein CpG island is an early sign of genetic abnormality in liver cirrhosis preceding hepatocarcinogenesis.

Important results for the understanding of the mechanism of γ-synuclein involvement in tumorgenesis were obtained by the methods of biochemistry and cell biology. In retinoblastoma cells, γ-synuclein is a centrosome-associated protein (Fig. 6.8) that regulates MAPK and Elk-1 pathways (Surguchov *et al.*, 2001b). γ-Synuclein has a dynamic intracellular localization and may translocate by cytokinesis to the midbody in astrocytoma and melanoma cell lines. Importantly, stress induces γ-synuclein shuttling between nucleus and cytoplasm (Fig. 6.7) (Surgucheva *et al.*, 2006).

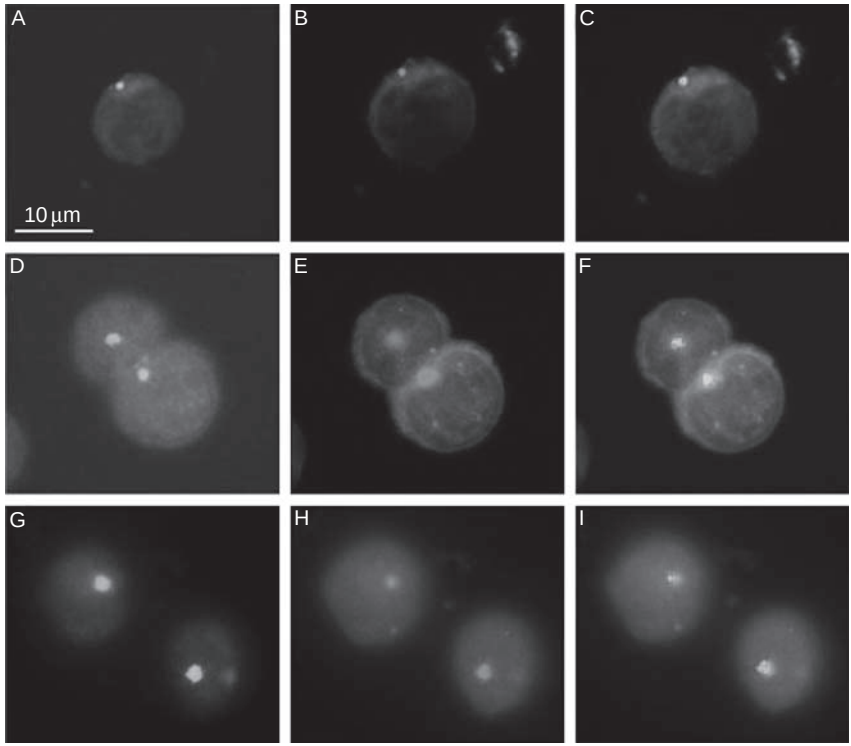

Figure 6.8 **Immunofluorescence microscopy demonstrating colocalization of γ-synuclein with centrosome markers in retinoblastoma Y79 cells. (A, D, G) Staining with γ-synuclein Ab. (B, E, H) Centrosome markers. (B) γ-Synuclein staining, (E) CTR-453 staining, (H) centrin 2 staining. (C, F, I) Merged images. (From Surguchov *et al.*, 2001b.)**

5.6. Synuclein pathology in ocular tissues

Abnormal synuclein localization was detected in the retina and in the optic nerve for α- and γ-synucleins using IHC methods. In the retina of Tg mice overexpressing α-synuclein under *thy-1* or PDGF-b promoters, α-synuclein accumulates in a subset of cells located in the inner nuclear layer and ganglion cell layer. A weaker staining was found in the inner segment of photoreceptor cells (Surguchov *et al.*, 2001a). In the optic nerve of Tg mice overexpressing α-synuclein, the accumulation of the protein deposits immunopositive for α-synuclein (Fig. 6.9) was detected (Surguchov *et al.*,

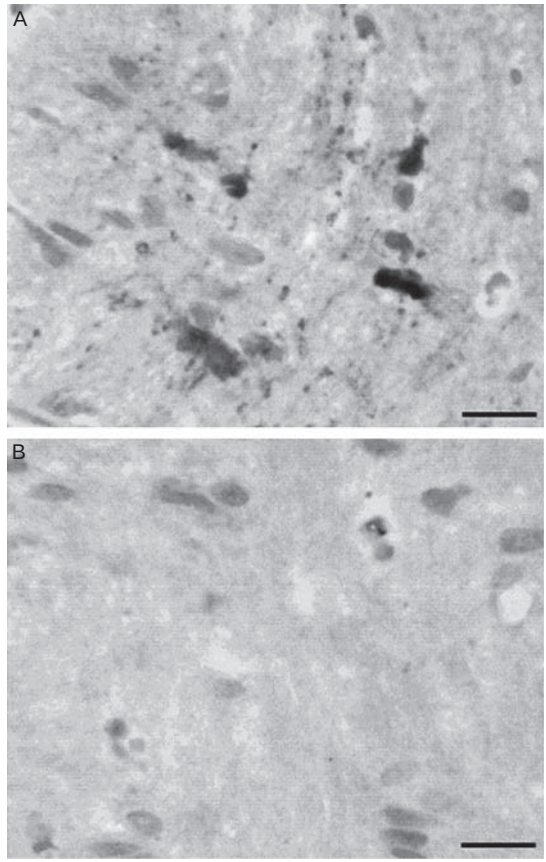

Figure 6.9 Immunohistochemical staining of optic nerve from Tg mouse overexpressing α-synuclein (A) and wild-type mice (B). α-Synuclein-immunopositive deposits were detected using DAB reagent (peroxidase; black); tissues were counterstained with hematoxylin (gray). Scale bar = 50 μm. (From Surguchov *et al.*, 2001a.)

2001a). The presence of similar deposits containing α-synuclein in the brain tissues is considered to play a causative role in NDDs (George, 2002; Goedert, 1999).

γ-Synuclein immunopathology was found in the retinas of AD patients. IHC staining for γ-synuclein revealed a partial loss of immunoreactivity in the NFL and the appearance of immunopositive staining in a subset of photoreceptor cells and cells of outer plexiform layer (Surguchov *et al.*, 2001a). The accumulation of γ-synuclein-positive inclusions also occurs in the glial cells of the optic nerve in glaucoma patients (Surgucheva *et al.*, 2002). Interestingly, γ-synuclein interacts with myocilin—a protein that is genetically linked with glaucoma inhibiting myocilin secretion and preventing the formation of high M_r forms of myocilin (Surgucheva *et al.*, 2005). Abnormality in γ-synuclein localization is also described in retinas of patients with retinoblastoma. Intensive immunoreactivity in NFL of control individuals almost disappears in the patient's retina with its strong accumulation in a subset of the RGC (Surgucheva *et al.*, 2008). Synuclein redistribution and cytoskeletal reorganization is also detected in the retina of patients with DLB (Maurage *et al.*, 2003).

6. Synuclein KO

Mice with the deletion of one or two synucleins are viable and exhibit little phenotypic changes in the majority of studies (Abeliovich *et al.*, 2000; Cabin *et al.*, 2002; Chandra *et al.*, 2004; Ninkina *et al.*, 2003; Surgucheva *et al.*, 2005). However, sometimes the results with KO mice generated by different approaches varied considerably. In α-synuclein KO mice, brain development and neuronal architecture, including the synapse, appeared normal and synaptic vesicle pools were normal, whereas some functional abnormalities in the dopaminergic system were found (Abeliovich *et al.*, 2000). The mutant mice did demonstrate a more rapid recovery of DA release after the second pulse in a paired stimulus depression paradigm. Behavioral studies were consistent with this observation that α-synuclein KO mice showed blunting of the increase in locomotor activity induced by amphetamines. Thus, α-synuclein may normally act to regulate the readily releasable pool of DA-containing vesicles negatively (Abeliovich *et al.*, 2000).

Cabin *et al.* (2002) generated α-synuclein-deficient mice by partially deleting the α-synuclein gene in embryonal stem cells and observed a dramatic loss of reserve vesicles and an increase in synaptic depression in α-synuclein KO mice. Electron microscopy of hippocampal sections and cultured hippocampal neurons showed a marked decrease in the pool of undocked synaptic vesicles in mice homozygous for the mutation. The

synaptic responses to prolonged, lower-frequency stimulation that would be expected to deplete reserve vesicle pools were significantly impaired in the mutant compared with the wt-mice. These results support the hypothesis that α-synuclein is required for the genesis, localization, and/or maintenance of at least some subset of vesicles that make up the reserve or resting pools of presynaptic vesicles.

Chandra *et al.* (2004) found that deletion of α- and β-synucleins in mice does not impair basic brain functions or survival. No significant changes in the ultrastructure of synuclein-deficient synapses, in short- or long-term synaptic plasticity, or in the pool size or replenishment of recycling synaptic vesicles were observed. Synaptic parameters, such as release of neurotransmitters and mobilization of synaptic vesicles were not impaired, but selective alterations in two synaptic signaling proteins complexins and 14-3-3 were found. Thus, synucleins may not be essential components of the basic machinery for neurotransmitter release but may contribute to the long-term regulation and/or maintenance of presynaptic function.

The study of glutamate release in KO mice demonstrated the weaker paired-pulse facilitations and the absence of frequency facilitation. These results suggest that lack of α-synuclein impairs mobilization of glutamate from the reserve pool. Thus, α-synuclein may play an important role in presynaptic mobilization of reserve pool neurotransmitter vesicles, not only for DA but also for glutamate (Gureviciene *et al.*, 2007).

Several studies showed that α-synuclein-deficient mice were resistant to MPTP neurotoxicity. The initial study suggested that a lack of α-synuclein interfered with the ability of MPP^+ to block complex I, by increasing monoamine vesicular transport (Dauer *et al.*, 2002). Mice lacking α-synuclein had an attenuated loss of DA but no loss of striatal VMAT2 (Drolet *et al.*, 2004). In mice lacking α-synuclein, MPTP induced metabolic activation, but behavioral symptoms and loss of DA neurons were almost completely abrogated. Thus, normal α-synuclein functions may be important to DA neuron viability and their alterations may modify the vulnerability of DA neurons to an environmental toxin.

Ellis *et al.* (2005) found that deletion of α-synuclein gene caused significant mitochondrial abnormalities. In mice lacking α-synuclein ($Snca^{-/-}$), total brain steady-state mass of the mitochondria-specific phospholipid, cardiolipin, is reduced and its acyl side chains show a considerable increase in saturated FAs. The abnormalities in mitochondrial membrane properties were associated with a 15% reduction in linked complex I/III activity of the electron transport chain. These findings suggest a relationship between α-synuclein's role in brain lipid metabolism, mitochondrial function, and PD.

Klivenyi *et al.* (2006) found that α-synuclein-deficient mice are resistant to MPTP-induced degeneration of DAN. There was dose-dependent protection against loss of both DA in the striatum and DAT-immunoreactive neurons in the SNc. These results suggest that α-synuclein plays a role of a

modulator of oxidative damage, which has been implicated in neuronal death produced by MPTP and other mitochondrial toxins.

Therefore, in spite of small phenotypic alterations in the majority of KO mice, they brought important information about synucleins. The absence of very clear phenotype in single and double KOs under basal conditions suggests that they may perform subtle regulatory functions and might become essential only under specific conditions of stress or malfunction, as shown, for example, by Chandra *et al.* (2005) who found an essential function for α-synuclein in CSPα-deficient mice (Chapter II, B and Chapter III, E).

7. Approaches to Reduce Pathological Action of Synucleins

7.1. α-synuclein

Based on the knowledge of α-synuclein biochemistry and molecular biology, different methods are considered to inhibit its pathogenic properties. They include methods to inhibit α-synuclein aggregation by reducing its expression, increasing its degradation, impairing the formation of toxic aggregates, or inhibiting its truncation. A number of different strategies have been proposed to control α-synuclein aggregation and toxicity *in vivo* and *in vitro*. They include the use of β-synuclein (Hashimoto *et al.*, 2001; Tsigelny *et al.*, 2007), Hsp70 (Klucken *et al.*, 2004), flavonoids (Zhu *et al.*, 2004), short antiaggregational peptides, vaccination (Masliah *et al.*, 2005), magnesium (Golts *et al.*, 2002), substance affecting proteasomal/autophagosomal clearance mechanisms, and some other agents.

7.1.1. The beneficial effect of β-synuclein

β-Synuclein is often considered to be a nonamyloidogenic member of the synuclein family since it lacks the nonamyloidogenic component domain (Fig. 6.2) thought to make α-synuclein prone to aggregation (El-Agnaf and Irvine, 2000; Jensen *et al.*, 1995). The beneficial effect of β-synuclein may be due to its ability to inhibit α-synuclein aggregation (Hashimoto *et al.*, 2001; Park and Lansbury, 2003), block the formation of α-synuclein dimers with subsequent inclusion into the membrane and organization into cation channels (Tsigelny *et al.*, 2007), or regulate Akt activity (Hashimoto *et al.*, 2004).

Alves da Costa *et al.* (2003) using stable clones of TSM1 neurons overexpressing this protein showed antiapoptotic effect of β-synuclein. β-Synuclein lowers the number of TUNEL-positive cells and DNA fragmentation and diminishes both caspase 3 activity and immunoreactivity. β-Synuclein also triggers a drastic reduction of p53 expression at a

posttranscriptional level. Thus, β-synuclein protects neurons from caspase activation in a p53-dependent manner. The authors speculate that β-synuclein could complement α-synuclein deficiency at least in the first stages of PD neuropathology.

In the cortex of mice overexpressing β-synuclein, a marked reduction in α-synuclein protein expression was observed without affecting its RNA levels (Fan *et al.*, 2006). This reduction in α-synuclein protein expression was not accompanied by decreases in α-synuclein mRNA expression. Overexpression of β-synuclein prevented the progression of impaired motor performance, reduced α-synuclein aggregation, and extended mice survival. The authors discuss their results with the downregulation of α-synuclein protein expression by β-synuclein is an appealing treatment option for synucleinopathies.

Although experiments with β-synuclein were important for understanding the mechanisms of α-synuclein toxicity, the initial enthusiasm about possible therapeutic use of β-synuclein is diminished, since according to Mor *et al.* (2003), it can induce autoimmune diseases. The authors found that immunization with β-synuclein peptide induced experimental autoimmune encephalomyelitis and uveitis in immunized rats. Autoimmunity to β-synuclein might play an inflammatory role in the pathogenesis of neurodegeneration (Mor *et al.*, 2003). Another reason reducing the enthusiasm about full-length β-synuclein use as a therapeutic agent concerns its intracellular concentration. A molar excess of β-synuclein is required to prevent fibrilization of very abundant α-synuclein, which can be problematic for a protein which should be present in brain cells.

7.1.2. Peptides preventing α-synuclein aggregation

El-Agnaf *et al.* (2004) used a library of overlapping seven-mer peptides spanning the entire α-synuclein sequence, and identified AA residues 64–100 of α-synuclein as the binding regg3 ion responsible for its self association. Modified short peptides containing α-synuclein AA sequences from part of this binding region (residues 69–72) were found to interact with full-length α-synuclein and block its assembly into both early oligomers and mature amyloid-like fibrils. Based on these findings, the authors developed a cell-permeable inhibitor of α-synuclein, using the polyarginine peptide delivery system. Amer *et al.* (2006) found several new peptides and identified small molecules that can inhibit α-synuclein oligomerization and toxicity *in vitro*. These compounds could serve as lead compounds for the design of new drugs for the treatment of PD and related disorders in the future.

Abe *et al.* (2007) used a method of silico panning and genetic algorithm to screen peptides able to bind to hydrophobic central region of α-synuclein and affect its aggregation. They selected an 11-mer peptide GAVVTGV-TAVA that is a part of NAC central hydrophobic region as a docking target. For the screening of binding peptides, the authors selected tetramer peptides

consisting of hydrophobic and polar AA that tended to form hydrogen bonds. After performing the binding analysis by surface plasmon residues measurements, the top peptides were found QSTQ, GSQQ, SQTQ, and AQTQ. These peptides bound to α-synuclein with low dissociation constants ($K_D = 19\ \mu M$ for QSTQ and AQTQ) and promoted α-synuclein fibrillation (Abe *et al.*, 2007). Since these peptides accelerate α-synuclein aggregation and fibrillation, they might be able to decrease α-synuclein cytotoxicity by decreasing the protofibrils amount.

7.1.3. Other substances reducing α-synuclein toxicity

A potent inhibitor of α-synuclein aggregation is flavonoid baicalein, the main component of a traditional Chinese herbal medicine *Scutellaria baicalensis* (Zhu *et al.*, 2004). α-Synuclein has one binding site with baicalein with K_d of 500 nM. Low micromolar concentrations of baicalein, and especially its oxidized forms, inhibit the formation of α-synuclein fibrils. Furthermore, existing fibrils of α-synuclein are disaggregated by baicalein. The product of the inhibition reaction is predominantly a soluble oligomer of α-synuclein, in which the protein molecules have been covalently modified by baicalein quinone to form a Schiff base with a lysine side chain in α-synuclein. According to AFM data, the disruption of the α-synuclein fibrils occurs not only from the ends of the fibril, as might be expected, but also from internal regions. Thus, baicalein causes both exo- and endodisaggregation of the fibrils.

Catechins from the bioactive green tea extracts possess protective effects against α-synuclein toxicity. One of the derivatives of catechins effectively inhibits α-synuclein filament formation with $IC_{50} = 9.8\ \mu M$ and is able to destabilize preformed fibrils (Ono and Yamada, 2006; Williams *et al.*, 2007). A cell-based method for screening compounds with therapeutic potential of PD was recently developed (Zhao *et al.*, 2007). The authors used human dopaminergic neuroblastoma cells SH-SYSY stably transfected with mutant $A^{53}T$ human α-synuclein and analyzed cell viability in the presence of MPP^+ and exogenous DA. Twelve compounds with therapeutic potential were found that decreased DA-induced cytotoxicity.

A valuable tool both as a diagnostic and for passive vaccination for treating PD may be a single chain Ab fragment against oligomeric α-synuclein (Emadi *et al.*, 2004, 2007). The importance of such Ab is in its specificity since Ab binds only to oligomeric form of α-synuclein and may neutralize the neurotoxic aggregates without interfering with beneficial functions of monomeric α-synuclein. Single chain Ab fragments (scFvs) were isolated from a phage-displayed Ab library against the target antigen using a novel biopanning technique. This method is based on AFM to image and immobilize specific morphologies of α-synuclein. scFv binds to dimmer, tetramer, and probably other oligomeric forms of α-synuclein and inhibits fibril formation and extracellular toxicity. The authors suggest that scFv

inhibits α-synuclein toxicity and formation of fibrils not by inhibiting nucleation sites or protein folding conformation but rather by specifically binding to an oligomeric form of α-synuclein preventing further aggregation to fibrils and blocking interactions of oligomers with the cell membrane. Thus, scFv Ab may have therapeutic value reducing α-synuclein misfolding and aggregation and preventing membrane damage (Emadi *et al.*, 2007).

The ability to reduce α-synuclein toxicity was detected for sirtuin inhibitors, which are members of the histone deacetylase family of proteins participating in a variety of cellular functions. Inhibition of SIRT2 rescued α-synuclein toxicity and modified inclusion morphology in a cellular model of PD (Outeiro *et al.*, 2006). Parkin may protect against the toxicity associated with mutant α-synuclein (Petrucelli *et al.*, 2002). Parkin gene therapy is considered as a possible treatment for a subset of PD patients who have mutations in the α-synuclein gene (Mochizuki, 2007).

Another approach based on the overexpression of proteins that enhance ER-to-Golgi transport may be also beneficial in synucleinopathies (Lashuel and Hirling, 2006). An unusual method has been recently proposed to reduce α-synuclein-mediated toxicity (Bodner *et al.*, 2006). The authors identified a compound B2 that promotes inclusion formation in cellular models that amazingly reduced α-synuclein-mediated toxicity. Hypothetically, B2 may alter some aspect of protein quality control. Thus, compounds that increase inclusion formation may actually lessen cellular pathology, suggesting a therapeutic approach for diseases caused by protein misfolding. These results support growing evidence for the protective effects of protein inclusions. α-Synuclein toxicity can be rescued by nonspecific inhibition of the caspases and RNAi knockdown of caspase-12 (Cappai *et al.*, 2005). Additionally, it also possible to abrogate α-synuclein toxicity with coexpression of Hsp70 (Yu *et al.*, 2005).

7.1.4. Potential application of the acidic tail of α-synuclein

The introduction of a peptide derived from the C-terminal acidic tail of α-synuclein (ATS) into different therapeutic proteins increases their stability and solubility (Lee *et al.*, 2005a). In other experiments, ATS protected a heat-labile protein, GST, from aggregation induced by different conditions or agents, that is elevated temperature, pH, and the presence of metals (Lee *et al.*, 2005a; Park *et al.*, 2004). The introduction of ATS peptide into the N-terminal antigenic portion of the nucleocapsid proteins of the viruses renders recombinant fusion proteins that are heat resistant and more convenient for diagnostic tests and seroepidemiological studies (Park and Kim, 2007). The results of these experiments suggest that ATS may be used to improve physicochemical properties of many medically important proteins that have low solubility or prone to aggregate. C-terminal fragments of other synucleins may also be used in peptide fusion technology for

preparing soluble, heat-resistant forms of different proteins used for the treatment and diagnostic of human diseases.

7.1.5. Autoantibodies to synucleins

Papachroni *et al.* (2007) examined the presence of autoantibodies (AAbs) against synuclein family members in the peripheral blood serum of PD patients and control individuals. Presence of AAb against β-synuclein or γ-synuclein did not showed association with PD. At the same time, multi-epitopic AAb against α-synuclein were detected in 65% of all patients tested and their presence strongly correlated with an inherited mode of the disease. The frequency of the presence of AAb in patients with sporadic form of PD was not significantly different from the frequency in the control group. However, very high proportion (90%) of patients with familial form of the disease was positive for AAb against α-synuclein, suggesting that these AAb could be involved in pathogenesis of the inherited form of PD.

7.1.6. Inhibition of synuclein expression

The finding that the higher gene dosage may cause PD suggests that pharmacological manipulations affecting α-synuclein expression level, for example antisense oligonucleotides, $sRNA_i$, might be considered as therapeutic or preventive strategies in susceptible individuals. Fountaine and Wade-Martins (2007) using siRNA to α-synuclein in human dopaminergic cellular model achieved 80% protein knockdown. Knockdown conferred resistance to the DAT-dependent MPP^+, decreased DA transport, reducing the maximal uptake velocity V (max) of DA and the surface density of its transporter by up to 50%. Therefore, RNAi-mediated α-synuclein knockdown alters cellular DA homeostasis in human cells and may suggest a mechanism for the increased survival in the presence of MPP^+.

7.2. γ-synuclein as a target for the development of anticancer drugs

γ-Synuclein is considered by some investigators as a key therapeutic target in the development of anticancer drugs due to its prominent role in the spindle assembly checkpoint pathway through its interaction with BubR. As briefly discussed in Chapter V, G, γ-synuclein expression is elevated in the advanced stages of many different types of solid tumors. Furthermore, in breast carcinoma, where γ-synuclein was first identified, it has been linked to stimulated proliferation, increased cell invasion, and metastasis. It is causatively linked to drug resistance in breast cancer. The aberrant expression of γ-synuclein and BubR1-mediated interference with the spindle assembly checkpoint complex together may play an inhibitory role to the action of antimicrotubule drugs. Based on this role of γ-synuclein in cancer, it is considered as a potential therapeutic target for an adjuvant

therapy through its inhibition by an ankyrin-based peptide. A novel peptide (ANK) based on an ankyrin-repeat domain binds to and inhibits γ-synuclein activity (Singh and Jia, 2008; Singh *et al.*, 2007).

The peptide conferred approximately three and a half times higher sensitivity to γ-synuclein positive drug-resistant cancer cells to antimicrotubule drugs. Development of a cell permeable version of this peptide (ANKtide) based on its attachment with HIV-TAT peptide is currently in progress (Singh and Jia, 2008).

8. Concluding Remarks

Twenty years of synuclein studies brought considerable progress in the understanding of their role in different human diseases and more modest progress in elucidation of their normal physiological functions. These studies brought exciting ideas about possible pharmacological approaches for the treatment of synucleinopathies. One of the examples of a promising translational research is the development of the single-chain Ab fragment against oligomeric α-synuclein.

The data presented in this chapter show that synucleins are very dynamic proteins, having the ability to adopt distinct structures under different conditions and easily change their intracellular localization. This feature may play an important role in their biological functions and sometimes explain conflicting results received by different investigators. Synuclein's involvement in NDDs and cancer may provide insights into the pathological processes implicated in these two groups of debilitating diseases, and present the possibility to use them as potential targets for early diagnosis and treatment.

Since the data on triple synuclein KOs are not yet available and single and double KOs of α-, β-, and γ-synucleins are viable and usually exhibit little phenotype, one can hypothesize about synuclein functions based on the current knowledge and waiting for triple KO results. α-Synuclein may be involved in the regulation of DA release and modulate a releasable pool of vesicles at the synapse (Larsen *et al.*, 2006). Recent results suggest that an essential function of α-synuclein is its ability to inhibit ''priming,'' a reaction that transfers morphologically docked vesicles to a fusion-competent state.

The manifestation of the physiological or pathological role of α-synuclein may depend on its local intracellular concentration and can be regulated by PTMs. α-Synuclein expressed at physiological level may function as a negative regulator of vesicle fusion and neurotransmitter release at the synapse. At the same time, when a certain level of α-synuclein is exceeded, this may lead to an inappropriate deployment of this function at the synapse (Gitler and Shorter, 2007). A new emerging area in synuclein studies is the

investigation of their role in the formation of ion channels (Conway *et al.*, 2000b; Ding *et al.*, 2002; Lashuel *et al.*, 2002; Quist *et al.*, 2005).

Overall, the studies of synucleins have enhanced our understanding of the pathogenesis of synucleinopathies, have led to the improvement of diagnostic tools for genetic forms of these diseases, and have opened new frontiers for the purposeful consideration of novel therapeutic targets.

Evidently, it is important for the normal function of α-synuclein to be better defined in order to understand the role of synucleins in pathology. A promising area in synuclein translational studies is the use of peptides to inhibit α-synuclein toxicity and the development of antitumor treatment based on γ-synuclein studies.

In summary, we believe that research in the third decade after the discovery of the first synuclein will bring a breakthrough in the pharmacological methods for the treatment of synucleinopathies. As a result, therapeutic interventions that halt or reverse the progression of these diseases will be developed.

ACKNOWLEDGMENTS

The author is grateful to Ms. Kristin Cain for the help in preparation of the manuscript. This work is supported by VA Merit Review grant, NIH grant EY 02687, and the Glaucoma Foundation grant.

REFERENCES

Abe, K., Kobayashi, N., Sode, K., and Ikebukuro, K. (2007). Peptide ligand screening of alpha-synuclein aggregation modulators by in silico panning. *BMC Bioinformatics* **8**(1), 451.

Abeliovich, A., Schmitz, Y., Fariñas, I., Choi-Lundberg, D., Ho, W. H., Castillo, P. E., Shinsky, N., Verdugo, J. M., Armanini, M., Ryan, A., Hynes, M., Phillips, H., *et al.* (2000). Mice lacking alpha-synuclein display functional deficits in the nigrostriatal dopamine system. *Neuron* **25**(1), 239–252.

Ahn, B.-H., Rhim, H., Kim, S. Y., Sung, Y.-M., Lee, M.-Y., Choi, J.-Y., Wolozin, B., Chang, J.-S., Lee, Y. H., Kwon, T. K., Chung, K. C., Yoon, S.-H., *et al.* (2002). α-Synuclein interacts with phospholipase D isozymes and inhibits pervanadate-induced phospholipase D activation in human embryonic kidney-293 cells. *J. Biol. Chem.* **277** (14), 12334–12342.

Ahn, M., Kim, S., Kang, M., Ryu, Y., and Kim, T. D. (2006). Chaperone-like activities of alpha-synuclein: Alpha-synuclein assists enzyme activities of esterases. *Biochem. Biophys. Res. Commun.* **346**(4), 1142–1149.

Ahn, T.-B., Kim, S. Y., Kim, J. Y., Park, S.-S., Lee, D. S., Min, H. J., Kim, Y. K., Kim, S. E., Kim, J.-M., Kim, H.-J., Cho, J., and Jeon, B. S. (2008). α-Synuclein gene duplication is present in sporadic Parkinson disease. *Neurology* **70,** 43–49.

Albani, D., Peverelli, E., Rametta, R., Batelli, S., Veschini, L., Negro, A., and Forloni, G. (2004). Protective effect of TAT-delivered α-synuclein: Relevance of the C-terminal domain and involvement of HSP70. *FASEB J.* **18**(14), 1713–1715.

Alberts, B., Johnson, A., Lewis, J., Raff, M., Roberts, K., and Walter, P. (2002). "Molecular Biology of the Cell." 4th ed. Garland Science, New York.

Alim, M. A., Hossain, M. S., Arima, K., Takeda, K., Izumiyama, Y., Nakamura, M., Kaji, H., Shinoda, T., Hisanaga, S., and Uéda, K. (2001). Tubulin seeds α-synuclein fibril formation. *J. Biol. Chem.* **277**(3), 2112–2117.

Alves da Costa, C., Ancolio, K., and Checler, F. (2000). Wild-type but not Parkinson's disease-related Ala-53 → Thr mutant α-synuclein protects neuronal cells from apoptotic stimuli. *J. Biol. Chem.* **275**(31), 24065–24069.

Alves da Costa, C., Paitel, E., Vincent, B., and Checler, F. (2002). α-Synuclein lowers p53-dependent apoptotic response of neuronal cells. *J. Biol. Chem.* **277**(52), 50980–50984.

Alves da Costa, C., Masliah, E., and Checler, F. (2003). β-Synuclein displays an antiapoptotic p53-dependent phenotype and protects neurons from 6-hydroxydopamine-induced caspase 3 activation: Cross-talk with alpha-synuclein and implication for Parkinson's disease. *J. Biol. Chem.* **278**(39), 37330–37335.

Amer, D. A., Irvine, G. B., and El-Agnaf, O. M. (2006). Inhibitors of alpha-synuclein oligomerization and toxicity: A future therapeutic strategy for Parkinson's disease and related disorders. *Exp. Brain Res.* **173**(2), 223–333.

Arai, H., Lee, V. M., Messinger, M. L., Greenberg, B. D., Lowery, D. E., and Trojanowski, J. Q. (1991). Expression patterns of beta-amyloid precursor protein (beta-APP) in neural and nonneural human tissues from Alzheimer's disease and control subjects. *Ann. Neurol.* **30**(5), 686–693.

Aravind, L., Iyer, L. M., and Koonin, E. V. (2006). Comparative genomics and structural biology of the molecular innovations of eukaryotes. *Curr. Opin. Struct. Biol.* **16**(3), 409–419.

Arima, K., Ueda, K., Sunohara, N., Arakawa, K., Hirai, S., Nakamura, M., Tonozuka-Uehara, H., and Kawai, M. (1998). NACP/alpha-synuclein immunoreactivity in fibrillary components of neuronal and oligodendroglial cytoplasmic inclusions in the pontine nuclei in multiple system atrophy. *Acta Neuropathol. (Berl)* **96**(5), 439–444.

Auluck, P. K., Chan, H. Y., Trojanowski, J. Q., Lee, V. M., and Bonini, N. M. (2002). Chaperone suppression of alpha-synuclein toxicity in a Drosophila model for Parkinson's disease. *Science* **295**(5556), 865–868.

Auluck, P. K., Meulener, M. C., and Bonini, N. M. (2005). Mechanisms of suppression of α-synuclein neurotoxicity by geldanamycin in *Drosophila*. *J. Biol. Chem.* **280**(4), 2873–2878.

Baba, M., Nakajo, S., Tu, P. H., Tomita, T., Nakaya, K., Lee, V. M., Trojanowski, J. Q., and Iwatsubo, T. (1998). Aggregation of alpha-synuclein in Lewy bodies of sporadic Parkinson's disease and dementia with Lewy bodies. *Am. J. Pathol.* **152**(4), 879–884.

Baptista, M. J., O'Farrell, C., Daya, S., Ahmad, R., Miller, D. W., Hardy, J., Farrer, M. J., and Cookson, M. R. (2003). Co-ordinate transcriptional regulation of dopamine synthesis genes by alpha-synuclein in human neuroblastoma cell lines. *J. Neurochem.* **85**(4), 957–968.

Beal, M. F. (2004). Commentary on "Alpha-synuclein and mitochondria: A tangled skein.". *Exp. Neurol.* **186**(2), 109–111.

Bennett, M. C. (2005). The role of alpha-synuclein in neurodegenerative diseases. *Pharmacol. Ther.* **105**(3), 311–331.

Beyer, K. (2006). Alpha-synuclein structure, posttranslational modification and alternative splicing as aggregation enhancers. *Acta Neuropathol. (Berl)* **112**(3), 237–251.

Beyer, K., and Ariza, A. (2007). Protein aggregation mechanisms in synucleinopathies: Commonalities and differences. *J. Neuropathol. Exp. Neurol.* **66**(11), 965–974.

Beyer, K., Humbert, J., Ferrer, A., Lao, J. I., Latorre, P., Lopez, D., Tolosa, E., Ferrer, I., and Ariza, A. (2007). A variable poly-T sequence modulates alpha-synuclein isoform expression and is associated with aging. *J. Neurosci. Res.* **85**(7), 1538–1546.

Biere, A. L., Wood, S. J., Wypych, J., Steavenson, S., Jiang, Y., Anafi, D., Jacobsen, F. W., Jarosinski, M. A., Wu, G.-M., Louis, J.-C., Martin, F., Narhi, L. O., *et al.* (2000). Parkinson's disease-associated α-synuclein is more fibrillogenic than β and γ-synuclein and cannot cross-seed its homologs. *J. Biol. Chem.* **275**(44), 34574–34579.

Bodner, R. A., Outeiro, T. F., Altmann, S., Maxwell, M. M., Cho, S. H., Hyman, B. T., McLean, P. J., Young, A. B., Housman, D. E., and Kazantsev, A. G. (2006). Pharmacological promotion of inclusion formation: A therapeutic approach for Huntington's and Parkinson's diseases. *Proc. Natl. Acad. Sci. USA* **103**(11), 4246–4251.

Bonini, N. M. (2002). Chaperoning brain degeneration. *Proc. Natl. Acad. Sci. USA* **99**(Suppl 4), 16407–16411.

Bonini, N. M., and Giasson, B. I. (2005). Snaring the function of alpha-synuclein. *Cell* **123**(3), 359–361.

Bönsch, D., Reulbach, U., Bayerlein, K., Hillemacher, T., Kornhuber, J., and Bleich, S. (2004). Elevated alpha synuclein mRNA levels are associated with craving in patients with alcoholism. *Biol. Psychiatry* **56**(12), 984–986.

Bönsch, D., Lederer, T., Reulbach, U., Hothorn, T., Kornhuber, J., and Bleich, S. (2005). Joint analysis of the NACP-REP1 marker within the alpha synuclein gene concludes association with alcohol dependence. *Hum. Mol. Genet.* **14**(7), 967–971.

Borghi, R., Marchese, R., Negro, A., Marinelli, L., Forloni, G., Zaccheo, D., Abbruzzese, G., and Tabaton, M. (2000). Full length alpha-synuclein is present in cerebrospinal fluid from Parkinson's disease and normal subjects. *Neurosci. Lett.* **287**(1), 65–67.

Braak, H., Sastre, M., and Del Tredici, K. (2007). Development of alpha-synuclein immunoreactive astrocytes in the forebrain parallels stages of intraneuronal pathology in sporadic Parkinson's disease. *Acta Neuropathol. (Berl)* **114**(3), 231–241.

Brenz Verca, M. S., Bahi, A., Boyer, F., Wagner, G. C., and Dreyer, J. L. (2003). Distribution of alpha- and gamma-synucleins in the adult rat brain and their modification by high-dose cocaine treatment. *Eur. J. Neurosci.* **18**(7), 1923–1938.

Brighina, L., Okubadejo, N. U., Schneider, N. K., Lesnick, T. G., de Andrade, M., Cunningham, J. M., Farrer, M. J., Lincoln, S. J., Rocca, W. A., and Maraganore, D. M. (2007). Beta-synuclein gene variants and Parkinson's disease: A preliminary case-control study. *Neurosci. Lett.* **420**(3), 229–234.

Bruening, W., Giasson, B. I., Klein-Szanto, A. J., Lee, V. M., Trojanowski, J. Q., and Godwin, A. K. (2000). Synucleins are expressed in the majority of breast and ovarian carcinomas and in preneoplastic lesions of the ovary. *Cancer* **88**(9), 2154–2163.

Bucciantini, M., Giannoni, E., Chiti, F., Baroni, F., Formigli, L., Zurdo, J., Taddei, N., Ramponi, G., Dobson, C. M., and Stefani, M. (2002). Inherent toxicity of aggregates implies a common mechanism for protein misfolding diseases. *Nature* **416**(6880), 507–511.

Buchman, V. L., Hunter, H. J., Pinõn, L. G., Thompson, J., Privalova, E. M., Ninkina, N. N., and Davies, A. M. (1998a). Persyn, a member of the synuclein family, has a distinct pattern of expression in the developing nervous system. *J. Neurosci.* **18**(22), 9335–9341.

Buchman, V. L., Adu, J., Pinõn, L., Ninkina, N., and Davies, A. (1998b). Persyn, a member of the synuclein family, influences neurofilament network integrity. *Nat. Neurosci.* **1**(2), 101–103.

Cabin, D. E., Shimazu, K., Murphy, D., Cole, N. B., Gottschalk, W., McIlwain, K. L., Orrison, B., Chen, A., Ellis, C. E., Paylor, R., Lu, B., and Nussbaum1, R. L. (2002).

Synaptic vesicle depletion correlates with attenuated synaptic responses to prolonged repetitive stimulation in mice lacking α-synuclein. *J. Neurosci.* **22**(20), 8797–8807.
Campbell, B. C., McLean, C. A., Culvenor, J. G., Gai, W. P., Blumbergs, P. C., Jäkälä, P., Beyreuther, K., Masters, C. L., and Li, Q. X. (2001). The solubility of alpha-synuclein in multiple system atrophy differs from that of dementia with Lewy bodies and Parkinson's disease. *J. Neurochem.* **76**(1), 87–96.
Campion, D., Martin, C., Heilig, R., Charbonnier, F., Moreau, V., Flaman, J. M., Petit, J. L., Hannequin, D., Brice, A., and Frebourg, T. (1995). The NACP/synuclein gene: Chromosomal assignment and screening for alterations in Alzheimer disease. *Genomics* **26**(2), 254–257.
Cao, S., Gelwix, C. C., Caldwell, K. A., and Caldwell, C. A. (2005). Torsin mediated protection from cellular stress in the dopaminergic neurons of Caenorhabditis elegans. *J. Neurosci.* **25,** 3801–3812.
Cappai, R., Leck, S. L., Tew, D. J., Williamson, N. A., Smith, D. P., Galatis, D., Sharples, R. A., Curtain, C. C., Ali, F. E., Cherny, R. A., Culvenor, J. G., Bottomley, S. P., *et al.* (2005). Dopamine promotes alpha-synuclein aggregation into SDS-resistant soluble oligomers via a distinct folding pathway. *FASEB J.* **19,** 1377–1379.
Castagnet, P. I., Golovko, M. Y., Barcelo-Coblijn, G. C., Nussbaum, R. L., and Murphy, E. J. (2005). Fatty acid incorporation is decreased in astrocytes cultured from α-synuclein gene-ablated mice. *J. Neurochem.* **94**(3), 839–849.
Chandra, S., Chen, X., Rizo, J., Jahn, R., and Südhof, T. C. (2003). A broken α-helix in folded α-synuclein. *J. Biol. Chem.* **278**(17), 15313–15318.
Chandra, S., Fornai, F., Kwon, H. B., Yazdani, U., Atasoy, D., Liu, X., Hammer, R. E., Battaglia, G., German, D. C., Castillo, P. E., and Südhof, T. C. (2004). Double-knockout mice for alpha- and beta-synucleins: Effect on synaptic functions. *Proc. Natl. Acad. Sci. USA* **101**(41), 14966–14971.
Chandra, S., Gallardo, G., Fernández-Chacón, R., Schlüter, O. M., and Südhof, T. C. (2005). Alpha-synuclein cooperates with CSPalpha in preventing neurodegeneration. *Cell* **123**(3), 383–396.
Chartier-Harlin, M. C., Kachergus, J., Roumier, C., Mouroux, V., Douay, X., Lincoln, S., Levecque, C., Larvor, L., Andrieux, J., Hulihan, M., Waucquier, N., Defebvre, L., *et al.* (2004). Alpha-synuclein locus duplication as a cause of familial Parkinson's disease. *Lancet* **364**(9440), 1167–1169.
Chen, L., and Feany, M. B. (2005). Alpha-synuclein phosphorylation controls neurotoxicity and inclusion formation in a Drosophila model of Parkinson disease. *Nat. Neurosci.* **8**(5), 657–663.
Chen, X., de Silva, H. A., Pettenati, M. J., Rao, P. N., St. George-Hyslop, P., Roses, A. D., Xia, Y., Horsburgh, K., Uéda, K., and Saitoh, T. (1995). The human NACP/alpha-synuclein gene: Chromosome assignment to 4q21.3-q22 and TaqI RFLP analysis. *Genomics* **26**(2), 425–427.
Chen, Q., Thorpe, J., and Keller, J. N. (2005). α-Synuclein alters proteasome function, protein synthesis, and stationary phase viability. *J. Biol. Chem.* **280**(34), 30009–30017.
Chiba-Falek, O., and Nussbaum, R. L. (2001). Effect of allelic variation at the NACP-Rep1 repeat upstream of the α-synuclein gene (SNCA) on transcription in a cell culture luciferase reporter system. *Hum. Mol. Genet.* **10**(26), 3101–3109.
Chiba-Falek, O., Touchman, J. W., and Nussbaum, R. L. (2003). Functional analysis of intra-allelic variation at NACP-Rep1 in the alpha-synuclein gene. *Hum. Genet.* **113**(5), 426–431.
Choi, W., Zibaee, S., Jakes, R., Serpell, L. C., Davletov, B., Crowther, R. A., and Goedert, M. (2004). Mutation E46K increases phospholipid binding and assembly into filaments of human alpha-synuclein. *FEBS Lett.* **576**(3), 363–368.

Choi, H. S., Lee, S. H., Kim, S. Y., An, J. J., Hwang, S.-I., Kim, D. W., Yoo, K.-Y., Won, M. H., Kang, T.-C., Kwon, H. J., Kang, J. H., Cho, S.-W., *et al.* (2006). Transduced Tat-α-synuclein protects against oxidative stress *in vitro* and *in vivo*. *J. Biochem. Mol. Biol.* **39**(3), 253–262.

Clayton, D. F., and George, J. M. (1998). The synucleins: A family of proteins involved in synaptic function, plasticity, neurodegeneration and disease. *Trends Neurosci.* **21**(6), 249–254.

Clough, R. L., and Stefanis, L. (2007). A novel pathway for transcriptional regulation of alpha-synuclein. *FASEB J.* **21**(2), 596–607.

Cole, R. N., and Hart, G. W. (2001). Cytosolic O-glycosylation in abundant in nerve terminals. *J. Neurochem.* **79**(5), 1080–1089.

Conway, K. A., Harper, J. D., and Lansbury, P. T., Jr. (1998). Accelerated *in vitro* fibril formation by a mutant alpha-synuclein linked to early-onset Parkinson disease. *Nat. Med.* **4**(11), 1318–1320.

Conway, K. A., Harper, J. D., and Lansbury, P. T., Jr. (2000a). Fibrils formed *in vitro* from alpha-synuclein and two mutant forms linked to Parkinson's disease are typical amyloid. *Biochemistry* **39**(10), 2552–2563.

Conway, K. A., Lee, S.-J., Rochet, J.-C., Ding, T. T., Williamson, R. E., and Lansbury, P. T., Jr. (2000b). Acceleration of oligomerization, not fibrillization, is a shared property of both α-synuclein mutations linked to early-onset Parkinson's disease: Implications for pathogenesis and therapy. *Proc. Natl. Acad. Sci. USA* **97**(2), 571–576.

Conway, K. A., Rochet, J. C., Bieganski, R. M., and Lansbury, P. T., Jr. (2001). Kinetic stabilization of the alpha-synuclein protofibril by a dopamine-alpha-synuclein adduct. *Science* **294**(5545), 1346–1349.

Cookson, M. R., and van der Brug, M. (2007). Cell systems and the toxic mechanism(s) of alpha-synuclein. *Exp. Neurol.* Epub ahead of print.

Cooper, A. A., Gitler, A. D., Cashikar, A., Haynes, C. M., Hill, K. J., Bhullar, B., Liu, K., Xu, K., Strathearn, K. E., Liu, F., Cao, S., Caldwell, K. A., *et al.* (2006). Alpha-synuclein blocks ER-Golgi traffic and Rab1 rescues neuron loss in Parkinson's models. *Science* **313** (5785), 324–328.

Croisier, E., Moran, L. B., Dexter, D. T., Pearce, R. K., and Graeber, M. B. (2005). Microglial inflammation in the parkinsonian substantia nigra: Relationship to alpha-synuclein deposition. *J. Neuroinflammation* **2,** 14.

Crowther, R. A., Jakes, R., Spillantini, M. G., and Goedert, M. (1998). Synthetic filaments assembled from C-terminally truncated alpha-synuclein. *FEBS Lett.* **436**(3), 309–312.

Dalfó, E., and Ferrer, I. (2005). Alpha-synuclein binding to rab3a in multiple system atrophy. *Neurosci. Lett.* **380**(1–2), 170–175.

Dalfó, E., Barrachina, M., Rosa, J. L., Ambrosio, S., and Ferrer, I. (2004). Abnormal alpha-synuclein interactions with rab3a and rabphilin in diffuse Lewy body disease. *Neurobiol. Dis.* **16**(1), 92–97.

Danzer, K. M., Schnack, C., Sutcliffe, A., Hengerer, B., and Gillardon, F. (2007). Functional protein kinase arrays reveal inhibition of p-21-activated kinase 4 by alpha-synuclein oligomers. *J. Neurochem.* Epub ahead of print.

Dauer, W., Kholodilov, N., Vila, M., Trillat, A.-C., Goodchild, R., Larsen, K. E., Staal, R., Tieu, K., Schmitz, Y., Yuan, C. A., Rocha, M., Jackson-Lewis, V., *et al.* (2002). Resistance of α-synuclein null mice to the parkinsonian neurotoxin MPTP. *Proc. Natl. Acad. Sci. USA* **99**(22), 14524–14529.

Davidson, W. S., Jonas, A., Clayton, D. F., and George, J. M. (1998). Stabilization of alpha-synuclein secondary structure upon binding to synthetic membranes. *J. Biol. Chem.* **273** (16), 9443–9449.

Dawson, T., Mandir, A., and Lee, M. (2002). Animal models of PD: Pieces of the same puzzle? *Neuron* **35**(2), 219–222.

Dev, K. K., Hofele, K., Barbieri, S., Buchman, V. L., and van der Putten, H. (2003). Part II: Alpha-synuclein and its molecular pathophysiological role in neurodegenerative disease. *Neuropharmacology* **45**(1), 14–44.

Dickson, D. W. (2001). Alpha-synuclein and the Lewy body disorders. *Curr. Opin. Neurol.* **14**(4), 423–432.

Ding, T. T., Lee, S. J., Rochet, J. C., and Lansbury, P. T., Jr. (2002). Annular alpha-synuclein protofibrils are produced when spherical protofibrils are incubated in solution or bound to brain-derived membranes. *Biochemistry* **41**(32), 10209–10217.

Dorval, V., and Fraser, P. E. (2006). Small ubiquitin-like modifier (SUMO) modification of natively unfolded proteins tau and α-synuclein. *J. Biol. Chem.* **281**(15), 9919–9924.

Drolet, R. E., Behrouz, B., Lookingland, K. J., and Goudreau, J. L. (2004). Mice lacking alpha-synuclein have an attenuated loss of striatal dopamine following prolonged chronic MPTP administration. *Neurotoxicology* **25**(5), 761–769.

Duda, J. E., Shah, U., Arnold, S. E., Lee, V. M., and Trojanowski, J. Q. (1999). The expression of alpha-, beta-, and gamma-synucleins in olfactory mucosa from patients with and without neurodegenerative diseases. *Exp. Neurol.* **160**(2), 515–522.

Duda, J. E., Giasson, B. I., Mabon, M. E., Lee, V. M., and Trojanowski, J. Q. (2002). Novel antibodies to synuclein show abundant striatal pathology in Lewy body diseases. *Ann. Neurol.* **52**(2), 205–210.

El-Agnaf, O. M., and Irvine, G. B. (2000). Review: Formation and properties of amyloid-like fibrils derived from alpha-synuclein and related proteins. *J. Struct. Biol.* **130**(2–3), 300–309.

El-Agnaf, O. M., Jakes, R., Curran, M. D., and Wallace, A. (1998a). Effects of the mutations Ala30 to Pro and Ala53 to Thr on the physical and morphological properties of alpha-synuclein protein implicated in Parkinson's disease. *FEBS Lett.* **440**(1–2), 67–70.

El-Agnaf, O. M., Jakes, R., Curran, M. D., Middleton, D., Ingenito, R., Bianchi, E., Pessi, A., Neill, D., and Wallace, A. (1998b). Aggregates from mutant and wild-type alpha-synuclein proteins and NAC peptide induce apoptotic cell death in human neuroblastoma cells by formation of beta-sheet and amyloid-like filaments. *FEBS Lett.* **440**(1–2), 71–75.

El-Agnaf, O. M. A., Salem, S. A., Paleologou, K. E., Cooper, L. J., Fullwood, N. J., Gibson, M. J., Curran, M. D., Court, J. A., Mann, D. M. A., Ikeda, S.-I., Cookson, M. R., Hardy, J., *et al.* (2003). α-Synuclein implicated in Parkinson's disease is present in extracellular biological fluids, including human plasma. *FASEB J.* **17**(13), 1945–1947.

El-Agnaf, O. M. A., Paleologou, K. E., Greer, B., Abogrein, A. M., King, J. E., Salem, S. A., Fullwood, N. J., Benson, F. E., Hewitt, R., Ford, K. J., Martin, F. L., Harriott, P., *et al.* (2004). A strategy for designing inhibitors of α-synuclein aggregation and toxicity as a novel treatment for Parkinson's disease and related disorders. *FASEB J.* **18**(11), 1315–1317.

El-Agnaf, O. M., Salem, S. A., Paleologou, K. E., Curran, M. D., Gibson, M. J., Court, J. A., Schlossmacher, M. G., and Allsop, D. (2006). Detection of oligomeric forms of α-synuclein protein in human plasma as a potential biomarker for Parkinson's disease. *FASEB J.* **20**(3), 419–425.

Ellis, C. E., Schwartzberg, P. L., Grider, T. L., Fink, D. W., and Nussbaum, R. L. (2001). α-Synuclein is phosphorylated by members of the Src family of protein-tyrosine kinases. *J. Biol. Chem.* **276**(6), 3879–3884.

Ellis, C. E., Murphy, E. J., Mitchell, D. C., Golovko, M. Y., Scaglia, F., Barceló-Coblijn, G. C., and Nussbaum, R. L. (2005). Mitochondrial lipid abnormality and

electron transport chain impairment in mice lacking alpha-synuclein. *Mol. Cell. Biol.* **25** (22), 10190–10201.

El Khoury, J. B., Moore, K. J., Means, T. K., Leung, J., Terada, K., Toft, M., Freeman, M.W., and Luster, A. D. (2003). CD36 mediates the innate host response to beta-amyloid. *J. Exp. Med.* **197**(12), 1657–1666.

Emadi, S., Liu, R., Yuan, B., Schulz, P., McAllister, C., Lyubchenko, Y., Messer, A., and Sierks, M. R. (2004). Inhibiting aggregation of alpha-synuclein with human single chain antibody fragments. *Biochemistry* **43**(10), 2871–2878.

Emadi, S., Barkhordarian, H., Wang, M. S., Schulz, P., and Sierks, M. R. (2007). Isolation of a human single chain antibody fragment against oligomeric alpha-synuclein that inhibits aggregation and prevents alpha-synuclein-induced toxicity. *J. Mol. Biol.* **368**(4), 1132–1144.

Engelender, S., Kaminsky, Z., Guo, X., Sharp, A. H., Amaravi, R. K., Kleinderlein, J. J., Margolis, R. L., Troncoso, J. C., Lanahan, A. A., Worley, P. F., Dawson, V. L., Dawson, T. M., *et al.* (1999). Synplilin-1 associates with alpha-synuclein and promotes the formation of cytosolic inclusions. *Nat. Genet.* **22**(1), 110–114.

Eyal, A., Szargel, R., Avraham, E., Liani, E., Haskin, J., Rott, R., and Engelender, S. (2006). Synphilin-1A: An aggregation-prone isoform of synphilin-1 that causes neuronal death and is present in aggregates from α-synucleinopathy patients. *Proc. Natl. Acad. Sci. USA* **103**(15), 5917–5922.

Fan, Y., Limprasert, P., Murray, I. V., Smith, A. C., Lee, V. M., Trojanowski, J. Q., Sopher, B. L., and La Spada, A. R. (2006). Beta-synuclein modulates alpha-synuclein neurotoxicity by reducing alpha-synuclein protein expression. *Hum. Mol. Genet.* **15**(20), 3002–3011.

Farkas, R. H., Qian, J., Goldberg, J. L., Quigley, H. A., and Zack, D. J. (2004). Gene expression profiling of purified rat retinal ganglion cells. *Invest. Ophthalmol. Vis. Sci.* **45**(8), 2503–2513.

Feany, M. B., and Bender, W. W. (2000). A Drosophila model of Parkinson's disease. *Nature* **404**(6776), 394–398.

Fernández-Chacón, R., Wölfel, M., Nishimune, H., Tabares, L., Schmitz, F., Castellano-Muñoz, M., Rosenmund, C., Montesinos, M. L., Sanes, J. R., Schneggenburger, R., and Südhof, T. C. (2004). The synaptic vesicle protein CSP alpha prevents presynaptic degeneration. *Neuron* **42**(2), 237–251.

Fleming, S. M., Salcedo, J., Fernagut, P.-O., Rockenstein, E., Masliah, E., Levine, M. S., and Chesselet, M.-F. (2004). Early and progressive sensorimotor anomalies in mice overexpressing wild-type human α-synuclein. *J. Neurosci.* **24**(42), 9434–9440.

Fleming, S. M., Fernagut, P.-O., and Chesselet, M.-F. (2005). Genetic mouse models of parkinsonism: Strengths and limitations. *NeuroRx* **2**(3), 495–503.

Forno, L. S. (1996). Neuropathology of Parkinson's disease. *J. Neuropathol. Exp. Neurol.* **55**(3), 259–272.

Fountaine, T. M., and Wade-Martins, R. (2007). RNA interference-mediated knockdown of alpha-synuclein protects human dopaminergic neuroblastoma cells from MPP(+) toxicity and reduces dopamine transport. *J. Neurosci. Res.* **85**(2), 351–363.

Frieling, H., Gozner, A., Römer, K. D., Lenz, B., Bönsch, D., Wilhelm, J., Hillemacher, T., de Zwaan, M., Kornhuber, J., and Bleich, S. (2007). Global DNA hypomethylation and DNA hypermethylation of the alpha synuclein promoter in females with anorexia nervosa. *Mol. Psychiatry* **12**(3), 229–230.

Fuchs, J., Tichopad, A., Golub, Y., Munz, M., Schweitzer, K. J., Wolf, B., Berg, D., Mueller, J. C., and Gasser, T. (2007). Genetic variability in the SNCA gene influences α-synuclein levels in the blood and brain. *FASEB J.* Epub ahead of print.

Fujita, M., Wei, J., Nakai, M., Masliah, E., and Hashimoto, M. (2006). Chaperone and anti-chaperone: Two-faced synuclein as stimulator of synaptic evolution. *Neuropathology* **26**(5), 383–392.

Fujita, M., Sugama, S., Nakai, M., Takenouchi, T., Wei, J., Urano, T., Inoue, S., and Hashimoto, M. (2007). alpha-Synuclein stimulates differentiation of osteosarcoma cells: Relevance to down-regulation of proteasome activity. *J. Biol. Chem.* **282**(8), 5736–5748.

Fujiwara, H., Hasegawa, M., Dohmae, N., Kawashima, A., Masliah, E., Goldberg, M. S., Shen, J., Takio, K., and Iwatsubo, T. (2002). alpha-Synuclein is phosphorylated in synucleinopathy lesions. *Nat. Cell Biol.* **4**(2), 160–164.

Fung, K. M., Rorke, L. B., Giasson, B., Lee, V. M., and Trojanowski, J. Q. (2003). Expression of alpha-, beta-, and gamma-synuclein in glial tumors and medulloblastomas. *Acta Neuropathol.* **106**(2), 167–175.

Furukawa, K., Matsuzaki-Kobayashi, M., Hasegawa, T., Kikuchi, A., Sugeno, N., Itoyama, Y., Wang, Y., Yao, P. J., Bushlin, I., and Takeda, A. (2006). Plasma membrane ion permeability induced by mutant alpha-synuclein contributes to the degeneration of neural cells. *J. Neurochem.* **97**(4), 1071–1077.

Galasko, D., Hansen, L. A., Katzman, R., Wiederholt, W., Masliah, E., Terry, R., Hill, L. R., Lessin, P., and Thal, L. J. (1994). Clinical-neuropathological correlations in Alzheimer's disease and related dementias. *Arch. Neurol.* **51**(9), 888–895.

Galvin, J. E. (2006). Interaction of alpha-synuclein and dopamine metabolites in the pathogenesis of Parkinson's disease: A case for the selective vulnerability of the substantia nigra. *Acta Neuropathol. (Berl)* **112**(2), 115–126.

Galvin, J. E., Uryu, K., Lee, V. M., and Trojanowski, J. Q. (1999). Axon pathology in Parkinson's disease and Lewy body dementia hippocampus contains alpha-, beta-, and gamma-synuclein. *Proc. Natl. Acad. Sci. USA* **96**(23), 13450–13455.

Galvin, J. E., Giasson, B., Hurtig, H. I., Lee, V. M.-Y., and Trojanowski, J. Q. (2000). Neurodegeneration with brain iron accumulation, type 1 is characterized by alpha-, beta-, and gamma-synuclein neuropathology. *Am. J. Pathol.* **157**(2), 361–368.

Galvin, J. E., Lee, V. M., and Trojanowski, J. Q. (2001a). Synucleinopathies: Clinical and pathological implications. *Arch. Neurol.* **58**(2), 186–190.

Galvin, J. E., Schuck, T. M., Lee, V. M., and Trojanowski, J. Q. (2001b). Differential expression and distribution of alpha-, beta-, and gamma-synuclein in the developing human substantia nigra. *Exp. Neurol.* **168**(2), 347–355.

George, J. M. (2002). The synucleins. *Genome Biol.* **3**(1), REVIEWS3002.

George, J. M., Jin, H., Woods, W. S., and Clayton, D. F. (1995). Characterization of a novel protein regulated during the critical period for song learning in the zebra finch. *Neuron* **15** (2), 361–372.

Giasson, B. I., Uryu, K., Trojanowski, J. Q., and Lee, V. M.-Y. (1999). Mutant and wild type human α-synucleins assemble into elongated filaments with distinct morphologies *in vitro*. *J. Biol. Chem.* **274**(12), 7619–7622.

Giasson, B. I., Duda, J. E., Murray, I. V., Chen, Q., Souza, J. M., Hurtig, H. I., Ischiropoulos, H., Trojanowski, J. Q., and Lee, V. M. (2000). Oxidative damage linked to neurodegeneration by selective alpha-synuclein nitration in synucleinopathy lesions. *Science* **290**(5493), 985–989.

Giasson, B. I., Murray, I. V., Trojanowski, J. Q., and Lee, V. M. (2001). A hydrophobic stretch of 12 amino acid residues in the middle of alpha-synuclein is essential for filament assembly. *J. Biol. Chem.* **276**(4), 2380–2386.

Giasson, B. I., Duda, J. E., Quinn, S. M., Zhang, B., Trojanowski, J. Q., and Lee, V. M. (2002). Neuronal alpha-synucleinopathy with severe movement disorder in mice expressing A53T human alpha-synuclein. *Neuron* **34**(4), 521–533.

Giasson, B. I., Mabon, M. E., Duda, J. E., Montine, T. J., Robertson, D., Hurtig, H. I., Lee, V. M., and Trojanowski, J. Q. (2003a). Tau and 14–3–3 in glial cytoplasmic inclusions of multiple system atrophy. *Acta Neuropathol.* **106**(3), 243–250.

Giasson, B. I., Forman, M. S., Higuchi, M., Golbe, L. I., Graves, C. L., Kotzbauer, P. T., Trojanowski, J. Q., and Lee, V. M. (2003b). Initiation and synergistic fibrillization of tau and alpha-synuclein. *Science* **300**(5619), 636–640.

Gispert, S., Del Turco, D., Garrett, L., Chen, A., Bernard, D. J., Hamm-Clement, J., Korf, H. W., Deller, T., Braak, H., Auburger, G., and Nussbaum, R. L. (2003). Transgenic mice expressing mutant A53T human alpha-synuclein show neuronal dysfunction in the absence of aggregate formation. *Mol. Cell. Neurosci.* **24**(2), 419–429.

Gitler, A. D., and Shorter, J. (2007). Prime time for alpha-synuclein. *J. Neurosci.* **27**(10), 2433–2434.

Glaser, C. B., Yamin, G., Uversky, V. N., and Fink, A. L. (2005). Methionine oxidation, alpha-synuclein and Parkinson's disease. *Biochim. Biophys. Acta* **1703**(2), 157–169.

Goedert, M. (1999). Filamentous nerve cell inclusions in neurodegenerative diseases: Tauopathies and alpha-synucleinopathies. *Philos. Trans. R. Soc. Lond. B Biol. Sci.* **354**(1386), 1101–1118.

Goers, J., Manning-Bog, A. B., McCormack, A. L., Millett, I. S., Doniach, S., Di Monte, D. A., Uversky, V. N., and Fink, A. L. (2003). Nuclear localization of α-synuclein and its interaction with histones. *Biochemistry* **42**(28), 8465–8471.

Goldberg, M. S., and Lansbury, P. T., Jr. (2000). Is there a cause-and-effect relationship between alpha-synuclein fibrillization and Parkinson's disease? *Nat. Cell Biol.* **2**(7), E115–E119.

Golovko, M. Y., Faergeman, N. J., Cole, N. B., Castagnet, P. I., Nussbaum, R. L., and Murphy, E. J. (2005). Alpha-synuclein gene deletion decreases brain palmitate uptake and alters the palmitate metabolism in the absence of alpha-synuclein palmitate binding. *Biochemistry* **44**(23), 8251–8259.

Golts, N., Snyder, H., Frasier, M., Theisler, C., Choi, P., and Wolozin, B. (2002). Magnesium inhibits spontaneous and iron-induced aggregation of α-synuclein. *J. Biol. Chem.* **277**(18), 16116–16123.

Gómez-Santos, C., Barrachina, M., Giménez-Xavier, P., Dalfó, E., Ferrer, I., and Ambrosio, S. (2005). Induction of C/EBP beta and GADD153 expression by dopamine in human neuroblastoma cells. Relationship with alpha-synuclein increase and cell damage. *Brain Res. Bull.* **65**(1), 87–95.

Graham, D. G., Tiffany, S. M., Bell, W. R., Jr., and Gutknecht, W. F. (1978). Autoxidation versus covalent binding of quinones as the mechanism of toxicity of dopamine, 6-hydroxydopamine, and related compounds toward C1300 neuroblastoma cells *in vitro*. *Mol. Pharmacol.* **14**(4), 644–653.

Greenbaum, E. A., Graves, C. L., Mishizen-Eberz, A. J., Lupoli, M. A., Lynch, D. R., Englander, S. W., Axelsen, P. H., and Giasson, B. I. (2005). The E46K mutation in α-synuclein increases amyloid fibril formation. *J. Biol. Chem.* **280**(9), 7800–7807.

Griffioen, G., Duhamel, H., Van Damme, N., Pellens, K., Zabrocki, P., Pannecouque, C., van Leuven, F., Winderickx, J., and Wera, S. (2006). A yeast-based model of alpha-synucleinopathy identifies compounds with therapeutic potential. *Biochim. Biophys. Acta* **1762**(3), 312–318.

Guo, J., Shou, C., Meng, L., Jiang, B., Dong, B., Yao, L., Xie, Y., Zhang, J., Chen, Y., Budman, D. R., and Shi, Y. E. (2007). Neuronal protein synuclein gamma predicts poor clinical outcome in breast cancer. *Int. J. Cancer* **121**(6), 1296–1305.

Gupta, A., Inaba, S., Wong, O. K., Fang, G., and Liu, J. (2003). Breast cancer-specific gene 1 interacts with the mitotic checkpoint kinase BubR1. *Oncogene* **22**(48), 7593–7599.

Gureviciene, I., Gurevicius, K., and Tanila, H. (2007). Role of alpha-synuclein in synaptic glutamate release. *Neurobiol. Dis.* **28**(1), 83–89.

Hamilton, R. L. (2000). Lewy bodies in Alzheimer's disease: A neuropathological review of 145 cases using alpha-synuclein immunohistochemistry. *Brain Pathol.* **10**(3), 378–384.

Hasegawa, M., Fujiwara, H., Nonaka, T., Wakabayashi, K., Takahashi, H., Lee, V. M., Trojanowski, J. Q., Mann, D., and Iwatsubo, T. (2002). Phosphorylated alpha-synuclein is ubiquitinated in alpha-synucleinopathy lesions. *J. Biol. Chem.* **277**(50), 49071–49076.

Hashimoto, M., Yoshimoto, M., Sisk, A., Hsu, L. J., Sundsmo, M., Kittel, A., Saitoh, T., Miller, A., and Masliah, E. (1997). NACP, a synaptic protein involved in Alzheimer's disease, is differentially regulated during megakaryocyte differentiation. *Biochem. Biophys. Res. Commun.* **237**(3), 611–616.

Hashimoto, M., Rockenstein, E., Mante, M., Mallory, M., and Masliah, E. (2001). Beta-synuclein inhibits alpha-synuclein aggregation: A possible role as an anti-parkinsonian factor. *Neuron* **32**(2), 213–223.

Hashimoto, M., Bar-On, P., Ho, G., Takenouchi, T., Rockenstein, E., Crews, L., and Masliah, E. (2004). Beta-synuclein regulates Akt activity in neuronal cells. A possible mechanism for neuroprotection in Parkinson's disease. *J. Biol. Chem.* **279**(22), 23622–23629.

Hatters, D. M., and Howlett, G. J. (2002). The structural basis for amyloid formation by plasma apolipoproteins: A review. *Eur. Biophys. J.* **31**(1), 2–8.

Heise, H., Hoyer, W., Becker, S., Andronesi, O. C., Riedel, D., and Baldus, M. (2005). Molecular-level secondary structure, polymorphism, and dynamics of full-length α-synuclein fibrils studied by solid-state NMR. *Proc. Natl. Acad. Sci. USA* **102**(44), 15871–15876.

Hirsch, E. C., Breidert, T., Rousselet, E., Hunot, S., Hartmann, A., and Michel, P. P. (2003). The role of glial reaction and inflammation in Parkinson's disease. *Ann. N. Y. Acad. Sci.* **991,** 214–228.

Hoyer, W., Cherny, D., Subramaniam, V., and Jovin, T. M. (2004). Impact of the acidic C-terminal region comprising amino acids 109–140 on alpha-synuclein aggregation *in vitro*. *Biochemistry* **43**(51), 16233–16242.

Hoyer, W., Antony, T., Cherny, D., Heim, G., Jovin, T. M., and Subramaniam, V. (2002). Dependence of alpha-synuclein aggregate morphology on solution conditions. *J. Mol. Biol.* **322**(2), 383–393.

Hsu, L. J., Sagara, Y., Arroyo, A., Rockenstein, E., Sisk, A., Mallory, M., Wong, J., Takenouchi, T., Hashimoto, M., and Masliah, E. (2000). α-Synuclein promotes mitochondrial deficit and oxidative stress. *Am. J. Pathol.* **157**(2), 401–410.

Ibáñez, P., Bonnet, A. M., Debarges, B., Lohmann, E., Tison, F., Pollak, P., Agid, Y., Dürr, A., and Brice, A. (2004). Causal relation between alpha-synuclein gene duplication and familial Parkinson's disease. *Lancet* **364**(9440), 1169–1171.

Inaba, S., Li, C., Shi, Y. E., Song, D. Q., Jiang, J. D., and Liu, J. (2005). Synuclein gamma inhibits the mitotic checkpoint function and promotes chromosomal instability of breast cancer cells. *Breast Cancer Res. Treat.* **94**(1), 25–35.

Iwai, A., Masliah, E., Yoshimoto, M., Ge, N., Flanagan, L., de Silva, H. A., Kittel, A., and Saitoh, T. (1995). The precursor protein of non-A beta component of Alzheimer's disease amyloid is a presynaptic protein of the central nervous system. *Neuron* **14**(2), 467–475.

Iwaki, H., Kageyama, S., Isono, T., Wakabayashi, Y., Okada, Y., Yoshimura, K., Terai, A., Arai, Y., Iwamura, H., Kawakita, M., and Yoshiki, T. (2004). Diagnostic potential in bladder cancer of a panel of tumor markers (calreticulin, gamma-synuclein, and catechol-O-methyltransferase) identified by proteomic analysis. *Cancer Sci.* **95**(12), 955–961.

Iwata, A., Maruyama, M., Akagi, T., Hashikawa, T., Kanazawa, I., Tsuji, S., and Nukina, N. (2003). Alpha-synuclein degradation by serine protease neurosin: Implication for pathogenesis of synucleinopathies. *Hum. Mol. Genet.* **12**(20), 2625–2635.

Jahn, R., and Scheller, R. H. (2006). SNAREs—engines for membrane fusion. *Nat. Rev. Mol. Cell Biol.* **7**(9), 631–643.

Jakes, R., Spillantini, M. G., and Goedert, M. (1994). Identification of two distinct synucleins from human brain. *FEBS Lett.* **345**(1), 27–32.

Jenco, J. M., Rawlingson, A., Daniels, B., and Morris, A. J. (1998). Regulation of phospholipase D2: Selective inhibition of mammalian phospholipase D isoenzymes by alpha- and beta-synucleins. *Biochemistry* **37**(14), 4901–4909.

Jensen, P. H., Sørensen, E. S., Petersen, T. E., Gliemann, J., and Ramsussen, L. K. (1995). Residues in the synuclein consensus motif of the α-synuclein fragment, NAC, participate in transglutaminase-catalysed cross-linking to Alzheimer-disease amyloid βA4 peptide. *Biochem. J.* **310**(Pt 1), 91–94.

Jensen, P. H., Hojrup, P., Hager, H., Nielsen, M. S., Jacobsen, L., Olesen, O. F., Gliemann, J., and Jakes, R. (1997). Binding of Abeta to alpha- and beta-synucleins: Identification of segments in alpha-synuclein/NAC precursor that bind Abeta and NAC. *Biochem. J.* **323**(Pt 2), 539–546.

Jensen, P. H., Nielsen, M. S., Jakes, R., Dotti, C. G., and Goedert, M. (1998). Binding of alpha-synuclein to brain vesicles is abolished by familial Parkinson's disease mutation. *J. Biol. Chem.* **273**(41), 26292–26294.

Jensen, P. H., Li, J. Y., Dahlström, A., and Dotti, C. G. (1999). Axonal transport of synucleins is mediated by all rate components. *Eur. J. Neurosci.* **11**(10), 3369–3376.

Jensen, P. J., Alter, B. J., and O'Malley, K. L. (2003). Alpha-synuclein protects naive but not dbcAMP-treated dopaminergic cell types from 1-methyl-4-phenylpyridinium toxicity. *J. Neurochem.* **86**(1), 196–209.

Ji, H., Liu, Y. E., Jia, T., Wang, M., Liu, J., Xiao, G., Joseph, B. K., Rosen, C., and Shi, Y. E. (1997). Identification of a breast cancer-specific gene, BCSG1, by direct differential cDNA sequencing. *Cancer Res.* **57**(4), 759–764.

Jia, T., Liu, Y. E., Liu, J., and Shi, Y. E. (1999). Stimulation of breast cancer invasion and metastasis by synuclein gamma. *Cancer Res.* **59**(3), 742–747.

Jiang, Y., Liu, Y. E., Lu, A., Gupta, A., Goldberg, I. D., Liu, J., and Shi, Y. E. (2003). Stimulation of estrogen receptor signaling by gamma synuclein. *Cancer Res.* **63**(14), 3899–3903.

Jiang, Y., Liu, Y. E., Goldberg, I. D., and Shi, Y. E. (2004). Gamma-synuclein, a novel heat-shock protein-associated chaperone, stimulates ligand-dependent estrogen receptor alpha signaling and mammary tumorigenesis. *Cancer Res.* **64**(13), 4539–4546.

Jin, H., and Clayton, D. F. (1997). Localized changes in immediate-early gene regulation during sensory and motor learning in zebra finches. *Neuron* **19**(5), 1049–1059.

Jo, E., Fuller, N., Rand, R. P., St George-Hyslop, P., and Fraser, P. E. (2002). Defective membrane interactions of familial Parkinson's disease mutant A30P alpha-synuclein. *J. Mol. Biol.* **315**(4), 799–807.

Junn, E., and Mouradian, M. M. (2002). Human alpha-synuclein over-expression increases intracellular reactive oxygen species levels and susceptibility to dopamine. *Neurosci. Lett.* **320**(3), 146–150.

Junn, E., Ronchetti, R. D., Quezado, M. M., Kim, S.-Y., and Mouradian, M. M. (2003). Tissue transglutaminase-induced aggregation of α-synuclein: Implications for Lewy body formation in Parkinson's disease and dementia with Lewy bodies. *Proc. Natl. Acad. Sci. USA* **100**(4), 2047–2052.

Kahle, P. J. (2007). Alpha-synucleinopathy models and human neuropathology: Similarities and differences. *Acta Neuropathol. (Berl)* Epub ahead of print.

Kahle, P. J., Neumann, M., Ozmen, L., Müller, V., Jacobsen, H., Spooren, W., Fuss, B., Mallon, B., Macklin, W. B., Fujiwara, H., Hasegawa, M., Iwatsubo, T., *et al.* (2002). Hyperphosphorylation and insolubility of α-synuclein in transgenic mouse oligodendrocytes. *EMBO Rep.* **3**(6), 583–588.

Kawashima, M., Suzuki, S. O., Doh-ura, K., and Iwaki, T. (2000). alpha-Synuclein is expressed in a variety of brain tumors showing neuronal differentiation. *Acta Neuropathol.* **99**(2), 154–160.

Kholodilov, N. G., Neystat, M., Oo, T. F., Lo, S. E., Larsen, K. E., Sulzer, D., and Burke, R. E. (1999). Increased expression of rat synuclein in the substantia nigra pars compacta identified by mRNA differential display in a model of developmental target injury. *J. Neurochem.* **73**(6), 2586–2599.

Khurana, R., Ionescu-Zanetti, C., Pope, M., Li, J., Nielson, L., Ramirez-Alvarado, M., Regan, L., Fink, A. L., and Carter, S. A. (2003). A general model for amyloid fibril assembly based on morphological studies using atomic force microscopy. *Biophys. J.* **85** (2), 1135–1144.

Kim, Y. S., and Joh, T. H. (2006). Microglia, major player in the brain inflammation: Their roles in the pathogenesis of Parkinson's disease. *Exp. Mol. Med.* **38**(4), 333–347.

Kim, T. D., Paik, S. R., and Yang, C. H. (2002). Structural and functional implications of C-terminal regions of alpha-synuclein. *Biochemistry* **41**(46), 13782–13790.

Kim, T. D., Choi, E., Rhim, H., Paik, S. R., and Yang, C. H. (2004). Alpha-synuclein has structural and functional similarities to small heat shock proteins. *Biochem. Biophys. Res. Commun.* **324**(4), 1352–1359.

Kirik, D., Rosenblad, C., Burger, C., Lundberg, C., Johansen, T. E., Muzyczka, N., Mandel, R. J., and Björklund, A. (2002). Parkinson-like neurodegeneration induced by targeted overexpression of α-synuclein in the nigrostriatal system. *J. Neurosci.* **22**(7), 2780–2791.

Klivenyi, P., Siwek, D., Gardian, G., Yang, L., Starkov, A., Cleren, C., Ferrante, R. J., Kowall, N. W., Abeliovich, A., and Beal, M. F. (2006). Mice lacking alpha-synuclein are resistant to mitochondrial toxins. *Neurobiol. Dis.* **21**(3), 541–548.

Kloepper, K. D., Zhou, D. H., Li, Y., Winter, K. A., George, J. M., and Rienstra, C. M. (2007a). Temperature-dependent sensitivity enhancement of solid-state NMR spectra of alpha-synuclein fibrils. *J. Biomol. NMR* Epub ahead of print.

Kloepper, K. D., Hartman, K. L., Ladror, D. T., and Rienstra, C. M. (2007b). Solid-state NMR spectroscopy reveals that water is nonessential to the core structure of alpha-synuclein fibrils. *J. Phys. Chem. B* Epub ahead of print.

Klucken, J., Shin, Y., Masliah, E., Hyman, B. T., and McLean, P. J. (2004). Hsp70 reduces alpha-synuclein aggregation and toxicity. *J. Biol. Chem.* **279**(24), 25497–25502.

Kontopoulos, E., Parvin, J. D., and Feany, M. B. (2006). Alpha-synuclein acts in the nucleus to inhibit histone acetylation and promote neurotoxicity. *Hum. Mol. Genet.* **15**(20), 3012–3023.

Kramer, M. L., and Schulz-Schaeffer, W. J. (2007). Presynaptic alpha-synuclein aggregates, not Lewy bodies, cause neurodegeneration in dementia with Lewy bodies. *J. Neurosci.* **27**(6), 1405–1410.

Krüger, R., Kuhn, W., Müller, T., Woitalla, D., Graeber, M., Kösel, S., Przuntek, H., Epplen, J. T., Schöls, L., and Riess, O. (1998). Ala30Pro mutation in the gene encoding alpha-synuclein in Parkinson's disease. *Nat. Genet.* **18**(2), 106–108.

Kuwahara, T., Koyama, A., Gengyo-Ando, K., Masuda, M., Kowa, H., Tsunoda, M., Mitani, S., and Iwatsubo, T. (2006). Familial Parkinson mutant α-synuclein causes dopamine neuron dysfunction in transgenic *Caenorhabditis elegans*. *J. Biol. Chem.* **281**(1), 334–340.

Lantos, P. L. (1998). The definition of multiple system atrophy: A review of recent developments. *J. Neuropathol. Exp. Neurol.* **57**(12), 1099–1111.

Larsen, K. E., Schmitz, Y., Troyer, M. D., Mosharov, E., Dietrich, P., Quazi, A. Z., Savalle, M., Nemani, V., Chaudhry, F. A., Edwards, R. H., Stefanis, L., and Sulzer, D. (2006). Alpha-synuclein overexpression in PC12 and chromaffin cells impairs

catecholamine release by interfering with a late step in exocytosis. *J. Neurosci.* **26**(46), 11915–11922.

Lashuel, H. A., and Hirling, H. (2006). Rescuing defective vesicular trafficking protects against alpha-synuclein toxicity in cellular and animal models of Parkinson's disease. *ACS Chem. Biol.* **1**(7), 420–424.

Lashuel, H. A., Petre, B. M., Wall, J., Simon, M., Nowak, R. J., Walz, T., and Lansbury, P. T., Jr. (2002). Alpha-synuclein, especially the Parkinson's disease-associated mutants, forms pore-like annular and tubular protofibrils. *J. Mol. Biol.* **322**(5), 1089–1102.

Lavedan, C. (1998). The synuclein family. *Genome Res.* **8**(9), 871–880.

Lavedan, C., Dehejia, A., Pike, B., Dutra, A., Leroy, E., Ide, S. E., Root, H., Rubenstein, J., Boyer, R. L., Chandrasekharappa, S., Makalowska, I., Nussbaum, R. L., *et al.* (1998a). Contig map of the Parkinson's disease region on 4q21-q23. *DNA Res.* **5**(1), 19–23.

Lavedan, C., Leroy, E., Dehejia, A., Buchholtz, S., Dutra, A., Nussbaum, R. L., and Polymeropoulos, M. H. (1998b). Identification, localization and characterization of the human gamma-synuclein gene. *Hum. Genet.* **103**(1), 106–112.

Lee, H.-J., and Lee, S.-J. (2002). Characterization of cytoplasmic α-synuclein aggregates. Fibril formation is tightly linked to the inclusion-forming process in cells. *J. Biol.Chem.* **277**(50), 48976–48983.

Lee, M. K., and Price, D. L. (2001). Advances in genetic models of Parkinson's disease. *Clin. Neurosci. Res.* **1,** 456–466.

Lee, V. M., and Trojanowski, J. Q. (2006). Mechanisms of Parkinson's disease linked to pathological alpha-synuclein: New targets for drug discovery. *Neuron* **52**(1), 33–38.

Lee, F. J., Liu, F., Pristupa, Z. B., and Niznik, H. B. (2001). Direct binding and functional coupling of alpha-synuclein to the dopamine transporters accelerate dopamine-induced apoptosis. *FASEB J.* **15**(6), 916–926.

Lee, H.-J., Choi, C., and Lee, S.-J. (2002a). Membrane-bound alpha-synuclein has a high aggregation propensity and the ability to seed the aggregation of the cytosolic form. *J. Biol. Chem.* **277**(1), 671–678.

Lee, M. K., Stirling, W., Xu, Y., Xu, X., Qui, D., Mandir, A. S., Dawson, T. M., Copeland, N. G., Jenkins, N. A., and Price, D. L. (2002b). Human α-synuclein-harboring familial Parkinson's disease-linked Ala-53 → Thr mutation causes neurodegenerative disease with α-synuclein aggregation in transgenic mice. *Proc. Natl. Acad. Sci. USA* **99**(13), 8968–8973.

Lee, G., Tanaka, M., Park, K., Lee, S. S., Kim, Y. M., Junn, E., Lee, S.-H., and Mouradian, M. M. (2004). Casein kinase II-mediated phosphorylation regulates α-synuclein/synphilin-1 interaction and inclusion body formation. *J. Biol. Chem.* **279**(8), 6834–6839.

Lee, E. N., Kim, Y. M., Lee, H. J., Park, S. W., Jung, H. Y., Lee, J. M., Ahn, Y. H., and Kim, J. (2005a). Stabilizing peptide fusion for solving the stability and solubility problems of therapeutic proteins. *Pharm. Res.* **22**(10), 1735–1746.

Lee, H.-J., Patel, S., and Lee, S.-J. (2005b). Intravesicular localization and exocytosis of alpha-synuclein and its aggregates. *J. Neurosci.* **25**(25), 6016–6024.

Li, J., Uversky, V. N., and Fink, A. L. (2001). Effect of familial Parkinson's disease point mutations A30P and A53T on the structural properties, aggregation, and fibrillation of human alpha-synuclein. *Biochemistry* **40**(38), 11604–11613.

Li, J., Uversky, V. N., and Fink, A. L. (2002). Conformational behavior of human alpha-synuclein is modulated by familial Parkinson's disease point mutations A30P and A53T. *Neurotoxicology* **23**(4–5), 553–567.

Li, W., Hoffman, P. N., Stirling, W., Price, D. L., and Lee, M. K. (2004a). Axonal transport of human alpha-synuclein slows with aging but is not affected by familial Parkinson's disease-linked mutations. *J. Neurochem.* **88**(2), 401–410.

Li, Z., Sclabas, G. M., Peng, B., Hess, K. R., Abbruzzese, J. L., Evans, D. B., and Chiao, P. J. (2004b). Overexpression of synuclein-gamma in pancreatic adenocarcinoma. *Cancer* **101**(1), 58–65.

Li, W., West, N., Colla, E., Pletnikova, O., Troncoso, J. C., Marsh, L., Dawson, T. M., Jäkälä, P., Hartmann, T., Price, D. L., and Lee, M. K. (2005). Aggregation promoting C-terminal truncation of α-synuclein is a normal cellular process and is enhanced by the familial Parkinson's disease-linked mutations. *Proc. Natl. Acad. Sci. USA* **102**(6), 2162–2167.

Li, W. W., Yang, R., Guo, J. C., Ren, H. M., Zha, X. L., Cheng, J. S., and Cai, D. F. (2007). Localization of alpha-synuclein to mitochondria within midbrain of mice. *Neuroreport* **18**(15), 1543–1546.

Liang, T., and Carr, L. G. (2006). Regulation of alpha-synuclein expression in alcohol-preferring and -non preferring rats. *J. Neurochem.* **99**(2), 470–482.

Liang, T., Spence, J., Liu, L., Strother, W. N., Chang, H. W., Ellison, J. A., Lumeng, L., Li, T. K., Foroud, T., and Carr, L. G. (2003). alpha-Synuclein maps to a quantitative trait locus for alcohol preference and is differentially expressed in alcohol-preferring and-non-preferring rats. *Proc. Natl. Acad. Sci. USA* **100**(8), 4690–4695.

Liani, E., Eyal, A., Avraham, E., Shemer, R., Szargel, R., Berg, D., Bornemann, A., Riess, O., Ross, C. A., Rott, R., and Engelender, S. (2004). Ubiquitylation of synphilin-1 and α-synuclein by SIAH and its presence in cellular inclusions and Lewy bodies imply a role in Parkinson's disease. *Proc. Natl. Acad. Sci. USA* **101**(15), 5500–5505.

Lin, X. J., Zhang, F., Xie, Y. Y., Bao, W. J., He, J. H., and Hu, H. Y. (2006). Secondary structural formation of alpha-synuclein amyloids as revealed by g-factor of solid-state circular dichroism. *Biopolymers* **83**(3), 226–232.

Lindersson, E., Beedholm, R., Højrup, P., Moos, T., Gai, W., Hendil, K. B., and Jensen, P. H. (2004). Proteasomal inhibition by alpha-synuclein filaments and oligomers. *J. Biol. Chem.* **279**(13), 12924–12934.

Lippa, C. F., Schmidt, M. L., Lee, V. M., and Trojanowski, J. Q. (1999). Antibodies to alpha-synuclein detect Lewy bodies in many Down's syndrome brains with Alzheimer's disease. *Ann. Neurol.* **45**(3), 353–357.

Liu, C.-W., Giasson, B. I., Lewis, K. A., Lee, V. M., DeMartino, G. N., and Thomas, P. J. (2005a). A precipitating role for truncated alpha-synuclein and the proteasome in alpha-synuclein aggregation: Implications for pathogenesis of Parkinson disease. *J. Biol. Chem.* **280**(24), 22670–22678.

Liu, H., Liu, W., Wu, Y., Zhou, Y., Xue, R., Luo, C., Wang, L., Zhao, W., Jiang, J. D., and Liu, J. (2005b). Loss of epigenetic control of synuclein-gamma gene as a molecular indicator of metastasis in a wide range of human cancers. *Cancer Res.* **65**(17), 7635–7643.

Liu, I. H., Uversky, V. N., Munishkina, L. A., Fink, A. L., Halfter, W., and Cole, G. J. (2005c). Agrin binds alpha-synuclein and modulates alpha-synuclein fibrillation. *Glycobiology* **15**(12), 1320–1331.

Liu, C., Fei, E., Jia, N., Wang, H., Tao, R., Iwata, A., Nukina, N., Zhou, J., and Wang, G. (2007). Assembly of lysine 63-linked ubiquitin conjugates by phosphorylated alpha-synuclein implies Lewy body biogenesis. *J. Biol. Chem.* **282**(19), 14558–14566.

Lo Bianco, C., Ridet, J. L., Schneider, B. L., Deglon, N., and Aebischer, P. (2002). alpha-Synucleinopathy and selective dopaminergic neuron loss in a rat lentiviral-based model of Parkinson's disease. *Proc. Natl. Acad. Sci. USA* **99**(16), 10813–10818.

Lotharius, J., and Brundin, P. (2002a). Impaired dopamine storage resulting from alpha-synuclein mutations may contribute to the pathogenesis of Parkinson's disease. *Hum. Mol. Genet.* **11**(20), 2395–2407.

Lotharius, J., and Brundin, P. (2002b). Pathogenesis of Parkinson's disease: Dopamine, vesicles and alpha-synuclein. *Nat. Rev. Neurosci.* **3**(12), 932–942.

Lotharius, J., Dugan, L. L., and O'Malley, K. L. (1999). Distinct mechanisms underlie neurotoxin-mediated cell death in cultured dopaminergic neurons. *J. Neurosci.* **19**(4), 1284–1293.

Lotharius, J., Barg, S., Wiekop, P., Lundberg, C., Raymon, H. K., and Brundin, P. (2002). Effect of mutant α-synuclein on dopamine homeostasis in a new human mesencephalic cell line. *J. Biol. Chem.* **277**(41), 38884–38894.

Lowe, R., Pountney, D. L., Jensen, P. H., Gai, W. P., and Voelcker, N. H. (2004). Calcium(II) selectively induces α-synuclein annular oligomers via interaction with the C-terminal domain. *Protein Sci.* **13**(12), 3245–3252.

Lu, A., Gupta, A., Li, C., Ahlborn, T. E., Ma, Y., Shi, E. Y., and Liu, J. (2001). Molecular mechanisms for aberrant expression of the human breast cancer specific gene 1 in breast cancer cells: Control of transcription by DNA methylation and intronic sequences. *Oncogene* **20**(37), 5173–5185.

Lu, A., Zhang, F., Gupta, A., and Liu, J. (2002). Blockade of AP1 transactivation abrogates the abnormal expression of breast cancer-specific gene 1 in breast cancer cells. *J. Biol. Chem.* **277**(35), 31364–31372.

Lu, L., Neff, F., Alvarez-Fischer, D., Henze, C., Xie, Y., Oertel, W. H., Schlegel, J., and Hartmann, A. (2005). Gene expression profiling of Lewy body-bearing neurons in Parkinson's disease. *Exp Neurol.* **195**(1), 27–39.

Lu, A., Li, Q., and Liu, J. (2006). Regulatory mechanisms for abnormal expression of the human breast cancer specific gene 1 in breast cancer cells. *Sci. China C Life Sci.* **49**(4), 403–408.

Lücke, C., Gantz, D. L., Klimtchuk, E., and Hamilton, J. A. (2006). Interactions between fatty acids and α-synuclein. *J. Lipid Res.* **47**(8), 1714–1724.

Lücking, C. B., and Brice, A. (2000). Alpha-synuclein and Parkinson's disease. *Cell. Mol. Life Sci.* **57**(13–14), 1894–1908.

Manning-Boğ, A. B., McCormack, A. L., Li, J., Uversky, V. N., Fink, A. L., and Di Monte, D. A. (2002). The herbicide paraquat causes up-regulation and aggregation of alpha-synuclein in mice: Paraquat and alpha-synuclein. *J. Biol. Chem.* **277**(3), 1641–1644.

Manning-Boğ, A. B., McCormack, A. L., Purisai, M. G., Bolin, L. M., and Di Monte, D. A. (2003). α-Synuclein overexpression protects against paraquat-induced neurodegeneration. *J. Neurosci.* **23**(8), 3095–3099.

Maraganore, D. M., de Andrade, M., Elbaz, A., Farrer, M. J., Ioannidis, J. P., Krüger, R., Rocca, W. A., Schneider, N. K., Lesnick, T. G., Lincoln, S. J., Hulihan, M. M., Aasly, J. O., *et al.* (2006). Collaborative analysis of α-synuclein gene promoter variability and Parkinson isease. *JAMA* **296**(6), 661–670.

Maroteaux, L., and Scheller, R. H. (1991). The rat brain synucleins; family of proteins transiently associated with neuronal membrane. *Brain Res. Mol. Brain Res.* **11**(3–4), 335–343.

Maroteaux, L., Campanelli, J. T., and Scheller, R. H. (1988). Synuclein: A neuron-specific protein localized to the nucleus and presynaptic nerve terminal. *J. Neurosci.* **8**(8), 2804–2815.

Marsh, J. A., Singh, V. K., Jia, Z., and Forman-Kay, J. D. (2006). Sensitivity of secondary structure propensities to sequence differences between alpha- and gamma-synuclein: Implications for fibrillation. *Protein Sci.* **15**(12), 2795–2804.

Martí, M. J., Tolosa, E., and Campdelacreu, J. (2003). Clinical overview of the synucleinopathies. *Mov. Disord.* **18**(Suppl 6), S21–S27.

Martin, L. J., Pan, Y., Price, A. C., Sterling, W., Copeland, N. G., Jenkins, N. A., Price, D. L., and Lee, M. K. (2006a). Parkinson's disease alpha-synuclein transgenic mice develop neuronal mitochondrial degeneration and cell death. *J. Neurosci.* **26**(1), 41–50.

Martin, T. A., Gomez, K., Watkins, G., Douglas-Jones, A., Mansel, R. E., and Jiang, W. G. (2006b). Expression of breast cancer specific gene-1 (BCSG-1/gamma-synuclein) is associated with tumour grade but not with clinical outcome of patients with breast cancer. *Oncol. Rep.* **16**(1), 207–212.

Martínez-Navarrete, G. C., Martín-Nieto, J., Esteve-Rudd, J., Angulo, A., and Cuenca, N. (2007). Alpha synuclein gene expression profile in the retina of vertebrates. *Mol. Vis.* **13,** 949–961.

Marui, W., Iseki, E., Nakai, T., Miura, S., Kato, M., Uéda, K., and Kosaka, K. (2002). Progression and staging of Lewy pathology in brains from patients with dementia with Lewy bodies. *J. Neurol. Sci.* **195**(2), 153–159.

Mash, D. C., Ouyang, Q., Pablo, J., Basile, M., Izenwasser, S., Lieberman, A., and Perrin, R. J. (2003). Cocaine abusers have an overexpression of alpha-synuclein in dopamine neurons. *J. Neurosci.* **23**(7), 2564–2571.

Masliah, E., Rockenstein, E., Veinbergs, I., Mallory, M., Hashimoto, M., Takeda, A., Sagara, Y., Sisk, A., and Mucke, L. (2000). Dopaminergic loss and inclusion body formation in alpha-synuclein mice: Implications for neurodegenerative disorders. *Science* **287**(5456), 1265–1269.

Masliah, E., Rockenstein, E., Veinbergs, I., Sagara, F., Mallory, M., Hashimoto, M., and Mucke, L. (2001). β-Amyloid peptides enhance α-synuclein accumulation and neuronal deficits in a transgenic mouse model linking Alzheimer's disease and Parkinson's disease. *Proc. Natl. Acad. Sci. USA* **98**(21), 12245–12250.

Masliah, E., Rockenstein, E., Adame, A., Alford, M., Crews, L., Hashimoto, M., Seubert, P., Lee, M., Goldstein, J., Chilcote, T., Games, D., and Schenk, D. (2005). Effects of alpha-synuclein immunization in a mouse model of Parkinson's disease. *Neuron* **46**(6), 857–868.

Matsuoka, Y., Vila, M., Lincoln, S., McCormack, A., Picciano, M., LaFrancois, J., Yu, X., Dickson, D., Langston, W. J., McGowan, E., Farrer, M., Hardy, J., *et al.* (2001). Lack of nigral pathology in transgenic mice expressing human alpha-synuclein driven by the tyrosine hydroxylase promoter. *Neurobiol. Dis.* **8**(3), 535–539.

Maurage, C. A., Ruchoux, M. M., de Vos, R., Surguchov, A., and Destee, A. (2003). Retinal involvement in dementia with Lewy bodies: A clue to hallucinations? *Ann. Neurol.* **54**(4), 542–547.

Mazzulli, J. R., Armakola, M., Dumoulin, M., Parastatidis, I., and Ischiropoulos, H. (2007). Cellular oligomerization of alpha-synuclein is determined by the interaction of oxidized catechols with a C-terminal sequence. *J. Biol. Chem.* **282**(43), 31621–31630.

McLean, P. J., Kawamata, H., Ribich, S., and Hyman, B. T. (2000). Membrane association and protein conformation of alpha-synuclein in intact neurons. Effect of Parkinson's disease-linked mutations. *J. Biol. Chem.* **275**(12), 8812–8816.

McNaught, K. S., Shashidharan, P., Perl, D. P., Jenner, P., and Olanow, C. W. (2002). Aggresome-related biogenesis of Lewy bodies. *Eur. J. Neurosci.* **16**(11), 2136–2148.

Mezey, E., Dehejia, A., Harta, G., Papp, M. I., Polymeropoulos, M. H., and Brownstein, M. J. (1998). Alpha synuclein in neurodegenerative disorders: Murderer or accomplice? *Nat. Med.* **4**(7), 755–757.

Miller, D. W., Hague, S. M., Clarimon, J., Baptista, M., Gwinn-Hardy, K., Cookson, M. R., and Singleton, A. B. (2004). Alpha-synuclein in blood and brain from familial Parkinson disease with SNCA locus triplication. *Neurology* **62**(10), 1835–1838.

Miller, D. W., Johnson, J. M., Solano, S. M., Hollingsworth, Z. R., Standaert, D. G., and Young, A. B. (2005). Absence of alpha-synuclein mRNA expression in normal and multiple system atrophy oligodendroglia. *J. Neural Transm.* **112**(12), 1613–1624.

Mochizuki, H. (2007). Gene therapy for Parkinson's disease. *Expert Rev. Neurother.* **7**(8), 957–960.

Monti, B., Polazzi, E., Batti, L., Crochemore, C., Virgili, M., and Contestabile, A. (2007). Alpha-synuclein protects cerebellar granule neurons against 6-hydroxydopamine-induced death. *J. Neurochem.* **103**(2), 518–530.

Moore, D. J., West, A. B., Dawson, V. L., and Dawson, T. M. (2005). Molecular pathophysiology of Parkinson's disease. *Annu. Rev. Neurosci.* **28,** 57–87.

Mor, F., Quintana, F., Mimran, A., and Cohen, I. R. (2003). Autoimmune encephalomyelitis and uveitis induced by T cell immunity to self β-synuclein. *J. Immunol.* **170**(1), 628–634.

Mori, F., Tanji, K., Yoshimoto, M., Takahashi, H., and Wakabayashi, K. (2002). Demonstration of alpha-synuclein immunoreactivity in neuronal and glial cytoplasm in normal human brain tissue using proteinase K and formic acid pretreatment. *Exp. Neurol.* **176**(1), 98–104.

Morrisett, J. D., Jackson, R. L., and Gotto, A. M., Jr. (1977). Lipid-protein interactions in the plasma lipoproteins. *Biochim. Biophys. Acta* **472**(2), 93–133.

Mosharov, E. V., Staal, R. G., Bové, J., Prou, D., Hananiya, A., Markov, D., Poulsen, N., Larsen, K. E., Moore, C. M. H., Troyer, M. D., Edwards, R. H., Przedborski, S., *et al.* (2006). Alpha-synuclein overexpression increases cytosolic catecholamine concentration. *J. Neurosci.* **26**(36), 9304–9311.

Moszczynska, A., Saleh, J., Zhang, H., Vukusic, B., Lee, F. J., and Liu, F. (2007). Parkin disrupts the alpha-synuclein/dopamine transporter interaction: Consequences toward dopamine-induced toxicity. *J. Mol. Neurosci.* **32**(3), 217–227.

Moussa, C. E.-H., Mahmoodian, F., Tomita, Y., and Sidhu, A. (2007). Dopamine differentially induces aggregation of A53T mutant and wild type α-synuclein: Insights into the protein chemistry of Parkinson's disease. *Biochem. Biophys. Res. Commun.* Epub ahead of print.

Mueller, J. C., Fuchs, J., Hofer, A., Zimprich, A., Lichtner, P., Illig, T., Berg, D., Wüllner, U., Meitinger, T., and Gasser, T. (2005). Multiple regions of alpha-synuclein are associated with Parkinson's disease. *Ann. Neurol.* **57**(4), 535–541.

Mukaetova-Ladinska, E. B., Hurt, J., Jakes, R., Xuereb, J., Honer, W. G., and Wischik, C. M. (2000). Alpha-synuclein inclusions in Alzheimer and Lewy body diseases. *J. Neuropathol. Exp. Neurol.* **59**(5), 408–417.

Murphy, D. D., Rueter, S. M., Trojanowski, J. Q., and Lee, V. M.-Y. (2000). Synucleins are developmentally expressed, and α-synuclein regulates the size of the presynaptic vesicular pool in primary hippocampal neurons. *J. Neurosci.* **20**(9), 3214–3220.

Murray, I. V., Giasson, B. I., Quinn, S. M., Koppaka, V., Axelsen, P. H., Ischiropoulos, H., Trojanowski, J. Q., and Lee, V. M. (2003). Role of alpha-synuclein carboxy-terminus on fibril formation *in vitro*. *Biochemistry* **42**(28), 8530–8540.

Naiki, H., Higuchi, K., Hosokawa, M., and Takeda, T. (1989). Fluorometric determination of amyloid fibrils *in vitro* using the fluorescent dye, thioflavin T1. *Anal. Biochem.* **177**(2), 244–2449.

Nakajo, S., Tsukada, K., Omata, K., Nakamura, Y., and Nakaya, K. (1993). A new brain-specific 14-kDa protein is a phosphoprotein. Its complete amino acid sequence and evidence for phosphorylation. *Eur. J. Biochem.* **217**(3), 1057–1063.

Nakamura, T., Yamashita, H., Nagano, Y., Takahashi, T., Avraham, S., Avraham, H., Matsumoto, M., and Nakamura, S. (2002). Activation of Pyk2/RAFTK induces tyrosine phosphorylation of alpha-synuclein via Src-family kinases. *FEBS Lett.* **521**(1–3), 190–194.

Narhi, L., Wood, S. J., Steavenson, S., Jiang, Y., Wu, G. M., Anafi, D., Kaufman, S. A., Martin, F., Sitney, K., Denis, P., Louis, J.-C., Wypych, J., *et al.* (1999). Both familial Parkinson's disease mutations accelerate α-synuclein aggregation. *J. Biol. Chem.* **274**(14), 9843–9846.

Neumann, M., Kahle, P. J., Giasson, B. I., Ozmen, L., Borroni, E., Spooren, W., Müller, V., Odoy, S., Fujiwara, H., Hasegawa, M., Iwatsubo, T., Trojanowski, J. Q., *et al.* (2002). Misfolded proteinase K–resistant hyperphosphorylated α-synuclein in aged transgenic mice with locomotor deterioration and in human α-synucleinopathies. *J. Clin. Invest.* **110**(10), 1429–1439.

Ninkina, N. N., Alimova-Kost, M. V., Paterson, J. W. E., Delaney, L., Cohen, B. B., Imreh, S., Gnuchev, N. V., Davies, A. M., and Buchman, V. L. (1998). Organisation, expression and polymorphism of the human persyn gene. *Hum. Mol. Genet.* **7,** 1417–1424.

Ninkina, N., Papachroni, K., Robertson, D. C., Schmidt, O., Delaney, L., O'Neill, F., Court, F., Rosenthal, A., Fleetwood-Walker, S. M., Davies, A. M., and Buchman, V. L. (2003). Neurons expressing the highest levels of gamma-synuclein are unaffected by targeted inactivation of the gene. *Mol. Cell. Biol.* **23**(22), 8233–8245.

Nishioka, K., Hayashi, S., Farrer, M. J., Singleton, A. B., Yoshino, H., Imai, H., Kitami, T., Sato, K., Kuroda, R., Tomiyama, H., Mizoguchi, K., Murata, M., *et al.* (2006). Clinical heterogeneity of alpha-synuclein gene duplication in Parkinson's disease. *Ann. Neurol.* **59** (2), 298–309.

Nonaka, T., Iwatsubo, T., and Hasegawa, M. (2005). Ubiquitination of alpha-synuclein. *Biochemistry* **44**(1), 361–368.

Nuscher, B., Kamp, F., Mehnert, T., Odoy, S., Haass, C., Kahle, P. J., and Beyer, K. (2004). α-Synuclein has a high affinity for packing defects in a bilayer membrane. *J. Biol. Chem.* **279**(21), 21966–21975.

Ogburn, K. D., and Figueiredo-Pereira, M. E. (2006). Cytoskeleton/endoplasmic reticulum collapse induced by prostaglandin J2 parallels centrosomal deposition of ubiquitinated protein aggregates. *J. Biol. Chem.* **281**(32), 23274–23284.

Ohtake, H., Limprasert, P., Fan, Y., Onodera, O., Kakita, A., Takahashi, H., Bonner, L. T., Tsuang, D. W., Murray, I. V. J., Lee, V. M.-Y., Trojanowski, J. Q., Ishikawa, A., *et al.* (2004). β-Synuclein gene alterations in dementia with Lewy bodies. *Neurology* **63**(5), 805–811.

Okochi, M., Walter, J., Koyama, A., Nakajo, S., Baba, M., Iwatsubo, T., Meijer, L., Kahle, P. J., and Haass, C. (2000). Constitutive phosphorylation of the Parkinson's disease associated α-synuclein. *J. Biol. Chem.* **275**(1), 390–397.

Ono, K., and Yamada, M. (2006). Antioxidant compounds have potent anti-fibrillogenic and fibril-destabilizing effects for alpha-synuclein fibrils *in vitro*. *J. Neurochem.* **97**(1), 105–115.

Orth, M., Tabrizi, S. J., Tomlinson, C., Messmer, K., Korlipara, L. V., Schapira, A. H., and Cooper, J. M. (2004). G209A mutant alpha synuclein expression specifically enhances dopamine induced oxidative damage. *Neurochem. Int.* **45**(5), 669–676.

Ostrerova, N., Petrucelli, L., Farrer, M., Mehta, N., Choi, P., Hardy, J., and Wolozin, B. (1999). α-Synuclein shares physical and functional homology with 14–3–3 proteins. *J. Neurosci.* **19**(14), 5782–5791.

Outeiro, T. F., and Lindquist, S. (2003). Yeast cells provide insight into alpha-synuclein biology and pathobiology. *Science* **302**(5651), 1772–1775.

Outeiro, T. F., Klucken, J., Strathearn, K. E., Liu, F., Nguyen, P., Rochet, J. C., Hyman, B. T., and McLean, P. J. (2006). Small heat shock proteins protect against alpha-synuclein-induced toxicity and aggregation. *Biochem. Biophys. Res. Commun.* **351**(3), 631–638.

Papachroni, K. K., Ninkina, N., Papapanagiotou, A., Hadjigeorgiou, G. M., Xiromerisiou, G., Papadimitriou, A., Kalofoutis, A., and Buchman, V. L. (2007). Autoantibodies to alpha-synuclein in inherited Parkinson's disease. *J. Neurochem.* **101**(3), 749–756.

Park, S. M., and Kim, J. (2007). A soluble and heat-resistant form of hantavirus nucleocapsid protein for the serodiagnosis of HFRS. *J. Virol Methods* Epub ahead of print.

Park, J. Y., and Lansbury, P. T., Jr. (2003). Beta-synuclein inhibits formation of alpha-synuclein protofibrils: A possible therapeutic strategy against Parkinson's disease. *Biochemistry* **42**(13), 3696–3700.

Park, S. M., Jung, H. Y., Chung, K. C., Rhim, H., Park, J. H., and Kim, J. (2002a). Stress-induced aggregation profiles of GST-alpha-synuclein fusion proteins: Role of the C-terminal acidic tail of alpha-synuclein in protein thermosolubility and stability. *Biochemistry* **41**(12), 4137–4146.

Park, S. M., Jung, H. Y., Kim, T. D., Park, J. H., Yang, C.-H., and Kim, J. (2002b). Distinct roles of the N-terminal-binding domain and the C-terminal-solubilizing domain of α-synuclein, a molecular chaperone. *J. Biol. Chem.* **277**(32), 28512–28520.

Park, S. M., Jung, H. Y., Kim, H. O., Rhim, H., Paik, S. R., Chung, K. C., Park, J. H., and Kim, J. (2002c). Evidence that alpha-synuclein functions as a negative regulator of Ca(++)-dependent alpha-granule release from human platelets. *Blood* **100**(7), 2506–2514.

Park, S. M., Ahn, K. J., Jung, H. Y., Park, J. H., and Kim, J. (2004). Effects of novel peptides derived from the acidic tail of synuclein (ATS) on the aggregation and stability of fusion proteins. *Protein Eng. Des. Sel.* **17**(3), 251–260.

Parsian, A., Racette, B., Zhang, Z. H., Chakraverty, S., Rundle, M., Goate, A., and Perlmutter, J. S. (1998). Mutation, sequence analysis, and association studies of alpha-synuclein in Parkinson's disease. *Neurology* **51**(6), 1757–1759.

Payton, J. E., Perrin, R. J., Woods, W. S., and George, J. M. (2004). Structural determinants of PLD2 inhibition by alpha-synuclein. *J. Mol. Biol.* **337**(4), 1001–1009.

Paxinou, E., Chen, Q., Weisse, M., Giasson, B. I., Norris, B. H., Rueter, S. M., Trojanowski, J. Q., Lee, V. M.-Y., and Ischiropoulos, H. (2001). Induction of α-synuclein aggregation by intracellular nitrative insult. *J. Neurosci.* **21**(20), 8053–8061.

Perez, R. G., Waymire, J. C., Lin, E., Liu, J. J., Guo, F., and Zigmond, M. J. (2002). A role for α-synuclein in the regulation of dopamine biosynthesis. *J. Neurosci.* **22**(8), 3090–3099. Erratum in: *J. Neurosci.* 22(20), 9142.

Perrin, R. J., Woods, W. S., Clayton, D. F., and George, J. M. (2000). Interaction of human α-synuclein and Parkinson's disease variants with phospholipids: Structural analysis using site-directed mutagenesis. *J. Biol. Chem.* **275**(44), 34393–34398.

Perrin, R. J., Woods, W. S., Clayton, D. F., and George, J. M. (2001). Exposure to long chain polyunsaturated fatty acids triggers rapid multimerization of synucleins. *J. Biol. Chem.* **276**(45), 41958–41962.

Petersen, K., Olesen, O. F., and Mikkelsen, J. D. (1999). Developmental expression of alpha-synuclein in rat hippocampus and cerebral cortex. *Neuroscience* **91**(2), 651–659.

Petrucelli, L., O'Farrell, C., Lockhart, P. J., Baptista, M., Kehoe, K., Vink, L., Choi, P., Wolozin, B., Farrer, M., Hardy, J., and Cookson, M. R. (2002). Parkin protects against the toxicity associated with mutant alpha-synuclein: Proteasome dysfunction selectively affects catecholaminergic neurons. *Neuron* **36**(6), 1007–1019.

Polymeropoulos, M. H., Lavedan, C., Leroy, E., Ide, S. E., Dehejia, A., Dutra, A., Pike, B., Root, H., Rubenstein, J., Boyer, R., Stenroos, E. S., Chandrasekharappa, S., *et al.* (1997). Mutation in the alpha-synuclein gene identified in families with Parkinson's disease. *Science* **276**(5321), 2045–2047.

Pountney, D. L., Lowe, R., Quilty, M., Vickers, J. C., Voelcker, N. H., and Gai, W. P. (2004). Annular alpha-synuclein species from purified multiple system atrophy inclusions. *J. Neurochem.* **90**(2), 502–512.

Pronin, A. N., Morris, A. J., Surguchov, A., and Benovic, J. L. (2000). Synucleins are a novel class of substrates for G protein-coupled receptor kinases. *J. Biol. Chem.* **275**(34), 26515–26522.

Qin, Z., Hu, D., Han, S., Hong, D. P., and Fink, A. L. (2007). Role of different regions of alpha-synuclein in the assembly of fibrils. *Biochemistry* **46**(46), 13322–13330.

Quist, A., Doudevski, I., Lin, H., Azimova, R., Ng, D., Frangione, B., Kagan, B., Ghiso, J., and Lal, R. (2005). Amyloid ion channels: A common structural link for protein-misfolding disease. *Proc. Natl. Acad. Sci. USA* **102**(30), 10427–10432.

Recchia, A., Debetto, P., Negro, A., Guidolin, D., Skaper, S. D., and Giusti, P. (2004). α-Synuclein and Parkinson's disease. *FASEB J.* **18**(6), 617–626.

Richfield, E. K., Thiruchelvam, M. J., Cory-Slechta, D. A., Wuertzer, C., Gainetdinov, R. R., Caron, M. G., Di Monte, D. A., and Federoff, H. J. (2002). Behavioral and neurochemical effects of wild-type and mutated human alpha-synuclein in transgenic mice. *Exp. Neurol.* **175**(1), 35–48.

Rochet, J. C., Outeiro, T. F., Conway, K. A., Ding, T. T., Volles, M. J., Lashuel, H. A., Bieganski, R. M., Lindquist, S. L., and Lansbury, P. T. (2004). Interactions among alpha-synuclein, dopamine, and biomembranes: Some clues for understanding neurodegeneration in Parkinson's disease. *J. Mol. Neurosci.* **23**(1–2), 23–34.

Rockenstein, E., Schwach, G., Ingolic, E., Adame, A., Crews, L., Mante, M., Pfragner, R., Schreiner, E., Windisch, M., and Masliah, E. (2005). Lysosomal pathology associated with alpha-synuclein accumulation in transgenic models using an eGFP fusion protein. *J. Neurosci. Res.* **80**(2), 247–259.

Saha, A. R., Hill, J., Utton, M. A., Asuni, A. A., Ackerley, S., Grierson, A. J., Miller, C. C., Davies, A. M., Buchman, V. L., Anderton, B. H., and Hanger, D. P. (2004). Parkinson's disease α-synuclein mutations exhibit defective axonal transport in cultured neurons. *J. Cell Sci.* **117**(Pt 7), 1017–1024.

Saito, Y., Kawai, M., Inoue, K., Sasaki, R., Arai, H., Nanba, E., Kuzuhara, S., Ihara, Y., Kanazawa, I., and Murayama, S. (2000). Widespread expression of alpha-synuclein and tau immunoreactivity in Hallervorden-Spatz syndrome with protracted clinical course. *J. Neurol. Sci.* **177**(1), 48–59.

Saito, Y., Kawashima, A., Ruberu, N. N., Fujiwara, H., Koyama, S., Sawabe, M., Arai, T., Nagura, H., Yamanouchi, H., Hasegawa, M., Iwatsubo, T., and Murayama, S. (2003). Accumulation of phosphorylated alpha-synuclein in aging human brain. *J. Neuropathol. Exp. Neurol.* **62**(6), 644–654.

Sampathu, D. M., Giasson, B. I., Pawlyk, A. C., Trojanowski, J. Q., and Lee, V. M. (2003). Ubiquitination of alpha-synuclein is not required for formation of pathological inclusions in alpha-synucleinopathies. *Am. J. Pathol.* **163**(1), 91–100.

Sangchot, P., Sharma, S., Chetsawang, B., Porter, J., Govitrapong, P., and Ebadi, M. (2002). Deferoxamine attenuates iron-induced oxidative stress and prevents mitochondrial aggregation and alpha-synuclein translocation in SK-N-SH cells in culture. *Dev. Neurosci.* **24**(2–3), 143–153.

Schneider, B. L., Seehus, C. R., Capowski, E. E., Aebischer, P., Zhang, S. C., and Svendsen, C. N. (2007). Over-expression of alpha-synuclein in human neural progenitors leads to specific changes in fate and differentiation. *Hum. Mol. Genet.* **16**(6), 651–666.

Serpell, L. C., Berriman, J., Jakes, R., Goedert, M., and Crowther, R. A. (2000). Fiber diffraction of synthetic α-synuclein filaments shows amyloid-like cross-β conformation. *Proc. Natl. Acad. Sci. USA* **97**(9), 4897–4902.

Shamoto-Nagai, M., Maruyama, W., Hashizume, Y., Yoshida, M., Osawa, T., Riederer, P., and Naoi, M. (2007). In parkinsonian substantia nigra, alpha-synuclein is modified by acrolein, a lipid-peroxidation product, and accumulates in the dopamine neurons with inhibition of proteasome activity. *J. Neural Transm.* Epub ahead of print.

Sharma, N., Brandis, K. A., Herrera, S. K., Johnson, B. E., Vaidya, T., Shrestha, R., and Debburman, S. K. (2006). alpha-Synuclein budding yeast model: Toxicity enhanced by impaired proteasome and oxidative stress. *J. Mol. Neurosci.* **28**(2), 161–178.

Sharon, R., Goldberg, M. S., Bar-Josef, I., Betensky, R. A., Shen, J., and Selkoe, D. J. (2001). Alpha-synuclein occurs in lipid-rich high molecular weight complexes, binds

fatty acids, and shows homology to the fatty acid-binding proteins. *Proc. Natl. Acad. Sci. USA* **98**(16), 9110–9115.

Sharon, R., Bar-Joseph, I., Mirick, G. E., Serhan, C. N., and Selkoe, D. J. (2003). Altered fatty acid composition of dopaminergic neurons expressing α-synuclein and human brains with α-synucleinopathies. *J. Biol. Chem.* **278**(50), 49874–49881.

Shibasaki, Y., Baillie, D. A., St Clair, D., and Brookes, A. J. (1995). High-resolution maping of SNCA encoding alpha-synuclein, the non-A beta component of Alzheimer's disease amyloid precursor, to human chromosome 4q21.3→q22 by fluorescence in situ hybridization. *Cytogenet. Cell Genet.* **71**(1), 54–55.

Shibayama-Imazu, T., Okahashi, T., Omata, K., Nakajo, S., Ochiai, H., Nakai, Y., Hama, T., Nakamura, Y., and Nakaya, K. (1993). Cell and tissue distribution and developmental change of neuron specific 14 kDa protein (phosphoneuroprotein 14). *Brain Res.* **622**(1–2), 17–25.

Shimura, H., Schlossmacher, M. G., Hattori, N., Frosch, M. P., Trockenbacher, A., Schneider, R., Mizuno, Y., Kosik, K. S., and Selkoe, D. J. (2001). Ubiquitination of a new form of alpha-synuclein by parkin from human brain: Implications for Parkinson's disease. *Science* **293**(5528), 263–269.

Shin, Y., Klucken, J., Patterson, C., Hyman, B. T., and McLean, P. J. (2005). The co-chaperone carboxyl terminus of Hsp70-interacting protein (CHIP) mediates alpha-synuclein degradation decisions between proteasomal and lysosomal pathways. *J. Biol. Chem.* **280**(25), 23727–23734.

Sidhu, A., Wersinger, C., and Vernier, P. (2004). alpha-Synuclein regulation of the dopaminergic transporter: A possible role in the pathogenesis of Parkinson's disease. *FEBS Lett.* **565**(1–3), 1–5.

Singh, V. K., and Jia, Z. (2008). Targeting synuclein-gamma to counteract drug resistance in cancer. *Expert Opin. Ther. Targets* **12**(1), 59–68.

Singh, V. K., Zhou, Y., Marsh, J. A., Uversky, V. N., Forman-Kay, J. D., Liu, J., and Jia, Z. (2007). Synuclein-gamma targeting peptide inhibitor that enhances sensitivity of breast cancer cells to antimicrotubule drugs. *Cancer Res.* **67**(2), 626–633.

Singleton, A. B., Farrer, M., Johnson, J., Singleton, A., Hague, S., Kachergus, J., Hulihan, M., Peuralinna, T., Dutra, A., Nussbaum, R., Lincoln, S., Crawley, A., *et al.* (2003). alpha-Synuclein locus triplication causes Parkinson's disease. *Science* **302**(5646), 841.

Smith, W. W., Margolis, R. L., Li, X., Troncoso, J. C., Lee, M. K., Dawson, V. L., Dawson, T. M., Iwatsubo, T., and Ross, C. A. (2005). α-Synuclein phosphorylation enhances eosinophilic cytoplasmic inclusion formation in SH-SY5Y cells. *J. Neurosci.* **25** (23), 5544–5552.

Snyder, H., Mensah, K., Hsu, C., Hashimoto, M., Surgucheva, I. G., Festoff, B., Surguchov, A., Masliah, E., Matouschek, A., and Wolozin, B. (2005). α-Synuclein reduces proteasomal inhibition by alpha-synuclein but not gamma-synuclein. *J. Biol. Chem.* **280**(9), 7562–7569.

Song, D. D., Shults, C. W., Sisk, A., Rockenstein, E., and Masliah, E. (2004). Enhanced substantia nigra mitochondrial pathology in human alpha-synuclein transgenic mice after treatment with MPTP. *Exp. Neurol.* **186**(2), 158–172.

Souza, J. M., Giasson, B. I., Chen, Q., Lee, V. M.-Y., and Ischiropoulos, H. (2000a). Dityrosine cross-linking promotes formation of stable α-synuclein polymers: Implication of nitrative and oxidative stress in the pathogenesis of neurodegenerative synucleinopathies. *J. Biol. Chem.* **275**(24), 18344–18349.

Souza, J. M., Giasson, B. I., Lee, V. M., and Ischiropoulos, H. (2000b). Chaperone-like activity of synucleins. *FEBS Lett.* **474,** 116–119.

Spadafora, P., Annesi, G., Pasqua, A. A., Serra, P., Ciro Candiano, I. C., Carrideo, S., Tarantino, P., Civitelli, D., De Marco, E. V., Nicoletti, G., Annesi, F., and Quattrone, A.

(2003). NACP-REP1 polymorphism is not involved in Parkinson's disease: A case-control study in a population sample from southern Italy. *Neurosci. Lett.* **351**(2), 75–78.

Spillantini, M. G., and Goedert, M. (2000). The alpha-synucleinopathies: Parkinson's disease, dementia with Lewy bodies, and multiple system atrophy. *Ann. N. Y. Acad. Sci.* **920,** 16–27.

Spillantini, M. G., Divane, A., and Goedert, M. (1995). Assignment of human alpha-synuclein (SNCA) and beta-synuclein (SNCB) genes to chromosomes 4q21 and 5q35. *Genomics* **27**(2), 379–381.

Spillantini, M. G., Schmidt, M. L., Lee, V. M., Trojanowski, J. Q., Jakes, R., and Goedert, M. (1997). Alpha-synuclein in Lewy bodies. *Nature* **388**(6645), 839–840.

Spillantini, M. G., Crowther, R. A., Jakes, R., Hasegawa, M., and Goedert, M. (1998a). alpha-Synuclein in filamentous inclusions of Lewy bodies from Parkinson's disease and dementia with Lewy bodies. *Proc. Natl. Acad. Sci. USA* **95**(11), 6469–6473.

Spillantini, M. G., Crowther, R. A., Jakes, R., Cairns, N. J., Lantos, P. L., and Goedert, M. (1998b). Filamentous alpha-synuclein inclusions link multiple system atrophy with Parkinson's disease and dementia with Lewy bodies. *Neurosci. Lett.* **251**(3), 205–208.

Spira, P. J., Sharpe, D. M., Halliday, G., Cavanagh, J., and Nicholson, G. A. (2001). Clinical and pathological features of a Parkinsonian syndrome in a family with an Ala53Thr alpha-synuclein mutation. *Ann. Neurol.* **49**(3), 313–319.

Stefanova, N., Reindl, M., Neumann, M., Haass, C., Poewe, W., Kahle, P. J., and Wenning, G. K. (2005). Oxidative stress in transgenic mice with oligodendroglial alpha-synuclein overexpression replicates the characteristic neuropathology of multiple system atrophy. *Am. J. Pathol.* **166**(3), 869–876.

Stefanova, N., Reindl, M., Neumann, M., Kahle, P. J., Poewe, W., and Wenning, G. K. (2007). Microglial activation mediates neurodegeneration related to oligodendroglial alpha-synucleinopathy: Implications for multiple system atrophy. *Mov. Disord.* Epub ahead of print.

Su, X., Maguire-Zeiss, K. A., Giuliano, R., Prifti, L., Venkatesh, K., and Federoff, H. J. (2007). Synuclein activates microglia in a model of Parkinson's disease. *Neurobiol. Aging* Epub ahead of print.

Sung, J. Y., Kim, J., Paik, S. R., Park, J. H., Ahn, Y. S., and Chung, K. C. (2001). Induction of neuronal cell death by Rab5A-dependent endocytosis of α-synculein. *J. Biol. Chem.* **276**(29), 27441–27448.

Sung, J. Y., Park, S. M., Lee, C.-H., Um, J. W., Lee, H. J., Kim, J., Oh, Y. J., Lee, S.-T., Paik, S. R., and Chung, K. C. (2005). Proteolytic cleavage of extracellular secreted α-synuclein via matrix metalloproteinases. *J. Biol. Chem.* **280**(26), 25216–25224.

Surgucheva, I., McMahan, B., Ahmed, F., Tomarev, S., Wax, M. B., and Surguchov, A. (2002). Synucleins in glaucoma: Implication of gamma-synuclein in glaucomatous alterations in the optic nerve. *J. Neurosci. Res.* **68**(1), 97–106.

Surgucheva, I., Sivak, J. M., Fini, M. E., Palazzo, R. E., and Surguchov, A. P. (2003). Effect of α-synuclein overexpression on matrix metalloproteinases in retinoblastoma Y79 cells. *Arch. Biochem. Biophys.* **410,** 167–176.

Surgucheva, I., Park, B. C., Yue, B. Y., Tomarev, S., and Surguchov, A. (2005). Interaction of myocilin with gamma-synuclein affects its secretion and aggregation. *Cell. Mol. Neurobiol.* **25**(6), 1009–1033.

Surgucheva, I., McMahon, B., and Surguchov, A. (2006). Gamma-synuclein has a dynamic intracellular localization. *Cell Motil. Cytoskeleton* **63**(8), 447–458.

Surgucheva, I., Shnyra, A., and Surguchov, A. (2008). α-Synuclein as a marker of the retinal ganglion cells (in preparation).

Surguchov, A., Surgucheva, I., Solessio, E., and Baehr, W. (1999). Synoretin—A new protein belonging to the synuclein family. *Mol. Cell. Neurosci.* **13**(2), 95–103.

Surguchov, A., McMahon, B., Masliah, E., and Surgucheva, I. (2001a). Synucleins in ocular tissues. *J. Neurosci. Res.* **65,** 68–77.

Surguchov, A., Palazzo, R. E., and Surgucheva, I. (2001b). Gamma synuclein: Subcellular localization in neuronal and non-neuronal cells and effect on signal transduction. *Cell Motil. Cytoskeleton* **49**(4), 218–228.

Suzuki, K., Iseki, E., Togo, T., Yamaguchi, A., Katsuse, O., Katsuyama, K., Kanzaki, S., Shiozaki, K., Kawanishi, C., Yamashita, S., Tanaka, Y., Yamanaka, S., *et al.* (2007). Neuronal and glial accumulation of alpha- and beta-synucleins in human lipidoses. *Acta Neuropathol.* **114**(5), 481–489.

Szargel, R., Rott, R., and Engelender, S. (2007). Synphilin-1 isoforms in Parkinson's disease: Regulation by phosphorylation and ubiquitylation. *Cell. Mol. Life Sci.* Epub ahead of print.

Takahashi, M., Ko, L. W., Kulathingal, J., Jiang, P., Sevlever, D., and Yen, S. H. (2007). Oxidative stress-induced phosphorylation, degradation and aggregation of alpha-synuclein are linked to upregulated CK2 and cathepsin D. *Eur. J. Neurosci.* **26**(4), 863–874.

Takeda, A., Mallory, M., Sundsmo, M., Honer, W., Hansen, L., and Masliah, E. (1998). Abnormal accumulation of NACP/alpha-synuclein in neurodegenerative disorders. *Am. J. Pathol.* **152**(2), 367–372.

Takeda, A., Hasegawa, T., Matsuzaki-Kobayashi, M., Sugeno, N., Kikuchi, A., Itoyama, Y., and Furukawa, K. (2006). Mechanisms of neuronal death in synucleinopathy. *J. Biomed. Biotechnol.* **2006**(3), 19365.

Tan, E. K., Chai, A., Teo, Y. Y., Zhao, Y., Tan, C., Shen, H., Chandran, V. R., Teoh, M. L., Yih, Y., Pavanni, R., Wong, M. C., Puvan, K., *et al.* (2004). Alpha-synuclein haplotypes implicated in risk of Parkinson's disease. *Neurology* **62**(1), 128–131.

Tanaka, Y., Engelender, S., Igarashi, S., Rao, R. K., Wanner, T., Tanzi, R. E., Sawa, A. L., Dawson, V., Dawson, T. M., and Ross, C. A. (2001). Inducible expression of mutant alpha-synuclein decreases proteasome activity and increases sensitivity to mitochondria-dependent apoptosis. *Hum. Mol. Genet.* **10**(9), 919–926.

Tanji, K., Imaizumi, T., Yoshida, H., Mori, F., Yoshimoto, M., Satoh, K., and Wakabayashi, K. (2001). Expression of alpha-synuclein in a human glioma cell line and its up-regulation by interleukin-1beta. *Neuroreport* **12**(9), 1909–1912.

Tartaglia, G. G., Cavalli, A., Pellarin, R., and Caflisch, A. (2005). Prediction of aggregation rate and aggregation-prone segments in polypeptide sequences. *Protein Sci.* **14**(10), 2723–2734.

Taylor, J. S., and Raes, J. (2004). Duplication and divergence: The evolution of new genes and old ideas. *Annu. Rev. Genet.* **38,** 615–643.

Thiruchelvam, M. J., Powers, J. M., Cory-Slechta, D. A., and Richfield, E. K. (2004). Risk factors for dopaminergic neuron loss in human alpha-synuclein transgenic mice. *Eur. J. Neurosci.* **19**(4), 845–854.

Tobe, T., Nakajo, S., Tanaka, A., Mitoya, A., Omata, K., Nakaya, K., Tomita, M., and Nakamura, Y. (1992). Cloning and characterization of the cDNA encoding a novel brain-specific 14-kDa protein. *J. Neurochem.* **59**(5), 1624–1629.

Tofaris, G. K., Layfield, R., and Spillantini, M. G. (2001). alpha-Synuclein metabolism and aggregation is linked to ubiquitin-independent degradation by the proteasome. *FEBS Lett.* **509**(1), 22–26.

Tofaris, G. K., Razzaq, A., Ghetti, B., Lilley, K. S., and Spillantini, M. G. (2003). Ubiquitination of α-synuclein in Lewy bodies is a pathological event not associated with impairment of proteasome function. *J. Biol. Chem.* **278**(45), 44405–44411.

Tompkins, M. M., Basgall, E. J., Zamrini, E., and Hill, W. D. (1997). Apoptotic-like changes in Lewy-body-associated disorders and normal aging in substantia nigral neurons. *Am. J. Pathol.* **150**(1), 119–131.

Touchman, J. W., Dehejia, A., Chiba-Falek, O., Cabin, D. E., Schwartz, J. R., Orrison, B. M., Polymeropoulos, M. H., and Nussbaum, R. L. (2001). Human and mouse α-synuclein genes: Comparative genomic sequence analysis and identification of a novel gene regulatory element. *Genome Res.* **11,** 78–86.

Tsigelny, I. F., Bar-On, P., Sharikov, Y., Crews, L., Hashimoto, M., Miller, M. A., Keller, S. H., Platoshyn, O., Yuan, J. X., and Masliah, E. (2007). Dynamics of alpha-synuclein aggregation and inhibition of pore-like oligomer development by beta-synuclein. *FEBS J.* **274**(7), 1862–1877.

Tu, P. H., Galvin, J. E., Baba, M., Giasson, B., Tomita, T., Leight, S., Nakajo, S., Iwatsubo, T., Trojanowski, J. Q., and Lee, V. M. (1998). Glial cytoplasmic inclusions in white matter oligodendrocytes of multiple system atrophy brains contain insoluble alpha-synuclein. *Ann. Neurol.* **44**(3), 415–422.

Uéda, K., Fukushima, H., Masliah, E., Xia, Y., Iwai, A., Yoshimoto, M., Otero, D. A., Kondo, J., Ihara, Y., and Saitoh, T. (1993). Molecular cloning of cDNA encoding an unrecognized component of amyloid in Alzheimer disease. *Proc. Natl. Acad. Sci. USA* **90**(23), 11282–11286.

Uéda, K., Saitoh, T., and Mori, H. (1994). Tissue-dependent alternative splicing of mRNA for NACP, the precursor of non-A beta component of Alzheimer's disease amyloid. *Biochem. Biophys. Res. Commun.* **205**(2), 1366–1372.

Ulmer, T. S., and Bax, A. (2005). Comparison of structure and dynamics of micelle-bound human α-synuclein and Parkinson disease variants. *J. Biol. Chem.* **280**(52), 43179–43187.

Ulmer, T. S., Bax, A., Cole, N. B., and Nussbaum, R. L. (2005). Structure and dynamics of micelle-bound human α-synuclein. *J. Biol. Chem.* **280**(10), 9595–9603.

Utton, M. A., Connell, J., Asuni, A. A., van Slegtenhorst, M., Hutton, M., de Silva, R., Lees, A. J., Miller, C. C., and Anderton, B. H. (2002). The slow axonal transport of the microtubule-associated protein tau and the transport rates of different isoforms and mutants in cultured neurons. *J. Neurosci.* **22**(15), 6394–6400.

Utton, M. A., Noble, W. J., Hill, J. E., Anderton, B. H., and Hanger, D. P. (2005). Molecular motors implicated in the axonal transport of tau and α-synuclein. *J. Cell Sci.* **118**(Pt 20), 4645–4654.

Uversky, V. N., Gillespie, J. R., and Fink, A. L. (2000). Why are ''natively unfolded'' proteins unstructured under physiologic conditions? *Proteins* **41**(3), 415–427.

Uversky, V. N., Li, J., and Fink, A. L. (2001a). Pesticides directly accelerate the rate of alpha-synuclein fibril formation: A possible factor in Parkinson's disease. *FEBS Lett.* **500**(3), 105–108.

Uversky, V. N., Lee, H.-J., Li, J., Fink, A. L., and Lee, S.-J. (2001b). Stabilization of partially folded conformation during α-synuclein oligomerization in both purified and cytosolic preparations. *J. Biol. Chem.* **276**(47), 43495–43498.

Uversky, V. N., Li, J., Souillac, P., Millett, I. S., Doniach, S., Jakes, R., Goedert, M., and Fink, A. L. (2002). Biophysical properties of the synucleins and their propensities to fibrillate: Inhibition of alpha-synuclein assembly by beta- and gamma-synucleins. *J. Biol. Chem.* **277**(14), 11970–11978.

van der Putten, H., Wiederhold, K.-H., Probst, A., Barbieri, S., Mistl, C., Danner, S., Kauffmann, S., Hofele, K., Spooren, W. P. J. M., Ruegg, M. A., Lin, S., Caroni, P., *et al.* (2000). Neuropathology in mice expressing human α-synuclein. *J. Neurosci.* **20**(16), 6021–6029.

Vila, M., Vukosavic, S., Jackson-Lewis, V., Neystat, M., Jakowec, M., and Przedborski, S. (2000). Alpha-synuclein up-regulation in substantia nigra dopaminergic neurons after administration of the parkinsonian toxin MPTP. *J. Neurochem.* **74**(2), 721–729.

Volkova, K. D., Kovalska, V. B., Balanda, A. O., Losytskyy, M. Y., Golub, A. G., Vermeij, R. J., Subramaniam, V., Tolmachev, O. I., and Yarmoluk, S. M. (2007).

Specific fluorescent detection of fibrillar alpha-synuclein using mono- and trimethine cyanine dyes. *Bioorg. Med. Chem.* Epub ahead of print.

Volles, M. J., Lee, S. J., Rochet, J. C., Shtilerman, M. D., Ding, T. T., Kessler, J. C., and Lansbury, P. T., Jr. (2001). Vesicle permeabilization by protofibrillar alpha-synuclein: Implications for the pathogenesis and treatment of Parkinson's disease. *Biochemistry* **40** (26), 7812–7819.

Volles, M. J., and Lansbury, P. T., Jr. (2002). Vesicle permeabilization by protofibrillar alpha-synuclein is sensitive to Parkinson's disease-linked mutations and occurs by a pore-like mechanism. *Biochemistry* **41**(14), 4595–4602.

Volles, M. J., and Lansbury, P. T., Jr. (2003). Zeroing in on the pathogenic form of alpha-synuclein and its mechanism of neurotoxicity in Parkinson's disease. *Biochemistry* **42**(26), 7871–7878.

Volles, M. J., and Lansbury, P. T., Jr. (2007). Relationships between the sequence of alpha-synuclein and its membrane affinity, fibrillization propensity, and yeast toxicity. *J. Mol. Biol.* **366**(5), 1510–1522.

von Coelln, R., Thomas, B., Andrabi, S. A., Lim, K. L., Savitt, J. M., Saffary, R., Stirling, W., Bruno, K., Hess, E. J., Lee, M. K., Dawson, V. L., and Dawson, T. M. (2006). Inclusion body formation and neurodegeneration are parkin independent in a mouse model of α-synucleinopathy. *J. Neurosci.* **26**(14), 3685–3696.

Wakabayashi, K., and Takahashi, H. (2006). Cellular pathology in multiple system atrophy. *Neuropathology* **26**(4), 338–345.

Wakabayashi, K., Yoshimoto, M., Tsuji, S., and Takahashi, H. (1998). Alpha-synuclein immunoreactivity in glial cytoplasmic inclusions in multiple system atrophy. *Neurosci. Lett.* **249**(2–3), 180–182.

Wakabayashi, K., Hayashi, S., Yoshimoto, M., Kudo, H., and Takahashi, H. (2000a). NACP/alpha-synuclein-positive filamentous inclusions in astrocytes and oligodendrocytes of Parkinson's disease brains. *Acta Neuropathol.* **99**(1), 14–20.

Wakabayashi, K., Fukushima, T., Koide, R., Horikawa, Y., Hasegawa, M., Watanabe, Y., Noda, T., Eguchi, I., Morita, T., Yoshimoto, M., Iwatsubo, T., and Takahashi, H. (2000b). Juvenile-onset generalized neuroaxonal dystrophy (Hallervorden-Spatz disease) with diffuse neurofibrillary and Lewy body pathology. *Acta Neuropathol. (Berl)* **99**(3), 331–336.

Wakabayashi, K., Tanji, K., Mori, F., and Takahashi, H. (2007). The Lewy body in Parkinson's disease: Molecules implicated in the formation and degradation of α-synuclein aggregates. *Neuropathology* **27,** 494–506.

Weinreb, P. H., Zhen, W., Poon, A. W., Conway, K. A., and Lansbury, P. T., Jr. (1996). NACP, a protein implicated in Alzheimer's disease and learning, is natively unfolded. *Biochemistry* **35**(43), 13709–13715.

Wenning, G. K., and Jellinger, K. A. (2005). The role of alpha-synuclein in the pathogenesis of multiple system atrophy. *Acta Neuropathol.* **109**(2), 129–140.

Williams, R. B., Gutekunst, W. R., Joyner, P. M., Duan, W., Li, Q., Ross, C. A., Wiliams, T. D., and Cichewicz, R. H. (2007). Bioactivity profiling with parallel mass spectrometry reveals an assemblage of green tea metabolites affording protection against human Huntingtin and alpha-synuclein toxicity. *J. Agric. Food Chem.* **55**(23), 9450–9456.

Willingham, S., Outeiro, T. F., DeVit, M. J., Lindquist, S. L., and Muchowski, P. J. (2003). Yeast genes that enhance the toxicity of a mutant huntingtin fragment or alpha-synuclein. *Science* **302**(5651), 1769–1772.

Winner, B., Rockenstein, E., Lie, D. C., Aigner, R., Mante, M., Bogdahn, U., Couillard-Despres, S., Masliah, E., and Winkler, J. (2007). Mutant alpha-synuclein exacerbates age-related decrease of neurogenesis. *Neurobiol. Aging* Epub ahead of print.

Withers, G. S., George, J. M., Banker, G. A., and Clayton, D. F. (1997). Delayed localization of synelfin (synuclein, NACP) to presynaptic terminals in cultered rat hippocampal neurons. *Brain Res. Dev. Brain Res.* **99**(1), 87–94.

Wong, K., Sidransky, E., Verma, A., Mixon, T., Sandberg, G. D., Wakefield, L. K., Morrison, A., Lwin, A., Colegial, C., Allman, J. M., and Schiffmann, R. (2004). Neuropathology provides clues to the pathophysiology of Gaucher disease. *Mol. Genet. Metab.* **82**(3), 192–207.

Wood, S. J., Wypych, J., Steavenson, S., Louis, J. C., Citron, M., and Biere, A. L. (1999). α-Synuclein fibrillogenesis is nucleation-dependent. Implications for the pathogenesis of Parkinson's disease. *J. Biol. Chem.* **274**(28), 19509–19512.

Woods, W. S., Boettcher, J. M., Zhou, D. H., Kloepper, K. D., Hartman, K. L., Ladror, D. T., Qi, Z., Rienstra, C. M., and George, J. M. (2007). Conformation-specific binging of alpha-synuclein to novel protein partners detected by phage display and NMR spectroscopy. *J. Biol. Chem.* Epub ahead of print.

Wu, K., Quan, Z., Weng, Z., Li, F., Zhang, Y., Yao, X., Chen, Y., Budman, D., Goldberg, I. D., and Shi, Y. E. (2007). Expression of neuronal protein synuclein gamma gene as a novel marker for breast cancer prognosis. *Breast Cancer Res. Treat.* **101**(3), 259–267.

Xu, J., Kao, S. Y., Lee, F. J., Song, W., Jin, L. W., and Yankner, B. A. (2002). Dopamine-dependent neurotoxicity of alpha-synuclein: A mechanism for selective neurodegeneration in Parkinson disease. *Nat. Med.* **8**(6), 600–606.

Xu, S., Zhou, M., Yu, S., Cai, Y., Zhang, A., Ueda, K., and Chan, P. (2006). Oxidative stress induces nuclear translocation of C-terminus of alpha-synuclein in dopaminergic cells. *Biochem. Biophys. Res. Commun.* **342**(1), 330–335.

Yazawa, I., Giasson, B. I., Sasaki, R., Zhang, B., Joyce, S., Uryu, K., Trojanowski, J. Q., and Lee, V. M. (2005). Mouse model of multiple system atrophy alpha-synuclein expression in oligodendrocytes causes glial and neuronal degeneration. *Neuron* **45**(6), 847–859.

Yoshida, H., Craxton, M., Jakes, R., Zibaee, S., Tavaré, R., Fraser, G., Serpell, L. C., Davletov, B., Crowther, R. A., and Goedert, M. (2006). Synuclein proteins of the pufferfish Fugu rubripes: Sequences and functional characterization. *Biochemistry* **45**(8), 2599–2607.

Yoshimoto, M., Iwai, A., Kang, D., Otero, D. A., Xia, Y., and Saitoh, T. (1995). NACP, the precursor protein of the non-amyloid beta/A4 protein (A beta) component of Alzheimer disease amyloid, binds A beta and stimulates A beta aggregation. *Proc. Natl. Acad. Sci. USA* **92**(20), 9141–9145.

Yu, F., Xu, H., Zhuo, M., Sun, L., Dong, A., and Liu, X. (2005). Impairment of redox state and dopamine level induced by alpha-synuclein aggregation and the prevention effect of hsp70. *Biochem. Biophys. Res. Commun.* **331,** 278–284.

Yu, S., Li, X., Liu, G., Han, J., Zhang, C., Li, Y., Xu, S., Liu, C., Gao, Y., Yang, H., Ueda, K., and Chan, P. (2007). Extensive nuclear localization of alpha-synuclein in normal rat brain neurons revealed by a novel monoclonal antibody. *Neuroscience.* **145**(2), 539–555.

Zach, S., Bueler, H., Hengerer, B., and Gillardon, F. (2007). Predominant neuritic pathology induced by viral overexpression of alpha-synuclein in cell culture. *Cell. Mol. Neurobiol.* **27**(4), 505–515.

Zakharov, S. D., Hulleman, J. D., Dutseva, E. A., Antonenko, Y. N., Rochet, J.-C., and Cramer, W. A. (2007). Helical α-synuclein forms highly conductive ion channels. *Biochemistry* Epub ahead of print.

Zarranz, J. J., Alegre, J., Gomez-Esteban, J. C., Lezcano, E., Ros, R., Ampuero, I., Vidal, L., Hoenicka, J., Rodriguez, O., Atares, B., Llorens, V., Gomez Tortosa, E., *et al.* (2004). The new mutation, E46K, of alpha-synuclein causes Parkinson and Lewy body dementia. *Ann. Neurol.* **55**(2), 164–173.

Zhang, W., Wang, T., Pei, Z., Miller, D. S., Wu, X., Block, M. L., Wilson, B., Zhang, W., Zhou, Y., Hong, J. S., and Zhang, J. (2005). Aggregated alpha-synuclein activates microglia: A process leading to disease progression in Parkinson's disease. *FASEB J.* **19**(6), 533–542.

Zhao, W., Liu, H., Liu, W., Wu, Y., Chen, W., Jiang, B., Zhou, Y., Xue, R., Luo, C., Wang, L., Jiang, J. D., and Liu, J. (2006). Abnormal activation of the synuclein-gamma gene in hepatocellular carcinomas by epigenetic alteration. *Int. J. Oncol.* **28**(5), 1081–1088.

Zhao, D. L., Zou, L. B., Zhou, L. F., Zhu, P., and Zhu, H. B. (2007). A cell-based model of alpha-synucleinopathy for screening compounds with therapeutic potential of Parkinson's disease. *Acta Pharmacol. Sin.* **28**(5), 616–626.

Zhou, Y., Gu, G., Goodlett, D. R., Zhang, T., Pan, C., Montine, T. J., Montine, K. S., Aebersold, R. H., and Zhang, J. (2004). Analysis of alpha-synuclein-associated proteins by quantitative proteomics. *J. Biol. Chem.* **279**(37), 39155–39164.

Zhou, Y., Inaba, S., and Liu, J. (2006). Inhibition of synuclein-gamma expression increases the sensitivity of breast cancer cells to paclitaxel treatment. *Int. J. Oncol.* **29**(1), 289–295.

Zhu, M., Rajamani, S., Kaylor, J., Han, S., Zhou, F., and Fink, A. L. (2004). The flavonoid baicalein inhibits fibrillation of alpha-synuclein and disaggregates existing fibrils. *J. Biol. Chem.* **79**(26), 26846–26857.

Zibaee, S., Jakes, R., Fraser, G., Serpell, L. C., Crowther, R. A., and Goedert, M. (2007). Sequence determinants for amyloid fibrillogenesis of human alpha-synuclein. *J. Mol. Biol.* **374**(2), 454–464.

This page intentionally left blank

CHAPTER SEVEN

Genetically Unstable Microsatellite-Containing Loci and Genome Diversity in Clonally Reproduced Unisexual Vertebrates

Alexei P. Ryskov

Contents

Abstract

There are more than 70 known unisexual species of fishes, amphibians, and reptiles. They are all-female populations of interspecific hybrid origin that reproduce without sex via altered gametogenetic mechanisms. They are either sperm independent as in parthenogenesis or sperm dependent as in gynogenesis or hybridogenesis, which causes clonal (or hemiclonal) inheritance. The first two modes of reproduction produce species composed of genetically isolated clones. In many previous papers, origin and ancestry, clonal diversity based on allozyme or mitochondrial DNA variation, ecology and evolution of unisexual vertebrates were discussed. This chapter reviews the role of

Institute of Gene Biology, Russian Academy of Sciences, 119334 Moscow, Russia

International Review of Cell and Molecular Biology, Volume 270
ISSN 1937-6448, DOI: 10.1016/S1937-6448(08)01407-X

mutations in genome diversity of some unisexual vertebrates revealed by DNA fingerprinting and/or by locus-specific PCR. It also describes recent data on molecular structure of unstable microsatellite loci and their allelic variants in parthenogenetic lizard species. The available data demonstrate that microsatellite mutations as well as point mutations in flanking regions make significant contribution in genome diversity of, at least some, clonaly reproduced vertebrates.

Key Words: Unisexual vertebrates, Genome diversity, Microsatellites, Mutations, Allelic variants, DNA fingerprinting, PCR.

1. Introduction

Unisexual vertebrates are of general interest because ''being abnormal, they provide a unique perspective on what is normal'' (Dawley, 1989). Biologists have always tried to understand the significance of sexual processes. Why in most species up to 50% of population consists of males which seem only to waste natural resources while the numerical strength of offspring is determined by females. There are many hypotheses on what makes bisexual species advantageous at the population level due to sexual reproduction and genetic changes it causes (Barton and Charlesworth, 1998; Hurst and Peck, 1996; Kondrashov, 1993; Otto and Lenormand, 2002). However, the lack of data, in particular, on deleterious mutation rates and on the amplitudes of fluctuations of selection in these species limits our understanding. The nature gives remarkable examples of all-female unisexual populations well adapted to various habitats. Unisexual vertebrates recognized first in 1932 (Hubbs and Hubbs, 1932) represent exciting cases of wild populations consisting of predominantly or exclusively females. According to Dawley (1989), they share four features: (1) they are of interspecific hybrid origin, (2) they are exclusively female or nearly so, (3) they reproduce via an aberrant gametogenetic mechanism (meiotic or premeiotic) that inhibits genetic recombination and causes clonal inheritance, and (4) they often include polyploids. Unisexual vertebrates are rather rare, compared with the total number of vertebrate species. The absence of genetic variation via recombination constitutes an evolutionary constraint on these populations. At present, there are more than 70 known unisexual vertebrate species and forms of fishes, amphibians, and reptiles (Table 7.1), distributed on five continents (Grebelnyi, 2005; Vasil'eva and Vasil'ev, 2000; Vrijenhoek *et al.*, 1989). The list of the best known unisexual taxa including their ploidy, ancestry, and reproductive mode was presented by Vrijenhoek *et al.* (1989). The hybrid nature of most unisexual vertebrates is shown by various means (Vrijenhoek *et al.*, 1989).

Table 7.1 Animal groups in which vertebrate unisexual species were found

Pisces	Amphibians	Reptiles
Atherinidae	Ambystomatidae	Agamidae
Cobitidae	Ranidae	Chameleonidae
Cyprinidae		Gekkonidae
Poeciliidae		Lacertidae
		Teiidae
		Typhlopidae
		Xantusiidae

Moreover, such hybridization was reproduced in the laboratory (Hotz *et al.*, 1985; Schultz, 1973; Wetherington *et al.*, 1987). The combination of two heterospecific genomes may skew the sex ratio in the hybrids toward females and alters gametogenesis such that hybrid females produce eggs without a recombination and often without reduction in ploidy founding clonal lineages. The molecular genetic mechanisms by which hybridizations altered gametogenesis remain unknown. Understanding these mechanisms is an important and rewarding task (Templeton, 1982).

Three modes of reproduction can be distinguished within the unisexual vertebrates whose reproductive mechanisms are understood (Fig. 7.1): (1) parthenogenesis, in which the hybrid genome is transmitted intact to the eggs, which develop into genetically identical offspring in the absence of sperm, (2) gynogenesis, in which sperm from a related bisexual ancestor activates development of the eggs but syngamy of egg and sperm does not occur and resulting offspring are genetically identical to their mother and to each other, and (3) hybridogenesis, in which the part of the hybrid genome derived from one parental species is inherited clonally, while the genome from the other parental species is lost and replaced in each generation through fertilization. Parthenogenetic and gynogenetic taxa are exclusively or predominantly females; hybridogenetic taxa can be of either or both sexes (Darevsky *et al.*, 1985). Within the vertebrates, clonal anamniotes may be either hybridogenetic or gynogenetic, while clonal taxa of reptiles are exclusively parthenogenetic. This probably reflects the need of anamniote ova for a special nonnuclear contribution from the sperm. It should be noted that low levels of recombination have been suggested for some unisexual amphibians (Graf and Polls Pelaz, 1989) and reptiles (Sites *et al.*, 1990), and incorporation of subgenomic amount of DNA from a bisexual host by microchromosomes in a gynogenetic fish has been described (Schartl *et al.*, 1995).

In unisexual vertebrates, polyploidy is one of the main features (Schultz, 1969). Although it may help to stabilize a unisexual lineage (Moritz *et al.*,

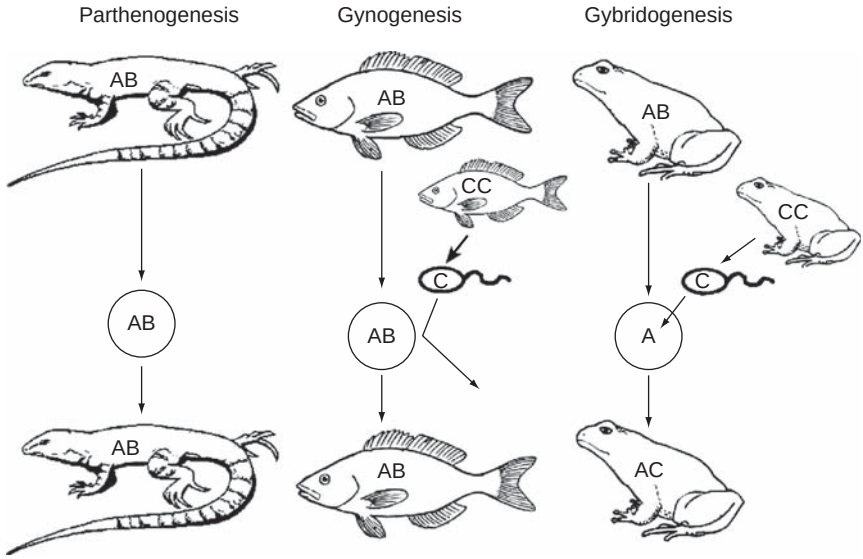

Figure 7.1 Schematic representation of the three unisexual modes of reproduction. In parthenogenesis, the genome AB is transmitted to the egg without genetic recombination; the egg develops without sperm into an offspring. In gynogenesis, the genome AB is transmitted to the egg without genetic recombination, but the egg requires sperm to stimulate embryogenesis without syngamy of egg and sperm. In hybridogenesis, one parental genome (A) is transmitted to the egg without genetic recombination, but the other parental genome (B) is lost and replaced in each generation through fertilization.

1989a,b) and mask deleterious alleles, the overall mutation rate per polyploid genome is higher and should result in higher mutation load in comparison with diploids (Kondrashov, 1997). Among a variety of clonal vertebrate taxa, only some are known to be diploid, others are either triploid or, more rarely, tetraploid. Of the 32 parthenogenetic taxa of reptiles that have been identified, some 15 forms are diploid, while 13 are triploid, and for 4, the ploidy is not determined (Darevsky *et al.*, 1985). The origin of polyploidy in a parthenogenetic system is in principle possible if unreduced gametes do mate (Fig. 7.2). It presupposes a very rare event, when sperm from a third bisexual species fertilizes some eggs and forms trihybrid triploids, which further reproduce parthenogenetically, without sperm, into clonal triploid offspring. Such triploid unisexual reptiles were recognized in nature and investigated using karyology, allozyme electrophoresis, tissue grafting, and restriction analysis of mtDNA (Darevsky *et al.*, 1985). In gynogenetic system, where the exposure of eggs to sperm is necessary to reproduce, syngamy occurs in about 1% of all eggs (Schultz and Kallman, 1968) and this produces triploids that differ from each other in third genome added from different bisexuals. Tetraploids are very rare

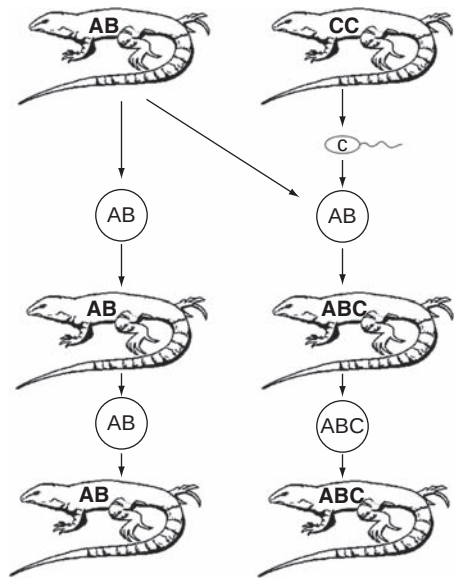

Figure 7.2 Schematic representation of origin of triploid unisexual. The unisexual female (AB) reproduces clonally, the egg (AB) develops into genetically identical offspring (AB). In rare cases, the egg (AB) is fertilized by sperm from a male (CC), yielded a triploid unisexual (ABC) that also reproduces clonally.

among unisexual vertebrates and they were only recognized in unisexual *Ambystoma*, *Carassius*, and *Cobitis* (Bohlen and Rab, 2001; Lowcock *et al.*, 1987; Vasil'ev *et al.*, 1989; Vasil'eva and Vasil'ev, 2000). This may suggest some genomic constrains in formation of stable tetraploid state. Up to now, the question which biological features of unisexual vertebrates depend on their clonal reproduction and which depend on their hybrid makeup or ploidy remains unclear.

According to Uzzell (1970), there is no direct correspondence between reproductive mode and cytological mechanism. For instance, gynogenesis can result from apomixis or premeiotic endomitosis, and premeiotic endomitosis can provide parthenogenesis or gynogenesis. All three unisexual reproductive modes suppress effects of genetic recombination, leading to reduced level of genome diversity in clonal populations. In particular, parthenogenesis and gynogenesis suppress the effects of crossing over between homologous chromosomes, random segregation of homologous chromosomes, and syngamy of egg and sperm pronuclei. In these cases, only spontaneous mutations and possible chromosomal genes rearrangements remain main sources of genetic and phenotypic variation. Hybridogenesis suppresses effects of the only first two forms of recombination. So syngamy yields additional genetic variation. In apomixes, eggs are produced by

mitosis, and fertilization by sperm is not necessary (Fig. 7.3A). After premeiotic cells duplication, chromosomal DNA duplicates, but homologous chromosomes do not pair and mitosis occurs producing an ovum with somatic ploidy level identical to mother cells.

According to Rasch *et al.* (1982), apomixis, not endoreduplication as previously reported by this group (Rasch *et al.*, 1970), is the cytological basis of reproduction in *Poecilia formoza* and its related, triploid biotypes. In some unisexual vertebrates, meiosis occurs but it involves modified step, called premeiotic endomitosis (Fig. 7.3B). Prior to meiosis, a chromosomal endoduplication occurs, producing pairs of identical chromosomes without cell division. After DNA duplication, identical chromosomes pair in meiosis I resulting in the formation of bivalents. Meiosis I then proceeds normally and the chromosomes reach meiosis II. After two maturation divisions, an ovum with the somatic ploidy level, identical to mother cells, is formed. Among unisexual vertebrates, the premeiotic endomitosis is known to occur in the parthenogenetic triploid lizard *Cnemidophorus uniparens* (Cuellar, 1971) and in triploid salamanders of the genus *Ambystoma* (Sessions, 1982).

At least two cytological mechanisms responsible for hybridogenetic reproduction mode are known (Fig. 7.3C). They involve premeiotic

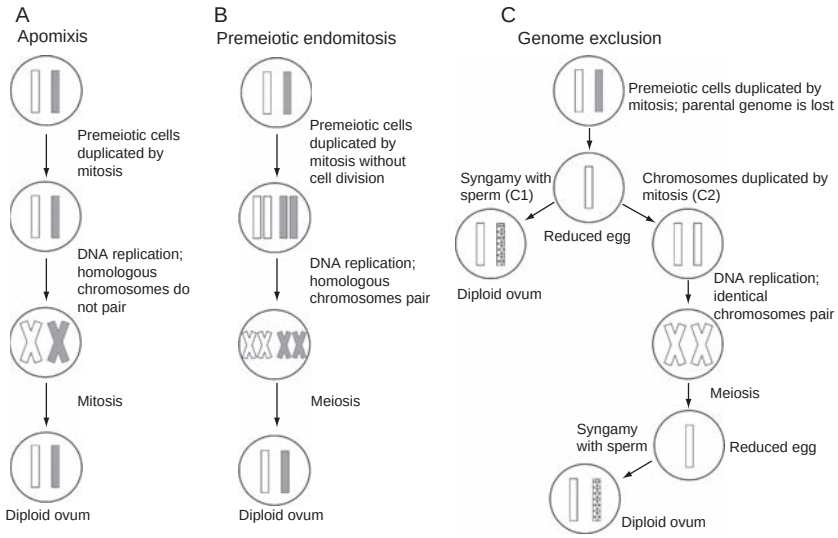

Figure 7.3 Schematic representation of cytological mechanisms of clonal reproduction in diploid unisexual vertebrates. (A) Apomixis, described in the gynogenetic fish *Poecilia formosa* (Rasch *et al.*, 1982); (B) Premeiotic endomitosis, described in the parthenogenetic triploid lizard *Cnemidophorus uniparens* (Cuellar, 1971); (C) Genome exclusion: C1, described in the hybridogenetic fish *Poecilopsis monacha-lucida* (Cimino, 1972a,b); C2, described in the hybridogenetic diploid amphibian *Rana esculenta* (Graf and Muller, 1979).

exclusion of one parental genome and produce a reduced egg that is subsequently fertilized and restored the diploid chromosome number. In diploid *Poeciliopsis monacha-lucidia* (Cimino, 1972a,b) during mitotic division prior to meiosis, a unipolar spindle attaches to chromosomes from only one parental species and draw them to one pole. Only these chromosomes enter an altered meiosis. The chromosomes from other parental species are lost. In diploid *Rana esculenta* (Graf and Muller, 1979), after premeiotic exclusion of one parental genome, the remaining genome is duplicated by a premeiotic endomitosis, DNA duplicates, identical chromosomes pair, and enter an altered meiosis. Cytological mechanisms responsible for unisexual reproduction were considered in many papers (Cuellar, 1971, 1974; Dawley, 1989; Grebelnyi, 2005; Monaco *et al.*, 1984; Sessions, 1982; Uzzell, 1970).

Clonal reproduction and clonal diversity are two features of unisexual vertebrates that make them useful as model organisms in such areas as evolutionary ecology, genetics, cellular, and molecular biology (Dawley, 1989; Vrijenhoek, 1994). Indeed (1) they represent greatly simplified systems for studying adaptive properties of genes; (2) environment effects on the phenotype or on the genotype fitness can be studied by comparing phenotypic characters or clonal frequencies over time; (3) captive reproduction of some unisexual species allows to control the effects of genetic variation in experiments; (4) comparison of initial and introduced into a new habitat unisexual populations can provide some possibilities for studying first stages of genetic divergence; (5) comparative investigations can be made with unisexual species and closely related bisexual ancestors providing valuable information on their evolution; (6) genetic dominance can be investigated by using clonal animals of different ploidy levels; (7) spontaneous or experimentally induced mutagenesis, as well as genetically unstable loci and karyotypes can be more easily detected and investigated in clonal populations, families, and next generations.

The principal fundamental problems concerning origin and ancestry, clonal diversity based on allozyme and mitochondrial DNA variation, ecology, and evolution of unisexual vertebrates were considered previously in detail (Avise *et al.*, 1992; Darevsky *et al.*, 1985; Fu *et al.*, 2000; Mateos and Vrijenhock, 2002; Mateos *et al.*, 2002; Moritz *et al.*, 1989a,b; Schultz, 1969; Turner, 1982; Vrijenhoek, 1984, 1989, 1994; Vrijenhoek *et al.*, 1989; Weeks, 1993).

Multiple independent origins of unisexuals are the primary source of clonal diversity (Butlin *et al.*, 1999). However, the genetic diversity of the majority of unisexual vertebrate species is low in comparison with their sexual progenitors. In this chapter, recent data concerning mutations in microsatellite-containing loci and their contribution in genome diversity of clonally reproduced vertebrates are considered.

2. DNA Fingerprinting in Studies of Genome Diversity

To study clonal and genome diversity in unisexual vertebrate populations, several approaches including histocompatibility analysis, extensive surveys of mtDNA and allozyme variations, and in more rare cases, DNA fingerprinting have been used. Of these techniques, histocompatibility analysis and DNA fingerprinting were clearly more sensitive. At the same time, in its present form, the histocompatibility technique is difficult to use on a survey scale.

2.1. Hypervariable mini- and microsatellites

Tandemly arranged repetitive DNA sequences of different types are widely represented in eukaryotic genomes. They vary in cluster length and repeat unit size. Among them, the most polymorphic are mini- and microsatellite DNAs, whose variability is displayed particularly in allelic variations of the number of repeat units. Jeffreys *et al.* (1985) were first to use the minisatellite probes 33.6 and 33.15 to detect numerous homologous loci in human DNA, and have demonstrated the individual-specific pictures of blot hybridizations that were termed DNA fingerprints. Later, the M13 family of minisatellites was characterized (Ryskov *et al.*, 1988; Vassart *et al.*, 1987), as well as a number of microsatellites (Epplen *et al.*, 1993; Limborska *et al.*, 1999; Tautz, 1989). It should be emphasized that many features of mini- and microsatellites and mechanisms of their variability are suggested to be different (Debrauwere *et al.*, 1997). In particular, microsatellites are more numerous and more randomly distributed in genome (Tautz and Renz, 1984; Toth *et al.*, 2000). The participations of recombination mechanisms has been shown for minisatellite variability (Bois, 2003; Jeffreys, 1997; Jeffreys *et al.*, 1997; Jurka and Gentles, 2006). The main models of microsatellite mutations are based on impaired DNA replication and repair (Brohede *et al.*, 2002; Debrauwere *et al.*, 1997; Djan, 1998; Ellegren, 2000, 2004; Hancock, 1999; Levinson and Gutman, 1987), although interaction of replication slippage and recombination in microsatellite variation are also discussed (Li *et al.*, 2002). If so, one can predict that in a clonal population, which lack effective genetic recombination, different levels of genomic diversity would be detected by DNA fingerprinting with mini- and microsatellite probes. At present, DNA fingerprinting is considered potentially very powerful tool for population studies of species whose genomes are poorly investigated. The features and possible applications of DNA fingerprinting were considered in earlier reviews (Jeffreys, 1997; Ryskov, 1999; Shabrova *et al.*, 2006). To date, only limited number of

unisexual fish and lizard species were investigated with the use of DNA fingerprinting.

2.2. Gynogenetic and hybridogenetic fishes

Turner *et al.* (1990) were the first to use DNA fingerprinting, based on microsatellite probes $(CAC)_5$ and $(GACA)_4$, to assess genetic variation in samples of two clonal fish species, gynogenetic *Poecilia formosa* and selfing hermaphrodite *Rivulus marmoratus*. The investigated material was taken from various laboratory lines and field collections. The DNA fingerprints obtained demonstrated very high levels of genetic variation in natural populations of both species. For example, a sample of 19 specimens of *P. formosa* from one station contained 16 fingerprint phenotypes (presumptive clones), while only 3 clones of *P. formosa* in the entire drainage system were discerned by allozyme survey (Turner *et al.*, 1983). The technique clearly differentiated allozymically identical laboratory lines of *R. marmoratus* that were previously distinguishable only by histocompatibility analysis (Vrijenhoek, 1985). At the same time, all fingerprints tested were clonally stable for at least three generations. To interpret very high level of genome and clonal diversity detected with DNA fingerprinting, the authors suggested that mutations, subsequent to the founding of clonal lineages, were important source of variation in investigated populations. They have also emphasized that the biological significance of the clonal heterogeneity detected with DNA fingerprinting should be a matter of laboratory and field comparison, not *a priori* judgments based on the nature of the fingerprint differences themselves. According to current ecological models, clones in a particular population have specializations that enable them to exist in distinct microhabitats (Schultz and Fielding, 1989; Vrijenhoek, 1984; Weeks, 1993). However, very high levels of genomic and clonal heterogeneity revealed by DNA fingerprinting in both species may suggest that their clonal composition is more strongly determined by stochastic factors, such as migration, founder effects, population size, and fluctuation, than particular clonal adaptations.

In extending study of seven Floridian populations of *R. marmoratus* (Turner *et al.*, 1992), DNA fingerprinting with an array of microsatellite [e.g., $(CT)_9$] and minisatellite (e.g., the 33.15 core sequence) probes also revealed very high genome and clonal diversity. There were 42 clones among 58 individuals surveyed. One sample of *R. marmoratus* was analyzed in more detail. All seven individuals (presumptive clones) could be resolved readily with probes $(CT)_9$, $(GT)_9$, and 33.15 at high hybridization stringency. Probably, the three hybridization probes, chosen arbitrarily, did not exhaust the repertoire of divergent bands that separated the clones. Four of these clones were subsequently fingerprinted with the *Drosophila* sequence $(AGAGGC)_4$ and the mouse sequence $(GGGCAGG)_4$, and several

additional divergent bands could be detected. The interpretation of these data was that most sympatric clones studied differed by multiple and independent mutational steps, and that regular mixing of individuals from different mutational lineages should exist.

Later, Laughlin *et al.* (1995) tried to clarify reasons of the extremely high levels of interclonal variation reported from natural Floridian populations of *R. marmoratus*. They investigated the clonal stability of laboratory lineages with regard to highly polymorphic loci. As a result, practically no mutations were observed with probes $(CAC)_5$ and $(CT)_9$ among 62 individuals from each of generations 19 and 20 (124 total). Only two divergent fragments were detected with probe $(GGCAGG)_4$ among the same 124 individuals. No mutation was observed with probes 33.15, $(CTG)_5$, and $(CAG)_5$. Based on these data, a maximum mutation rate of 3.5×10^{-4} for loci detected by probe $(GCCAGG)_4$ was calculated in laboratory lines of *R. marmoratus*. These results do not support a hypothesis of clonal diversification of *R. marmoratus*, due to mutation alone. So, authors confirmed the previous suggestion (Turner *et al.*, 1992) that high levels of migration with lineage mixing together with mutations might be important explanations for the very high interindividual variation observed in Floridian populations of this species. At the same time, critical consideration of these data allows to suggest that some other, more appropriate probes might be chosen for mutation detection in the laboratory lineages studied. It should also take into account that germinal mutations inherited in all offspring will provide identical fingerprints in population samples. More direct information about *de novo* mutations might be obtained from comparison of maternal and offspring fingerprints on a large-scale family analysis.

The *Phoxinus eos/Phoxinus neogaeus* hybrid gynogen complex of cyprinid fishes appears to represent an example of extreme clonal uniformity. Because gynogenesis is not 100% efficient in the *Phoxinus* complex, hybrids exist as diploid clonal lineages and triploid biotypes (Goddart *et al.*, 1989). mtDNA analysis of limited numbers of individuals from geographically distinct hybrid populations suggested relatively recent, repeated origination of these gynogens (Goddart *et al.*, 1989). The fin graft histocompatibility analysis led Goddart *et al.* (1989) to suggestion that local populations of *Phoxinus* gynogens were composed of only a single clonal lineage. Using multilocus DNA fingerprinting, Elder and Schlosser (1995) reported definitive evidence of an extreme lack of population genetic variation in this species/gynogen complex in a north Minnesota stream drainage. Gynogens were sampled from three habitats in each of four different pond types in a single drainage. The abundance of gynogens relative to sexual fishes varied with pond type (from 13.4% to 48.6%). DNA fingerprinting of 464 individual gynogens detected only one clone. DNA fingerprint patterns, generated sequentially by using three probes, $(CAC)_5$, $(GACA)_4$, and 33.15, all revealed the same unprecedented lack of variation. The authors did not rule

out the possibility that a more complex community of gynogenetic clones existed in the described system in the past, and the current presence of only a single clone could be due to either selective or stochastic forces.

Only 1 clone was recently detected among 20 triploid gynogens of genus *Cobitis* (Cobitidae) sampled from the Moscow River (near Zvenigorod) and fingerprinted with minisatellite probe 33.15 and 7 different microsatellite probes (Lebedeva *et al.*, 2005). The resulting fingerprints were identical with all probes used. The authors inferred that monoclonality of this population might be a result of recent local introduction and reproduction of a new single individual or selection adaptation of the most fitness clone.

Multilocus DNA fingerprinting with probes $(GGAT)_4$, $(GACA)_4$, $(GATA)_4$, $(GAA)_6$, and $(CA)_8$ was also performed for studying two different laboratory lines and two single broods of *P. formosa* (Schartl *et al.*, 1991). The lines were derived from single females and propagated in population stocks of 40–100 individuals. When individuals from the same line were compared over several generations, a very similar overall fingerprint pattern was obtained with subtle differences. Small fingerprint differences in the laboratory lines indicated mutations that occurred in microsatellite-containing loci. Such mutations were seen in succeeding generations and therefore were clonally transmitted and stable. By analyzing siblings of a single brood, it was found that all individuals display almost identical fingerprint patterns. However, with the $(GATA)_4$ probe, a truly hypervariable locus was detected, which gave rise to variable restriction fragment length. The authors proposed that variable fragments could arise due to mutations occurred during early stages of embryogenesis. The low level of mutations observed by these authors in two single broods appears to be not surprising. The probability to find mutant fingerprint fragment in siblings of only two families is very low, practically equal to zero. Besides, as it was pointed out above, *de novo* mutations might be more effectively detected by comparing sibling fingerprint patterns with maternal fingerprint on a large-scale family analysis.

Umino *et al.* (1997) examined the frequency of gynogenetic triploid ginbuna in a total of 118 specimens belonging to the *Carassius* species (*Carassius langsdorfii*), caught in Kurose River, Hirosima. Combining the results from the cytogenetics, the flow cytometry, and erythrocyte measurements, 96 triploids (81%) and 22 diploids (19%) were detected. In the total of 77 triploid specimens fingerprinted, 51 (66%), 2 (3%), and 13 (17%) individuals had identical DNA fingerprints, respectively, and were concluded to be different three clones. The average band sharing index was relatively low between these clones. This implied that 86% of the triploid ginbuna in the Kurose River were the clonal progeny of only three females.

Alves *et al.* (1998) described genetic analysis of the progeny from diploid and triploid females of the *Rutilus alburnoides* complex taken from the Sorraia River of the Tejo Basin and from the Degebe River of the

Guadiana Basin. The mechanisms by which different *R. alburnoides* hybrids are perpetuated in nature are not yet well understood. Preliminary results obtained with allozyme markers revealed that triploid females from the Tejo basin mated to *Leuciscus pyrenaicus* (parental species) males produced diploid and triploid progeny, which showed evidence of sperm incorporation (Alves *et al.*, 1996, 1997; Carmona *et al.*, 1997). This suggested that triploid females might reproduce by hybridogenesis. In a study by Alves *et al.* (1998), diploid and triploid females were experimentally crossed with nonhybrid and *L. pyrenaicus* males, and the progeny was fingerprinted with minisatellite probes 33.6 and 33.15. The results obtained, together with the data of allozyme analysis, allowed the authors to conclude that the reproductive modes of diploid and triploid female *R. alburnoides* cannot be conveniently placed into the three categories generally recognized for unisexual vertebrates. Like the gynogenetic vertebrates, diploid females clonally transmit their hybrid genomes, but sperm is apparently incorporated and expressed in all offspring. Triploid females present a modified hybridogenesis (named ''meiotic hybridogenesis''), in which one genome is discarded in each generation without recombination, but inheritance is not hemiclonal. Meiosis involved random segregation and recombination between the homospecific genomes, and genetically distinct haploid and diploid eggs are produced. Moreover, unlike what happens in hybridogenesis, a sperm genome that is incorporated into the progeny may remain in the hybrid lineages longer than one generation—it is clonally transmitted by the diploid females to their diploid eggs. Thus, in addition to the genotypic diversity that results from paternal genome incorporation in each generation, *R. alburnoides* also possesses genotypic diversity resulting from the occurrence of meiosis in triploid females. High genetic variability introduced by different reproductive modes of diploid and triploid females may explain in part the ecological success of *R. alburnoides*, which is one of the most abundant and widespread minnows of central and southern Iberian freshwaters.

Summarizing, one can conclude that genome diversity and clonal composition of natural unisexual fish species is determined by mutations together with mixing of individuals from different lineages and migrating populations.

2.3. Parthenogenetic lizard populations

Among the amniotes, unisexual species of reptiles are the only vertebrates known to reproduce by true parthenogenesis. Of the 32 parthenogenetic species of reptiles that have been at least tentatively identified (Darevsky, 1993; Darevsky *et al.*, 1985), some have been extensively studied, but almost nothing is known about many. The basic biology including comparative anatomy, chromosome cytology, biochemical genetics, ecology,

and biogeography have been studied in details in some of these species (Arribas, 1999; Cuellar, 1971, 1974; Darevsky, 1985, 1993; Moritz *et al.*, 1989a,b, 1993; Parker *et al.*, 1989; Sites *et al.*, 1990; Suomalainen *et al.*, 1987; Vyas *et al.*, 1990). However, only four diploid parthenogenetic lizard species of the genus *Darevskia* and one triploid parthenogenetic species of the genus *Leiolepis* were investigated by DNA fingerprinting technique. Among them, Caucasian rock lizards *Darevskia dahli*, *D. armeniaca*, *D. unisexualis*, and *D. rostombekovi* were most extensively studied. Note that these species were only recently attributed to the newly nominated taxon *Darevskia* gen.nov. (Arribas, 1999), and I. S. Darevsky was the first who recognized them as parthenogenetic species in 1958. Meiotic parthenogenesis dominates in the eggs of such species, producing finally the diploid chromosome sets (Darevsky *et al.*, 1985). Hence, the progeny includes only genetically identical females, with clonal inheritance in next generations. Diploid males with notably decreased fertility appear in populations rarely and spontaneously [1 male per 1000 females (Darevsky *et al.*, 1985)]. Previously, some degree of allozyme variation (Fu *et al.*, 1998, 2000; MacCulloch *et al.*, 1995, 1997; Murphy *et al.*, 1997) and low variability of mtDNA (Moritz *et al.*, 1992) in parthenogenetic *Darevskia* lizard species were described. For example, one to seven clones were found in these species by allozyme electrophoresis. Theoretically, possible sources of such variations in parthenogenetic populations may be associated with mutations, rare new hybridization events, some low level of genetic recombination, or with the plural origin of clones from different pairs of founders (Cole *et al.*, 1983; Fu *et al.*, 2000; Moritz *et al.*, 1989a,b; Parker, 1979; Parker and Selander, 1976). However, contribution of these events in overall genetic variation remains unknown.

Parthenogenetic lizards *D. dahli* from two populations of Armenia were first fingerprinted using hybridization probes M13 DNA, $(TCC)_{50}$, $(GACA)_4$, and $(CAC)_5$ (Kan *et al.*, 1998; Tokarskaya *et al.*, 2001). DNA fingerprints produced by minisatellite probe M13 DNA were practically identical for all specimens in each population, while some interpopulation differences were observed. Microsatellite probes also produced species-specific fingerprints but a number of variable fragments were clearly detected in both populations. Out of 25 individuals of *D. dahli* analyzed, 17 (68%) yielded 5 fingerprint phenotypes (clones), represented by 6 (24%), 4 (16%), 3 (12%), and 2 (8%) individuals. The mean index of similarity (MIS) between these clones, estimated using the overall data matrix for all probes, was 0.962. The other eight animals did not belong to any of these clones and differed among themselves by several fingerprint fragments. Similar analysis was performed with *D. armeniaca* (Martirosyan *et al.*, 2003; Tokarskaya *et al.*, 2001) and *D. unisexualis* (Kan *et al.*, 2000; Ryskov *et al.*, 2000, 2003; Tokarskaya *et al.*, 2000, 2001) lizards. Out of 36 individuals of *D. armeniaca* from three populations of Armenia, 19 (52.7%) were classified

into 6 clones represented by 5 (13.8%), 4 (11%), 3 (8%), 2 (5.5%), and 2 (5.5%) lizards. The MIS between clones was 0.975. The remaining 17 (47.3%) specimens constituted 17 other clones. The MIS between these individuals was 0.953. Out of 40 lizards of *D. unisexualis* from three Armenian populations analyzed with M13DNA and $(GATA)_4$ probes, 28 (70%) were assigned to 4 clones consisting of 16 (40%), 7 (17.5%), 3 (7.5%), and 2 (5%) individuals, respectively. The MIS between them was 0.972. The other 12 individuals (30%) showed more divergent fingerprint patterns (MIS = 0.907). The most polymorphic, practically individual-specific fingerprints were observed when *D. unisexualis* populations were analyzed with the $(TCC)_{50}$ and $(TCT)_5$ probes (Ryskov *et al.*, 2000, 2003) (Fig. 7.4). The MIS value for TCC fingerprints was 0.824. Interestingly, a number of fragments in the fingerprint patterns detected by $(TCC)_{50}$ also hybridized with $(TCT)_5$. It means that some variable fragments of *D. unisexualis* possessed internal structural heterogeneity of microsatellite motifs containing both $(TCC)_n$ and $(TCT)_n$ polypyrimidine clusters and the possibility exists that observed variability of polypyrimidine-containing loci is connected with its specific structural organization. Nevertheless, the reasons of enhanced genomic variability of *D. unisexualis* remain unclear. According to one explanation, it may depend on the origin of unisexual species, namely on interspecies hybridization that combines two parent genomes. The resulting hybrid karyotypes and genomes in unisexuals may possess different stability (Kupriyanova, 1999). Another possible explanation is that *D. unisexualis* lizards may be deficient in some enzymatic activities, for example, in some DNA repair activities.

Darevsky *et al.* (1998) have compared one population of *D. armeniaca* from Armenia with *D. armeniaca* population originated after the introduction of these lizards from Armenia to Ukraine in 1963. The use of M13 DNA probe could reveal only 1 fingerprint phenotype among 21 lizards of

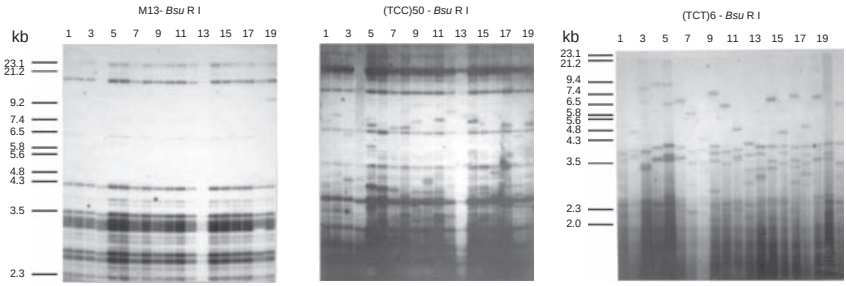

Figure 7.4 Typical pictures demonstrating enhanced variability of *Darevskia unisexualis* DNA fingerprints produced with microsatellite probes [adapted data from Ryskov *et al.* (2000) and Tokarskaya *et al.* (2001)]. Minisatellite probe M13 DNA produces monomorphic fingerprint patterns, microsatellite probes $(TCC)_{50}$ and $(TCT)_6$ produce highly polymorphic fingerprint patterns.

Armenian population and 2 fingerprint phenotypes differing in 1 fragment among 11 individuals of Ukrainian population. The authors suggested that the appearance of the second fingerprint phenotype in the Ukrainian population was not connected with mutation but might be result of accumulation of a minor variant (present in initial population) in the course of adaptation of the introduced population to environmental changes.

Variation of mini- and microsatellites-containing loci in populations of parthenogenetic lizards *D. rostombekovi* was studied by Martirosyan *et al.* (2002). Previously, the allozyme data for 35 loci of *D. rostombekovi* (sample of 65 animals from three Armenian populations) did not show any variation (MacCulloch *et al.*, 1997). Therefore, *D. rostombekovi* was considered a monoclonal species. In contrast, DNA fingerprinting with M13 minisatellite, $(GATA)_4$ and $(TCC)_{50}$ microsatellite probes in samples of 21 animals from 3 isolated populations of North Armenia and in a sample of 5 animals from relict population of Sevan Lake indicated that relict population of Sevan Lake was different from other populations with the interpopulation MIS about 0.536 (Martirosyan *et al.*, 2002). The authors suggested that hybrid karyotype of *D. rostombekovi* generated a series of chromosomal mutations that might lead to the appearance of a geographically isolated chromosome clone in the population inhabiting Sevan Lake. This conclusion was also confirmed by data of RAPD (Random Amplified Polymorphic DNA) and mitochondrial DNA analysis (Malysheva *et al.*, 2006a).

Recently, DNA fingerprinting in Southern Asian lizards belonging to the genus *Leiolepis*—bisexual species *L. reevesii* and parthenogenetic triploid species *L. guentherpetersi*—was first carried out (Malysheva *et al.*, 2006b). The genus *Leiolepis* comprises seven species, including four bisexual diploid species (*L. belliana*, *L. guttata*, *L. peguensis*, and *L. reevesii*) and three parthenogenetic species, one of which is diploid (*L. boehmei*) and two are triploid (*L. guentherpetersi* and *L. triploida*). Morphological and karyological characteristics of the *Leiolepis* species (Darevsky and Kupriyanova, 1993) as well as the mitochondrial DNA data (Schmitz *et al.*, 2001) indicated that *L. guentherpetersi* was formed as a result of hybrid mating of diploid parthenogenetic mother to the male from diploid bisexual species. The maternal diploid form was not found in nature and is thought to be extinct. The presumptive parental form is *L. reevesii*. DNA fingerprints with probes $(GACA)_4$, $(GGCA)_4$, and $(CAC)_5$ produced practically identical patterns in *L. guentherpetersi* lizards (MIS = 0.960) (Malysheva *et al.*, 2006a). Unexpected results were obtained in this study when the same *L. guentherpetesi* samples were fingerprinted with the $(GATA)_4$ probe (Fig. 7.5). The variability of $(GATA)_n$ loci in *L. guentherpetersi* and *L. reevesii* was similar (MIS = 0.460). The nature of high variability of $(GATA)_n$-containing loci in *L. guentherpetersi* remains obscure. Possible explanation assume that these loci should be more prone to different mutations and chromosomal rearrangements, leading to DNA restriction fragment length polymorphism

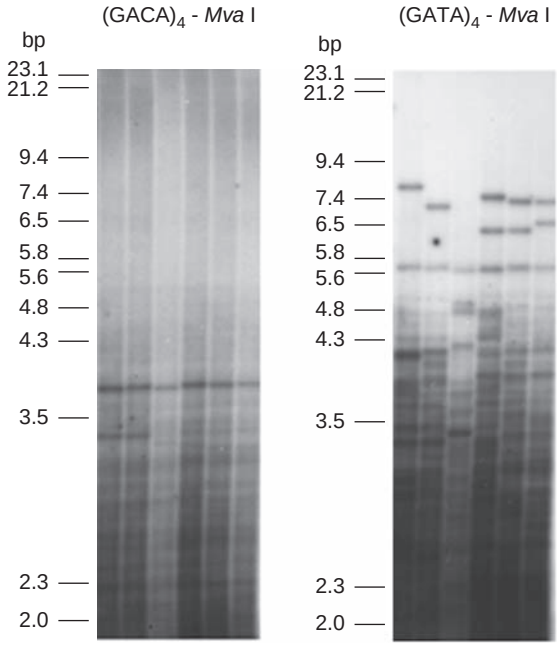

Figure 7.5 Typical pictures demonstrating enhanced variability of *Leolepis guentherpetersi* DNA fingerprints produced with GATA-microsatellite probe [adapted data from Malysheva *et al.* (2006b)]. In contrast to other microsatellite probes, the $(GATA)_4$ produces highly polymorphic fingerprint patterns. This can suggest enhanced instability of $(GATA)_n$-containing loci in parthenogenetic triploid lizards *L. guentherpetersi*.

(RFLP) and to diversity of fingerprint patterns. It is evident that instability of such loci in *L. guentherpetersi* can be directly demonstrated by further multilocus and/or single-locus analysis of parthenogenetic families. Adapted data on genetic variation in some parthenogenetic lizard species are summarized in the Table 7.2.

It should be mentioned that the biological significance of genetic heterogeneity detected by DNA fingerprinting of natural populations of parthenogenetic lizards with respect to clonal differentiation remains uncertain. For example, there are two widespread and equally abundant color varieties (with pale yellow and bright yellow bellies) in populations of *D. dahli*. Neither allozyme data (Murphy *et al.*, 1997) nor fingerprinting assays (Tokarskaya *et al.*, 2001) can distinguish between these two differently pigmented clones. Thus, it seems unlikely that fingerprint variability always coincides with phenotype variation and clonal differentiation in morphological and/or physiological characters. It is more likely that the observed fingerprint variability illustrates the process of spontaneous mutagenesis at the unstable loci and initial stages of clonal differentiation.

Table 7.2 Genetic variation in some parthenogenetic lizard species based on DNA fingerprinting data[a]

Species	Number of specimens	Probes	MIS
Darevskia dahli	25	M13 DNA	0.943
	25	$(TCC)_{50}$	0.973
	25	$(GACA)_4$	0.969
	25	United	0.962
D. armeniaca	36	M13 DNA	0.974
	36	$(TCC)_{50}$	0.967
	36	$(GACA)_4$	0.944
	36	United	0.966
D. unisexualis	40	M13 DNA	0.992
	40	$(TCC)_{50}$	0.825
	40	$(GATA)_4$	0.862
	40	United	0.952
D. rostombekowi	21	M13 DNA	0.981
	21	$(TCC)_{50}$	0.962
	21	$(GATA)_4$	0.901
	21	United	0.875
Leiolepis guenterpetersi	6	$(GACA)_4$	0.950
	6	$(GGCA)_4$	0.980
	6	$(CAC)_5$	0.970
	6	United	0.960
	6	$(GATA)_4$	0.350

[a] Adapted data from Kan *et al.* (1998), Tokarskaya *et al.* (2000, 2001), Martirosyan *et al.* (2002, 2003), Ryskov *et al.* (2000, 2003), and Malysheva *et al.* (2006b).

2.4. Parthenogenetic lizard families

To date, only parthenogenetic families of *D. armeniaca* and *D. unisexualis* consisting of mother and their progeny of first generation were investigated by multilocus DNA fingerprinting. Malysheva *et al.* (2007) have fingerprinted 43 *D. armeniaca* families (131 siblings) using $(GACA)_4$, $(GGCA)_4$, $(GATA)_4$, and $(CAC)_n$ probes, and revealed mutant fingerprints in 4 families (16 siblings) that differed from their mothers in several restriction DNA fragments. It is interesting that some mutant fingerprint fragments detected in siblings were also observed as polymorphic ones in fingerprints of population samples. One can infer that mutant fingerprint fragments are fixed, forming overall population polymorphism of fingerprint spectra. Mutation rate for new restriction fragment length estimated by these probes varied from 0.8×10^{-2} to 4.9×10^{-2} per fragment/sibling. As a rule, identical mutant fingerprints were observed in all siblings of one family.

It means that the most variations, detected as RFLPs, had germ line origin, but somatic changes of $(CAC)_n$ fingerprints were also found.

In similar experiments, rather high intrafamily variation of $(GATA)_n$, $(TCT)_n$, and $(TCC)_n$ containing DNA fragments was shown for cogeneric parthenogenetic species *D. unisexualis* (Kan *et al.*, 2000; Ryskov *et al.*, 2003; Tokarskaya *et al.*, 2003, 2004). For instance, mutation rate for new $(GATA)_n$-containing fragments, revealed in 25 families (overall 84 siblings), was as high as 0.9×10^{-2} per fragment/sibling. The case of somatic variation of $(GATA)_n$ detectable loci in adult *D. unisexualis* lizards was also described (Tokarskaya *et al.*, 2003, 2004). Typical pictures of intrafamily variability of DNA fingerprints are shown in Figure 7.6.

It is clear that differences in fragment size detected as RFLP appear to be too large to reflect microsatellite repeat number variation and seem likely to reflect mutations and/or epigenetic modifications in restriction sites, or other kinds of genomic alterations, which may occur during somatic development. Theoretically, instability of the hybrid karyotype characteristic of parthenogenetic species of the genus *Darevskia* (Kupriyanova, 1997) may also lead to chromosomal rearrangements resulting in the observed population and intrafamily variability of DNA fingerprints.

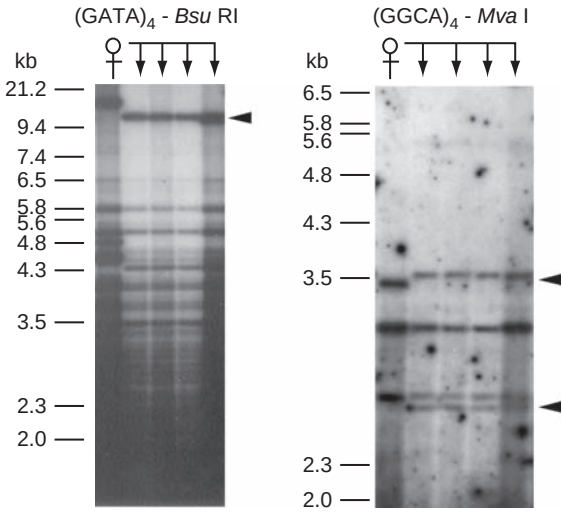

Figure 7.6 Typical pictures demonstrating intrafamily variability of DNA fingerprints: (A) *Darevskia unisexualis*; (B) *Darevskia armeniaca* [adapted data from Malysheva *et al.* (2007) and Tokarskaya *et al.* (2004)]. Intrafamily variation detected by microsatellite probes as restriction fragment length polymorphism can reflect mutations in restriction sites or various genomic alterations in loci containing these microsatellites. Triangles show mutant restriction fragments in siblings.

Summarizing, DNA fingerprinting studies provide some indirect evidence for existing unstable regions in parthenogenetic genomes detectable with microsatellite probes. To obtain more direct information about instability and molecular structure of microsatellite-containing loci in clonal species, new molecular approaches such as DNA cloning and sequencing should be applied.

3. Characterization of Individual Microsatellite Loci in Parthenogenetic Lizards

Despite the continued accumulation of data on mutation rate and sequence organization of microsatellite-containing loci in various species (Cleary *et al.*, 2002; Colson and Goldstein, 1999; Neff and Gross, 2001; Orti *et al.*, 1997), the general picture of their instability remains largely unclear. Recent studies have shown that different processes are actually involved in the creation of microsatellite-containing loci variability. Among such processes, there are sister chromatid exchange, asymmetry and polarity in the distribution of mutations, single nucleotide substitutions, deletions and insertions in flanking regions, and genesis of mobile elements (Ellegren, 2000, 2004; Goldstein and Pollock, 1997; Li *et al.*, 2002; Wilder and Hollocher, 2001). It is evident that DNA cloning and sequencing of allelic variants of microsatellite-containing loci may give detailed information on the nature of their variability. At present, very limited information is available concerning structural organization and allelic polymorphism of individual microsatellite loci in unisexual vertebrates.

3.1. Organization and polymorphism of individual microsatellite loci

Wilmhoff *et al.* (2003) have cloned and sequenced 16 variable dinucleotide microsatellite loci to quantify genetic variation in the parthenogenetic gecko, *Lepidodactylus lugubris*. The genetic diversity at these loci, analyzed by locus-specific PCR, was unusually high for an asexual species. Subsets of individuals produced identical genotypes across all loci. Substantial genetic differences were detected among subgroups, indicating the presence of distinct clonal lineages. Some individuals produced triploid haplotypes at two or more loci, in agreement with previous reports of triploid karyotypes in *L. lugubris* (Moritz *et al.*, 1993). Individual loci revealed differences between observed and expected heterozygosity, indicating the presence of null alleles.

Gardner *et al.* (2004) have isolated and sequenced six successfully amplified polymorphic loci containing $(AAC)_n$ and $(AAG)_n$ microsatellites from a triploid parthenogenetic form of the Australian lizard *Menetia greyii*. Observed heterozygosity for two populations ranges from 0.171 to 0.917 with an average of 0.609. Only one locus showed significant heterozygous difference indicating that most of the loci show no evidence for null alleles. A test of linkage disequilibrium within the populations was not significant, thus indicating the loci segregate independently. Authors reported the potential use of these loci across various sexual species within the *M. greyii* complex. However, in these two studies, the nucleotide sequences of the allelic variants were not investigated.

3.2. Variability of allelic variants of microsatellite loci

The more extensive information was followed from our studies of parthenogenetic *Darevskia* lizards. Korchagin *et al.* (2007) have cloned and sequenced a number of $(GATA)_n$ microsatellite loci of *D. unisexualis*. Among several loci analyzed in detail, two (Du 215 and Du 281) were polymorphic. Three and six allelic variants were detected among 65 lizards investigated for Du 215 and Du 281, respectively. Sequencing the PCR products amplified from these variants showed that allelic differences at the polymorphic loci were caused by variation in a number of tandem repeats and point mutations in microsatellite cluster as well as point mutations in the flanking regions. Comparison of polymorphic and monomorphic $(GATA)_n$-containing loci showed that the monomorphic ones contained more point mutations in microsatellite clusters as well as degenerative $(GATA)_n$-like sequences in the vicinity of these clusters or large insertions of $(GACA)_n$ in the middle of $(GATA)_n$ cluster. These data are consistent with the view that loci containing less perfect microsatellites are more stable and vice versa. Authors carried out cross-species analysis of polymorphic Du 215 and Du 281 and monomorphic Du 323 indicating that the PCR priming sites at the *D. unisexualis* were conserved in other parthenogenetic and bisexual species of genus *Darevskia*. Using these locus-specific primers, 8 allelic variants at Du 215 and 3 allelic variants at Du 281 among 26 individuals of *D. dahli* were found (Davoyan *et al.*, 2007). High interpopulation differences revealed in *D. dahli* probably reflected some differences in environmental conditions in which isolated populations were existed. Similar analysis revealed only 3 allelic variants at Du 215 among 127 specimens of *D. armeniaca* (Malysheva *et al.*, 2007). Sequencing of these allelic variants showed that they differed from each other by the size and composition of microsatellite cluster and by single nucleotide substitutions in flanking DNA. In several cases, significant differences among orthologues were found. For example, Du 215 in *D. armeniaca* contained not only $(GATA)_n$ but also $(GACA)_n$ cluster, which was absent in *D. unisexualis* (Table 7.3).

Table 7.3 Microsatellites in the allelic variants of orthological loci of some *Darevskia* lizard species[a]

Species, allelic variants	Allelic size (bp)	Locus, microsatellite cluster	Haplotype
D. unisexualis		Du281	
1	200	$(GATA)_9(GAT)(GATA)(TA)(GATA)$	T–A–T
2	204	$(GATA)_{10}(GAT)(GATA)(TA)(GATA)$	T–A–T
3	208	$(GATA)_{11}(GAT)(GATA)(TA)(GATA)$	T–A–T
4	212	$(GATA)_{12}(GAT)(GATA)(TA)(GATA)$	T–A–T
5	201	$(GATA)_{11}(TA)(GATA)$	C–G–C
6	197	$(GATA)_{10}(TA)(GATA)$	C–G–C
D. raddei		Du281	
1–4	184–204	$(GATA)_{5–10}(GAT)(GATA)(TA)(GATA)$	T–A–T
D. valentini		Du281	
1–5	183–199	$(GATA)_{8–12}$	C–G–C
D. dahli		Du281	
1	225	$(GATA)_9(GAT)(GATA)(GGTA)_2(GAT)(GATA)_4$	C–G–T
2	195	$(GATA)_{10}$	C–G–C
3	191	$(GATA)_8$	C–G–C
D. unisexualis		Du215	
1	227	$(GAT)(GATA)_4(GAT)(GATA)_7(GCAA)_2$	A–A
2	220	$(GAT)(GATA)_{10}(GCAA)_2$	T–G
3	216	$(GAT)(GATA)_9(GCAA)_2$	T–G
D. armeniaca		Du215	
1	236	$(GAT)(GACA)(GATA)_8(GACA)_5(GATA)(GCAA)$	T–G–C
2	232	$(GAT)(GACA)(GATA)_7(GACA)_5(GATA)(GCAA)$	T–G–C
3	192	$(GAT)\ (GATA)_5$	A–C–T
D. unisexualis		Du323	
1	199	$(AC)_6$-$(GATA)_7(GAT)(GATA)_2$-$(GA)_4$	C–T

(*continued*)

Table 7.3 (*continued*)

Species, allelic variants	Allelic size (bp)	Locus, microsatellite cluster	Haplotype
D. dahli		Du323	
1	215	$(AC)_6$-$(GATA)_{11}$(GAT) $(GATA)_2$-$(GA)_4$	C–T
2	211	$(AC)_6$-$(GATA)_{10}$(GAT) $(GATA)_2$-$(GA)_4$	C–T
3	184	$(AC)_5$-(GATA)(GGT) $(GATA)_3$(GAT)(GATA)-$(GA)_4$	A–C

[a] Data adapted from Korchagin *et al.* (2007), Davoyan *et al.* (2006), Malysheva *et al.* (2007), and Vergun *et al.* (2007).

The haplotypes were also identified among the allelic variants of Du 215, Du 281, and among their orthologues in the parental species *D. raddei* and *D. valentini* providing new evidence for the cross-species origin of *D. unisexualis* (Davoyan *et al.*, 2006, 2007; Korchagin *et al.*, 2007; Malysheva *et al.*, 2007). These haplotypes were further used as specific allelic markers in studies of inheritance of these alleles as well as in detection of mutant alleles in parthenogenetic progeny of *D. unisexualis*.

3.3. Microsatellite mutations in parthenogenetic lizard progeny

Badaeva *et al.* (2006) have analyzed 217 lizards representing 49 families (168 siblings) by monolocus PCR. Among them, mutant alleles were revealed in the progeny of four families (15 siblings) at Du 281 locus. A comparison of cloned and sequenced alleles of the mother and two offspring of one such family showed that the mutations lead to changes in the size of microsatellite clusters (insertion of the GATA monomer), with mutant alleles being identical in both siblings. This is apparently indicative of a greater probability of such mutations to emerge in the germ line cells. By the example of the family analyzed, the results demonstrate that the variability of alleles in the parthenogenetic offspring is limited by the microsatellite cluster and does not extend to the flanking regions. This means that it is the errors that arise owing to DNA polymerase slippage at microsatellite sites in DNA during replication that lead to the appearance of mutant alleles and that may be one of the factors that determine clonal and genetic diversity of unisexual populations. According to Badaeva (personal communication), similar mutations (deletion or insertion of one GATA monomer in Du 281 microsatellite clusters) were observed in the mutant alleles of the siblings

from three other *D. unisexualis* families analyzed. Microsatellite mutations found in *D. unisexualis* progeny of first generation fits well with the stepwise mutation model (Ohta and Kimura, 1973), which assumes that all mutation events involve a change in a single microsatellite repeat. At the same time, new data in favor of two phase model (Di Rienzop *et al.*, 1994) may be obtained in further studies of *de novo* mutant microsatellite alleles. In any case, the above-considered data provide first direct information on the contribution of mutations in genome diversity of parthenogenetic lizard populations.

4. Concluding Remarks

There are a variety of unisexual all-female vertebrates that display remarkable diversity in their genetic features, modes, and cytological mechanisms of reproduction, population structures, ecological adaptation, and perpetuation of clonal lineages. Clonal reproduction and clonal diversity are two features of unisexual vertebrates that make them exceptionally useful as model organisms in genetic and ecological studies. Although the questions concerning genetic variation and factors determining clonal and genomic diversity of unisexual vertebrate populations have received considerable attention, data obtained remain insufficient and conflicting. In fact, precise origin of many variant clones recognized by various means in many such species is unknown. This may depend on undetected complexity of some unisexual systems and nonadequate analyzing methods applied. Thus, the DNA fingerprinting method reveals much higher level of genome variation in true clonal populations (gynogenetic and parthenogenetic) in comparison to allozyme and mtDNA analysis. It seems that high genome diversity revealed in various clonal populations by DNA fingerprinting associated with different factors, including the plural origin of clones from different pairs of founders, outcrossing events, some low level of genetic recombination, and mutations. The clonal diversity that is arisen due to different hybrid combinations of ancestral egg and sperm or as a consequence of new outcrossing events must be a matter of additional laboratory and field comparisons. The DNA fingerprinting method is exceptionally powerful tool that can be used strategically to complement less conclusive results obtained from other data. In particular, this method is useful for revealing small genomic variation in clonal populations, detecting *de novo* mutations in next generations, and unstable loci in hybrid genomes. Population variability of both minisatellite- and microsatellite-derived fingerprints in gynogenetic fishes implies that not only mutations but also plural clonal origin as well as some levels of migration with lineage mixing may be responsible for overall genomic variation. The data on intrapopulation identity of minisatellite-derived fingerprints in parthenogenetic lizards of

genus *Darevskia* are not consistent with plural origin of their clones. On the other hand, population variability of microsatellite-derived fingerprints in the same lizard samples would mainly reflect mutational diversity of their genotypes. Whether such mutations are fixed providing new clonal lineages and thus higher clonal diversity remains unclear and needs further study of the fate of unstable loci in the second and next generations. While limited, recent data on molecular nature of mutations and composition of allelic variants of polymorphic loci in parthenogenetic lizards of genus *Darevskia* directly show that microsatellite mutations as well as point mutations in flanking regions make significant contribution in genome diversity of these populations. Although this may involve substantial work, continued characterization of different unisexual vertebrates with various techniques should greatly facilitate our knowledge about genome and clonal diversity of these species.

ACKNOWLEDGMENTS

I am thankful to members of my laboratory for their collaboration on the Darevskia lizards research project, to I. A. Martirosyan for useful suggestions on the manuscript, and to M. A. Baukova for help in preparing the manuscript.

REFERENCES

Alves, M. J., Coelho, M. M., and Collares-Pereira, M. J. (1996). Evidence for nonclonal reproduction in triploid *Rutilus alburnoides*. *Isozyme Bull.* **29,** 23.

Alves, M. J., Coelho, M. M., and Collares-Pereira, M. J. (1997). The *Rutilus alburnoides* complex (Cyprinidae): Evidence for a hybrid origin. *J. Zool. Syst. Evol. Res.* **35,** 1–10.

Alves, M. J., Coelho, M. M., and Collares-Pereira, M. J. (1998). Diversity in the reproductive modes of females of the *Rutilus alburnoides* complex (Teleostei, Cyprinidae): A way to avoid the genetic constrains of uniparentalism. *Mol. Biol. Evol.* **15,** 1233–1242.

Arribas, O. J. (1999). Phylogeny and relationship of the mountain lizards of Europe and the Near East (*Archaeolacerta* Mertens 1921, *sencu lato*) and their relationships among the Eurasian Lacertid lizards. *Russ. J. Herpetology* **6,** 1–22.

Avise, J. C., Quanttro, J. M., and Vrijenhoek, R. C. (1992). Molecular clones within organismal clones. *Evolutionary Biology* **26,** 225–246.

Badaeva, T. N., Korchagin, V. I., Tokarskaya, O. N., and Ryskov, A. P. (2006). Identification and molecular characteristics of mutant alleles at the Du281 locus in parthenogenetic progeny of *Darevskia unisexualis*. *Dokl. Biochem. Biophys.* **409,** 197–199.

Barton, N. H., and Charlesworth, B. (1998). Why sex and recombination? *Science* **281,** 1986–1990.

Bohlen, J., and Rab, P. (2001). Species and hybrid richness in spined loaches of the genus *Cobitis* (Teleostei: Cobitidae), with a checklist of European forms and suggestion for conservation. *J. Fish Biol.* **59,** 75–89.

Bois, P. (2003). Hypermutable minisatellites, a human affair? *Genomics* **81,** 349–355.

Brohede, J., Primmer, C. R., Moller, A., and Ellegren, H. (2002). Heterogeneity in the rate and pattern of germline mutations at individual microsatellite loci. *Nucl. Acids Res.* **30,** 1997–2003.

Butlin, R. K., Schoen, I., and Martens, K. (1999). Origin, age and diversity of clones. *J. Evol. Biol.* **12,** 1020–1022.

Carmona, J. A., Sanjur, O. I., Doadrio, I., Machordom, A., and Vrijenhoek, R. C. (1997). Hybridogenetic reproduction and maternal ancestry of polyploid Iberian fish: The *Tropidophoxinellus alburnoides* complex. *Genetics* **146,** 983–993.

Cimino, M. C. (1972a). Egg production, polyploidization and evolution in a diploid all-female fish of the genus Poeciliopsis. *Evolution* **26,** 294–306.

Cimino, M. C. (1972b). Meiosis in a triploid all-female fish (Poeciliopsis, Poeciliidae). *Science* **175,** 1484–1486.

Cleary, J. D., Nichol, K., Wang, Y.-H., and Pearson, C. E. (2002). Evidence of *cis*-acting factors in replication-mediated trinucleotide repeat instability in primate cells. *Nat. Genet.* **31,** 37–46.

Cole, C. J., Dessauer, H. C., and Barrowclough, G. F. (1983). Isozymes reveal hybrid origin of neotropical unisexual lizards. *Isozyme Bull.* **16,** 74.

Colson, I., and Goldstein, D. B. (1999). Evidence for complex mutations at microsatellite loci in *Drosophila*. *Genetics* **152,** 617–627.

Cuellar, O. (1971). Reproduction and the mechanism of meiotic restitution in the parthenogenetic lizard *Chnemidophorus uniparens*. *J. Morphol.* **133,** 139–166.

Cuellar, O. (1974). The origin of parthenogenesis in vertebrates: The cytogenetic factors. *Am. Nat.* **108,** 625–648.

Darevsky, I. S. (1985). Natural parthenogenesis in certain subspecies of rock lizards (*Lacerta saxicola* Eversmann). *Dokl. Akad. Nauk SSSR* **122,** 730–732 (in Russian).

Darevsky, I. S. (1993). Evolution and ecology of parthenogenesis in reptiles. *In* "Current Research in Biology of Amphibians and Reptiles" (K. Adler, ed.), pp. 209–257. Oxford, Ohio.

Darevsky, I. S., and Kupriyanova, L. A. (1993). Two new all-female lizard species of the genus *Leiolepis* (Sauria: Uromastycidae) from Thailand and Vietnam. *Herpetozoa* **6,** 1–20.

Darevsky, I. S., Kupriyanova, L. A., and Uzzell, T. (1985). Parthenogenesis in reptiles. *In* "Biology of the Reptilia" (C. Gans and F. Billett, eds.), pp. 412–526. Weley and Sons, New York.

Darevsky, I. S., Kan, N. G., Rybinina, N. L., Martirosyan, I. A., Tokarskaya, O. N., Grechko, V. V., Scherback, N. N., Danielyan, F. D., and Ryskov, A. P. (1998). Biological and molecular–genetic characteristics of the parthenogenetic lizard *Lacerta armeniaca* (Mehely) introduced to Ukraine from Armenia. *Dokl. Biol. Sci.* **363,** 599–601.

Davoyan, A. G., Aslanyan, A. V., Danielyan, F. D., Darevsky, I. S., and Martirosyan, I. A. (2006). Study of allelic variants' structure of loci Du281 in *Darevskia dahli* (Lacertidae) parthenogenetic lizard populations. *Electron. J. Nat. Sci. Natl. Acad. Sci. RA (Mol. Biol.)* **2,** 38–41.

Davoyan, A. G., Aslanyan, A. V., Danielyan, F. D., Darevsky, I. S., and Martirosyan, I. A. (2007). Revealing of allelic polymorphism in populations of parthenogenetic lizards *Darevskia dahli* (Lacertidae) using locus-specific PCR. *Russ. J. Genet.* **43,** 20–23.

Dawley, R. M. (1989). An introduction to unisexual vertebrates. *In* "Evolution and Ecology of Unisexual Vertebrates" (R. M. Dawley and J. P. Bogart, eds.), pp. 1–18. New York State Museum, Albany, New York.

Debrauwere, H., Gendrel, C. G., Lechat, S., and Dutreix, M. (1997). Differences and similarities between various tandem repeat sequences: Minisatellites and microsatellites. *Biochimie* **79,** 577–586.

Di Rienzop, A., Peterson, A. C., Garza, J. C., Valdes, A. M., Slatkin, M., and Freimer, N. B. (1994). Mutational processes of simple-sequence repeat loci in human populations. *Proc. Natl. Acad. Sci. USA* **91,** 3166–3170.

Djan, P. (1998). Evolution of simple repeats in DNA and their relation to human disease. *Cell* **94,** 155–160.

Elder, J. F., and Schlosser, I. J. (1995). Extreme clonal uniformity of *Phoxinus eos/neogaeus* gynogens (Pisces: Cyprinidae) among variable habitats in northern Minnesota beaver ponds. *Proc. Natl. Acad. Sci. USA* **92,** 5001–5005.

Ellegren, H. (2000). Microsatellite mutations in the germline: Implications for evolutionary inference. *Trends Genet.* **16,** 551–558.

Ellegren, H. (2004). Microsatellites: Simple sequences with complex evolution. *Genetics* **5,** 435–445.

Epplen, C., Melmer, G., Siedlaczck, I., Schwaiger, F. W., Mäueler, W., and Epplen, J. T. (1993). On the essence of meaningless simple repetitive DNA in eukaryotic genomes. *In* "DNA Fingerprinting: State of the Science" (S. D. J. Pena, P. Chakraborty, J. T. Epplen, and A. J. Jeffreys, eds.), pp. 29–45. Birkhäuser Verlag, Basel, Switzerland.

Fu, J., MacCulloch, R. D., Murphy, R. W., Darevsky, I. S., Kupriyanova, L. A., and Danielyan, F. D. (1998). The parthenogenetic rock lizard *Lacerta unisexualis*: An example of limited genetic polymorphism. *J. Mol. Evol.* **46,** 127–130.

Fu, J., MacCulloch, R. D., Murphy, R. W., Darevsky, I. S., and Tuniyev, B. S. (2000). Allozyme variation patterns and multiple hybridization origins: Clonal variation among four parthenogenetic Caucasian rock lizards. *Genetica* **108,** 107–112.

Gardner, M. G., Ottewell, K., and Adams, M. (2004). Isolation of microsatellites in parthenogenetic lizard *Menetia greyii* (Scincidae) and their utility in sexual species of the *Menetia greyii* complex. *Mol. Ecol. Notes* **4,** 219–221.

Goddart, K. A., Dawley, R. M., and Dowling, T. E. (1989). Origin and genetic relationships of diploid, triploid, and diploid-triploid mosaic biotypes in the *Phoxinus cos-neogaeus* unisexual complex. *In* "Evolution and Ecology of Unisexual Vertebrates" (R. M. Dawley and J. P. Bogart, eds.), pp. 268–280. New York State Museum, Albany, New York.

Goldstein, D. B., and Pollock, D. D. (1997). Launching microsatellites: A review of mutation processes and methods of phylogenetic inference. *J. Hered.* **88,** 335–342.

Graf, J.-D., and Muller, W. P. (1979). Experimental gynogenesis provides evidence of hybridogenetic reproduction in the *Rana esculenta* complex. *Experientia* **35,** 1574–1576.

Graf, J.-D., and Polls Pelaz, M. (1989). Evolutionary genetics in the *Rana esculenta* complex. *In* "Evolution and Ecology of Unisexual Vertebrates" (R. M. Dawley and J. P. Bogart, eds.), pp. 289–301. New York State Museum, Albany, New York.

Grebelnyi, S. D. (2005). How many clonal species are there in the world. Part 1. The difference between clonal forms and bisexual species. *Invertebr. Zool.* **2,** 79–102.

Hancock, J. M. (1999). Microsatellites and other simple sequences: Genomic context and mutational mechanisms. *In* "Microsatellites: Evolution and Applications" (D. B. Goldstein and C. Scholötterer, eds.), pp. 1–9. Oxford University Press, Oxford.

Hotz, H., Mancino, G., Bucciinnocenti, S., Ragghianti, M., Berger, L., and Uzzell, T. M. (1985). *Rana ridibunda* varies geographically in inducing clonal gametogenesis in inter-species hybrids. *J. Exp. Zool.* **236,** 199–210.

Hubbs, C. L., and Hubbs, L. C. (1932). Apparent parthenogenesis in nature, in a form of fish of hybrid origin. *Science* **76,** 628–630.

Hurst, L. D., and Peck, J. R. (1996). Recent advances in understanding of the evolution and maintenance of sex. *Trends Ecol. Evol.* **11,** 46–52.

Jeffreys, A. J. (1997). Spontaneous and induced minisatellite instability in the human genome (Bayer Lecture). *Clin. Sci.* **93,** 383–390.

Jeffreys, A. J., Wilson, V., and Thein, S. L. (1985). Individual-specific fingerprints of human DNA. *Nature* **316,** 76–79.

Jeffreys, A. J., Bois, P., Buard, J., Collick, A., Dubrova, Y., Hollies, C. R., May, C. A., Murray, J., Neil, D. L., Neumann, R., Stead, J. D., Tamaki, K., and Yardley, J. (1997). Spontaneous and induced minisatellite instability. *Electrophoresis* **18,** 1501–1511.

Jurka, J., and Gentles, A. J. (2006). Origin and diversification of minisatellites derived from human Alu sequences. *Gene* **365,** 21–26.

Kan, N. G., Petrosyan, V. G., Martirosyan, I. A., Ryskov, A. P., Darevsky, I. S., Danielyan, F. D., Grechko, V. V., Ryabinin, D. M., and Tokarskaya, O. N. (1998). Genomic polymorphism of mini- and microsatellite loci of the parthenogenic *Lacerta dahli* revealed by DNA Fingerprinting. *Mol. Biol. (Moscow)* **32,** 672–678.

Kan, N. G., Martirosyan, I. A., Darevsky, I. S., Danielyan, F. D., Arakelyan, M. S., Aslanyan, A. V., Grechko, V. V., Tokarskaya, O. N., and Ryskov, A. P. (2000). Detection of genetically unstable loci in parthenogenic families of lizards of the *Lacerta* genus by DNA fingerprinting. *Mol. Biol. (Moscow)* **34,** 707–711.

Kondrashov, A. S. (1993). Classification of hypotheses on the advantage of amphimixis. *J. Hered.* **84,** 372–387.

Kondrashov, A. S. (1997). Evolutionary genetics of life cycles. *Annu. Rev. Ecol. Syst.* **28,** 391–435.

Korchagin, V. I., Badaeva, T. N., Tokarskaya, O. N., Martirosyan, I. A., Darevsky, I. S., and Ryskov, A. P. (2007). Molecular characterization of allelic variants of $(GATA)_n$ microsatellite loci in parthenogenetic lizards *Darevskia unisexualis* (Lacertidae). *Gene* **392,** 126–133.

Kupriyanova, L. A. (1997). Some cytogenetical regular trends in reticular (hybridogenous) speciation in unisexual lizards (Reptilia: Lacertilian) and other groups of vertebrates. *Cytologia* **39,** 1089–1108 (in Russian).

Kupriyanova, L. A. (1999). Genetic variations in hybrid unisexual species and forms of the genus *Lacerta* (Lacertidae, Reptilia): Possible cytogenetic mechanisms, cytogenetics of meiosis in natural polyploid forms. *Cytologia* **41,** 1038–1046 (in Russian).

Laughlin, T. F., Lubinski, B. A., Park, E. -H., Taylor, D. S., and Turner, B. J. (1995). Clonal stability and mutation in the self-fertilizing hermaphroditic fish, *Rivulus marmoratus*. *J. Hered.* **86,** 399–402.

Lebedeva, E. B., Vasil'ev, V. P., and Ryskov, A. P. (2005). The gynogenetic form of fish from the genus *Cobitis* (Cobitidae) in a region of its geographic range is monoclonal: DNA fingerprinting data. *Dokl. Biol. Sci.* **401,** 107–109.

Levinson, G., and Gutman, G. A. (1987). Slipped-strand mispairing: A major mechanism for DNA sequences evolution. *Mol. Boil. Evol.* **4,** 203–221.

Li, Y.-C., Korol, A. B., Fahima, T., Beiles, A., and Nevo, E. (2002). Microsatellites: Genomic distribution, putative functions and mutational mechanisms: A review. *Mol. Ecol.* **11,** 2453–2465.

Limborska, S. A., Prosnyak, M. I., Bocharova, T. N., Smirnova, E. M., and Ryskov, A. P. (1999). The properties of human DNA fingerprints produced by polymeric monocore probes (PMC probes). *Genet. Anal. Biomol. Eng.* **15,** 19–24.

Lowcock, L. A., Light, L. E., and Bogart, J. P. (1987). Nomenclature in hybrid complexes of *Ambystoma* (Urodela: Ambystomatidae): No case for the erection of hybrid species. *Syst. Zool.* **36,** 328–336.

MacCulloch, R. D., Murphy, R. W., Kupriyanova, L. A., Darevsky, I. S., and Danielyan, F. D. (1995). Clonal variation in the parthenogenetic rock lizard *Lacerta armeniaca*. *Genome* **38,** 1057–1060.

MacCulloch, R. D., Murphy, R. W., Kupriyanova, L. A., and Darevsky, I. S. (1997). The Caucasian rock lizard *Lacerta rostombekovi*: A monoclonal parthenogenetic vertebrate. *Biochem. Syst. Ecol.* **25,** 33–37.

Malysheva, D. N., Tokarskaya, O. N., Petrosyan, V. G., Daniyelyan, F. D., and Ryskov, A. P. (2006a). Genetic differentiation of parthenogenetic lizards *Darevskia rostombekowi* (family Lacertidae) as determined using nuclear and mitochondrial DNA markers. *Dokl. Biochem. Biophys.* **410,** 304–307.

Malysheva, D. N., Darevsky, I. S., Tokarskaya, O. N., Petrosyan, V. G., Martirosyan, I. A., and Ryskov, A. P. (2006b). Analysis of genetic variation in unisexual and bisexual lizard species of the genus *Leiolepis* from Southeast Asia. *Russ. J. Genet.* **42,** 463–467.

Malysheva, D. N., Vergun, A. A., Tokarskaya, O. N., Sevast'yanova, G. A., Darevsky, I. S., and Ryskov, A. P. (2007). Nucleotide sequences of the microsatellite locus *Du215 (arm)* allelic variants in the parthenospecies *Darevskia armeniaca* (Lacertidae). *Russ. J. Genet.* **43,** 116–120.

Martirosyan, I. A., Ryskov, A. P., Petrosyan, V. G., Arakelyan, M. S., Aslanyan, A. V., Danielyan, F. D., Darevsky, I. S., and Tokarskaya, O. N. (2002). Variation of mini- and microsatellite DNA markers in populations of parthenogenetic rock lizard *Darevskia rostombekovi*. *Russ. J. Genet.* **38,** 691–698.

Martirosyan, I. A., Kan, N. G., Petrosyan, V. G., Malysheva, D. N., Trofimova, A. A., Danielyan, F. D., Darevsky, I. S., Korochkin, L. I., Ryskov, A. P., and Tokarskaya, O. N. (2003). Variation of mini-and microsatellite DNA repeat in parthenogenetic lizard *Darevskia armeniaca* as revealed by DNA fingerprinting analysis. *Russ. J. Genet.* **39,** 159–165.

Mateos, M., and Vrijenhock, R. C. (2002). Ancient versus reticulate origin of a hemiclonal lineage. *Evolution* **56,** 985–992.

Mateos, M., Sanjur, O. I., and Vrijenhock, R. C. (2002). Historical biogeography of the fish genus *Poeciliopsis* (Cypriodontiformes). *Evolution* **56,** 972–984.

Monaco, P. J., Rasch, E. M., and Balsano, J. S. (1984). Apomictic reproduction in the Amazone mollie, *Poecilia formosa*, and its triploid hybrids. *In* "Evolutionary Genetics of Fishes" (B. J. Turner, ed.), pp. 311–328. Plenum Press, New York.

Moritz, C., Brown, W. M., Densmore, L. D., Wright, J. W., Vyas, D., Donnellan, S., Adams, M., and Baverstock, P. (1989a). Genetic diversity and the dynamics of hybrid parthenogenesis in *Cnemidophorus* (Teiidae) and *Heteronotia* (Gekkonidae). *In* "Evolution and Ecology of Unisexual Vertebrates" (R. M. Dawley and J. P. Bogart, eds.), pp. 24–31. New York State Museum, Albany, New York.

Moritz, C., Donnelan, S., Adams, M., and Baverstock, P. R. (1989b). The origin and evolution of parthenogenesis in *Heteronotia binoei* (Gekkonidae): Extensive genotypic diversity among parthenogens. *Evolution* **43,** 994–1003.

Moritz, C., Uzzell, T., Spolsky, C., Hotz, H., Darevsky, I. S., Kupriyanova, L. A., and Danielyan, F. D. (1992). The maternal ancestry and approximate age of parthenogenetic species of Caucasin rock lizards (*Lacerta:* Lacertidae). *Genetica* **84,** 53–62.

Moritz, C., Case, T. J., Bolger, D. T., and Donnellan, S. (1993). Genetic diversity and the history of Pacific island house geckos (*Hemidactylus* and *Lepidodactylus*). *Biol. J. Linn. Soc.* **48,** 113–133.

Murphy, R. W., Darevsky, I. S., MacCulloch, R. D., Fu, J., Kupriyanova, L. A., Upton, D. E., and Danielyan, F. D. (1997). Old age, multiply formations or genetic plasticity? Clonal diversity in the uniparental Caucasian rock lizard, *Lacerta dahli*. *Genetica* **101,** 125–130.

Neff, B. D., and Gross, M. R. (2001). Microsatellite evolution in vertebrates: Inference from AC dinucleotide repeats. *Evolution* **55,** 1717–1733.

Ohta, T., and Kimura, M. (1973). A model of mutation appropriate to estimate the number of electrophoretically detectable alleles in a finite population. *Genet. Res.* **22,** 201–204.

Orti, G., Pearse, D. E., and Avise, J. C. (1997). Phylogenetic assessment of length variation at microsatellite locus. *Proc. Natl. Acad. Sci. USA* **94,** 10745–10749.

Otto, S. P., and Lenormand, T. (2002). Resolving the paradox of sex and recombination. *Nat. Rev. Genet.* **3,** 252–261.

Parker, E. D. (1979). Phenotypic consequences of parthenogenesis in *Cnemidophorus* lizards. I. Variability in parthenogenetic and sexual populations. *Evolution* **33,** 1150–1166.

Parker, E. D., and Selander, R. K. (1976). The organization of genetic diversity in the parthenogenetic lizard *Cnemidophorus tesselatus*. *Genetics* **84,** 791–805.

Parker, E. D., Walker, J. M., and Paulissen, M. A. (1989). Clonal diversity in *Cnemidophorus:* Ecological and morphological consequences. *In* "Evolution and Ecology of Unisexual Vertebrates" (R. M. Dawley and J. P. Bodart, eds.), pp. 72–86. NewYork State Museum, Albany, New York.

Rasch, E. M., Prehn, L. M., and Rasch, R. W. (1970). Cytogenetic studies of *Poecilia* (Pisces) II. Triploidy and DNA levels in naturally occurring populations associated with gynogenetic teleost *Poecilia formosa* (Garard). *Chromosoma* **31,** 18–40.

Rasch, E. M., Monaco, P. J., and Balsano, J. S. (1982). Cytophotometric and autoradiographic evidence for functional apomixis in a gynogenetic fish, *Poecilia formosa* and its related, triploid unisexuals. *Histochemistry* **73,** 515–533.

Ryskov, A. P. (1999). Multilocus DNA fingerprinting in the genetic studies of biodiversity (Review). *Mol. Biol. (Moscow)* **33,** 880–892.

Ryskov, A. P., Jincharadze, A. G., Prosnyak, M. I., Ivanov, P. L., and Limborska, S. A. (1988). M13 phage DNA fingerprinting of animals, plants, and microorganisms. *FEBS Lett.* **233,** 388–392.

Ryskov, A. P., Kan, N. G., Martirosyan, I. A., Darevsky, I. S., Danielyan, F. D., Petrosyan, V. G., and Tokarskaya, O. N. (2000). High variability of $(TCC)_n$ microsatellite loci in populations of parthenogenetic lizard *Lacerta unisexualis* Darevsky. *Russ. J. Genet.* **36,** 1262–1266.

Ryskov, A. P., Martirosyan, I. A., Badaeva, T. N., Korchagin, V. I., Danielyan, F. D., Petrosyan, V. G., Darevsky, I. S., and Tokarskaya, O. N. (2003). Hyperinstability of $(TCT/TCC)_n$ microsatellite DNAs in parthenogenetic lizard *Darevskia unisexualis* (Lacertidae). *Russ. J. Genet.* **39,** 986–992.

Schartl, M., Schlupp, I., Schartl, A., Meyer, M. K., Nanda, I., Schmid, M., Epplen, J. T., and Parzefall, J. (1991). On the stability of dispensable constituents of the eukaryotic genome: Stability of coding sequences versus truly hypervariable sequences in a clonal vertebrate, the amazon molly, *Poecilia formosa*. *Proc. Natl. Acad. Sci. USA* **88,** 8759–8763.

Schartl, M., Nanda, I., Schlupp, I., Wilde, B., Epplen, J. T., Schmid, M., and Parzefall, J. (1995). Incorporation of subgenomic amounts of DNA as compensation for mutational load in a gynogenetic fish. *Nature* **373,** 68–71.

Schmitz, A., Vences, M., and Weitkus, S. (2001). Recent maternal divergence of the parthenogenetic lizard *Leiolepis guentherpetersii* from *L. guttata*: Molecular evidence (Reptilia: Squemata: Agamidae). *Zool. Abh. Mus. Tierkde* **51,** 355–360.

Schultz, R. J. (1969). Hybridization, unisexuality and polyploidy in the teleost *Poeciliopsis* (Poeciliidae) and other vertebrates. *Am. Nat.* **103,** 605–619.

Schultz, R. J. (1973). Unisexual fish: Laboratory synthesis of a "species.". *Science* **179,** 180–181.

Schultz, R. J., and Fielding, E. (1989). Fixed genotypes in variable environment. *In* "Evolution and Ecology of Unisexual Vertebrates" (R. M. Dawley and J. P. Bogart, eds.), pp. 32–38. New York State Museum, Albany, New York.

Schultz, R. J., and Kallman, K. D. (1968). Triploid hybrids between the all-female teleost *Poecilia formosa* and *Poecilia sphenops*. *Nature* **219,** 280–282.

Sessions, S. K. (1982). Cytogenetics of diploid and triploid salamanders of the *Ambystoma jeffersonianum* complex. *Chromosoma* **84,** 599–621.

Shabrova, E. V., Limborska, S. A., and Ryskov, A. P. (2006). Multilocus DNA fingerprinting-genotyping based on micro-and minisatellite polymorphisms. *In* "Focus on DNA Fingerprinting Research" (M. M. Read, ed.), pp. 1–60. Nova Science Publishers, Inc., New York.

Sites, J. W., Jr., Peccinini-Seale, D., Moritz, C., Wright, J. W., and Brown, W. M. (1990). The evolutionary history of the parthenogenetic *Cnemidophorus lemniscatus* (Sauria, Teiidae). I. Evidence for a hybrid origin. *Evolution* **44,** 906–921.

Suomalainen, E., Saura, A., and Lokki, J. (1987). "Cytology and Evolution in Parthenogenesis." CRC Press, Boca Ration, Florida.

Tautz, D. (1989). Hypervariability of simple sequences as a general source for polymorphic DNA markers. *Nucl. Acids Res.* **17,** 6463–6471.

Tautz, D., and Renz, M. (1984). Simple sequences are ubiquitous repetitive components of eukaryotic genomes. *Nucl. Acids Res.* **12,** 4127–4138.

Templeton, A. R. (1982). The prophecies of parthenogenesis. *In* "Evolution and Genetics of Life Histories" (H. Dingle and J. P. Hegmann, eds.), pp. 75–102. Springer-Verlag, Berlin-Heidelberg-New York.

Tokarskaya, O. N., Kan, N. G., Petrosyan, V. G., Martirosyan, I. A., Danielyan, F. D., Darevsky, I. S., and Ryskov, A. P. (2000). Variation of GATA -microsatellite DNA in populations of the parthenogenetic species of lizard *Lacerta unisexualis* Darevsky. *Russ. J. Genet.* **36,** 563–567.

Tokarskaya, O. N., Kan, N. G., Petrosyan, V. G., Martirosyan, I. A., Grechko, V. V., Danielyan, F. D., Darevsky, I. S., and Ryskov, A. P. (2001). Genetic variation in parthenogenetic Caucasian rock lizards of the genus *Lacerta* (*L. dahli*, *L. armeniaca*, *L. unisexualis*), analyzed by DNA fingerprinting. *Mol. Gen. Genomics* **265,** 812–819.

Tokarskaya, O. N., Darevsky, I. S., Martirosyan, I. A., Badaeva, T. N., Korochkin, L. I., Danielyan, F. D., Petrosyan, V. G., and Ryskov, A. P. (2003). Genetic instability of $(GATA)_n$ microsatellite DNAs and somatic mosaicism in unisexual lizard, *Darevskia unisexualis*. *Dokl. Biochem. Biophys.* **388,** 64–66.

Tokarskaya, O. N., Martirosyan, I. A., Badaeva, T. N., Malysheva, D. N., Korchagin, V. I., Darevsky, I. S., Danielyan, F. D., and Ryskov, A. P. (2004). $(GATA)_n$ microsatellite instability in the parthenogenetic Caucasian rock lizard *Darevskia unisexualis* (Lacertidae). *Mol. Gen. Genomics* **270,** 509–513.

Toth, G., Gaspari, Z., and Jurka, J. (2000). Microsatellites in different eukaryotic genomes: Survey and analysis. *Genome Res.* **10,** 967–981.

Turner, B. J. (1982). The evolutionary genetics of a unisexual fish *Poecilia formosa*. *In* "Mechanisms of Speciation" (C. Barigozzi, ed.), pp. 265–305. Alan Liss., New York.

Turner, B. J., Balsano, J. S., Monaco, P. J., and Rasch, E. M. (1983). Clonal diversity and evolutionary dynamics in a diploid-triploid breeding complex of unisexual fishes (*Poecilia*). *Evolution* **37,** 798–809.

Turner, B. J., Elder, J. F., Jr., Laughlin, T. F., and Davis, W. P. (1990). Genetic variation in clonal vertebrates detected by simple-sequence DNA fingerprinting. *Proc. Natl. Acad. Sci. USA* **87,** 5653–5657.

Turner, B. J., Elder, J. F., Jr., Laughlin, T. F., Davis, W. P., and Taylor, D. S. (1992). Extreme clonal diversity and divergence in populations of selfing hermaphroditic fish. *Evolution* **89,** 10643–10647.

Umino, T., Arai, K., Maeda, K., Zang, Q., Sakac, K., Niwase, I., and Nakagawa, H. (1997). Natural clones detected by multilocus DNA fingerprinting in gynogenetic triploid ginbuna *Carrassius langsdorfii* in Kurose River, Hiroshima. *Fish. Sci.* **63,** 147–148.

Uzzell, T. (1970). Meiotic mechanisms of naturally occurring unisexual vertebrates. *Am. Nat.* **104,** 433–445.

Vasil'eva, E. D., and Vasil'ev, V. P. (2000). The origin and taxonomic status of the triploid form of the gold fish, *Carrassius auratus* (Ciprinidae). *J. Ichtiology* **40,** 553–563 (in Russian).

Vasil'ev, V. P., Vasil'eva, E. D., and Osinov, A. G. (1989). Evolution of diploid-triploid-tetraploid complexes in fishes of the genus *Cobitis* (Pisces, Cobitidae). *In* "Evolution and Ecology of Unisexual Vertebrates" (R. M. Dawley and J. P. Bogart, eds.), pp. 153–169. New York State Museum, Albany, New York.

Vassart, G., Georges, M., Monsieur, R., Brocas, H., Lequarre, A. S., and Christophe, D. (1987). A sequence in M13 phage detects hypervariable minisatellites in human and animal DNA. *Science* **235,** 683–684.

Vergun, A. A., Markelova, E. S., and Martirosyan, I. A. (2007). Molecular-genetic characteristics of the Du323 locus containing various microsatellite types in the parthenogenetic lizard *Darevskia dahli* (Lacertidae). *Dokl Biochem Biophys* **416,** 278–280.

Vrijenhoek, R. C. (1984). Ecological differentiation among clones: The frozen niche variation model. *In* "Population Biology and Evolution" (K. Wohrmann and V. Loeschcke, eds.), pp. 217–231. Springer-Verlag, Heidelberg.

Vrijenhoek, R. C. (1985). Homozygosity and interstrain variation in the self-fertilizing hermaphroditic fish, *Rivulus marmoratus*. *J. Hered*. **76,** 82–84.

Vrijenhoek, R. C. (1989). Genetic and ecological constraints on the origins and establishment of unisexual vertebrates. *In* "Evolution and Ecology of Unisexual Vertebrates" (R. Dawley and J. Bogart, eds.), pp. 24–31. New York State Museum, Albany, New York.

Vrijenhoek, R. C. (1994). Unisexual fish: Models for studying ecology and evolution. *Annu. Rev. Ecol. Syst*. **25,** 71–96.

Vrijenhoek, R. C., Dawley, R. M., Cole, C. J., and Bogart, J. P. (1989). A list of the known unisexual vertebrates. *In* "Evolution and Ecology of Unisexual Vertebrates" (R. M. Dawley and J. P. Bogart, eds.), pp. 19–23. New York State Museum, Albany, New York.

Vyas, D. K., Moritz, G., Peccinini-Seale, D. M., Wright, J. W., and Brown, W. M. (1990). The evolution history of parthenogenetic *Chnemidophorus lemniscatus* (Sauria: Teiidae). II. Maternal origin and age inferred from mitochondrial DNA analysis. *Evolution* **44,** 922–932.

Weeks, S. C. (1993). The effects of recurrent clonal formation on clonal invasion patterns and sexual persistence: A Monte Carlo simulation of the frozen niche variation model. *Am. Nat*. **141,** 409–427.

Wetherington, J. D., Kotora, K. E., and Vrijenhoek, R. C. (1987). A test of the spontaneous heterosis hypothesis for unisexual vertebrates. *Evolution* **41,** 721–731.

Wilder, J., and Hollocher, H. (2001). Mobile elements and genesis of microsatellites in Dipterians. *Mol. Biol. Evol*. **18,** 384–392.

Wilmhoff, C. D., Csepeggi, C. E., and Petren, K. (2003). Characterization of dinucleotide microsatellite markers in the parthenogenetic mourning gecko (*Lepidodactylus lugubris*). *Mol. Ecol. Notes* **3,** 400–402.

This page intentionally left blank

Index

T

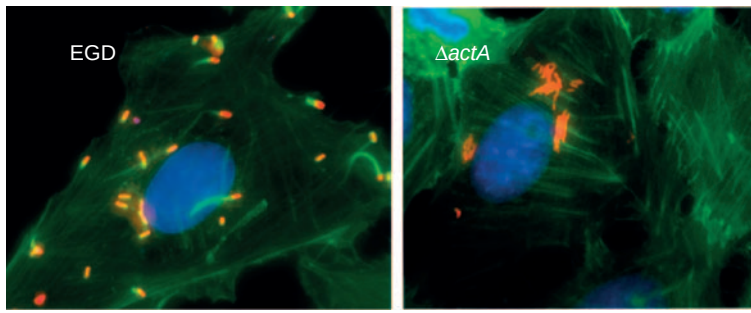

Olivier Dussurget, Figure 1.2 Vero cells infected with *L. monocytogenes* EGD (left panel) or its isogenic *actA* mutant (right panel). Cells were processed for triple fluorescence microscopy 5 h after infection. Bacteria were labeled with a polyclonal anti-*Listeria* antibody (black), actin with FITC-phalloidin (dark gray), and nuclei with DAPI (light gray). Actin accumulates around the parental strain EGD, leading to the formation of typical comet tails. In cells infected with the *actA* mutant, bacteria are unable to induce actin polymerization and multiply in the cytoplasm forming perinuclear microcolonies.

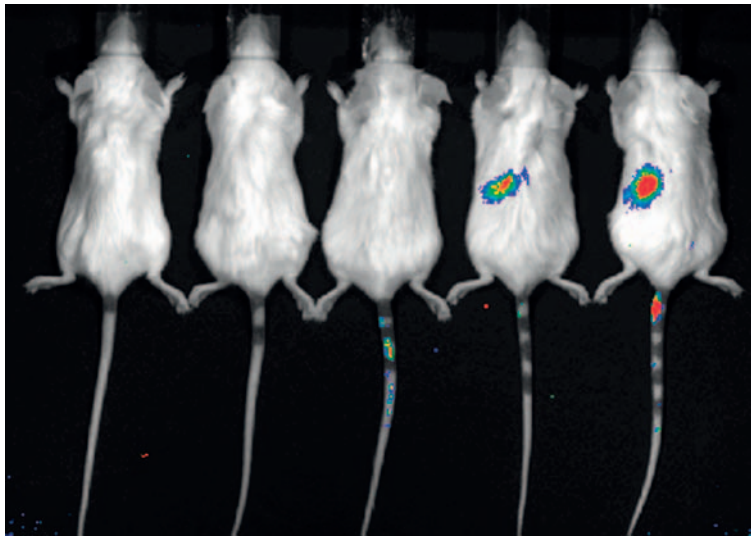

Olivier Dussurget, Figure 1.4 Noninvasive bioluminescence imaging of listeriosis in BALB/c mice. Bioluminescent splenic signals corresponding to bacterial replication foci were detected 48 h after intravenous inoculation of 8×10^3, 4×10^4, 2×10^5, 10^6, and 5×10^6 *L. monocytogenes* from left to right.